Contact Angle, Wettability, and Adhesion

The Kendall Award Symposium
honoring William A. Zisman
sponsored by the Division of
Colloid and Surface Chemistry
at the 144th Meeting of the
American Chemical Society
Los Angeles, Calif., April 2–3, 1963

Frederick M. Fowkes, *Symposium Chairman*

Publication Date: January 1, 1964 | doi: 10.1021/ba-1964-0043.fw001

ADVANCES IN CHEMISTRY SERIES 43

AMERICAN CHEMICAL SOCIETY
WASHINGTON, D.C. 1964

Publication Date: January 1, 1964 | doi: 10.1021/ba-1964-0043.fw001

Library of Congress Catalog Card 63–14481

PRINTED IN THE UNITED STATES OF AMERICA

Advances in Chemistry Series

Robert F. Gould, *Editor*

Advisory Board

AMERICAN CHEMICAL SOCIETY

APPLIED PUBLICATIONS

Publication Date: January 1, 1964 | doi: 10.1021/ba-1964-0043.fw001

In Contact Angle, Wettability, and Adhesion; Fowkes, F.;
Advances in Chemistry; American Chemical Society: Washington, DC, 1964.

PREFACE

This symposium is in honor of the 1963 recipient of the Kendall Award, W. A. Zisman, Naval Research Laboratory.

Dr. Zisman has an unusual combination of talents; he is by training a physicist, is an active scientific investigator, and an efficient administrator of the Naval Research Laboratory's Chemistry Division, but most of all he is a surface chemist and a very outstanding one. Although his doctoral and postdoctoral research with the late P. W. Bridgeman was devoted to the physics of high pressure phenomena in minerals, and though his career at Harvard would have led him to a professorship in geophysics, Dr. Zisman was so infatuated with the exciting developments in surface chemistry pioneered by Langmuir, Rideal, and Harkins that he abandoned geophysics in order to work in surface chemistry. During the depression of the 1930's, Dr. Zisman sought vainly for opportunities for a career in surface chemistry as he worked in a Washington social service headquarters. In 1938 the urge to do surface chemistry became so great that he left his job and financed himself for a year of study in the laboratory of Dr. Goranson at the Carnegie Geophysical Laboratory. Finally, in 1939 Dr. Zisman persuaded a research director that a research program in surface chemistry would be of value, and he was hired by the Naval Research Laboratory.

Dr. Zisman's earliest contribution in surface chemistry was the development of a vibrating condenser method of measuring contact potential (done as a master's thesis at MIT). This method has been widely used ever since. At the Naval Research Laboratory, his prewar work on the spreading of oils on water resulted in three publications, which have become a worthwhile and lasting addition to this subject. During the war, his research led him into a thorough investigation of lubricants and lubrication. Under his guidance, many new synthetic lubricants were developed. He is regarded as one of the world's experts in lubrication, friction, and the use of surface active additives in lubricants. His studies with adsorbed oleophobic monolayers on metals led to his major interest in low energy surfaces, contact angles, and wettability. His studies in this field, aided by his group of very capable chemists and physicists, have produced an enormous body of literature which is best described by the title of this Kendall Award Symposium. This work has led a large collection of excellent data on wettability, and to a new understanding of the relationship of surface tensions in wettability, and has promoted considerable interest in low energy solids and liquids such as the silicones, the fluorocarbons, and fluorochemicals.

Coupled with this research program has been a continuing effort to apply the results of his research to practical problems. The practical applications have been very successful and led to the highest standards of lubrication and the protection of weapons and vessels from the very wide range of temperatures, weather, and corrosive conditions encountered by the Navy. One interesting example occurred recently when an aircraft carrier nearing completion in the Brooklyn Naval Yard caught fire and in the process of putting out the fire all of the expensive

Publication Date: January 1, 1964 | doi: 10.1021/ba-1964-0043.pr001

In Contact Angle, Wettability, and Adhesion; Fowkes, F.;
Advances in Chemistry; American Chemical Society: Washington, DC, 1964.

and delicate electronic equipment was damaged by smoke, oil, and sea water. Dr. Zisman's group was called in, and thanks to their background of practical applications in surface chemistry, they devised a cleaning solution which displaced contamination from the electrical apparatus, leaving it in as good condition as new. This one application saved the Navy millions of dollars.

The literature in surface chemistry is greatly enriched by the 95 publications by Dr. Zisman. There are also 22 patents in his name, mainly on lubricants and protective treatments for surfaces.

Dr. Zisman was nominated for the Kendall Award because of his contributions in the whole field of surface chemistry. While some of us had hoped that this symposium could cover all the fields in which he had worked, it soon became obvious that five full days would be needed, whereas we were allotted only two. Consequently, we had to narrow the scope of the symposium to just one part of his work. Several surface chemists (including Professor LaMer) were disappointed that their particular field in surface chemistry was excluded from this symposium, because they wished to honor Dr. Zisman by participation in the program. Seldom has a chairman had such an enthusiastic response to requests for papers for a symposium. Many of those who have not contributed have written letters expressing their appreciation of Dr. Zisman.

Frederick M. Fowkes

Sprague Electric Co.
North Adams, Mass.

Publication Date: January 1, 1964 | doi: 10.1021/ba-1964-0043.pr001

In Contact Angle, Wettability, and Adhesion; Fowkes, F.;
Advances in Chemistry; American Chemical Society: Washington, DC, 1964.

1

Relation of the Equilibrium Contact Angle to Liquid and Solid Constitution

W. A. ZISMAN

U. S. Naval Research Laboratory
Washington 25, D. C.

Publication Date: January 1, 1964 | doi: 10.1021/ba-1964-0043.ch001

A review of the author's investigations of the equilibrium contact angles of pure liquids on low- and high-energy solid surfaces, both bare and covered with a condensed monomolecular adsorbed film, includes the critical surface tension of wetting and the effect of homology on spreading by pure liquids, the causes of nonspreading on high-energy surfaces, and the existence and properties of autophobic liquids and oleophobic monolayers. Constitutive relationships are summarized in a table of critical surface tensions of wetting. The theory and application of the retraction method of preparing adsorbed monolayers from solution and the conditions for mixed films are presented. Studies of the wetting behavior of solutions of various surfactants and the resultant explanation of the function of a wetting agent are generalized to include nonaqueous systems. Following estimates of the reversible work of adhesion of liquids to solids, the part played by wetting in obtaining optimum adhesion by adhesives is outlined, and a fundamental explanation is given of constitutive effects in the development of strong adhesive joints. Future areas of research on wetting and adhesion are indicated.

In his classic investigation of capillarity, Laplace [76] explained the adhesion of liquids to solids in terms of central fields of force between the volume elements of a continuous medium. This approach was illuminating about the origin of surface tension and energy and their relation to the internal pressure, and it resulted in the fundamental differential equation of capillarity which has been the basis of all

In Contact Angle, Wettability, and Adhesion; Fowkes, F.;
Advances in Chemistry; American Chemical Society: Washington, DC, 1964.

methods of measuring liquid surface tension. For nearly a century this essentially mechanical treatment was elaborated by Gauss, Neumann, Poisson, Kelvin, Rayleigh, van der Waals, and many others; Bakker [3] has summarized their results.

Eventually, the Laplace treatment was abandoned because: in the resulting differential and integral relations among the surface tension, internal pressure of the liquid, the density, and its gradient, the parameters defining the interparticle field of force were not experimentally obtainable; the theory was unsuccessful in explaining common phenomena, some of which are the concern of this symposium; and as the molecular structure of liquids and solids became better understood, the central field of force approach became recognized as an oversimplification which had to be replaced by an electromagnetic and wave mechanics description of intermolecular fields of force. Even today knowledge of the force field in the vicinity of the molecules of a liquid is not precise enough for such calculations—except possibly in the case of the liquefied rare gases. The status of the statistical mechanical treatment of the subject and the mathematic problem to be solved is well indicated in the review of Hirshfelder, Curtiss, and Bird [60].

Over 150 years ago Thomas Young [104] proposed treating the contact angle of a liquid as the result of the mechanical equilibrium of a drop resting on a plane solid surface under the action of three surface tensions (Figure 1)—γ_{LV} at the interface of the liquid and vapor phases, γ_{SL} at the interface of the solid and the liquid, and γ_{SV} at the interface of the solid and vapor. Hence,

$$\gamma_{SV} - \gamma_{SL} = \gamma_{LV} \cos \theta \qquad (1)$$

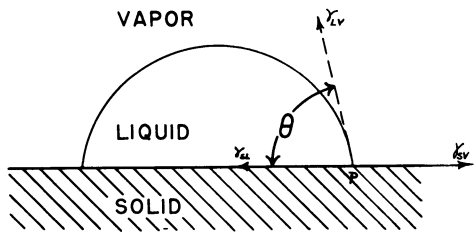

Figure 1. Contact angle of a sessile drop

The concept of the contact angle and its equilibrium was valuable because it gave a definition to the notion of wettability and indicated the surface parameters needing measurement. Today when we say that a liquid is nonspreading, we simply mean that $\theta \neq 0°$; and when the liquid wets the solid completely and spreads freely over the surface at a rate depending on the liquid viscosity and solid surface roughness, we say that $\theta = 0°$. A host of early experiments revealed that every liquid wets every solid to some extent—that is, $\theta \neq 180°$. Another way to express this point is that there is always some adhesion of any liquid to any solid. On a homogeneous solid surface, angle θ is independent of the volume of the liquid drop. Obviously, since the tendency for the liquid to spread increases as θ decreases, the contact angle is a useful inverse measure of spreadability or wettability.

Publication Date: January 1, 1964 | doi: 10.1021/ba-1964-0043.ch001

Young's equation is deceptively simple; actually, there are present conceptual and experimental difficulties; and Equation 1 has been the source of many arguments. In the definition of γ_{SL} and γ_{SV}, neither of which we can conveniently and reliably measure, there is the difficulty that any tensile stresses existing in the surface of a solid would rarely be a system in equilibrium. Solids are rare whose surfaces are free of stresses which have penetrated from below the surface layer. Lester [77] has recently given a sophisticated treatment of Young's equation and has shown that it is correct so long as the drop of liquid rests on a solid which is not too deformable.

Another approach avoids specifying the field of intermolecular force between solid and liquid and instead resorts to thermodynamics. The first application of thermodynamics to capillarity appears to have been made by Thompson [101,102]; later came the classic and general treatment by J. Willard Gibbs [50]. Nearly 60 years had elapsed after Young's treatment before Dupré [31] introduced the reversible work of adhesion of liquid and solid, W_A, and its relation to γ_{SV} and γ_{SL} :

$$W_A = \gamma_{SV} + \gamma_{LV} - \gamma_{SL} \tag{2}$$

This equation is simply the thermodynamic expression of the fact that the reversible work of separating the liquid and solid phases must be equal to the change in the free energy of the system. Therefore, a correct derivation implies that the three terms on the right of Equation 2 are the nature of free energies per unit surface area of the solid-vapor, liquid-vapor, and solid-liquid interfaces, respectively.

As Sumner showed 25 years ago [99], the Young equation can also be derived thermodynamically for the ideal plane solid surface of Figure 1, provided that the system is treated as one in thermal and mechanical equilibrium and the quantities γ_{SL}, γ_{SV} , and γ_{LV} are defined as follows:

$$\begin{aligned} \gamma_{SL} &= \left(\frac{\partial F}{\partial A_{SL}}\right) T,\ \mu_i \\ \gamma_{SV} &= \left(\frac{\partial F}{\partial A_{SV}}\right) T,\ \mu_i \\ \gamma_{LV} &= \left(\frac{\partial F}{\partial A_{LV}}\right) T,\ \mu_i \end{aligned} \tag{3}$$

where F is the Helmholtz free energy (or the work function) of the system, A_{SV} is the area of the solid-vapor interface, etc., T is the temperature, and μ_i is the chemical potential of each component in the phases present. Implicit in this treatment, and also in Young's derivation, is the assumption that the contact angle is independent of the volume of the drop and depends only on the temperature and the nature of the liquid, solid, and vapor phases in contact. Later investigators have given more general thermodynamic derivations of the Young and Dupré equations, most noteworthy being those by Shuttleworth and Bailey [98] and Johnson [64].

It was not until 1937 that Bangham and Razouk [4,5] called attention to the importance of not neglecting the adsorption of vapor on the

surface of the solid phase in deriving the equilibrium relations concerning the contact angle; and they were the first to derive the following widely used forms of the Young and Dupré equations. Here the more precise system of subscripts due to Boyd and Livingston [25] is used in order to distinguish between the solid-vacuum and solid-liquid interfaces. Thus, γ_{S° is the free energy at the solid-vacuum interface, γ_{SV° the corresponding term for the interface of the solid with the saturated vapor, and γ_{LV° that for the interface of the liquid with the saturated vapor.

$$\gamma_{SV^\circ} - \gamma_{SL} = \gamma_{LV^\circ} \cos \theta \tag{4a}$$

$$W_A = \gamma_{S^\circ} + \gamma_{LV^\circ} - \gamma_{SL} \tag{4b}$$

and hence,

$$W_A = \left(\gamma_{S^\circ} - \gamma_{SV^\circ}\right) + \gamma_{LV^\circ} (1 + \cos \theta) \tag{4c}$$

Most textbooks neglect the first term on the right side of Equation 4c. Obviously, the quantity

$$W_{A*} \equiv \gamma_{LV^\circ} (1 + \cos \theta) \tag{4d}$$

is the reversible work of adhesion of the liquid to the solid when coated with an adsorbed film of the saturated vapor. The first parenthetical term in Equation 4c is simply the free energy decrease on immersion of the solid in the saturated vapor phase; for it Bangham and Razouk derived the following expression when the vapor obeys the ideal gas law:

$$\gamma_{S^\circ} - \gamma_{SV^\circ} = RT \int_0^{p_o} \Gamma d(\ln p) \tag{5}$$

where p_o is the pressure of the saturated vapor, R the gas constant, T the absolute temperature, and Γ the Gibbs absorption excess per unit area of the vapor on the solid.

Two investigators of the spreading of insecticides on leaves, Cooper and Nuttall [29], were the originators of the well-known condition for the spreading of a liquid substance, b, on a solid or liquid substance, a:

$$\text{For spreading} \quad S > 0$$

$$\text{For nonspreading} \quad S \leqq 0$$

where

$$S = \gamma_a - (\gamma_{ab} + \gamma_b) \tag{6}$$

or using the subscripts just introduced,

$$S = \gamma_{SV^\circ} - (\gamma_{SL} + \gamma_{LV^\circ}) \tag{7}$$

Publication Date: January 1, 1964 | doi: 10.1021/ba-1964-0043.ch001

Harkins soon afterwards [55-58] developed fully the usefulness of their concept, named S the "initial spreading coefficient," and from it derived the two relations

$$S = W_A - W_C \tag{8}$$

and

$$S = -\left(\frac{\partial F}{\partial A}\right)_{T,\ \mu_i} \tag{9}$$

Here W_C is the reversible work of cohesion of the liquid; from the Dupré equation for a liquid-liquid interface it is simple to show that W_c is twice the liquid surface tension. Equations 8 and 9 are especially suggestive about the physical cause of spreading; however, like Equation 1, they are deceptively simple. As Harkins pointed out, an "initial value" of the spreading coefficient exists for the condition that spreading can initiate; a "final coefficient" exists for the conditions that once spreading has occurred the liquid can remain spread. It turns out that much experimental information is needed to determine the final spreading coefficient.

Assuming that no surface electrification is involved, the above group of equations are the basic thermodynamic relations for describing the equilibrium contact angle and wetting phenomena. In so far as details of molecular structure of the substances and surfaces play an important part, these purely thermodynamic equations would not be expected to suffice to permit us to describe the wetting, spreading, and adhesion of liquids on solids.

Despite many attempts, little was learned about the constitutive aspects of the wetting and spreading of liquids on solids until the past two decades. Practically every investigator was engulfed in the difficulties of obtaining reproducible and significant contact angles. The oldest experimental difficulty, and the source of many controversies, was the occurrence of large differences between the contact angle, θ_A, observed in advancing the liquid boundary over a dry clean surface and the value, θ_R, observed in receding the liquid boundary over the previously wetted surface. There was much concern until very recently about which contact angle was more significant, and if both were significant, what function of the two was useful.

Some clarification of this problem resulted after Wenzel [103] developed a relation between the macroscopic roughness of a solid surface and the contact angle. Wenzel discussed the roughness factor, r (defined as the ratio of the true area of the solid to the apparent area or envelope), and its relation to the apparent or measured contact angle, θ', between the liquid and the envelope to the surface of the solid and to the true contact angle, θ, between the liquid and the surface at the air-liquid-solid contact boundary. He derived the well known relation

$$r = \frac{\cos \theta'}{\cos \theta} \tag{10}$$

from the Young equation and from the definition of r; hence, Equation 10 is essentially a thermodynamic requirement. This relation is important,

Publication Date: January 1, 1964 | doi: 10.1021/ba-1964-0043.ch001

because surfaces having r = 1.00 rarely are encountered; perhaps the nearest to such a smooth surface is that of freshly fire-polished glass or freshly cleaved mica; usually r is significantly greater than 1.0. Wenzel's equation has been derived more generally and applied to woven and other regular structures by Cassie and Baxter [28] and by Shuttleworth and Bailey [98].

Several general consequences of Wenzel's equation should influence all research on contact angles. First, when $\theta < 90°$, Equation 10 indicates $\theta' < \theta$. But most organic liquids exhibit contact angles of less than 90° on clean polished metals; hence, the effect of roughening the metals is to make the apparent contact angle, θ', between the drop and the envelope to the metal surface less than the true contact angle, θ. In other words, each liquid will appear to spread more when the metal is roughened. Secondly, when $\theta > 90°$, Equation 10 indicates $\theta' > \theta$. Since pure water makes a contact angle of 105° to 110° with a smooth paraffin surface, the effect of roughening the surface tends to make θ' greater than 110°; θ' values of 140° have been observed. Thirdly, the experimental problem of accurately measuring the true contact angle is made difficult by the surface roughness, and Wenzel's equation makes it possible to estimate the resulting error. When $\theta = 10°$, the difference, $\theta - \theta'$, between the real and apparent angles will be 5° if r = 1.02. When $\theta = 45°$, the same 5° difference between θ and θ' will occur when r = 1.1. When $\theta = 80°$, the 5° difference in θ and θ' will occur when r = 2.0. This means that, in order to measure small contact angles accurately, the surface used must be much smoother than when large contact angles are measured. Unfortunately, this requirement has rarely been given sufficient attention.

Langmuir's Observations

Langmuir's investigations [71] had a profound influence on all research concerned with surface properties of solids and liquids. In his research prior to 1916 on the adsorption of gases and solids under high vacuum conditions, he had found good evidence that the major changes in the surface properties of solids had occurred with the adsorption of a monomolecular layer. He also had reasoned from the early x-ray findings about the structure of solids that the forces causing adsorption originated from the uncompensated field emanating from the atoms in the surface and that usually this adsorptive field of force was the residual electrical field of the valence electrons belonging to the surface atoms. In view of these conclusions and the fact, well known to chemists, that the fields of force giving rise to secondary valences in a compound are so localized that, for reaction to occur, the contact of atoms was necessary, he stated in 1916 [72] that: (i) such short-range force fields are responsible for nearly all types of adsorption, and (ii) a solid or liquid surface should have its adsorbing properties completely altered when covered by one layer of foreign atoms or molecules.

Langmuir's conclusion that the forces between molecules and the adsorbing surface come into play only at the immediate area of contact made predicting surface interactions much simpler than trying to compute quantities of interest through a precise knowledge of the central field of force between all of the molecules in the solid or liquid. In effect, he had discovered a convenient approximate method for investigating

Publication Date: January 1, 1964 | doi: 10.1021/ba-1964-0043.ch001

the constitutional aspects of adsorption as well as other surface properties. Langmuir later concluded that the adsorptive properties of the surface were determined essentially by the nature and packing of the atoms or groups of atoms in the surface of a solid or liquid, and he often referred to this concept as "the principle of independent surface action." Many years later, because he realized that its theoretical foundation might receive firmer support through use of the more recent scientific developments, he derived in a less widely known paper a limited justification for this principle [70].

Langmuir reported [75] in his famous 1919 lecture to the Faraday Society that an adsorbed monolayer of an organic polar compound could radically change the frictional and wetting properties of solid surfaces. He also emphasized the need for developing experimental methods to study oil films of solids, especially their adhesion and the effects of the resulting oil film on the contact angle with water. A method was described for depositing a condensed monolayer of oleic acid from its position as a compressed film on the surface of water, so that it would adsorb on a clean glass solid as it was withdrawn edgewise through the floating film. Such a monolayer always made glass and many other clean solids act hydrophobic and also lowered the coefficient of friction to only 0.1. Smooth clean surfaces of stearic acid, paraffin wax, myristyl alcohol, and cetyl palmitate exhibited large hydrophobic contact angles, the value for the last three substances being 110°. Langmuir expressed some surprise because the contact angles with the various waxy surfaces were not independent of the nature of the underlying solid; he had expected that they would depend only on the nature of the outermost hydrocarbon groups and so would be similar.

In two later addresses [73,74] Langmuir added other highly significant observations about the effects of adsorbed films on the wettability of solids. A trimolecular stearate film (prepared by the Langmuir-Blodgett technique) exhibited a contact angle of 55.4° with a white mineral oil, 51.7° with ethyl myristate, 48.7° with carbon tetrachloride, 48° with benzene, 1.5° with n-hexane, and 50° with water. The contact angle of this oil with barium stearate multilayers varied little with the number of monolayers in the film—e.g., it was 52° on a monolayer, 55.4° on three layers, and 55.9° on seven layers.

Langmuir offered the following highly suggestive explanation of why the mineral oil rolled off these monolayers: "The probable explanation is that the molecules are so tightly packed into an area of about 20 sq. A. per molecule that only the CH_3 groups at the end of the molecules are exposed on the surface. The properties of CH_3 may well be so different from CH_2 that a liquid consisting mostly of CH_2 does not wet a surface consisting entirely of CH_3." He also reported that as a drop of cetyl alcohol moved over the clean dry surface of glass, a monolayer of alcohol was left which the liquid could not wet. The following interesting observations were added later: "Stearic acid, however, when melted on the glass surface forms drops which show a large contact angle against the glass (oleic acid on glass gives a practically zero contact angle)," and also: "Molten stearic acid on chromium draws up into drops and leaves on the metal a monolayer which has a contact angle for water ($\theta > 90°$) and about 30° for petrolatum." These were the earliest reliable observations of adsorbed films which were hydrophobic and oleophobic.

Publication Date: January 1, 1964 | doi: 10.1021/ba-1964-0043.ch001

Retraction Method and Wetting Properties of Resulting Films

Following an observation in 1941 that dilute solutions of pure heptadecylamine in white mineral oil exhibited considerable contact angles on the glass walls of the containing flask, Pickett and I [23] found that a monolayer of heptadecylamine could be adsorbed from solution on a polished clean solid glass slide or flat metal surface and also that the resulting coated surface could be slowly removed with the plane held vertically (see Figure 2) so that the solution was not transported along with it; the same phenomenon resulted when the heptadecylamine was adsorbed from any of a variety of nonpolar solvents. Any of numerous types of paraffinic polar compounds could be adsorbed and isolated from solution in the same way as the heptadecylamine.

Publication Date: January 1, 1964 | doi: 10.1021/ba-1964-0043.ch001

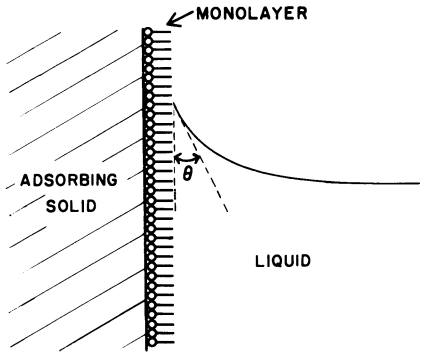

Figure 2. Retraction method

Later using a multiple dip method, Bigelow, Pickett, and I [23] adsorbed octadecylamine on a polished platinum foil dipper from a dilute solution in dicyclohexyl and proved that the average cross-sectional area per adsorbed molecule of the retracted film was 30 sq. A. and hence that the film was a condensed monolayer. In general, in order that such films could form, we found that the polar group had to be located at one extremity of the solute molecule with one or more methyl groups located at the opposite extremity and that the solute molecules must adsorb on the smooth solid surface with sufficient closeness of packing so that the outermost portion of the film is densely populated with methyl groups. A molecular configuration like a long rod or flat plate with a polar group attached to one end of the rod or the rim of the plate, and one or more methyl groups attached to the other end, satisfied these requirements. At my suggestion during World War II, Brockway and Karle examined retracted monolayers by electron diffraction [27,67] and found that the paraffinic polar compounds, octadecylamine and stearic acid, were oriented essentially along the normal to the solid surface with a random tilt of several degrees in the principal axis. These findings were confirmed and studied further by Bigelow and Brockway [21] and also by Menter and Tabor [83]. Further analysis of the data led Epstein [38] to suggest that the adsorbed polar molecules were clustered into two-dimensional, micelle-like, brush heaps.

In a subsequent study of the effect of temperature on the retraction and wetting process with Bigelow and Glass [22], we found a method by which the energy of adsorption of the polar molecule could be estimated and obtained values of from 10 to 14 kcal. per mole for stearyl derivatives; these obviously corresponded to a physical adsorption process. Furthermore, the molar energy of adsorption increased linearly with the number of carbon atoms in the polar molecule, and the energy increment per carbon atom was in reasonable accord with estimates of the energy of intermolecular cohesion per CH_2 group in adlineated (or crystalline) paraffinic compounds. An unexpected observation was that a wide variety of such polar paraffinic compounds could be adsorbed on smooth clean glass and metals by retraction from the molten compound; this made available an experimental method for preparing by retraction adsorbed condensed monolayers of the pure compound. Since this technique avoided any possibility that solvent molecules could remain trapped in the monolayer, it became a valuable method which was frequently used in subsequent comparisons of the properties of monolayers on solids.

Measurements of the wetting properties of various polished surfaces coated by retraction with condensed monolayers proved illuminating. Like Langmuir's observations on barium stearate monolayers and multilayers, these films were found to be both hydrophobic and oleophobic. A variety of organic liquids besides water and mineral oil were found unable to spread on such uncoated surfaces, and the contact angles exhibited were highly reproducible and independent of the nature of the solid substrate upon which a monolayer had been coated during the retraction process. Our results on the surface properties of these monolayers and the process by which they were produced obviously deserved attention because the retracted films were obtained under conditions of adsorption equilibrium at the solid-liquid interface; such films could and did occur in the arts and technology, whereas the Langmuir-Blodgett multilayers [71] are produced only by their one method; they do not occur at the solid-solution interface, and so despite their interesting properties they appear to be artifacts.

The large and reproducible contact angles observed on these retracted monolayers stimulated us to investigate if similar films could be adsorbed and retracted from solutions of various polar-nonpolar compounds in water [93]. In these and later experiments a simple platinum foil chimney was used to prevent inadvertently picking up by the Langmuir-Blodgett process any undissolved floating film-forming solute or contaminate [2,84,92]. It had been known for a long time that metals, glass, and minerals adsorbed a film when immersed in an aqueous solution of a polar adsorptive compound containing a hydrophobic group or radical such that upon removing the solid the aqueous solution would roll off the surface exhibiting a large contact angle. Our experiments confirmed our suspicion that usually the films retracted from aqueous solution are monomolecular and, when the solute concentration is not too low or the pH not inappropriate, are in the condensed state. Since water has such a high surface tension, it was not unexpected to find that by retraction from aqueous solutions one can isolate monolayers of hydrophobic polar compounds having the greatest variety in molecular structures [43,92].

Various experimental studies [2,78,92] revealed that the contact angle of any liquid on a condensed monolayer adsorbed on a polished

solid surface was generally independent of whether it had been retracted from an aqueous or nonaqueous solution. For example, Table I summarizes the results obtained with Levine [78] on the wettability of a solid coated by using a variety of techniques to adsorb and retract a condensed monolayer of n-octadecylamine on platinum, stainless steel, and borosilicate glass. The identical packing of methyl groups in the condensed monolayer formed under each condition is demonstrated by the nearly constant value of the contact angle exhibited by methylene iodide (the maximum variation in the contact angle of 2° is the experimental uncertainty in our contact angle measurements).

Table I. Effect of Method of Film Preparation on Wettability of Octadecylamine Monolayers

Films Prepared by	Methylene Iodide Contact Angle, °
Retraction from molten amine	69
Vapor phase adsorption	69
Retraction from hexadecane soln.	70
Retraction from dicyclohexyl soln.	68
Retraction from nitromethane soln.	69
Retraction from aqueous soln. of $C_{18}H_{37}NH_3Cl$	69

The interesting observation was made [2,92,93] on long-chain paraffinic films retracted from aqueous solution, that the contact angle of water on the resulting condensed film was 90° when the drop was advancing or receding! When the same compound was retracted from a nonaqueous solution in a nonpolar liquid, the advancing contact angle was 101° and the receding contact angle was 90° (see Table II). Water is a nearly unique liquid, in that it readily permeates between the long, adlineated, hydrocarbon chains of a close-packed monolayer of a fatty

Table II. Comparison of Hydrophobic Films of Amines

n-Alkylamine	N[a]	Retracted Films Prepared from: Molten Compound: Thermal-Gradient Method[b] θ_A,°	Thermal-Gradient Method[b] θ_R,°	Isothermal Method[b] θ_A,°	Isothermal Method[b] θ_R,°	Hexadecane Solution: Oleophobic Method[b] θ_A,°	Oleophobic Method[b] θ_R,°	Water Solution: Hydrophobic Method $\theta_A = \theta_R$,°
Butylamine	4	55	48	55	51	--	--	52[c]
Octylamine	8	81	67	74	69	73	68	69[c]
Dodecylamine	12	90	83	89	83	89	83	85[c]
Tetradecylamine	14	91	84	92	87	90	86	86[c]
Hexadecylamine	16	96	87	96	89	96	89	89[c]
Octadecylamine	18	102	89	102	91	101	90	90[b]

[a]Total number of carbon atoms per molecule.
[b]Measurements made at 20.0° ± 0.1°C.
[c]Measurements made at 25° ± 1°C.

Publication Date: January 1, 1964 | doi: 10.1021/ba-1964-0043.ch001

acid, alcohol, or primary amine. Therefore, when the film was adsorbed from aqueous solution, it was saturated with water; hence the drop of water was moving over a water-saturated surface regardless of whether it was advancing or receding, and therefore θ_A and θ_R had to be equal. On one hand, because the monolayer adsorbed from the nonaqueous liquid was devoid of solvent molecules (including water), the drop of water was advancing over an anhydrous film and so the advancing contact angle had the higher value of 101°. On the other hand, the receding drop was moving over a surface which had become saturated with water abstracted by vapor transfer from the water drop during its prior advance, and it should have the same value as the water-soaked film retracted for the aqueous solution. The condition that the advancing and receding contact angles are different on condensed organic monolayers is unusual, and it occurs with a water drop simply because of the great permeability of condensed monolayers to molecularly dispersed water. When the liquid drop is not water, liquid molecules are usually too large to permeate into the condensed monolayer; hence $\theta_A = \theta_R$.

Especially significant about these early results was the wealth of reliable experimental evidence revealing the condition when contact angles were reproducible and interpretable in terms of the structure and composition of the surface phases. Ample justification existed for broadening the range of solid surfaces studied by means of the equilibrium contact angle.

Wetting of Low-Energy Solid Surfaces

In considering the wetting properties of solid surfaces, Fox and I found it helpful to coin a few convenient terms to identify the extremes of the specific surface free energies of solids [46]. As is well known, the specific surface free energies of liquids (excluding the liquid metals) are less than 100 ergs per sq. cm. at ordinary temperatures. But hard solids have surface free energies ranging from about 5000 to 500 ergs per sq. cm., the value being higher the greater the hardness and the higher the melting point. Examples are the ordinary metals, metal oxides, nitrides, and sulfides, silica, glass, ruby, and diamond. Soft organic solids have much lower melting points and the specific surface free energies are generally under 100 ergs per sq. cm. Examples are waxes, solid organic polymers, and in fact, most solid organic compounds. Solids having high specific surface free energies may be said to have "high-energy surfaces," and solids having low specific surface free energies have "low-energy surfaces." This terminology has since been widely adopted.

Because of the comparatively low specific surface free energies of organic and most inorganic liquids, one would expect them to spread freely on solids of high surface energy, since there would result a large decrease in the surface free energy of the system, and this is most often found to be true. But since the surface free energies of such liquids are comparable to those of low-energy solids, among these liquids should be found those exhibiting nonspreading on low-energy solids.

Our previous work on the retraction of monolayers from organic liquids and their oleophobic properties led us to propose that when any

Publication Date: January 1, 1964 | doi: 10.1021/ba-1964-0043.ch001

organic liquid would not spread on a high-energy surface, it did so because it contained a dissolved polar-nonpolar compound from which an oleophobic film had adsorbed on the surface. However, measurements on organic liquids from which polar-nonpolar adsorbable impurities had been carefully removed demonstrated that pure liquids like tri-o-cresyl phosphate and benzyl phenylundecanoate would not spread on high-energy surfaces. Because of these unexpected and at the time inexplicable results, a temporary detour was made to seek the missing information by studying the spreading of pure liquids on well defined low-energy surfaces.

Equilibrium contact angles of a variety of pure liquids were studied with Fox [46,47,48] and later Ellison [33,34] on surfaces of solid organic polymers free of contaminants, monomer, or plasticizers—examples are polytetrafluoroethylene, polyethylene, poly(vinyl chloride), poly(ethylene terephthalate), etc. Because of the large percentage error in low contact angles resulting from the surface roughness, great care was exercised in preparing the surfaces of these polymers in extremely clean and glossy-smooth condition. Each liquid used in observing contact angles on such surfaces was percolated slowly through columns packed with adsorbents to remove adsorptive contaminants. Using such solids and liquids it was found, in disagreement with past reports on contact angle phenomena, that these systems behaved reproducibly; furthermore, the advancing and receding contact angles were identical so long as the liquid drop was advancing or receding sufficiently slowly to be reasonably close to an equilibrium condition.

A comparison was made between the results of measurements of the contact angles of various volatile liquids on polytetrafluoroethylene when measured in air saturated with the liquid vapor and when measured in the open air. No significant differences were found in the contact angles of the n-alkanes until pentane or lower boiling homologs were used. Differences became significant in the series of dimethyl silicones only when homologs below the tetramer were used. This means that the adsorptivity of these vapors on polytetrafluoroethylene was so low at ordinary temperatures that the condensed vapor did not significantly affect the spreading of the liquid drop on the solid. Therefore, so long as attention was confined to measurements of the contact angles of the high boiling liquids on this and other low-energy surfaces, the measurements could be made in the open air rather than in a saturated atmosphere of the liquid vapor.

In general, a rectilinear relation was established empirically between the cosine of the contact angle, θ, and the surface tension, γ_{LV°, for each homologous series of organic liquids. Figure 3 illustrates the results with the n-alkanes on polytetrafluoroethylene [46]. The critical surface tension for wetting by each homologous series was defined by the intercept of the horizontal line $\cos \theta = 1$ with the extrapolated straight-line plot $\cos \theta$ vs. γ_{LV°, and it was denoted by γ_c. This intercept was found more valuable than the slope of the rectilinear graph for correlations between wettability and constitution. Even when $\cos \theta$ was plotted against γ_{LV° for a variety of nonhomologous liquids, the graphical points fell close to a straight line or collected around it in a narrow rectilinear band (see Figures 4 and 5). Certain low-energy surfaces, such as on polytetrafluoroethylene (Figures 6 and 7), exhibit curvature of this band for values of γ_{LV° above 50 dynes per cm. But

Publication Date: January 1, 1964 | doi: 10.1021/ba-1964-0043.ch001

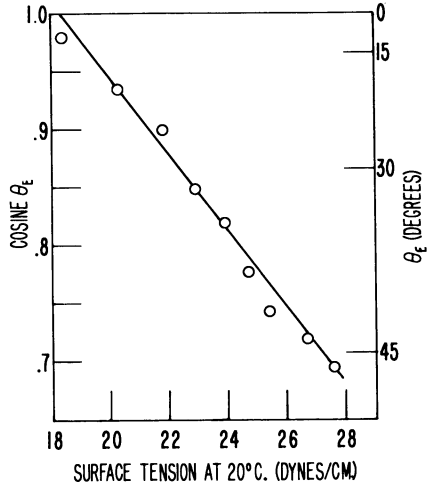

Figure 3. Wettability of polytetrafluoroethylene by the n-alkanes [46]

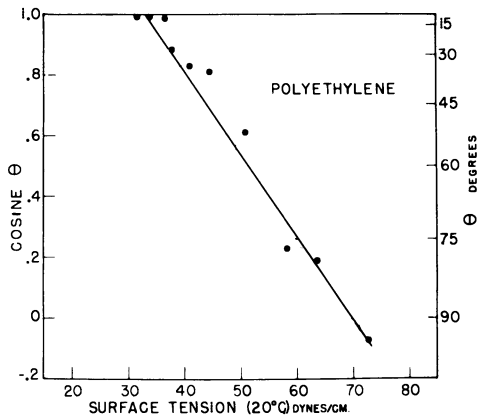

Figure 4. Wettability of polyethylene [48]

in those cases we found that the curvature results because weak hydrogen bonds form between the molecules of liquid and those in the solid surface. This is most likely to happen with liquids of high surface tension, because they are always hydrogen-bonding liquids. In general, the graph of cos θ vs. γ_{LV}° for any low-energy surface is always a straight line (or a narrow rectilinear band) as in Figure 4, unless the molecules in the solid surface form hydrogen bonds.

When rectilinear bands are obtained in this type of graph, the intercept of the lower limb of the band at cos θ = 1 is chosen as the critical surface tension, γ_c, of the solid. Although this intercept is less precisely defined than the critical surface tension of a homologous

Publication Date: January 1, 1964 | doi: 10.1021/ba-1964-0043.ch001

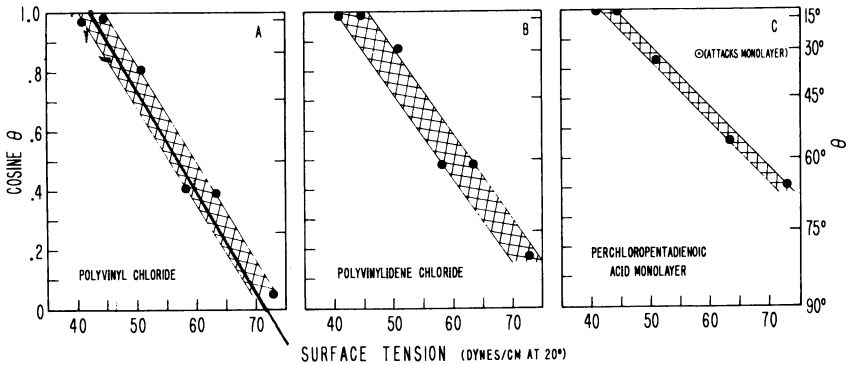

Figure 5. Wettability by various liquids on surface of:

A. Poly(vinyl chloride)
B. Poly(vinylidene chloride)
C. Close-packed monolayer of perchloropentadienoic acid [33]

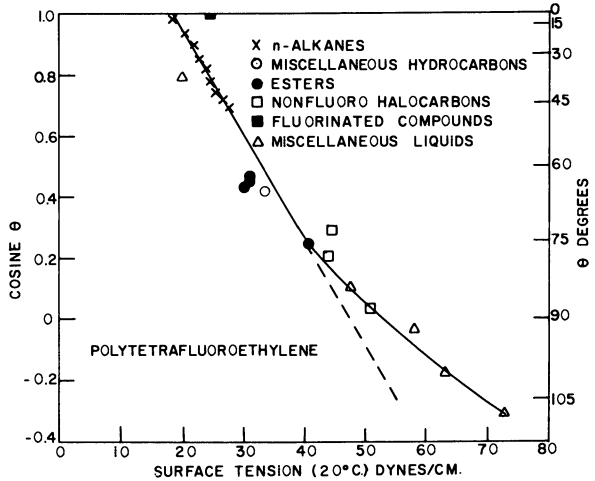

Figure 6. Wettability of polytetrafluoroethylene by various liquids [47]

series of liquids, nevertheless it is an even more useful parameter because it is a characteristic of the solid surface. It has proved to be a useful empirical parameter whose relative values act as one would expect of γ_{S^o}, the specific surface free energies of the solid. The widespread occurrence of the rectilinear relationship between cos θ and γ_{LV^o} in the rapidly growing body of reliable experimental data led us to use γ_c to characterize and compare the wettabilities of a variety of low-energy surfaces.

By comparing values of γ_c of structurally "homologous" or "analogous" solids, such as unbranched polyethylene and its various chlorinated

Publication Date: January 1, 1964 | doi: 10.1021/ba-1964-0043.ch001

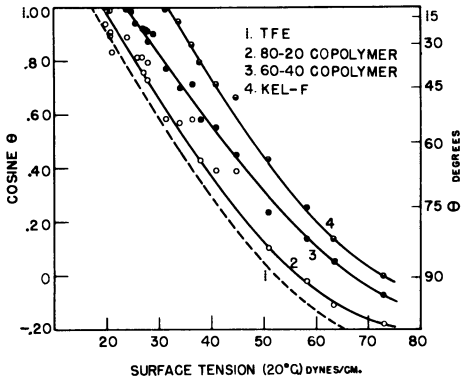

Figure 7. Wettability of copolymers of polytetrafluoroethylene and polychlorotrifluoroethylene [47]

or fluorinated analogs (see Table III) and by making the usually reasonable assumption that the surface composition of the solid polymer was the same as that of the horizontally oriented polymer molecule, it was possible to measure the effect of surface constitution on the wettability.

In the upper curve of Figure 8, γ_c values for polyethylene, poly(vinyl chloride), and poly(vinylidene chloride) are plotted against the atom per cent replacement of hydrogen by chlorine. Although the introduction of the first chlorine atom in the monomer causes γ_c to rise from 31 to 39 dynes per cm., the addition of a second chlorine increases γ_c only to 40 dynes per cm. On comparing the upper and lower curves, striking differences are evident in the effect on γ_c of chlorine or fluorine replacement of hydrogen, both as to the direction of the change and the effect of progressive halogenation. Although polytetrachloroethylene does not exist, an organic coating with an outermost surface comprised of close-packed covalent chlorine atoms was prepared [33] by the retraction method to form a condensed, adsorbed, and oriented monolayer of perchloropentadienoic acid (CCl_2 = CCl-CCl = CCl-COOH) on the clean polished surface of glass or platinum. Not only is the graph of cos θ vs. γ_{LV}° for such a surface similar to those of the above-mentioned chlorinated polyethylenes, but the corresponding value of γ_c (43 dynes per cm.) is shifted in the appropriate direction—i.e., to higher values of γ_c. Extrapolation of the line defined by the experimental points for the two chlorinated polymers in Figure 8 to the value of γ_c for 100% hydrogen replacement indicates a value of 42 dynes per cm. Thus, the hypothetical polytetrachloroethylene surface should have a critical surface tension of wetting of 42 dynes per cm., which is only 1 dyne per cm. less than the experimental value found for the perchloropentadienoic acid monolayer. This shows how closely the wetting properties of the latter surface approximate those of a fully chlorinated polymeric solid surface.

Since the same results were obtained regardless of the nature of the polished solid substrate on which the perchloropentadienoic acid monolayer was adsorbed, it was evident that the wettability of these monolayer coated surfaces is determined by the nature and packing of

Publication Date: January 1, 1964 | doi: 10.1021/ba-1964-0043.ch001

Table III. Critical Surface Tensions of Halogenated Polyethylenes [33]

Polymer	Structural Formula	Critical Surface Tension, Dynes/Cm.
Poly(vinylidene chloride)	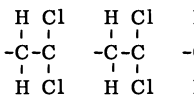	40
Poly(vinyl chloride)	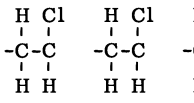	39
Polyethylene	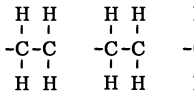	31
Poly(vinyl fluoride)	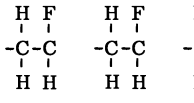	28
Poly(vinylidene fluoride)	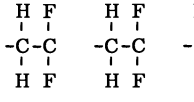	25
Polytrifluoroethylene	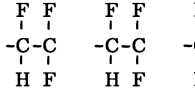	22
Polytetrafluoroethylene (Teflon)	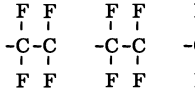	18

the outermost atom in exposed groups of atoms in the coating and not by the nature and arrangements of atoms in the solid substrate 10 to 20A. below the surface layer. This will exemplify the extreme localization of the fields of force of covalent bonded atoms responsible for the adhesion of liquids to organic solids.

In the upper curve of Figure 9 is plotted cos θ for each of the n-alkane liquids on a close-packed retracted monolayer of prim-octadecylamine on platinum or glass [94]. Comparable data for the surface of polyethylene cannot be shown here because the alkane liquids exhibit zero contact angles on this solid. In other words, the graph is so much above that of octadecylamine that it cannot be shown in this plot. The second curve gives the analogous results for polytetrafluoroethylene [46]. By structural analogy, one can reason that since the surface of close-packed $-CH_3$ groups is much less wettable than one of $-CH_2-$ groups, a surface of $-CF_3$ groups should also be much less wettable than one of $-CF_2-$ groups. This simple argument led Schulman and me [91] to study the wettability of close-packed adsorbed films of

Publication Date: January 1, 1964 | doi: 10.1021/ba-1964-0043.ch001

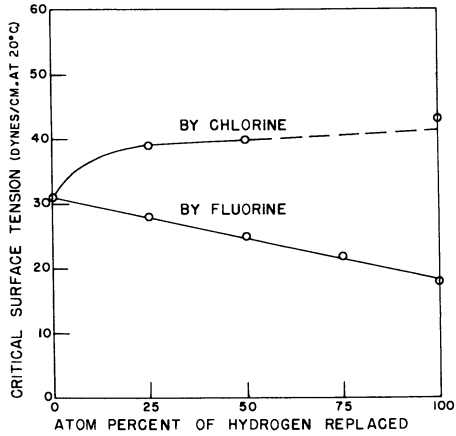

Figure 8. Effect of progressive halogen substitution on wettability of polyethylene-type surfaces [96]

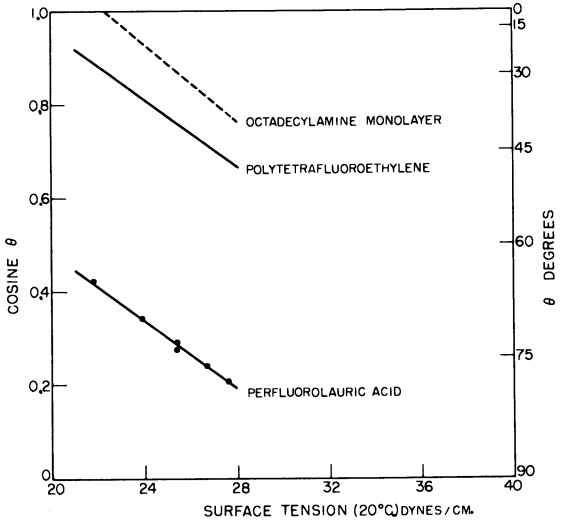

Figure 9. Comparison of effects of $-CH_3$, $-CH_2-$, and $-CF_3$ groups on wettability by n-alkanes [105]

perfluorodecanoic (or ϕ-decanoic) acid. This acid had only recently been prepared by the Simon's process of electrochemical fluorination. Soon afterward a study was made with Shafrin and Hare [53] of the homologous family of perfluoro fatty acids, and we then found that a condensed monolayer of perfluorolauric acid, $F_3C(CF_2)_{10}COOH$, was the most nonwettable surface ever reported; on it every liquid we studied was unable to spread. Figure 10 shows that very large contact angles

Publication Date: January 1, 1964 | doi: 10.1021/ba-1964-0043.ch001

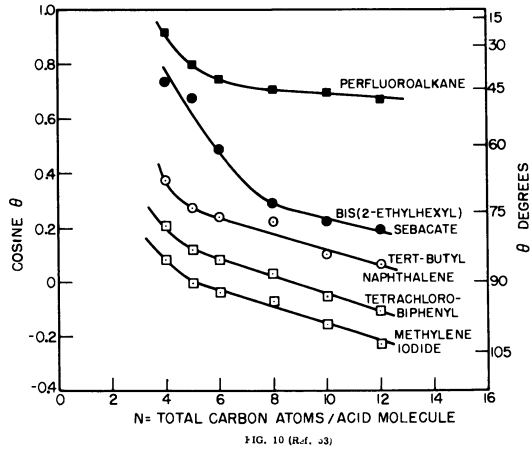

FIG. 10 (Ref. 53)

Figure 10. Wettability of condensed monolayers of perfluoroalkanoic acids by various liquids [53]

are exhibited by common types of organic liquids upon retracted monolayers of any of the perfluoroalkanoic acids.

Since Berry [18] had succeeded in preparing the interesting and related ψ-alkanoic acids

$$HF_2C(CF_2)_nCOOH$$

we investigated their behavior as condensed monolayers adsorbed by retraction on polished platinum foil [32]. As expected, such coated surfaces also exhibited large contact angles with all liquids. Figure 11

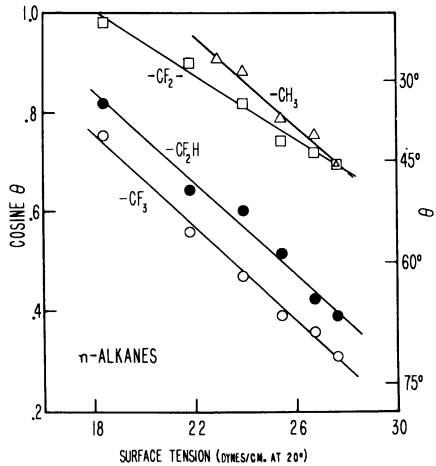

Figure 11. Effect of progressive fluorination of ω-CH_3 group on wettability by n-alkanes [32]

compares the cos θ vs. γ_{LV} graphs for the n-alkanes on surfaces coated with close-packed $-CF_3$, $-CF_2H$, $-CF_2-$, and $-CH_3$ groups. Just as the hydrogen-donating liquids—water, glycerol, glycol, and formamide—all formed weak hydrogen bonds with the fluorine atoms in the surface of polytetrafluoroethylene, the same effect occurred in wetting surfaces covered with monolayers having outermost $-CF_3$ and $-CF_2H$ groups [32,53,91].

Our results on the wettability of surfaces covered with highly fluorine-substituted alkyl groups stimulated several research laboratories to apply these surface properties to polymeric coating materials for textile fibers and fabrics as a means of imparting to them nonstaining, oil-, and water-resistant properties. Such products are becoming very prominent today and the contact angle is used for product control and trade specifications [1].

Regularities in the cos θ vs. γ_{LV} graphs of various fluorine-rich surfaces are illustrated in Figure 12. From the cos $\theta = 1$ intercepts

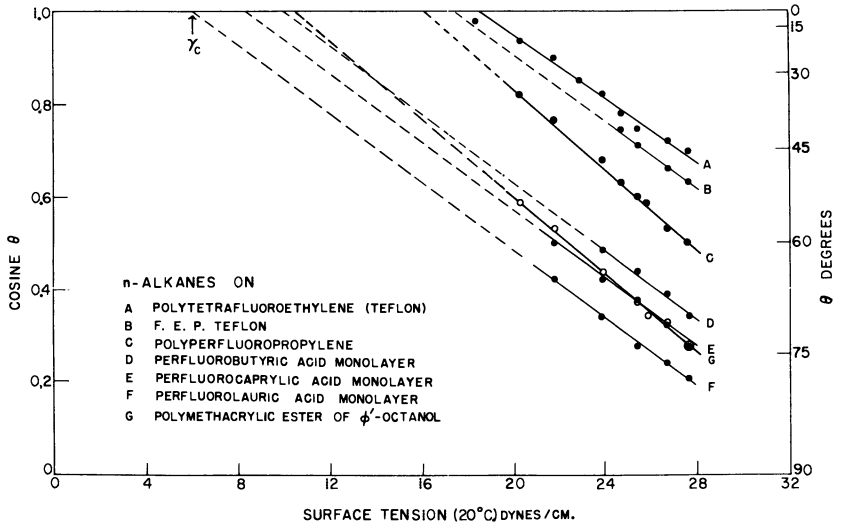

Figure 12. Contact angles for n-alkanes on various fluorinated surfaces [17,96]

on Figure 12, it is evident that γ_c has a value of about 18.5 dynes per cm. for the n-alkanes on the surface of Teflon. Values of about 17 and 15 dynes per cm. are obtained from curves B and C—i.e., the introduction of the perfluoromethyl group as a side chain in the polymer reduces γ_c, the reduction becoming greater the higher the surface concentration of exposed $-CF_3$ groups. An adsorbed, close-packed monolayer of a perfluoro fatty acid (curves D, E, and F) is an example of such a surface. The values of γ_c for such surfaces are, therefore, much lower than for surfaces comprised only of $-CF_2-$ groups. The closer the packing of the aliphatic chains of the adsorbed molecules, the closer the packing of the exposed terminal $-CF_3$ groups, and hence the lower γ_c. Thus, the value for a condensed monolayer of perfluorolauric acid

Publication Date: January 1, 1964 | doi: 10.1021/ba-1964-0043.ch001

(curve F) is only 6 dynes per cm., and this is the lowest value yet encountered; only the condensed inert gases could spread on such a surface. The value of 10.6 dynes per cm. for the polymethacrylic ester of perfluorooctanol (curve G) is the lowest encountered with any solid polymer [17].

Results to date of wettability studies on clean, smooth, plasticizer-free, polymeric solids of general interest are summarized in Table IV. Included in this table is the value for poly(vinyl alcohol) (γ_c = 37 dynes per cm.) reported by Ray, Anderson, and Scholz [88]; the same investigators also found a range in γ_c of 40 to 45 dynes per cm. for a series

Table IV. Critical Surface Tensions of Various Polymeric Solids [106]

Polymeric Solid	γ_c, Dynes/Cm. at 20°C.	Ref.
Polymethacrylic ester of ϕ'-octanol	10.6	[17]
Polyhexafluoropropylene	16.2	[16]
Polytetrafluoroethylene	18.5	[46]
Polytrifluoroethylene	22	[33]
Poly(vinylidene fluoride)	25	[33]
Poly(vinyl fluoride)	28	[33]
Polyethylene	31	[48]
Polytrifluorochloroethylene	31	[47]
Polystyrene	33	[34]
Poly(vinyl alcohol)	37	[88]
Poly(methyl methacrylate)	39	[61]
Poly(vinyl chloride)	39	[33]
Poly(vinylidene chloride)	40	[33]
Poly(ethylene terephthalate)	43	[34]
Poly(hexamethylene adipamide)	46	[34]

of hydroxyl-rich surfaces of the starch polymer type [90]. These values of γ_c are reasonably close to that of 43 dynes per cm. reported for the oxygen-rich surface of poly(ethylene terephthalate). Among the early reliable studies of contact angle vs. surface tension for smooth surfaces of various waxes, resins, and cellulose derivatives were those reported by Bartell and Zuidema [8]. If the cosines of their contact angles are plotted against γ_{LV}°, good straight lines are obtained. The values of γ_c for their resin surfaces rich in exposed oxygen-containing groups fit in well with the data presented here on the relative wettability of oxygen-rich surfaces. Nylon, with its many exposed amide groups, has the highest γ_c value of the common plastics we have reported [34]. Since γ_c for all the polymers of Table IV are well below the surface tension of water (72.8 dynes per cm.), all are hydrophobic.

Effect of Constitution on Wetting of Low-Energy Surfaces

The widespread occurrence of the rectilinear relationship between cos θ and γ_{LV} in the large body of experimental data and the fact that these straight lines diverge away from the cos θ = 1 axis have made it possible to use γ_c to characterize the wettability of each low-energy surface. In Table V are presented the results of values of γ_c obtained from some comparative studies [96,105] of the wettability of a number of well-defined, low-energy, solid surfaces. In the first column is

Publication Date: January 1, 1964 | doi: 10.1021/ba-1964-0043.ch001

Table V. Critical Surface Tensions of Low-Energy Surfaces [96]

Surface Constitution	γ_c, Dynes/Cm. at 20°	Ref.
A. Fluorocarbon Surfaces		
$-CF_3$	6	[53]
$-CF_2H$	15	[32]
$-CF_3$ and $-CF_2-$	17	[15, 16]
$-CF_2-$	18	[46]
$-CH_2-CF_3$	20	[95]
$-CF_2-CFH-$	22	[33]
$-CF_2-CH_2-$	25	[33]
$-CFH-CH_2-$	28	[33]
B. Hydrocarbon Surfaces		
$-CH_3$ (crystal)	22	[48]
$-CH_3$ (monolayer)	24	[94]
$-CH_2-$	31	[48]
$-CH_2-$ and —CH—	33	[43]
—CH— (phenyl ring edge)	35	[43]
C. Chlorocarbon Surfaces		
$-CClH-CH_2-$	39	[33]
$-CCl_2-CH_2-$	40	[33]
$=CCl_2$	43	[33]
D. Nitrated Hydrocarbon Surfaces [45]		
$-CH_2ONO_2$ (crystal) [110]	40	[45]
$-C(NO_2)_3$ (monolayer)	42	[45]
$-CH_2NHNO_2$ (crystal)	44	[45]
$-CH_2ONO_2$ (crystal) [101]	45	[45]

given the constitution of the atoms or organic radicals in the solid surface arranged in the order of increasing values of γ_c. Literature references are given in the third column. Data have been grouped under the subheadings emphasizing the surface chemical constitution—i.e., fluorocarbons, hydrocarbons, chlorocarbons, and nitrated hydrocarbons.

Some important results included in Table V deserve a brief discussion. The surface of lowest energy ever found (and hence having the lowest γ_c) is that comprised of closest packed $-CF_3$ groups. The replacement of a single fluorine atom by a hydrogen atom in a terminal $-CF_3$ group more than doubles γ_c. A parallel and regular increase in γ_c has been observed with progressive replacement of fluorine by hydrogen atoms in the surfaces of bulk polymers. Data for polytetrafluoroethylene $(-CF_2-CF_2-)_n$, polytrifluoroethylene $(-CF_2-CFH-)_n$, poly(vinylidene fluoride) $(-CF_2-CH_2-)_n$, and poly(vinyl fluoride) $(-CFH-CH_2-)_n$ are listed in the order of increasing values of γ_c; however, this is also the order of decreasing fluorine content. As pointed out earlier, a plot of γ_c against the atom per cent replacement of hydrogen in the monomer by fluorine results in a straight line (Figure 8).

Publication Date: January 1, 1964 | doi: 10.1021/ba-1964-0043.ch001

Among the hydrocarbons the lowest values of γ_c are found in surfaces comprising close-packed, oriented, methyl groups. The lowest value of 22 dynes per cm. results when the methyl groups are packed in the close-packed array found in the easiest cleavage plane of a single crystal of a higher paraffin such as n-hexatriacontane. The less closely packed arrangement found in a condensed adsorbed monolayer of a high molecular weight fatty acid is characterized by a γ_c value of about 24 dynes per cm. The great sensitivity of the contact angle (and hence of γ_c) to such subtle changes in the packing of the methyl groups comprising the surface of the solid is remarkable, and it has much significance in technological aspects of wetting and adhesion. The transition from a surface comprised of $-CH_3$ groups to one of $-CH_2-$ groups results in an increase in γ_c of some 10 dynes per cm.; this is to be compared with the increase of 12 dynes per cm. observed in going from a surface of $-CF_3$ to one of $-CF_2-$ groups. The presence of aromatic carbon atoms in the hydrocarbon surface also increases γ_c. Thus, the introduction of a significant proportion of phenyl groups in the surface in going from polyethylene to polystyrene raises γ_c from 31 to 33 dynes per cm. A further increase to 35 dynes per cm. results when the surface is composed solely of phenyl groups, edge on, as in the cleavage surface of naphthalene.

The results of many experiments summarized in Table V make it evident that the wettability of low-energy organic surfaces, or of high-energy surfaces coated by organic films is determined essentially by the nature and packing of the exposed surface atoms of the solid and is otherwise independent of the nature and arrangements of the underlying atoms and molecules. These findings exemplify the extreme localization of the attractive field of force around the solid surfaces of covalent-bonded atoms which are responsible for the adhesion of a great variety of liquids to solids; the field of force becomes unimportant at a distance of only a few atom diameters and hence there is little contribution to the adhesion by atoms not in the surface layers. However, when the constitution of the solid, or of the adsorbed monolayer, is such that either ions or large, uncompensated, permanent dipoles are located in the outermost portion of the surface monolayer, the residual field of force of the surface is much less localized.

Recent examples will be found in the unexpectedly strong wetting behavior of a solid coated with an adsorbed terminally fluorinated monolayer of a fatty acid or amine [95]. The outermost group of atoms (the $-CF_3$ group) has a strong dipole whose electrostatic field is not compensated by adjacent dipoles within the same molecule; hence, the external field of force is effective over much greater distances than that of nonpolar substances, so that the principle of localized action no longer holds. A solid coated with such a film is much more wettable by all liquids than is a coating made up of the fully fluorinated acid in which there is internal compensation of local dipoles. Subsequent similar studies with Shafrin [97] of a series of progressively fluorinated fatty acids synthesized by Brace [26] showed that only after the seven outermost carbon atoms were fully fluorinated, did the contact angles of various liquids on the surface approach those of a perfluoro fatty acid monolayer. In summary, our studies of wetting demonstrate that although there are understandable exceptions to Langmuir's "principle of independent surface action" it is usually true.

Publication Date: January 1, 1964 | doi: 10.1021/ba-1964-0043.ch001

Wetting of High-Energy Surfaces

Many years ago Harkins and Feldman [57], extrapolating from measurements of the spreading coefficients of liquids on water and mercury [56,58], concluded that practically all liquids should spread on clean metals and other inorganic high-melting solids. But the research already summarized here has shown that when the liquid in contact with a high-energy surface is made up in whole or in part of polar-nonpolar molecules of certain types, there will be produced through adsorption at the solid-liquid interface a low-energy surface on which the liquid will not spread. When the adsorbed film comprises long-chain, unbranched, polar molecules, which are able to form a close-packed array with terminal $-CH_3$, $-CF_2H$, or $-CF_3$ groups, the resulting surfaces permit spreading only by liquids having low surface tensions. When the adsorbed molecules are branched or cyclic structures [43], the resulting surfaces permit spreading by all liquids except those having high surface tensions.

It seemed possible to us by 1954 to explain the essential features of the wetting behavior of each organic liquid on high-energy surfaces, provided that information is available on the over-all configuration and packing of the adsorbed molecules of liquid. Therefore, the wetting behavior of over a hundred pure liquids comprising a great variety of organic and inorganic liquids was examined at 20°C. on surfaces of polished clean platinum, stainless steel, brass, fused silica, borosilicate glass, and synthetic sapphire (α-Al_2O_3). Some of the results obtained with Fox and Hare are summarized [44] in a condensed form in Tables VI and VII.

From a study of these data two problems were recognized, but their solution took several years of research. The first problem was defined by Hare and me [54] when we established that liquids such as 1-octanol, 2-octanol, 2-ethyl-1-hexanol, trichlorodiphenyl, and tri-o-cresyl phosphate exhibited appreciable contact angles on all these high-energy surfaces, no matter what extremes of purification were used. Examples of the observed equilibrium contact angles are given in Table VII. Our further investigation revealed that each liquid was nonspreading because the molecules adsorbed on the solid to form a film whose critical surface tension of wetting was less than the surface tension of the liquid itself. In short, each liquid was unable to spread upon its own adsorbed oriented monolayer; hence, we named such substances "autophobic liquids."

It followed logically that liquids which are not autophobic should have surface tensions which are less than the critical surface tensions of wetting of their adsorbed monolayers, and the data on γ_c vs. constitution agreed with this conclusion. For example, the polymethylsiloxane liquids spread on all high-energy surfaces because the surface tensions of 19 to 20 dynes per cm. [42] are always less than the critical surface tensions of their own adsorbed films. This follows because an adsorbed close-packed monolayer of such silicone molecules has an outermost surface of methyl groups which are not quite as closely packed as those in a single crystal of a paraffin. Since γ_c of close-packed stearic acid or octadecylamine is about 24 dynes per cm., the value of γ_c for the silicone monolayer must exceed 22; actually, it is 24 or more, dependent on packing [106]. Because γ_{LV}° of this class of silicones is below

Publication Date: January 1, 1964 | doi: 10.1021/ba-1964-0043.ch001

Table VI. Survey of Wettability by

Class of Liquid	Liquid Surface Tension, Dynes/Cm. at 20°C.
Open-chain aliphatic hydrocarbons	27 - 31
Open-chain methyl silicones	19 - 20
Open-chain aliphatic ethers	28 - 30
Open-chain aliphatic monoesters	27 - 29
Open-chain aliphatic diesters	28 - 34
Cyclic, saturated hydrocarbons	26 - 35
Aromatic-aliphatic hydrocarbons	28 - 38
Cyclic esters (dumbbell)	36 - 42
Cyclic esters (one ring)	30 - 35
Cyclic ethers	33 - 44
Phosphate esters (aromatic)	40 - 44
Phosphate esters (chlorinated aromatic)	44 - 46
Polychlorobiphenyls	42 - 46

20 dynes per cm., $\gamma_{LV} < \gamma_c$ and hence these silicones cannot be autophobic. A similar argument using the critical surface tension of polyethylene of 31 dynes per cm. and the fact that the surface tensions of liquid aliphatic hydrocarbons are always less than 30 dynes per cm., leads us at once to understand why such hydrocarbons cannot be autophobic.

The second problem encountered was to explain why all pure liquid esters spread completely upon the metals studied, yet as Tables VI and VII indicate, some spread on glass, silica, and α-Al_2O_3 and others did not. A careful investigation with Hare and Fox [44] finally revealed that the cause of these differences in spreadability is the hydrolysis of the ester immediately after the molecule has adsorbed upon hydrated surfaces such as those of glass, fused silica, and α-Al_2O_3. This is not surprising, since the polar group of the ester would be expected to adsorb on immediate contact with the solid surface unless prevented by steric hindrance, and since the surface molecules of the water of hydration and adsorption of the glass (being oriented) should be more effective in causing hydrolysis than bulk water. Hence, as the result of surface hydrolysis, two fragments of the ester result. The fragment which has a greater average lifetime of adsorption is more likely to remain, and eventually this molecular species coats the surface with a close-packed monolayer. Rapidly the surface becomes blocked or "poisoned" by the coating of the hydrolysis product and so the hydrolysis reaction ceases. Obviously, under these circumstances the volume concentration of hydrolyzed ester is too small to be measured by ordinary analytical methods. When the resulting adsorbed monolayer has a critical surface tension of wetting less than the surface tension

Higher Boiling Liquids [44]

Spreadability on		
Metals	Fused SiO_2	α-Al_2O_3
Spread	Spread	Spread
Spread	Spread	Spread
Spread	Spread	Spread
Spread	(No + yes)	(No + yes)
Spread	No	No
Spread	Spread	Spread
Spread	(No + yes)	(No + yes)
No	No	No
(No and yes)	No	No
No	(No and yes)	(No and yes)
No	No	No
No	No	No
No	No	No

of the ester, nonspreading behavior is observed—i.e., the ester is unable to spread upon the adsorbed film of its own hydrolysis product. Esters having a great variety of structures have been studied, and in every instance of nonspreading on glass, fused silica, and α-Al_2O_3, we have been able to give a similar explanation of the behavior.

As an example, consider the ability of bis(2-ethylhexyl) sebacate to spread freely on metals and its inability to spread on fused silica, glass, or α-Al_2O_3. On these hydrated nonmetallic surfaces the diester hydrolyzes to form 2-ethylhexanoic acid. The critical surface tension

Table VII. Some Autophobic Liquids and Their Contact Angles on High-Energy Surfaces [54]

Liquid	γ_{LV} at 20°C.	θ at 20°C., °			
		18.8 stainless steel	Platinum	Fused silica	α-Al_2O_3
1-Octanol	27.8	35	42	42	43
2-Octanol	26.7	14	29	30	26
2-Ethyl-1-hexanol	26.7	< 5	20	26	19
2-Butyl-1-pentanol	26.1	-	7	20	7
n-Octanoic acid	29.2	34	42	32	43
2-Ethylhexanoic acid	27.8	< 5	11	17	12
Tri-o-cresyl phosphate	40.9	-	7	14	18
Tri-o-chlorophenyl phosphate	45.8	-	7	19	21

Publication Date: January 1, 1964 | doi: 10.1021/ba-1964-0043.ch001

of wetting of a close-packed monolayer of 2-ethylhexanoic acid is about 28 dynes per cm. [44]. Since the surface tension of this diester is 31.1 dynes per cm. at 20°C., $\gamma_{LV} > \gamma_c$, and the diester cannot spread on the film of its hydrolyzed product. When adsorbed on metals at ordinary conditions of relative humidity, the diester is not in contact with hydrated water and so cannot hydrolyze; nevertheless, following de Boer's ideas [30], the molecule should be adsorbed lying on the surface as flat as possible to allow contact of the greatest number of polarizable atoms. The resulting adsorbed monolayer, because of the presence of the ester groups, must have a critical surface tension of wetting greater than that of polyethylene; in other words, γ_c is considerably greater than 31 dynes per cm. Hence, $\gamma_{LV} < \gamma_c$, and the diester must spread freely over its own adsorbed film and over the metal surface.

Once these two classes of nonspreading liquids were understood, it proved possible to explain the wetting and spreading properties of all of the many liquids investigated. To summarize the results of our investigations on the wetting of high-energy surfaces: Every liquid having a low specific surface free energy always spreads freely on specularly smooth, clean, high-energy surfaces at ordinary temperatures unless the film adsorbed by the solid converts it into a low-energy surface having a critical surface tension less than the surface tension of the liquid. Because of the highly localized nature of the forces between each solid surface and the molecules of a liquid and also between the molecules of each liquid, a monolayer of adsorbed molecules is always sufficient to give the high-energy surface the same wettability properties as the low-energy solid having the same surface constitution.

Theory of Retraction Method and Some Related Topics

After learning how to explain the spreading and wetting behavior of liquids upon high-energy solid surfaces, it soon was recognized [43,96,105] that the retraction method of preparing adsorbed monolayers is a logical consequence of the above-mentioned constitutive law of wetting. In essence, the retraction method is a process by which a clean, high-energy, plane solid is brought in contact with a liquid containing adsorbable polar-nonpolar molecules; adsorption occurs at the solid-liquid interface, and the surface is covered with a film which converts it to a lower energy surface. When the coated solid is held approximately vertically during withdrawal from the bulk liquid phase, the adhering layer of liquid exhibits an appreciable contact angle and then peels back or retracts, leaving the withdrawn, solid, low-energy surface dry but still coated with the monolayer. The monolayer-coated surface can be removed from the liquid unwetted only when the contact angle, θ, of the liquid with the solid is greater than zero; the permissible rate of removal can be faster the greater the value of θ. However, θ exceeds zero only for those liquids having surface tensions greater than the critical surface tension of the solid. Therefore, the necessary and sufficient condition for retraction is that $\gamma_{LV} > \gamma_c$. Adsorbed monolayers can thus be isolated from any liquid having a surface tension, γ_{LV}, greater than the γ_c value of the low-energy surface created by the initial adsorption process.

This explanation provides helpful guidance about the solvents one may use in the preparation of films by retraction from solution. The

Publication Date: January 1, 1964 | doi: 10.1021/ba-1964-0043.ch001

principal requirement is that γ_{LV} exceed γ_c; the greater the difference between γ_{LV} and γ_c, the larger the contact angle (according to the cos θ vs. γ_{LV} relation) and the easier it is to perform the retraction operation to isolate the adsorbed film on the solid. In order that the adsorbed monolayer should emerge from the solution unwetted, it is usually advantageous to choose a solvent with a surface tension sufficiently in excess of γ_c of the adsorbed monolayer so that the solution exhibits a contact angle with the coated solid of 30° or more.

The earliest experiments with the retraction method [23] led to the conclusion that retraction was not possible when the polar-nonpolar solute had one or more cis double bonds—for example, oleic acid could not be isolated by retraction. Evidently, our difficulty arose from the fact that γ_c for an adsorbed film of oleic acid must be greater than for stearic acid; hence the solvent used for retraction of oleic acid must have a surface tension higher than that used with stearic acid. As the hexadecane used as the solvent in the early unsuccessful experiments with oleic acid had γ_{LV} = 27.7 dynes per cm., a solvent with a much higher surface tension is needed (a nonhydrocarbon would be preferable). It is now evident why on using liquids of high surface tensions such as water, ethylene glycol, and methylene iodide, it is possible to retract polar solutes as condensed monolayers having a wide variety of organic structures, including branched or cyclic types. Examples of cos θ vs. γ_{LV} plots for such films [43] are given in Figure 13.

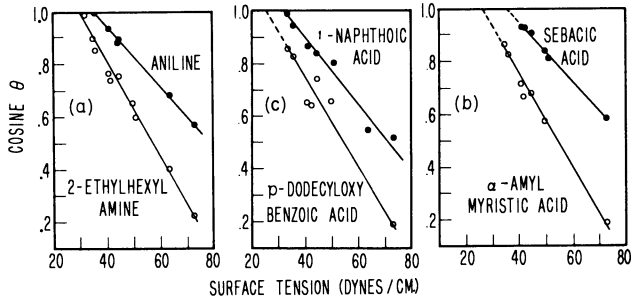

Figure 13. Wettability of various monolayers on platinum prepared by retraction from aqueous solution [43]

A method described earlier for preparing adsorbed monolayers on solids by retraction from the molten state of the pure compound [22] represents, in effect, an application of the autophobic property of the liquid; each of these compounds is autophobic or nonspreading at all temperatures in the portion of the liquidus range of the material in which the liquid surface tension exceeds γ_c of the adsorbed monolayer. A variant on the retraction technique [2] is the tilted plate method, in which the molten compound is placed along the inclined hotter edge. As the melt runs down the plane it cools and solidifies. A retracted monolayer forms on the surface near the hot edge. This method has advantages over the vertical plate retraction method when the contact angle is small (but not zero).

Publication Date: January 1, 1964 | doi: 10.1021/ba-1964-0043.ch001

A temperature, τ, was found by us experimentally [22] above which it was no longer possible to use the retraction method to isolate the monolayer from the molten compound. The values of τ for each homologous series of aliphatic compounds were a rectilinear increasing function of the number of carbon atoms per molecule. For most pure homologous liquids not too near the critical temperature, the surface tension vs. temperature relations can be represented by a series of straight lines of negative slope. In contrast, the effect of raising the temperature of an adsorbed film by a few degrees is to decrease the surface density and lower adhesion very little; hence, γ_c increases only slightly per degree of rise. At a sufficiently high temperature, the condition is reached at which $\gamma_{LV} > \gamma_c$ and retraction is possible no longer. Hence, the temperature limit, τ, corresponds to the condition when γ_{LV} of the molten compound equals γ_c of the adsorbed film.

In the homologous series of fatty acids, only small variations were found in the value of γ_c characteristic of the acid monolayer at temperature τ. Whereas an increase in chain length in going from octanoic to octadecanoic acid resulted in a rise in τ from 23° to 106°, the corresponding change in γ_c was only to decrease from 28 to 25 dynes per cm. Since these values do not greatly exceed the value of γ_c characteristic of hydrocarbon surfaces in closest packing, they indicate that the adsorbed film is wetted by the melt at temperatures at which the adsorbed films are still relatively intact.

Formation of Mixed Films and Their Metastability

If in retracting a monolayer of stearic acid or octadecylamine from a solution in hexadecane, a mixed film of solute and solvent molecules is produced, it is not possible to detect the presence of the solvent molecules in the film by means of contact angle measurements using an appropriate liquid drop such as water, methylene iodide, etc. This result is a consequence of the fact we had already established that the wettability of an adsorbed monolayer is determined by the nature and packing of the outermost surface atoms or organic radicals. Bartell and Ruch [9,10], using an optical interference spectrometer, proved that octadecylamine films adsorbed and retracted from hexadecane solutions on polished chromium can comprise mixtures of solute and solvent. Levine and I [79] found shortly afterwards that such mixed films could also be formed by retraction on fire-polished glass surfaces and distinguished readily from films of solute by multiple-traverse boundary friction measurements. The mixed films prepared from solution in hexadecane of either stearic acid or octadecylamine proved to be metastable, for they did not occur if sufficient immersion time was allowed before retraction to approximate adsorption equilibrium. An immersion time of 24 hours was required for the adsorbed film to be free of hexadecane molecules. When the solvent used had a molecular structure such that it could not form adlineated films with the solute molecules, mixed films were not encountered. For example, either stearic acid or octadecylamine adsorbed and retracted from solutions in nitromethane, carbon tetrachloride, dicyclohexyl, or benzene showed no evidence of containing solvent molecules.

Recently Bewig and I have successfully used changes in the contact potential difference between metals for studying the formation of mixed

Publication Date: January 1, 1964 | doi: 10.1021/ba-1964-0043.ch001

films by retraction [20]. This method consists of measuring the change in the contact potential differences (between a clean metal electrode and a stabilized gold reference electrode) resulting from the adsorption of a condensed organic monolayer. The adsorbed monolayer studied was deposited on the clean metal electrode (platinum, nickel, or chromium) by retraction from a variety of pure solvents. Plots of contact potential difference, ΔV, vs. the length of time of immersion of the metal electrode in the solution readily distinguished between films free from or containing the solvent molecules. Our earlier results with the friction method [79] were verified. It was found that if the number of carbon atoms per molecule in the alkane solvent differed too much, mixed film formation became less prominent; it became insignificant when there was a difference of five carbon atoms per molecule. Solvents such as 1-phenyldodecane and methylene iodide did not form adlineated films with octadecylamine under any condition. Aliphatic solvents having methyl- branches, such as pristane and squalane, although less able to adlineate than unbranched alkanes, still formed mixed films with octadecylamine.

In summary, mixed films of solute and solvent can be prepared as retracted films; however, these are always transient or metastable systems, the probability of whose formation becomes greater the more fully does molecular adlineation of solute and solvent occur. If the concentration of polar solute is high enough, the film eventually becomes free of solvent as adsorption equilibrium is approached, and the retracted film is then free of solvent molecules. Where the solute and solvent molecules are so different in shape or size that the intermolecular cohesion between them through London dispersion forces becomes a minor factor, mixed films are never formed. Therefore, mixed films occur by the retraction process under special conditions; nonetheless, when they can be produced, a useful technique is available for studying the intermolecular interaction of solute and solvent molecules in the adsorbed state.

A by-product of the study of mixed films is better guidance in the selection of liquids suitable for reliable measurements of the wetting properties of adsorbed films. Whenever a liquid drop is placed upon a film, there is always the possibility that molecules of the drop will permeate into the film to form a mixed film system and so create the condition that the contact angle observed is dependent on other factors than the surface composition and packing of the original film. As pointed out earlier [2,92,93], this is precisely one of the limitations in the use of water for contact angle measurements in studying monolayers of paraffinic derivatives, and it gives rise to differences in the advancing and receding contact angles (see Table II). From the preceding discussion, it is evident that hexadecane or any other n-alkane liquid may also be able to permeate into and adlineate with the polar molecules in films of paraffinic polar compounds. For these reasons Levine and I concluded that it is generally preferable to use a nonlinear large molecule having a high surface tension as the reference liquid for many contact angle studies on adsorbed films and even on surfaces of plastics [78, 79]. Since methylene iodide has a surface tension of 50.8 dynes per cm. at 20°C., and a boiling point of 180°C., it will exhibit large contact angles with most organic surfaces and will not evaporate too rapidly. Furthermore, since the molecule is roughly spherical,

Publication Date: January 1, 1964 | doi: 10.1021/ba-1964-0043.ch001

it has little ability to adlineate to form mixed films. Its size is enough greater than that of the water molecule to limit greatly permeation into anything but loosely packed films. For these reasons we have used the equilibrium contact angle of methylene iodide very widely in our investigations of the properties of adsorbed films and other low-energy surfaces.

Wetting by Solutions - Aqueous and Nonaqueous

Present theories about the wetting ability of surface-active agents in aqueous systems either state or imply that spreading results because the wetting agent becomes selectively adsorbed on the surface so as to orient the hydrophilic group toward the aqueous solution [41,85]. Our studies on adsorption at solid-air and solid-liquid interfaces made it increasingly improbable that the major mechanism of wetting is the result of the ability of the nonpolar group of the wetting agent to adsorb by its hydrocarbon "tail" on the low-energy surfaces and so convert it into a high-energy surface. A more reasonable assumption is that spreading on low-energy surfaces is caused by the lowering of the surface tension of water. If the solute molecules do adsorb at the solid-liquid interface, it is one of the results of wetting—not the cause. Hence, changes in γ_{SL} must play a minor role in the presence of solutions of wetting agents. Therefore, we assumed that the ability of the aqueous solution to spread on such low-energy surfaces is determined by the value of the critical surface tension, γ_c, of the solid to be wetted and the amount of the wetting agent which must be dissolved in the water to depress the surface tension of water below γ_c.

These ideas were verified in experiments on two low-energy solids, polyethylene ($\gamma_c \approx 31$ dynes per cm.) and polytetrafluoroethylene ($\gamma_c \approx 18$ dynes per cm.), using a variety of well-defined aqueous solutions [14]. Pure water ($\gamma_{LV} = 71.9$ dynes per cm. at 25°C.) will not spread on either of these two surfaces. Fischer and Gans [39] have pointed out that conventional surface-active agents (derived from aliphatic or aromatic hydrocarbons) do not lower the surface of tension of water at 25°C. below between 26 and 27 dynes per cm. It follows from the definition of the critical surface tension that whenever any wetting agent lowers the liquid surface tension below 31 dynes per cm., the solution will spread on the surface of smooth clean polyethylene. However, aqueous solutions containing conventional wetting agents should not spread on polytetrafluoroethylene, since a wetting agent capable of depressing the surface tension below 18 dynes per cm. would be needed. Wetting agents used in our experiments included all three classes—i.e., anionic, cationic, and nonionic—and as many diversified hydrocarbon structures as feasible in order to show properties or general trends common to conventional surface-active agents.

Figure 14 shows the knee-shaped curve of solution surface tension vs. concentration characteristic of aqueous surface-active agents; the steeper the curve, the more efficient the wetting agent. It is generally assumed that the bend of the curve coincides with the critical micelle concentration (c.m.c.) of the respective compound in the aqueous medium. Since the discontinuities in the slopes of the individual curves of Figure 14 occur in the region of the c.m.c. values reported by various

Publication Date: January 1, 1964 | doi: 10.1021/ba-1964-0043.ch001

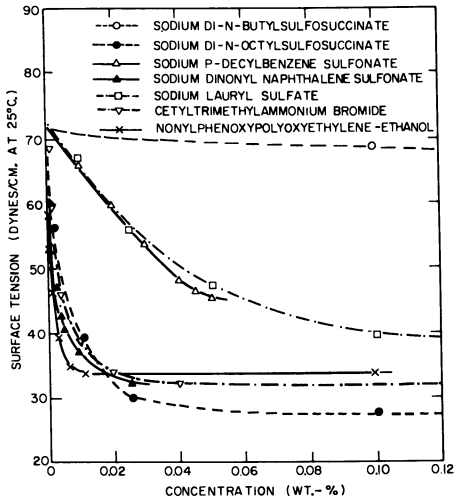

Figure 14. Surface tensions of conventional wetting agents in aqueous solution [13]

investigators, the above assumption can be made again for the agents discussed here.

Curves of surface tension vs. cos θ, obtained for wetting agents on polyethylene, are given in Figure 15, A and B. Analogous results using smooth polytetrafluoroethylene surfaces are given in Figure 16, A and B. At the critical surface tension (cos θ = 1) there is only a narrow

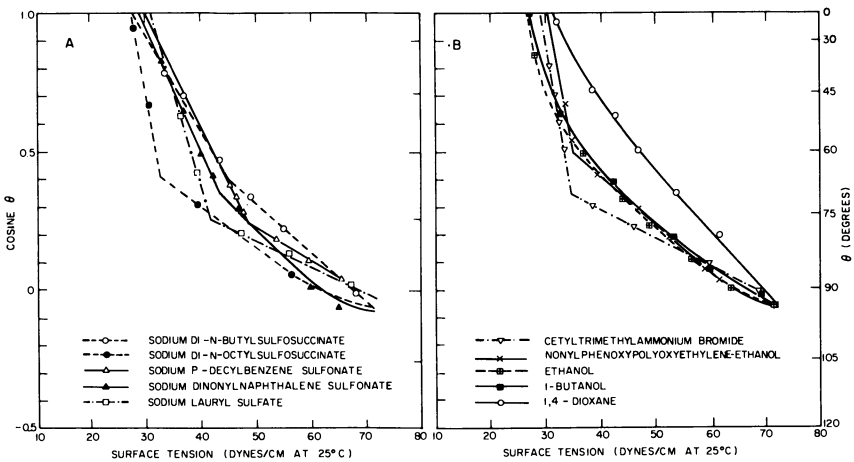

Figure 15. Wettability of polyethylene by aqueous solutions [13]

A. Anionic wetting agents
B. Other wetting agents

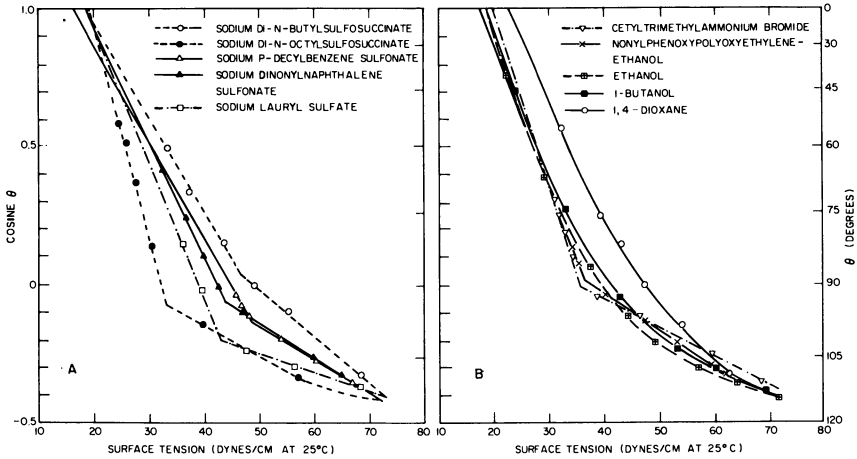

Figure 16. Wettability of polytetrafluoroethylene by aqueous solutions [13]

A. Anionic wetting agents
B. Other wetting agents

spread of the converging curves for each organic surface. From these intercepts one can estimate γ_c values for polytetrafluoroethylene as between 16.5 and 19.5 dynes per cm. and for polyethylene as between 27.5 and 31.5 dynes per cm. These are in reasonable accord with the values reported in Table V, which are based on the wettability by pure organic liquids. Only solutions whose surface tensions were lower than 30 dynes per cm. spread freely on polyethylene. No aqueous solution of a conventional hydrocarbon derivative wetting agent had a surface tension low enough to spread freely on polytetrafluoroethylene. Hence, our observations agreed with the assumption that aqueous solutions will spread on a low-energy surface when the surface tension is less than the γ_c value of the solid.

Whereas the curves for the various wetting agents grouped in a narrow band intercepting the line $\cos \theta = 1$ at the value of γ_c, they did not converge to a point, as would be anticipated, at the value of γ_{LV} = 71.9 dynes per cm. for pure water but also exhibited a spread in θ of 2°, which is well within the experimental error in measuring θ. An unexpected and new phenomenon, however, was the abrupt change in slope in the middle zone of each of the curves of Figures 15 and 16. The data in the first two columns of Table VIII (calculated from Figures 14, 15, and 16) revealed that the discontinuities in slope for polytetrafluoroethylene occurred at approximately equal concentrations for a given wetting agent. Hence, the discontinuities in slope are determined by the constitution of the wetting agent and not by that of the solid. When the surface tension corresponding to each such discontinutiy was referred to the curve of surface tension vs. concentration in Figure 14, it was found that it corresponded to the concentration in the region of greatest curvature. Therefore, there was a close relation between the concentration at which discontinuity in the slope occurs in each wetting

Publication Date: January 1, 1964 | doi: 10.1021/ba-1964-0043.ch001

Table VIII. Concentrations at Discontinuities in Slope for Various Wetting Agents and Surfaces at 25°C. [13]

Compound	Concn., Moles/Liter		
	Polyethylene	Polytetra-fluoroethylene	C.m.c.
Na di-n-butyl sulfosuccinate	5.0×10^{-2}	4.2×10^{-2}	2×10^{-1}
Na di-n-octyl sulfosuccinate	6.8×10^{-4}	4.5×10^{-4}	6.8×10^{-4}
Na p-decyl benzene-sulfonate	1.2×10^{-3}	1.2×10^{-3}	3×10^{-3} at 50°
Na lauryl sulfate	3.0×10^{-3}	2.7×10^{-3}	8×10^{-3}
Cetyltrimethyl-ammonium bromide	4.3×10^{-4}	3.8×10^{-4}	1×10^{-3} at 60°

curve of Figures 15 and 16 and the c.m.c. of the wetting agent in the same solution. The last column of Table VIII gives the best literature values of the c.m.c. of each of these wetting agents at or near the temperature used. There is a fair correlation between the concentration corresponding to the discontinuity in slope in the wetting curve and the reported c.m.c.; also it appears that the c.m.c. is always slightly higher.

The correctness of the preceding interpretation of the slope discontinuities in the curves of γ_{LV} vs. cos θ was supported by experiments on solutions of the following pure polar compounds which are not able to form micelles: ethanol, 1-butanol, 1,4-dioxane, propylene carbonate, diacetone alcohol, dipropylene glycol, 2-butanone, and tetrahydrofuran. Surface tensions for these compounds agreed well with the available literature values [87]. None of these polar solutes form micelles in water and, as can be seen in Figures 15, B, and 16, B, no discontinuities in the slopes of the curves of cos θ vs. γ_{LV} were observed for either solid surface. It was concluded, therefore, that no discontinuities in slope occur without the formation of micelles.

Each intercept at cos $\theta = 1$ fell within the expected range of γ_c values (Figure 16, B), with the exception of the intercept for the

Table IX. Critical Surface Tensions by Aqueous Solutions of Non-Micelle-Forming Compounds at 25°C. [13]

Solute	γ_{LV}, Dynes/Cm., Pure Solute	γ_c, Dynes/Cm.	
		Polyethylene	Polytetra-fluoroethylene
Ethanol	21.4	27.5	18.5
1-Butanol	23.7	27.5	18.5
2-Butanone	24.4	27.5	---
Tetrahydrofuran	27.4	29.5	---
Diacetone alcohol	30.2	29.0	17.0
1,4-Dioxane	32.4	31.5	22.5
Dipropylene glycol	33.1	30.0	18.0
Propylene carbonate	40.5	29.5	19.5

Publication Date: January 1, 1964 | doi: 10.1021/ba-1964-0043.ch001

1,4-dioxane curve which occurred at the higher value of 22.5 dynes per cm. Wetting curves on polyethylene were almost coincident for 1,4-dioxane and propylene carbonate, for diacetone alcohol and 2-butanone, and for dipropylene glycol and tetrahydrofuran, and were very similar for ethanol and 1-butanol (Figure 15, B). Table IX shows the intercepts at $\cos \theta = 1$ for the compounds for polytetrafluoroethylene and polyethylene. It has been found in previous work [46,48] that the γ_c value of any one solid surface varies somewhat among the various homologous series of liquids.

Since discontinuities at the c.m.c. occur in curves of surface tensions vs. concentration and of either $\cos \theta$ vs. concentration or $\cos \theta$ vs. surface tension, the generalization is proposed that micelle-forming compounds will produce discontinuities in the slopes of other surface properties of surface active agents when plotted against either the concentration or the surface tension of the solution. For example, it may be that such will occur in plots of the interfacial tension vs. the concentration of the surface active solute in the aqueous phase.

Because of their hydrophobic-hydrophilic structures, each of the most effective wetting agents adsorbs to form a thin film on the free surface of the aqueous solution. At sufficiently high solute concentrations, this film will make the aqueous liquid appear to be a hydrocarbon liquid whose surface is comprised of the oriented, packed, hydrophobic groups characteristic of the organic structure of the wetting agent. Our experiments lead to the conclusion that bringing the low-energy surface of polytetrafluoroethylene (or polyethylene) into contact with this film-coated water did not change the orientation or packing of the film adsorbed at the water-air interface. Fowkes and Harkins [41] had reached essentially the same conclusion about paraffin when they found that the force-area curves for films of butyl alcohol, butyric acid, and butylamine adsorbed at the paraffin-water interface were nearly the same as those for adsorption at the air-water interface.

From these considerations one can predict that γ_{SL} will decrease as adsorption of the wetting agent increases. At high solute concentrations, γ_{SL} will become small because the interface will be between an organic low-energy solid and a hydrocarbon-like liquid. In other words, the much greater adhesion of the polar groups to the water and the much lower adhesion of the hydrocarbon groups to the low-energy solid surface will have caused the interface determining spreading and wetting to become the hydrocarbon-like outer surface of the film of adsorbed wetting agent. Hence, γ_{SL} will decrease with increased solute concentration and will become nearly constant at high concentrations as the adsorbed film approaches closest packing. Thus, the value of γ_c will vary with the nature of the wetting agent only in so far as there are differences in the nature and packing of the hydrocarbon groups of the wetting agent in the adsorbed state at the water-air interface. One would expect γ_c to be least for n-alkane long-chain derivatives; it will be greater on each surface for branched hydrocarbon derivatives; and it will be largest for aromatic polar compounds. Solutes like 1,4-dioxane or propylene carbonate (or the others in Table IX) adsorb a film at the water-air interface which has a higher free surface energy than one containing only hydrocarbon groups. Any discontinuity in the slope or first-order phase change of the force-area curve in the film

Publication Date: January 1, 1964 | doi: 10.1021/ba-1964-0043.ch001

adsorbed at the water-air interface will be accompanied by a discontinuity in the slope of the cos θ vs. γ_{LV} curve, in view of the conclusion that the contact angle is essentially that of a liquid having the same outermost hydrocarbon structure as the adsorbed solute. It is now evident why the discontinuity in the slope occurs at a concentration which is dependent only on the nature of the wetting agent and not on the nature of the solid surface.

The same experimental approach and conclusions should apply to the wetting of poly(vinyl chloride), polystyrene, and other low-energy solid surfaces. In previous studies we had shown that even a single, close-packed, adsorbed monolayer is sufficient to convert the wetting properties of a high-energy surface into those of a low-energy surface. One cannot predict that the same rule will hold for the wettability of any such film-coated surface by an aqueous solution. In predicting the spreading properties on low-energy surfaces of aqueous solutions of wetting agents, one cannot neglect γ_{SL} at solute concentrations so low that the liquid surface phase consists essentially of water; but at concentrations high enough for the surface of the water to approximate close packing of adsorbed solute molecules, γ_{SL} becomes constant and small in value, and the wetting behavior becomes predictable by the critical surface tension approach.

One might rate the effectiveness of any hydrocarbon-type wetting agent by the minimum concentration necessary at 25°C. to cause the solution to spread on smooth polyethylene (γ_c = 31 dynes per cm.). Another interesting measure of wetting efficiency is the minimum concentration of the agent necessary to wet the smooth clean surface of polytetrafluoroethylene (γ_c = 18 dynes per cm.); however, conventional wetting agents could not be so rated, since they do not decrease γ_{LV} below 26 to 27 dynes per cm. A sufficiently large depression of the surface tension of water necessitates use of a soluble surface-active agent whose hydrophobic group is an appropriately fluorinated hydrocarbon. Some of the properties of these rather "exotic" wetting agents have been reported by Scholberg, Guenthner, and Coon [89] and Klevens and Raison [68]. The low surface energies of films of such compounds have been discussed by us [53]. Results of an investigation of aqueous solutions of such agents for wetting low-energy surfaces have been reported with Bernett [14]. A measure of wetting efficiency of intermediate value is the minimum solute concentration necessary to spread an aqueous solution on the surface of a single crystal of hexatriacontane (γ_c = 22 dynes per cm.). Polystyrene (γ_c = 33 dynes per cm.) and poly(vinyl chloride) (γ_c = 34 dynes per cm.) might also be considered useful low-energy surfaces for relatively rating the wetting agents incapable of lowering γ_{LV} below 30 dynes per cm. The value of such a scheme for rating aqueous wetting agents is that it is quantitative and objective, requires small amounts of solution, has fundamental significance, and need not be confused by other properties such as detergency, capillarity, and surface roughness.

Of especial interest is that the same approach in defining wetting agents in aqueous solutions can also apply to nonaqueous solutions. Increasing interest has been shown in the behavior of surface-active agents at organic liquid-air interfaces. Many of the earliest such studies were made on compounds previously found effective as surface-

Publication Date: January 1, 1964 | doi: 10.1021/ba-1964-0043.ch001

active agents in aqueous solutions. Thus, McBain and Perry [81] showed that low concentrations of laurylsulfonic acids lowered slightly the surface tensions of a group of hydrocarbons. Jones and Saunders [65] later measured the surface tensions of a series of n-aliphatic acids in nitromethane, and Kaminski [66] observed the adsorption of lauric acid and lauryl alcohol at the mineral oil—air interface using the McBain microtome technique. In recent years it has been found that many silicones and fluorochemicals are remarkably surface active in organic liquids and so depress the surface tensions of organic liquids considerably. Banks [6,7] reported the formation of stable, insoluble films of polydimethylsiloxanes on oleic acid, olive oil, triacetin, or ethylene glycol. Almost simultaneously Ellison and I [35,36] demonstrated with an all-Teflon film balance the monomolecular nature of films of the linear polymethylsiloxanes and certain perfluorocarbon derivatives adsorbed as insoluble films on mineral oil, n-hexadecane, and tricresyl phosphate. Other silicones as well as various polyacrylates, polyalkylene ethers, organosilanes, and zein were also surface active on certain organic substrates. Scholberg, Guenthner, and Coon [89] found that certain fluorocarbon derivatives which were surface-active agents in water were also very effective in lowering the surface tensions of organic liquids. Blake, Ahlbrecht, and Bryce [24] reported the surface tension—reducing effects of a series of polyfluoroquaternary ammonium compounds in selected organic liquids. The preparation and physical properties of some partially fluorinated esters and ethers, which had been designed to have an organophobic-organophilic balance suitable for high surface activity, were described with O'Rear [107]; and with Ellison [37] and Jarvis [12,61,62,63] subsequent reports were made of a series of studies of the surface activity of these fluoro- compounds when dissolved in various organic liquids.

Estimates of Reversible Work of Adhesion

Bangham and Razouk's Equations 4c and 5 for the reversible work of adhesion and f_{SV° were used by Boyd and Livingston [25] and by Harkins et al. [11,59,80] to calculate W_A from experimental vapor adsorption isotherms for various liquids on a number of metallic and nonmetallic surfaces. Their results, summarized in Tables X and XI, show that in every instance f_{SV° is of the same magnitude as W_{A*} and so cannot be neglected in the calculation of W_A. Each of these solids is a highly adsorptive, finely divided material, and excluding graphite, each is a hydrophilic high-energy surface.

Unfortunately, f_{SV° has not yet been measured for any well-defined, smooth, low-energy, solid surface. But one should not assume from the results in these tables that in dealing with low-energy solids f_{SV° will also be an important correction term in Equation 4c. On the contrary, there is good experimental evidence that whenever a liquid exhibits a large contact angle on a solid there is negligible adsorption of the vapor. Recent measurements with Bewig [19], using a special reference electrode for studying adsorption by contact potential changes, have demonstrated that negligible adsorption of most vapors occurs at ordinary temperatures on smooth clean surfaces of polytetrafluoroethylene. Extensive room-temperature adsorption measurements over

Publication Date: January 1, 1964 | doi: 10.1021/ba-1964-0043.ch001

Table X. Literature Values of f_{sv° for Nonmetallic High-Energy Surfaces[a] (Ergs/Sq. Cm. at 25°C.)

Solid	Liquid	$f_{sv^\circ} \equiv \gamma_{s^\circ} - \gamma_{sv^\circ}$	W_A
TiO_2	Water	300 (196[b])	370 (340[b])
	1-Propanol	114 (108[b])	138 (154[b])
	Benzene	85	114
	n-Heptane	58 (46[b])	78 (86[b])
SiO_2	Water	316	388
	1-Propanol	134	158
	Acetone	109	133
	Benzene	81	110
	n-Heptane	59	79
$BaSO_4$	Water	318	390
	1-Propanol	101	125
	n-Heptane	58	78
Fe_2O_3	n-Heptane[c]	54	94
SnO_2	Water	292 (220[b])	364 (364[b])
	1-Propanol	104 (117[b])	128 (163[b])
	Propyl acetate[b]	104	151
	n-Heptane[c]	54	94
Graphite	Water	64	136
	1-Propanol	95	118
	Benzene	76	96
	n-Heptane	57[c]	97[c]

[a]Data from [25] unless otherwise indicated.
[b][80].
[c][11].

Table XI. Literature Values of f_{sv° for Metallic High-Energy Surfaces[a] (Ergs/Sq. Cm. at 25°C.)

Solid	Liquid	$f_{sv^\circ} \equiv \gamma_{s^\circ} - \gamma_{sv^\circ}$	W_A
Mercury	Water	101	174
	1-Propanol	108	132
	Acetone	86	110
	Benzene	119	148
	n-Octane	101	123
Copper	n-Heptane[b]	29	69
Silver	n-Heptane[b]	37	77
Lead	n-Heptane[b]	49	89
Iron	n-Heptane[b]	53	93
Tin	Water[c]	168	312
	n-Heptane[c]	50	90
	1-Propanol[c]	83	129

[a]Data from [25] unless otherwise indicated.
[b][59].
[c][80].

Publication Date: January 1, 1964 | doi: 10.1021/ba-1964-0043.ch001

the entire vapor pressure range of p/p_o up to 1.0 by Martinet [82] and Graham [51] have also led to the conclusion that the vapor adsorption for the gaseous substances studied on this low-energy solid surface is but a small fraction of a monolayer. Hence, we have concluded [106] that f_{SV° is a small term in comparison with W_{A*} for each liquid and solid whenever γ_{LV° is greater than γ_c. The same conclusion should also apply to other low-energy solids at ordinary temperatures such as polyethylene, polystyrene, poly(vinyl chloride), etc.

Therefore, it was proposed that as regards any low-energy solid surface: liquids having γ_{LV° much greater than γ_c have W_A essentially equal to W_{A*}; as γ_{LV° closely approaches γ_c but exceeds it, $W_A - W_{A*}$ becomes more significant; and liquids having γ_{LV° less than or equal to γ_c may have appreciable values of $W_A - W_{A*}$. The same conclusions about the negligible value of f_{SV° apply to any high-energy surface which has been converted to a low-energy surface by the adsorption of a suitable condensed organic monolayer, with the one reservation that f_{SV° may become more significant if the molecule of the liquid is small enough to be able to penetrate readily through the condensed monolayer and so adsorb on the high-energy surface beneath.

In dealing with the adhesion of a liquid to a plane, nonporous, solid surface, according to Equation 4d, W_{A*} is given by $W_{A*} = \gamma_{LV^\circ}(1 + \cos\theta)$. However, experiments show that for any homologous series of liquid compounds and for all values of $\gamma_{LV^\circ} > \gamma_c$, the contact angle is related to γ_{LV° by the straight-line equation

$$\cos\theta = a - b\gamma_{LV^\circ} \tag{11}$$

Since γ_{LV° approaches γ_c as θ approaches zero, Equation 11 can be written

$$\cos\theta = 1 + b(\gamma_c - \gamma_{LV^\circ}) \tag{12}$$

Upon eliminating $\cos\theta$ between Equations 5 and 12, there results [106]:

$$W_{A*} = (2 + b\gamma_c)\,\gamma_{LV^\circ} - b\gamma_{LV^\circ}^2 \tag{13}$$

This is the equation of a parabola with the concave side toward the surface tension axis; it has a maximum value of W_{A*} occurring at

$$\gamma_{LV^\circ} = \frac{1}{b} + \frac{1}{2}\gamma_c \tag{14}$$

and the maximum value is given by

$$W_{A*} = \frac{1}{b} + \gamma_c + \frac{1}{4}b\gamma_c^2 \tag{15}$$

For example, consider smooth polyethylene for which $\gamma_c = 31$ dynes per cm. and $b = 0.026$ [48]; the maximum of W_{A*} occurs at $\gamma_{LV^\circ} = 54$ dynes per cm. and is about 76 ergs per sq. cm.

It is of interest to compute the value of W_{A*} for the many liquid-solid combinations reported in the past. Figures 17 to 20 show how

Publication Date: January 1, 1964 | doi: 10.1021/ba-1964-0043.ch001

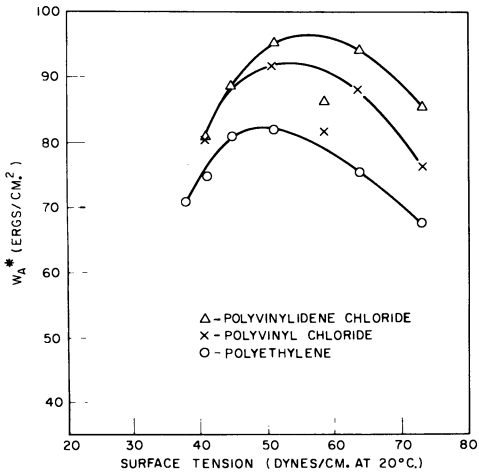

Figure 17. Effect of liquid surface tension on W_{A*} for chlorinated polyethylene [106]

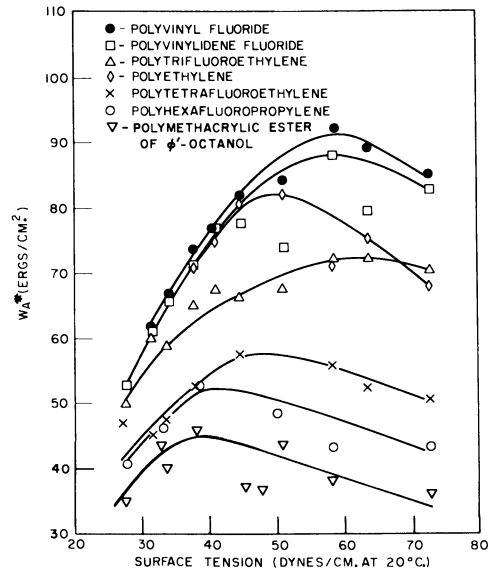

Figure 18. Effect of liquid surface tension on W_{A*} for fluorinated plastics [106]

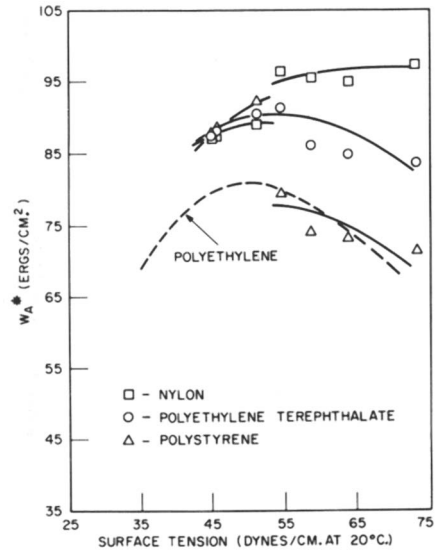

Figure 19. Effect of liquid surface tension on W_{A*} for some common plastics [106]

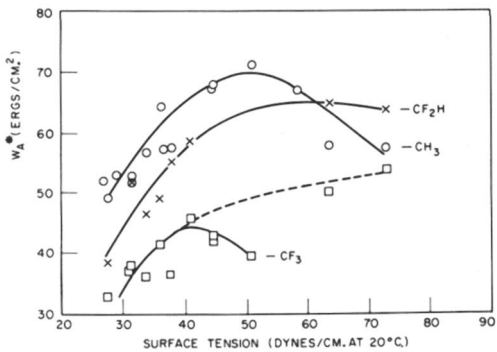

Figure 20. Effect of liquid surface tension on W_{A*} for a solid coated with a condensed monolayer [106]

W_{A*} varies as a function of γ_{LV°. In every case there results a parabolic curve with a maximum. However, in a few instances, such as in the case of polytrifluoroethylene (Figure 18), the decrease of W_{A*} after reaching the maximum value is greatly moderated by the effect of the hydrogen bonding action of the liquids of high surface tension—i.e., water, glycerol, and formamide, each of which is an effective hydrogen-donating compound. Similar effects are seen in the curve of Figure 20 for the close-packed monolayers terminated by $-CF_2H$ groups and $-CF_3$ groups. In the latter case, if the data points for the hydrogen-donating liquids are excluded, the curve is seen to form a parabola with its

Publication Date: January 1, 1964 | doi: 10.1021/ba-1964-0043.ch001

maximum occurring at about 40 dynes per cm. It is also seen that the maximum values of W_{A*} for $-CH_3$, $-CF_2H$, and $-CF_3$ coated surfaces are approximately 70, 65, and 44 ergs per cm. sq., respectively. Inspection of Figures 17 to 20 also reveals that the extreme variation in W_{A*} among all the low-energy solid surfaces reported is only about threefold.

Relation of Wetting to Adhesives Art

Only in this century has the art of using adhesives been based on the properties and applications of liquid adhesives other than old glue formulations from fish and animal products or cements made from inorganic slurries or solutions. The subject of adhesives assumed a new stature with the advent of synthetic polymers having readily controlled and understood properties. However, there are many unanswered questions about the principles underlying the subject and accepted methods of application.

Figure 21 is a simplified diagram of a typical adhesive joint comprising two plane solid surfaces, identified usually as the "adherends," and a thin layer of liquid, the "adhesive." If the adhesive, while in the

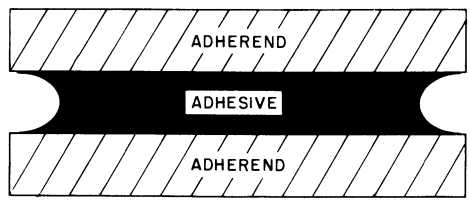

Figure 21. Idealized adhesive joint [106]

liquid state, has a zero contact angle, it will spread spontaneously over the solid to make intimate intermolecular contact with the surface of each adherend. Each adhesive is designed to increase in viscosity with the passage of time until it becomes solid; this may occur through freezing, evaporation of a volatile solvent, or polymerization. If the thermal expansion coefficients of adhesive and adherends are not too different, and if there is not too large a change in the density during solidification, internal stresses developed in the area during solidification of the adhesive will not be sufficient to shatter the joint or cause cracking. Obviously, a good joint must have sufficient strength to endure large externally applied stresses.

Tabor [100] has pointed out that according to Equation 4c, W_A for any system having $\theta = 0$ will be equal to or greater than twice the surface tension of the liquid; a simple calculation, assuming that the field of force emanating from the solid vanishes in about 3 A., and that the surface tension of the adhesive is 30 dynes per cm., results in an average tensile strength of the adhesive joint of 2000 kg. per sq. cm. This value is much greater than the tensile strength of common adhesives, for Kraus and Manson [69] obtained for polyethylene a tensile strength of 183 kg. per sq. cm. Therefore, the joint must break by cohesive

Publication Date: January 1, 1964 | doi: 10.1021/ba-1964-0043.ch001

rather than adhesive failure. Since the correction term, f_{SV°, in Equation 4c makes the adhesional energy even greater than $2\gamma_{LV^\circ}$, it is apparent that when $\theta = 0$ the theoretical adhesive strength will always be much more than the observed tensile or shear strength of the adhesive material.

Real solid surfaces are neither flat nor free of pores and crevices, and no treatment of adhesion can disregard the realities of surface structure. Each adherend has a true surface area which is r times greater than the apparent or envelope area; hence the work of adhesion should be expected to be r times greater than that for the apparent surface area. However, the larger the contact angle the more difficult it becomes to make the liquid flow over the surface of each adherend to fill completely every crevice and pore in the surface. More often there are air pockets trapped in the hollows and crevices. Such difficulties with the formation of gas bubbles and pores are, of course, greatly amplified in dealing with viscous adhesives which solidify shortly after being applied to form the joint. Hence in practice the true value of W_{A*} lies somewhere between the value obtained from Equation 4c by using the apparent contact angle and r times that value. Where there are accessible pores, crevices, and capillaries in the surface of the adherend, the viscous liquid adhesive may penetrate to some extent and so increase adhesion, provided it does not harden too soon and an adequate supply of the liquid is available. However, in order to obtain the maximum adhesion, the adhesive should obviously be able to penetrate into each capillary and fill it.

An obvious approximation is to assume that the capillary rise equation

$$h = \frac{k\gamma_{LV^\circ} \cos\theta}{\rho R} \tag{16}$$

can be used (R is the equivalent radius of the capillary, $k = 2/981$, and ρ is the density of the liquid) and also that the liquid still wets the capillary wall according to the $\cos\theta$ vs. γ_{LV° relation of Equation 11. Eliminating $\cos\theta$ from the two equations results in the equation for the parabola [106]:

$$h = \frac{k\gamma_c}{\rho R}(b + \gamma_c + 1) - \frac{(bk)}{R\rho}\gamma_{LV^\circ}^2 \tag{17}$$

where h has a maximum when

$$\gamma_{LV^\circ} = \frac{1}{2}\left(\gamma_c + \frac{1}{b}\right) \tag{18}$$

For example, in smooth polyethylene the maximum capillary rise will occur when $\gamma_{LV^\circ} = 1/2\ (31 + 38.4) = 34.7$ dynes per cm.; this value is only 3.7 dynes per cm. more than γ_c. Despite the unrealistic assumption made, this analysis reveals again that W_{A*} may go through a maximum as γ_{LV° increases, even when a porous interfacial surface is involved.

Publication Date: January 1, 1964 | doi: 10.1021/ba-1964-0043.ch001

As the result of the intense localization of the residual field of force emanating from both the adherend and adhesive, when a liquid adhesive solidifies, the value of W_A for the joint should remain close to the value computed for the adhesive in the liquid state if stress concentrations do not develop in the process. Since the forces causing adhesion are effective to little more than the depth of one molecule in both surfaces, they will be unaffected by changes of state of the bulk phases so long as allowance is made for any resulting changes in the surface density or molecular orientation occurring at the joint interface [106]. The former can be estimated from the change of density on solidification, but the latter may be difficult to compute, since reorientation effects could originate through any crystallization process starting at or near the interface. It is also usual for internal stresses and stress concentrations to develop when the adhesive solidifies, the most common cause being the difference in the thermal expansion coefficients of adhesive and adherend. In some applications, care is taken to match the thermal expansion coefficients of adhesive and adherend; however, in others this matching process is not critical. Hence, the actual strength of the adhesive joint is usually considerably less than the theoretical (or thermodynamic) value because of the development of internal stress concentrations.

Mylonas [86] has shown that in a lap joint poor wetting of the adherend tends to produce a greater stress concentration at the free surface of the adhesive where failure is most likely to be initiated. As the contact angle, θ, becomes large, the maximum stress concentration increases and moves toward the edge where the adhesive makes contact with the adherend, the stress concentration factor increasing from about 1.2 when $\theta = 30°$, to about 2.5 when $\theta = 90°$ (Figure 22). Furthermore, Griffith [52] has shown that failure of the adhesive may occur at a relatively small applied stress if there are air bubbles, solid inclusions, or surface defects; it occurs because stress concentrations result which are much higher than the mean stress applied across the specimen. His conclusion is very important, because the most probable effect of poor wetting is the development of air pockets or voids at the adhesive-adherend interface. Even when $\theta = 0$, there may be gas pockets formed at the adhesive-adherend interface around which stress concentrations can build up, for if the adhesive is too viscous when

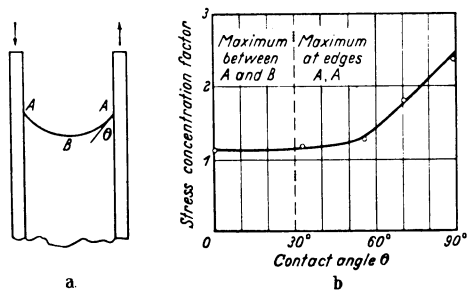

Figure 22. Variation of stress concentration maxima in lap joint adhesive with angle of contact [86]

Publication Date: January 1, 1964 | doi: 10.1021/ba-1964-0043.ch001

applied, it may never penetrate the accessible surface pores before polymerizing. Of course, this situation is the more aggravated the larger the contact angle or the rougher the surface.

In adhesives technology it is common practice to roughen the surface of each adherend, or "give it tooth," and so obtain a stronger joint. This practice can be justified theoretically, with certain limitations, by the following considerations. If the gas pockets formed in the surface depressions of the adherend are all nearly in the same plane and are not far apart (as on the upper adherend of Figure 23) there may be crack propagation from one pocket to the next, and the joint may break as if it had a built-in "zipper." Therefore, if roughness must be accepted, the kind of roughness shown on the lower adherend would be preferable because crack propagation along a plane would be less probable.

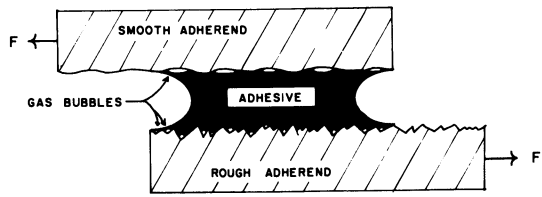

Figure 23. Effect of surface roughness on coplanarity of gas bubbles [106]

"Abhesives" are materials used in the form of films or coatings which are applied to one solid to prevent—or greatly decrease—the adhesion to another solid in intimate contact with it. Such materials are employed in molding, casting, or rolling operation; therefore, it is also common to refer to the film as the "parting," "mold-release," or "antistick" agent. Examples of materials commonly used for such purposes are the polymethylsiloxanes; the high molecular weight fatty acids, amines, amides, and alcohols; various types of highly fluorinated fatty acids and alcohols; and the fluorocarbon resins. Usually a condensed monolayer or thin film of the agent is sufficient to cause the optimum parting effect. Table XII gives the γ_c values of each of these films. Each abhesive coating will convert the solid into a low-energy surface, and any liquid placed on such a coated surface will exhibit an equilibrium contact angle which will be larger as $\gamma_{LV^\circ} - \gamma_c$ increases. When θ is large enough, such poor adhesion results on solidification of the liquid that the application of a modest external stress suffices for

Table XII. Critical Surface Tensions of Wetting of Surfaces Coated with Abhesive Films [106]

Coating Material	γ_c, Dynes/Cm. at 20°C.
Polymethylsiloxane film	24
Fatty acid monolayer	24
Polytetrafluoroethylene film	18
Ψ'-Fatty acid monolayer	15
Polymethacrylic ester of Φ'-octanol	10.6
Perfluorolauric acid monolayer	6

Publication Date: January 1, 1964 | doi: 10.1021/ba-1964-0043.ch001

parting or splitting of the joint along the adhesive-adherend interface. The excellent and easy parting action usually achieved is the result of the formation of a deliberately weakened joint; it should be explainable by any general theory of adhesives.

It was pointed out earlier that W_A exhibits a maximum variation among the various low-energy surfaces of about threefold in going from the least to the most adhesive liquids. Such a range is too small to explain the effectiveness and easy parting action of a good abhesive. However, this range of values of W_A is for flat, nonporous, smooth, solid surfaces. The roughness factor, r, of the uncoated surface of the mold could raise W_A by a factor of at least 1.5 to 3, and it could be much larger the less smooth the surface finish; however, if the material to be molded is (or becomes) viscous rapidly during mold injection or application of the liquid adhesive, poor wetting will cause voids or gas pockets to be produced at the interface between the material molded and the adhesive, and thereby the adhesion will be greatly decreased through stress concentrations by some unknown fraction, 1/g. Furthermore, if $\theta > 30°$, the resulting stress concentration factor of from 1.2 to 2.5 at the adhesive-plastic interface will contribute an additional decrease in the adhesion, and so the adhesional work per unit area of the apparent or envelope area at the molding interface will be $(r/gs)W_A$. Therefore, for both reasons the greater the value of θ, the greater the effectiveness of the release agent in weakening the joint formed.

The large values of θ encountered with the various types of organic liquids on such low-energy surfaces as those shown in Table XII are good evidence in favor of this explanation of abhesive action. As a general proposition, any low-energy surface will be more effective as a release agent (or abhesive) the lower its γ_c value [106]. It can also be concluded that the smoother the finish of the outer coating of the mold and the lower the surface tension and viscosity of the material being molded (or the lower its contact angle with the adhesive), the greater will be the external stress required to cause the desired parting action. In conclusion, a good adhesive joint can be made on any low-energy surface, including any abhesive surface, if the surface is not too rough or if the adhesive has $\gamma_{LV} < \gamma_c$—i.e., if there is good wetting by the adhesive.

There has been much discussion about the necessity for using adhesives capable of forming chemical bonds with the adherends. But the preceding considerations concerning the relation of wetting to adhesion have made it evident that the energy involved in the physical adsorption to the adherend of molecules of adhesive is more than sufficient to form joints which are stronger than the cohesive strength of existing adhesives. Of course, chemical bonding may offer advantages other than that of increasing the joint strength—for example, greater heat, water, or chemical resistance may result. Under some circumstances a few monolayers of water adsorbed on the adherend can be tolerated because they are readily displaced by the adhesive or absorbed in the adherend or adhesive; but usually bulk water cannot be tolerated because of its low shear strength and its adverse effect on spreading of the adhesive. However, it is usually a great advantage, when selecting an adhesive for a given application, to be released from the very limiting requirement of finding a material capable of chemically bonding to the adherends.

Publication Date: January 1, 1964 | doi: 10.1021/ba-1964-0043.ch001

In summary, for optimum or theoretical joint strength, it is essential to keep the contact angle between the liquid adhesive and the adherends as small as possible in order to obtain good spreading and to minimize the buildup of stress concentrations. Obviously, the interface of each adherend must be kept as smooth and free as possible of low-energy surface films and dust, in order to prevent forming voids, gas pockets, or occlusions. In applying liquid adhesives the viscosity should be as low as possible, in order to increase the extent of capillary flow into pores and crevices. Maximum spreading and capillarity will be obtained with adhesives having the highest surface tension compatible with obtaining a low contact angle. When conditions of complete wetting and freedom from the formation of gas pockets and occlusions prevail, the adhesion to either high-energy or low-energy surfaces will usually be ample, and generally failures of the joint will be in cohesion. If the surface of the adherend is to be roughened, it is better done in such a way as to keep any surface gas pockets formed from being coplanar or nearly so over a large region. When difficulties are encountered in finding a suitable adhesive for a specific application, or in seeking new adhesives, it should be helpful to try an adhesive having a γ_{LV} value (while in the liquid state), which is less than the γ_c value of the adherend surface, and, of course, to apply it under conditions that will minimize the tendency to occlude gas bubbles in the surface.

Publication Date: January 1, 1964 | doi: 10.1021/ba-1964-0043.ch001

Future Research on Wetting and Adhesion

An exciting beginning has been made in explaining the wetting, spreading, and adhesive behavior of liquids on solids. We have established that the observation of the equilibrium contact angles of liquids on solids, under appropriately controlled and now well understood conditions, is a powerful method of investigating the surface properties of either solid surfaces or adsorbed monolayers. From the diversity of new surface chemical phenomena revealed by our investigations, it should be apparent why many past investigations of wetting and adhesion have foundered or gone astray. It is hoped that a solid foundation has been laid for a more understanding experimental and theoretical treatment of many other properties of solid-liquid interfaces. For example, the calorimetric measurement of heats of wetting to characterize either wetting properties or solid surface states will be much more revealing now that we understand the major effects arising from adsorbed films on the surfaces or from trace impurities or additives in the liquids.

Langmuir's "principle of independent surface action" has been found useful and often correct, and the conditions under which it should not be used are now more evident. Our experimental results on the effect of surface constitution on the spreading and adhesive properties of liquids on solid surfaces or on adsorbed films are convincing examples of the wide occurrence in solids and liquids of extremely localized surface forces. Our Table V of critical surface tensions, although empirical and approximate in nature, has proved a powerful tool for describing and predicting important properties of solid surfaces and adsorbed films; undoubtedly, future investigations and applications will be guided by such considerations.

With these new concepts we have been able to develop a simple general treatment of the wetting properties of solutions—both aqueous and nonaqueous. Undoubtedly, the principal function of a wetting agent is to lower the surface tension of the solution below the critical surface tension of wetting of the solid surface to be wetted. One of the most interesting by-products of our investigations has been the recognition of the major part played by incomplete wetting and by low-energy surfaces in the adhesives and related arts. When Griffith's important effect of stress concentrations around voids or gas pockets was coupled with our results on the effects of surface composition on wetting and spreading by the liquid adhesives, a general and useful theoretical treatment of adhesional joints and adhesives emerged.

Many applications in research and industry have already been made of the results of the investigations reviewed here; undoubtedly many more will be made. These include: studies of other physical and chemical properties of adsorbed retracted monolayers, a full exploration of the nonspreading properties of watch, clock, and fuse oils; the all-Teflon film balance for investigating the mechanical properties of surface films on organic liquids; the development of new and improved treatments for chemical-, oil- and water-repellent finishes for clothing, canvas, etc.; improved finishes for textile fibers and tire cords; an explanation and generalization of the many processes based on mold-release agents or abhesives, which are important in the plastic and paper industries; an explanation of the spreading properties of printing inks and the key to developing better inks as well as those capable of writing on greasy surfaces; both improved and new adhesives; improved polishes and cleaners for plastic floor coverings and tile; and a long-sought explanation of the relation of wetting properties of liquids to their effectiveness as lubricants.

Despite these many advances, certain aspects of the subject of this paper have been neglected and further investigation is much needed. No reliable data are available on the effect of temperature on the equilibrium contact angles of any systems; all of the measurements reported here were made at 20°C. and 50% relative humidity. However, several general effects of variations in the temperature and humidity on the contact angle can be outlined. It is well known that the surface tensions, γ_{LV°, of pure organic liquids decrease linearly with rising temperature until close to the critical temperatures. Hence, if the temperature is T, then

$$\gamma_{LV^\circ} = C_1 - C_2T$$

But we have shown that $\cos \theta_E = a - b\gamma_{LV^\circ}$, when the surface composition of the solid is constant. Here C_1, C_2, a, and b are positive. Therefore,

$$\cos \theta_E = (a - bC_1) + bC_2T$$

and $\cos \theta_E$ must increase (or θ_E decrease) with increasing temperature. In addition, the effect of raising the temperature will be to cause surface expansion and increased desorption of any physically adsorbed compounds. Temperature increase will therefore decrease the packing of such adsorbed films, and this will raise the critical surface tension of the system and thus cause θ_E to decrease with rising temperatures.

In Contact Angle, Wettability, and Adhesion; Fowkes, F.;
Advances in Chemistry; American Chemical Society: Washington, DC, 1964.

When the temperature becomes high, there may result chemical changes in the liquids, such as hydrolysis, oxidation, and pyrolysis, or there may develop surface-chemical changes in the solid due to oxidation, dehydration, or crystallographic rearrangement. The products of chemical reaction in the liquids may be highly adsorbable and may cause the formation of new low-energy surface films on which the liquids will not spread. This effect may overbalance the above-mentioned normal decrease in θ_E with rising temperature. The oxidation or dehydration of these inorganic solid surfaces may greatly alter the wetting behavior of the liquids. But if the chemical reactivity or adsorptivity of the liquid is little changed thereby, no large change in wettability is to be expected.

Decreasing the relative humidity at ordinary temperatures will have little effect on θ_E unless the atmosphere is made so dry as to dehydrate the solid surface (as in silica and α-alumina). But usually long exposure to very dry air will be required to change the contact angles significantly. As the relative humidity approaches 100%, increased condensation of water on the surfaces of both metals and metallic oxides will invite the hydrolysis *in situ* of some adsorbed liquids, and so the wetting properties of these surfaces will become more like those of such highly hydrated surfaces as glass, silica, and alumina.

Obviously, data are needed on the values of f_{SV° for a variety of low-energy solid surfaces; with these and the values of W_{A*} given here, one would no longer have to estimate W_A, and hence our knowledge of adhesion would become more precise.

The empirical nature of γ_c is obvious, and it would be helpful to replace γ_c by parameters having a sound basis in thermodynamic or statistical mechanical considerations. Recent efforts by Fowkes [40] to relate γ_c to the dispersion forces between molecules at the interface have been especially promising in leading to tractable equations. An interesting direct correlation has been recently pointed out to us by Gardon [49] between the value of γ_c of a solid polymer and the Hildebrand solubility parameter, δ, which is defined as the square root of the molar energy density—i.e., $\delta = \sqrt{E/\rho'}$. A simple consideration of the Young equation and the definition of γ_c indicates that when cos $\theta = 1$,

$$\gamma_{SV^\circ} - \gamma_{SL} \doteq \gamma_c$$

Unfortunately, the effect of constitution on either γ_{SV° or γ_{SL} is still unknown, and neither quantity can be studied until a satisfactory experimental method for measuring it has been found. However, neither quantity appears to be a simple function of the constitution of the solid and liquid phases. A more precise theory of wetting of low-energy surfaces should at least include γ_{SL}. Probably the lateral spread in the data points of our graphs of cos θ vs. γ_{LV} for a given solid surface is due to the variation of γ_{SL} among the liquids used.

Finally, our investigations have been concerned with the wetting of a solid by one liquid, and nothing has been said about the classic problem of the competitive wetting and adhesion of two immiscible liquids with respect to a given solid surface. However, it is obvious that the findings reported here for the simpler systems should prove helpful in learning more about the more complex.

Publication Date: January 1, 1964 | doi: 10.1021/ba-1964-0043.ch001

Literature Cited

(1) Am. Assoc. Textile Chemists and Colorists, Piedmont Section, Am. Dyestuff Reptr. **53**, 25 (Feb. 4, 1963).
(2) Baker, H. R., Shafrin, E. G., Zisman, W. A., J. Phys. Chem. **56**, 405 (1952).
(3) Bakker, G., "Kapillarität und Oberflächenspannung," in Wien-Harms "Handbuch der Experimental Physik," Vol. VI, Academischer Verlag, Leipzig, 1928.
(4) Bangham, D. H., Trans. Faraday Soc. **33**, 805 (1937).
(5) Bangham, D. H., Razouk, R. I., Ibid., **33**, 1459 (1937).
(6) Banks, W. H., Nature **174**, 365 (1954).
(7) Banks, W. H., Proc. 2nd Intern. Congr. Surface Activity, Vol. I, p. 16, Academic Press, New York, 1957.
(8) Bartell, F. E., Zuidema, H. H., J. Am. Chem. Soc. **58**, 1451 (1936).
(9) Bartell, L. S., Ruch, R. J., J. Phys. Chem. **60**, 1231 (1956).
(10) Ibid., **63**, 1045 (1959).
(11) Basford, P. R., Harkins, W. D., Twiss, S. B., Ibid., **58**, 307 (1954).
(12) Bernett, M. K., Jarvis, N. L., Zisman, W. A., Ibid., **66**, 328 (1962).
(13) Bernett, M. K., Zisman, W. A., Ibid., **63**, 1241 (1959).
(14) Ibid., p. 1911.
(15) Ibid., **64**, 1292 (1960).
(16) Ibid., **65**, 2266 (1961).
(17) Ibid., **66**, 1207 (1962).
(18) Berry, K. L., U.S. Patent **2,559,629** (July 10, 1951).
(19) Bewig, K., Zisman, W. A., Advan. Chem. Ser., No. **33**, 100 (1961).
(20) Bewig, K., Zisman, W. A., J. Phys. Chem. **67**, 130 (1963).
(21) Bigelow, W. C., Brockway, L. O., J. Colloid Sci. **11**, 60 (1956).
(22) Bigelow, W. C., Glass, E., Zisman, W. A., Ibid., **2**, 563 (1947).
(23) Bigelow, W. C., Pickett, D. L., Zisman, W. A., Ibid., **1**, 513 (1946).
(24) Blake, G. G., Ahlbrecht, A. H., Bryce, H. Y., "Quaternary Ammonium Compounds from Fluorinated Acids," Division of Industrial and Engineering Chemistry, 126th Meeting, A.C.S., New York, N. Y., September 1954.
(25) Boyd, G. E., Livingston, H. K., J. Am. Chem. Soc. **64**, 2383 (1942).
(26) Brace, N. O., J. Org. Chem. **27**, 4491 (1962).
(27) Brockway, L. O., Karle, J., J. Colloid Sci. **2**, 277 (1947).
(28) Cassie, A. B., Baxter, S., Trans. Faraday Soc. **40**, 546 (1944).
(29) Cooper, W. A., Nuttall, W. A., J. Agr. Sci. **7**, 219 (1915).
(30) De Boer, J. H., Advan. Colloid Sci. **3**, 27 (1950).
(31) Dupré, A., "Théorie Méchanique de la Chaleur," p. 369, Gauthier-Villars, Paris, 1869.
(32) Ellison, A. H., Fox, H. W., Zisman, W. A., J. Phys. Chem. **57**, 622 (1953).
(33) Ellison, A. H., Zisman, W. A., Ibid., **58**, 260 (1954).
(34) Ibid., p. 503.
(35) Ibid., **59**, 1233 (1955).
(36) Ibid., **60**, 416 (1956).
(37) Ibid., **63**, 1121 (1959).
(38) Epstein, H. T., Ibid., **54**, 1053 (1950).
(39) Fischer, E. K., Gans, D. M., Ann. N. Y. Acad. Sci. **46**, 371 (1946).
(40) Fowkes, F. M., Advan. Chem. Ser., No. 43, 99 (1963).
(41) Fowkes, F. M., Harkins, W. D., J. Am. Chem. Soc. **62**, 3377 (1940).
(42) Fox, H. W., Taylor, P. W., Zisman, W. A., Ind. Eng. Chem. **39**, 1401 (1947).
(43) Fox, H. W., Hare, E. F., Zisman, W. A., J. Colloid Sci. **8**, 194 (1953).
(44) Fox, H. W., Hare, E. F., Zisman, W. A., J. Phys. Chem. **59**, 1097 (1955).
(45) Fox, H. W., Levine, O., private communication.
(46) Fox, H. W., Zisman, W. A., J. Colloid Sci. **5**, 514 (1950).
(47) Ibid., **7**, 109 (1952).
(48) Ibid., p., 428.
(49) Gardon, J. L., J. Phys. Chem. **67**, 1935 (1963).
(50) Gibbs, J. Willard, Trans. Connecticut Acad. **3** (1876-1878); "Collected Works," Vol. I, Longmans, Green, New York, 1928.

Publication Date: January 1, 1964 | doi: 10.1021/ba-1964-0043.ch001

(51) Graham, D., J. Phys. Chem. **66**, 1815 (1962).
(52) Griffith, A. A., Phil. Trans. Roy. Soc. (London) **A221**, 163 (1920).
(53) Hare, E. F., Shafrin, E. G., Zisman, W. A., J. Phys. Chem. **58**, 236 (1954).
(54) Hare, E. F., Zisman, W. A., Ibid., **59**, 335 (1955).
(55) Harkins, W. D., Chem. Revs. **29**, 408 (1941).
(56) Harkins, W. D., Ewing, W. W., J. Am. Chem. Soc. **42**, 2539 (1920).
(57) Harkins, W. D., Feldman, A., Ibid., 44, 2665 (1922).
(58) Harkins, W. D., Grafton, E. H., Ibid., **42**, 2534 (1920).
(59) Harkins, W. D., Loeser, E. H., J. Chem. Phys. **18**, 556 (1950).
(60) Hirshfelder, J. D., Curtiss, C. F., Bird, R. B., "Molecular Theory of Gases and Liquids," Wiley, New York, 1954.
(61) Jarvis, N. L., Fox, R. B., Zisman, W. A., Advan. Chem. Ser., No. 43, 317 (1963).
(62) Jarvis, N. L., Zisman, W. A., J. Phys. Chem. 63, 727 (1959).
(63) Ibid., 64, 150, 157 (1960).
(64) Johnson, R. E., Ibid., **63**, 1655 (1959).
(65) Jones, D. C., Saunders, L., J. Chem. Soc. 1951, 2944.
(66) Kaminski, A., Stanford Research Inst. Rept. 2, Contract N60ri-15402, Jan. 12, 1948.
(67) Karle, J., Brockway, L. O., J. Chem. Phys. **15**, 213 (1947).
(68) Klevens, H. B., Raison, M., J. Chim. Phys. **51**, 1 (1954).
(69) Kraus, G., Manson, J. E., J. Polymer Sci. **6** (5), 625 (1951).
(70) Langmuir, I., Chem. Revs. **6**, 451 (1929).
(71) Langmuir, I., "Collected Works," Pergamon Press, New York, 1960.
(72) Langmuir, I., J. Am. Chem. Soc. **38**, 2221 (1916).
(73) Langmuir, I., J. Franklin Inst. **218**, 143 (1934).
(74) Langmuir, I., Science 87, 493 (1938).
(75) Langmuir, I., Trans. Faraday Soc. **15** (3), 62 (1920).
(76) Laplace, P., "Méchanique Céleste," Suppl. 10th Vol., 1806.
(77) Lester, G. R., J. Colloid Sci. **16**, 315 (1961).
(78) Levine, O., Zisman, W. A., J. Phys. Chem. **61**, 1068 (1957).
(79) Ibid., p. 1188.
(80) Loeser, E. H., Harkins, W. D., Twiss, S. B., Ibid., **57**, 251 (1953).
(81) McBain, M. E. L., Perry, L. H., J. Am. Chem. Soc. **62**, 989 (1940).
(82) Martinet, J. M., "Adsorption des Composés Organiques Volatiles par le Polytétrafluor Éthylene," Commissariat à l'Énergique Atomique, Rapport CEA 888, Centre d'Etudes Nucleáires de Socloy, 1958.
(83) Menter, J. W., Tabor, D., Proc. Roy. Soc. (London) **A204**, 151 (1951).
(84) Merker, R., Zisman, W. A., J. Phys. Chem. **56**, 399 (1952).
(85) Moilliet, J. L., J. Oil Colour Chemists' Assoc. **38**, 463 (1955).
(86) Mylonas, C., Proc. VII Intern. Congr. Appl. Mech., London, 1948.
(87) Quayle, O. R., Chem. Revs. **53**, 439 (1959).
(88) Ray, B. R., Anderson, J. R., Scholz, J. J., J. Phys. Chem. **62**, 1220 (1958).
(89) Scholberg, H. M., Guenthner, R. A., Coon, R. I., Ibid., **57**, 923 (1953).
(90) Scholz, J. J., Ray, B. R., Anderson, J. R., Ibid., **62**, 1227 (1958).
(91) Schulman, F., Zisman, W. A., J. Colloid Sci. **7**, 465 (1952).
(92) Shafrin, E. G., Zisman, W. A., "Hydrophobic Monolayers and Their Adsorption from Aqueous Solutions," p. 129, in "Monomolecular Layers," Am. Assoc. Advance. Sci., Washington, D. C., 1954.
(93) Shafrin, E. G., Zisman, W. A., J. Colloid Sci. **4**, 571 (1949).
(94) Ibid., **7**, 166 (1952).
(95) Shafrin, E. G., Zisman, W. A., J. Phys. Chem. **61**, 1046 (1957).
(96) Ibid., **64**, 519 (1960).
(97) Ibid., **66**, 740 (1962).
(98) Shuttleworth, R., Bailey, G. L., Discussions Faraday Soc. 1948, No. **3**, 16.
(99) Sumner, C. G., "Symposium on Detergency," p. 15, Chemical Publ. Co., New York, 1937.
(100) Tabor, D., Rept. Progr. Appl. Chem., Soc. Chem. Ind., London **36**, 621 (1951).
(101) Thompson, W., Phil. Mag. (4) **17**, 61 (1858).

Publication Date: January 1, 1964 | doi: 10.1021/ba-1964-0043.ch001

(102) Thompson, W., Proc. Roy. Soc. (London) **9**, 255 (1858).
(103) Wenzel, R. N., Ind. Eng. Chem. **28**, 988 (1936).
(104) Young, Thomas, Phil. Trans. Roy. Soc. (London) **95**, 65 (1805).
(105) Zisman, W. A., "Relation of Chemical Constitution to the Wetting and Spreading of Liquids on Solids," p. 30 in "A Decade of Basic and Applied Science in the Navy," U. S. Government Printing Office, Washington, D. C., 1957.
(106) Zisman, W. A., "Constitutional Effects in Adhesion and Abhesion," in "Symposium on Adhesion and Cohesion," P. Weiss, ed., Elsevier, New York, 1962.
(107) Zisman, W. A., O'Rear, J. G., U. S. Patent 2,824,141 (Feb. 18, 1958).

Received April 16, 1963.

2

The Chemical Structure of Solid Surfaces as Deduced from Contact Angles

N. K. ADAM

Department of Chemistry,
University of Southampton,
Southampton, England

Publication Date: January 1, 1964 | doi: 10.1021/ba-1964-0043.ch002

The relation between equilibrium contact angles at a solid surface, and the adhesion between solid and liquid, is reviewed. The information deducible as to the chemical nature of the groups exposed at the surface is summarized.

This brief review surveys our knowledge, and the methods by which it has been obtained, of the chemical composition of some solid surfaces, mostly of the low-energy type, as learned from measurements of contact angles.

The basic equations were known over 150 years ago, and can be found in Thomas Young's classical treatise, "On the Cohesion of Fluids" [18]. They were given in words rather than in algebraic form; for this reason some seem to have missed the fact that Young's exceptional insight enabled him to see that the contact angle gives the relation between the adhesion of the liquid to the solid, and its cohesion to itself, as expressed in Equation 2. When the adhesion is less than the self-cohesion of the liquid, there is a contact angle, the larger the smaller the adhesion. When the adhesion is equal to or greater than the cohesion, the angle is zero. The equations for finite angles are

$$\gamma_S = \gamma_{SL} + \gamma_L \cos\theta \quad (1)$$

and

$$W_{SL} = \gamma_L (1 + \cos\theta) \quad (2)$$

γ_S, γ_L, γ_{SL} are the free energies per square centimeter of the solid, liquid, and solid-liquid interfaces—i.e., their surface tensions; W_{SL} is the work of adhesion—i.e., the work required to separate the liquid from the solid; and θ is the contact angle measured in the liquid.

The name "Young's equation" has been given to both Equations 1 and 2, although it is more commonly given to 1, especially in America. But we would do more honor [1] to Thomas Young by giving his name to Equation 2, rather than to 1, since Equation 1 is obvious to anyone who regards surfaces as being in tension—the concept of surface tension

In Contact Angle, Wettability, and Adhesion; Fowkes, F.;
Advances in Chemistry; American Chemical Society: Washington, DC, 1964.

was generally accepted in Young's time, but the concept of free energy had not been introduced. Equation 2 is much less obvious. Moreover, 2 is far more useful than 1, since it contains on the right-hand side only measurable quantities, whereas 1 contains two solid surface tensions, γ_S and γ_{SL}, which are almost impossible to measure.

The term γ_S in Equation 1 needs clarification. As Bangham and Razouk [6] pointed out, the vapor of the liquid will be adsorbed on the solid surface, often considerably decreasing its surface free energy. In Equation 1, and also in Dupré's Equation 3,

$$W_{SL} = \gamma_S + \gamma_L - \gamma_{SL} \tag{3}$$

which, when combined with 1 gives 2, we should write

$$\gamma_S = \gamma_S^\circ - \pi_{SV}$$

where π_{SV} is the surface pressure of this adsorbed film of the vapor of the liquid, and γ_S° is the free energy of a film-free solid surface. Since the part of the surface relevant for contact angle equilibrium is infinitesimally distant from the edge of the liquid, we can safely assume that this adsorbed film is in equilibrium with the saturated vapor pressure of the liquid. We rewrite Equations 1 and 3 thus:

$$\gamma_S^\circ - \pi_{SV} = \gamma_{SL} + \gamma_L \cos\theta \tag{1a}$$

$$W_{SLV} = \gamma_S^\circ - \pi_{SV} + \gamma_L - \gamma_{SL} \tag{3a}$$

but Young's second equation (Equation 2) remains unchanged, provided that W_{SL} in 2 is taken as the work of adhesion, W_{SLV}, of the liquid to a solid surface covered by an adsorbed film.

$$W_{SLV} = \gamma_L (1 + \cos\theta) \tag{2a}$$

The work of adhesion to the film-covered solid surface is of much greater practical importance than the work of adhesion, W_{SLO}, to a film-free solid, and is the only work that can be directly measured. If W_{SLO} is required, since $W_{SLO} = W_{SLV} + \pi_{SV}$, π_{SV} must be determined. This is likely to be very difficult, but could conceivably be done [5] by measuring the amount, Γ, of vapor adsorbed at several pressures of the vapor, from near zero up to the saturated vapor pressure of the liquid, and using the integrated form of the Gibbs adsorption equation

$$\pi_{SV} = RT \int_0^{p^\circ} \Gamma \, d \ln p$$

where p° is the saturated vapor pressure of the liquid.

Equations 1 and 2 assume that thermodynamic equilibrium exists between the liquid and the solid surface. In practice, however, equilibrium is rather rarely attainable experimentally, and there is a difference, sometimes considerable, between the larger angle given by a liquid advancing over a dry solid surface, and the smaller angle when the liquid is receding from a previously wetted surface. This is not

Publication Date: January 1, 1964 | doi: 10.1021/ba-1964-0043.ch002

the place to attempt a complete discussion of the numerous causes which have been suggested for this difference, or "hysteresis" of the contact angle. My experience, however, is that one of the commonest causes—unaccountably omitted from some recent discussions of hysteresis, although it was recognized by all the earlier workers—is that the liquid soaks into the upper layers of the solid, increasing its attraction for the liquid. It is very easy to observe that the contact angle of most solids is lowered by being left in contact with the liquid for some time. On extremely porous solids such as textile yarns, Cassie [6] has stated that the receding angle is unstable and not reproducible, since water soaks into the pores so quickly. Another cause may be surface films or other impurities on the solid, which can be easily removed by the liquid. It can be shown mathematically [16] that roughening a solid surface should increase hysteresis or even cause it to appear on a surface which, if smooth, would not show hysteresis. Any or all of these causes may contribute to hysteresis in a particular case. Among other causes suggested is friction between solid and liquid [4], but a permanent frictional force seems improbable because of the mobility of the liquid. Langmuir suggested that, in certain cases, the surface molecules overturn when in contact with water, so that their more polar ends point outwards [13].

Many workers record only a single angle; in other cases, where both advancing and receding angles have been recorded, their mean may be taken as a fairly satisfactory approach to the equilibrium angle. This procedure receives some justification from the fact that the mean angle is more consistent than either the advancing or receding angle [3], and there is often good agreement between the mean angle and the single angle given by those who recorded only one angle. These are the angles given in what follows.

Contact angles seem to vary very little with temperature. Studies on the temperature variation of contact angles are confined to ascertaining that close temperature control is unnecessary in measuring the angles. Fowkes and Harkins [9] state, without any details, that the angle between water and graphite or paraffin wax increases by 0.06° per degree centigrade; Adam and Elliott [3] found no detectable variation for water and various solid hydrocarbons between 20° and 35°C.

Rewriting Equation 2

$$\cos \theta = W_{SL}/\gamma_L - 1$$

it appears that temperature affects the surface tension and the adhesion to the solid to very nearly the same proportionate extent. Increase in the thermal motions of the liquid is the cause of decrease in its surface tension, and therefore in its work of cohesion, $2\gamma_L$, and the adhesion to the solid appears to be decreased in the same proportion. This suggests that the decrease in the adhesive field of force with rising temperature is much less in solids than in liquids, and is due principally or wholly to translatory motions.

It has been known for a very long time that water forms a large angle on paraffinic surfaces. Angles from 105° to 114° have been recorded for paraffin wax, the higher angles with very carefully purified specimens. Probably 112° to 114° is the best value for really pure paraffin wax; Fox and Zisman [12] found 111° with crystalline

Publication Date: January 1, 1964 | doi: 10.1021/ba-1964-0043.ch002

hexatriacontane; Ray and Bartell [15] obtained 112°, and Adam and Elliott [3] 114° for very carefully purified wax.

Polyethylene, according to Fox and Zisman [12], gives 94°, a value confirmed by Adam and Elliott. The question naturally arises whether the large difference between paraffin wax and polyethylene is due to the wax exposing methyl groups almost exclusively, the polyethylene, with its much higher molecular weight, little but methylene groups. To examine whether there is any difference between the adhesion of water to methyl and methylene groups, Adam and Elliott [3] measured the angle on several rare, fully saturated solid aliphatic hydrocarbons. Hexamethylethane, which has nothing but methyl groups to be exposed, gave 115°, only a degree higher than the highest value found with paraffin wax. But three specimens of higher cycloparaffins, with 15, 16, and 17 $-CH_2-$ groups only, each gave 104.5°, indicating that methylene groups have a higher attraction for water than methyl groups, about 30% higher according to Equation 2.

Norcamphane, which contains five $-CH_2-$ and two tertiary $-\dot{C}H-$ groups, gave 102°; and adamantane and tricyclodecane, each with six $-CH_2-$ and four $-\dot{C}H-$ groups, gave 98°, indicating that $-\dot{C}H-$ groups adhere to water more strongly than $-CH_2-$ groups.

A possible reason for the difference in attraction for water of CH_3, $-CH_2-$, and $-\dot{C}H-$ groups may be that the water molecules can approach closer to the carbon atoms when there are fewer hydrogens present, as if the hydrogens formed a partial screen to the major attractive forces.

Although methylene groups have, by Equation 2, about 30% greater attraction for water than methyl groups, the difference is only half that required (60%) to account for the low angle obtained with polyethylene. We must conclude that probably even the best specimens of polyethylene have traces of polar, strongly water-attracting material present in or very near their surface. Similar trace amounts of polar material could account for the variation of angle between 105° and 114° found with different specimens of paraffin wax; the lowest angles were obtained with ordinary commercial waxes.

Fox and Zisman [10] showed that replacement of all the hydrogen by fluorine considerably increases the angle, water giving 108° with polytetrafluoroethylene; but replacement of only one of the four fluorines in this polymer by chlorine decreases the angle to 90°, even lower than for polyethylene. Probably a fully fluorinated, and very highly purified, "paraffin wax" would show an angle of about 120°, which seems likely to be the highest possible angle which could be given by water on a smooth surface. On a rough surface, or one regularly perforated with small holes [1, 8], much higher apparent angles can be obtained. These, however, do not depend on extra low adhesion of water to the solid, but are due to the surface in contact with water consisting partly of solid and partly of air, the water being unable to penetrate into the air-filled spaces except under rather high pressure.

Long-chain acids and alcohols, when allowed to solidify naturally, give an angle of contact [4] with water nearly as high as that shown by commercial paraffin wax. If, however, a fresh surface is formed by cutting with a knife, the cut surface has areas with widely differing angles, varying from 50° to 105°. The explanation is that these substances crystallize in parallel bimolecular sheets, each sheet consisting of two condensed monolayers with the polar groups sandwiched

Publication Date: January 1, 1964 | doi: 10.1021/ba-1964-0043.ch002

between the long hydrocarbon chains. At a naturally solidified surface, or one cut by a knife traveling more or less parallel to these sheets, only methyl groups are exposed and the angle is high; but if the knife travels across the sheets, one polar group per molecule will be exposed and the angle is much lower.

When hexadecyl alcohol was allowed to solidify in contact with water, in the hope of producing a surface with the molecules oriented so that only hydroxyl groups, closely packed, were exposed, again two kinds of surface were found, one with angle about 55°, other parts showing 105°. The lower angle indicates sheets more or less perpendicular to the surface; the higher angle indicates sheets parallel to the surface with methyl groups exposed. There was no sign of a surface with only hydroxyl groups exposed; such a surface would be expected to show a very low angle, probably zero. Although, during solidification, the hydroxyl groups were no doubt oriented to the water, this outer layer would adhere to the water much more strongly than it would adhere to the underlying solid by its end methyl groups, and would be detached from the solid when this is removed from the water.

Monolayers of long-chain substances with a polar group at one end, adsorbed on glass or other strongly water-attracting solids, give contact angles with water of the order of 90° if the chains are 12 carbon atoms long or more. That contact angles are unaffected, or at most very slightly affected, by attraction from groups more than a few atoms below the surface, is shown by the following observations. Wark and Cox [17] found that isoamyl xanthate produces angles up to 90° when adsorbed on various minerals; Levine and Zisman [14] found that the angle given by methylene iodide on an adsorbed monolayer of perfluoro-octanoic acid on glass was actually higher than that on polytetrafluoroethylene. Evidently a hydrocarbon chain five to seven carbons long can act as a nearly complete screen to attractive forces arising from a highly polar surface below.

Publication Date: January 1, 1964 | doi: 10.1021/ba-1964-0043.ch002

Literature Cited

(1) Adam, N. K., Endeavour **17**, 40 (1958).
(2) Adam, N. K., Nature 180, 809 (1957).
(3) Adam, N. K., Elliott, G. E. P., J. Chem. Soc. 1962, 2206.
(4) Adam, N. K., Jessop, G., Ibid., 1925, 1863.
(5) Adam, N. K., Livingston, H. K., Nature **182**, 128 (1958).
(6) Bangham, D. H., Razouk, R. I., Trans. Faraday Soc. **33**, 1459 (1937).
(7) Cassie, A. B. D., Discussions Faraday Soc. **3**, 14 (1948).
(8) Cassie, A. B. D., Baxter, S., Trans. Faraday Soc. 40, 546 (1944).
(9) Fowkes, F. M., Harkins, W. D., J. Am. Chem. Soc. **62**, 3377 (1940).
(10) Fox, H. W., Zisman, W. A., J. Colloid Sci. **5**, 514 (1950).
(11) Ibid., **7**, 109 (1952).
(12) Ibid., p. 431.
(13) Langmuir, I., Science **87**, 493 (1938).
(14) Levine, O., Zisman, W. A., J. Phys. Chem. **61**, 1188 (1957).
(15) Ray, B. R., Bartell, F. E., J. Colloid Sci. **8**, 214 (1953).
(16) Shuttleworth, R., Bailey, G. L. J., Discussions Faraday Soc. **3**, 16 (1948).
(17) Wark, I. W., Cox, A. B., Am. Inst. Mining Met. Engr. Tech. Publ. **461** (1932).
(18) Young, T., Phil. Trans. Roy. Soc. **84** (1805).

Received April 3, 1963.

Publication Date: January 1, 1964 | doi: 10.1021/ba-1964-0043.ch003

3

The Status of Contact Angle as a Thermodynamic Property

ARTHUR W. ADAMSON and IRENE LING

Department of Chemistry,
University of Southern California,
Los Angeles 7, Calif.

The Young and Dupré equation for the angle of contact of a liquid resting on a solid surface may be derived as a thermodynamic relationship, but the testing of its validity for the real situation of a nonequilibrium and usually heterogeneous surface presents difficulties. These are discussed first in terms of two simple molecular models and secondly in terms of thermodynamic relationships that should permit an independent verification of the contact angle relationship.

The present remarks are directed primarily towards a consideration of the thermodynamic usefulness of the equation generally written for the situation illustrated in Figure 1—namely, that of a liquid resting on a solid surface. The equation is, for the case where the third phase is gaseous,

$$\gamma_{LV}^0 \cos\theta = \gamma_{SV}^0 - \gamma_{SL} \quad (1)$$

Here, γ_{LV}^0 denotes the usual surface tension of the liquid (the superscript zero being a reminder that in principle the liquid is saturated

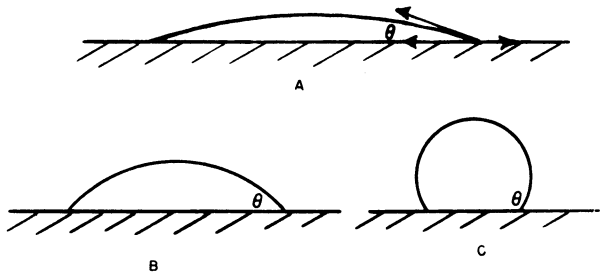

Figure 1. Sequence of isosteric shapes for gravity-free liquid drop

In Contact Angle, Wettability, and Adhesion; Fowkes, F.;
Advances in Chemistry; American Chemical Society: Washington, DC, 1964.

with the solid species), and the term $\gamma_{SV^0} - \gamma_{SL}$ denotes the free energy of exchanging unit geometric area of solid-vapor interface for solid-liquid interface. The antecedents of this relationship are old and its naming has been a matter of occasional discussion [1]; we prefer the usage: Young and Dupré [2, p. 265; 8].

The derivation of Equation 1 is often considered obvious, in that it follows directly from equating the horizontal components of surface tensional forces (indicated in Figure 1). The presence of some such forces is not to be denied; indeed, what should be the vertical component of γ_{LV^0} has been observed in the pulling up of the surface of deformable solids such as soft silica gel [27] and thin mica sheets [32] along the line of three-phase contact.

Equation 1 may also be derived in terms of the conformation of minimum free energy. The gravity-free case is straightforward. As illustrated in Figure 1, the sequence of possible drop shapes is that of truncated spheres and the condition of surface free energy minimization leads directly to Equation 1 [18]. The same result is shown below to be obtained by a similar analysis of the case of a very large drop, such that the surface becomes essentially horizontal in the middle. Gibbs also cites Equation 1 [16], and a detailed general thermodynamic proof has been offered by Johnson [24]. Thus, despite occasional claims to the contrary [7, 30], the equation appears to be potentially sound thermodynamically.

There remains the question of the physical–i.e., operational [9]–definition of the terms. It appears to the writers that the derivation as a force balance is merely intuitional, and, as a consequence, it leaves the quantities γ_{SL} and γ_{SV^0} undefined operationally. Thus, if these be viewed as forces parallel to the solid surface, one must ask with what property of the solid they are to be identified. Unlike the case with liquids, there is for solids a surface or stretching tension (the work per unit stretching of the surface [20, 25, 28]), in general nonisotropic. If this is what is involved, liquid drops on a crystalline surface of low symmetry should not be circular in cross section; this is apparently contrary to observation. From the thermodynamic derivation, however, we see that one is dealing with the work of exchanging one type of solid interface for another, and that surface free energies, not stretching tensions, are the proper quantities.

Again, contact angles are known to depend on surface roughness [6]. It has been pointed out [18] that the equation [2, p. 275]

$$\cos \theta_{rough} = r \cos \theta_{smooth}$$

where r is the roughness factor, appears naturally and immediately from a free energy approach. Likewise in the case of heterogeneous surfaces, perhaps an extreme example of which would be a porous or sievelike surface, the surface free energy approach readily provides an analysis at least approximately confirmed by experiment [10], where a force balance treatment seems never to have been attempted.

Such observations suggest that while the one can always be viewed as the mathematical construct of the other, surface free energy is a more rational quantity than surface force in the context of a contact angle situation. The former has also the merit of carrying some specific implications. The Young and Dupré equation is obtained by setting

Publication Date: January 1, 1964 | doi: 10.1021/ba-1964-0043.ch003

equal to zero the free energy change for a small displacement of the system from equilibrium–i.e., for a process involving a small exchange of amounts of the three interfaces. For such a process to have thermodynamic meaning, it would seem necessary that the surfaces involved in it be well defined thermodynamically. They should therefore uniquely be determined by the specification of the thermodynamic variables of composition, temperature, and pressure.

The liquid phase must be expected to be in equilibrium with the adjacent solid-vapor interface. Harkins and Livingston [22] were certainly justified in insisting on this requirement; if it does not hold, one can well ask just how the state of the solid-vapor interface is to be defined thermodynamically. A further significance of the thermodynamic derivation is that $\gamma_{SV^0} - \gamma_{SL}$ need not be viewed as the difference of independent quantities. Given a certain solid and liquid, the one value should determine the other, if equilibrium prevails. One can furthermore now defend this difference as having thermodynamic status without requiring that the solid surface *per se* be an equilibrium one.

The point here is that the surfaces of solids actually dealt with usually cannot be considered to be equilibrium ones. Even if crystalline, they will not usually display those faces demanded by the macroscopic minimizing of surface free energy [23]. Further, one expects for the equilibrium surface an optimization of the thermodynamic combination of entropy and energy, and hence a distribution of imperfections, surface waves and humps [33], etc. Most solids are incapable of adjusting to such equilibrium conformations and in practice their surface structure will be largely a frozen-in record of an arbitrary past history.

Even though nonequilibrium in this larger sense, the solid surface can come to a local equilibrium with molecules of an adjacent phase, in terms of chemical and van der Waals interactions, exchange of thermal energy, etc. The difference $\gamma_{SV^0} - \gamma_{SL}$ can thus be viewed as arising from the microscopic or local interactions between the molecules in the solid and vapor and the solid and liquid phases. On this basis, it is only indirectly and may be only incidentally related to the surface free energy of the pure solid. Indeed, it is different to define operationally the surface free energy of a nonequilibrium solid surface.

The conclusion at this point is that it is futile to seek a general thermodynamic connection between contact angle and the surface free energy of the pure solid. Any success in relating the two must come from theory based on specific molecular models. In this respect, then, the writers deny thermodynamic value to the Young and Dupré equation.

A Model for Treating γ_{SV^0}

Although, thermodynamically, it appears that only the difference $\gamma_{SV^0} - \gamma_{SL}$ has significance, the separate terms can be formulated when certain models for interfacial interactions are invoked. The following is a particularly simple one, adapted from the approach used by Girifalco and Good [17].

We assume that we are dealing with molecules of about the same size, and that only nearest neighbor interactions are of importance. Let the free energy of each be denoted by ε_{ij}. Consider, then, two phases, of S and L type molecules, and that the packing in each is such that there are n_1 molecules in the plane of a given molecule, and n_2 in

Publication Date: January 1, 1964 | doi: 10.1021/ba-1964-0043.ch003

the planes immediately above and below, as nearest neighbors. For cubic close packing n_1 and n_2 would be 6 and 3, respectively. Then for the surface free energy of phase L, per sq. cm.,

$$2\,\gamma_L\,V^{2/3} = (n_1 + 2n_2)\,\epsilon^0_{LL} - (n_1 + n_2)\,\epsilon^0_{LL} = n_2\,\epsilon^0_{LL} \qquad (3)$$

where V is the molecular volume, so defined that $V^{2/3}$ gives the molecular area. Equation 3 gives the free energy to bring an interior molecule to the surface, corrected for the area per molecule. The factor of 2 enters, because on applying the above process to a collection of molecules each interaction enters twice. Similarly, the surface free energy of phase S is

$$2\,\gamma_S\,V^{2/3} = n_2\,\epsilon^0_{SS} \qquad (4)$$

Consider now the process whereby an S-L interface is separated to give pure L and pure S surfaces; the free energy for this process, W_{SL}, is then given by

$$\begin{aligned} 2\,W_{SL}\,V^{2/3} &= (n_1 + n_2)\,\epsilon^0_{LL} + n_2\,\epsilon^0_{SL} + (n_1 + n_2)\,\epsilon^0_{SS} + n_2\,\epsilon^0_{SL} \\ &\quad - (n_1 + n_2)\,\epsilon^0_{LL} - (n_1 + n_2)\,\epsilon^0_{SS} \qquad (5) \\ &= 2\,n_2\,\epsilon^0_{SL} \end{aligned}$$

If the geometric mean rule--i.e., $\epsilon^0_{SL} = \sqrt{\epsilon^0_{SS}\,\epsilon^0_{LL}}$—is invoked, Equations 3 and 4 may be combined to give

$$\epsilon^0_{SL} = \frac{2V^{2/3}}{n_2}\sqrt{\gamma_S\,\gamma_L} \qquad (6)$$

which in combination with the expression for W_{SL} and Equation 5 yields

$$\gamma_{SL} = \gamma_S + \gamma_L - W_{SL} = \gamma_S + \gamma_L - 2\sqrt{\gamma_S\,\gamma_L} \qquad (7)$$

The above relationship was obtained by Girifalco and Good as a first approximation. Actually, it is doubtful if any greater generality than that of replacing the coefficient 2 in Equation 7 by an empirical constant is justified. As an illustration of this point, Fowkes [13] suggests that if L denotes a substance capable only of dispersion-type interactions, ϵ^0_{SL} probably involves only dispersion forces between S and L type molecules, even though the former may be hydrogen-bonded, etc. The consequence is that in Equation 7, the term $\sqrt{\gamma_S\,\gamma_L}$ is to be taken to involve hypothetical γ_S and γ_L values.

If we now consider a contact angle situation, Equation 1 may be written in the form

$$\gamma_L\,\cos\theta = \gamma_S - \pi - \gamma_{SL} \qquad (8)$$

where π denotes the film pressure of adsorbed vapor, $\gamma_s - \gamma_{sv^o}$, and we suppose the liquid-vapor interface to be that of pure liquid, for simplicity. We suppose further that the adsorbed layer of species L in equilibrium with its saturation vapor pressure, P^0, is less than a

Publication Date: January 1, 1964 | doi: 10.1021/ba-1964-0043.ch003

monolayer, and that, as an approximation, the Langmuir adsorption isotherm applies. We then write

$$\Gamma = \frac{1}{V^{2/3}} \frac{bP}{1 + bP} \tag{9}$$

where Γ denotes molecules per sq. cm., and $b = b' e^{n_2 \varepsilon^0_{SL}/kT}$. The film pressure of the adsorbed layer may next be calculated by means of the Gibbs equation,

$$\pi = kT \int_0^{P^0} \Gamma \, d \ln P \tag{10}$$

Insertion of Equation 9 into 10 and integration yield

$$\pi = \frac{kT}{V^{2/3}} \ln (1 + bP^0) \tag{11}$$

Equation 11 can be put in the form

$$\pi = \frac{kT}{V^{2/3}} \ln \left[1 + \beta \, e^{n_2(\varepsilon^0_{SL} - \varepsilon^0_{LL})/kT}\right] \tag{12}$$

where β is unity if the frequency and accommodation coefficients are the same as for the evaporation-condensation process of liquid L on itself–i.e., if the entropy of condensation is the same for L on L as for L on S, apart from the assumption that the adsorbed film is localized [2, p. 470]. With dissimilar molecules, the accommodation coefficient for adsorption could well be less than for self-condensation, so that β might be much less than unity.

On combining Equations 12, 3, 4, and 6, one obtains

$$\pi = \frac{kT}{V^{2/3}} \ln \left[1 + \beta \exp.\left(\frac{2V^{2/3}}{kT} \left\{\sqrt{\gamma_S \gamma_L} - \gamma_L\right\}\right)\right] \tag{13}$$

On insertion of this result into Equation 8, a transcendental relationship is obtained for cos θ which, while difficult to verify as to form by fitting of data, leads to some limiting predictions which are of interest. Thus, taking β to be unity, the following cases obtain:

Case 1. $\gamma_L << \sqrt{\gamma_S \gamma_L} >>$ ca. 10

whence

$$\pi = 2 (\sqrt{\gamma_S \gamma_L} - \gamma_L), \cos \theta = 1$$

Case 2. $\gamma_L = \sqrt{\gamma_S \gamma_L}$; $\pi = 0.69 \frac{kT}{V^{2/3}}$

(or π has the value of about 9 ergs per sq. cm. for 25°C. and a molecular area of 30 sq. A.).

Publication Date: January 1, 1964 | doi: 10.1021/ba-1964-0043.ch003

Case 3. $\gamma_L > \sqrt{\gamma_S \gamma_L}$

π decreases towards zero.

Fowkes has made the point that, particularly in the case of hydrogen-bonded phases in contact with non-hydrogen-bonded ones—e.g., water *vs.* hydrocarbons—the potentials involved in determining the surface free energies of the former may be different (and presumably greater) than those for the interaction between the two. The effect is to replace everywhere the term $\sqrt{\gamma_S \gamma_L}$ by $\sqrt{\gamma_S^w \gamma_L^w}$, where superscript w denotes the dispersion or van der Waals potential component only. Thus for hydrocarbons on water, or aqueous silica gel as a solid stand-in for water [28], the term γ_S^w would be estimated at about 20 ergs per sq. cm.—i.e., as being about the same as for a liquid hydrocarbon. This then corresponds to Case 2, for which a π value of about 9 ergs per sq. cm. is predicted.

Actual π values for hydrocarbon liquids on liquid water or on water immobilized in a silica gel matrix are small, in contradiction to the above prediction. This situation of a very low π value may be special. The entire field of surface area determination by gas adsorption rests on the fact that low energy adsorbates (hydrocarbons, nitrogen, rare gases, etc.) give thick adsorbed layers on all variety of solids at pressures approaching the saturation pressure. The interesting question then arises as to whether it may be the liquid state of the adsorbent in the above-cited instances that leads to a distinctly different behavior than that expected from general experience with solids. In a formal way, the observed low π values are interpreted as meaning low β values or small condensation coefficients for hydrocarbon vapors on a liquid water surface, whether free or immeshed in a gel matrix. The point could be clarified by adsorption studies using ice as the solid.

In general, there seems to be no theoretical basis for supposing that for circumstances other than corresponding to Case 3, negligibly small π values should pertain. In particular, the presence of a finite contact angle should in no way characterize a system for which π will be very small.

As a specific example, Harkins and coworkers [21] observed π values of 20 ergs per sq. cm. or more in the case of graphites in near-saturated water vapor. The fact that the graphite surfaces involved were heterogeneous is immaterial, since, as noted further below, the contact angle Equation [1] then involves the average $\overline{\gamma_{SV^0} - \gamma_{SL}}$, which will certainly be reduced from $\overline{\gamma_S - \gamma_{SL}}$ if there is a nonzero average π value calculated from the Gibbs integration of the adsorption isotherm. The case of low energy liquids on lower energy solids, such as hydrocarbons on fluorocarbon surfaces, may or may not resemble the situation with the former on water; the matter is best decided by actual adsorption studies. It is possibly significant, however, that such substances as CF_4, argon, and N_2 show considerable adsorption on polytetrafluoroethylene [19].

Preliminary Approach to Obtaining $\gamma_{SV^0} - \gamma_{SL}$

The preceding treatment, however simple, is relatively consistent, in that all interactions invoked are restricted to nearest neighbor ones. There is no reason, however, to suppose that the adsorbed film need be

Publication Date: January 1, 1964 | doi: 10.1021/ba-1964-0043.ch003

submonolayer in nature and it is desirable to find some way of handling the more general situation where the film may be multilayer. One approach lies through recognizing that the dispersion potential experienced by a molecule near a solid-vapor interface will be, in the limit of large distances, inverse cube in distance–i.e.,

$$\epsilon_{SL} = \frac{\epsilon^0_{SL}}{(x/d_{SL})^3} \tag{14}$$

where x is the distance from the surface of a semi-infinite solid and d_{SL} is the nearest neighbor distance. Equation 14 can be only approximate, since the inverse cube law does not hold strictly at small distances from a lattice. Nonetheless, if it is used in combination with a simple Polanyi type treatment of adsorption in which one supposes that condensation of the vapor will occur to a depth x such that

$$\epsilon_{SL}(x) = kT \ln P^0/P \tag{15}$$

(see [2, p. 265] for more detail), one then obtains the following expression for Γ:

$$\Gamma = \frac{1}{V_L^{2/3}} (\epsilon^0_{SL}/kT)^{1/3} (1/\ln P^0/P)^{1/3} \tag{16}$$

The general picture is illustrated in Figure 2. The dashed line in Figure 2, B, indicates that below a critical pressure, P', only submonolayer adsorption (or vapor compression in the potential field) occurs; at P' condensation begins, and a liquid-like adsorbed film deepens towards infinite thickness as P approaches P^0.

Such an infinitely thick film, however, would not allow for a contact angle situation. Frumkin [15], in fact, concluded that for a nonzero contact angle to be possible, a continuous transition from adsorbed film to bulk liquid must not be possible. There is experimental evidence that equilibrium adsorbed films do not approach infinite thickness at P^0 [11, 15]. It is desirable, therefore, to consider at least qualitatively how a treatment might be formulated which would correctly predict a discontinuity between adsorbed film and adjacent bulk liquid in a contact angle situation.

The detailed approach would require a meticulous summation of all molecule-molecule interactions. Consider the situation, shown schematically in Figure 3, of a deep layer of adsorbate, j molecules thick. The particular molecule shown in the ith layer experiences a potential given by the sum of interactions with the semi-infinite solid and the interactions with other adsorbate molecules, infinite in two dimensions, but finite in the third. The last was approximated in Equation 16 by treating the adsorbed film as normal liquid in state. The detailed analysis would involve complete potential functions, radial distributions, and structural information, and would then lead to some total expression for the free energy of an adsorbed film as a function of its thickness. From the corresponding partial molar free energy, a relationship to kT ln P^0/P could in principle be obtained.

As a semi-empirical expedient, however, assume that this function can be separated into that part given by Equation 16 and that representing

Publication Date: January 1, 1964 | doi: 10.1021/ba-1964-0043.ch003

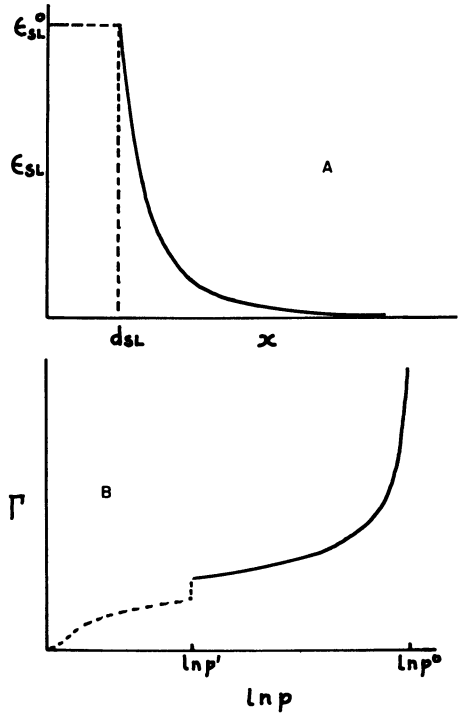

Figure 2. A. Assumed variation of ϵ_{SL} *with distance*

B. Variation of Γ *with pressure*

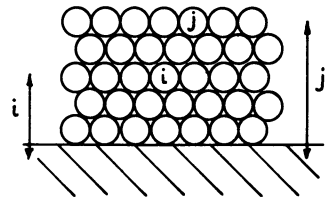

Figure 3. Summations involved for a film of stacked spheres

the adsorbate-adsorbate interactions. Assume further that this last can be expressed as a deviation from normal liquid by means of an effective vapor pressure, $P^{0'}$, which approaches P^0 for infinite film thickness. Equations 14 and 15 then become:

$$kT \ln P^{0'}/P = \frac{\epsilon^0_{SL}}{(x/d_{SL})^3} \qquad (17)$$

Publication Date: January 1, 1964 | doi: 10.1021/ba-1964-0043.ch003

If this deviation of the film from liquid in state be regarded as a propagation originating at the solid-film boundary, it seems reasonable to approximate its decay to zero with increasing distance from the surface as exponential in nature–i.e.,

$$kT \ln P^{0'}/P^{0} = \Delta e^{-aX} \tag{18}$$

where Δ might be either positive or negative. Essentially this type of behavior was proposed by Fletcher [12] for the progression from surface to interior structure in the case of liquid water.

The complete equation then becomes:

$$kT \ln P^{0}/P = \frac{\epsilon^{0}_{SL}}{(x/d_{SL})^{3}} - \Delta e^{-aX} \tag{19}$$

The general appearance of this function is shown in Figure 4, and it is seen that for Δ positive–i.e., for $P^{0'} > P^{0}$–a discontinuity is possible, in that film of finite thickness x^{0} can be in equilibrium with an infinitely thick liquid layer–i.e., bulk liquid–at $P = P^{0}$. In combination with the Gibbs equation, we then have:

$$\pi_{sv^{0}} = \gamma_{s} - \gamma_{sv^{0}} = kT \int_{x=o}^{x=x^{0}} \Gamma \, d \ln P \tag{20}$$

where x^{0} is obtained by setting the right-hand side of Equation 19 equal to zero, and

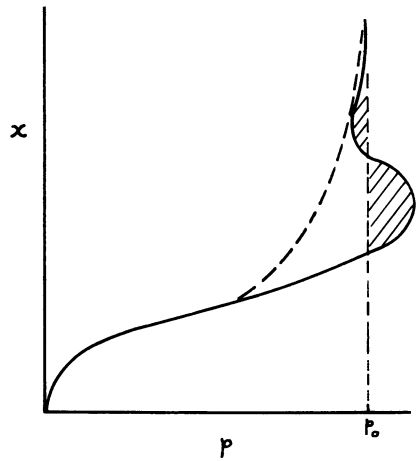

Figure 4. Variation of film thickness with pressure

Publication Date: January 1, 1964 | doi: 10.1021/ba-1964-0043.ch003

$$\pi_{SL} = \gamma_S - (\gamma_{SL} + \gamma_{LV}) = kT \int_{x=0}^{x=\infty} \Gamma \, d \ln P \tag{21}$$

with Γ related to x as before. On carrying out the integrations,

$$\pi_{SL} - \pi_{SV^0} = \frac{\epsilon^0_{SL}}{V^{2/3}} \left(\frac{1}{2x^{02}} - \frac{1}{ax^{03}} \right) \tag{22}$$

In effect, we have determined directly the difference $\pi_{SL} - \pi_{SV^0}$, equal to the net of the shaded areas in Figure 4, so that the absolute surface free energy of the solid is not really involved. Furthermore, the exact formulation of Equation 19 for small x values should be important, since this portion of the area in the Γ *vs.* ln P plot cancels out in Equation 22.

A preliminary analysis of the detailed summations of van der Waals interactions between a film and a semi-infinite solid indicates that if ϵ^0_{ij} has the same interpretation as in the preceding section, in Equations 14 through 23 x ϵ^0_{SL} is actually $(\epsilon^0_{SL} - \epsilon^0_{LL})$.

The expression for cos θ now becomes:

$$\cos \theta = 1 + \frac{\epsilon^0_{SL}}{\gamma_L V_L^{2/3} x^{02}} \left(\frac{1}{2} - \frac{1}{ax^0} \right) \tag{23}$$

Thus wetting will always occur if Δ is negative–i.e., if $P^{0'} < P^0$– and with Δ positive, a finite contact angle is predicted if ax^0 is less than 2. For layers as thick as Derjaguin [11] reports–namely, 20 to 60 molecules in depth in the case of organic vapors adsorbed on glass–the propagation constant, a, would have to be less than 5% per layer for a finite contact angle to be possible. Since his systems were probably all ones in which spreading occurs, the 5% figure is then a lower limit.

The above analysis, while very tentative, indicates that vapor adsorption determinations are a desirable part of the study of contact angle systems. In fact, through such data, it may be possible to develop a sufficiently valid analysis to allow prediction from them of contact angle values. In any event, the above approach suggests that the fundamental quantity in determining a contact angle is the difference, $\gamma_{SV^0} - \gamma_{SL}$, as such, and not either quantity separately, in the sense of being viewed as independent. Complications that may arise with a two-component liquid are discussed further below.

Another line of investigation of potential interest would be that of contact angle measurements on various faces of single crystals. The first, and perhaps both right-hand terms of Equation 19 (or some more exact form), should show a dependence on and very likely a proportionality to the surface density of atoms for the solid.

Verification of Young and Dupré Equation

Just as it was interesting to verify experimentally the Gibbs adsorption equation in the case of solution-vapor interfaces [26], it should be worthwhile to verify such aspects of the Young and Dupré Equation 1 as are experimentally accessible. The approaches outlined above are not thermodynamic in the sense that particular molecular models are

Publication Date: January 1, 1964 | doi: 10.1021/ba-1964-0043.ch003

invoked. We are concerned now with verifications that do not involve such specific assumptions.

A direct testing of Equation 1 by determinations of γ_{SV^0} and γ_{SL} separately presents all of the difficulties of estimating experimentally the surface free energy of a solid. Studies on the contraction of wires near their melting points, in nonwetting liquid and in saturated vapor, might have some success, as they apparently do in giving the pure metal surface free energies [3]. The highly ingenious approach of Michaels and Dean [27] of using silica gel as a stand-in for water does not fully lay to rest doubts, mentioned above, as to whether a solid surface of water substance may be qualitatively different from a liquid surface.

A rather different procedure lies in a testing of the temperature dependence of contact angle. From the second law equations, $(\partial F^S/\partial T)_P = -S^S$, and $F^S = E^S - TS^S$, one finds, in combination with Equation 1:

$$q = E_{SV^0} - E_{SL} = E_{LV} \cos\theta - T\gamma_{LV^0}\left(\frac{\partial \cos\theta}{\partial T}\right)_P \qquad (24)$$

where q is the integral heat of immersion of unit area of solid-vapor interface. In fact, the correctness of Equation 22 was assumed by Bartell and Fu [4] (neglecting, however, the term involving the temperature dependence of cos θ) in their proposal of an "absolute" method of surface area determination–that is, by comparing the q obtained by means of Equation 24 with an experimental heat of immersion per gram of powdered solid, the specific surface area of the latter was obtained. An actual verification of Equation 24 should be possible in better defined systems and using current gas adsorption methods for independent surface area determination.

A more complex line of approach is that involving the use of two-component liquid systems, the dilute component of which is surface active. Thus Fowkes and Harkins [14] measured the contact angles of aqueous solutions of n-butyl alcohol at various solid-air interfaces. The film pressure at the solution-solid interface was then given by:

$$\pi_{SL'} = \gamma_{SL} - \gamma_{SL'} = \pi_{SV^0'} + \gamma_{LV'} \cos\theta' - \gamma_{LV} \cos\theta \qquad (25)$$

where the primes denote values for solution. Equation 25 was assumed correct (with the first term taken to be zero). Again, an independent verification would be possible through direct studies of the adsorption of the solute at the solid-solution interface, combined with the use of the Gibbs equation [10], to give an independent evaluation of $\pi_{SL'}$.

A question that arises immediately, however, is that of the extent to which the solute component is also present at the solid-vapor surface–i.e., the extent to which an equilibrium mixed adsorbed film is present. Qualitative observations by Bartell and Fu tended to suggest that in their cases very little adsorption at the solid-vapor interface occurred, justifying their neglect of $\pi_{SV^0'}$. It would take the independent verification procedure suggested, however, to confirm the correctness of this assumption and of Equation 25. A complete study should include adsorption experiments with appropriate mixed vapors, so as to obtain $\pi_{SV^0'}$ independently.

Publication Date: January 1, 1964 | doi: 10.1021/ba-1964-0043.ch003

Some experiments very similar to these outlined above were carried out by Ruch and Bartell [31]. Metal surfaces were equilibrated with aqueous decylamine, and the air-liquid-solid contact angles were then measured, using small air bubbles. The degree of adsorption of the decylamine was determined by optical measurements of the thickness of the film, but could be only approximately related to actual amounts adsorbed. While the results correlated well with a semi-empirical analysis, they unfortunately do not allow a verification of Equation 25. As shown in Figure 5, a qualitative calculation of π_{SL}', using the solution adsorption data, then allows calculation of π_{SV^0}', assuming Equation 25 to hold. Clearly this last quantity is far from zero, as opposed to the situation assumed by Fowkes and Harkins for their system. Ruch and Bartell in fact took the adsorbed film to be identical in nature at the SL and the SV interfaces, but without any independent verification of the assumption.

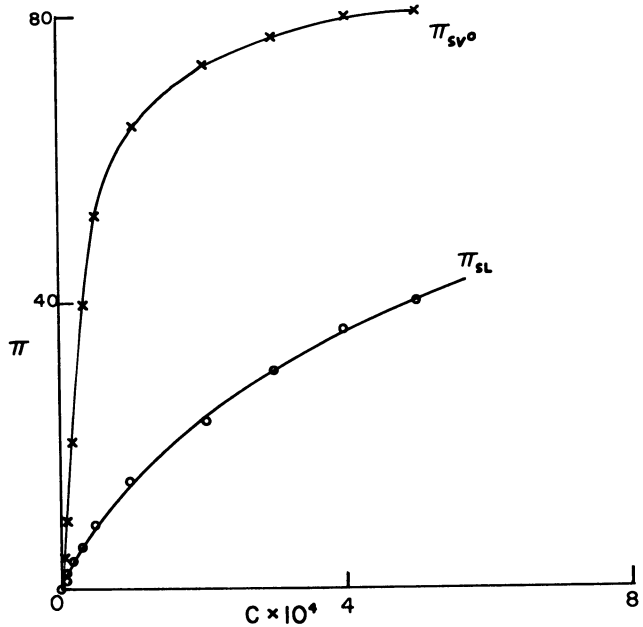

Figure 5. Calculated film pressures for the adsorption of decylamine on platinum

Data of Figure 3 [31]

It would certainly be desirable to see some definitive work establishing the validity of Equation 25 in at least a few systems. The above two examples suggest, furthermore, that it may be entirely possible to have metastable films at one or the other solid interface–for example, if the liquid-film transition involves a structural phase change [11], so that nucleation may be required to produce an equilibrium film.

Heterogeneous Surfaces

The derivation of Equation 1 by the surface free energy minimization procedure, both for the gravity-free case and for the one given in the discussion of the case of a very large drop, makes it clear that the quantity determining $\gamma_L \cos \theta$ is the net reversible work of replacing unit film covered surface by unit solid-liquid interface. If the surface is grossly heterogeneous, there will be a driving force for local contact angles to be the local equilibrium ones, different on various portions of the surface. As a result, varying local curvatures would be introduced in the liquid surface, which must be compensated if the net curvature and hence the mechanical pressure within the liquid is to be purely hydrostatic. Hence there will be a tendency for liquid to extend over low contact angle regions and to retreat from high contact angle ones, as illustrated in Figure 6. For liquids of ordinary viscosity, the requirement of uniform hydrostatic pressure should be overriding, and the various local contact angles may represent some compromise demanded by this condition. The average contact angle, by whatever experimental procedure it be defined, will then reflect the topology of surface heterogeneities, and it is difficult to see how the various thermodynamic tests discussed above could be experimentally formulated, let alone succeed.

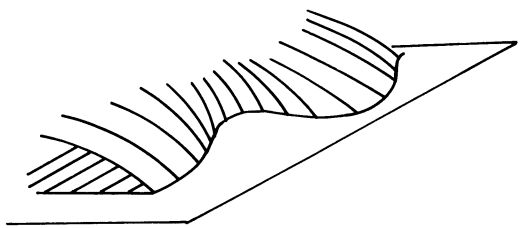

Figure 6. Shape assumed by a drop on a heterogeneous surface

For microscopically heterogeneous surfaces, in the limit, polyatomic solids, three types of behavior can be distinguished. The liquid boundary may preferentially rest on one or the other type of surface, so that the contact angle approximates the minimum or the maximum available local values. In fact, the postulation of this type of behavior has been a basis for an explanation of hysteresis [29]. A second possibility is that there are locally varying angles, but on so small a scale as quickly to average to a single observable one. In a formal way one may then write

$$\bar{\theta} = \sum_{\theta_{min.}}^{\theta_{max.}} f(\theta)\, \theta \qquad (26)$$

where $f(\theta)$ is an appropriately defined distribution function. Here again the topology of the heterogeneities would be involved and it is doubtful if thermodynamic relationships such as Equations 24 and 25 can be expected

to hold. Finally, it may happen that the average value, $\overline{\gamma_{SV^0} - \gamma_{SL}}$, determines cos θ–i.e.,

$$\gamma_L \overline{\cos \theta} = \overline{\gamma_{SV^0} - \gamma_{SL}} \quad (27)$$

Favorable conditions would seem to be heterogeneities of molecular dimensions and a mobile adsorbed film such that molecules near the boundary experience only an average potential in so far as an equation of state such as 19 is concerned. Where Equation 27 does apply, the various thermodynamic verifications outlined above should succeed; the circumstance is essentially that the solid-liquid and the solid-vapor interfaces behave as though a single and not a collection of states were involved. Studies of contact angles on cleavage surfaces of pure and of mixed crystals might shed some light on the type of average that occurs with heterogeneities of molecular dimensions.

Finally, a note of caution on the danger of oversimplifying the role of surface roughness might be raised. Equation 2 follows if it is assumed that $F_{SV^0} - F_{SL}$ will, for the extension of liquid over unit geometric surface, be proportional to the ratio of true to apparent area–i.e., to the roughness factor–of solid surfaces otherwise identical. The integrals involved in Equations 20 and 21, however, are based on an implicit assumption of a plane surface. To the extent that the curvatures in the surface are not negligible in comparison to the depth of film involved, the potential functions will cease to be functions only of distance normal to the macroscopic plane of the surface. Under such conditions, the detailed nature of the roughness will be woven into the functions themselves, and it will not be true that a simple roughness factor will factor out. Bikerman [7] has noted, for example, that in extreme situations such as surface grooves, it becomes obvious that the topology of roughness and not just the roughness factor must be considered. For rough surfaces, then (and this could mean nearly all experimental surfaces), the thermodynamic status of the Young and Dupré equation is clouded.

Summary and Conclusions

The general philosophy of the present paper is that the question of whether the Young and Dupré equation is a thermodynamic one is meaningless unless there exist in principle experiments capable of deciding the point in any given case. We conclude that, apart from possible special cases such as wires near their melting point, there is little likelihood of providing such answers by determinations of the separate surface free energies of the solid-liquid and solid-vapor interfaces. In the usual circumstance of solids not near their melting point, these interfaces will not be equilibrium ones, so that it appears operationally meaningless even to apply the term of surface free energy to them.

It appears, however, that since the difference $\gamma_{SV^0} - \gamma_{SL}$ is involved, this quantity may be capable of definition independently of the question of whether the solid surface itself is an equilibrium one. From a molecular point of view, the matter becomes one of estimating the difference between solid-liquid and solid-vapor interactions, and two simple models were considered. They are capable of at least some experimental reinforcements in the form of vapor adsorption studies, and

Publication Date: January 1, 1964 | doi: 10.1021/ba-1964-0043.ch003

it may therefore prove possible to make useful interpretations of contact angle values by means of them. As a negative example, the critical surface tension quantity used by Zisman and coworkers [5]–i.e., the surface tension of that liquid in a related series which just wets a particular solid–does not seem to be directly related to the surface free energy of the pure solid surface, but rather it marks a critical stage, in the progression from one liquid to another, in the shape of the x *vs.* P curve (see Figure 4). In terms of the specific potential function of Equation 19, wetting depends on the quantity ax^0, which is not simply related to either the liquid or solid surface free energy.

With respect to purely thermodynamic tests of the Young and Dupré equation, a study of the temperature dependence of contact angles, combined with calorimetric and surface area measurements, offers some promise. This would provide a classical second law test.

The case of contact angles of solutions is more difficult, but offers more scope for thermodynamic predictions that would be in principle verifiable. In addition to temperature-dependence studies, it is now possible to make independent determinations of changes in γ_{SV^0} and γ_{SL} with solution composition and hence of the expected changes in contact angle.

The question of the thermodynamic status of the Young and Dupré equation is not a trivial one. On the one hand, if the thermodynamic state of the interfaces involved is not uniquely defined by the terms in the Young and Dupré equation, as may be true for rough and for heterogeneous surfaces and possibly for some situations with multicomponent systems, the thermodynamic tests will fail. The same would be true if at the three-phase boundary stretching tensions and not purely surface free energy quantities are important. From such thermodynamic studies may then emerge a recognition of what additional conditions are implicit in the equation. This in turn should greatly assist in the formulation of better molecular models. Alternatively, if in some classes of situations the thermodynamic tests succeed, one gains indirect methods for obtaining contact angles or changes in contact angles.

Case of a Very Large Drop

The derivation of Equation 1 for the gravity-free case is straightforward and need not be given here. It is mentioned by Pethica and Pethica [30]. The case of a very large drop may be proved as follows.

In the limiting case of a very large drop, one radius of curvature becomes infinite, so that, as illustrated in Figure 7, only the curvature of a cross section need be considered. In addition, the second radius of curvature approaches infinite at the center–i.e., the middle of the drop becomes flat–and area terms involving the curved rim can be neglected.

The total free energy then becomes:

$$F^S_{total} = 1/2\ h\rho gV + A_{LV}\ \gamma_{LV} + A_{SL}\ \gamma_{SL} + (A_{total} - A_{SL})\ \gamma_{SV^0} \quad (28)$$

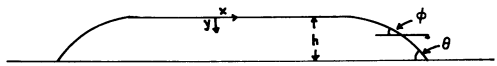

Figure 7. Profile for a very large drop

Publication Date: January 1, 1964 | doi: 10.1021/ba-1964-0043.ch003

The first term gives the gravitational potential; also, neglecting rim areas, $A_{LV} = A_{SL}$ and $hA_L = V$. Making these substitutions, and setting the derivative of F^S_{total} with respect to h equal to zero, one obtains:

$$\left(\frac{h}{a}\right)^2 = \frac{\gamma_{LV} + \gamma_{SL} - \gamma_{SV^0}}{\gamma_{LV}} \tag{29}$$

where $a^2 = 2\gamma_{LV}/\rho g$

Turning to the analysis of the drop shape, the Laplace equation may be put in the form:

$$\frac{2y}{a^2} = p \frac{dp/dy}{(1 + p^2)^{3/2}} \tag{30}$$

where $p = dy/dx$. This may be integrated to give

$$\left(\frac{y}{a}\right)^2 = \frac{1}{(1 + p^2)^{1/2}} + \text{constant} \tag{31}$$

where the constant is equal to unity if $p = 0$ at $y = 0$. Since $p = \tan \varphi$, Equation 31 may also be written as

$$(y/a)^2 = 1 - \cos \varphi \tag{32}$$

or, when $y = h$,

$$\left(\frac{h}{a}\right)^2 = 1 - \cos \theta \tag{33}$$

Equations 29 and 33 combine to give the Young and Dupré relationship.

Literature Cited

(1) Adam, N. K., Nature 180, 809 (1957).
(2) Adamson, A. W., "Physical Chemistry of Surfaces," Interscience, New York, 1960.
(3) Alexander, B. H., Dawson, M. H., Kling, H. P., J. Appl. Phys. 22, 439 (1951).
(4) Bartell, F. E., Fu, Y., "The Specific Surface Area of Activated Carbon and Silica," in "Colloid Symposium Annual," Vol. III, H. B. Weiser, ed., Wiley, New York, 1930.
(5) Bernett, M. K., Zisman, W. A., J. Phys. Chem. 64, 1292 (1960).
(6) Bikerman, J. J., J. Phys. Colloid Chem. 54, 653 (1950).
(7) Bikerman, J. J., "Proceedings of Second International Congress on Surface Activity," Vol. II, p. 125, Butterworth, London, 1957.
(8) Boyd, G. E., "Surface Chemistry," Am. Assoc. for Advancement of Science, Publ. 21, 128 (1943).
(9) Bridgeman, P. W., "The Logic of Modern Physics," Macmillan, New York, 1961.
(10) Cassie, A. B. D., Baxter, S., Trans. Faraday Soc. 40, 546 (1944).
(11) Derjaguin, B. V., Zorin, Z. M., "Proceedings of Second International Congress on Surface Activity," Vol. II, pp. 145, 224, Butterworth, London, 1957.
(12) Fletcher, N. H., Phil. Mag. (8) 7, 255 (1962).

Publication Date: January 1, 1964 | doi: 10.1021/ba-1964-0043.ch003

(13) Fowkes, F. M., J. Phys. Chem. 66, 382 (1962).
(14) Fowkes, F. M., Harkins, W. D. J. Am. Chem. Soc. 62, 3377 (1940).
(15) Frumkin, A., J. Phys. Chem. (Moscow) 12, 337 (1938).
(16) Gibbs, J. W., "Collected Works," p. 326, Longmans, Green, New York, 1928.
(17) Girifalco, L. A., Good, R. J., J. Phys. Chem. 61, 904 (1957).
(18) Good, R. J., J. Am. Chem. Soc. 74, 5041 (1952).
(19) Graham, D., J. Phys. Chem. 66, 1815 (1962).
(20) Gurney, C., Proc. Phys. Soc. (London) A62, 639 (1949).
(21) Harkins, W. D., "Physical Chemistry of Surface Films," pp. 286-91, Reinhold, New York, 1952.
(22) Harkins, W. D., Livingston, H. K., J. Chem. Phys. 10, 342 (1942).
(23) Herring, C., Phys. Rev. 82, 87 (1951).
(24) Johnson, R. E., Jr., J. Phys. Chem. 63, 1655 (1959).
(25) Lennard-Jones, J. E., Dent, R. M., Proc. Roy. Soc. (London) A109, 476 (1925); A121, 247 (1928).
(26) McBain, J. W. Swain, R. C., Ibid., A154, 608 (1936).
(27) Michaels, A. S., Dean, S. W., Jr., J. Phys. Chem. 66, 1790 (1962).
(28) Nicholson, M. M., Proc. Roy. Soc. (London) A228, 490 (1955).
(29) Pease, D. C., J. Phys. Chem. 49, 107 (1945).
(30) Pethica, B. A., Pethica, T. J. P., "Proceedings of Second International Congress on Surface Activity," Vol. III, p. 131, Butterworth, London.
(31) Ruch, R. J., Bartell, L. S., J. Phys. Chem. 64, 513 (1960).
(32) Second International Congress on Surface Activity, Vol. III, p. 189, Butterworth, London, 1957.
(33) Temperley, H. N. V., Proc. Cambridge Phil. Soc. 48, 683 (1952).

Received April 15, 1963. Investigations supported in part by a grant from the Petroleum Research Fund of the American Chemical Society.

4

Theory for the Estimation of Surface and Interfacial Energies

VI. Surface Energies of Some Flurocarbon Surfaces from Contact Angle Measurements

ROBERT J. GOOD

Space Science Laboratory
General Dynamics/Astronautics
San Diego, Calif.

Publication Date: January 1, 1964 | doi: 10.1021/ba-1964-0043.ch004

The surface free energy of a solid can be estimated from the contact angles of liquids on the solid, by means of the equation

$$\gamma_{so} = \frac{\left[\gamma_1(1 + \cos\theta) + \pi_e\right]^2}{4\Phi^2\gamma_1}.$$

The constant, Φ, which is a property of the particular liquid-solid system, can be calculated from the molecular properties of the two substances: dipole moment, polarizability, ionization energy, and molecular radius. Free energies have been calculated from contact angle data for the following solids: polytetrafluoroethylene, polyhexafluoropropylene, poly(trifluoromonochloro)ethylene, and a monolayer of perfluorolauric acid.

Zisman's extensive studies of contact angles and wetting led him and his associates [15] to the conclusion that the surface free energy of a solid, γ_{so}, is approximated by a "critical surface tension," γ_c, which is the surface tension that divides the liquids forming zero contact angle on the solid from those forming contact angles greater than zero. A more detailed theoretical justification of this conclusion was given by Good and Girifalco [16, 20], who also showed that for "regular" interfaces—i.e., systems for which the cohesive forces of the two phases, and the adhesive forces across the interface, are of the same type—the contact angle of the liquid on the solid is related to the surface energies of the liquid and the solid. Fowkes [12, 13] has extended the treatment of Good and Girifalco to certain cases where the cohesive forces

In Contact Angle, Wettability, and Adhesion; Fowkes, F.;
Advances in Chemistry; American Chemical Society: Washington, DC, 1964.

are of unlike type. He found that the component of solid surface energy due to dispersion forces could be estimated from contact angle data, using a modified form of the equations of Good et al.

Very recently, Good [17] has extended the theory of interfacial energies [16] to include an explicit account of the different types of intermolecular forces: dispersion, dipole induction, and dipole orientation. In the present paper, we will use the theory, as extended [17], to show how the actual surface free energies of certain solids can be calculated from contact angle data, including Fox and Zisman's critical surface tensions.

Solubility effects in interfacial tension have been treated very recently [18]. For low-energy solids such as polytetrafluoroethylene, the correction for solubility effects will be negligible with most liquids. However, for metal-metal systems such as liquid bismuth vs. copper the effect of solubility on the liquid-solid interfacial tension is very marked [19]. For solids that are swelled by the liquids, or for monolayers that are penetrated or filled out by molecules of the wetting liquid–e.g., octadecylamine by alkanes [2, 3, 20]–the solubility correction will be important. Such systems will be treated in a later publication.

Theory

Good and Girifalco [16, 20] showed that the interfacial tension between the liquid and solid phases was given by

$$\gamma_{s1} = \gamma_{so} + \gamma_1 - 2\Phi\sqrt{\gamma_{so}\,\gamma_1} \tag{1}$$

where γ_{so} is the surface free energy of the solid in vacuum.

This equation was combined with Young's equation [32] to give the expression:

$$\cos\theta = 2\Phi\sqrt{\frac{\gamma_{so}}{\gamma_1}} - 1 - \frac{\pi_e}{\gamma_1} \tag{2}$$

$$\simeq 2\Phi\sqrt{\frac{\gamma_{so}}{\gamma_1}} - 1 \tag{3}$$

where θ is the equilibrium contact angle and π_e is the equilibrium spreading pressure ($\pi_e = \gamma_{so} - \gamma_{sv}$). Φ is a function of the molecular properties of the two substances. It is clear from Equation 3 that if Φ is a constant for a series of liquids–e.g., the alkanes–on a given solid, if $\pi_e \simeq 0$, and if γ_c is the critical surface tension for that series, then $\gamma_c = \Phi^2\gamma_{so}$.

To discuss how Φ may be evaluated, we note first that for interfaces other than those involving solids, the equations by which Φ is evaluated are symmetrical. Hence the subscripts 1, 2, and 12 are employed, rather than s, l, and sl, to refer to the respective phases. It was originally proposed that, for "regular" interfaces,

$$\Phi \equiv \frac{-\Delta F^{a}}{\left(\Delta F_1^{c} \Delta F_2^{c}\right)^{1/2}} = \frac{(r_1 r_2)}{r_{12}^2} \tag{4a}$$

$$= \frac{4 r_1 r_2}{(r_1 + r_2)^2} \simeq \frac{4(V_1 V_2)^{1/3}}{\left(V_1^{1/3} + V_2^{1/3}\right)^2} \tag{4b}$$

where r_1 and r_2 are the molecular radii corresponding to the equilibrium distances between the centers of force of the molecules, and V_1 and V_2 are the molar volumes. ΔF^{a} is the free energy of adhesion, and ΔF_1^{c} and ΔF_2^{c} are the free energies of cohesion of the separate phases.

Φ is approximately unity for "regular" interfaces, as defined above. But for systems in which the types of intermolecular forces in the two molecules are markedly different, it was shown [16] that Φ may be appreciably less than unity. The most general expression that can be derived from the present model is of the form

$$\Phi = \frac{4 r_1 r_2}{(r_1 + r_2)^2} \times \frac{\Sigma A_{12}}{(\Sigma A_{11}\ \Sigma A_{22})^{1/2}} \tag{5}$$

where the A's are the attractive constants in an r^{-6} potential energy function. Thus in a Lennard-Jones potential,

$$E = \frac{B}{r^{12}} - \frac{\Sigma A}{r^6} \tag{6}$$

where $\Sigma A = A_{(\text{dispersion})} + A_{(\text{induction})} + A_{(\text{dipole orientation})}$. When the intermolecular forces in each phase are of these familiar types [22,23], and when the molar volume expression for the r's is employed, Equation 4 has the more explicit form,

$$\Phi = \frac{4(V_1 V_2)^{1/3}}{\left(V_1^{1/3} + V_2^{1/3}\right)^2} \times \frac{\frac{3}{4}\alpha_1\alpha_2 \times \frac{2 I_1 I_2}{I_1 + I_2} + \alpha_1 \mu_2^2 + \alpha_2 \mu_1^2 + \frac{2}{3}\frac{(\mu_1 \mu_2)^2}{kT}}{\left[\left(\frac{3}{4}\alpha_1^2 I_1 + 2\alpha_1 \mu_1^2 + \frac{2}{3}\frac{\mu_1^4}{kT}\right)\left(\frac{3}{4}\alpha_2^2 I_2 + 2\alpha_2 \mu_2^2 + \frac{2}{3}\frac{\mu_2^4}{kT}\right)\right]^{1/2}} \tag{7}$$

Here the α's are polarizabilities, the μ's are dipole moments, and the I's are ionization energies. When $\mu_1 = 0$, Equation 7 reduces to

Publication Date: January 1, 1964 | doi: 10.1021/ba-1964-0043.ch004

$$\Phi = \frac{4(V_1V_2)^{1/3}}{\left(V_1^{1/3} + V_2^{1/3}\right)^2}\left[\left(\frac{\frac{3}{4}\alpha_2^2 I_2}{\frac{3}{4}\alpha_2^2 I_2 + 2\alpha_2\mu_2^2 + \frac{2}{3}\frac{\mu_2^4}{kT}}\right)^{1/2} \times \frac{2(I_1I_2)^{1/2}}{I_1 + I_2} + \frac{\mu_2^2}{\left[\frac{3}{4}I_1\left(\frac{3}{4}\alpha_2^2 I_2 + 2\alpha_2\mu_2^2 + \frac{2}{3}\frac{\mu_2^4}{kT}\right)\right]^{1/2}}\right] \quad (8)$$

This expression is only slightly dependent on the molecular properties of phase 1 (the nonpolar phase), since the molar volumes and ionization energies of substances of interest do not vary widely, and the second term in brackets is generally considerably smaller than the first.

If both μ_1 and μ_2 are zero–i.e., if the only forces are of the London dispersion type–then

$$\Phi = \frac{4(V_1V_2)^{1/3}}{\left(V_1^{1/3} + V_2^{1/3}\right)^2} \times \frac{2(I_1I_2)^{1/2}}{I_1 + I_2} \quad (9)$$

Solving Equation 2 for γ_{so}, we have

$$\gamma_{so} = \frac{\left[\gamma_1(1 + \cos\theta) + \pi_e\right]^2}{4\Phi^2\gamma_1} \quad (10)$$

$$\simeq \frac{\gamma_1(1 + \cos\theta)^2}{4\Phi^2} \quad (11)$$

For most low-energy surfaces, on which adsorption is small, π_e is probably negligible in comparison to γ_1 [15]. (However, for metal-metal systems, π_e cannot be neglected, as shown by Bailey and Watkins [1] for lead on copper.) Since γ_{so} is a property of the solid only, the right-hand side of Equation 11 should be equal to a constant.

Application of Theory

The surface free energies were calculated by Equation 11 for polytetrafluoroethylene (Teflon), polyhexafluoropropylene, poly(trifluoromonochloro)ethylene (Kel-F), and a perfluorolauric acid monolayer on an inert substrate such as platinum. Figures 1 to 5 show the results of this calculation. In each figure, the calculated value of γ_{so} is plotted against the surface tension of the liquid, γ_1. According to the discussion of Equation 11, above, the best horizontal line through the data points should correspond to the surface free energy of the solid, γ_{so}. The narrowness of the dispersion of points around that line should be a measure of the quality of the entire treatment, and of the correctness of choice of the parameters μ, α, I, and V, employed in Equation 7, 8, or 9.

Publication Date: January 1, 1964 | doi: 10.1021/ba-1964-0043.ch004

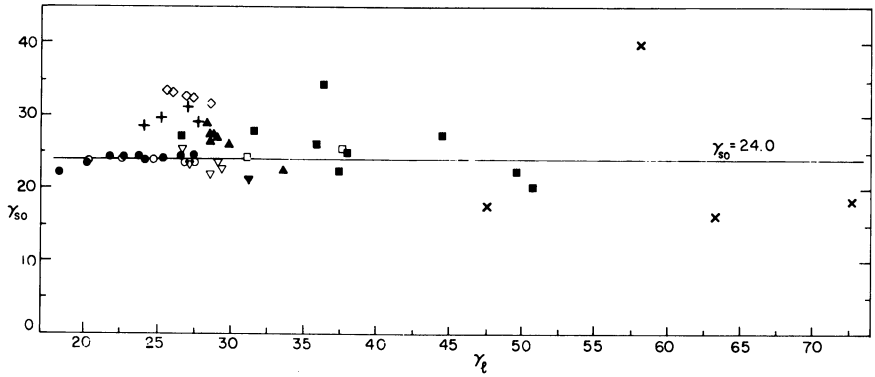

Figure 1. Surface free energy of Teflon γ_{so} calculated on basis of $\mu = 1.2$

- ● Alkanes
- ▲ Alkylaryl compounds
- ■ Halogenated hydrocarbons
- o Dialkyl ethers
- × Water, glycerol, Ethylene glycol, formamide
- ▽ Fatty acids
- ◇ Alcohols
- \+ Amines
- □ Esters
- ▼ CS_2

Contact angle data, and the surface tensions of the test liquids, were taken from the work of Zisman et al. [4, 5, 8, 9, 14, 15, 22]. Data for the computation of Φ, to use in Equation 11, were from the following sources: Ionization energies were from Field and Franklin [11] and (for fluorocarbons) from Reed [28]. Dipole moments were taken from Smyth [29] and from the compilation of Wesson [30]. Polarizabilities were computed from refractive indices by the formula

$$\alpha = \frac{n^2 - 1}{n^2 + 2} \times \frac{3}{4\pi N} \times \frac{M}{D} \qquad (12)$$

where M was taken to be the group-molecular weight, for each compound, corresponding to the size of the group that would act as a unit (or center of force) in nearest-neighbor attractive interactions. Table I lists the substances and the groups that were considered to act as units, for this purpose. (The same choices were made in determining the V's for use in the molar volume term in Equations 7, 8, and 9.)

TABLE I. Substances Acting as Units

Substance	Group Considered in Choice of M, Eq. 12
Teflon	CF_2
Polyhexafluoropropylene	CF_3
Kel-F	CF_2 (CFCl also tried. See below)
Perfluorolauric acid monolayer	CF_3

Publication Date: January 1, 1964 | doi: 10.1021/ba-1964-0043.ch004

TABLE I. Substances Acting as Units—Continued

Substance	Group Considered in Choice of M, Eq. 12
Alkanes	CH_3
Alkyl ethers	CH_3 (-O- also tried)
Alkylaromatic compounds	Aryl ring
Chlorinated hydrocarbons	C-Cl
Brominated hydrocarbons	C-Br
Iodinated hydrocarbons	C-I
H_2O	Molecule as a whole
Alcohols (including polyhydric)	C-OH
Fatty acids	CH_3 (CO_2H also tried)
Alkyl amines	CH_3 (same as NH_2)
Esters	CO_2C; or for aryl esters, aryl ring

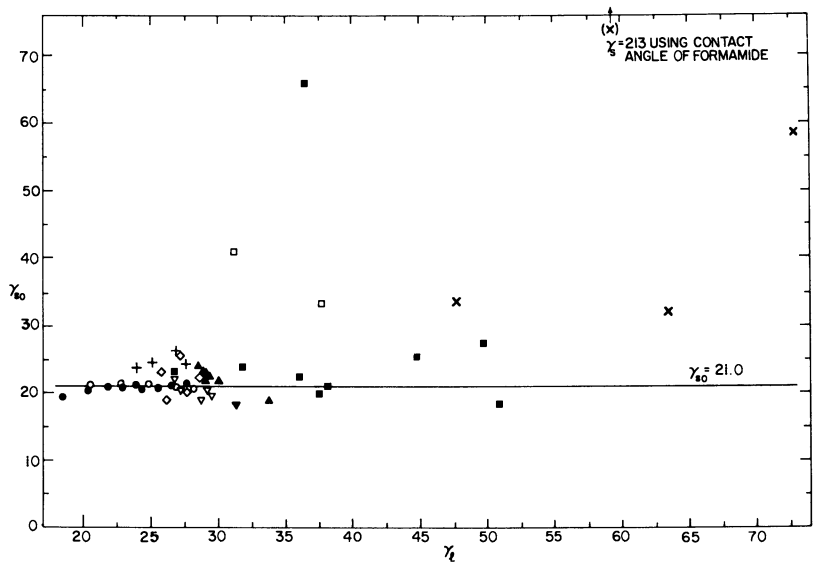

Figure 2. Surface free energy of Teflon γ_{so} calculated on basis of $\mu = 0$

- ● Alkanes
- ▲ Alkylaryl compounds
- ■ Halogenated hydrocarbons
- o Dialkyl ethers
- × Water, glycerol, ethylene glycol, formamide
- ▽ Fatty acids
- ◇ Alcohols
- \+ Amines
- □ Esters
- ▼ CS_2

Table II summarizes the results of the computations for the four substrates. No estimates of probable errors are reported. A statistical treatment seemed inappropriate in view of the widely divergent molecular interactions involved for the various different species, which is discussed below.

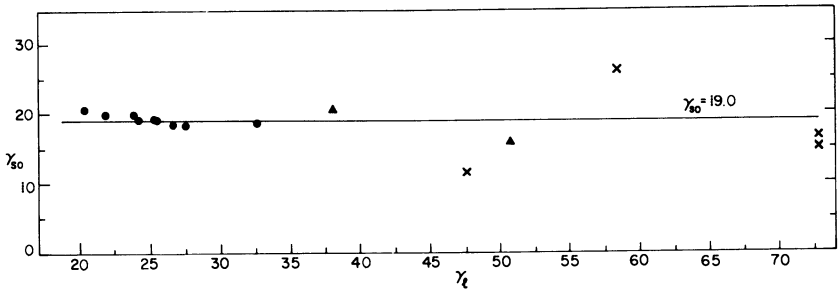

Figure 3. Surface free energy of polyhexafluoropropylene γ_{so} calculated on basis of $\mu = 1.2$

- ● Alkanes
- ▲ Alkylaryl compounds
- × Water, ethylene Glycol, formamide

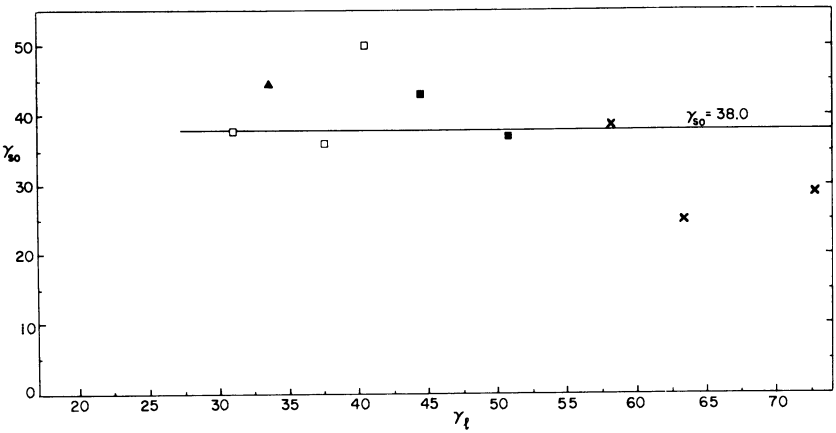

Figure 4. Surface free energy of Kel-F γ_{so} calculated on basis of $\mu = 1.2$

- ■ Halogenated hydrocarbons
- □ Esters
- × Water, glycerol, formamide

Publication Date: January 1, 1964 | doi: 10.1021/ba-1964-0043.ch004

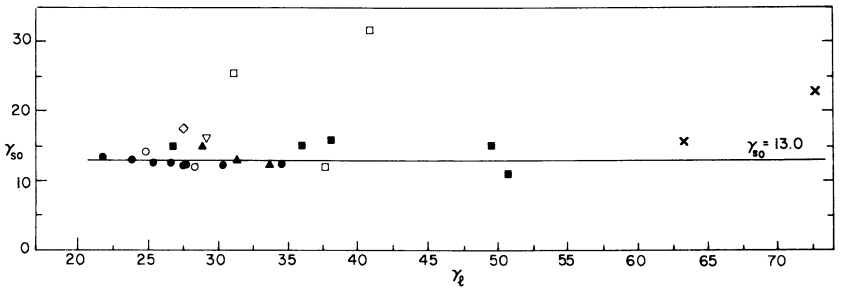

Figure 5. Surface free energy of perfluorolauric acid monolayer γ_{so} calculated on basis of $\mu = 1.0$

- ● Alkanes
- ▲ Alkylaryl compounds
- ■ Halogenated hydrocarbons
- O Dialkyl ethers
- × Water, glycerol
- ▽ Fatty acids
- □ Esters

TABLE II. Results of Computations

Solid Surface	Calculated γ_{so}, Ergs/Sq. Cm.
Polytetrafluoroethylene (Teflon)	24
Polyhexafluoropropylene	19
Perfluorolauric acid monolayer	13
Poly(trifluoromonochloro)ethylene (Kel-F)	38

Discussion of Results

The imposing number of substances whose contact angle on Teflon, etc., had been reported by Zisman et al. precludes a detailed discussion of each compound at this time. (Indeed, it was in part for this reason that the present study was restricted to only four substrates.)

It is evident from Equations 7, 8, and 9 that the results of this treatment are dependent on the choice of molecular parameters: the dipole moments, the polarizabilities, the ionization energies, and the molar (or group-molar) volumes. Consequently this treatment should, in principle, be a method of examining molecular interactions on a microscopic scale. If correct assumptions are made for every compound, about the nature of the interactions—e.g., dipole-dipole attraction, etc.—the same value of the surface free energy should result. However, it would be out of the question to adjust four parameters freely in order to minimize the dispersion in calculated values of γ_{so}. In this study, only physically reasonable values of these parameters were employed in the treatment, and the dipole moments of the substance forming the solid phase were the only parameters for which any attempt at further adjustment was made. For nonpolar substances and halogenated hydrocarbons, the "goodness of fit" to a horizontal straight line was not appreciably altered (beyond the experimental scatter to be expected from the data) by choice of one physically reasonable value of the dipole moment or another. On the other hand, the calculations

Publication Date: January 1, 1964 | doi: 10.1021/ba-1964-0043.ch004

made from contact angles of more highly polar liquids yielded definite indications for the polar nature of a solid fluorocarbon surface.

(While contact angle data are reproducible when extreme care is taken—e.g., when different laboratories use the same materials and technique—still the values of the adhesion tension, $\gamma_1\cos\theta$, are ordinarily reproducible to a precision of only about ±1 erg per sq. cm. Also, it is evident that the sensitivity of the term, $\gamma_1\cos\theta$, to errors in θ increases in proportion to $\sin\theta$. Since θ increases with increasing γ_1, the uncertainty in the calculated value of γ_{so}, due to experimental errors in θ, increases toward the right in Figures 1 to 5).

For Teflon (Figure 1) computations were made assuming a dipole moment of 1.2 debyes, corresponding to the group moment of a C-F bond [29]. In other words, the quadrupole and other higher orders of moments of the fluorocarbon molecules were considered. Such a model of the surface is physically reasonable, in the first place because the bond dipole must always be directed with the negative pole "outward" from the carbon chain; and in the second place, the crystallinity and spiral structure of the polymer [6, 24] ensure the presence of C-F dipoles in essentially fixed orientations such that the surface will have a net dipole moment. An examination of molecular models leads to the conclusion that it is impossible to attain an exact compensation of dipole fields. In Figure 2, zero dipole moment (which, as just noted, is physically less reasonable) was assumed. Clearly, the choice of $\mu = 1.2$ (Figure 1) leads to a much narrower dispersion in the calculated γ_{so}; in particular, substances such as water, formamide, and $C_2H_2Cl_4$ yield γ_{so} values that are fairly consistent with those obtained with nonpolar liquids, whereas when $\mu = 0$ is employed, water and formamide yield γ_{so}'s that are three to ten times as large.

A similar better consistency of calculated values of γ_{so} was noted when calculations were made employing bond dipole moments for polyhexafluoropropylene, for the perfluorolauric acid monolayer, and for Kel-F, as opposed to calculations made using $\mu = 0$. Since poly-(trifluoromonochloro)ethylene must have a spiral structure with shorter period than that of polytetrafluoroethylene, the reasoning just given regarding the surface polarity of Teflon must hold a fortiori for Kel-F. Polyhexafluoropropylene and a perfluorolauric acid monolayer both have CF_3 groups populating the surface, and so a net surface dipole moment is most certainly to be expected. Resolution of bond-dipole vectors [29] shows that the moment should be approximately 1.2 debyes per molecule.

It should be possible in an extensive and carefully planned study of contact angles of various liquids on a single solid, to examine the fine structure of the liquid-solid interface and of the surface of the bare solid. For example, molecules such as those of a fatty acid, amine, or alcohol can be expected to pack to a considerable extent as parallel chains in the interface, with the methyl groups toward the fluorocarbon. Hence the value of $\mu = 0.4$ debye [29], corresponding to the moment of a CH_3 grouping, should be chosen for such molecules, rather than the actual dipole moment of the molecule as a whole, since the carboxylic acid group, or the amine or alcohol group, can be expected to be oriented toward the interior of the liquid phase. The -OH groups, etc., should form hydrogen bonds to like groups within the liquid, since this would be energetically more favorable, rather than orienting toward the

Publication Date: January 1, 1964 | doi: 10.1021/ba-1964-0043.ch004

C-F dipoles. The calculated γ_{so}'s from data on alcohols, acids, and amines were actually in better agreement with the results obtained from contact angles of nonpolar compounds, when $\mu = 0.4$ was used rather than the actual moments of the molecules. The improvement was by about 3 to 5 ergs in γ_{so}, which is a large enough effect to consider significant, and which qualitatively confirms the expectations just mentioned as to orientation.

Relationship to Other Recent Developments

Method of Fowkes. Fowkes [12, 13] has proposed that "the surface tensions [are] a measure of the attractive forces between surface layers and liquid phase, and that such forces and their contribution to the free energy are additive." From this he concluded that the surface tension of a liquid could be resolved into additive terms–e.g., for water,

$$\gamma_1 = \gamma_1^h + \gamma_1^w \tag{13}$$

where superscript h refers to hydrogen bonding, and w to dispersion. He then proposed that an expression of the form of our Equation 1, with $\Phi = 1$, be applied to each component of the surface tension. For example, for the interface between water and a saturated hydrocarbon,

$$\gamma_{12} = \gamma_1 + \gamma_2 - 2\sqrt{\gamma_1^w \gamma_2} \tag{14}$$

This treatment is in principle quite consistent with ours [18], except for the omission of the term $2(I_1 I_2)^{1/2}/(I_1+I_2)$, which is included in Equation 9. (The importance of the term in the I's, Equation 5, was not discussed [18] until after Fowkes' paper had been published.) Further, this term in the I's is itself an approximation. Pitzer and Donath [7, 26] have discussed the London [25] expression for dispersion energy,

$$A_{11} = \frac{3}{4}\alpha_1^2 I_1$$

$$A_{12} = \frac{3}{4}\alpha_1\alpha_2 \times \frac{2I_1I_2}{I_1 + I_2} \tag{15}$$

They pointed out that I should be replaced by a new energy term, U, which arises in the perturbation treatment of the interaction, corresponding to the fact that more than one electron may be promoted to the continuum. U may be several times as large as I; but except for the simplest atoms, it is not practical at this time to evaluate the U's.

Fowkes' expression (Equation 14) is justified for most molecules because [18] the effective group radii are not very different, and the ionization energies of most common molecules fall in the range of about 9 to 12 e.v. Hence the expression for Φ (Equation 9) leads to values between about 0.97 and 1 for most common nonpolar molecules. However, systems in which one phase is a fluorocarbon constitute an exception. For example, if the ionization energy of a fluorocarbon is

Publication Date: January 1, 1964 | doi: 10.1021/ba-1964-0043.ch004

17.8 e.v. [28] and that of benzene is 9.24 e.v. [10], the calculated value of Φ is 0.92. (This calculation assumes dispersion forces only.)

Fowkes discusses his treatment in another article [11]. But it should be pointed out here that the γ_{so}'s calculated by Equation 3 (or Equation 2 if π_e is appreciable) together with Equation 7, are the specific surface free energies of the solid—e.g.,

$$\gamma_{so} = \gamma_{s(\text{dispersion})} + \gamma_{s(\text{induction})} + \gamma_{s(\text{dipole orientation})} \quad (16)$$

The first term on the right is the quantity which Fowkes' method calculates.

Limitations on Method of Estimating Surface Energies

Entropy Effects. Interfacial orientation such as suggested for the fatty acids, alcohols, and amines (and which would be present with certain other series of compounds also) should lead to a negative contribution to the interfacial entropy, σ_{s1}. The interfacial tension will be greater than in the absence of the orientation, since

$$\gamma_{s1} = \epsilon_{s1} - T\sigma_{s1} \quad (17)$$

A similar orientation will exist in the liquid-vapor interface, with similar incremental effect on γ_1. However, the increases in γ_1 and γ_{s1} will not necessarily be of equal magnitude. Equation 1 does not recognize orientation; so the value of γ_{s1} calculated by Equation 1 will be incorrect because the γ_1 used in Equation 1 is unduly large, and because an increment must be added to the calculated value of γ_{s1} on account of orientational entropy at the solid-liquid interface.

If the excess components of γ_1 and γ_{s1}, due to orientational entropy, are, respectively, δ_1 and δ_{s1}—i.e., excess surface entropy over that corresponding to a "normal" Eötvos constant [17]—Equation 1 becomes

$$\gamma_{s1} - \delta_{s1} = \gamma_{so} + \gamma_1 - \delta_1 + 2\Phi\sqrt{\gamma_{so}(\gamma_1 - \delta_1)} \quad (18)$$

Combining Equation 18 with Young's equation (in the case when $\pi_e = 0$),

$$\gamma_{s1} = \gamma_{so} - \gamma_1\cos\theta \quad (19)$$

$$\gamma_{so} \simeq \frac{\left[\gamma_1(1 + \cos\theta) - \delta_1 + \delta_{s1}\right]^2}{4\Phi^2(\gamma_1 - \delta_1)} \quad (20)$$

No quantitative basis exists at present for determining the value of δ_{s1}, and indeed, only a very rough estimate can be made for δ_1. But it is evident that δ_1 and δ_{s1} should be of about the same magnitude, and hence they will tend to cancel, in Equation 20. As a result, the method for estimating surface energies may not be extremely sensitive to the effect of orientation on surface entropy.

Publication Date: January 1, 1964 | doi: 10.1021/ba-1964-0043.ch004

Errors in Potential Functions. Equation 7 will yield the correct value of Φ only if the potential energy functions making up A_{11}, A_{22}, and A_{12} are correctly stated there. For example, the question about the use of I_1 and I_2 has already been mentioned. If, in addition, types of force other than dispersion, induction, and dipole-dipole orientation make significant contributions to the surface energy, Equation 7 will be in error and the results invalidated to the extent of the other contributions. (The Sinanoglu-Pitzer treatment of dispersion forces, which involves a third-order perturbation treatment of three interacting bodies, has not as yet been put in suitable form for application to complex molecules. Hence this effect was not included in the treatment above or in [18].)

A further limitation is in the fact that the attractive potential term, Equation 6, is in r^{-6}. If the other types of forces obey a law in r^{-n} with $n \neq 6$, then the term in molecular radii (Equation 5) will involve a different power of the r's. In particular, if $n \leq 4$, the quadruple integration employed in deriving Equation 5 breaks down. Such is actually the case for dipoles in fixed orientation, for which the attractive term is

$$E = \frac{-\mu_1\mu_2 \sin\beta}{r^3} \tag{21}$$

where β is the angle between the axes of the dipoles.

Fortunately, for most common molecules at their equilibrium separation, this term makes a contribution to the energy of interaction that is of approximately the same size as that for rotating dipoles,

$$E = \frac{-2(\mu_1\mu_2)^2}{3kTr^6} \tag{22}$$

(This was found to be true, in particular, for the interaction of halogen-carbon dipoles with water [18].) And dipoles outside the first coordination sphere of a given polar molecule are usually not so strongly oriented as to cause Equation 21 to apply to them.

This point was examined at some length [18] for systems of various organic liquids vs. water. The discussion above of the orientation of group dipoles—i.e., of quadrupole and higher order pole effects—constitutes an extension of the earlier discussion [18]. To complete this theoretical treatment, it will be necessary to examine in detail the group-dipole interactions in fixed orientations, in a model for the system where nearest-neighbor interactions are considered separately from the attractions of further-removed molecules.

Summary of Limitations on This Treatment. The calculated values of γ_{so} will represent the true surface energy of the solid, if the following conditions hold:

The liquid does not perturb the solid.

The contact angles employed are true equilibrium angles.

The spreading pressure, π_e, is negligible. (In principle, negative as well as positive values of π_e are possible.)

Errors due to orientational entropy effects, as discussed above, are not important.

Publication Date: January 1, 1964 | doi: 10.1021/ba-1964-0043.ch004

The potential functions that determine the attractive molecular interactions are known, and correctly stated (see above).

Second-nearest-neighbor interactions either follow the same laws as the nearest-neighbor interaction or are negligible.

Errors due to concentration gradients (both at the interface and at the surfaces of the separate condensed phases) are negligible or else cancel.

The solid surface is homogeneous, in that defects, dislocations, edges, corners, etc., do not make important contributions to the surface energy. (This limitation also applies to the calculation of the dispersion contribution to the surface energy.)

Most, and hopefully all, of these limitations are of such kind that experimental examination of their importance will be possible. Results previously reported for liquid-liquid interfaces [18] indicate that these limitations may lead to an over-all error as small as 1 or 2 ergs per sq. cm.

Publication Date: January 1, 1964 | doi: 10.1021/ba-1964-0043.ch004

Acknowledgment

Thanks are expressed to Carl Hubbard for assistance with the computations, and to M. K. Bernett for making available contact angle data on polyhexafluoropropylene.

Literature Cited

(1) Bailey, G. L. J., Watkins, H. C., Proc. Roy. Soc. (London) 63B, 350 (1950).
(2) Bartell, L. S., Ruch, R. J., J. Chem. Phys. 60, 1231 (1956).
(3) Ibid., 63, 1045 (1959).
(4) Bernett, M. K., U.S. Naval Research Laboratory, personal communication.
(5) Bernett, M. K., Zisman, W. A., J. Phys. Chem. 65, 2266 (1961).
(6) Bunn, C. W., Howells, E R., Nature 174, 549 (1954).
(7) Donath, W. E., Ph. D. thesis, University of California, Berkeley, Calif., 1958.
(8) Ellison, A. H., Fox, H. W., Zisman, W. A., J. Phys. Chem. 57, 622 (1953).
(9) Ellison, A. H., Zisman, W. A., Ibid., 58, 260 (1954).
(10) Field, F. H., Franklin, J. L., "Electron Impact Phenomena," Academic Press, New York, 1957.
(11) Fowkes, F. W., Advan. Chem. Ser., No. 43, 99 (1963).
(12) Fowkes, F. W., Division of Colloid and Surface Chemistry, 141st Meeting, ACS, Washington, D.C., March 1962.
(13) Fowkes, F. W., J. Phys. Chem. 66, 382 (1962).
(14) Fox, H. W., Zisman, W. A., J. Colloid Sci. 7, 109 (1952).
(15) Ibid., p. 428.
(16) Girifalco, L. A., Good, R. J., J. Phys. Chem. 61, 904 (1957).
(17) Good, R. J., Ibid., 61, 810 (1957).
(18) Good, R. J., 142nd Meeting, American Chemical Society, Atlantic City, N. J., September 1962.
(19) Good, R. J., unpublished results.
(20) Good, R. J., Girifalco, L. A., J. Phys. Chem. 64, 561 (1960).
(21) Hare, E. F., Shafrin, E. G., Zisman, W. A., Ibid., 58, 236 (1954).
(22) Hildebrand, J. H., Scott, R. L., "Regular Solutions," Prentice-Hall, Englewood Cliffs, N.J., 1962.
(23) Hildebrand, J. H., Scott, R. L., "Solubility of Non-Electrolytes," 3rd ed., Reinhold, New York, 1950.
(24) Iwasaki, M., J. Polymer Sci. A1, 1099 (1963).
(25) London, F., Trans. Faraday Soc. 33, 8 (1937).
(26) Pitzer, K. S., Advan. Chem. Phys. 2, 59-84 (1959).

(27) Pitzer, K. S., Sinanoglu, O., J. Chem. Phys. **32**, 1279 (1950).
(28) Reed, T. M., III, J. Phys. Chem. **59**, 428 (1955).
(29) Smyth, C. P., "Dielectric Behavior and Structure," McGraw-Hill, New York, 1955.
(30) Wesson, L. G., "Tables of Electric Dipole Moments," Technology Press, Mass. Institute of Technology, Cambridge, Mass., 1948.
(31) Young, T., Trans. Roy. Soc. (London) **95**, 65 (1805).

Received April 3, 1963. Work partly supported by the U.S. Atomic Energy Commission under Contract AT(04-3)-297.

5

Wettability by Heats of Immersion

A. C. ZETTLEMOYER AND J. J. CHESSICK

Surface Chemistry Laboratory
Lehigh University, Bethlehem, Pa.

Publication Date: January 1, 1964 | doi: 10.1021/ba-1964-0043.ch005

Heats of immersion are effective in rating the average polarity or field strength of polar surfaces, and in assaying different batches of the same type of fine powders, whether pigment, catalyst, or filler. The technique of following heats of immersion as a function of precoverage provides one of the simplest ways of ascertaining the heterogeneity of surfaces; it is useful whether the heterogeneities take up a very minor or large fractions of the surface area. The wetting of surfactants for low energy surfaces can be readily rated by heats of immersion; the change with surface concentration as given by tracer measurements and the effect of added counterions have been followed. Differences between heats of immersion of Graphon into hexanoic acid and into the sodium salt yield directly estimates of heats of formation of the double layer at the solid-solution interface.

This commentary on the current status of research on heats of immersion begins where our review written in 1958 concludes [6]. The classification of heats of immersion of solids into liquids as a function of precoverage is expanded to include two new types of curves. Several difficulties in heat of immersion research are discussed. Then, current applications of heats of immersion to determine the average polarity of solid surfaces, heterogeneities on solid surfaces, wetting by surfactants, hydrophilicity of solid surfaces, and thermodynamics of the specific interaction of molecules from solution onto solid surfaces are described.

Heats of immersion can provide information on energies of interaction for systems in cases of spreading wetting or zero contact angles. The approach is particularly suitable for mapping the energetics of surfaces which, of course, are invariably somewhat heterogeneous. Even if the liquid has a very low vapor pressure, and consequently low equilibrium pressures to be employed in preconditioning to follow heats of immersion with coverage, ample time can be allowed to reach the required state; the bulbs containing the solid are sealed off and taken

In Contact Angle, Wettability, and Adhesion; Fowkes, F.;
Advances in Chemistry; American Chemical Society: Washington, DC, 1964.

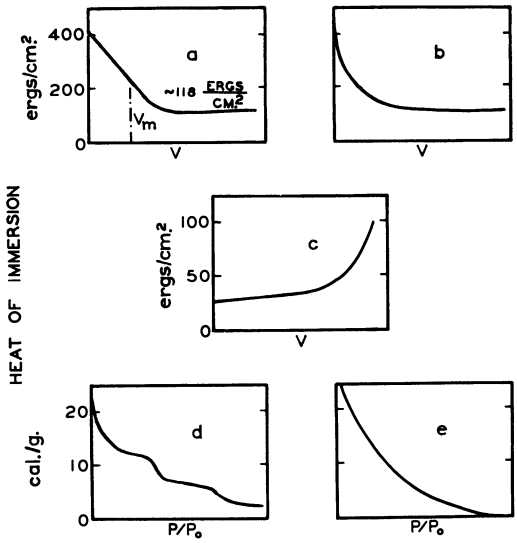

Figure 1. Classification of heat of immersion curves as a function of preadsorbed wetting liquid

a. Essentially homogeneous surface. Water on chrysotile asbestos [40]
b. Heterogeneous surface. Water on anatase titanium dioxide. Classic case given by Harkins [11]
c. Low-energy surface possessing isolated polar sites. Water on Graphon [31] or some polymers
d. Swelling of stratified mineral. Polar adsorbate such as water absorbing at rather definite pressures. Water on and in Wyoming bentonite [39]
e. Gradual filling of pores, leaving no appreciable area and so a negligible heat effect at high relative pressures. Methanol on charcoal [21]. Benzene on graphitized black [19]

Publication Date: January 1, 1964 | doi: 10.1021/ba-1964-0043.ch005

to the calorimeter only after the absorbate has been distributed to the appropriate sites. Calorimeters can give precise results only for powders, except for the most sensitive types which can handle coarse materials measuring only a few hundredths of a square meter per gram.

Classification

The previous classification [6] is repeated in Figure 1.

A sixth type of heat of immersion curve can be predicted from the isosteric heats determined by Graham [9] for carbon tetrafluoride and other gases on polytetrafluorethylene. The prediction can readily be made from the equation:

$$\frac{h_{i(SL)} - h_{i(SfL)}}{\Gamma} = \int_0^{\Gamma} q_{st}\, d\Gamma + \Delta H_L \qquad (1)$$

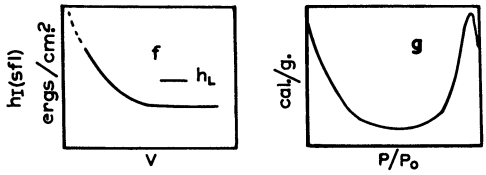

Figure 2. New types of heat of immersion curves

f. Weak adsorption such as CF_4 on polytetrafluoroethylene
g. Swelling of aggregates at high relative pressures

where $h_{i\,(SL)}$ and $h_{i\,(SfL)}$ refer to the heats liberated in ergs per square centimeter on immersion of the bare and film-covered solid, respectively, into the liquid, Γ is the surface coverage in moles per square centimeter, q_{st} is the isosteric heat of adsorption (from two temperature isotherms), and ΔH_L is the heat of liquefaction per mole. Heterogeneities plus low energies of adsorption yield a heat of immersion curve which starts above the heat of liquefaction but then falls below, as in Figure 2,f. Such a curve has not yet been directly measured.

A seventh type as predicted from Kiselev's measurements of gas-solid interactions [15] is depicted in Figure 2,g. Here, the commonly found decrease of heat of immersion with coverage is followed by a rising portion, which is believed to be due to the expansion of aggregates and possibly consequent energy release.

Problems in Heat of Immersion Technique

A number of difficulties in measurement and interpretation of heats of immersion have come to the fore in recent years. These problems are sometimes pertinent to the other techniques as well. They must be taken into account if valid results are to be obtained.

Polar solids collect organic contaminants from the air merely on exposure in the laboratory. They may also become contaminated during manufacture, or by stopcock grease. It is sometimes exceedingly difficult to solve this problem. The organic impurities can be eliminated from titanium dioxide, for example, by heating in a vacuum at 450°C. [13]. A liquid nitrogen trap must be inserted between the final stopcock and the sample being outgassed. If the solid is washed with an organic solvent or series of solvents to remove contaminants, the surface may be left even dirtier than at the start. This situation is particularly prevalent in the case of oxides.

The removal of impurities by outgassing may include reduction of the surface. Thus, oxygen deficiencies are created in the surface of rutile TiO_2 by outgassing at 450° in a vacuum; the reduction is indicated very sensitively by the gray color produced. When oxygen is returned to the surface by admitting it to the hot sample, the color returns to white. Oxygen is much less readily removed by outgassing if organic contaminants are kept from the surface. The heat of immersion of the deficient surface was about 50 ergs per square centimeter greater than for the stoichiometric surface in the case of one TiO_2 sample studied [13]. Both problems of surface contamination and deficiencies must be attacked if proper wetting results are to be obtained.

A prevalent problem is interpretation of the interaction occurring in the calorimeter as physical or chemical. Coupled with this problem

Publication Date: January 1, 1964 | doi: 10.1021/ba-1964-0043.ch005

is the omnipresent water which tenaciously holds to high-energy solids. Physical adsorption is not all that can occur during the wetting process. A particular difficulty arises if heats of immersion obtained after activation at several temperatures are compared. After low temperature activation, the interaction may be entirely physical, whereas after high temperature activation some of the interaction may be chemical. Such effects have been well explored in the case of silicas [13, 30] interacting with water, and oxides such as titania [15] and alumina [25, 26, 27] interacting with water or with organic molecules such as alcohols. Yet, the complication of chemisorption as higher and higher activation temperatures are employed is not always quantitatively considered [25, 26, 27].

A plea should be made that other techniques should be brought to bear on the problem whenever any unknown system is investigated. A well established heat of immersion value in itself is not sufficient. As indicated by the classification, heat of immersion followed as a function of precoverage reveals far more about the wetting characteristics of the system. But very different studies are also helpful. For example, butyl chloride was earlier believed to stand upright in close-packed array on rutile, as does the hydroxide or amine [35]. Recent adsorption isotherms, however, indicate that it lies flat [13]. Infrared spectroscopy is a powerful tool, when the powder is sufficiently fine, in determining the number per unit area and the nature of the hydroxyls on silicas [12, 16, 20] and alumina [17]. Water vapor isotherms locate the number of hydrophilic sites on an otherwise hydrophobic surface, such as presented by graphitized blacks [32], flame-hydrolyzed silicas [35], or silver halides [10, 38], and this is a useful technique even for rather low area solids. In addition, as determined by Kiselev *et al.* [1], ground quartz agglomerated in such a fashion that the ground samples yielded much lower nitrogen areas than water areas as estimated from the isotherms. In this case, the heats of immersion per unit area (based on nitrogen) would be higher than if the total area available to the water molecules was used.

The large decrease in heats of immersion of the same oxide in water or hexane as a function of increase in surface area (decrease in particle size), as reported by Wade and Hackerman [25, 26, 27], cannot be explained by Kiselev's finding. In fact, the trend is opposite in the case of the silicas, aluminas, and titanias which they investigated. It appears, instead, that the less amorphous, coarser granules orient several layers of adsorbate. For silica-water systems, for example, the difference between low and high area silicas can be 500 ergs per square centimeter or more. Such a difference amounts to 7 kcal. per mole, if all of the extra energy is ascribed to the first adsorbed layer. Contrariwise, this additional interaction energy may be distributed over several layers. The suggestion is made that an icelike structure is developed over the crystalline faces of the coarse particles. NMR might reveal such structure; Pethica [18] has found a surprising amount of icelike structure around micelles using this tool.

Application of Heats of Immersion

The average polarity of solid surfaces can be estimated from heats of immersion into selected liquids, usually n-butyl derivatives possessing

Publication Date: January 1, 1964 | doi: 10.1021/ba-1964-0043.ch005

a single functional group. From the slope of the line of heat of immersion (or better, heats of adsorption obtained by substracting the enthalpy of the liquids, h_L) *vs.* dipole moment, the surface force field, F, emanating from the solid can be estimated. The first such curve [4] obtained for a rutile is given in Figure 3. Additional values reported by Zettlemoyer, Chessick, and Hollabaugh [35], by Romo [22], and by Dear, Eley, and Johnson [8] are listed in Table I.

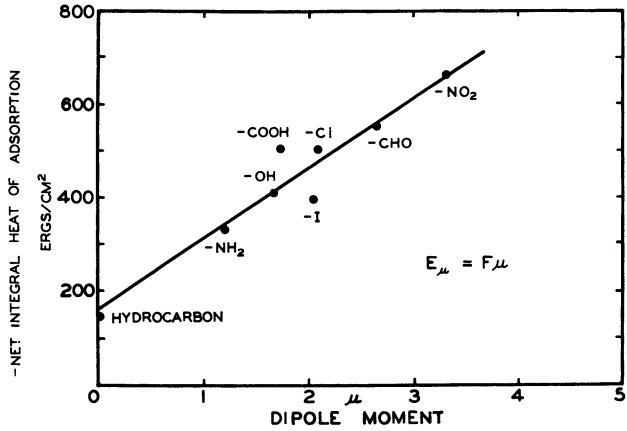

Figure 3. Determination of polarity of solid surface (rutile)

Chemisorption must be avoided. Close-packed, perpendicular array and same distance from dipole to surface assumed. Chloride lies flat on this substrate [13]

Table I. Electrostatic Field Strengths, F, and Dispersion Energies, E_W

Powder	BET Area, Sq. M./G.	F, E.S.U./Sq.Cm. $\times 10^{-5}$	E_W, Ergs/Sq.Cm.	Ref.
Rutile (bare?)	7.7	2.7	145	[3]
(bare)	6.4	2.0	125	[22]
(Al_2O_3-SiO_2 coated)	11.2	3.2	135	[22]
CaF_2	12.7	2.5	105	[35]
SiO_2 (Aerosil)	120	1.1	75	[35]
Al_2O_3 (40 A. on Al)	0.4	1.9	335	[8]
Graphon	95	0	80	[3]
Teflon	9.0	0	25	[5]
Iron blue (high strength)	87	2.2	105	[33]
Chrome yellow (med.)	6.7	1.9	105	[33]
Barium lithol (str. med. tone)	41	(1.7)	105	[33]
Carbon black (short channel)	120	0.7	105	[33]

Publication Date: January 1, 1964 | doi: 10.1021/ba-1964-0043.ch005

These results are not discussed in detail here.

The Aerosil silica was 75% hydrophobic, as indicated by $100 \times \Sigma_{H_2O}/\Sigma_{N_2}$; thus, surface regions of very different polarity are averaged in the value of 1.1×10^5 e.s.u. per sq. cm. The graphitic surface of Graphon displays no metallic character toward the dipoles employed; graphite had earlier been classified with metals as to adsorption characteristics [2]. The dispersion energy for the alumina on aluminum is usually large, as discussed by Eley [8]. Our values for rutile are probably less reliable than Romo's, because it has recently been concluded that a truly bare rutile surface is exceedingly difficult to prepare. A most important application of the F values will doubtless be to compare different samples of the same material and to relate them to other properties such as flocculation tendencies in organic media. It would also be interesting to compare F values for the different surface area samples studied by Wade and Hackerman. Finally, very little application and analysis of the E_W values have yet been made; they were calculated by subtracting 25 ergs per sq. cm. for the enthalpy of the hydrocarbon from the intercepts.

Heterogeneities in Site Energies

These heterogeneities can be assayed by exploring the variation in heat of immersion with coverage. For example, the acid sites on cracking catalysts can be explored by following the heat of immersion into liquid butylamine as a function of precoverage with butylamine from the vapor state. Rather, the reverse is done and the powder is first saturated with the vapor, so that all the active sites are covered after pumping at 25°C. Typically, about 50% of the surface retains butylamine. To prepare successive samples for heat of immersion determinations, increasing temperature are employed for outgassing. The derivative of the heat of immersion curve provides a differential heat curve, and the differential of the latter curve yields, when inverted, an approximate site energy distribution [34]:

$$\frac{dN_A}{d(\Delta H_d)} = g(\epsilon) \qquad (2)$$

Two such curves are plotted in Figure 4. The catalyst with the larger number of low energy sites was also the most active in cracking. The original heat of immersion curves, rather than these derived curves, reflect the site energy distributions. In an interesting sidelight, it was found that the differential heat curve for a kaolin catalyst [34] contained a maximum at 0.4 θ. This maximum was suspected to be caused by lateral interactions, even though $\theta = 1$ for butylamine corresponded to 50% coverage. To explore this possibility, sterically hindered diethylamine and pyridine were employed as adsorbates. Only about 40% coverage was retained in these cases, suggesting strongly that the acid sites were close neighbors and so occurred in patches.

Wetting Ability of Surfactants

The wetting ability of surfactants for low energy surfaces shows great promise and has only begun to be explored [20, 24, 36, 37]. Graphon

Publication Date: January 1, 1964 | doi: 10.1021/ba-1964-0043.ch005

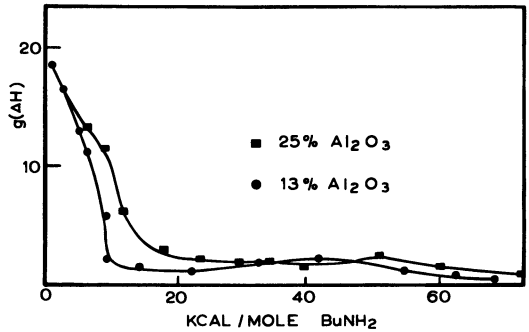

Figure 4. Site energy distribution from heats of immersion into n-butylamine as a function of precoverage

25% Al_2O_3 catalyst showed greater activity

has been employed as the powder to be wetted, because it presents a large and uniform surface. Measurements were first made on a series of surfactants to examine the utility of the method. Then, sodium dodecyl sulfate (NaDS) and sodium dodecylbenzene sulfonate (NaDBS) were studied in detail; the amounts adsorbed were also monitored as a function of concentration. The NaDS adopted two preferred packings, the closer one occurring at higher concentrations or when salt was added. When the heats of immersion were put on a molar basis, the values in Table II were calculated. Heats of dissolution were negligible. The lower energy value obtained at the closer packing apparently reflects repulsion between the head groups.

Table II. Surfactant Heats of Adsorption on Graphon

	Area per Anion, Sq. A.	$-\Delta H_W$, Kcal./Mole
NaDS	37	7.6
	67	9.5
NaDBS	48	8.8

If calcium is added to the solution, an even closer packing results. Trace calcium had a large effect on either the heats or the packing. Indeed, the Graphon flocculated markedly even at a few parts per million. To avoid traces of polyvalent ions, an all-plastic calorimeter was developed, as depicted in Figure 5.

Hydrophilic Nature of Surfaces

The hydrophilic nature of surfaces deserves separate attention, if only because water is omnipresent. Except for silica surfaces, little is yet known about the precise nature of its interaction with solids. Figure 1,a, is exemplified by the interaction of water with hydrophilic asbestos [40]; the heat of immersion falls in equal increments, indicating

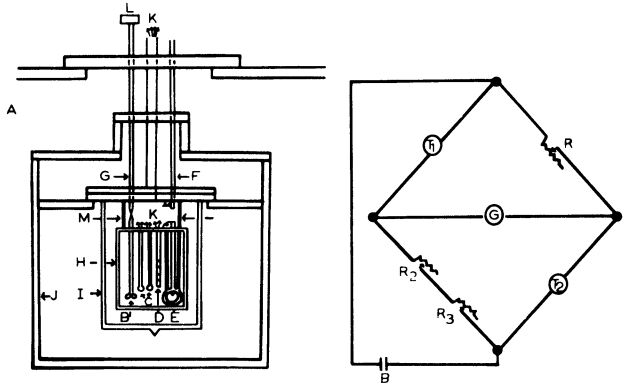

Figure 5. Plastic calorimeter for measuring heats of immersion of low-energy surfaces in surfactant solutions

Multivalent ions avoided
Sensitivity. 0.01 cal. ± 3%, with electronic galvanometer

a homogeneous surface (for water), to the value of 118.5 ergs per sq. cm., the enthalpy of liquid water. Figure 1,c, typifies an essentially hydrophobic surface possessing a few hydrophilic sites; in the case of Graphon, about 1/1500 of the nitrogen area accepts water and the coverage curve rises from about 32 to 37 ergs per sq. cm. when equilibrated at 0.95 relative pressure before immersion [32]. Water interacts, in this case, more energetically with the precoated surface; however, the water is adsorbed in isolated patches. Polar sites provided by surfactants and the like on polymer and essentially hydrophobic organic coatings will interact with water in a similar manner. This interaction may be the precursor to undesired attack of ambients on surfaces, or it may be desired, as with cloud nucleants such as silver iodide [16, 32, 38]. Curiously, this solid is largely hydrophobic (75%), in contrast to the hydrophilic character previously assigned by cloud physicists [10, 32, 38].

The nature of the interactions of water with oxides or hydroxyl groups on oxides remains largely unsettled. In the case of titania, it is not yet certain whether hydroxyls exist on the surface (Ti-OH in solution is unknown). An intriguing break in the curve of heat of immersion *vs.* activation temperature, recently found, is depicted in Figure 6. It occurs between 120° and 130°C., and its magnitude is about 10%. The strange finding is that alumina-coated titania behaves in the same way; and so do other oxide-coated titanias. Other techniques are needed to help to decide whether the 120° to 130° range under vacuum separates physically adsorbed molecules from the surface and leaves only chemisorbed molecules behind. When such a finding is made for each material, it suggests an experimental artifact; none has yet been found. For example, no appreciable change in heat of bulb breaking was discovered in the 120° to 130° range.

Some attempt has been made recently to separate the total heat of immersion due to changes in the adsorbent and that due to changes in

Publication Date: January 1, 1964 | doi: 10.1021/ba-1964-0043.ch005

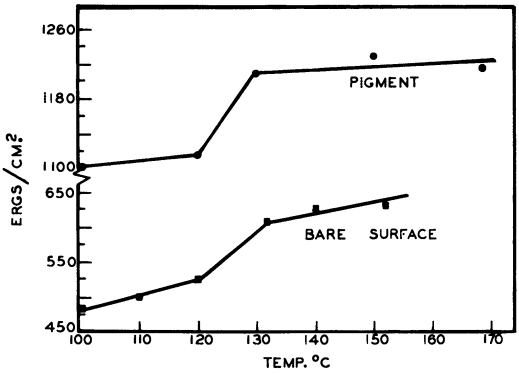

Figure 6. Heat of immersion of rutile as a function of activation temperature

Break found for bare surface as well as oxide-coated rutiles.
Upper curve. Alumina-coated rutile

the adsorbate for the $BaSO_4/H_2O$ system [7, 29]. The free energy and entropy changes in both were obtained.

Solution Adsorption Studies

Solution adsorption studies also deserve to be set apart. A start was made in 1956 by following 1-butanol adsorption out of water onto Graphon by heat of immersion measurements [31]. A model of preferential adsorption of the butanol, plus the measured adsorption isotherm and measured heat effects due to wetting of the adsorbed film at various pertinent concentrations, allowed the heats of immersion to be calculated. Interaction between molecules in the adsorbed film were taken to be the same as in the bulk solution. The calculated values were in excellent agreement with the experimental heats of immersion, as illustrated in Figure 7. No further studies of this kind have been performed on other functional groups, different chain lengths, or other molecular structures.

An incremental analysis of the contributions of various groups can be made by the heat of immersion technique. Heat of interaction of adsorbed layers with the equilibrium solutions can be directly determined by removing the equilibrated solid from the solution, drying it, and then re-immersing it into the equilibrium solution in the calorimeter. Lateral interactions can be determined from measurements at low and high coverages.

Heats of immersion have been useful in elucidating the adsorption of heptyl derivatives out of paraffin oil onto a polar silica [28]. It was established that heptyl chloride is not adsorbed from solution in this system, and that the other polar derivatives, such as the alcohol and amine, form close-packed monolayers.

Heats of formation of double layers are being determined [14] by comparing the heats of immersion of Graphon in solutions of fatty acids at high (double layer forms) and low pH (un-ionized).

Publication Date: January 1, 1964 | doi: 10.1021/ba-1964-0043.ch005

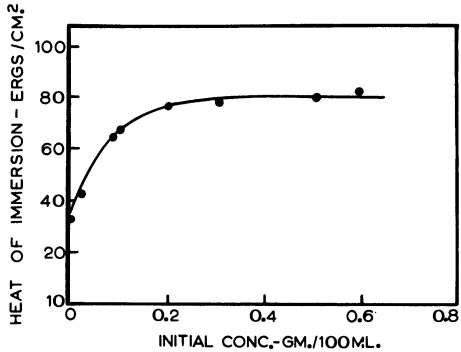

Figure 7. Heats of immersion of Graphon into 1-butanol in water solutions

● Experimental points
—— Calculated on basis of simple model

Rovinskaya and Koganovskiĭ [23] have recently made an incremental analysis of the effects of functional groups on the free energy of adsorption of benzene derivatives from water solutions on charcoal. This effort suffers from the use of an inhomogeneous and porous substrate. Furthermore, wetting of the adsorbed films and lateral interactions were not accounted for. By measuring the required heat effects at several temperatures, using a more satisfactory adsorbent, the entire thermodynamic picture could be unfolded.

Summary

Applications of the heat of immersion technique to determinations of polarity of surfaces, site heterogeneities, wetting of surfactants, hydrophilicity, and the interaction of specific groups from solution with solids are on the increase. The technique is certain to provide new and valuable information about the solid-liquid interface in the near future.

Literature Cited

(1) Aleksandrova, G. I., Kiselev, V. F., Maiorova, M. P., Colloid J. (USSR) **24**, 3 (1962); J. Phys. Chem. (USSR), No. 9, 2031 (1961); No. 10, 2234 (1961).
(2) de Boer, J. H., Advan. Catalysis 8, 102 (1956).
(3) Chessick, J. J., J. Phys. Chem. **66**, 762 (1962).
(4) Chessick, J. J., Healey, F. H., Zettlemoyer, A. C., Can. J. Chem. **33**, 251 (1955).
(5) Chessick, J. J., Healey, F. H., Zettlemoyer, A. C., J. Phys. Chem. 60, 1345 (1956).
(6) Chessick, J. J., Zettlemoyer, A. C., Advan. Catalysis **11**, 263 (1959).
(7) Copeland, L. E., Yound, T. F., Advan. Chem. Ser., No. 33, 348 (1961).
(8) Dear, D. J. A., Eley, D. D., Johnson, B. C., Trans. Faraday Soc. **59**, 713 (1963).

(9) Graham, D., J. Phys. Chem. 66, 1815 (1962)
(10) Hall, P. G., Tompkins, F. C., Trans. Faraday Soc. 58, 1734 (1962).
(11) Harkins, W. D., Jura, G., "Physical Chemistry of Surface Films," p. 256, Reinhold, New York, 1952.
(12) Hockey, J. A., Pethica, B. A., Trans. Faraday Soc. 57, 2247 (1961).
(13) Hollabaugh, C. M., Chessick, J. J., J. Phys. Chem. 65, 109 (1961).
(14) Iyer, S.R., Zettlemoyer, A.C., Narayan, K.S., National Colloid Symposium, Ottawa, Canada, June 1963; J. Phys. Chem. 67, 2112 (1963).
(15) Kiselev, A. V., private communication.
(16) Kiselev, A. V., Lygin, V. I., Kolloidn. Zh. 22, No. 4 (1960).
(17) Perri, J. B., Hannan, R. B., J. Phys. Chem. 69, 1526 (1960).
(18) Pethica, B. A., private communication.
(19) Pierce, W. C., Mooi, J., Harris, R. E., J. Phys. Chem. 62, 655 (1958).
(20) "Proceedings of Second International Congress on Surface Activity," Vol. 2, p. 204, Academic Press, New York, 1957.
(21) Razouk, R. I., J. Phys. Chem. 45, 190 (1941).
(22) Romo, L. A., J. Colloid Sci. 16, 139 (1961).
(23) Rovinskaya, T. M., Koganovskiĭ, A. M., Kollidn. Zh. 24, 67—74 (1962); 23, No. 5 (1961).
(24) Skewis, J. D., Zettlemoyer, A. C., "Proceedings of 3rd International Congress on Surface Activity," Vol. II, p. 401, 1960.
(25) Wade, W.H., Cole, H.D., Meyer, D.E., Hackerman, N., Advan. Chem. Ser., No. 33, 35 (1961).
(26) Wade, W. H., Hackerman, N., Ibid., No. 43, 222 (1963).
(27) Wade, W. H., Hackerman, N., J. Phys. Chem. 66, 1823 (1962).
(28) Wightman, J. P., Chessick, J. J., Ibid., 66, 1217 (1962).
(29) Wu, Y. C., Copeland, L. E., Advan. Chem. Ser., No. 33, 357 (1961).
(30) Young, G. J., J. Colloid Sci. 13, 67 (1958).
(31) Young, G.J., Chessick, J.J., Healey, F.H., J. Phys. Chem. 60, 394 (1956).
(32) Young, G. J., Chessick, J. J., Healey, V. H., Zettlemoyer, A. C., Ibid., 58, 313 (1954).
(33) Zettlemoyer, A. C., Offic. Digest Federation Paint Varnish Prod. Clubs 28, 1238 (1957).
(34) Zettlemoyer, A. C., Chessick, J. J., J. Phys. Chem. 64, 1131 (1960).
(35) Zettlemoyer, A.C., Chessick, J.J., Hollabaugh, C.M., Ibid., 62, 489 (1958).
(36) Zettlemoyer, A. C., Schneider, C. H., Skewis, J. D., "Proceedings of 2nd International Congress on Surface Activity," Vol. III, p. 472, Academic Press, New York, 1957.
(37) Zettlemoyer, A. C., Skewis, J. D., Chessick, J. J., J. Am. Oil Chemists' Soc. 39, 280 (1962).
(38) Zettlemoyer, A. C., Tcheurekdjian, N., Chessick, J. J., Nature 192, 653 (1961).
(39) Zettlemoyer, A. C., Young, G. J., Chessick, J. J., J. Phys. Chem. 59, 962 (1955).
(40) Zettlemoyer, A. C., Young, G. J., Chessick, J. J., Healey, F. H., Ibid., 57, 649 (1953).

Received May 6, 1963.

6

Dispersion Force Contributions to Surface and Interfacial Tensions, Contact Angles, and Heats of Immersion

FREDERICK M. FOWKES

Sprague Electric Co.
North Adams, Mass.

Publication Date: January 1, 1964 | doi: 10.1021/ba-1964-0043.ch006

Dispersion forces account for interactions between liquid or solid saturated hydrocarbons and other substances (polar, metallic, etc.), as measured by interfacial tensions and contact angles. Consequently the magnitude of the dispersion force contribution to surface energy, γ^d, in many liquids and solids can be determined by measuring interfacial tension and contact angles, using saturated hydrocarbons as the primary reference phase. Free energies and heats of adsorption of gases on solids, as measured from adsorption isotherms and heats of immersion, can be used to determine γ_S^d for high energy solids. Values for graphite agree well with those determined from contact angles. The intermolecular forces in fluorocarbons (solid and liquid) consist of dispersion forces and some special force which functions between fluorocarbons but not between fluorocarbons and hydrocarbons. Contact angle measurements on low energy solids can be used to determine γ^d values for polar organic molecules; in many polar liquids the intermolecular attractions are essentially due to dispersion forces.

Surface tensions, interfacial tensions, and contact angles can be used as laboratory tools for the evaluation of the various intermolecular forces that determine cohesion in a single phase or adhesion between two dissimilar materials at an interface. By the use of these tools, considerable information about the magnitude of various intermolecular forces may become available. Basic understanding of means to determine interfacial forces has sprung from the principle of additivity of intermolecular forces at surfaces and interfaces [4, 6].

In Contact Angle, Wettability, and Adhesion; Fowkes, F.;
Advances in Chemistry; American Chemical Society: Washington, DC, 1964.

Additivity of Intermolecular Forces at Interfaces

Intermolecular forces in saturated hydrocarbons are practically entirely due to the London dispersion forces. These forces are the result of the interaction of fluctuating electric dipoles with the induced dipoles; they contribute to the cohesion in all substances, but their magnitude depends on the type of material and its density. Many substances have other intermolecular forces in addition to the dispersion forces. In the case of mercury, the interatomic forces involve the dispersion forces and the metallic bond; in the case of water, they involve dispersion forces and dipole interactions (mainly hydrogen bonds). Since the dispersion forces are not appreciably influenced by other intermolecular forces, one can assume dispersion forces and other intermolecular forces generally to be additive. Thus, in the case of the surface tension of water, the surface tension can be considered the sum of a contribution resulting from dispersion forces, γ^d, and a contribution resulting from the dipole interactions, mainly hydrogen bonds, γ^h:

$$\gamma_{H_2O} = \gamma_{H_2O}^{d} + \gamma_{H_2O}^{h}$$

Similarly, in the case of mercury:

$$\gamma_{Hg} = \gamma_{Hg}^{d} + \gamma_{Hg}^{m}$$

(The electrons involved in the dispersion interactions of metals are not the conduction electrons.)

Since interactions in saturated hydrocarbons involve only dispersion forces and these materials interact with other materials almost exclusively by dispersion force interactions, these become good primary standards for determining the magnitude of γ^d contributions in more complex liquids and solids.

Liquid-Liquid Interfaces

Interfacial regions actually have a greater depth than one molecular layer in each phase, but since nearly all of the interfacial characteristics are confined to the first layer, these regions are referred to as monolayers. Although surface and interfacial tensions are discussed, these terms may be replaced by surface and interfacial free energies without affecting the argument or equations.

At an interface between a hydrocarbon and an immiscible liquid, the interface is composed of two monolayers, as indicated in Figure 1. At the interface, the adjacent layers of dissimilar molecules are in a different force field than the bulk liquid, and consequently, the molecules or atoms in these layers have a different pressure, intermolecular spacing, and chemical potential [5]. If the molecules in one of these monolayers are less strongly attracted by the adjacent phase than by its bulk liquid, the molecules in the interfacial layer have an increased intermolecular distance and are in tension. However, if the attraction by the adjacent phase is greater than that of the bulk liquid, the molecules of the interfacial monolayer have a shorter intermolecular distance and are under a two-dimensional pressure. The measured tension of the interface is always the sum of the tensions in the two interfacial

Publication Date: January 1, 1964 | doi: 10.1021/ba-1964-0043.ch006

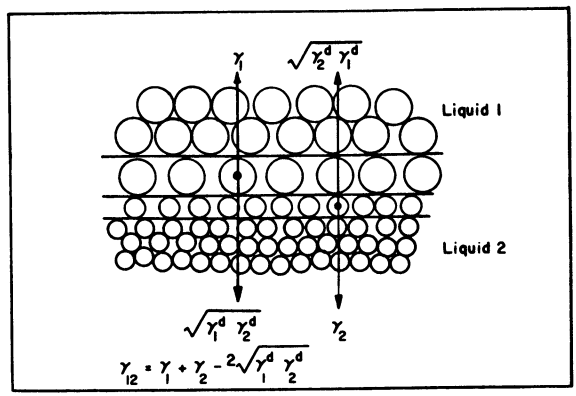

Figure 1. Diagram of two monolayers at liquid-liquid interface in which tension resides

monolayers. In the case illustrated in Figure 1, we have a situation similar to cetane on water. The cetane molecules are less strongly attracted by water than by other cetane molecules and consequently the intermolecular spacing in the interfacial phase is greater and a tension exists in this layer. (The arrows in Figure 1 indicate the direction of attraction of adjacent bulk liquids on the surface region. The resulting tensions or pressures are added as scalar quantities.) Similarly, the interfacial layer of water molecules is less strongly attracted by cetane than by water, the intermolecular distance is greater, and a tension exists in this layer also. The interfacial tension is the sum of the tensions in the two monolayers. In the case of a mercury-cetane interface, a somewhat different situation exists. Here, although the layer of mercury atoms next to cetane has an increased interatomic distance and is under tension, the layer of cetane molecules next to the mercury is more strongly attracted by mercury than by cetane; this results in a decreased intermolecular distance and a two-dimensional pressure. In this case, the interfacial tension is the sum of the tension in the mercury layer minus the two-dimensional pressure in the cetane layer.

The magnitude of the interaction of dispersion forces between two phases may be predicted from the values of the dispersion force contribution to the surface tensions of the two liquids (γ_1^d and γ_2^d).

The surface monolayer of liquid 1 has a tension γ_1 resulting from the unopposed attraction of the bulk liquid. An interfacial monolayer of liquid 1 is attracted by its bulk liquid in an identical manner, but this attraction is opposed by the attraction of liquid 2. The result is a decrease of tension in the interfacial monolayer of liquid 1, and the amount of this decrease is some average of the tensions representing the interacting intermolecular forces. The most obvious average to use is the geometric mean of Berthelot, which has been used so successfully for predicting intermolecular energy in solutions [17]. When the interacting forces are entirely dispersion forces (such as between saturated hydrocarbons and water or mercury), then the decrease in tension in the interfacial monolayer of liquid 1 resulting from the presence of liquid 2 is $\sqrt{\gamma_1^d \gamma_2^d}$. Consequently

Publication Date: January 1, 1964 | doi: 10.1021/ba-1964-0043.ch006

the tension in the interfacial monolayer of liquid 1 is $\gamma_1 - \sqrt{\gamma_1^d \gamma_2^d}$, and in the interfacial monolayer of liquid 2 is $\gamma_2 - \sqrt{\gamma_1^d \gamma_2^d}$, which leads to the equation:

$$\gamma_{12} = \gamma_1 + \gamma_2 - 2\sqrt{\gamma_1^d \gamma_2^d} \quad (1)$$

This equation is somewhat similar to that of Girifalco and Good [11], except that these authors used a parameter Φ in the last term ($-2\Phi\sqrt{\gamma_1 \gamma_2}$) and did not distinguish between surface tensions resulting from various types of intermolecular forces. The values of Φ were about 0.5 for water-hydrocarbon interfaces. The Berthelot relation in Equation 1 is not exact, as can be shown by the London pair potentials, but is seldom in error by more than 2%, and the geometric mean is applied to only the interacting contributions to the surface tension.

Application of the above equation to the experimental values of γ_{12} for eight saturated hydrocarbons (where $\gamma_2^d = \gamma$) *vs.* water leads to $\gamma_{H_2O}^d = 21.8 \pm 0.7$ dynes per cm. at 20°C. [7]. Similarly, with mercury *vs.* 10 hydrocarbons (including aromatics), $\gamma_{Hg}^d = 200 \pm 7$ dynes per cm. at 20°C. [7]. This is an example of how hydrocarbons can be used as primary standards for determining values of γ^d. These values of γ^d lead to the evaluation of $\gamma_{H_2O}^h$ (51.0 dynes per cm. at 20°) and γ_{Hg}^m (284 dynes per cm. at 20°). Thus we have a method of evaluating quantitatively the contribution of various intermolecular forces to the cohesion in liquids. For example, we see that in mercury (at 20°) 41% of the interatomic forces are dispersion forces. These are stronger dispersion forces than one ordinarily considers; the heat of surface formation attributable to dispersion forces is 2.8 kcal. per gram-atom and thus the dispersion force contribution to the heat of vaporization is about 6 kcal. per gram-atom of mercury.

The values of $\gamma_{H_2O}^d$ and γ_{Hg}^d determined with hydrocarbons as primary standards can be used to calculate $\gamma_{H_2O/Hg}$. This is possible because the hydrogen bonds of water do not interact with mercury and the metallic bonds in mercury do not interact with water. Thus the intermolecular attraction is expected to be almost entirely dispersion forces ($\sqrt{\gamma_{Hg}^d \gamma_{H_2O}^d}$), and Equation 1 predicts the interfacial tension to be 424.8 ± 4.4 dynes per cm. at 20° as compared with the best experimental values [7] of 426 to 427 dynes per cm.

Contact Angles of Hydrocarbons on Various Solids

At the interface between a liquid and solid, the interfacial monolayer of liquid is attracted by the bulk liquid from one side and from the other side by the intermolecular forces which interact between the two materials. In the case of saturated hydrocarbon liquids which can interact with a solid only by dispersion forces, the interfacial attraction results in a decrease of tension ($\sqrt{\gamma_L^d \gamma_S^d}$) in the liquid interfacial layer (where γ_L^d and γ_S^d are the dispersion force contributions to the surface

Publication Date: January 1, 1964 | doi: 10.1021/ba-1964-0043.ch006

tension of the liquid and the solid, respectively). The concept of a surface tension of a solid appears difficult to define; however, the concept of a dispersion force contribution to the surface tension of a solid (γ_S^d) appears more acceptable, since it can be defined in terms of the interaction with the dispersion forces of an adjacent liquid. The surface tension of the solid (γ_S) is difficult to define, since one should take into account defects, mechanical stresses, and other deviations from equilibrium which are present. The Young equation may be written as

$$\gamma_L \cos\theta = \gamma_S - \gamma_{LS} - \pi_e$$

where π_e is the reduction of γ_S resulting from vapor adsorbed on the solid surface. If the liquid and solid interact by dispersion forces only, then

$$\gamma_{LS} = \gamma_L + \gamma_S - 2\sqrt{\gamma_L^d \gamma_S^d} \quad (2)$$

and by substitution into the Young equation γ_S is cancelled:

$$\gamma_L \cos\theta = -\gamma_L + 2\sqrt{\gamma_L^d \gamma_S^d} - \pi_e \quad (3)$$

Rearrangement of Equation 3 leads to a more easily graphed relation

$$\cos\theta = -1 + \frac{2\sqrt{\gamma_L^d \gamma_S^d}}{\gamma_L} - \pi_e$$

$$= -1 + 2\sqrt{\gamma_S^d} \times \frac{\sqrt{\gamma_L^d}}{\gamma_L} - \frac{\pi_e}{\gamma_L} \quad (4)$$

The value of spreading pressure, π_e, in the above equations is very often zero, although there are a few systems in which π_e must be taken into consideration. There has been no successful prediction of the magnitude of spreading pressures from known values of intermolecular forces; however, it appears possible to make some useful predictions based on our knowledge of spreading pressures on liquids, where we have the most trustworthy data. In the case of spreading pressures on water, saturated hydrocarbons with surface tensions less than $\gamma_{H_2O}^d$ have spreading pressures on water which are close to, though somewhat less than, the value of the spreading coefficient, S, of liquid 1 on liquid 2:

$$S_{2/1} = \gamma_1 - (\gamma_2 + \gamma_{12})$$

$$= 2\sqrt{\gamma_1^d \gamma_2^d} - 2\gamma_2$$

Similarly, in the case of mercury, the spreading pressure of hydrocarbons on mercury is 0.8 to 0.9 of S [20, 21]. These results in liquid systems in which the adsorbed materials have only dispersion forces and can interact with the solids only by dispersion forces show that the value of π_e is always less than S. Consequently, whenever liquid 2 does not spread over liquid 1, we may expect π_e to be zero. Another way of

Publication Date: January 1, 1964 | doi: 10.1021/ba-1964-0043.ch006

expressing this is to say that high energy materials cannot adsorb on low energy materials so as to reduce the surface tension of the latter. If we apply this principle to the spreading of hydrocarbons on solid surfaces, we must conclude that whenever the contact angle θ is greater than zero, π_e is zero and the last term of Equations 2, 3, and 4 also becomes zero.

However, when adsorbing vapors have other types of intermolecular interactions, there is a possibility of appreciable spreading pressures in excess of S, including situations where the liquid does not spread, and θ is finite. Examples with water vapor are (1) on mercury where liquid water does not spread and π_e is about 45 to 50 dynes per cm. [20, 21, 22], and (2) on graphite where the contact angle is 85.7° and π_e is 19 dynes per cm. [13]. In these cases the substrate has a greater dispersion energy than the water, and this leads to adsorption of the vapor. However, the hydrogen-bonding forces in liquid water increase its cohesion so greatly that it will not spread over the surface. Thus, we may expect appreciable spreading pressures for nonspreading liquids only in cases where the vapors can interact with a substrate of greater dispersion energy and where the liquids have additional intermolecular forces great enough to prevent spreading. Therefore, except under these uncommon conditions, the last term in Equation 4 may be omitted.

Equation 4 (with the last term omitted) predicts a useful method of graphing contact angles of a variety of liquids (with surface tensions γ_L) on a low energy surface with a dispersion force contribution to surface tension γ_S^d. If cos θ is plotted as a function of $\sqrt{\gamma_L^d}/\gamma_L$, we see that the experimental points should fall on a straight line with an origin of -1 and with slope 2 $\sqrt{\gamma_S^d}$. The value of γ_S^d is not the total value of the surface tension of the solid, but only the dispersion force contribution to the surface tension. This method of graphing contact angles also indicates that from a single contact angle of a hydrocarbon on a low energy solid the contact angle of any other hydrocarbon and also the value of γ_S^d can be predicted.

Figure 2 shows some of Zisman's [1, 10, 12, 23, 24] data plotted in the above-described manner. Results are shown for a variety of hydrocarbons and for some other organic liquids in which γ_L^d equals γ_L. On each of the five substrates, the experimental points fall extremely close to a straight line and give intercepts at cos θ + 1 which are close to but somewhat different from the "critical surface tension for the wetting" (γ_c) of Zisman and coworkers. Figure 3 shows that this method of graphing is successful both for low energy hydrocarbon solids and for monolayers of fluorochemicals adsorbed on platinum. Some points are also shown for contact angles of water on solid hydrocarbons where the value of γ_L^d obtained from interfacial tensions (21.8 dynes per cm.) was used to determine the abscissa. Consideration of the tendency of water vapor to adsorb on these surfaces and lower their surface tension suggests that in the case of paraffin waxes the spreading pressure is negligibly small. The value of the contact angle of water on paraffin wax is predicted to be 111°, using $\gamma_{H_2O}^d$ = 21.8 dynes per cm. and γ_S^d for the paraffin wax equals 25 dynes per cm., as predicted by Zisman's measurements with liquid hydrocarbons; this is an especially close agreement, since experimental values of the contact angles of water and paraffin wax are 110° ± 2° [8].

Publication Date: January 1, 1964 | doi: 10.1021/ba-1964-0043.ch006

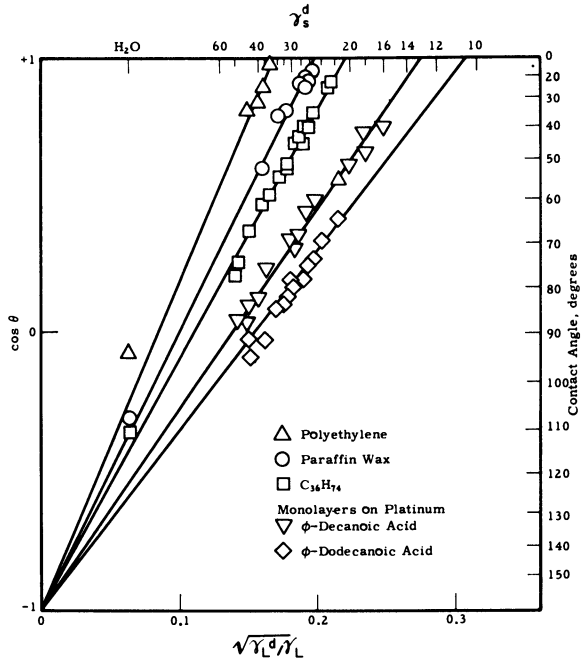

FIGURE 2. Contact angles of a number of liquids on five low energy surfaces, plotted according to equation 4.

Figure 2. Contact angles of a number of liquids on five low energy surfaces

Plotted according to Equation 4

Interaction of Fluorocarbons at Interfaces

The interaction of fluorocarbons with hydrocarbons in solution is not well understood [17]. Their deviations from predictions of solubility are much greater than with other nonelectrolytes. Fluorocarbons are poorer solvents for hydrocarbons than predicted by heats of vaporization; this means that the actual interactions are weaker than predicted. The same is observed at interfaces—for example, a fluorinated lubricating oil was found to have a surface tension of 22.4 dynes per cm. [9]. If we assume that the intermolecular forces are entirely dispersion forces ($\gamma = \gamma^d$), then the interfacial tension with water should be 50.3 dynes per cm., according to Equation 1; however, the experimental interfacial tension is 57.7 dynes per cm., which indicates a weaker than predicted interaction with water. If γ^d is calculated with Equation 1 using the interfacial tension of 57.7 dynes per cm. the result is 15.4 dynes per cm. as compared with the experimental γ of 22.4 dynes per cm. These findings are in good agreement with solution studies, although they do not explain the discrepancy.

Similar findings arise in contact angle studies with solid fluorocarbons or adsorbed monolayers of fluorochemicals [1, 10, 12, 23, 24].

Publication Date: January 1, 1964 | doi: 10.1021/ba-1964-0043.ch006

Contact angles of hydrocarbons on these surfaces, when graphed as in Figure 2, give very low γ_S^d intercepts. However, contact angles of highly fluorinated liquids on these surfaces lead to larger γ_S^d intercepts (Figure 3). One might question which γ_S^d really involves only dispersion force interactions; it is reasonable to assume that the lower value obtained with liquid hydrocarbons is the better measure of dispersion force interaction and to explain the larger value obtained with liquid fluorocarbons as including some additional (though undetermined) interaction.

Very similar findings resulted in a contact angle study of a perfluorinated lubricating oil on paraffin wax. The surface tension, γ, was 20.2 dynes per cm., but the contact angles on two wax surfaces gave γ_L^d values of 13.5 dynes per cm. (see Figure 4).

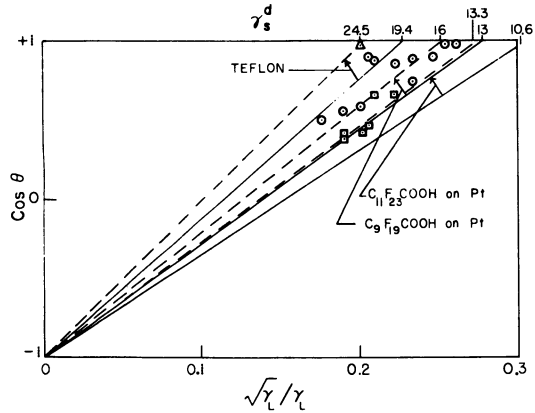

Figure 3. Contact angles of liquid fluorocarbons on solid fluorocarbons

——— Predicted from γ_L^d values determined with liquid hydrocarbons
------ Determined

Interaction of Polar Liquids with Other Phases

Polar liquids interact with other phases by various intermolecular forces in addition to dispersion forces. However, by choosing a suitable reference material, it is usually possible to evaluate γ^d of the polar liquid.

Mercury is a good reference for aromatic hydrocarbons and organic bases; the interaction with mercury is entirely by dispersion forces and these materials are found to have $\gamma^d = \gamma$ [7]. On the other hand, acidic organic compounds, divalent sulfur compounds, and organic halides (especially iodides and bromides) interact with mercury by polar interactions of appreciable magnitude, though never as strong an interaction as results from dispersion forces. Mercury has promise as a reference liquid for contact angle measurement on high energy solids.

Water is sometimes useful as a reference material, either for a liquid interface or by contact angle measurement. However, water

sometimes forms polar bonds with liquids which have only dispersion force interactions in the bulk liquid—for example, strong hydrogen bonds are formed with amines and pi-bonds with aromatics. Furthermore, on some solids unwetted by water appreciable spreading pressures are observed—for example, on graphite where $\theta = 85.7$, π_e is 19 dynes per cm. [8, 13].

Saturated hydrocarbons are theoretically the best standards for determining γ^d. However, many polar organic liquids are soluble in hydrocarbons and so interfacial tensions cannot be used. On the other hand, many solid hydrocarbons (and even some solid fluorocarbons) can be used as good standards for determining the γ_L^d values from contact angles. Figure 4 illustrates this point with examples of contact angles on nine different solids with water ($\gamma_L^d = 22$, $\gamma_L = 72.8$ dynes per cm.), glycerol ($\gamma_L^d = 36$, $\gamma_L = 63.4$ dynes per cm.), 1-bromonaphthalene ($\gamma_L^d = 44$ to 45, $\gamma_L = 44.6$ dynes per cm.), du Pont's Fluorolube FCD-330 ($\gamma_L^d = 13.5$, $\gamma_L = 20.2$ dynes per cm.), and the pentamer of dimethyl silicone ($\gamma_L^d = 16.5$, $\gamma_L = 19.9$ dynes per cm.). In Figure 4 the arrow for each liquid points at a subscale of values of γ_L^d computed from the known value of γ_L (number under subscale) and the abscissa values of $\sqrt{\gamma_L^d}/\gamma_L$. In this manner it can be shown that methylene iodide, tricresyl phosphate, and most esters have γ_L^d values indistinguishably different (by contact angle measurement) from their surface tensions.

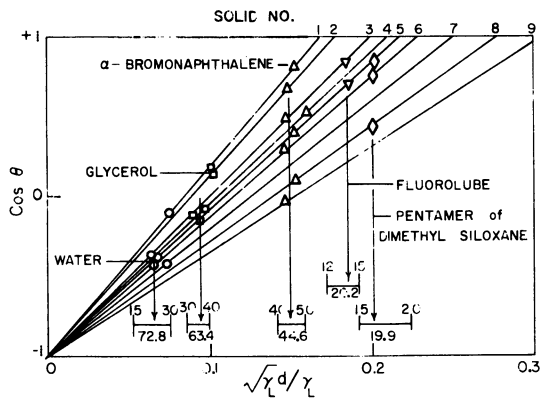

Figure 4. Method of determining γ_L^d of polar liquids by contact angle measurements

Low energy surfaces

1. Polyethylene
2. Kel-F
3. Paraffin wax
4. $C_{18}H_{37}NH_2$ monolayer on Pt
5. $C_{36}H_{74}$
6. Teflon
7. Polyhexafluoropropylene
8. $C_9F_{19}COOH$ monolayer on Pt
9. $C_{11}F_{23}COOH$ monolayer on Pt

Publication Date: January 1, 1964 | doi: 10.1021/ba-1964-0043.ch006

High Energy Solid Surfaces

Most contact angle studies have been limited to low energy solids, usually organic materials or sulfide minerals. However, high energy solids are of considerable interest as adsorbents and catalysts, and are important in electronic devices. Studies with mercury surfaces point up the importance in preventing contamination of high energy surfaces [20, 21, 22], for organic vapors in the air are rapidly and strongly adsorbed, mainly by the strong dispersion force interactions resulting from the very large value of γ^d for mercury (200 dynes per cm.). By proper choice of a standard liquid (so that π_e is either zero or measurable, and the interfacial interaction is confined to dispersion forces) it is possible through contact angle studies to determine γ^d values for a variety of high energy solids. Once these values are known, the pathway to prediction of free energies and heats of immersion and adsorption becomes clear.

A useful example is graphite. The contact angle of water on graphite was found to be 85.7° and π_e was 19 dynes per cm. [8, 13]. If we assume that graphite and water interact entirely by dispersion forces, we can use Equation 4, rearranged as

$$\gamma_S^d = [\gamma_L(1 + \cos\theta) + \pi_e]^2/4\gamma_L^d \tag{5}$$

and obtain a γ_S^d of 109 dynes per cm. However, since water interacts with graphite by π-bonding (as with benzene, where such bonds decrease interfacial tension by 16 dynes per cm. from the predicted value for dispersion force interactions), the value of γ_S^d for graphite should be about 93 dynes per cm.

On the other hand, we can use the π_e of n-heptane on graphite (58 dynes per cm.) measured by Loeser [14] and assume that it equals the spreading coefficient, S (as did Harkins [13]), which leads to

$$\gamma_S^d = (S + 2\gamma_L)^2/4\gamma_L^d = 119 \text{ dynes per cm.} \tag{6}$$

The free energy of immersion, ΔF_i (for solids and liquids interacting entirely by dispersion forces), is:

$$\Delta F_i = \gamma_{SL} - \gamma_S = \gamma_L - 2\sqrt{\gamma_L^d \gamma_S^d}$$

from which the heat of immersion, ΔH_i, for such systems is given by

$$\Delta H_i = \Delta F_i - T\frac{d\Delta F_i}{dT}$$

$$= \gamma_L - 2\sqrt{\gamma_L^d \gamma_S^d} - T\left[\frac{d\gamma_L}{dT} - 2\sqrt{\gamma_L^d} \times \frac{d\sqrt{\gamma_S^d}}{dT} - 2\sqrt{\gamma_S^d}\,\frac{d\sqrt{\gamma_L^d}}{dT}\right] \tag{7}$$

All of the data needed to implement Equation 7 are available for some systems, with the exception of the temperature coefficient of γ_S^d; someday the temperature coefficients of contact angles will be measured and then this can be evaluated. In the meantime the value can be

estimated from coefficients of thermal expansion, using the relation observed in liquid hydrocarbons that the surface tension increases as the fourth power of the density; this term is the smallest in Equation 7 and amounts to only 2% of ΔH_i.

Figure 5 shows calculated heats of immersion for graphite and rutile (TiO_2) in saturated hydrocarbon liquids for a range of γ_S^d values. The value of ΔH_i is shown to be rather sensitive to γ_S^d but not very sensitive to γ_L^d. Thus ΔH_i for hexane, heptane, and octane should be nearly identical, as was observed by Healey [16] for rutile (squares), though not for graphite (circles). These observed values of heats of immersion for graphite indicate that γ_S^d lies between 97 and 120 dynes per cm, which agrees well with the 93 from contact angle measurement and the 119 from a π_e value calculated from adsorption isotherms.

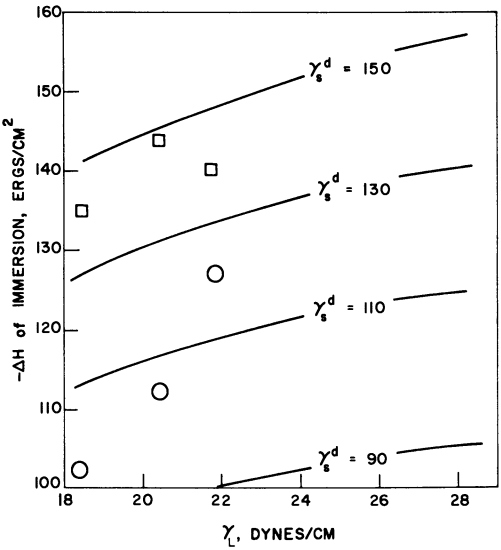

Figure 5. Dependence of heats of immersion on γ_S^d and γ_L

○ Graphite

□ Rutile

Equation 7 may also be tested with heats of immersion of Teflon in n-heptane; however, for such soft solids the temperature coefficient of γ_S^d becomes more important. For a coefficient of thermal expansion of 10^{-4} per degree, the calculated ΔH_i is -28 ergs per sq. cm. as compared with an experimental -58 ergs per sq. cm. [2].

From studies with high energy solids and saturated hydrocarbons, the π_e values obtained from adsorption isotherms by Harkins and coworkers [14, 15], and the ΔH_i values obtained calorimetrically by Zettlemoyer and coworkers [2, 16], we can obtain preliminary γ_S^d values for higher energy solids (using Equations 6 and 7):

Graphite	110 dynes/cm.
Rutile	140 dynes/cm.
Iron	105 dynes/cm.
Iron oxide	107 dynes/cm.
Silver	76 dynes/cm.

The above value for rutile (and probably iron oxide) includes polarization force of these surfaces on hydrocarbons [3]. Since both the dispersion force and polarization force depend on the polarizability of the hydrocarbon, these two terms should be additive. The value of the polarization force can be determined by measurements with polar molecules; the field strength of the surface is indicated by the increase in interfacial interaction with dipole moment [3]. As there is no appreciable dipole effect on interfacial tensions between many polar organic substances and mercury, it appears that with mercury (and perhaps other metals without oxide surfaces) the γ^d values include no polarization term.

Heats of adsorption (ΔH_{ads}) may be calculated for monolayers bound to surfaces by dispersion forces by assuming that the free energy of adsorption (per unit area of adsorbent) at $p/p_o = 1$ is given by $\Delta F_{ads} = -S$ as Harkins [13] and Chessick [3] have done:

$$\Delta H_{ads} = -S + T\frac{dS}{dT}, \quad \text{where} \quad S = 2\sqrt{\gamma_S^d \gamma_L^d} - 2\gamma_L .$$

$$= 2\gamma_L - 2\sqrt{\gamma_S^d \gamma_L^d} - 2T\left[\frac{d\gamma_L}{dT} - \sqrt{\gamma_L^d}\,\frac{d\sqrt{\gamma_S^d}}{dT} - \sqrt{\gamma_S^d}\,\frac{d\sqrt{\gamma_L^d}}{dT}\right] \qquad (8)$$

For the adsorption of hexane on graphite we may use the experimental results of Isirikyan and Kiselev [18], who found that on graphitized carbon black (Graphon) n-hexane occupies 54 sq. A. per molecule and has a heat of adsorption (with liquid hexane as standard state) of 5.0 kcal. per mole. The value of γ_S^d for graphite which gives a heat of adsorption of 5.0 kcal. per mole is found by Equation 8 to be 108 dynes per cm.

Experimental values of γ_S^d at 25° for graphite, determined on crystalline graphite and on graphitized carbon black, are:

Method	γ_S^d, *Dynes/Cm.*
Contact angle	93
Free energy of adsorption (π_e)	119
Heat of immersion (calorimetric)	97, 105, 120
Heat of adsorption (isosteric)	108

Publication Date: January 1, 1964 | doi: 10.1021/ba-1964-0043.ch006

Literature Cited

(1) Bernett, M. K., Zisman, W. A., J. Phys. Chem. **65**, 2266 (1961).
(2) Chessick, J. J., Healey, F. H., Zettlemoyer, A. C., Ibid., **60**, 1345 (1956).
(3) Chessick, J. J., Zettlemoyer, A. C., Healey, F. H., Young, G. J., Can. J. Chem. **33**, 251 (1955).
(4) Fowkes, F. M., J. Phys. Chem. **66**, 382 (1962).
(5) Ibid., P. 1863.
(6) Ibid., in press (1963).
(7) Fowkes, F. M., to be published.
(8) Fowkes, F. M. Harkins, W. D., J. Am. Chem. Soc. **62**, 3377 (1940).
(9) Fowkes, F. M., Sawyer, W. M., J. Chem. Phys. 20, 1650 (1952).
(10) Fox, H. W., Zisman, W. A., J. Colloid Sci. 5, 514 (1950); 7, 428 (1952).
(11) Girifalco, L. A., Good, R. J., J. Phys. Chem. **61**, 904 (1957).
(12) Hare, E. F., Shafrin, E. G., Zisman, W. A., Ibid., 58, 236 (1954).
(13) Harkins, W. D., "Physical Chemistry of Surface Films," Reinhold, New York, 1952.
(14) Harkins, W. D., Jura, G., Loeser, E. H., J. Am. Chem. Soc. 68, 554 (1946).
(15) Harkins, W. D., Loeser, E. H., J. Chem. Phys. **18**, 556 (1950).
(16) Healey, F. H., Chessick, J. J., Zettlemoyer, A. C. Young, G. J., J. Phys. Chem. **58**, 887 (1954).
(17) Hildebrand, J. H., Scott, R. L., "Solubility of Non-Electrolytes," 3rd ed. Reinhold, New York, 1950; "Regular Solutions," Prentice-Hall, Edgewood Cliffs, N. J., 1962.
(18) Isirikyan, A. A., Kiselev, A. V., J. Phys. Chem. **66**, 210 (1962).
(19) Jura, G., Loeser, E. H., Basford, P. R., Harkins, W. D., J. Chem. Phys. 13, 535 (1945); 14, 117 (1946).
(20) Kemball, C., Proc. Roy. Soc. **187**A, 73 (1946); 190A, 117 (1947).
(21) Kemball, C., Rideal, E. K., Ibid., A187, 53 (1946).
(22) Nicholas, M. E., Joyner, P. A., Tessem, B. M., Olsen, M. D., J. Phys. Chem. **65**, 1373 (1961).
(23) Schulman, F., Zisman, W. A., J. Colloid Sci. **7**, 465 (1952).
(24) Shafrin, E. G., Zisman, W. A., Ibid., **7**, 166 (1952).

Received April 3, 1963

7

Contact Angle Hysteresis

I. Study of an Idealized Rough Surface

RULON E. JOHNSON, Jr., and ROBERT H. DETTRE

Organic Chemicals Department, Jackson Laboratory
E. I. du Pont de Nemours & Co., Inc., Wilmington, Del.

Publication Date: January 1, 1964 | doi: 10.1021/ba-1964-0043.ch007

The effect of roughness on the wettability of an idealized sinusoidal surface has been studied with a digital computer. The equations of Wenzel and of Cassie and Baxter are discussed in relation to the model. The heights of the energy barriers between metastable states of a drop are seen to be of utmost importance in determining the magnitude of contact angle hysteresis.

This paper describes a computer study of the wettability of idealized surfaces. The theories of Wenzel [9], Cassie and Baxter [2], Shuttleworth and Bailey [8], and Good [5] are analyzed in terms of a surface of specific geometry. The concept of an energy barrier between metastable states associated with contact angles, first introduced by Shuttleworth and Bailey [8], and discussed by Bikerman [1], Good [5], and Schwartz and Minor [7], is shown to be of utmost importance in determining hysteresis. A second paper describes correlations with measurements on surfaces of controlled roughness. The model surface was suggested by Good [5].

Description of System

Solid Surface. We use cylindrical coordinates (x, z, Ψ) to describe the system. The solid surface is circularly symmetrical about the z axis. Figure 1 is a cross section through the origin. Its equation is

$$z = z_o \left(1 + \cos \frac{2\pi x}{x_o}\right) \quad (1)$$

where $2z_o$ is the height of a ridge and x_o is the period of the surface.

We assume that the volume of the drop is constant, that the drop always meets the surface with a constant, intrinsic angle, θ (at equilibrium), and that gravitational forces are absent. For simplicity we also assume that the liquid consists of a single component and that the solid is insoluble in the liquid. The radius of the drop is assumed to be much greater than the separation of asperities.

In Contact Angle, Wettability, and Adhesion; Fowkes, F.;
Advances in Chemistry; American Chemical Society: Washington, DC, 1964.

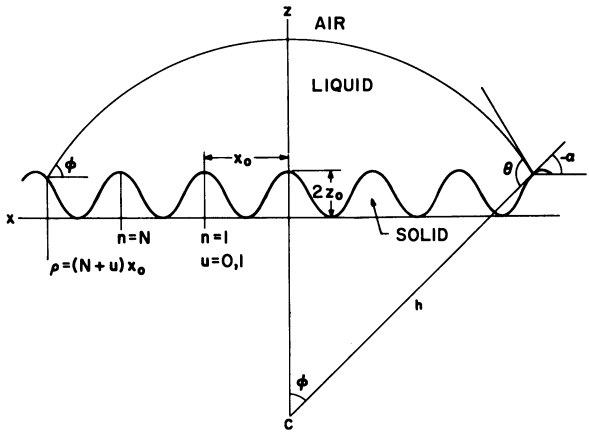

Figure 1. Drop on idealized rough surface

Relationship of Observed Angles to Intrinsic Angle. As stated by Shuttleworth and Bailey [8], the experimentally observed contact angle, ϕ, is the sum of the intrinsic angle, θ, plus the slope angle, α, of the surface at the point of contact:

$$\phi = \theta + \alpha \tag{2}$$

From Figure 1,

$$\tan \alpha = - \frac{\partial z}{\partial x} \tag{3}$$

The slope angle, α, can be positive or negative.

Maximum Possible Hysteresis. The maximum possible angle, ϕ_{max}, is observed where α is a maximum and the minimum is observed where α is a minimum. Whereas Shuttleworth and Bailey [8] associated these values with advancing and receding angles, it is improbable that ϕ_{max} and ϕ_{min} will actually be observed in a real system.

The slope angle, α, for any given value of x is found by differentiating Equation 1 and substituting in Equation 3.

$$\alpha = \tan^{-1} \left(\frac{2\pi z_o}{x_o} \sin \frac{2\pi x}{x_o} \right) \tag{4}$$

Since α is a maximum where $\sin 2\pi x/x_o = 1$ and a minimum where $\sin 2\pi x/x_o = -1$,

$$\alpha_{max} = -\alpha_{min} = \tan^{-1} \frac{2\pi z_o}{x_o} \tag{5}$$

Table I gives values of α_{max} for various ratios of z_o/x_o. The heading r stands for Wenzel's roughness ratio, defined by Equation 16.

Publication Date: January 1, 1964 | doi: 10.1021/ba-1964-0043.ch007

Table I. Maximum Possible Hysteresis for Various Rough Surfaces

r	z_o/x_o	α_{max}, degrees
1.001	0.01	3.60
1.092	0.1	32.13
1.321	0.2	51.48
1.618	0.3	62.07
1.952	0.4	68.30
	0.5	72.35
2.670	0.6	75.13
	0.7	77.18
3.421	0.8	78.75
	0.9	79.96
4.189	1.0	80.97

If we consider the ratio z_o/x_o to be a measure of roughness, it is clear that possible hysteresis decreases as surface roughness decreases, and that the maximum and minimum possible angles are symmetrical about the intrinsic contact angle, θ. Furthermore, the ratio z_o/x_o, rather than the absolute value of either z_o or x_o, determines the maximum possible hysteresis.

Free Energy of Metastable Configurations. A quantity of importance in this analysis is the difference in Helmholtz free energy between two configurations of the system. The term "configuration" refers to a state in which the drop is at rest in a position of metastable equilibrium. Associated with each configuration is a characteristic contact angle, ϕ, and a characteristic Helmholtz free energy, F. For a given configuration:

$$F_j = \underset{\text{all phases}}{\Sigma} (-PV)_j + \underset{\text{all phases}}{\Sigma} (n^*\mu)_j + \underset{\text{all interfaces}}{\Sigma} (\gamma\Omega)_j \quad (6)$$

where j refers to the jth configuration
μ is the chemical potential of a component
n* is the number of moles of a component
V is the volume of a phase
P is the pressure in a phase
γ is the interfacial tension of an interface
Ω is the area of an interface

$$\Delta F = F_j - F_k = \underset{\text{all phases}}{\Delta\Sigma} (-PV) + \underset{\text{all phases}}{\Delta\Sigma} (n^*\mu) + \underset{\text{all interfaces}}{\Delta\Sigma} (\gamma\Omega) \quad (7)$$

It can be seen from the Gibbs-Duhem equation that at constant temperature and volume the first two terms of the right-hand side of Equation 7 are equal and opposite, so that

$$\Delta F = \underset{\text{all interfaces}}{\Sigma} (\gamma\Omega)_j - \underset{\text{all interfaces}}{\Sigma} (\gamma\Omega)_k \quad (8)$$

Publication Date: January 1, 1964 | doi: 10.1021/ba-1964-0043.ch007

For the system of our model

$$\Delta F = \gamma^{la}\left(\Omega_2^{la} - \Omega_1^{la}\right) + \gamma^{sl}\left(\Omega_2^{sl} - \Omega_1^{sl}\right) + \gamma^{sa}\left(\Omega_2^{sa} - \Omega_1^{sa}\right) \quad (9)$$

Superscripts la, sl, and sa refer to the liquid-air, solid-liquid, and solid-air interfaces, respectively. The subscripts refer to two different configurations. Now,

$$\Omega^{sl} + \Omega^{sa} = \Omega^{surface} = \text{constant} \quad (10)$$

$$\Omega_2^{sl} - \Omega_1^{sl} = \Omega_1^{sa} - \Omega_2^{sa} \quad (11)$$

From Young's equation,

$$\gamma^{la} \cos\theta = \gamma^{sa} - \gamma^{sl} \quad (12)$$

Combining Equations 9, 10, 11, and 12,

$$\Delta F = \gamma^{la}\left\{\left(\Omega_2^{la} - \Omega_2^{sl}\cos\theta\right) - \left(\Omega_1^{la} - \Omega_1^{sl}\cos\theta\right)\right\} \quad (13)$$

Let F^{rel} be defined for any configuration by

$$F^{rel} = \Omega^{la} - \Omega^{sl}\cos\theta \quad (14)$$

F^{rel} has the significance that the difference in the values of γ^{la} F^{rel} for any two configurations is the difference in free energy between these states. F^{rel} has dimensions in square centimeters and can be considered to be an effective area.

The area of the spherical surface of a drop on a flat surface is given by

$$\Omega^{la} = \frac{2\pi\rho^2}{1 + \cos\phi} \quad (15)$$

where ρ is the value of x at which the liquid meets the solid. Let A^{sl} be the projection of the solid surface on the (x, Ψ) plane. Wenzel's ratio, r, is defined by

$$r = \frac{\Omega^{sl}}{A^{sl}} \quad (16)$$

Assuming r is not a function of ρ (see calculations),

$$\Omega^{sl} = rA^{sl} = r\pi\rho^2 \quad (17)$$

Combining Equations 14, 15, and 17 yields

$$F^{rel} = \frac{2\pi\rho^2}{1 + \cos\phi} - \pi r\rho^2\cos\theta \quad (18)$$

Equation 18 is the fundamental equation for the study of metastable states.

Publication Date: January 1, 1964 | doi: 10.1021/ba-1964-0043.ch007

Discrete Positions of Metastable Equilibrium. For purposes of discussion, it is convenient to divide x into two parts,

$$x = (n + u)\, x_o \tag{19}$$

where n is an integer which counts the number of crests of the surface from the origin, and u is the fraction of the distance along the x axis between adjacent crests. The radius of the drop is then

$$\rho = (N + u)\, x_o \tag{20}$$

where N is the number of crests on the surface between the origin and the edge of the drop.

Not all values of ϕ between ϕ_{max} and ϕ_{min} are possible. The boundary conditions of constant volume and constant θ limit ϕ to $2N_{max}$ values. N_{max} is the value of N in Equation 20, where ρ has its maximum value. For each trough there are two positions of equilibrium, one metastable and one unstable. The metastable configuration is always with the edge of the drop closest to the top of the ridge. This is shown schematically in Figure 2. Let A and B be the positions of equilibrium—i.e., the vector sum $\vec{\gamma}^{sa} + \vec{\gamma}^{la} + \vec{\gamma}^{sl} = 0$. As the drop edge moves from A to C, the resultant vector is such as to move the drop back to A. As the drop edge moves from B to D, the resultant is such as to move the edge still farther from D. Computer calculations confirm that position B is indeed a maximum in the free energy. There are, thus, N_{max} positions of metastable equilibrium.

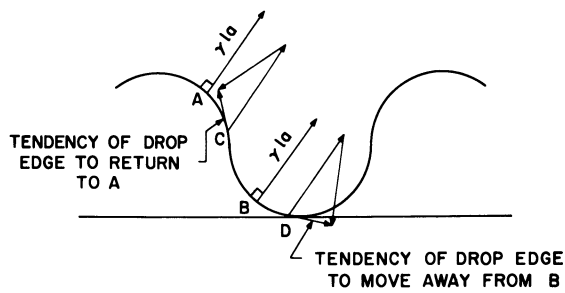

Figure 2. Positions of stable and unstable equilibrium for drop on rough surface

Calculation of F^{rel} as a Function of ϕ. Expressions relating F^{rel} to ϕ cannot be obtained in closed form. They must be calculated by successive approximations. The details of this calculation are given below (Calculation of F^{rel}). Figure 3 shows curves of F^{rel} vs. ϕ for five surfaces of different roughness. In each case θ is 120° and V is 0.05 ml. ($\rho >> x_o$). Wenzel roughness ratios have been calculated for each surface. Scale models of the surfaces can be seen in Figure 6. Although the curves are plotted as continuous, it should be remembered that there are only a finite number of allowed values of ϕ. Curves 1, 2, and 3 have minima (at W-1, W-2, and W-3) where predicted by Wenzel's

Publication Date: January 1, 1964 | doi: 10.1021/ba-1964-0043.ch007

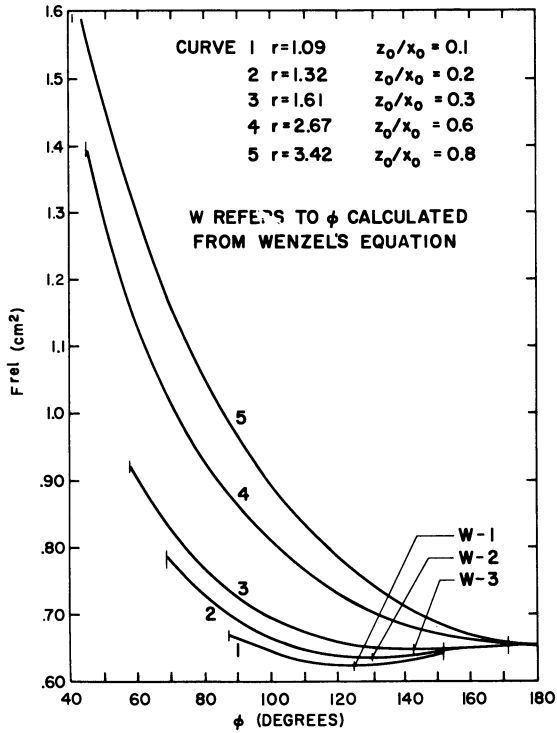

Figure 3. Free energy vs. contact angle for drop on noncomposite surface
θ = 120°
v = 0.05 ml.

equation. The vertical lines at the end of the curves are ϕ_{max} and ϕ_{min} (see Derivation of Expressions for Minima in Free Energy Curves). Curves 4 and 5 have no minima; the lowest free energy is observed at ϕ = 180°. This behavior is discussed in the section on composite surfaces. Wenzel's equation, itself, fails for extremely rough surfaces, since it leads to cosines greater than +1 or smaller than -1.

Figure 4 shows curves of F^{rel} vs. ϕ for three surfaces when θ is 45°. Curves 1 and 2 show minima (W-1, W-2) where predicted by Wenzel's equation. Curve 3 has no minimum, but approaches -∞ as ϕ approaches 0. This behavior implies surface wicking. The necessary condition for surface wicking is

$$r \geq \frac{1}{\cos \theta} \quad (\text{for } \theta < 90°) \tag{21}$$

Equation 21 says that when r is greater than 1.414, surface wicking can occur (for θ = 45°). This is true for curve 3 but not for curves 1 and 2.

Publication Date: January 1, 1964 | doi: 10.1021/ba-1964-0043.ch007

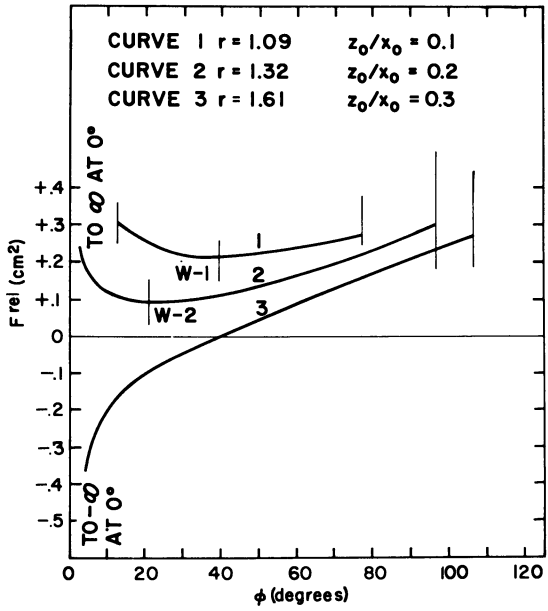

Figure 4. Free energy vs. contact angle for drop on noncomposite surface

$\theta = 45°$
v = 0.05 ml.

Condition for Wicking on a Rough Surface. F^{rel} for a noncomposite surface can be written as

$$F^{rel} = \pi\rho^2\left\{\frac{2}{1 + \cos\phi} - r\cos\theta\right\} \tag{22}$$

The requirement for spontaneous wicking is that

$$F^{rel} \rightarrow -\infty \text{ as } \rho \rightarrow \infty \tag{23}$$

Condition 23 can be written as

$$r\cos\theta > \frac{2}{1 + \cos\phi} \tag{24}$$

Now, as

$$\rho \rightarrow \infty;\ \phi \rightarrow 0;\ \cos\phi \rightarrow 1 \tag{25}$$

Hence, the condition for spontaneous wicking becomes

$$r\cos\theta > 1 \text{ or } r > \frac{1}{\cos\theta} \tag{26}$$

Publication Date: January 1, 1964 | doi: 10.1021/ba-1964-0043.ch007

Energy Barriers between Metastable States. The reason why any system does not automatically assume Wenzel's configuration is that free energy barriers separate positions of metastable equilibrium. For a drop to remain in a position of metastable equilibrium, it is necessary that the vibrational energy of the drop be small compared with the height of the barrier. The shape of a free energy barrier can be calculated from the work required to move a drop from one configuration to the next (see Calculation of Free Energy Barriers). Figure 5 shows two energy barriers computed for two values of ϕ of curve 1 in Figure 3. The barrier in Figure 5, A, was computed for a ϕ near the minimum in curve 1–i.e., at $\phi = \hat{\phi}$–and the barrier in Figure 5, B, was computed for a ϕ near ϕ_{max} in curve 1. ($\hat{\phi}$ is the value of ϕ for the configuration having the lowest free energy of all possible configurations of a given drop and surface.) The barrier heights approach zero as ϕ approaches ϕ_{max} and ϕ_{min}. For this reason, neither ϕ_{max} nor ϕ_{min} is likely to be observed in real systems. The actual values of the advancing and receding angles depend on the barrier heights and the vibrational state of the drop. As a first approximation, the barriers are proportional to z_o and independent of x_o.

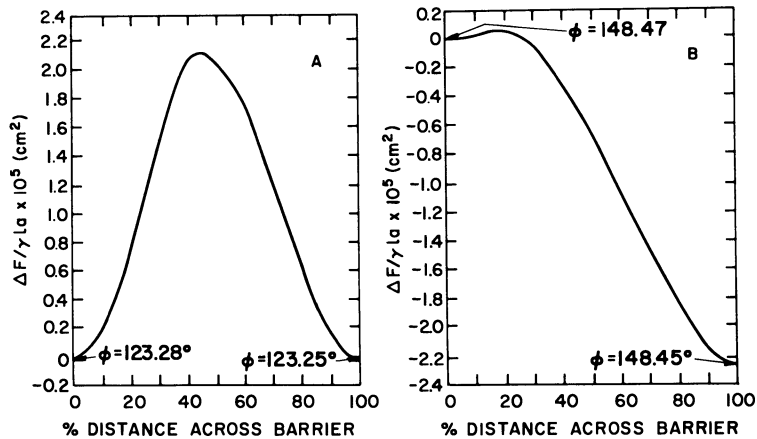

Figure 5. Free energy barriers for system

$\theta = 120°$
$z_o/x_o = 10^{-4}$ cm.
v = 0.05 ml.
See curve 1, Figure 3

Extension to Composite Surfaces. It was pointed out in the discussion of Figure 3 that for very rough surfaces–e.g., $z_o/x_o = 0.6, 0.8$–there is no minimum in the F^{rel} vs. ϕ curve. This does not describe the behavior of real systems. It can be seen from Figure 6 that, as the surface roughness increases, it becomes possible for the system to assume configurations in which the liquid does not penetrate into the troughs. The rougher the surface, the less the liquid penetrates into troughs. Equation 77 gives the calculation of F^{rel} for a composite

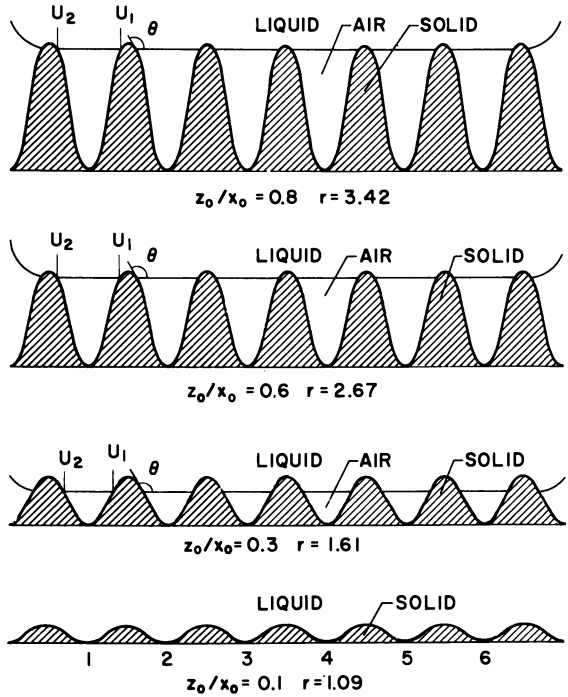

Figure 6. Scale drawings of cross section of idealized surfaces of various roughnesses

surface. The name "composite" refers to the fact that the interfaces under the drop are both liquid-air and liquid-solid. It is possible for the system to achieve a composite configuration, if and only if, there is a slope of the surface such that

$$\theta = 180° - |\alpha| \tag{27}$$

We define u_1 and u_2 in Figure 6 to be the values of u at which the internal liquid-air interfaces meet the solid surface, at equilibrium. There are two positions in each trough in which it is geometrically possible for composite surfaces to be formed. Just as with the noncomposite case, the configuration with the liquid farthest out of the trough is metastable, while that farthest in is unstable.

Figure 7 compares the free energies of composite and noncomposite configurations for two different roughnesses. A minimum in the curve for $z_o/x_o = 0.8$ now appears for the composite calculation where none appeared before. Whereas for very rough surfaces, the composite configuration leads to states of lower free energy, the curves for $z_o/x_o = 0.3$ show that for surfaces of intermediate roughness the noncomposite configuration can still be in a lower energy state than the composite. This means that, even though it is geometrically possible for the system to become composite (by Equation 27), it may be energetically

Publication Date: January 1, 1964 | doi: 10.1021/ba-1964-0043.ch007

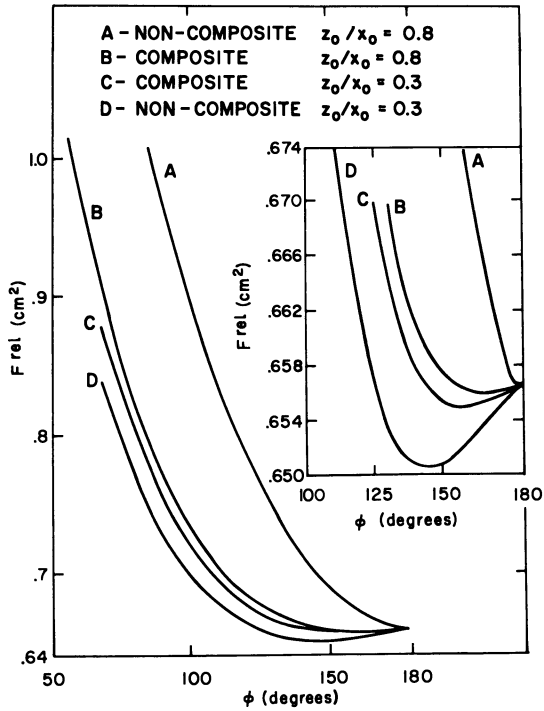

Figure 7. Comparison of curves of free energy vs. contact angle for composite and noncomposite surfaces

preferable for the liquid to penetrate into the troughs. The curves also show that the free energies of composite configurations are much less sensitive to the degree of roughness than those of the noncomposite—e.g., curves B and C are much closer than A and D. This behavior is related to the very small area of the solid-liquid interface in the composite configuration.

The minima in curves B and C are given by the equation of Cassie and Baxter [2],

$$\cos \phi = r' \cos \theta - \eta \tag{28}$$

$$r' = \frac{\Omega^{sl}}{A} \tag{29}$$

where the prime refers to composite configurations and

$$\eta = \frac{\Omega^{la}_{int}}{A} \tag{30}$$

where Ω^{la}_{int} refers to the liquid-air interface under the drop (see discussion of derivation of expressions for minima).

Publication Date: January 1, 1964 | doi: 10.1021/ba-1964-0043.ch007

With little error, η is given for our model by

$$\eta = u_2 - u_1 \tag{31}$$

Both r' and η depend on θ, since u_1 and u_2 depend on θ.

Energy Barriers and Hysteresis of Composite Configurations. Figure 8 compares energy barriers for noncomposite and composite configurations (see Calculations of Free Energy Barriers). The calculation for Figure 8 is made at a surface roughness of $z_o/x_o = 0.6$ and with $\phi = 90°$. Of extreme importance for the wetting behavior of composite surfaces is the large lowering of free energy barriers as the system becomes composite. The lowering in this example is by a factor of about 28. This is equivalent to reducing the roughness of a noncomposite surface from r = 2.67 to r = 1.001. In contrast to the noncomposite case, the free energy barriers actually become lower as the surface becomes rougher.

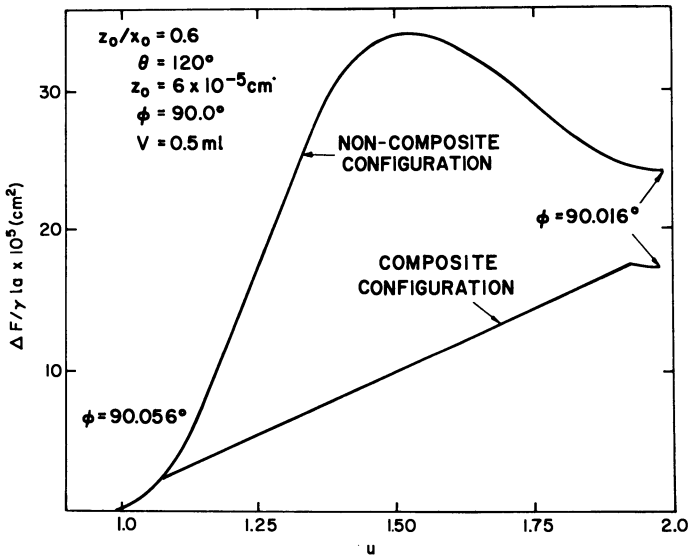

Figure 8. Comparison of energy barriers for composite and noncomposite systems

Calculations and Derivations

Calculation of Wenzel's r Ratio. Since our system is circularly symmetrical, the total area of a circular region of radius ρ about the origin is given by

$$\Omega^{s1} = \int_0^{\rho} 2\pi x \left[1 + \left(\frac{\partial z}{\partial x}\right)^2\right]^{1/2} dx \tag{32}$$

Publication Date: January 1, 1964 | doi: 10.1021/ba-1964-0043.ch007

The area of the projection of this area on the (x, Ψ) plane is

$$A = \pi\rho^2 \tag{33}$$

Wenzel's ratio, r, is defined by

$$r = \frac{\Omega^{sl}}{A} \tag{34}$$

Taking the derivative of Equation 1 and combining with Equations 32, 33, and 34 gives

$$r = \frac{4\pi z_o}{x_o \rho^2} \int_o^\rho \left\{ \frac{x_o^2 x^2}{4\pi^2 z_o^2} + x^2 \sin^2 \frac{2\pi x}{x_o} \right\}^{1/2} dx \tag{35}$$

Equation 35 cannot be solved in closed form, but must be solved by a numerical integration. Although r is not exactly constant over the surface, a series of numerical calculations showed that the error in assuming r to be constant is less than 1 part in 10^5.

Calculation of F^{rel}

Noncomposite Surface. The calculation of F^{rel} by Equation 18 requires ϕ as a function of ρ at constant volume. The volume of a drop on the model surface can be derived from consideration of Figure 1. Let c be the center of curvature of the liquid surface and h the radius of curvature. Let the z coordinate of c be -a. The included angle between the z axis and the radius to the edge of the drop is then $\phi = (\theta + \alpha)$. Let z' be the value of z at the liquid-solid interface and z'' the value of z at the liquid-air interface. The volume of the liquid is given by

$$V = 2\pi \int_o^\rho (z'' - z')\, x\, dx \tag{36}$$

From geometrical considerations,

$$z'' = (h^2 - x^2)^{1/2} - a \tag{37}$$

and

$$h = \rho / \sin \phi \tag{38}$$

Equation 1 gives z'. Combining Equations 1 and 36, 37, and 38,

$$V = 2\pi \int_o^\rho \left\{ (h^2 - x^2)^{1/2} - a - z_o \cos \frac{2\pi x}{x_o} - z_o \right\} x\, dx \tag{39}$$

and

$$a = h \cos \phi - z_o \left(1 + \cos \frac{2\pi\rho}{x_o} \right) = \rho \cot \phi - z_o \left(1 + \cos \frac{2\pi\rho}{x_o} \right) \tag{40}$$

Publication Date: January 1, 1964 | doi: 10.1021/ba-1964-0043.ch007

Combining Equations 39 and 40, integrating, and simplifying, give

$$V = 1/3\ \pi\rho^3\left(\frac{\cos^3\phi - 3\cos\phi + 2}{\sin^3\phi}\right) + z_o\left(\pi\rho^2 - \frac{x_o^2}{2\pi}\right)\cos\frac{2\pi\rho}{x_o}$$

$$- x_o z_o \rho\left(\sin\frac{2\pi\rho}{x_o}\right) + \frac{x_o^2 z_o}{2\pi} \qquad (41)$$

The first term in the equation is the volume of a drop on a plane surface; the remaining terms are corrections due to roughness. Since Equation 41 cannot be solved for either ϕ or ρ explicitly, the computer is programmed to find them by successive approximations. For most of our calculations, we are satisfied when ρ and ϕ are found which give the chosen volume to 1 part in 10^5. F^{rel} is then computed from Equation 18 with these values of ϕ and ρ.

Composite Surface. Equation 14 is valid for a composite surface but Equation 18 is not. To derive the equation for F^{rel} for the composite surface it is necessary to develop corresponding equations for Ω^{la} and Ω^{sl}.

Figure 6 gives some scale drawings of a composite surface. Let u_1 and u_2 be the values of u at which the internal solid-liquid-air boundaries meet. The other symbols are defined in Figure 1. The total solid-liquid interfacial area is the sum of the areas of all troughs.

$$\Omega^{sl} = \sum_{n=0}^{N-1}\left\{\int_{nx_o}^{(n+u_1)x_o} B\,dx + \int_{(n+u_2)x_o}^{(n+1)x_o} B\,dx\right\} + \int_{Nx_o}^{\rho} B\,dx \qquad (42)$$

where

$$B = 2\pi x\left[1 + \left(\frac{\partial z}{\partial x}\right)^2\right]^{1/2} \qquad (43)$$

Define r'_n by

$$r'_n \equiv \frac{1}{A_n}\int_{nx_o}^{(n+u_1)x_o} B\,dx + \int_{(n+u_2)x_o}^{(n+1)x_o} B\,dx \qquad (44)$$

where

$$A_n = \int_{nx_o}^{(n+1)x_o} 2\pi x\,dx \qquad (45)$$

Therefore,

$$\Omega^{sl} = \sum_{n=0}^{N-1} A_n r'_n + \int_{Nx_o}^{\rho} B\,dx \qquad (46)$$

Publication Date: January 1, 1964 | doi: 10.1021/ba-1964-0043.ch007

Now, if

$$r'_1 = r'_2 = r'_n = r' \tag{47}$$

$$\Omega^{s1} = \pi N^2 x_o^2 r' + \int_{Nx_o}^{\rho} B dx \tag{48}$$

If we then make the approximation,

$$\int_{Nx_o}^{\rho} B dx \cong r' \int_{Nx_o}^{\rho} 2\pi x dx \tag{49}$$

then,

$$\Omega^{s1} = r' \pi \rho^2 \tag{50}$$

Equation 47 has been verified by machine calculation. The change in r'_n over a range of 10 to 1000 cycles is considerably less than 1 part in 5000. Any error introduced by the use of Equation 49 is less than that.

The symbol Ω^{la}_{int} refers to the liquid-air interface underneath the drop. Therefore,

$$\Omega^{la} = \frac{2\pi\rho^2}{1 + \cos\phi} + \Omega^{la}_{int} \tag{51}$$

We assume the internal liquid-vapor interface to be planar. This is not exactly true, since this interface has the same curvature as the external surface. Little error will be introduced when $\rho >> x_o$. As before, the total internal area is the sum of the internal areas of all the troughs,

$$\Omega^{la}_{int} = \sum_{n=0}^{N-1} \int_{(n+u_1)x_o}^{(n+u_2)x_o} 2\pi x dx \tag{52}$$

Integrating, simplifying, and noting that

$$\sum_{n=0}^{N-1} n = \frac{N}{2}(N - 1) \tag{53}$$

Equation 52 becomes

$$\Omega^{la}_{int} = N\pi x_o^2(u_2^2 - u_1^2) + \pi x_o^2(u_2 - u_1) N(N - 1) \tag{54}$$

Combining Equations 14, 50, and 51 gives the desired equation for F^{rel}, for the composite surface,

$$F^{rel}_{composite} = \frac{2\pi\rho^2}{1 + \cos\phi} + N\pi x_o^2(u_2^2 - u_1^2) + \pi x_o^2(u_2 - u_1) N(N - 1) - \pi\rho^2 r' \cos\theta \tag{55}$$

Publication Date: January 1, 1964 | doi: 10.1021/ba-1964-0043.ch007

Equation 55 must be evaluated at constant volume. To do this, relationships between ρ, θ, and V must be determined for the composite configuration.

Equation 41 gives the volume of a drop on a noncomposite surface. We can modify this expression by subtracting the volume of air under the drop. Let subscript n refer to the nth trough. Let subscript j refer to the total volume (solid + air) above the (x, Ψ) plane and below the internal liquid air interface. Let subscript k refer to the volume of solid surface under the internal liquid-air interface and above the (x, Ψ) plane. Let subscript s refer to the volume of air under the liquid-air interface. These definitions are shown schematically in Figure 9.

Definition of terms:

$$V_{sn} = V_{jn} - V_{kn} \tag{56}$$

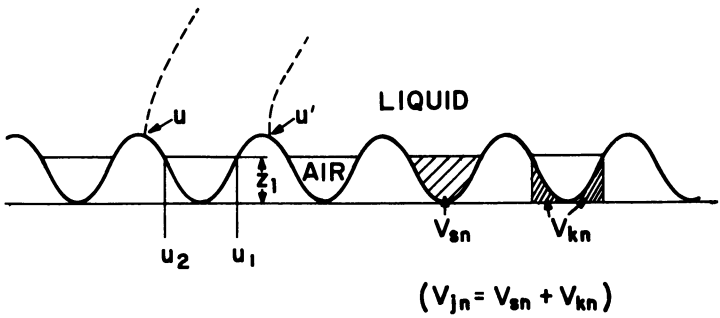

Figure 9. Notation for calculation of volume of drop on idealized composite surface

$$V_s = \sum_{n=0}^{N-1} V_{sn} = \sum_{n=0}^{N-1} V_{jn} - \sum_{n=0}^{N-1} V_{kn} \tag{57}$$

and

$$V_c = V - V_s \tag{58}$$

where V_c is the volume of a drop on a composite surface and V is the volume of a drop on a noncomposite surface.

$$V_{jn} = \int_{(n+u_1)x_o}^{(n+u_2)x_o} 2\pi x z_1 dx \tag{59}$$

Integrating and summing over n,

$$V_j = \pi z_1 x_o^2 (u_2 - u_1) \left\{ N(u_2 + u_1) + N(N - 1) \right\} \tag{60}$$

where z_1 is defined in Figure 9. Similarly,

$$V_{kn} = \int_{(n+u_1)x_o}^{(n+u_2)x_o} 2\pi x z dx \tag{61}$$

Publication Date: January 1, 1964 | doi: 10.1021/ba-1964-0043.ch007

where x is defined by Equation 19 and

$$z = z_o(1 + \cos 2\pi u) \tag{62}$$

Integrating and summing over n,

$$V_k = \pi z_o x_o^2 \left\{ N(N-1) \left[(u_2 - u_1) + \frac{1}{2\pi} (\sin 2\pi u_2 - \sin 2\pi u_1) \right] + N \left[\left(u_2^2 - u_1^2 \right) + \frac{1}{2\pi^2} (\cos 2\pi u_2 - \cos 2\pi u_1 + 2\pi u_2 \sin 2\pi u_2 - 2\pi u_1 \sin 2\pi u_1) \right] \right\} \tag{63}$$

Combining Equations 60 and 63 with Equation 41 and noting that

$$V_c = V - V_j + V_k \tag{64}$$

yield

$$V_c = \frac{1}{3} \pi \rho^3 \left(\frac{\cos^3 \phi - 3 \cos \phi + 2}{\sin^3 \phi} \right) + z_o \left(\pi \rho^2 - \frac{x_o^2}{2\pi} \right) \cos \frac{2\pi\rho}{x_o} - x_o z_o \rho \sin \left(\frac{2\pi\rho}{x_o} \right) + \frac{x_o^2 z_o}{2\pi} - \pi x_o^2 \left\{ N(N-1) \left[(u_2 - u_1)(z_1 - z_o) - \frac{z_o}{2\pi} (\sin 2\pi u_2 - \sin 2\pi u_1) \right] + N \left[\left(u_2^2 - u_1^2 \right) (z_1 - z_o) - \frac{z_o}{2\pi^2} \times (\cos 2\pi u_2 - \cos 2\pi u_1 + 2\pi u_2 \sin 2\pi u_2 - 2\pi u_1 \sin 2\pi u_1) \right] \right\} \tag{65}$$

As before, ρ and ϕ are evaluated by successive approximations. An accuracy of 1 part in 10^5 is usually assumed adequate.

Derivation of Expressions for Minima in Free Energy Curves, Equation of Wenzel. Wenzel [9] first derived an equation for the effect of surface roughness on contact angles. His basic assumption was that a rough surface can be treated as a smooth surface of surface energy $r\gamma^{sa}$ or $r\gamma^{s1}$, depending on the interface. With this assumption, Wenzel's equation can be derived using the same techniques as in the derivation of Young's equation itself [4]. Shuttleworth and Bailey [8] pointed out that roughness made it possible to have more than one metastable position of equilibrium. The contact angle given by Wenzel's equation was correctly stated to give the angle corresponding to the lowest free energy. The derivation of Young's equation and the derivation of Wenzel's equation are essentially different. Young's equation is derived by Gibbs using a variational technique which compares an equilibrium position with adjacent, infinitesimally close, nonequilibrium states. The derivation of Wenzel's equation, on the other hand, compares adjacent states which are all in metastable equilibrium. It is instructive to list explicitly the assumptions that must be made to derive Wenzel's equation by the

Publication Date: January 1, 1964 | doi: 10.1021/ba-1964-0043.ch007

methods of Shuttleworth and Bailey [8] and of Good [5]. The assumptions are:

1. The free energy is a continuous function of ϕ.
2. $d\Omega^{sl} = rdA$ (66)
3. $d\Omega^{sl} = -d\Omega^{sa}$ (67)
4. $d\Omega^{la} = dA \cos \phi$ (68)

From these assumptions and the condition that $dF = 0$ for a minimum, Wenzel's equation,

$$\cos \hat{\phi} = r \cos \theta \tag{69}$$

is readily derived.

Approximation 1 is not true, but it does not lead to a serious error when the roughness is small compared with the drop size. Condition 2 is not true except when the differential of A corresponds to exactly one period of the surface. Condition 3 demands that the surface be noncomposite. Condition 4 is true only in the absence of a gravitational field. (This is an indication, but not proof that Wenzel's equation may not be valid in a gravitational field.)

Equation of Cassie and Baxter. Cassie and Baxter [2] extended Wenzel's treatment to composite surfaces. The same assumptions necessary for the derivation of Wenzel's equation are necessary, except that Equation 66 is replaced by 70, and Equation 68 is replaced by 71. These two changes are direct consequences of the difference between the geometry of composite and noncomposite surfaces.

$$d\Omega^{sl} = r' dA \tag{70}$$

$$d\Omega^{la} = dA(\cos \phi + \eta) \tag{71}$$

These assumptions lead directly to Cassie and Baxter's equation,

$$\cos \hat{\phi} = r' \cos \theta - \eta \tag{72}$$

In the notation of Cassie and Baxter,

$$r' = f_1 \text{ and } \eta = f_2$$

Equation 73 defines η,

$$\eta = \frac{\Omega_{int}^{la}}{\pi \rho^2} \tag{73}$$

where Ω_{int}^{la} is given by Equation 54. In most cases,

$$N(N - 1) >> N \tag{74}$$

and

$$\pi \rho^2 \cong \pi x_o^2 N(N - 1) \tag{75}$$

Publication Date: January 1, 1964 | doi: 10.1021/ba-1964-0043.ch007

With these approximations, Equation 73 becomes

$$\eta = (u_2 - u_1) \tag{76}$$

Calculation of Free Energy Barriers

Noncomposite Surfaces. We assume that the free energy difference between two states of the system, equilibrium or not, is given by

$$\Delta F = \int_{\Omega_1^{1a}}^{\Omega_2^{1a}} \gamma^{1a}\, d\Omega^{1a} + \int_{\Omega_1^{s1}}^{\Omega_2^{s1}} \gamma^{s1}\, d\Omega^{s1} + \int_{\Omega_1^{sa}}^{\Omega_2^{sa}} \gamma^{sa}\, d\Omega^{sa} \tag{77}$$

We assume, during the motion from one position to another, that the periphery of the drop moves uniformly, that the liquid-air interface remains a section of a sphere, and that the motion is slow enough that kinetic energy can be ignored. The angle θ' which the liquid makes with the solid at any point is given by

$$\theta' = \phi - \alpha \tag{78}$$

When the drop size is large compared with the roughness of the surface, ϕ changes very little as the drop edge moves over one cycle of the surface. We assume this change in ϕ to be linear,

$$\phi = \phi_2 + (\phi_1 - \phi_2)\left(\frac{u_2 - u}{u_2 - u_1}\right) \tag{79}$$

Then,

$$d\Omega^{sa} = -d\Omega^{s1} \tag{80}$$

and

$$d\Omega^{1a} = \cos\theta'\, d\Omega^{s1} \tag{81}$$

Therefore,

$$\Delta F = \int_{\Omega_1^{s1}}^{\Omega_2^{s1}} (\gamma^{1a}\cos\theta' + \gamma^{s1} - \gamma^{sa})\, d\Omega^{s1} \tag{82}$$

or,

$$\Delta F = \int_{\Omega_1^{s1}}^{\Omega_2^{s1}} \gamma^{1a}\left(\cos\theta' + \frac{\gamma^{s1} - \gamma^{sa}}{\gamma^{1a}}\right) d\Omega^{s1} \tag{83}$$

or,

$$\frac{\Delta F}{\gamma^{1a}} = \int_{\Omega_1^{s1}}^{\Omega_2^{s1}} (\cos\theta' - \cos\theta)\, d\Omega^{s1} \tag{84}$$

Publication Date: January 1, 1964 | doi: 10.1021/ba-1964-0043.ch007

Now,

$$\alpha = \tan^{-1}\left(\frac{2\pi z_o}{x_o}\sin 2\pi u\right) \tag{85}$$

$$d\Omega^{s1} = \frac{4\pi^2 z_o}{x_o}\left\{\frac{x_o^2 x^2}{4\pi^2 z_o^2} + x^2 \sin^2(2\pi u)\right\}^{1/2} dx \tag{86}$$

Combining Equations 78, 79, 84, 85, 86, and 64, 65 yields

$$\Delta F/\gamma^{1a} = 2\pi \int_{u_1}^{u_2} \left\{-\cos\theta + \cos\left[\phi_2 + (\phi_1 - \phi_2)\left(\frac{u_2 - u}{u_2 - u_1}\right) - \tan^{-1}\left(\frac{2\pi z_o}{x_o}\sin 2\pi u\right)\right]\right\} \times \left\{1 + \frac{4\pi^2 z_o^2}{x_o^2}\sin^2(2\pi u)\right\}^{1/2} (N + u)\, x_o^2\, du \tag{87}$$

Equation 87 is programmed for numerical integration by means of Simpson's rule. In most calculations, states 1 and 2 are metastable configurations. Intermediate values of ΔF are calculated by having the computer add up any desired number of Simpson's rule areas.

Composite Surfaces. Consider Figure 9. Let u, u_1, and u_2 have their usual meaning. Let u' be the value of u at an adjacent position of metastability. As the drop contracts, the edge of the drop follows the solid surface until it reaches u_2. The free energy change in this process is ΔF_1. At u_2 the drop no longer follows the solid surface but jumps from u_2 to u_1. This free energy change is ΔF_2. The drop edge then follows the solid surface to an equilibrium position at u'. This free energy change is ΔF_3. The total free energy difference between the two points is

$$\Delta F = \Delta F_1 + \Delta F_2 + \Delta F_3 \tag{88}$$

ΔF_1 and ΔF_3 are computed from Equation 87 using appropriate limits of integration. $\Delta F_2/\gamma^{1a}$ is equal to $\Delta\Omega^{1a}$ as u goes from u_2 to u_1. Now,

$$\Delta\Omega^{1a} = \int_{\rho_2}^{\rho_1} 2\pi\rho\cos\phi\, d\rho + \pi\left(\rho_1^2 - \rho_2^2\right) \tag{89}$$

For most purposes, the following approximations give results of adequate accuracy:

1. ϕ remains constant throughout the region of integration.
2. $N >> u$.

Integrating Equation 89, assuming constant ϕ, and using the relation $\rho = (N + u)\, x_o$ yields

Publication Date: January 1, 1964 | doi: 10.1021/ba-1964-0043.ch007

$$\Delta\Omega^{1a} = \pi x_o^2(1 + \cos\phi)\left\{2N(u_1 - u_2) + u_1^2 - u_2^2\right\} \quad (90)$$

Using approximation 2,

$$\frac{\Delta F_2}{\gamma^{1a}} = 2N\pi x_o^2(1 + \cos\phi)(u_1 - u_2) \quad (91)$$

It was mentioned above that the energy barrier actually decreases for a composite configuration as the roughness increases. The height of the energy barrier is directly related to the distance the drop edge moves in going from u to u_2. As the roughness increases, the liquid penetrates less deeply into the grooves, which in turn moves u_2 closer to u, lowering the barrier.

Discussion and Conclusions

The analysis of this idealized surface shows that roughness leads to a large number of metastable configurations. The configuration having the lowest free energy is given by Wenzel's equation (or Cassie and Baxter's for composite configurations). Each metastable state is separated from an adjacent state by an energy barrier. These barriers are a maximum at $\tilde{\phi}$ and go to zero at ϕ_{max} and ϕ_{min}. The heights of the energy barriers are approximately directly proportional to the height of the asperities and approximately independent of their separation. The energy barriers for composite surfaces are very much lower than for noncomposite surfaces.

Contact angle hysteresis on rough surfaces can be qualitatively explained by assuming that the advancing and receding angles are determined by a balance between the macroscopic vibrational energy of the drop and the heights of the energy barriers. As the energy barriers become smaller (or the vibrational energy becomes greater), hysteresis becomes less.

These comments are summarized in Figures 10 and 11. Figure 10 shows curves of contact angle vs. roughness for $\theta = 120°$, while Figure 11 is for $\theta = 45°$. Curves B are plots of $\hat{\phi}$. In Figure 10, B consists of two curves. The curve at small roughnesses is calculated from Wenzel's equation, while at higher roughnesses Cassie and Baxter's equation is used. The intersection of the two curves indicates the point of transition from a noncomposite to a composite surface. The solid portion of curve B indicates the configurations of lower free energy. Curves A give the maximum and minimum angles that are geometrically possible. These would be advancing and receding angles in the treatment of Shuttleworth and Bailey. Curves C and D are possible advancing and receding angles which might be observed on a real system having the geometry of our model. The exact shapes of C and D depend on the heights of the energy barriers and the vibrational state of the drop. For this model, curves A and B depend on only the surface roughness ratio, r, while curves C and D depend on both r and the absolute magnitude of the surface asperities. Curves C and D of Figure 10 show that when composite configurations are energetically preferred, the hysteresis becomes dramatically less. This is a direct reflection

Publication Date: January 1, 1964 | doi: 10.1021/ba-1964-0043.ch007

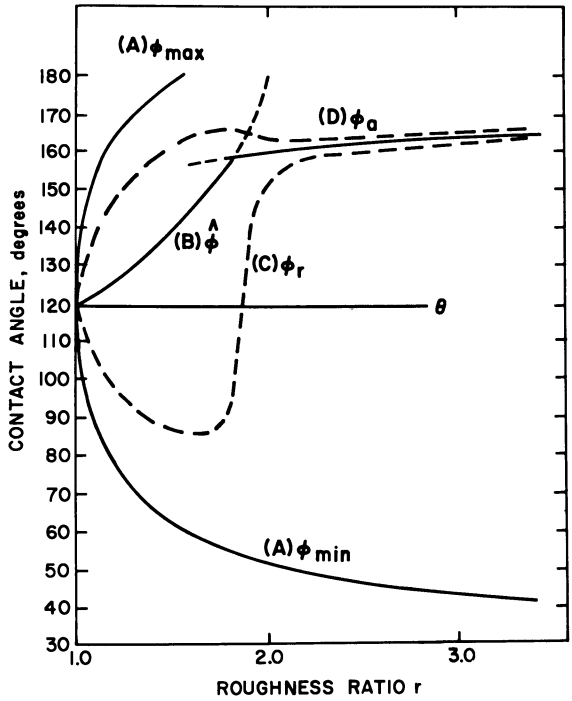

Figure 10. Effect of roughness on contact angle for θ = 120°

A. Maximum and minimum possible angles
B. Most probable contact angles, $\hat{\phi}$
   Lower. Calculated from Wenzel's equation
   Upper. Calculated from Cassie and Baxter's equation
C. Possible curve of receding angles
D. Possible curve of advancing angles

of the very low free energy barriers for the composite configurations. This large decrease in hysteresis for composite surfaces offers a means for testing the hypothesis of energy barrier control of hysteresis. This question is examined experimentally in another paper [3].

It is not possible to obtain composite surfaces for θ less than 90° for our model. (This is not true for all surfaces–for example, one composed of parallel fibers.) Accordingly, there is no drastic decrease in hysteresis in Figure 11 as is observed in Figure 10. On the other hand, when θ is less than 90°, there is a surface roughness at which surface wicking tends to occur. This occurs when $\hat{\phi}$ = 0. Whether or not wicking actually occurs depends on the vibrations in the drop and on the nature of the energy barriers.

We are not implying with this analysis that surface roughness is the only or even the most important source of contact angle hysteresis. Since it is a common source of hysteresis, it is necessary to understand the effect of roughness in order to interpret experimental results

Publication Date: January 1, 1964 | doi: 10.1021/ba-1964-0043.ch007

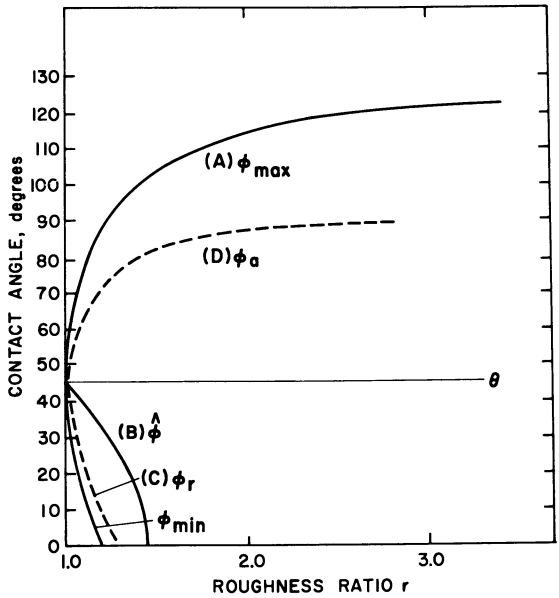

Figure 11. Effect of roughness of contact angles for $\theta = 45°$

A. Maximum and minimum possible angles
B. Most probable contact angles, $\hat{\phi}$, calculated from Wenzel's equation
C. Possible curve of receding angles
D. Possible curve of advancing angles

rationally. A similar study of the relation between surface heterogeneity and contact angle hysteresis will soon be published.

GLOSSARY OF TERMS

Name	Symbol	Definition
Contact angle	θ or ϕ	Angle (measured through liquid) which liquid makes with solid
Intrinsic contact angle	θ	Contact angle given by $\gamma^{la} \cos \theta = \gamma^{sa} - \gamma^{sl}$
Observed contact angle	ϕ	Contact angle experimentally observed
Advancing contact angle	ϕ_a	Largest experimentally measured angle of liquid on solid
Receding contact angle	ϕ_r	Smallest experimentally measured angle of liquid on solid
Maximum possible angle	ϕ_{max}	Maximum contact angle that could be observed; deduced from geometrical considerations

Publication Date: January 1, 1964 | doi: 10.1021/ba-1964-0043.ch007

Name	Symbol	Definition
Minimum possible angle	ϕ_{min}	Minimum contact angle that could be observed; deduced from geometrical considerations
Most probable contact angle	$\hat{\phi}$	Contact angle corresponding to lowest value of F^{rel} for given surface and drop
Hysteresis	$\phi_a - \phi_r$	Qualitatively, fact that many different contact angles can be observed for a given liquid on a given surface. Quantitatively, difference between advancing and receding angles
Solid-air interfacial tension	γ^{sa}	See [6] for detailed discussion and definitions
Liquid-air interfacial tension	γ^{la}	
Solid-liquid interfacial tension	γ^{sl}	
Solid-liquid interfacial area	Ω^{sl}	Total area of solid-liquid interface
Solid-air interfacial area	Ω^{sa}	Total area of solid-air interface
Liquid-air interfacial area	Ω^{la}	Total area of liquid-air interface
Internal liquid-air interfacial area	Ω^{la}_{int}	Area of liquid-air interface under surface of drop
Plane area	A	Area of (x, ψ) plane under drop $(A = \pi\rho^2)$
Surface area ratio (Wenzel's)	r	Ω^{sl}/A (for noncomposite surface)
Surface area ratio (composite)	r'	Ω^{sl}/A (for composite surface)
Internal liquid-air surface ratio	η	Ω^{la}_{int}/A (for composite surface)
Relative free energy	F^{rel}	Helmholtz free energy (referred to special reference state) of configuration divided by γ^{la}
Configuration		Position of metastable equilibrium of drop on rough surface
Composite surface		System (see Figure 6) which has air-liquid, and air-solid interfaces, as well as solid-liquid, under surface of drop
Radius of drop	ρ	Radius of projection of drop on (x, ψ) plane
Height of ridge on surface	$2z_o$	(z_o = amplitude of sine wave)
Period of surface	x_o	Distance between ridges
Number of ridges under drop	N	
	n	Number of ridges from origin to arbitrary point on surface
Fraction of distance between two adjacent ridges	u	e.g., $\rho = (N + u)\, x_o$
	u_1, u_2	Positions of contact of interior liquid-air interface with surface (Figure 6)

Publication Date: January 1, 1964 | doi: 10.1021/ba-1964-0043.ch007

Acknowledgment

We acknowledge the assistance of William Saadeh, who programmed the equations for the digital computer.

Literature Cited

(1) Bikerman, J. J., J. Phys. Chem. **54**, 653 (1950).
(2) Cassie, A. B. D., Baxter, S., Trans. Faraday Soc. **40**, 546 (1944).
(3) Dettre, R. H., Johnson, R. E., Jr., Advan. Chem. Ser., No. **43**, 136 (1963).
(4) Gibbs, J. W., "Collected Works of J. Willard Gibbs," Vol. I, "Thermodynamics," pp. 314–31, Yale University Press, New Haven, Conn., 1928.
(5) Good, R. J., J. Am. Chem. Soc. **74**, 504 (1952).
(6) Johnson, R. E., Jr., J. Phys. Chem. **63**, 1655 (1959).
(7) Schwartz, A. M., Minor, F. W., J. Colloid Sci. **14**, 584 (1959).
(8) Shuttleworth, R., Bailey, G. L. J., Discussions Faraday Soc. **3**, 16 (1948).
(9) Wenzel, R. N., Ind. Eng. Chem. **28**, 988 (1936); J. Phys. Colloid Chem. **53**, 1466 (1949).

Received March 22, 1963. Contribution 312.

8

Contact Angle Hysteresis

II. Contact Angle Measurements on Rough Surfaces

ROBERT H. DETTRE and RULON E. JOHNSON, JR.

Organic Chemicals Department
E. I. du Pont de Nemours & Co., Inc., Wilmington, Del.

Publication Date: January 1, 1964 | doi: 10.1021/ba-1964-0043.ch008

An experimental study of the wettability of rough surfaces over an extremely wide range of roughness is described. The theoretical wettability behavior of an idealized, rough surface agrees well with that of real surfaces. The theoretically predicted minimum in the curve of receding contact angle vs. roughness, for systems of high intrinsic contact angle, is experimentally verified.

A computer study of a liquid drop on an idealized, rough surface [8] showed that the heights of the energy barriers which exist between the metastable configurations suggested by Shuttleworth and Bailey [12] increase from zero, at both the largest and the smallest possible contact angles, to a maximum at an angle corresponding to the lowest free energy for the system. It was suggested that the advancing and receding contact angles and consequently the magnitude of the hysteresis are determined by a balance between the vibrational energy of the drop and the heights of the energy barriers.

For a liquid with a high intrinsic contact angle, the idealized, rough surface shows a transition from a noncomposite to a composite surface as roughness increases, accompanied by a pronounced decrease in the heights of the energy barriers. If energy barriers control contact angle hysteresis, this should result in a dramatic increase in the receding angle and a concomitant decrease in hysteresis.

Experimental studies of the effect of surface roughness on contact angle hysteresis have been reported by a number of investigators [1–4, 6, 10, 11]. The work of Cassie and Baxter [6] on extremely rough, porous surfaces and that of Bartell and Shepard [2, 3, 11] on surfaces of moderate roughness have given quantitative measures of this effect. The results of a computer study [8] encouraged us to consider solid surfaces whose range of roughness is sufficiently wide to include both of the above types of surface. In the present paper we describe wettability studies on surfaces having an extremely wide range of roughness

In Contact Angle, Wettability, and Adhesion; Fowkes, F.;
Advances in Chemistry; American Chemical Society: Washington, DC, 1964.

and compare the contact angle behavior with that predicted from the idealized model [8]. All of the symbols and terms used in this paper are defined in the previous paper [8].

Experimental

Apparatus and Methods. Contact angles were measured on profiles of sessile drops using a microscope fitted with a goniometer eyepiece [7]; magnification was about 20 X. Error in angle measurements by this method is estimated to be about ± 1°. Drops were added and sizes changed using a hypodermic syringe. Advancing angles were measured after the drop size was increased and the periphery advanced over the surface; receding angles were measured after the drop size was reduced and the periphery receded. Unless otherwise stated, readings were taken within 30 seconds of drop formation or size change and drop volumes were between 0.05 and 0.1 ml. Receding angles were measured on drops that had been in contact with the surface for some time before receding and on fresh drops which were placed on the surface and immediately reduced in size. There was little difference between these two methods as long as the drop size was kept below 0.1 ml.

Each contact angle value is the average of at least eight measurements. The lengths of the vertical lines on the points in the graphs represent the magnitudes of the standard deviations. The ± values in Table I are also standard deviations.

All measurements were made at 24° ± 1°C. and 50% relative humidity.

TABLE I. Liquid Contact Angles on Roughest and Smoothest Wax Surfaces Available in This Study

Surface		Water		Methylene Iodide		Hexadecane	
		Φ_a	Φ_r	Φ_a	Φ_r	Φ_a	Φ_r
TFE-methanol telomer wax	Rough	159±2	157±2	143±1	139±2	85±4	0
	Smooth	111±1	95±1	87±4	75±3	52±4	40±4
TFE-silicone oil telomer wax	Rough	158±3	157±2	99±4	0	39±3	0
	Smooth	111±1	98±2	--	--	40±1	23±2
Paraffin wax	Rough	158±1	153±2	60±4	0	0	0
	Smooth	110±1	103±1	51±2	46±4	22±3[a]	0[a]

[a]Evidence of solution of wax in hexadecane.

Materials. Both paraffin and fluorocarbon wax surfaces were studied. The paraffin was a household wax distributed by Esso, Inc. Two fluorocarbon waxes, telomers of tetrafluoroethylene (TFE), were used. One, a methanol telomer, had a crystalline melting point of 278°C. and an approximate molecular weight of 2000 [5]; the other, a telomer of polydimethylsiloxane (Dow Corning DC 200 silicone oil), had a crystalline melting point of 275°C. [13].

The distilled water used in the contact angle measurements had a surface tension of 72.1 dynes per cm. at 24°C. The methylene iodide was Eastman White Label grade; its surface tension at 24°C. was 50.1

Publication Date: January 1, 1964 | doi: 10.1021/ba-1964-0043.ch008

dynes per cm. Olefin-free hexadecane, from Matheson, Coleman and Bell, had a purity greater than 99% as determined by vapor phase chromatography; its surface tension was 27.4 dynes per cm. at 24°C. Surface tensions were determined by the Wilhelmy plate method.

Surface Preparation and Treatment. The roughest fluorocarbon wax surfaces were prepared by spraying the telomer waxes, dispersed in trichlorotrifluoroethane, onto glass microscope slides. These surfaces were made progressively smoother by heating in an oven. Although the time and temperature for each heat treatment were chosen to give a noticeable smoothing of the surface, the change in roughness was not necessarily the same for each treatment. The TFE-methanol telomer surface was heated from 200° to 280°C. over a 2 1/2-hour period; the TFE-silicone oil telomer surface was heated from 150° to about 290°C. over a 13 1/2-hour period.

The roughest paraffin wax surface (Figure 3, E) was obtained by spraying a warm (50°C.) mixture of a 10% wax (in hexane) solution and 10-micron glass beads onto a glass microscope slide. The glass beads were 10% by weight of the total sprayed mixture. A slightly smoother surface (Figure 3, D) was obtained by spraying the above solution without the 10-micron glass beads. Surface C was prepared by spreading 10-micron glass beads on a glass microscope slide, completely covering them with a warm 5% solution of the wax in toluene, and then allowing the toluene to evaporate. A second treatment with the wax solution was made to ensure complete coverage by the wax. Surface B is that of frozen paraffin wax and A is a specular surface prepared by pressing the softened wax against a glass microscope slide. All of the paraffin and fluorocarbon wax coatings described above were 0.1 to 0.2 mm. thick.

Results

Fluorocarbon Wax Surfaces. Figure 1 shows the variation of water contact angle with roughness for the TFE-methanol telomer wax surface. The TFE-silicone oil telomer wax surface showed the same behavior. Although no absolute value is known for surface roughness at each heat treatment, it was established from examination of photomicrographs of the surfaces that roughness changed in the direction indicated on the graph. This is illustrated in Figure 2 by a series of photomicrographs of the wax surfaces of Figure 1.

Air was observed beneath the water drops on the surfaces represented by the points to the right of the minimum in Figure 1. On the surfaces where n.h.t. = 0 to 3, water drops as small as 0.01 ml. were exceptionally mobile and contact angles were independent of drop size. As the number of heat treatments increased, the mobility of these small drops decreased and receding contact angles became sensitive to drop size. For example, at n.h.t. = 6 in Figure 1, the advancing angle remained unchanged when the drop volume was increased from 0.05 to 0.6 ml. but the receding angle changed from 143° ± 3° to 93° ± 31°. Penetration of water into the wax surface was observed as the drop was increased in size. The high sensitivity of the receding angles to roughness, in the above example and in Figure 1, is indicated by the large standard deviations for these angles. Table I lists contact angles for water, methylene iodide, and hexadecane on the smoothest and roughest fluorocarbon wax surfaces prepared in this study. They are averages

Publication Date: January 1, 1964 | doi: 10.1021/ba-1964-0043.ch008

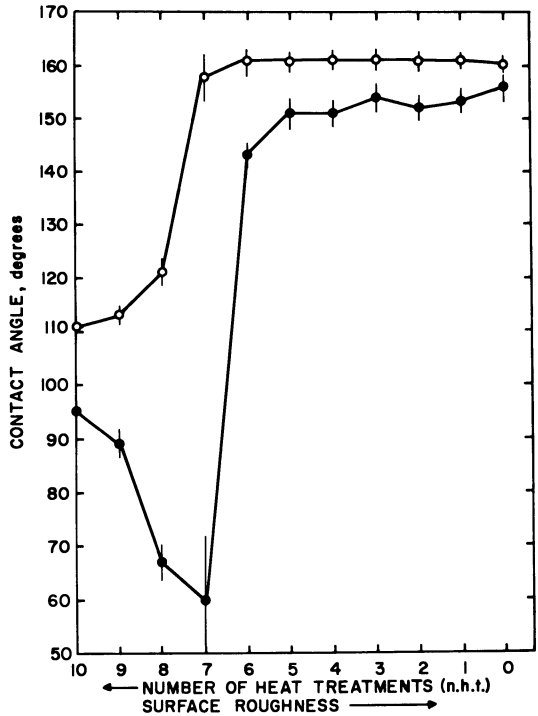

Figure 1. Water contact angles on TFE-methanol telomer wax surface as a function of roughness

○ Advancing angle
● Receding angle

of values obtained on several surfaces of the same type. Air was observed under the methylene iodide drops on the rough TFE-methanol telomer wax surfaces. Both rough fluorocarbon wax surfaces showed a slow wicking of liquid into the surface around the peripheries of the hexadecane drops.

Paraffin Wax Surfaces. Figure 3 shows the variation of water contact angle with surface roughness for paraffin wax surfaces. As with the fluorocarbon waxes, the roughness scale is a relative one; the positions of the various surfaces on this scale were obtained from microscopic examination of the surfaces. Air was observed under the water drops on surfaces D and E.

Table I gives the contact angles of water, methylene iodide, and hexadecane on the smoothest and roughest surfaces of Figure 3. The zero advancing angle for hexadecane on the roughest surface was apparent as a spontaneous and rapid wicking of the entire 0.05-ml. drop into the surface.

Wettability Studies of Bartell and Shepard. In Figures 4 and 5 we have plotted the contact angle data of Bartell and Shepard [2, 3, 11] as a function

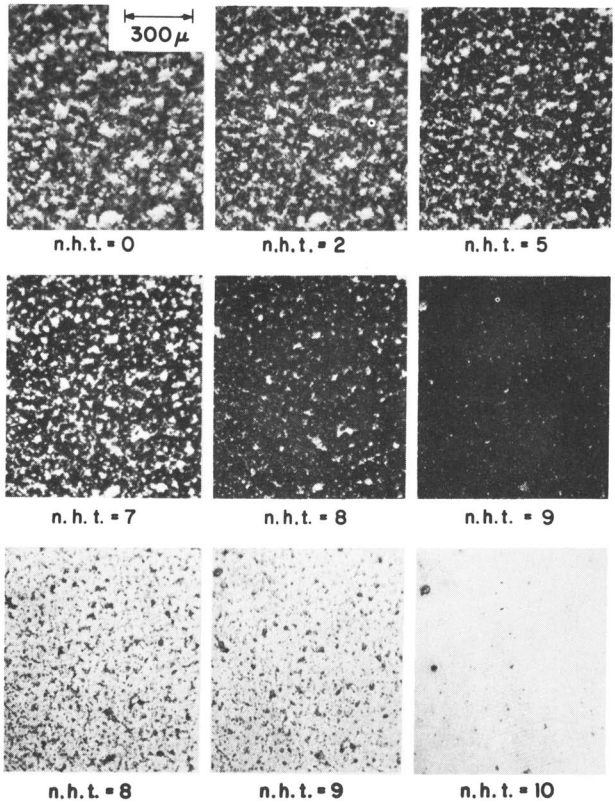

Figure 2. Photomicrographs of TFE-methanol telomer wax surface of Figure 1

n.h.t. No. of heat treatments

Same region of surface shown in each photomicrograph. Transmitted light used for bottom three photomicrographs; others taken with reflected light, with angle of illumination about 15° to plane of wax surface.

of Wenzel's roughness ratio, r, for various liquids on paraffin wax surfaces of controlled roughness. The vertical lines represent the magnitudes of the standard deviations. The values for water in Figure 4 are averages of all their reported data. Although they discarded some extreme values, we have included them, since we believe that a large spread in values is characteristic of such systems. The data were originally reported as a function of the angle of inclination of the sides of the asperities with respect to the horizontal plane of the solid surface; the roughness ratio is equal to the secant of this angle.

Contact Angle Hysteresis on Smooth, Specular Wax Surfaces. The contact angle hysteresis observed on the smooth, specular wax surfaces

Publication Date: January 1, 1964 | doi: 10.1021/ba-1964-0043.ch008

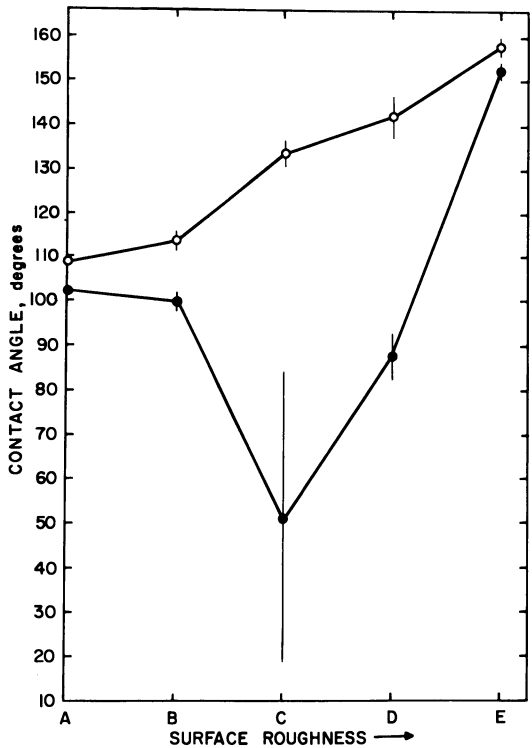

Figure 3. Water contact angles on paraffin wax as a function of surface roughness

○ Advancing angle
● Receding angle

of Table I is probably due to surface heterogeneity. Ray and Bartell [10] have shown that smooth surfaces of purified paraffin wax show no contact angle hysteresis with water. The effect of surface heterogeneity on contact angle hysteresis will be discussed in another article [9].

Discussion

Noncomposite Surfaces. In the noncomposite region of roughness, the wettability behavior of the idealized surface [8] is consistent with the observed behavior described by Figures 1, 3, 4, and 5–i.e., the advancing angles increase and the receding angles decrease with increasing roughness. In Figures 4 and 5 the observed advancing angles are all less than the maximum possible value, ϕ_{max}, calculated from the geometry of the surface and the receding angles (nonzero values) are all greater than the minimum possible value, ϕ_{min}. The existence of energy barriers which increase in height below ϕ_{max} and above ϕ_{min}, and the concept that the observed advancing and receding angles are determined by a balance between the vibrational energy of the drop and the heights of these barriers, can explain these observations.

Publication Date: January 1, 1964 | doi: 10.1021/ba-1964-0043.ch008

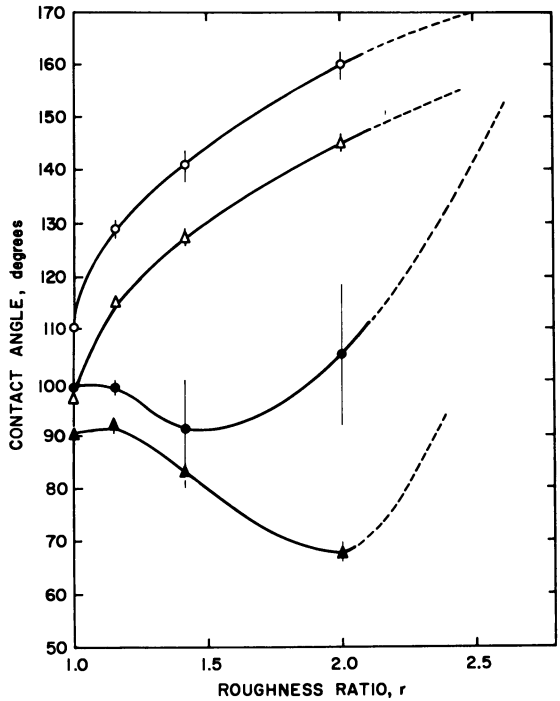

Figure 4. Data of Bartell and Shepard plotted against roughness ratio

○ Advancing angles for water
● Receding angles for water
△ Advancing angles for glycerol
▲ Receding angles for glycerol

The decrease in advancing angle for methanol on paraffin wax (Figure 5) can be accounted for by surface wicking. In the present study, whenever surface wicking occurred on rough wax surfaces, the advancing angle always decreased with time. Considering the geometry of the surfaces studied by Bartell and Shepard, one would expect the rate of wicking to increase with roughness so that the observed angle would appear to decrease with roughness. The condition for wicking [8] requires that r = 1.35 for methanol on paraffin wax. The decrease in advancing angle in Figure 5 begins somewhere between r = 1.16 and r = 1.41.

Composite Surfaces. In Figures 1 and 3 the increase in receding angle with increasing roughness reflects transitions from noncomposite to composite surfaces. The accompanying decrease in contact angle hysteresis is in agreement with the idealized model [8], which explains this effect on the basis of a drastic decrease in the heights of the energy barriers separating metastable drop configurations. The very high angles shown here are similar to those observed by Cassie and Baxter on paraffin-coated wire gratings [6]. The good agreement which they

Publication Date: January 1, 1964 | doi: 10.1021/ba-1964-0043.ch008

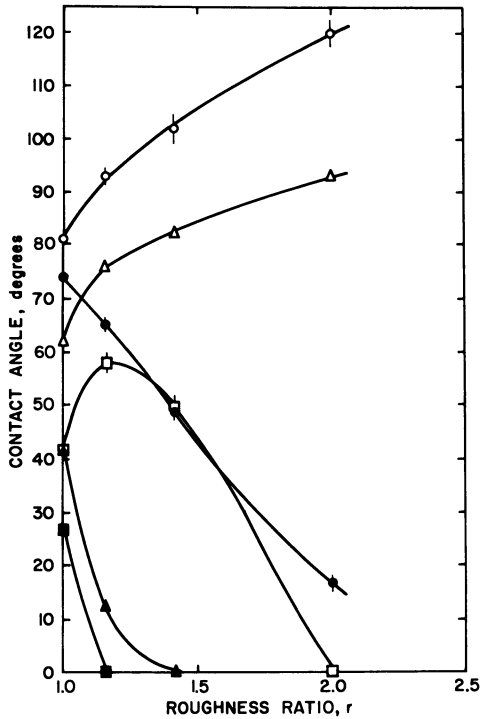

Figure 5. Data of Shepard and Bartell plotted against roughness ratio

○ Advancing angles for ethylene glycol
● Receding angles for ethylene glycol
△ Advancing angles for methyl Cellusolve
▲ Receding angles for methyl Cellosolve
□ Advancing angles for methanol
■ Receding angles for methanol

found between measured angles and those calculated from their equation is consistent with the existence of small energy barriers for composite surfaces.

The results of Bartell and Shepard for water on rough paraffin wax surfaces show the increase in receding angle (Figure 4) anticipated for the formation of a composite surface. The dashed lines in Figure 4 represent possible angles for higher roughness ratios. An increase in receding angle with roughness for 3M calcium chloride solutions on paraffin wax surfaces, reported by Bartell and Shepard [3], is also due to the composite nature of the surface under the liquid drop.

Comparison of Idealized, Rough Surface with Real Surfaces. An essential difference between an actual, rough surface and the idealized model [8] is that the former is usually a random distribution of surface

projections or asperities, but the latter consists of a system of concentric crests and troughs. Another difference is that the idealized system ignores gravity. The pressure of the liquid will cause increased penetration into a composite surface. This accounts for the increase in hysteresis with drop size which was described previously. The pressure of the liquid will also tend to increase the rate of surface wicking. Both of the above effects are accentuated when the spacing between asperities becomes large. A third difference, of lesser importance, is the fact that a real surface has a wide range of asperity heights but the idealized surface does not.

Consider a liquid drop on an idealized surface and on a real surface, both surfaces having identical average asperity heights and roughness ratios. The angle, $\hat{\phi}$, calculated from Wenzel's equation or from the equation of Cassie and Baxter, is the same for both systems. Both have metastable states on either side of $\hat{\phi}$, with energy barriers separating them. When a liquid drop spreads over the real surface, liquid moves between the asperities as well as over them, but on the idealized surface liquid movement can take place only over the crests. This should cause the energy barriers for the real surface to be lower than those for the idealized model. Even though this results in smaller hysteresis for the real surface, the qualitative behavior of the two will be the same.

Publication Date: January 1, 1964 | doi: 10.1021/ba-1964-0043.ch008

Literature Cited

(1) Allan, A. J. G., Roberts, R., J. Polymer Sci. 31, 1 (1959).
(2) Bartell, F. E., Shepard, J. W., J. Phys. Chem. 57, 211 (1953).
(3) Ibid., p. 455.
(4) Bikerman, J. J., Ibid., 54, 653 (1950).
(5) Brady, J. D. (to E. I. du Pont de Nemours & Co.), U. S. Patent 3,067,262 (1962).
(6) Cassie, A. B. D., Baxter, S., Trans. Faraday Soc. 40, 546 (1944).
(7) Fox, H. W., Zisman, W. A., J. Colloid Sci. 5, 514 (1950).
(8) Johnson, R. E., Jr., Dettre, R. H., Advan. Chem. Ser., No. 43, 112 (1963).
(9) Johnson, R. E., Jr., Dettre, R. H., to be published.
(10) Ray, B. R., Bartell, F. E., J. Colloid Sci. 8, 214 (1953).
(11) Shepard, J. W., Bartell, F. E., J. Phys. Chem. 57, 458 (1953).
(12) Shuttleworth, R., Bailey, G. L. J., Discussions Faraday Soc. 3, 16 (1948).
(13) Spiegler, L. (to E. I. du Pont de Nemours & Co.), U. S. Patent 3,069,280 (1962).

Received March 22, 1963. Research Contribution No. 345.

9

Upper Limits to the Contact Angles of Liquids on Solids

ELAINE G. SHAFRIN and WILLIAM A. ZISMAN

U. S. Naval Research Laboratory
Washington 25, D. C.

Publication Date: January 1, 1964 | doi: 10.1021/ba-1964-0043.ch009

Graphical plots of the cosine of the equilibrium contact angle *vs.* the difference in the surface tension of a pure liquid and the critical surface tension of wetting of the solid group data for each liquid into a zone bounded by a straight line passing through the origin ($\cos \theta = 1$; $\gamma_{LV} - \gamma_c = 0$). From the parameters defining this straight line the limiting contact angles for each liquid can be estimated. They indicate that the maximum contact angle possible for water is 156°; for hexadecane, 109°. A rectilinear relation between liquid surface tension and the minimum value of ($\gamma_{LV} - \gamma_c$) required for a surface to exhibit a 90° contact angle can be extended to provide a good fit to available data for a pure liquid metal like mercury.

Data on the equilibrium contact angles, θ, at 20°C. obtained under comparable and well-controlled experimental conditions are available for many dozens of pure liquids on over 100 different solid surfaces [26, 32, 33]. In previous studies of wetting the primary interest was in the variation of θ among many liquids with respect to a specific solid surface. This paper concerns the variation in the wetting behavior of a single liquid with respect to many solid surfaces. Specifically, answers are sought to the following questions:

What is the range of contact angles observed experimentally?

What is the effect on the range of contact angles on changing the solid surface composition?

What is the maximum contact angle that can be expected for the specified liquid on any solid surface?

Eight pure liquids (water, methylene iodide, n-hexadecane, formamide, hexachloropropylene, tert-butylnaphthalene, dicyclohexyl, and n-decane) were chosen for this investigation, with special emphasis on the data for the first three.

Water is an obvious choice not only because of the importance of the hydrophobic behavior of organic surfaces in science, technology,

In Contact Angle, Wettability, and Adhesion; Fowkes, F.;
Advances in Chemistry; American Chemical Society: Washington, DC, 1964.

and the arts, but also because of its high surface tension (and the associated large contact angles on many surfaces) and its extremely small molecular size, which makes it capable of penetrating adsorbed monolayers [2] as well as many bulk solids [1, 17].

n-Hexadecane was chosen because it is a nonpolar liquid of low surface tension which is incapable of forming hydrogen bonds and it exemplifies a liquid whose cohesive and adhesive properties are in some ways ideally simple, since only London dispersion forces are usually involved. Although the large size of the hexadecane molecule makes penetration of molecular pores in bulk solids difficult, its linear structure and molecular flexibility make it able to adlineate with itself or with other molecules containing similar molecular chains-e.g., in an adsorbed monolayer of a polar paraffinic compound.

Methylene iodide was chosen as the third reference liquid because, although it has a high surface tension, it cannot adlineate, and its large size and molecular shape generally preclude permeation into closely packed, adsorbed, organic monolayers [19].

Properties of the three liquids of special interest are compared in Table I. The liquid surface tension, γ_{LV}, for these reference liquids covers almost a threefold range at 20°C. In this same range are the surface tensions at 20°C. for the five other freshly purified liquids, formamide, hexachloropropylene, tert-butylnaphthalene, dicyclohexyl, and decane (58.2, 38.1, 33.7, 32.8, and 23.9 dynes per cm., respectively).

TABLE I. Comparison of Physical

Liquid Property	Dimension
Spatial	
Molecular volume at 20°C. (mol. wt./density)	Cu. A./molecule
Minimum effective cross-sectional area	Sq. A./molecule
Dielectric	
Dipole moment at 20°C. (exp. condition)	Debyes
Polarizability	Cu. A.
Capillary	
Surface tension at 20°C.	Dynes/cm.
Spreading behavior on clean, high-energy surfaces	--

[a]Estimated from Stuart-Briegleb ball models.

All of the contact angles included in this paper are for smooth surfaces and were obtained by slowly advancing a sessile drop of the liquid in order to provide a good approximation to the equilibrium contact

Publication Date: January 1, 1964 | doi: 10.1021/ba-1964-0043.ch009

angle. The results were generally free from difficulties with hysteresis and the few exceptions are discussed in the reference papers.

The data were obtained principally from published papers in which are given full details about the preparation and cleaning of the solid surfaces. Two types of monolayer-coated surfaces have not been reported previously. Polydimethylsiloxane films were prepared by contact of freshly acid-cleaned Aloe glass microscope slides with a 2.5×10^{-4} solution (by weight) in benzene of polydimethylsiloxane (DC No. 200; 350 cs. at 25°C.) for 30 minutes. Following retraction of the solution, the monolayer-coated glass slide was heated for 30 minutes at 220°C. Contact angle measurements made after the slide had cooled to 20°C. indicated that γ_c = 24 dynes per cm. Monolayers of selected terminally perfluoroalkyl-substituted undecanoic and hexanoic acids [6] were prepared by adsorption from the melt onto metallographically polished chromium surfaces under conditions identical to those used to prepare films of the terminally perfluoroalkyl-substituted heptadecanoic acids [27].

In the following discussion the low-energy surfaces are grouped into four main classes, based on surface atomic composition. In general, this corresponds to the order of increasing (although overlapping) values of their critical surface tension, γ_c:

Surfaces exposing any F atoms (γ_c = 6 to 31 dynes per cm., with surfaces exposing only F and C atoms having $\gamma_c < 20$ dynes per cm.).

Surfaces exposing only C and H atoms (γ_c = 22 to 35 dynes per cm.).

Properties of Reference Liquids Investigated

Reference Liquid					
Water		Methylene iodide		n-Hexadecane	
30.0	[14]	133.8	[14]	485.2	[14]
7[a]		17[a]		21.3 (liquid) 18.5 (crystal)	[11] [18]
1.84 (gaseous)	[28]	1.14 (in hexane)	[28]	0	[28]
1.48	[20]	12	[22]	30	[13]
72.8	[14]	50.8	[16]	27.6	[29]
Spreading	[8]	Nonspreading	[7, 19]	Spreading	[8]

Surfaces exposing halogen atoms but not including F (γ_c = 38 to 44 dynes per cm.).

Surfaces exposing O or N atoms (γ_c = 35 to 45 dynes per cm.).

Publication Date: January 1, 1964 | doi: 10.1021/ba-1964-0043.ch009

Hydrophobic Behavior of Low-Energy Surfaces

Reliable equilibrium contact angles of water have been reported for over 100 well-defined, low-energy organic-solid surfaces or adsorption-modified high-energy surfaces; of these, data on γ_c are available for at least 60. The cosine of the hydrophobic contact angle of each surface is conveniently plotted in Figure 1,a, against the difference between the surface tension, γ_{LV}, of water and γ_c of the solid. The data in Figure 1,a, are for wetting by only one liquid (water). All but nine of the data were obtained at 20°C.; for nine bulk polymers exposing only C and F atoms the contact angles [3–5] were obtained at 25°C. Since comparison measurements on polytetrafluoroethylene surfaces at 20° and 25°C. indicated that the effect of this small change in temperature on θ does not significantly exceed the experimental error of measurement, the 25°C. data are included in Figure 1,a, even though only a single value of the surface tension of water is used (72.8 dynes per cm. at 20°C.). On the same graph are plotted the values of γ_c decreasing to a zero value toward the right, as shown across the top of the chart. For easy reference, the value of θ is also indicated along the ordinate axis at the right.

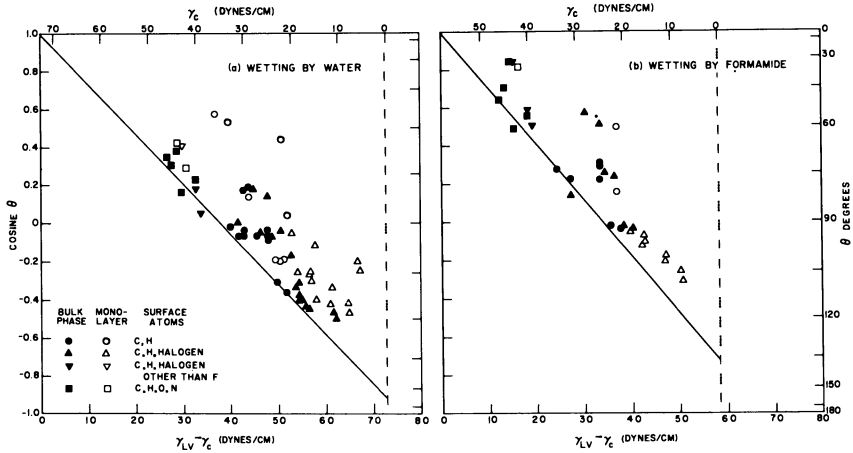

Figure 1. Wetting behavior of hydrogen-bonding liquids on low-energy surfaces of varied surface composition

Each datum point of Figure 1,a, represents the hydrophobic behavior of a single solid surface. Symbols of different shapes distinguish the solid surfaces according to their surface atomic composition. Filled symbols designate surfaces of bulk organic solids (single crystals, polymers, etc.) and open symbols refer to low-energy surfaces created by adsorption of monomolecular films.

The largest water angle observed is 120° on the CF_3-rich surface of a thin coating of a polymethacrylic ester having perfluorinated side chains [5]; close to this is the 118° angle reported for both a related polymeric surface (an acrylic ester with perfluorinated side chains) [5]

and a monolayer of 11-(perfluorodecyl)undecanoic acid adsorbed on a mirror-smooth chromium surface. No hydrophobic angle lower than 108° is found for any homo- or copolymer exposing C and F atoms only; lower angles are invariably obtained upon introducing any additional atomic species.

The second most hydrophobic class of surfaces is the one containing only C and H atoms, but the largest water angles are well below those on the fluorocarbons. The largest contact angle on a hydrocarbon is the 111° obtained on a cleavage plane of a single crystal of n-hexatriacontane [10], a surface comprising $-CH_3$ groups in the highly condensed packing characteristic of the crystal lattice. Hydrophobic angles of 108° to 110° are common on white paraffin surfaces ($-CH_2-$ and $-CH_3$ groups) [10], the higher value of θ resulting when there is a higher concentration of $-CH_3$ groups. The highest water angle observed on a condensed, adsorbed monolayer of polar paraffinic molecules is 101°, the difference between this and 111° reflecting the difference in the packing of the terminal $-CH_3$ groups of aliphatic chains when crystallization does not occur. An identical angle of 101° also is obtained on an adsorbed, condensed monolayer of an open-chain polydimethylsiloxane, indicating that the methyl groups exposed by the silicone film are sufficiently close-packed to shield the Si-O linkages effectively from the wetting interface. The water contact angle drops to 94° for a polyethylene surface, paralleling the decrease in θ observed between a $-CF_3$ and a $-CF_2-$ surface previously noted for fluorocarbon surfaces.

Greater water wettability is observed for surfaces exposing atoms other than C, H, or F. Despite their generally high values of γ_c, these surfaces are still usefully hydrophobic and angles larger than 65° are the rule for surfaces sufficiently insoluble in or impermeable to water to give stable angles showing no hysteresis effects after several minutes' contact with the water drop. The smallest such stable water angle included in Figure 1,a, is 68° for a single crystal of cyclotrimethylene trinitramine (γ_c = 44 dynes per cm.) [9]. Less stable angles are observed for surfaces dissolved by water (cf. poly(vinyl alcohol) with γ_c = 37 dynes per cm. reported by Ray, Anderson, and Scholz [23]).

The distribution of filled and open symbols for surfaces of the same composition indicates that the monolayers generally are less hydrophobic than the atomically comparable bulk solids. This may result from the greater penetration by the water molecules and the possibility that this interstitial water facilitates overturning of the polar molecules in the monolayers as shown by Rideal and Tadayon [24] and more recently by Gaines [12] and Yiannos [31]. The distribution of data points in Figure 1,a, shows that cos θ is larger the closer γ_c is to γ_{LV}. By definition, any solid surface with γ_c exactly equal to or larger than the γ_{LV} of the liquid will be spread upon by that liquid. Hence, water should spread on any surface having $\gamma_c > 72.8$ dynes per cm. This is in good agreement with the well-known spreading of water on high-energy surfaces which are free of organic contamination [8].

As ($\gamma_{LV} - \gamma_c$) increases—i.e., as γ_c decreases—the surfaces become more hydrophobic. At larger values of ($\gamma_{LV} - \gamma_c$) the majority of the data points tend to lie within a relatively narrow range of cos θ values and to concentrate toward the lower end of that range. This is surprising, since a wider range of water contact angles becomes possible as the difference between γ_c and γ_{LV} is increased and there is no

Publication Date: January 1, 1964 | doi: 10.1021/ba-1964-0043.ch009

a priori reason why two different surfaces having the same value of γ_c should necessarily exhibit identical water angles.

An envelope to the minimum cos θ values toward which the data points of Figure 1,a, tend to concentrate can be drawn which is a straight line passing through or close to a large number of experimental points as well as through the point cos $\theta = 1$; $(\gamma_{LV} - \gamma_c) = 0$ as required by theory. Despite the extreme variations in surface chemical composition and hydrophobic behavior, an empirical relation as simple as a straight line appears to represent adequately the minimum cos θ observed experimentally for water. As drawn in Figure 1,a, this limiting envelope lies on or below all but two of the data points [for poly(ethylene terephthalate) and poly(vinyl chloride)] and these also are close–i.e., within 3° to 4° of falling on the line. Thus it appears possible to predict what the maximum water contact angle might be for a surface having a given value of γ_c; of course, the actual angle may prove smaller. Conversely, for any specific value of θ–e.g., $\theta \geq 90°$ to prevent capillary penetration–the intersection of the limiting line of Figure 1,a, with the appropriate ordinate–e.g., cos 90°–provides an indication of the smallest difference between γ_c and γ_{LV} for which an angle of 90° is possible–namely, $\gamma_{LV} - \gamma_c = 38.2$ dynes per cm. The existence of this minimum difference eliminates from consideration surfaces for which $(\gamma_{LV} - \gamma_c) < 38.2$ dynes per cm. and, hence, for which $\gamma_c > 34.6$ dynes per cm. Finally, by extrapolation of this limiting line to the maximum possible value of $(\gamma_{LV} - \gamma_c)$ (see vertical dashed line of Figure 1,a), which corresponds to allowing γ_c to approach zero, the maximum hydrophobic contact angle possible appears to be 156°.

Wetting of Low-Energy Surfaces by Methylene Iodide

Equilibrium contact angle data are available for methylene iodide on a somewhat smaller number of solid surfaces than for water (about 80); they range from a maximum of 101° to 103° on a condensed film of $-CF_3$ terminal groups to a minimum of 29° on surfaces not dissolved or attacked by the sessile drop [poly(vinylidene chloride), $\gamma_c = 40$ dynes per cm.].

In Figure 2,a, are plotted the data for methylene iodide comparable to those for water in Figure 1,a; in general, the distribution of data points is similar. The group of surfaces exhibiting maximum hydrophobicity also exhibits the largest methylene iodide contact angles: $\theta \geq 90°$ on condensed $-CF_3$ groups, whether bulk material–e.g., polyhexafluoropropylene–or monolayers comprising molecules with terminal perfluoroalkyl groups of five or more carbon atoms. For monolayers with perfluoroalkyl moieties shorter than this and for polymers with significant proportions of $-CF_2-$ groups, $\theta < 90°$. The lowest θ on a bulk surface comprising only C and F atoms is 82° [3]. Contact angles on hydrocarbon surfaces, although large, are far lower than those on fluorinated surfaces. The largest methylene iodide contact angle on a hydrocarbon surface is only 77° for the CH_3-rich surface of a single crystal [10]; a maximum value of 71° is characteristic of close-packed monolayers of adsorbed aliphatic derivatives [19], again showing the sensitivity of θ to the packing of the terminal methyl groups.

In Figure 2,a, as in Figure 1,a, the lower limit to the data is well represented by a straight line passing through the point cos $\theta = 1$;

Publication Date: January 1, 1964 | doi: 10.1021/ba-1964-0043.ch009

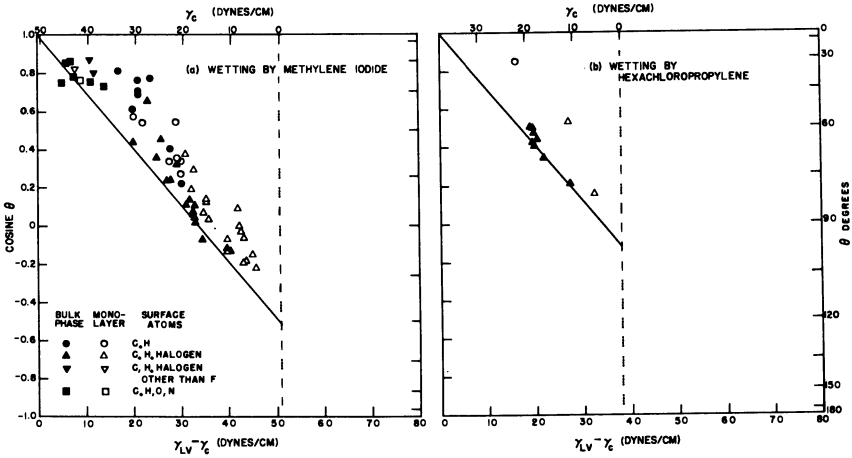

Figure 2. Wetting behavior of halocarbons on low-energy surfaces of varied surface composition

$(\gamma_{LV} - \gamma_c) = 0$. Although the datum point for any given solid surface necessarily lies closer to the left side of Figure 2,a, than in Figure 1,a, comparison of the two figures reveals that, for any given difference between γ_{LV} and γ_c, methylene iodide exhibits a larger contact angle than does water. Since the slope of the limiting straight line is steeper for methylene iodide than for water, the value of $(\gamma_{LV} - \gamma_c)$ required for methylene iodide to exhibit a particular contact angle is less than for water. Accordingly, a surface must have $\gamma_c < 17$ dynes per cm. for a 90° methylene iodide angle, whereas the corresponding value for a 90° water angle is $\gamma_c < 34.6$ dynes per cm. If the limiting straight line of Figure 2,a, is extrapolated to the maximum possible value of $(\gamma_{LV} - \gamma_c)$, a maximum value of $\theta = 121°$ is indicated for methylene iodide on a hypothetical surface for which $\gamma_c = 0$. Thus, although the limiting line is steeper than for water, it terminates before intersecting the $\cos \theta = -1$ axis and indicates a maximum angle which is smaller than that indicated for water.

Wetting of Low-Energy Surfaces by n-Hexadecane

In Figure 4,a, is a similar plot of $\cos \theta$ vs. $(\gamma_{LV} - \gamma_c)$ for n-hexadecane. There are fewer data points because there are not many low-energy surfaces with values of γ_c less than the surface tension of hexadecane–i.e., relatively few types of surfaces exhibit nonzero contact angles to hexadecane or other low-surface-tension oils. On the basis of their γ_c values, only two major classes of surfaces can be expected to exhibit substantial oil contact angles: the hydrocarbon surfaces and the fluorine-containing surfaces, providing no other types of halogen atoms are present.

The largest hexadecane angles observed experimentally range from 75° to 78° on surfaces comprising condensed $-CF_3$ groups; the largest angle on a hydrocarbon surface (46°) is obtained on the analogous

Publication Date: January 1, 1964 | doi: 10.1021/ba-1964-0043.ch009

CH_3- surfaces. A straight line can be drawn which passes through or close to many of the data points in Figure 4,a, representing the minimum values of cos θ observed for hexadecane on various solid surfaces. The scatter of the data points relative to this straight line is less than for water or methylene iodide and there is no consistent displacement of open symbols relative to filled symbols (distinguishing between monolayer-coated and bulk surfaces) for atomically comparable surfaces as was observed for the former two liquids.

Only London dispersion force (or induced polarization) interactions with the solid surface are possible for a liquid like hexadecane which has no permanent electric moment and is not capable of hydrogen-bond formation. The data points representing its wetting behavior must therefore lie very close to the straight-line cos θ vs. γ_{LV} relations used to determine the values of γ_c for the different solid surfaces. When such data are transformed to plots of cos θ vs. $(\gamma_{LV} - \gamma_c)$, coincidence of the data points at any single value of $(\gamma_{LV} - \gamma_c)$ is possible only for those systems having identical cos θ vs. γ_{LV} relations (a common occurrence, to judge from many of the data in Figure 4,a). A second consequence of the transformation is that a straight-line relation between cos θ and $(\gamma_{LV} - \gamma_c)$ is possible only if the original cos θ vs. γ_{LV} relations are parallel, the slope of the cos θ vs. $(\gamma_{LV} - \gamma_c)$ relation being identical to the slopes of the set of parallel relations. Thus, the strong tendency of the data of Figure 4,a, to cluster along a single straight line shows how nearly parallel many of the cos θ vs. γ_{LV} relations are, despite wide variations in solid surface composition and physical form. The clustering of data points toward the lower values of cos θ indicates that the steeper slopes are the more characteristic for cos θ vs. γ_{LV} relations for the n-alkanes. Indeed, the narrow radial spread of the data in Figure 4,a, is indicative of how small or how constant is the interfacial tension γ_{SL} between hexadecane and most low-energy surfaces. This is in contrast with the data for a hydrogen-bonding liquid like water, for example, which show (Figure 1,a) considerable radial divergence.

The slope of the limiting line in Figure 4,a, is even steeper than that observed in Figure 1,a, or 2,a. In order for hexadecane to exhibit a contact angle of 90° on a solid surface, the difference between γ_c and γ_{LV} needs only to be larger than 20.8 dynes per cm.; however, this corresponds to requiring that the solid surface have a critical surface tension of 6.8 dynes per cm. or less. Extrapolation of the linear relation to its termination at the maximum possible value of $(\gamma_{LV} - \gamma_c)$, which is γ_{LV}, indicates that the largest hexadecane angle possible would be 109° on a hypothetical surface of zero critical surface tension.

Limiting Wetting Behavior of Other Liquids on Low-Energy Surfaces

Similar plots were prepared to the same scale for five additional organic liquids: formamide (Figure 1,b), hexachloropropylene (Figure 2,b), tert-butylnaphthalene (Figure 3,a), dicyclohexyl (Figure 3,b), and n-decane (Figure 4,b). Fewer data are available for each of these liquids than for water, methylene iodide, or hexadecane, but the resulting plots all show the same characteristic features and are therefore treated analogously. The sequence of graphs in Figures 1 to 4 is arranged in the order of decreasing surface tension of the reference liquid. This is

Publication Date: January 1, 1964 | doi: 10.1021/ba-1964-0043.ch009

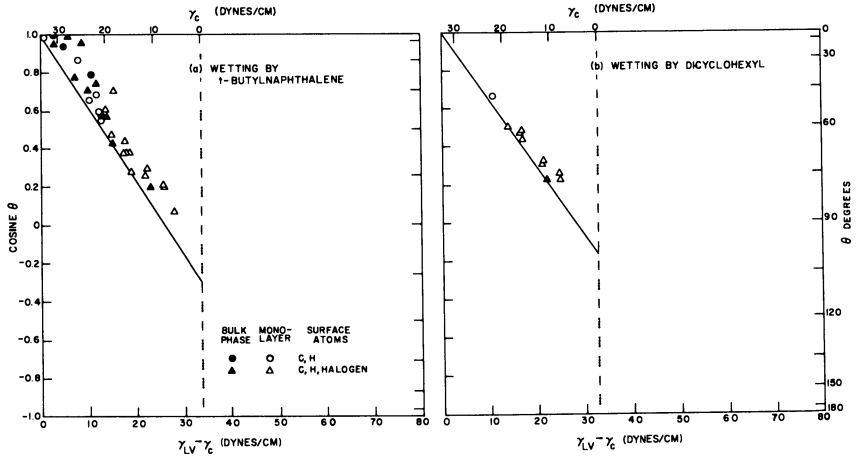

Figure 3. Wetting behavior of cyclic hydrocarbons on low-energy surfaces of varied surface composition

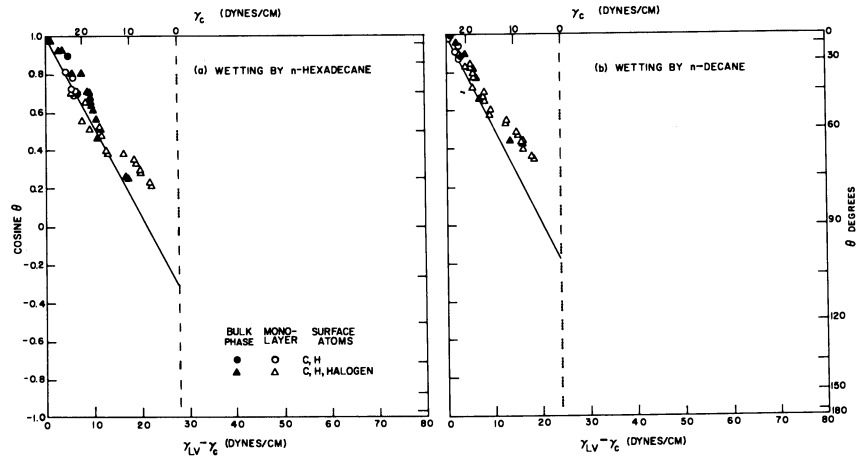

Figure 4. Wetting behavior of aliphatic hydrocarbons on low-energy surfaces of varied surface composition

found to be the same order in which the slope of the limiting straight line becomes steeper; also, it is approximately the order of the decrease in the maximum contact angle possible on a hypothetical surface of zero critical surface tension.

Relatively few data are available for the wetting of low-energy surfaces by liquid metals. Reliable contact angles are available, however, for mercury (γ_{LV} = 485 dynes per cm.) on three different surfaces. When plotted as a function of ($\gamma_{LV} - \gamma_c$), their data points suggest that a linear limiting relation also characterizes the wetting properties of this liquid metal.

Publication Date: January 1, 1964 | doi: 10.1021/ba-1964-0043.ch009

Discussion

The same general pattern in plots of cos θ vs. $(\gamma_{LV} - \gamma_c)$ appears characteristic of the available data for the nine liquids discussed here. Furthermore, the parameters involved in the straight lines bounding such plots show systematic changes with the surface tension of the reference liquid. Thus, as γ_{LV} decreases, the slope of the limiting straight line becomes greater, there is a decrease in the value of $(\gamma_{LV} - \gamma_c)$ required for a liquid to exhibit any given contact angle, and the maximum contact angle indicated for a hypothetical surface with $\gamma_c = 0$ tends to become smaller.

The effect of the liquid surface tension on the minimum value of $(\gamma_{LV} - \gamma_c)$ required for $\theta = 90°$ is illustrated in Figure 5. Each datum point corresponds to a single reference liquid. The data for all nine liquids (from decane with the lowest value of γ_{LV} to mercury with the highest) plot very close to a straight line passing through the origin at $\gamma_{LV} = 0$. This result is remarkable when it is realized that γ_{LV} varies by 25-fold. Among the nine liquids studied, the minimum value of $(\gamma_{LV} - \gamma_c)$ required for a 90° contact angle was never less than half of the surface tension of the liquid; thus, the slope of the line in Figure 5 is close to, but not quite as low as one half. From these data there results the following interesting generalization for the design of solid-liquid systems in which capillary penetration is not possible–i.e., $\theta \geq 90°$–the minimum value of $(\gamma_{LV} - \gamma_c)$ which is required to get a 90° contact angle must be more than half of the surface tension of the liquid and therefore the solid must be chosen for which γ_c is less than $1/2\ \gamma_{LV}$.

In Figure 5 a slight displacement upward (relative to the straight line) is observed for data points for some of the liquids of low γ_{LV}.

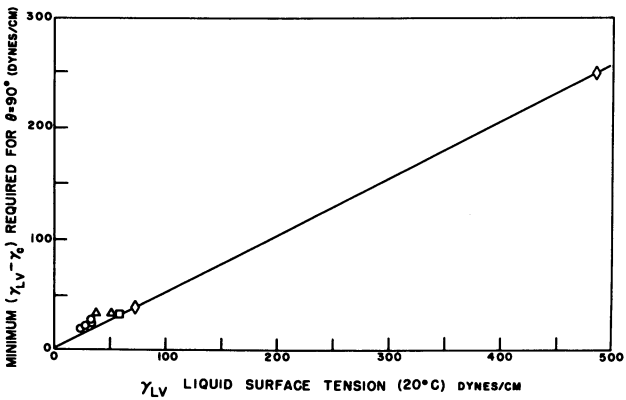

Figure 5. Effect of liquid surface tension on a parameter characterizing limiting wetting behavior

O *Hydrocarbons*
△ *Halocarbons*
□ *Formamide*
◇ *Water and mercury*

Publication Date: January 1, 1964 | doi: 10.1021/ba-1964-0043.ch009

For these liquids, the minimum difference between γ_{LV} and γ_c required for $\theta = 90°$ corresponds to a fraction of γ_{LV} larger than half and hence to a proportionately smaller γ_c ($<< 1/2\,\gamma_{LV}$). Since γ_{LV} is already small for these liquids, this is a serious limitation; relatively few surfaces are available for which γ_c is of the order of only a few dynes per centimeter. For example, the data of Figure 4,b, for n-decane indicate that, although a maximum contact angle of 100° is indicated for a hypothetical surface having $\gamma_c = 0$, a solid would require $\gamma_c < 3.6$ dynes per cm. before there was any chance for decane to exhibit a 90° contact angle. The largest angle observed experimentally for decane is 70° on a perfluorolauric acid monolayer with $\gamma_c = 5.6$ dynes per cm. [15].

The maximum contact angle for a hypothetical surface having $\gamma_c = 0$ also shows a marked dependence on γ_{LV} (Figure 6), increasing rapidly with the surface tension at low values of γ_{LV}, but becoming nearly constant at higher values. From the curve in Figure 6 a rough estimate can be made of the maximum contact angle for a liquid of any given surface tension on the least wettable surface ($\gamma_c = 0$); additionally, one can indicate the liquids for which a contact angle as large as 90° is not possible—namely, those with surface tensions less than about 20 dynes per cm. To indicate how realistic these maximum contact angles are, there are plotted in Figure 6 data points corresponding to the largest contact angles observed experimentally at this laboratory for each liquid on a surface for which critical surface tensions have been determined. These experimental values show the same correlation with γ_{LV} as do the values of the limiting contact angles extrapolated to $\gamma_c = 0$, although they are invariably smaller, since no real surface is available for which $\gamma_c = 0$. Examples of real surfaces having critical surface tensions approaching zero are the adsorbed monolayers of fully fluorinated acids, which show a linear decrease in γ_c with increasing chain length, N [27], for homologs through perfluorolauric acid ($\gamma_c = 5.6$ dynes per cm.) [15];

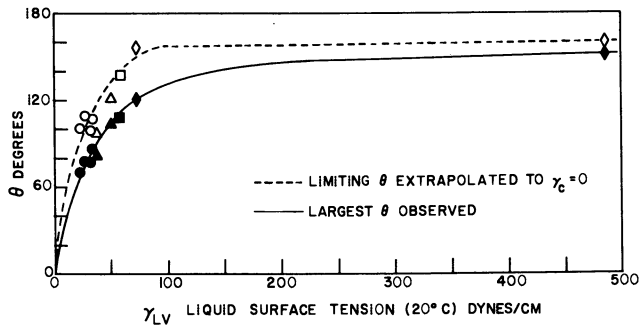

Figure 6. Effect of liquid surface tension on maximum contact angles

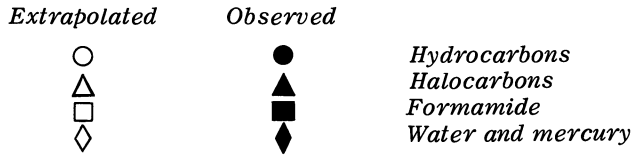

Publication Date: January 1, 1964 | doi: 10.1021/ba-1964-0043.ch009

if this γ_c vs. N relation is extrapolated linearly, it intersects the $\gamma_c = 0$ axis at a value of N corresponding to an acid slightly more than 24 carbon atoms long. The cos θ vs. N data for hexadecane on perfluorinated acid monolayers are essentially linear through N = 12; extrapolation to N = 24 leads to a maximum contact angle of 92°. This is larger than the 78° observed experimentally on perfluorolauric acid monolayers but is still considerably smaller than the 109° predicted as the limiting angle on a surface of $\gamma_c = 0$.

These values are of interest when compared with the contact angles recently reported by Ryan, Kunz, and Shepard for N-ethyl-N-perfluorooctane-sulfonylglycine monolayers chemisorbed on the one metal, aluminum [25]. Their hexadecane contact angle of 110° is larger than any previously reported and is close to the limiting maximum indicated in Figure 6. The same surface, however, exhibited a methylene iodide contact angle of 160°, far above the limiting angle predicted here of 121°. This suggests that although the adsorption experiments were carried out on initially smooth metal surfaces, chemisorption may have resulted in sufficient roughening of the surface to enhance the observed contact angle in accordance with Wenzel's equation [30]. If this is the explanation of the remarkably large apparent contact angles obtained, it indicates that the true angle for hexadecane on a completely smooth surface would still have to exceed 90°.

Relations of the types graphed in Figures 5 and 6 are suggestive and may prove useful in predicting the limiting wetting behavior of new or unusual liquids. Using the surface tension value for gallium of 735 dynes per cm. [21], extrapolation of the graphical relation in Figure 5 indicates that a minimum value of $(\gamma_{LV} - \gamma_c)$ of more than 373 dynes per cm. would be required for gallium to exhibit a contact angle of 90°; this corresponds to a surface for which γ_c needs to be less than 362 dynes per cm. The largest gallium contact angle possible on polyethylene (γ_c = 31 dynes per cm.) is 153°, while that for Teflon (γ_c = 18.5 dynes per cm.) is 157°. The maximum possible contact angle on a surface having $\gamma_c = 0$ is 163°, only slightly larger than that for mercury (160°) despite the 50% increase in liquid surface tension.

Literature Cited

(1) Adam, N. K., Elliott, G. E. P., J. Chem. Soc. (London) 1962, 2206.
(2) Baker, H. R., Shafrin, E. G., Zisman, W. A., J. Phys. Chem. **56**, 405 (1952).
(3) Bernett, M. K., Zisman, W. A., Ibid., **64**, 1292 (1960).
(4) Ibid., **65**, 2266 (1961).
(5) Ibid., **66**, 1207 (1962).
(6) Brace, N. O., J. Org. Chem. **27**, 4491 (1962).
(7) Cottington, R. L., Shafrin, E. G., Zisman, W. A., J. Phys. Chem. **62**, 513 (1958).
(8) Fox, H. W., Hare, E. F., Zisman, W. A., Ibid., **59**, 1097 (1955).
(9) Fox, H. W., Levine, O., U.S. Naval Research Laboratory, Washington, D.C., private communication.
(10) Fox, H. W., Zisman, W. A., J. Colloid Sci. **7**, 428 (1952).
(11) Francis, F., Piper, S. H., "Applications of the X-Ray Method to the Study of the Paraffin Hydrocarbons," p. 1203, in A. E. Dunstan, A. W. Nash, B. T. Brooks, H. T. Tizard, eds., "Science of Petroleum, Vol. II," Oxford University Press, London, 1938.
(12) Gaines, G. L., Jr., Nature **186**, 384 (1960).
(13) Groves, L. G., Sugden, S., J. Chem. Soc. (London) 1937, 1992.

Publication Date: January 1, 1964 | doi: 10.1021/ba-1964-0043.ch009

(14) "Handbook of Chemistry and Physics," 42nd ed., Chem. Rubber Pub. Co., Cleveland, Ohio, 1960-61.
(15) Hare, E.F., Shafrin, E. G., Zisman, W. A., J. Phys. Chem. 58, 236 (1954).
(16) International Critical Tables, McGraw-Hill, New York, 1922.
(17) Kawasaki, K., J. Colloid Sci. 17, 169 (1962).
(18) Kurz, S. S., Jr., Sankin, A., "Density and Refractive Index of Hydrocarbons," p. 27 in A. Farkas, ed., "Physical Chemistry of the Hydrocarbons," Vol. II, Academic Press, New York, 1953.
(19) Levine, O., Zisman, W. A., J. Phys. Chem. 61, 1068 (1957).
(20) London, F., Trans. Faraday Soc. 33, 8 (1937).
(21) Mack, G. L., Davis, J. K., Bartell, F. E., J. Phys. Chem. 45, 846 (1941).
(22) Miller, G. A., Bernstein, R. B., Ibid., 63, 710 (1959).
(23) Ray, B. R., Anderson, J. R., Scholz, J. J., Ibid., 62, 1220 (1958).
(24) Rideal, E., Tadayon, J., Proc. Roy. Soc. (London) A225, 346 (1954).
(25) Ryan, J. P., Kunz, R. J., Shepard, J. W., J. Phys. Chem. 64, 525 (1960).
(26) Shafrin, E. G., Zisman, W. A., Ibid., 64, 519 (1960).
(27) Ibid., 66, 740 (1962).
(28) Stuart, H. A., "Die Struktur des Freien Moleküls," Springer-Verlag, Berlin, 1952.
(29) Vogel, A. I., J. Chem. Soc. (London) 1946, 133.
(30) Wenzel, R. N., Ind. Eng. Chem. 28, 988 (1936).
(31) Yiannos, P. N., J. Colloid Sci. 17, 334 (1962).
(32) Zisman, W. A., "Relation of Chemical Constitution to the Wetting and Spreading of Liquids on Solids," p. 30, in "A Decade of Basic and Applied Science in the Navy," U.S. Government Printing Office, Washington, D. C., 1957.
(33) Zisman, W. A., Advan. Chem. Ser., No. 43, 1 (1963).

Received May 8, 1963

10

Evidence for Solid-Fluid Interfacial Tensions from Contact Angles

J. C. MELROSE

Field Research Laboratory
Socony Mobil Oil Co., Inc.
Dallas, Tex.

Publication Date: January 1, 1964 | doi: 10.1021/ba-1964-0043.ch010

Contact angle data for several low energy solids are examined, to estimate surface tensions for the bare solid, and solid-liquid interfacial tensions. A basic assumption is that film pressures for organic liquids may not be neglected. Evidence for this assumption is reviewed. In particular, information derived from contact angle observations involving two immiscible liquids is employed. For the solid-liquid interfacial tensions, estimates are obtained from experiments involving crystallization rate phenomena. Using these results and the assumptions, the surface tensions for the bare solids are estimated to be: polytetrafluoroethylene, 34; paraffin, 45; and polyethylene, 55 dynes per cm. The contact angle observations reported by Zisman and coworkers for homologous series of compounds are also discussed. The conclusion is that, when spreading occurs, Young's equation is no longer applicable.

Contact angle measurements represent one of the oldest techniques for studying the nature of solid surfaces. Yet, until the recent contributions of Zisman and coworkers [13, 14, 25, 26, 27, 32–35, 41, 60, 61, 69], surprisingly little progress in the interpretation and use of such measurements had been made. Even at present, there is no general agreement as to the magnitude of the solid-vapor or solid-liquid interfacial tensions for any solid for which reliable contact angle observations have been reported. However, if Young's equation is to be believed, the magnitude of the contact angle in a given case depends directly upon the values of these two parameters. Thus, there is yet to be achieved a systematic approach to the use of such data, when reliable values for the tensions subsisting in solid-fluid interfaces are desired.

In Contact Angle, Wettability, and Adhesion; Fowkes, F.;
Advances in Chemistry; American Chemical Society: Washington, DC, 1964.

The difficulty encountered is well known. The use of Young's equation together with measured values of the contact angle must be supplemented by some additional technique or approach. The latter must yield information as to the value of one or the other of the two interfacial tensions involving the solid surface. To date suitable techniques have not been devised.

The purpose of the present work is to bring together and to examine and assess information from several sources which bear upon this problem. Evidence is presented which leads to the estimation of values for the solid-vapor and solid-liquid tensions for several cases of interest. The values thus obtained, although tentative, are consistent with a wide range of experimental facts.

Relevant to the arguments put forward is the relationship introduced by Girifalco and Good [36, 39]. Their expression relates the interfacial tension for two immiscible liquid phases to the surface tensions of the individual liquids. The application of this approach to the interpretation of contact angle data was suggested in a later paper by these authors [38]. Our approach, however, is developed under somewhat different basic assumptions and with rather different results.

Any discussion leading to the interpretation of contact angle measurements, such as that presented below, presupposes the existence of a body of reliable experimental data. Such data are now available, due to the efforts of Zisman and his collaborators at the Naval Research Laboratory. This situation is the result of solving a number of problems connected with the preparation of suitable solid surfaces. These problems had presented major difficulties in the field of contact angle studies ever since its inception and hence had prevented any substantial progress.

In addition to overcoming experimental difficulties, the Naval Research Laboratory group has contributed many important generalizations and new concepts–for example, the concepts of low energy solid [33, 69], critical surface tension [33, 61], and autophobic liquid [32, 41]. These developments have also stimulated the search for an interpretative scheme capable of yielding values of solid-vapor and solid-liquid interfacial tensions.

Such an objective implies, of course, an acceptance of the validity of Young's equation. (Although recent literature frequently refers to this relation as the Young-Dupré equation, no support for this designation may be obtained from any adequate review of the classical work in this field, such as that of Bakker [4]. If any modification is justified, it would seem far more suitable to refer to the relation as the Young-Gauss equation.) Support for this standpoint is provided by several recent discussions [21, 47, 49, 50, 52] of the theoretical foundation of the equation. Lester [49], in particular, has investigated the inadequacy of Young's equation when the solid phase is appreciably deformable. In this connection the experiments with silica aquagels reported by Michaels and Dean [53] are of interest. The evidence provided by these experiments suggests that in most cases the defect in Young's equation arising from solid phase deformability is not important.

The exhaustive theoretical study of fluid interfaces, which is due to Buff [17], has clarified the complementary roles of hydrostatics and thermodynamics in the theory of capillarity. More importantly, the relationship of these phenomenological descriptions to rigorous molecular

Publication Date: January 1, 1964 | doi: 10.1021/ba-1964-0043.ch010

theory is developed. In particular, the concepts of superficial tension and surface free energy, long confused in the literature, have been carefully and precisely differentiated.

The viewpoint regarding Young's equation which follows from Buff's investigation is that it provides the condition for hydrostatic equilibrium at the three-phase line of contact, or confluent zone, at which a meniscus meets a solid surface. Young's equation thus constitutes a one-dimensional principle of hydrostatics, analogous to Laplace's equation for fluid interfaces and to Pascal's law for bulk fluids. The surface and/or interfacial tensions in the equation refer specifically to the matter in the immediate neighborhood of the confluent zone. This local nature of the equilibrium condition given by Young's equation has important consequences for the interpretation of contact angle data, as indicated below.

Publication Date: January 1, 1964 | doi: 10.1021/ba-1964-0043.ch010

Notation and Nomenclature

Notation. The usual discussion of the thermodynamic surface properties involved in Young's equation and related expressions employs a notation which is at best unwieldy. We introduce in the present discussion, therefore, a notation which appears to be somewhat simpler than those previously used.

To handle the case of two immiscible liquid phases, in contact with each other and with a solid phase, it is necessary from the outset to distinguish between them. Hence, such phases are denoted by subscripts 1 and 2. Phase 1 is taken to be that having the larger surface tension. Each of the two liquids is either pure, and hence has but a single component, or is saturated with the other liquid. Subscripts 1 and 2 then refer also to components 1 and 2. Finally, the solid phase is denoted by subscript 3. It is assumed that this phase is composed of a single component, which furthermore exists neither in the vapor nor in either liquid phase.

A property referred to the interface between a given pure phase and its vapor is denoted by a single subscript. When the property refers to the interface between two phases, a double subscript is used. Either of the liquid phase components can, by adsorption from the vapor, modify the surface properties of the other liquid or of the solid. In similar fashion, adsorption from one of the liquid phases, when it is saturated with the other liquid, can modify the solid-liquid interfacial properties of that liquid. The surface and interfacial properties so modified are denoted by a subscripted comma, followed by 1 or 2, denoting the component adsorbed.

Nomenclature. To illustrate the notation adopted, let us write Young's equation for the three cases of interest. Using σ to denote either surface or interfacial tension and θ to denote the contact angle, we have (see Figure 1):

$$\sigma_{3,i} = \sigma_{i3} + \sigma_i \cos \theta_{i3} \quad (i = 1, 2) \tag{1a}$$

$$\sigma_{13,2} = \sigma_{23,1} + \sigma_{12} \cos \theta_{123} \tag{1b}$$

Here, the subscripts used for the contact angles denote either an angle measured through the liquid phase, for a single liquid in contact with

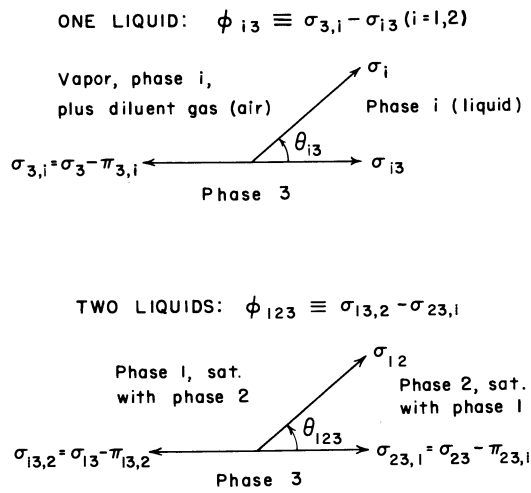

Figure 1. Notation and rector diagrams for Young's equation

the solid (two subscripts), or else, for two liquids in contact, an angle measured through the phase denoted by the middle subscript.

In accord with the critique of Young's equation introduced by Bangham and Razouk [7], Equations 1 explicitly recognize the adsorption of components 1 and 2 at the appropriate interfaces. The notation just discussed permits this to be done with economy and precision.

It is, of course, understood that Equations 1 are subject to the following conditions:

$$\sigma_i \geq |\sigma_{3,i} - \sigma_{i3}| \quad (i = 1, 2) \tag{2a}$$

$$\sigma_{12} \geq |\sigma_{13,2} - \sigma_{23,1}| \tag{2b}$$

These conditions arise from the interpretation of Young's equation as a condition for hydrostatic equilibrium at a three-phase line of contact. (The general status of conditions for hydrostatic equilibrium in the theory of capillarity is fully discussed by Buff [17].) When spreading occurs, such an equilibrium is not established. Hence, Young's equation is not applicable.

One may thus interpret Equations 2, written with the inequality signs, as giving the condition for nonspreading, while the equality signs refer to a condition of metastable spreading. Some authors have accepted the validity of Young's equation even in the absence of an equilibrium situation involving a three-phase line of contact. This point of view and evidence suggesting that it is not generally correct are discussed below. There may, of course, arise cases of spreading where Equations 2, written with the equality signs, may be approximately true.

We now turn to the representation of the film pressures associated with the adsorption processes at the various interfaces so far considered. Taking the symbol π to indicate a film pressure, the usual definitions give

Publication Date: January 1, 1964 | doi: 10.1021/ba-1964-0043.ch010

$$\pi_{3,i} = \sigma_3 - \sigma_{3,i} \qquad (i = 1, 2) \tag{3a}$$

$$\pi_{i3,j} = \sigma_{i3} - \sigma_{i3,j} \qquad (i,j = 1, 2) \tag{3b}$$

The film pressures defined by Equations 3 may be taken as referring to physical contexts in which the vapor phases, as well as the liquid phases, are saturated with the adsorbing component. This is so because measured values of contact angles involving a single liquid phase, with which Equation 1a is concerned, depend on the state of the interfacial matter in the immediate neighborhood of the three-phase confluent zone. Clearly, the vapor space in this region is saturated, or nearly so, with the liquid component. Hence the solid-vapor interface which is effective in establishing the value of the contact angle is subjected to a film pressure corresponding to saturation conditions. This point, not usually discussed in the literature, has been emphasized in a note by Adam and Livingston [2]. The viewpoint that Young's equation has only a local validity is supported, as noted previously, by the theoretical studies due to Buff [17].

In a fashion analogous to Equations 3 the several adhesion tensions can be written, choosing ϕ to represent this quantity. (The term "spreading pressure," as proposed by Harkins and Livingston [44], is perhaps to be avoided, since in the literature it is sometimes used to refer to the quantity denoted here by ϕ and sometimes to that denoted by π.) These definitions are as follows:

$$\phi_{i3} = \sigma_{3,i} - \sigma_{i3} \qquad (i = 1, 2) \tag{4a}$$

$$\phi_{123} = \sigma_{13,2} - \sigma_{23,1} \tag{4b}$$

The quantity ϕ_{123} has no well-established name; it is suggested that the term "two-liquid adhesion tension" be used.

The definitions represented by Equations 3 and 4 can be combined to give the following relationships:

$$\sigma_3 = \pi_{3,i} + \sigma_{i3} + \phi_{i3} \qquad (i = 1, 2) \tag{5a}$$

$$\sigma_{13} = \pi_{13,2} - \pi_{23,1} + \sigma_{23} + \phi_{123} \tag{5b}$$

Similarly, Equations 1 and 3 can be combined. Comparing the result with Equations 5, it is seen that, whenever Equations 2 are satisfied,

$$\phi_{i3} = \sigma_i \cos \theta_{i3} \qquad (i = 1, 2) \tag{6a}$$

$$\phi_{123} = \sigma_{12} \cos \theta_{123} \tag{6b}$$

Several interesting operations with Equations 5 now suggest themselves. Writing 5a for each of the liquid phases 1 and 2, and then subtracting, we obtain

$$\sigma_{13} - \sigma_{23} = \pi_{3,2} - \pi_{3,1} + \phi_{23} - \phi_{13} \tag{7}$$

Combining this result with 5b then gives

$$\phi_{123} - (\phi_{23} - \phi_{13}) = \pi_{3,2} - \pi_{3,1} - \pi_{13,2} + \pi_{23,1} \tag{8}$$

Publication Date: January 1, 1964 | doi: 10.1021/ba-1964-0043.ch010

This result is recognized as the Bartell-Osterhof [9] relation. It is written, however, taking into account the various film pressures. As originally proposed, the equation neglected these terms; hence the right-hand side of Equation 8 was set equal to zero.

Review of Assumptions

Available Experimental Techniques. Examination of Equation 5a shows that in order to evaluate the surface tension of the bare solid, σ_3, it is necessary to have independent knowledge of three quantities, $\pi_{3,i}$, ϕ_{i3}, and σ_{i3} (i = 1, 2). Only the first two of these quantities are experimentally accessible by the conventional techniques of surface chemistry.

The experimental approach to the quantity $\pi_{3,i}$ is well known. As pointed out by Bangham [6], adsorption data can be employed, using the appropriate integrated form of the Gibbs adsorption isotherm. Accurate measurements thus require that the solid phase be in a finely divided form, so as to exhibit a large surface area. This, of course, means that identical samples cannot be used to measure both $\pi_{3,i}$ and ϕ_{i3}, since the latter quantity must be obtained from a contact angle measurement on an extremely smooth surface. Here, also, the limitation imposed by the requirement of nonspreading—i.e., Equation 2a—must be recognized.

In view of these difficulties, it is hardly surprising that $\pi_{3,i}$ and ϕ_{i3} have rarely been obtained simultaneously for a given solid-liquid pair. The best known attempts have been made in the case of the charcoal-water and graphite-water systems [8, 16, 30, 43, 67].

Faced with these problems, previous authors have usually adopted one of two alternative assumptions. This paper discusses these two assumptions in some detail.

HBL Assumption. The first of these may be called the Harkins-Boyd-Livingston (HBL) assumption [16, 44]. These workers focused their attention primarily (but not exclusively) on cases which involved liquids spreading on the solid surfaces chosen for investigation. This situation no doubt provided the motivation for the following assumption:

$$\text{If } \theta_{i3} = 0, \text{ then } \sigma_{3,i} = \sigma_i + \sigma_{i3} \tag{9}$$

The implication of Equation 9 should be clearly understood. Whereas Equation 2a stated the conditions for nonspreading and also for the validity of Equation 1a, the effect of Equation 9 is to relax these conditions, in so far as the validity of Equation 1a is concerned. In other words, even when spreading occurs, Young's equation retains its validity.

The justification presented originally for the HBL assumption was not based on experimental evidence, nor can it be, with the present state of knowledge regarding solid-fluid interfacial tensions. The argument adduced is based upon a postulated equilibrium between a "duplex film," having a surface free energy of $\sigma_i + \sigma_{i3}$, and the solid surface with its adsorbed film. But when spreading occurs, the physical basis of such a postulated equilibrium disappears. Thus the original argument presented to support the HBL assumption is clearly circular and without foundation.

The effect of adopting the HBL assumption is to make possible, for liquid-solid pairs which involve spreading, the computation of the

Publication Date: January 1, 1964 | doi: 10.1021/ba-1964-0043.ch010

work of adhesion and the related surface properties defined by Harkins [42]. Such computations under this assumption require only the experimental determination of the film pressure.

The HBL assumption is equivalent to assuming that the Antonoff rule holds. This rule can be written as follows:

$$\sigma_{i3} = |\sigma_i - \sigma_{3,i}| \quad (i = 1, 2) \tag{10}$$

As pointed out by Elton [28], this may be combined with Equation 1a to yield:

$$\text{If } \sigma_i > \sigma_{3,i}, \text{ then } \sigma_{3,i} = \frac{1}{2}\sigma_i (1 + \cos \theta_{i3}) \tag{11a}$$

$$\text{If } \sigma_{3,i} > \sigma_i, \text{ then } \theta_{i3} = 0 \tag{11b}$$

But in the latter case, Equation 10 is identical with Equation 9. This implies that Young's equation is valid for situations involving spreading, as well as for nonspreading. Elton's proposal that the Antonoff rule be applied to solid-liquid pairs is thus seen to lead to the HBL assumption as a special case.

The range of validity of the Antonoff rule, as applied to the spreading of organic liquids on water, has been studied by Donahue and Bartell [23]. Their work indicates that the rule is followed only for those liquids which, when the phases are mutually saturated, do not form lenses—i.e., exhibit spreading. This would suggest that the Antonoff rule might be applicable under the condition of Equation 11b but not under that of Equation 11a.

Fox and Zisman [34] have demonstrated the failure of Equation 11a for the low energy surfaces studied by them. They further concluded, however, that the rule has no validity, even for cases of spreading. This position was based on the fact that their results involved various homologous series of organic liquids. Thus accepting the Antonoff rule only for those members of a given series which spread, while rejecting it for higher members which do not spread, can hardly be justified.

FZ Assumption. We now turn to an alternative assumption which we shall call the Fox-Zisman (FZ) assumption [33]. These workers studied the effect of the partial vapor pressure of the liquid phase component on the contact angles of several organic liquids on polytetrafluoroethylene. No difference was observed between the angles measured in air having a negligible partial vapor pressure and those measured in air saturated with vapor. This result led to the conclusion that the film pressures were of vanishing magnitude for the cases studied. Generalizing from this experimental evidence, we may state the following assumption:

$$\text{If } \theta_{i3} > 0, \text{ then } \pi_{3,i} \cong 0 \tag{12}$$

Under this assumption, it is again possible to compute the work of adhesion and other related properties.

Any effort, such as that of Good and Girifalco [38], to interpret contact angle data in terms of the relevant solid-fluid interfacial tensions, is also faced with a similar problem with respect to assigning

Publication Date: January 1, 1964 | doi: 10.1021/ba-1964-0043.ch010

values to the film pressures. Good and Girifalco, and also Fowkes [29], have adopted the FZ assumption in their discussions.

On the other hand, in the earlier literature opinions to the contrary have been expressed. Both Bangham [5] and Cassel [18] have suggested that systems exist for which the FZ assumption cannot hold. Further, one may cite the adhesion tension data for water on graphite reported by Fowkes and Harkins [30] and the corresponding film pressures determined by Harkins, Jura, and Loeser [43].

Adsorption isotherm measurements for water on a partially graphitized carbon black, Graphon, have also been reported by Young et al. [67]. The contact angle for this system is close [19] to that found by Fowkes and Harkins for graphite. In this case, as for the adsorption of water on polytetrafluoroethylene [19], the observed adsorption has been attributed to hydrophilic heterogeneities in the solid surface. Thus, the experimental evidence for the general validity of the FZ assumption is somewhat conflicting and is subject to various interpretations.

More pertinent, however, is the consideration introduced above relating to the vapor saturation conditions applicable to experimental measurements of contact angles. Such a measurement involves a liquid drop resting on a solid surface and forming a three-phase line of contact. But in the immediate vicinity of the contact line, the adsorbed film on the solid surface must be exposed to vapor which is saturated [2]. Hence, the insensitivity of the contact angles in the experiments reported by Fox and Zisman [33] to the saturation conditions of the bulk vapor is to be expected. The results therefore, are not conclusive evidence for negligible values of the film pressures.

Assumptions Used in Present Work. In view of the criticism of the FZ assumption just discussed, this paper proposes and uses below a less restrictive form of this assumption. Instead of Equation 12, we adopt the following:

$$\text{Modified FZ assumption: If } \phi_{i3} < 0, \text{ then } \pi_{3,i} \cong 0 \qquad (13)$$

Since negative adhesion tensions arise when the contact angle θ_{i3} is greater than 90°, this assumption has reference only to water or other highly associated liquids in contact with the most hydrophobic of low energy solids [33, 34, 35]. This assumption is in accord with the dictum of Pierotti and Halsey [56]. These authors suggested that water, because of its very high self-interaction, would not adsorb on any solid surface with which it could not form hydrogen bonds.

For the adhesion tension data considered below, the liquid phase denoted by subscript 1 will in all cases be water. Hence, for present purposes, Equation 13 can be written as

$$\pi_{3,1} \cong 0 \qquad (14)$$

The liquid phases denoted by subscript 2 will in all cases, where adhesion tension data are concerned, be restricted to hydrocarbons.

Attention is now drawn to a further assumption which will prove useful in dealing with two-liquid adhesion tension data. It involves the film pressures defined by Equation 3b, which refer to adsorption at solid-liquid interfaces. This further assumption is that these film pressures are also of negligible magnitude. Thus,

Publication Date: January 1, 1964 | doi: 10.1021/ba-1964-0043.ch010

$$\pi_{i3,j} \cong 0 \quad (i,j = 1,2) \tag{15}$$

As a justification for this assumption, let us consider first the case of $\pi_{23,1}$. Consistency with Equation 14 requires that the assumption represented by 15 be valid in this case.

In the other case, the possibility of the adsorption of the organic liquid component at the interface between liquid water and a low energy solid is more difficult to exclude. Such adsorption would give rise to a film pressure denoted by $\pi_{13,2}$. In this case, however, it may be argued that the solid-liquid water interfacial tension would be of the same order of magnitude as water-hydrocarbon liquid interfacial tensions. Hence, an appreciable decrease in interfacial tension could not be effected by an adsorption process.

As a result of the various assumptions introduced in this section, the basic relations given in the previous section can be somewhat simplified. Under the assumption given by Equation 14, Equation 5a can now be written as

$$\sigma_3 = \sigma_{13} + \phi_{13} \tag{16a}$$

$$\sigma_3 = \pi_{3,2} + \sigma_{23} + \phi_{23} \tag{16b}$$

Similarly, Equation 5b becomes, using Equation 15,

$$\sigma_{13} = \sigma_{23} + \phi_{123} \tag{17}$$

while Equation 8 now reads

$$\phi_{123} - (\phi_{23} - \phi_{13}) = \pi_{3,2} \tag{18}$$

Survey of Adhesion Tensions and Related Data

Adhesion Tensions. Among the surfaces chosen for discussion are the glassy fluorocarbon studied by Fowkes and Sawyer [31] and polytetrafluoroethylene, for which extensive data have been reported by Fox and Zisman [33]. For the latter material values of the adhesion tensions with a series of alkylnaphthalenes and a series of alkyl biphenyls have also been presented by Bascom and Singleterry [10]. These data, along with the glassy fluorocarbon data and a selection of the Fox and Zisman polytetrafluoroethylene data, are given in Table I.

For the two surfaces in question, plots of adhesion tension versus the surface tension of the liquid phase are given in Figure 2. Of special note are the nearly constant values of the adhesion tensions for various homologous series of hydrocarbon liquids in contact with polytetrafluoroethylene.

Regarded from the point of view of Young's equation, Equation 16b, three important aspects of the behavior illustrated in Figure 2 emerge. The first concerns the approximately constant value for the adhesion tension for a given homologous series. This suggests that either the film pressure, $\pi_{3,2}$, and the solid-liquid interfacial tension, σ_{23}, are individually nearly constant for a given series, or alternatively, that the sum of the two quantities is nearly constant.

Publication Date: January 1, 1964 | doi: 10.1021/ba-1964-0043.ch010

TABLE I. Adhesion Tensions for Solid Surfaces

Liquid	Liquid Surface Tension, σ_i, Dynes/Cm.	Observed Adhesion Tensions, ϕ_{i3}, Dynes/Cm.			
		Glassy Fluorocarbon [31]	Polytetrafluoroethylene[a]	Paraffin[b]	Polyethylene[b]
n-Alkanes					
Hexane	18.4		18.1		
Heptane	20.3		19.1		
Octane	21.8		19.6		
Nonane	22.9		19.4	Sp	
Decane	23.9		19.6	23.7	
Undecane	24.7		19.2		
Dodecane	25.4		18.9	24.3	
Tetradecane	26.7		19.2	24.6	
Hexadecane	27.6		19.2	24.6	Sp
n-Alkylbenzenes					
Benzene	28.9	15.5	20.1	26.4	28.9
Methylbenzene	28.5		20.9		
Ethylbenzene	29.0		19.4		
Propylbenzene	29.0		19.0		
Butylbenzene	29.2		19.2		
Hexylbenzene	30.0		18.5		
Alkylnaphthalenes					
Dinonylnaphthalene	31.2		12.2		
Nonylnaphthalene	32.6		12.2		
t-Butylnaphthalene	33.6		12.6	26.6	33.4
t-Amylnaphthalene	34.3		12.3		
1-Ethylnaphthalene	37.6		11.6		
1,6-Dimethylnaphthalene	37.7		11.0		
1-Methylnaphthalene	38.5	9.0	11.3		
Alkyl biphenyls					
Diphenyldodecane	32.5		10.6		31.8
Amylbiphenyl	34.2		10.6		
Isopropylbiphenyl	34.8		10.2		32.2
α-Methylbiphenyl	36.4		10.0		32.2
1,1-Diphenylethane	37.7		9.8		32.3
Water	72.8	-32.7	-22.5	-22.5	-5.1

[a]n-Alkanes, n-alkylbenzenes, and water [33]; alkylnaphthalenes and alkyl biphenyls [10].
[b]All liquids except alkyl biphenyls [35]; for latter [10].

The second aspect which deserves comment is the appreciable decrease in values of the adhesion tensions shown by the alkylnaphthalenes and alkyl biphenyls. In the light of Equation 16b, the reason for this must be a corresponding increase in either the film pressure or the solid-liquid tension (or in their sum).

The final aspect of the adhesion tension data to be discussed here is the following. The diagonal line shown in Figure 2 represents values

Publication Date: January 1, 1964 | doi: 10.1021/ba-1964-0043.ch010

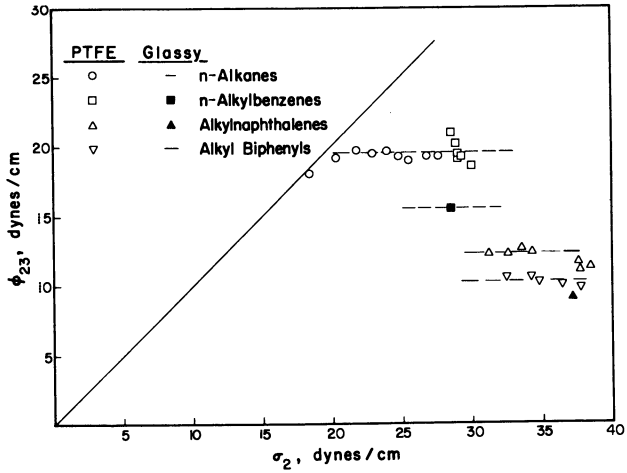

Figure 2. Adhesion tensions for fluorocarbon surfaces

of the adhesion tension corresponding to contact angles equal to zero. According to the discussion of the validity of Young's equation presented above, points lying to the left of this line represent liquid-solid pairs for which spreading occurs. The adhesion tensions for such pairs cannot, of course, be observed. On the other hand, if Young's equation is assumed to retain its validity for situations involving spreading, with zero values for the contact angles, the points representing such systems will lie on the diagonal line of Figure 2. Now, in a homologous series of liquids, with those of lower surface tension spreading and those of higher surface tension exhibiting finite contact angles, there seems to be no reasonable basis for supposing that the plot of adhesion tension vs. surface tension would show a sharp change in slope. This is strong evidence for the contention that Young's equation is in fact limited in validity to cases of nonspreading. This argument, of course, is closely related to the point of view expressed by Fox and Zisman [34] and discussed above.

In addition to the two fluorocarbon surfaces, it is informative to consider data for two hydrocarbon solid surfaces: paraffin and polyethylene. Adhesion tension data for these surfaces have been presented by Fox and Zisman [35]. Selections of these data are given also in Table I, as are some additional data of Bascom and Singleterry for polyethylene [10].

Although the data available are not so extensive as those for polytetrafluoroethylene, similar behavior for several homologous series of hydrocarbon liquids is observed. This is also shown in Figure 3. There are, however, some differences in behavior to be noted. For both

Publication Date: January 1, 1964 | doi: 10.1021/ba-1964-0043.ch010

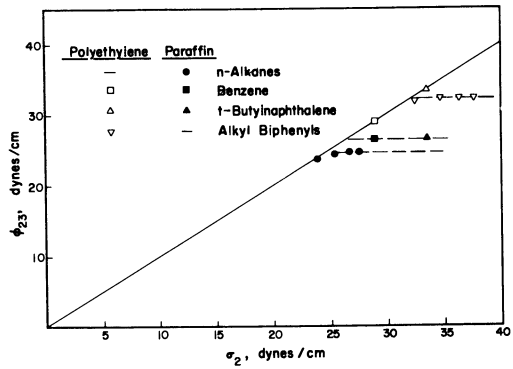

Figure 3. Adhesion tensions for hydrocarbon surfaces

paraffin and polyethylene the results for the homologous series having higher liquid surface tensions do not exhibit a decrease in the values of the adhesion tension, as compared with series having lower surface tensions. Of interest, also, is the value for benzene on polyethylene. In comparison with the bulk of the data presented, this value seems somewhat low. Its magnitude, however, has been confirmed by measurements reported by Speece, Rutkowski, and Gaines [63].

Interaction Parameters. A valuable approach to the problem of interpreting contact angle data has been initiated by Good and Girifalco [38]. As noted above, this approach is based on an expression relating the interfacial tension for two immiscible phases to the surface tensions of the individual phases [36, 37]. If one of the phases is a solid, this expression is

$$\sigma_{i3} = \sigma_i + \sigma_3 - 2Z_{i3}(\sigma_i \sigma_3)^{1/2} \quad (i = 1, 2) \tag{19}$$

The factor denoted in these equations by Z_{i3} is called here the interaction parameter. (The symbol Φ was employed for this quantity by Good and Girifalco.)

Considerations arising from statistical mechanics and the theory of intermolecular forces can be used to estimate values of the interaction parameter. The pertinent theory has been discussed by Girifalco and Good [36] and independently by Moelwyn-Hughes [54]. However, this approach can be justified only for phases composed of spherical molecules which do not differ greatly in size. The actual importance and usefulness of the interaction parameter are consequently for purposes of correlating existing experimental data.

This application has only a limited scope in connection with adhesion tension studies, because of the need for an independent approach to the solid-vacuum and solid-liquid interfacial tensions. There exists, however, one case where an application of this approach is of considerable use: the glassy fluorocarbon solid surface studied by Fowkes

Publication Date: January 1, 1964 | doi: 10.1021/ba-1964-0043.ch010

and Sawyer [31] (see Table I). The interaction parameters can be estimated here because interfacial tension data were also obtained for a series of liquid fractions of the fluorinated lubricating oil from which the glassy fraction was obtained. This fact has also been exploited in the work of Good and Girifalco [38].

These authors, as noted above, adopted the FZ assumption regarding the magnitude of the film pressures. They did not choose to use the adhesion tension value for water, ϕ_{13}. The present approach, on the contrary, uses the value of ϕ_{13}, since it is assumed that $\pi_{3,1}$ can be neglected. Thus, eliminating σ_{13} between Equations 16a and 19 yields

$$\sigma_3 = (\sigma_1 + \phi_{13})^2 / 4\sigma_1 Z_{13}^2 \qquad (20)$$

Upon the establishment of the value of the surface tension for the bare solid, the assumption of negligible film pressures for the other two liquids may be relaxed. Equation 19 is used to obtain values of the solid-liquid tension, σ_{23}, and Equation 16b can then be solved for the film pressure, $\pi_{3,2}$.

The results found by this approach, as well as the liquid-liquid interfacial tensions upon which they are based, are given in Table II. The film pressures for the hydrocarbon liquids, although small, are not negligible. The values of the solid-liquid interfacial tensions are essentially identical with the corresponding liquid-liquid values. The solid-vacuum tension, however, is slightly increased.

Two-Liquid Adhesion Tensions and Film Pressures. Another avenue leading to information bearing on the problem under discussion has recently been opened by the studies of Bascom and Singleterry [11] on two-liquid adhesion tensions. Here, the concern is with the phenomena of relative spreading. Water may spread completely over a surface which is, originally, in contact with a hydrocarbon liquid, or the reverse may occur, or the two liquid phases may form a stable three-phase line of contact, with a corresponding measurable value of the contact angle, θ_{123}.

TABLE II. Interaction Parameters for Fluorocarbon Fractions [31]

Liquid Fraction	Liquid Surface Tension, σ_2, Dynes/Cm.	Interfacial Tensions, σ_{12}, Dynes/Cm. and Interaction Parameters, Z_{12}					
		Benzene		1-Methylnaphthalene		Water	
		σ_{12}	Z_{12}	σ_{12}	Z_{12}	σ_{12}	Z_{12}
124–135 BPR	21.8	7.8	0.853	12.7	0.813	57.0	0.465
135–145 BPR	22.3	7.8	0.853	12.5	0.816	56.3	0.474
145–155 BPR	22.8	7.9	0.852	12.9	0.809	58.4	0.449
155–165 BPR	22.6	7.5	0.859			59.3	0.438
Average Z_{12}			0.854		0.813		0.456
		Computed Quantities[a]					
	σ_3	σ_{23}	$\pi_{3,2}$	σ_{23}	$\pi_{3,2}$	σ_{13}	$\pi_{3,1}$
Glassy fr.	25.7	8.0	2.2	12.7	4.0	58.4	0

[a]Surface and interfacial tensions, σ_3 and σ_{i3}, and film pressures, $\pi_{3,i}$, dynes/cm.

Publication Date: January 1, 1964 | doi: 10.1021/ba-1964-0043.ch010

The present discussion is restricted to two of the surfaces studied by Bascom and Singleterry–i.e., polytetrafluoroethylene and polyethylene. Data for two hydrocarbon liquids–n-decane and isopropylbiphenyl–which had nonzero contact angles on each of these surfaces are given in Table III. Also given are the appropriate one-liquid adhesion tensions from Table I.

The two-liquid adhesion tension data are of particular value in the event that the one-liquid values for each of the liquids are also available. From Table III it is seen that this is the case for both liquids on polytetrafluoroethylene and for isopropylbiphenyl alone on polyethylene. Application of the modified Bartell-Osterhof relation, Equation 18, gives values for the film pressure, $\pi_{3,2}$, which are recorded in Table III.

TABLE III. Two-Liquid Adhesion Tensions and Film Pressures

Liquid	Interfacial Tension, σ_{12}, Dynes/Cm.	Adhesion Tensions and Film Pressures, Dynes/Cm.					
		Polytetrafluoroethylene			Polyethylene		
		ϕ_{i3}	ϕ_{123}	$\pi_{3,i}$	ϕ_{i3}	ϕ_{123}	$\pi_{3,i}$
n-Decane	51.1	19.6[a]	50.9[b]	8.8	Sp[c]	50.8[b]	?
Isopropylbiphenyl	42.8	10.2[d]	42.5[b]	9.8	32.2[d]	42.6[b]	5.3
Water	-	-22.5[a]	-	0	-5.1[c]	-	0

[a][33]. [b][11]. [c][35]. [d][10].

Use of the Bartell-Osterhof relation to arrive at values for the film pressure of an organic liquid in contact with a low energy solid has not been attempted before. The assumptions under which this approach can be used are those leading to Equation 18, as discussed above. It is therefore appropriate to turn to the question of the reliability of the two-liquid adhesion tension data. The film pressures found for each of the two liquids on polytetrafluoroethylene are of the order of 10 dynes per cm. Hence, if the film pressures, $\pi_{3,2}$, were in fact negligible, the reported two-liquid adhesion tensions would be necessarily about 10 dynes per cm. too large. But this would imply that the true contact angles, measured through phase 1, are in the range of 140° to 145°. The difference between such values and those reported (173° to 175°) is clearly far greater than any possible experimental error. Furthermore, the Bascom and Singleterry measurements have been confirmed in our laboratory [24] by a method involving large sessile drops of water.

A possible objection to the results in question lies in the nearness with which a spreading condition is approached. It might conceivably be argued that a continuous thick film of hydrocarbon liquid (phase 2) is trapped on the solid surface by some mechanism such as surface roughness. Such a situation would lead to a contact angle which is actually zero, measured through phase 2. That this is not the case, however, has been demonstrated by Baker, Bascom, and Singleterry [3]. True spreading of phase 2 may be detected by comparing the behavior of large sessile drops of water immersed in the hydrocarbon or organic liquid in question with similar drops immersed in benzene. In the latter

Publication Date: January 1, 1964 | doi: 10.1021/ba-1964-0043.ch010

case, the interfacial tension is sufficiently low that benzene may be expected to spread, in competition with water, on a wide variety of low energy solids.

The evidence obtained from measurements of two-liquid adhesion tensions seems to point very strongly to the existence of film pressures of the order of 5 to 10 dynes per cm. on low energy surfaces. In fact, no alternative explanation of the observations suggests itself. Therefore, there follows a discussion of some direct measurements of film pressures which have been reported and which bear on the problem.

Unfortunately, adsorption studies on low energy surfaces have been limited in number and in scope. Pertinent to the present work are the measurements reported recently by Graham [40]. In this work adsorption isotherms were obtained for argon, nitrogen, and carbon tetrafluoride on polytetrafluoroethylene. The portions of the isotherms out to monolayer coverage were used to compute film pressures corresponding to such coverage. For each of the adsorbates, the film pressure was from 9.5 to 10.0 dynes per cm. Another case of interest is the study of Zettlemoyer, Chand, and Gamble [68], of the adsorption of nitrogen and krypton on polyethylene. In this work film pressures were not reported. The data were, however, fitted to a BET isotherm and the BET constants evaluated. Based on the assumption that the fit is good out to monolayer coverage, an analytical integration gives a value of 13.6 dynes per cm. for the film pressure of nitrogen at this coverage.

Two questions arise in attempting to extrapolate the information from the studies just quoted to the case of high boiling liquids adsorbed on low energy solids. The first is how much additional film pressure results from adsorption beyond monolayer coverage, and the second is how can a film pressure for a substance like n-decane be related to that for nitrogen. For answers to these questions it is necessary to turn to adsorption studies on a material such as graphite, where much more experimental information is available. The application of these results to such low energy surfaces as are of interest in the present discussion can, however, only be qualitative.

The adsorption of nitrogen on graphite and closely related materials, such as Graphon, has been widely studied. Joyner and Emmett [48] treated their data for Graphon according to the BET prescription. Assuming again that the fit is sufficiently good below monolayer coverage permits the reported BET constants to be used with analytical integration to find a film pressure of 19.1 dynes per cm. at this coverage. For the higher coverages, adsorption data in this region have been discussed by Pierce [55]. Since the Frenkel-Halsey-Hill isotherm can be used to fit such data, again an analytical integration can be employed. From the constants reported by Pierce, the film pressure corresponding to the region from monolayer coverage to saturation was found to be 31.7 dynes per cm. Combining this value with the Joyner and Emmett results yields a film pressure at saturation of about 51 dynes per cm.

As an example of a high boiling adsorbate, adsorption data for n-heptane on graphite may be considered. Harkins, Jura, and Loeser [43] reported a film pressure at saturation of 63 dynes per cm. for this system. For comparison, we may cite the value for monolayer coverage given by Chessick, Zettlemoyer, and Wu [20], which was 27.6 dynes per cm. Thus, the relative contributions of monolayer adsorption and multilayer adsorption to the film pressures at saturation are quite comparable

Publication Date: January 1, 1964 | doi: 10.1021/ba-1964-0043.ch010

for nitrogen and n-heptane on graphite. Also, the film pressure for n-heptane is only some 20 to 50% greater than that for nitrogen on this surface.

The various results quoted do not provide conclusive evidence as to the magnitudes of film pressures of high boiling liquids on low energy solids such as polyethylene and polytetrafluoroethylene. On the other hand, film pressures of the order of 10 dynes per cm., as obtained by use of the Bartell-Osterhof relation, do not seem unreasonable. Other adsorption studies in which film pressures have been reported and which support the arguments just presented are those of Harkins and coworkers [12, 45, 51].

Yet another interesting conclusion may be derived from the two-liquid adhesion tension data of Bascom and Singleterry [11] which are recorded in Table III. If Equation 17 is applied to each of two different hydrocarbon liquids, the difference between the two solid-liquid interfacial tensions is just the (negative) difference between the respective two-liquid adhesion tensions. Thus, from the values given in Table III, the solid-liquid tension for isopropyl biphenyl is 8 dynes per cm. greater than that for n-decane. This difference is the same for both polytetrafluoroethylene and polyethylene.

In relation to this result, it is of interest to refer to the solid-liquid interfacial tensions evaluated previously for the glassy fluorocarbon surface studied by Fowkes and Sawyer [31]. From Table II, we note that the difference between the solid-liquid tensions for benzene and 1-methylnaphthalene on this surface is about 5 dynes per cm.

Solid-Liquid Interfacial Tensions. For such systems as are of interest in the present discussion, the solid-liquid interfacial tensions, like the surface tensions of the bare solids, cannot be evaluated by the usual techniques of surface chemistry. In the case of the solid-liquid tensions, however, there remains an avenue of approach which has been, as yet, rather ignored by workers in this field: the study of crystallization rate phenomena.

The approach in question has been pursued primarily by investigators interested in metals, notably Turnbull [65]. According to the theory of homogeneous nucleation in supercooled liquids, the frequency of nucleation is related to the amount of undercooling and also to the solid-liquid interfacial tension. Thus measurements of frequency as a function of undercooling can be utilized to evaluate the solid-liquid tension. In some cases the measurement of the undercooling alone suffices. It has been found from studies of this type with liquid metals [65] and with a number of organic liquids [64] that the solid-liquid tensions so obtained correlate well with molar heats of fusion. Molecular theory, utilizing a rather crude model, tends to confirm this correlation [46].

Fortunately, several hydrocarbon liquids which are of interest in the present discussion have been among those studied. Turnbull and Cormia [66] report a value of 9.6 dynes per cm. for the solid-liquid interfacial tension of n-octadecane and 7.2 dynes per cm. for n-heptadecane. They suggest that these two values are characteristic of the higher n-alkanes with even and odd numbers of carbon atoms, respectively. That is, for each series, the solid-liquid tension is independent of the number of carbon atoms. Data for other hydrocarbons are given by Thomas and Stavely [64]. They report values of 20.4 dynes per cm. for benzene, 24.0 for biphenyl, and 30.1 for naphthalene.

Publication Date: January 1, 1964 | doi: 10.1021/ba-1964-0043.ch010

In the method employed in obtaining these data, any effect of temperature on the solid-liquid interfacial tension is ignored. For the n-alkanes [66] the amount of undercooling was only 12° to 13°C. Hence, applying any reasonable temperature coefficient–e.g., -0.05 dyne per cm. per degree–would not have a significant effect. It is therefore suggested that a satisfactory estimate of the solid-liquid tension for n-decane on solid hydrocarbon surfaces would be 10 dynes per cm.

In the case of benzene [64], the observed undercooling was about 70°C. Hence, we might expect an interfacial tension which is several dynes less than the value quoted. On the other hand, Skapski, Billups, and Casavant [62] have reported a direct determination of the solid-liquid interfacial tension for benzene. The value found is about 22 dynes per cm. This is the only direct measurement known to the writer, and it provides an interesting confirmation of the result obtained from undercooling experiments.

In view of the uncertainty regarding the effect of temperature on the benzene result and because the hydrocarbon surfaces of interest are paraffinic rather than aromatic, any estimate for the solid-liquid tension for solid-benzene pairs is less satisfactory than the n-decane value. Nevertheless, it is of interest to make such estimates for several other hydrocarbon liquids as well as for benzene. The increase in solid-liquid interfacial tension for aromatic compounds, which is indicated by the undercooling experiments, can at least be reflected in such estimates. Since both one-liquid and two-liquid adhesion tension data are available for isopropylbiphenyl, an estimate for this liquid is desirable. For comparison, and because one-liquid adhesion data exist, tert-butylnaphthalene has been chosen as another case for which an estimate of the solid-liquid interfacial tension has been made.

These estimates are given in Table IV. Also presented are estimates appropriate to fluorocarbon surfaces. In the latter case, the values for benzene and tert-butylnaphthalene are chosen to correspond with the results obtained by use of the interaction parameter method, as given in Table II. For both the fluorocarbon surfaces and the hydrocarbon surfaces, the estimates given are also in agreement with the differences between the values for n-decane and isopropylbiphenyl, as deduced from two-liquid adhesion tension data.

The estimates given in Table IV are based on evidence which is admittedly indirect in nature. Yet, the values have the virtue of being consistent with several independent lines of evidence.

TABLE IV. Estimates for Solid-Liquid Interfacial Tensions

Liquid	Solid-Liquid Interfacial Tensions, σ_{23}, Dynes/Cm.	
	Fluorocarbon Surfaces	Hydrocarbon Surfaces
n-Decane	6	10
Benzene	8	12
tert-Butylnaphthalene	13	17
Isopropylbiphenyl	14	18

Publication Date: January 1, 1964 | doi: 10.1021/ba-1964-0043.ch010

Estimates for Solid-Vacuum Tensions and Related Quantities

Referring to the form in which Young's equation was finally expressed (Equation 16b), it is seen that with the information at hand it is possible to obtain estimates of the surface tensions of the bare solids. The discussion is restricted to three of the solid surfaces for which data were given in Table I. The data for the glassy fluorocarbon surface have been fully treated by the method of interaction parameters, as given in Table II. The liquids of interest for the three surfaces are those for which solid-liquid interfacial tension estimates are given in Table IV, and, in addition, water.

According to Equation 16b, the remaining quantity for which knowledge is required is the film pressure, $\pi_{3,2}$. This quantity should be known for at least one liquid in contact with each solid. Data for $\pi_{3,2}$ are given in Table III for two of the liquids on polytetrafluoroethylene and for one liquid on polyethylene. Employing these results and those of Tables I and IV allows values of the solid-vacuum tensions to be calculated from Equation 16b. The results are presented in the first row of Table V. The solid-liquid interfacial tensions for water in contact with the solids are given in the second row. These are computed from the solid-vacuum tensions, using Equation 16a.

In the case of paraffin, no film pressures are available, since two-liquid adhesion tension data are lacking. Thus, it was necessary to assume a film pressure for one of the liquids in contact with paraffin. For this, a value of 1 dyne per cm. was taken as the film pressure of tert-butylnaphthalene. If a higher value had been chosen, the solid-vacuum and solid-liquid water tensions would have been correspondingly higher. Since the interfacial tension with water in this case seems already high, in comparison with liquid-liquid interfacial tensions for paraffin hydrocarbons [23], the quoted film pressure was adopted.

The film pressures which were either taken from Table III or else assumed are also given in Table V. In the other cases, the film pressures were computed from Equation 16b, using the tabulated values of the solid-vacuum surface tensions.

Table V. Estimated Solid-Vacuum Interfacial Tensions and Related Quantities[a]

	Polytetrafluoroethylene		Paraffin		Polyethylene	
σ_3, dynes/cm.	34		45		55	
σ_{13}, dynes/cm.	57		68		60	
	$\pi_{3,i}$	Z_{i3}	$\pi_{3,i}$	Z_{i3}	$\pi_{3,i}$	Z_{i3}
n-Decane	9[b]	0.91	11	0.90	?	0.95
Benzene	6	0.88	7	0.86	14	0.90
tert-Butylnaphthalene	8	0.81	1[c]	0.79	5	0.83
Isopropylbiphenyl	10[b]	0.80	?	0.78	5[b]	0.82
Water	0[c]	0.51	0[c]	0.44	0[c]	0.54

[a] Film pressures, $\pi_{3,i}$, dynes/cm.; interaction parameters, Z_{i3}.
[b] From Table III.
[c] Assumed.

Publication Date: January 1, 1964 | doi: 10.1021/ba-1964-0043.ch010

It is possible, from the estimates obtained, to proceed to evaluate the interaction parameters for the systems considered. For this, Equation 19 is employed, and the results are also given in Table V. The trend of estimated solid-liquid interfacial tensions for the series of five liquids on each of the solids is roughly parallel to the trend of liquid surface tensions (Table I). Hence, the similar trends found for the interaction parameters on each of the solids are to be expected.

Discussion and Conclusions

The estimates given in Table V for the solid-vacuum tensions of the three solids vary considerably among themselves. Also, the polytetrafluoroethylene result is somewhat higher than the estimate found by Good and Girifalco [38], which was 28 dynes per cm. These authors also give 30 dynes per cm. as the surface tension of an octadecylamine monolayer adsorbed on platinum. This is markedly lower than the present estimate for paraffin.

It is not possible to cite other estimates for the quantities in question. To the writer's knowledge, no previous discussions suggesting magnitudes for the surface tensions of low energy solids, other than those quoted, have been published.

Good and Girifalco assign to the values estimated by them an uncertainty of ± 2 dynes per cm. An uncertainty of perhaps ± 4 dynes per cm. applies to the present estimates. Thus, there remains a wide divergence between the values estimated here and those of Good and Girifalco. This is to be accounted for by the difference in basic assumptions adopted and in procedures followed.

Possibly the most direct route to resolving discrepancies of the magnitude in question would be a theoretical calculation of the surface tension of one of the solids under discussion. For this purpose a calculation for the case of paraffin would offer distinct advantages. These arise as the result of considerable prior effort which has been devoted to carrying out such calculations for the energy of sublimation of paraffin crystals. Recently, these calculations have been reviewed and extended by Salem [57], who obtained good agreement with experiment [15].

In view of the close chemical similarity between paraffin and polyethylene, the large difference in the estimates of the solid surface tensions is rather unexpected and deserves comment. This difference is, by virtue of the assumptions and related estimates used in the present approach, reflected in the rather different contact angles observed for water on these two solids. This contact angle difference has been confirmed and commented on by Adam and Elliott [1]. They attribute the difference from the expected behavior for polyethylene to the presence of traces of polar impurities.

An alternative possibility arises from considerations related to the development of crystalline structure in polyethylene [22]. The main feature of this structure is the periodic folding of the polymer chains in the crystal. Theoretically this is explained within the context of the kinetics of crystal nucleation and growth from solution. According to Cormia, Price, and Turnbull [22], the fold-surface energy in polyethylene crystals is comparable to the end-interfacial energy of rod-shaped nuclei. These surface free energies are of the order of 10 to

Publication Date: January 1, 1964 | doi: 10.1021/ba-1964-0043.ch010

15 times larger than the solid-liquid interfacial tensions for unfolded chains. Hence, even if only a small fraction of the solid surface is occupied by chain-folding sites, the surface tension of the bare solid should be appreciably larger than for crystals in which such sites are absent.

Complications such as these extend also to the case of polytetrafluoroethylene. The large difference in estimated solid-vacuum tensions between this polymer and polyethylene is not unexpected, since a proportionately large difference exists for the liquid surface tensions of hydrocarbons and fluorocarbons having five to eight carbon atoms [58]. The underlying cause of this difference is, however, more obscure. The intermolecular forces for fluorocarbons apparently have features which lead to anomalous behavior, at least from the point of view of solubility parameter theory [59]. Thus, theoretical calculations of the surface tension for the bare solid in the case of polytetrafluoroethylene would face a number of difficulties not encountered with paraffin crystals.

Conclusions. The present paper offers an approach to an interpretive scheme by which contact angle measurements can furnish information as to more fundamental properties of interfaces involving solid phases. As in most other approaches, the basis chosen for the interpretation is Young's equation. The following conclusions are reached:

When spreading occurs, Young's equation is no longer valid.

When spreading does not occur, the film pressure for the (single) liquid phase cannot be neglected, unless the contact angle is greater than 90°.

For two liquid phases in contact with a solid, both film pressures can be neglected.

Based on Young's equation and the conclusions just stated, the interpretation of available experimental evidence leads to the following further conclusions:

Film pressures can be estimated from a combination of one-liquid and two-liquid adhesion tension data, using the modified Bartell-Osterhof relation. For high boiling liquids on low energy solids, film pressures in the range of 5 to 10 dynes per cm. are obtained.

Solid-liquid interfacial tensions can be estimated from experiments involving crystallization rate phenomena. For hydrocarbon surfaces, the estimated values range from 10 to 18 dynes per cm., while for fluorocarbon surfaces the range is from 6 to 14 dynes per cm.

Surface tensions for the bare solids are estimated to be: polytetrafluoroethylene, 34; paraffin, 45; and polyethylene, 55 dynes per cm.

Verification of the estimates presented will be aided by further experimental studies, particularly direct measurements of film pressures. Also of distinct interest will be theoretical calculations of the solid-vacuum tension for a paraffin crystal.

Acknowledgment

Many valuable discussions with Peggy M. Dunlap contributed much to the development of the approach presented in this paper. Appreciation is also expressed to the Socony Mobil Oil Co., Inc., for permitting publication of this work.

Literature Cited

(1) Adam, N. K., Elliott, G. E. P., J. Chem. Soc. 1962, 2206.
(2) Adam, N. K., Livingston, H. K., Nature 182, 128 (1958).
(3) Baker, H. R., Bascom, W. D., Singleterry, C. R., J. Colloid Sci. 17, 477 (1962).
(4) Bakker, G., "Kapillarität und Oberflächenspannung," in "Handbuch der Experimentalphysik," Vol. VI, Akademische Verlagsgesellschaft, Leipzig, 1928.
(5) Bangham, D. H., J. Chem. Phys. 14, 352 (1946).
(6) Bangham, D. H., Trans. Faraday Soc. 33, 805 (1937).
(7) Bangham, D. H., Razouk, R. I., Ibid., 33, 1459 (1937).
(8) Ibid., p. 1463.
(9) Bartell, F. E., Osterhof, H. J., Colloid Symp. Monograph 5, 113 (1927).
(10) Bascom, W. D., Singleterry, C. R., J. Phys. Chem. 65, 1683 (1961).
(11) Ibid., 66, 236 (1962).
(12) Basford, P. R., Harkins, W. D., Twiss, S. B., Ibid., 58, 307 (1954).
(13) Bernett, M. K., Zisman, W. A., Ibid., 63, 1241 (1959).
(14) Ibid., p. 1911.
(15) Billmeyer, F. W., Jr., J. Appl. Phys. 28, 1114 (1957).
(16) Boyd, G. E., Livingston, H. K., J. Am. Chem. Soc. 64, 2383 (1942).
(17) Buff, F. P., "The Theory of Capillarity," in "Handbuch der Physik," Vol. X, Springer-Verlag, Berlin, 1960.
(18) Cassel, H. M., J. Chem. Phys. 14, 217 (1946).
(19) Chessick, J. J., Healey, F. H., Zettlemoyer, A. C., J. Phys. Chem. 60, 1345 (1956).
(20) Chessick, J. J., Zettlemoyer, A. C., Wu, Y.-F., Ibid., 64, 530 (1960).
(21) Collins, R. E., Cooke, C. E., Jr., Trans. Faraday Soc. 55, 1602 (1959).
(22) Cormia, R. L., Price, F. P., Turnbull, D., J. Chem. Phys. 37, 1333 (1962).
(23) Donahue, D. J., Bartell, F. E., J. Phys. Chem. 56, 480 (1952).
(24) Dunlap, P. M., Paper S.P.-13, 18th Southwest Regional Meeting, ACS, Dallas, Dec. 6–8, 1962.
(25) Ellison, A. H., Fox, H. W., Zisman, W. A., J. Phys. Chem. 57, 622 (1953).
(26) Ellison, A. H., Zisman, W. A., Ibid., 58, 260 (1954).
(27) Ibid., p. 503.
(28) Elton, G. A. H., J. Chem. Phys. 19, 1066 (1951).
(29) Fowkes, F. M., J. Phys. Chem. 66, 382 (1962).
(30) Fowkes, F. M., Harkins, W. D., J. Am. Chem. Soc. 62, 3377 (1940).
(31) Fowkes, F. M., Sawyer, W. M., J. Chem. Phys. 20, 1650 (1952).
(32) Fox, H. W., Hare, E. F., Zisman, W. A., J. Phys. Chem. 59, 1097 (1955).
(33) Fox, H. W., Zisman, W. A., J. Colloid Sci. 5, 514 (1950).
(34) Ibid., 7, 109 (1952).
(35) Ibid., p. 428.
(36) Girifalco, L. A., Good, R. J., J. Phys. Chem. 61, 904 (1957).
(37) Good, R. J., Paper 31, Division of Colloid and Surface Chemistry, 142nd Meeting ACS, Atlantic City, Sept. 12, 1962.
(38) Good, R. J., Girifalco, L. A., J. Phys. Chem., 64, 561 (1960).
(39) Good, R. J., Girifalco, L. A., Kraus, G., Ibid., 62, 1418 (1958).
(40) Graham, D., Ibid., 66, 1815 (1962).
(41) Hare, E. F., Zisman, W. A., Ibid., 59, 335 (1955).
(42) Harkins, W. D., J. Chem. Phys. 9, 552 (1941).
(43) Harkins, W. D., Jura, G., Loeser, E. H., J. Am. Chem. Soc. 68, 554 (1946).
(44) Harkins, W. D., Livingston, H. K., J. Chem. Phys. 10, 342 (1942).
(45) Harkins, W. D., Loeser, E. H., Ibid., 18, 556 (1950).
(46) Jackson, K. A., Chalmers, B., Can. J. Phys. 34, 473 (1956).
(47) Johnson, R. E., Jr., J. Phys. Chem. 63, 1655 (1959).
(48) Joyner, L. G., Emmett, P. H., J. Am. Chem. Soc. 70, 2353 (1948).
(49) Lester, G. R., J. Colloid Sci. 16, 315 (1961).
(50) Li, T., J. Chem. Phys. 36, 2369 (1962).
(51) Loeser, E. H., Harkins, W. D., Twiss, S. B., J. Phys. Chem. 57, 251 (1953).

Publication Date: January 1, 1964 | doi: 10.1021/ba-1964-0043.ch010

(52) McNutt, J. E., Andes, G. M., J. Chem. Phys. 30, 1300 (1959).
(53) Michaels, A. S., Dean, S. W., Jr., J. Phys. Chem. 66, 1790 (1962).
(54) Moelwyn-Hughes, E. A., J. Colloid Sci. 11, 501 (1956).
(55) Pierce, C., J. Phys. Chem. 63, 1076 (1959).
(56) Pierotti, R. A., Halsey, G. D., Jr., Ibid., 63, 680 (1959).
(57) Salem, L., J. Chem. Phys. 37, 2100 (1962).
(58) Scholberg, H. M., Guenthner, R. A., Coon, R. I., J. Phys. Chem. 57, 923 (1953).
(59) Scott, R. L., Ibid., 62, 136 (1958).
(60) Shafrin, E. G., Zisman, W. A., J. Colloid Sci. 7, 166 (1952).
(61) Shafrin, E. G., Zisman, W. A., J. Phys. Chem. 64, 519 (1960).
(62) Skapski, A., Billups, R., Casavant, D., J. Chem. Phys. 31, 1431 (1959).
(63) Speece, A. L., Rutowski, C. P., Gaines, G. L., Jr., Rev. Sci. Instr. 28, 636 (1957).
(64) Thomas, D. G., Stavely, L. A. K., J. Chem. Soc. 1952, 4569.
(65) Turnbull, D., J. Appl. Phys. 21, 1022 (1950).
(66) Turnbull, D., Cormia, R. L., J. Chem. Phys. 34, 820 (1961).
(67) Young, G. J., Chessick, J. J., Healey, F. H., Zettlemoyer, A. C., J. Phys. Chem. 58, 313 (1954).
(68) Zettlemoyer, A. C., Chand, A., Gamble, E., J. Am. Chem. Soc. 72, 2752 (1950).
(69) Zisman, W. A., "Relation of Chemical Constitution to the Wetting and Spreading of Liquids on Solids," in "A Decade of Basic and Applied Science in the Navy," Office of Naval Research, U. S. Government Printing Office, Washington, D. C., 1957.

Received April 1, 1963

11

The Relationship between Wetting and Adhesion

J. R. HUNTSBERGER

Fabrics and Finishes Department
E. I. du Pont de Nemours & Co., Inc.
Wilmington 98, Del.

Publication Date: January 1, 1964 | doi: 10.1021/ba-1964-0043.ch011

Adhesion of polymers was determined as a function of temperature. The influence of the bonding times and temperatures indicates that the performance is established largely by the extent of wetting at the polymer-substrate interface. Considerations based on surface free energies show that most practical systems should exhibit complete wetting at equilibrium. The problem appears to involve establishing factors which retard or preclude wetting. Low substrate surface energy, high polymer viscosity, substrate topography, selective adsorption, and coacervation may be involved.

When two solid materials are brought together in such a way that intimate molecular contact between the phases is achieved, they should adhere strongly to each other. Many authors have shown that dispersion forces alone are sufficient to lead to high values for the work of adhesion; consequently, relatively good adhesion should be exhibited despite the chemical nature of the materials.

In practice examples of very poor adhesion are frequently observed. The objective of this paper is to show that in many such cases interfacial equilibrium has not been achieved and that incomplete wetting is a major factor in establishing the performance. This proposal is based on the adhesive performance of many polymer-substrate combinations observed as a function of temperature [4].

Discussion

Wetting may be thought of as the process of achieving molecular contact. The extent of wetting may be defined as the number of molecular contacts between the two phases comprising the system relative to

In Contact Angle, Wettability, and Adhesion; Fowkes, F.;
Advances in Chemistry; American Chemical Society: Washington, DC, 1964.

that exhibited when wetting is complete. This definition, in contradistinction to one which equates wetting with spreading, is preferable for discussion of relationships between wetting and adhesion.

Equilibrium contact angles are functions of the surface free energies of the solid substrate and the liquid in contact with it and of the free energy of the interface between the two phases. Much useful information can be obtained through studies of contact angles. This equilibrium, however, represents the extent to which a liquid spreads over the substrate and not the extent of wetting at the interface.

In practice the fluid adhesives are spread over the substrates and constrained in some way so that the problem is to determine whether the surface free energies and interfacial energy of the phases in question will lead to complete wetting. A fluid adhesive spread over a "real" (nonplanar) substrate is shown schematically in Figure 1. The system is depicted in a state in which the solid is not completely wetted (upper) and the wetted state (lower).

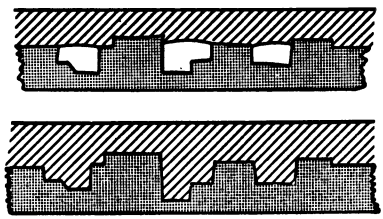

Figure 1. Wetting of solid substrate by fluid adhesive

Upper. Substrate incompletely wetted
Lower. Substrate completely wetted

Johnson and Dettre [5] have investigated the thermodynamics of wetting for specific nonplanar surfaces and have shown that both stable and metastable equilibria can be encountered in systems exhibiting incomplete wetting.

By considering the change in surface free energy associated with the change from any given nonwetted state to the wetted state for a single asperity, it is easy to find a criterion for wetting. Energy changes in other parts of the system will be negligible if the volume of the asperity or not wetted void is small compared to the total volume of the adhesive layer and will not invalidate this treatment.

Neglecting gravitational effects, adsorption, and any thermal effects associated with the morphology of the adhesive, the change in free energy accompanying the wetting of the substrate in any single asperity is given by:

$$\Delta F = \Omega^{SV} F_{SL} - \left[\Omega^{SV} F_{SV} + A^{LV} F_{LV}\right] \quad (1)$$

where Ω^{SV} and A^{LV} are the integrated or actual area of the solid-vapor interface and the area of the liquid-vapor interface, respectively, in

Publication Date: January 1, 1964 | doi: 10.1021/ba-1964-0043.ch011

the nonwetted state. F_{SV} and F_{LV} are the surface free energies of the solid and liquid phases, respectively, in equilibrium with the saturated vapor phase. F_{SL} is the free energy of the solid-liquid interface.

Under the above assumptions the Young-Dupré equation can be written in terms of surface free energies:

$$F_{SV} - F_{SL} = F_{LV} \cos \theta \quad (2)$$

substituting this value for $F_{SV} - F_{SL}$ in Equation 1 gives:

$$\Delta F = -F_{LV} \left[1 + \left(\Omega^{SV}/A^{LV}\right) \cos \theta\right] \quad (3)$$

Equation 3 shows that at equilibrium complete wetting is expected unless $(\Omega^{SV}/A^{LV}) \cos \theta < -1$. It is important to note that this criterion establishes whether the minimum surface free energy is exhibited by the wetted or the particular given nonwetted state. Some surface geometries could be found which during the wetting process would lead to stable equilibria exhibiting surface free energies lower than either the initial or wetted states given above [5]. For most practical adhesive systems, the adhesive will exhibit equilibrium contact angles with the substrate of less than 90°. Cos θ will be positive; and thermodynamic equilibrium will correspond to a completely wetted state.

Experimental Procedures and Results

The adhesive performance of poly(n-butyl methacrylate) adhered to cold-rolled steel substrates was determined as a function of temperature. The polymer exhibited an inherent viscosity of 0.57 (0.5% in chloroform). Films were applied to the steel substrates by casting from 40% solid solution in reagent grade toluene. To obviate stretching and tearing during testing, 2-mil-thick glass fabric was embedded within the polymer by casting two coats, pressing the glass fabric into the second coat immediately after casting the film. The films were applied using an applicator with a 20-mil clearance. The resulting structure was 9 mils thick with approximately 7 mils of polymer below the fabric. The cold-rolled steel was abraded with 600A silicon carbide abrasive and rinsed in acetone.

The peel strength was determined using the apparatus shown in Figure 2. The 1-inch-wide substrate panels were placed in Teflon TFE-fluorocarbon resin lined tracks. The free end of the film was passed around the roller and attached to a line which extended through a small tubular opening out of the oven and around a ball-bearing pulley to the loading container.

Tests were carried out by adding lead shot slowly to the container until peeling proceeded at a rate of 2 to 3 mm. per minute. As the films were peeled, the substrate panels slid in the tracks under a second small retaining roller. The peel angle was set by the nature of the system and was observed to be somewhat less than 90°.

The precision of this test is a function of the temperature and of the strain geometry. It can be defined most conveniently by grouping the data for cohesive failures and for apparent interfacial failure separately. The coefficient of variation for the mean of duplicate tests was ±4.3% when failure was cohesive and ± 9.0% when failure appeared to

Publication Date: January 1, 1964 | doi: 10.1021/ba-1964-0043.ch011

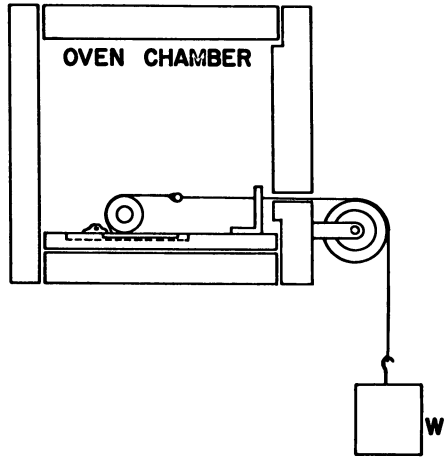

Figure 2. Schematic diagram of apparatus for measuring peel strength at various temperatures

occur at the interface. The data are plotted as the log of the load required for peeling *vs.* reciprocal absolute temperature. The points are based on the mean values of the duplicate tests.

Two sets of samples were prepared. After 3 hours had been allowed for solvent evaporation, the adhesive bonds were formed by holding one set for an hour at 100°C. and the second for an hour at 150°C. The results are shown in Figure 3.

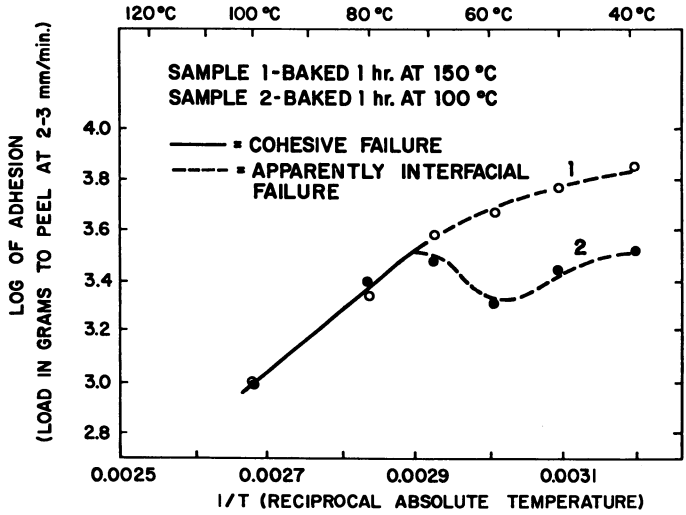

Figure 3. Force required to peel poly(n-butyl methacrylate) from steel vs. reciprocal absolute temperature

Publication Date: January 1, 1964 | doi: 10.1021/ba-1964-0043.ch011

At temperatures above ~72°C. the performance was identical for the two samples. Failure occurred cohesively within the polymer. At temperatures below ~72°C. the peel strength of the sample bonded at 150°C. continued to increase with decreasing temperature but at a reduced rate, and the locus of failure shifted to or close to the interface. The sample bonded at 100°C., however, exhibited decreasing peel strength with decreasing temperature, reaching a minimum at ~50°C. Below 50°C. the peel strength again increased. Below 72°C. the failure appeared to occur at the interface.

This behavior appears to be satisfactorily explained by the following hypothesis:

The two major factors influencing the performance are the viscoelastic response of the polymer and the extent of interfacial contact. The difference in the behavior of the two samples is attributed to the fact that the sample bonded at 150°C. had reached or at least very closely approached interfacial equilibrium and had achieved nearly maximum interfacial contact or "wetting." The sample bonded at 100°C. did not approach equilibrium, and discontinuities existed in the interface of such magnitude that stress concentration occurred at their edges when the effective strain rate of the test exceeded the relaxation rate of the polymer. For this test and with these particular samples the effective strain rate and relaxation rate were equal at ~72°C. Above this temperature cohesive failure occurred through polymer relaxation. At temperatures below 72°C. stress concentration arose and increased with decreasing temperature as the relaxation rate of the polymer decreased and its modulus increased. Failure occurred when the stress at the "microedges" of the discontinuities in the sample prepared at 100°C. exceeded either the interfacial bond strength or the cohesive strength of the polymer, depending on the locus of failure. For the sample prepared at 150°C. concentration of normal stresses occurred only at the sample edges; hence only a small deviation in the performance was observed at temperatures below 72°. The stresses were greatest at or very near the interface, however, because of the nature of the deformation of the sample during testing. This resulted in the shift of the locus of failure.

The preceding hypothesis is substantiated by data for many systems obtained through peeling tests and tests involving cleavage of lap joints. A particularly interesting example is provided by the behavior of poly(n-butyl methacrylate) bonded to a substrate exhibiting a low surface energy. The low energy substrate was achieved by coating a steel panel with 52% soybean oil alkyd resin with an acid number of 6. The resin was cured by baking for 0.5 hour at 200°C. The surface energy was appraised using the technique of Fox and Zisman for evaluating γ_c. This gave a value of γ_c ~31 dynes per cm. Three sets of samples were prepared using bonding temperatures of 120°, 150°, and 180°C. Bonding time was 1 hour. The data are shown in Figure 4. The point of greatest interest is the similarity of the performance as compared with that exhibited on the high energy steel substrates. The important difference is that higher temperatures were required at equal bonding times to reach equivalent performance. This is what would be expected if the bonding were a "wetting" process.

Another interesting example is given by the behavior of 0.5×0.5 inch lap joints comprising $0.25 \times 0.5 \times 5$ inch steel bars bonded with

Publication Date: January 1, 1964 | doi: 10.1021/ba-1964-0043.ch011

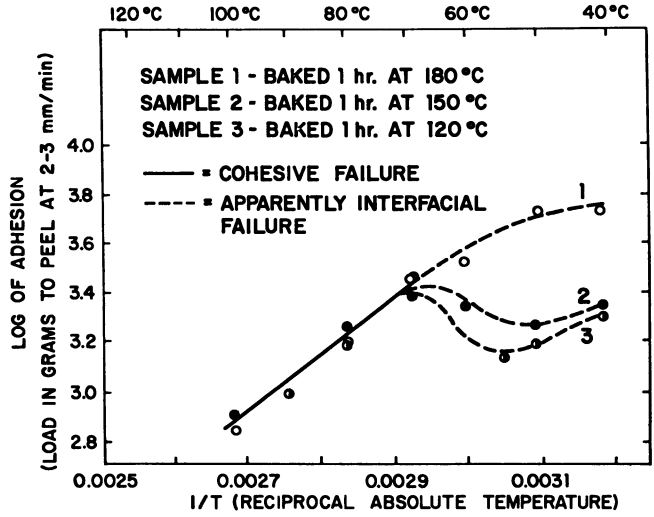

Figure 4. Force required to peel poly(n-butyl methacrylate) from an alkyd resin vs. reciprocal absolute temperature

poly(methyl methacrylate) exhibiting a viscosity average molecular weight of ~90,000 and plasticized with various amounts of benzyl butyl phthalate. The samples were bonded by holding under a load of 10 pounds for 3 hours at 150°C. After this time the samples were cooled slowly and tested *in situ* at various temperatures as the cooling proceeded. This avoided a history of thermal cycling. The apparatus is shown diagrammatically in Figure 5. (The sample-holding device has been eliminated for clarity.) The tests were carried out by adding lead shot to a container attached to the end of the test line at a rate of 100 grams per second. The data are shown in Figure 6. The solid lines again indicate cohesive failure, and the dashed lines indicate apparent interfacial separation.

The shift of the position of the maximum to lower temperatures with increasing plasticizer content is consistent with the interpretation given above. The smaller decrease at temperatures below the maxima with increasing plasticizer content may reflect increasing proximity to equilibrium, since all samples were prepared by holding at 150°C. for 3 hours.

These three sets of experiments all appear to be in complete harmony with the proposed explanation. A satisfactory independent determination of the extent of interfacial contact would be very desirable, however, in order to establish the validity of the hypothesis.

The physical dimensions of the interfacial discontinuities appear to be such that they cannot be detected by visible optics, nor have first attempts to show their existence by capacitance measurements been fruitful. Thus far it has been necessary to rely on data which support the proposition but do not provide unequivocal evidence that incomplete "wetting" is primarily responsible for the observed performance. An example is the "activation energy" of the bonding process. This has

Publication Date: January 1, 1964 | doi: 10.1021/ba-1964-0043.ch011

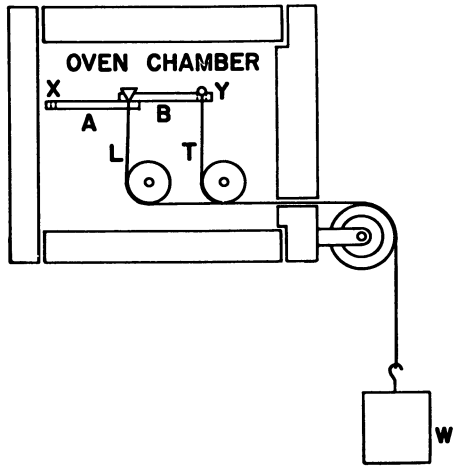

Figure 5. Schematic diagram of apparatus for measuring force required to cleave lap joints at various temperatures

L. Line for application of load for bond formation. T. Line for application of test load

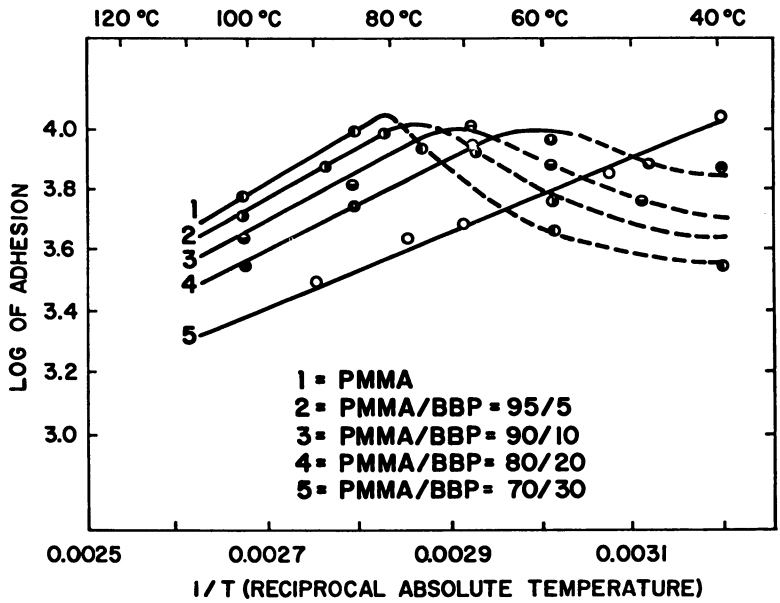

Figure 6. Force required to cleave 0.5 × 0.5 inch lap joints comprising 0.25-inch thick steel rods bonded with plasticized poly(methyl methacrylate) vs. reciprocal absolute temperature

been determined for the bonding of poly(vinyl acetate) to steel, giving a value of 42 kcal. This appears to be in fair agreement with data reported for the activation energy for flow (39 kcal.). A similar observation has been made recently by Gusman [3].

If the wetting process involves viscous flow, at some thickness level the thickness of the polymer film should exert a detectable influence on the rate of bonding. The rate of leveling of surface scratches in lacquer films, for example, has been shown to increase with increasing film thickness. By analogy the rate of bonding at the liquid-solid interface might be expected to decrease with decreasing film thickness. Such an effect was observed with both poly(n-butyl methacrylate) and polyethylene films when they were 50 to 1000 A. thick. This lends strong support to the concept that wetting rather than chemical interaction is frequently involved in the bonding process.

If these hypotheses are correct, one of the major problems is to establish the factors which restrict or limit the interfacial contact.

Consider first the case of fluid low molecular weight polymers of moderate viscosity which may be applied without solvents and "cured" *in situ* to give useful films or adhesives. If no external pressure is applied, the only driving force leading to wetting is the capillary pressure. Zisman [6] has shown that a maximum capillary pressure exists for capillary pores in a given material when

$$\gamma_{LV} = \frac{1}{2b} + \frac{1}{2}\gamma_c \tag{4}$$

Constant b in Equation 4 is a measure of the interaction between the solid and liquid phases when cos θ is approximately a linear function of γ_{LV}, cos $\theta = 1 + b(\gamma_c - \gamma_{LV})$, and γ_c is the "critical surface tension" of wetting of the solid [1].

γ_c is related to the surface free energy of the solid:

$$\gamma_c = \varphi^2 F_{SV} \tag{5}$$

where φ is a measure of the departure from regularity in the interfacial interaction between the solid and the liquid [2].

The maximum capillary pressure is given by:

$$p_{max} = \left(\frac{1}{2b} + \frac{\gamma_c}{2}\right)\left(\frac{1}{r_1} + \frac{1}{r_2}\right) \tag{6}$$

where r_1 and r_2 are the principal radii of curvature of the liquid-vapor interface in the nonwetted regions of the solid-liquid interface.

For organic substrates the first term will generally be about 20 to 70 dynes per cm. The second indicates a profound influence for surface topography. This term could have a large positive value for small porelike asperities but very small or even negative values for some configurations. This may explain in part the improved adhesion often observed for sand-blasted or etched surfaces in contradistinction to sanded or polished surfaces. Certain topographical configurations may lead to metastable mechanical equilibria which would halt the wetting process.

Publication Date: January 1, 1964 | doi: 10.1021/ba-1964-0043.ch011

The nonwetted portions of the interface comprise small closed gas- or vapor-filled volumes bounded by the substrate and the adhesive. If these volumes are of such size that they contain a sufficiently large number of molecules in the vapor phase to exert nearly normal pressures, these will act against the capillary pressures and diminish the rate of wetting. It is conceivable that diffusion of these molecules into the adhesive layer could be rate-limiting under certain circumstances.

Also in general the resistance to viscous flow will increase at a faster rate than the capillary pressures increase as the pore or channel dimensions become smaller. This is of real significance in the case of hot-melt adhesives, which are frequently applied at relatively high viscosity and remain fluid for only a brief time.

For polymers applied from solution there is a possibility that the solvent may be selectively adsorbed. If this were the case, intimate contact between the polymer and substrate could be achieved only after desorption of the solvent. If desorption occurred when the solvent concentration was relatively small, the viscosity of the solution could be very high, precluding wetting within the time the solution exhibited sensible fluid characteristics.

If coacervation were to occur in the solution in the vicinity of the solution-substrate interface, the fluid phase containing relatively little polymer would wet and fill the surface asperities. After evaporation of the solvent the voids would remain unfilled.

Publication Date: January 1, 1964 | doi: 10.1021/ba-1964-0043.ch011

Conclusions

Virtually all practical systems should exhibit complete wetting at equilibrium. In practice, however, interfacial equilibrium is frequently not achieved. Under these circumstances high stress concentration at the interfacial discontinuities leads to poor performance. The stress concentration is determined by the viscoelastic response of the adhesive and the time-temperature characteristics of the test used to assess the performance.

Some factors which may retard the wetting and preclude attainment of equilibrium are a combination of low capillary pressures and high fluid viscosities, metastable equilibria, selective adsorption, and coacervation.

Literature Cited

(1) Fox, H. W., Zisman, W. A., J. Colloid Sci. **7**, 428 (1952).
(2) Good, R. J., Girifalco, L. A., J. Phys. Chem. **64**, 561 (1960).
(3) Gusman, S., Offic. Dig. Federation Soc. Paint Technol. **34**, 884 (1962).
(4) Huntsberger, J. R., J. Polymer Sci. **1a**, 2241 (1963).
(5) Johnson, R. E., Jr., Dettre, R. H., Advan. Chem. Ser., No. **43**, 112 (1963).
(6) Zisman, W. A., General Motors Symposium on Adhesion and Cohesion, July 24-25, 1961.

Received March 14, 1963.

12

Surface Energetics, Adhesion, and Adhesive Joints

LOUIS H. SHARPE and HAROLD SCHONHORN

Bell Telephone Laboratories, Inc.
Murray Hill, N. J.

Publication Date: January 1, 1964 | doi: 10.1021/ba-1964-0043.ch012

Certain aspects of the adsorption theory of adhesion are developed more fully than has been done previously. The consequences of nonreciprocity of spreading are pointed out, and are used to develop a more general practical point of view with respect to the adhesive bonding of materials of low-surface free energy. The system epoxy adhesive–(nonsurface-treated) polyethylene, normally considered nonadherent, is investigated experimentally in some detail. It is shown how this system, without material modification, can be made adherent. An area of study for possible adhesives for materials of low-surface free energy is suggested.

At present three theories of adhesion exist—the adsorption theory [9], the diffusion theory [24, 25, 26], and the electrostatic theory [10, 23]. The majority of those who have concerned themselves with the subject of adhesion lean toward the adsorption theory, if for no other reason than a recognition that the phenomenon of wetting is intimately related to adhesion. The word "adhesion" (unmodified) here means strictly an interfacial phenomenon, while "practical adhesion" means the strength with which two materials stick together—that is, the force required to separate them, or joint strength.

We develop certain aspects of the adsorption theory of adhesion more fully than has been done previously, based solely on (free) surface energetics, and show how they can be applied to real or practical systems. As a consequence, it is shown that the deBruyne adhesion rule [7] is incorrect in part. Our concern is mainly with what we believe to be the most important problem in the making of adhesive bonds—that is, the achievement of extensive and proper (no intermediate phase) interfacial contact. We discuss also the breaking strength of certain adhesive joints where this is necessary to the development of our thesis. However, the processes of making and breaking adhesive joints bear no

In Contact Angle, Wettability, and Adhesion; Fowkes, F.;
Advances in Chemistry; American Chemical Society: Washington, DC, 1964.

direct fundamental relation to each other, although the breaking strength of an adhesive joint is, in general, a consequence of how it is made.

The adhesion and practical adhesion of combinations of (organic) low-surface free energy materials (< 100 ergs per sq. cm.) mainly are discussed, since these, in general, present the most difficulty in bonding, and there exists the most confusion concerning them. High-surface free energy materials (metals, metal oxides, glasses, etc.) are not discussed in detail, since the principles discussed can be directly extended to include these materials.

Theoretical

Thermodynamics. Consider an equilibrium closed system of a liquid, L_2, in contact with a plane surface of an isotropic solid, S_1 (which is not soluble in L_2), and saturated vapor, V_2°, of liquid L_2. The Young-Dupré equation is

$$\gamma_{S_1V_2^\circ} - \gamma_{S_1L_2} = \gamma_{L_2V_2^\circ} \cos\theta \quad (1)$$

where the γ's are surface tensions and θ is the usually defined contact angle. Let us further consider the surface of the solid to be an equilibrium surface. Under these circumstances the surface tension and surface free energy of the solid are the same and we can write

$$F_{S_1V_2^\circ} - F_{S_1L_2} = F_{L_2V_2^\circ} \cos\theta \quad (2)$$

where the F's are now surface free energies.

The maximum reversible work of adhesion of L_2 to S_1 is

$$W_{adh} = F_{S_1^\circ} + F_{L_2V_2^\circ} - F_{S_1L_2} \quad (3)$$

where $F_{S_1^\circ}$ is the surface free energy of the solid, S_1, in vacuum. Upon substituting in Equation 3 the value of $F_{S_1L_2}$ from Equation 2, we obtain

$$W_{adh} = \left(F_{S_1^\circ} - F_{S_1V_2^\circ}\right) + F_{L_2V_2^\circ}(1 + \cos\theta) \quad (4)$$

As has been pointed out by Bangham and Razouk [3], this is the work required to strip the liquid from the solid so as to leave a surface on the solid which is identically the equilibrium surface on the solid in a vacuum. This work of adhesion is different from the work of adhesion required to strip the liquid from the solid so as to leave the equilibrium adsorbed film of vapor V_2 on the solid surface. This latter work of adhesion is

$$W'_{adh} = F_{L_2V_2^\circ}(1 + \cos\theta)$$

and differs from W_{adh} by the term $\left(F_{S_1^\circ} - F_{S_1V_2^\circ}\right)$. Now $F_{S_1^\circ}$ must always be greater than $F_{S_1V_2^\circ}$; hence the term $\left(F_{S_1^\circ} - F_{S_1V_2^\circ}\right)$ is always positive [3]. This means that the work required to strip the liquid from the solid completely is greater than that required to strip the liquid

Publication Date: January 1, 1964 | doi: 10.1021/ba-1964-0043.ch012

from the solid so as to leave an equilibrium film of adsorbed vapor of the liquid.

Since the work of cohesion of L_2 is given by

$$W_{coh} = 2F_{L_2v_2^\circ} \tag{6}$$

Equation 4 tells us that if $\theta = 0$—that is, if liquid L_2 spreads on solid S_1—the maximum reversible work of adhesion is always in excess of the work of cohesion by an amount at least $\left(F_{S_1^\circ} - F_{S_1v_2^\circ}\right)$; we say at least because Equation 4 is valid only for $\theta > 0$.

Now assume that by some means we cause liquid L_2 to solidfy on solid S_1 in such a manner that we again have an equilibrium system, this time of solid S_1 in contact with solid S_2 in the presence of saturated vapor of S_2. The Young-Dupré equation for this system is

$$\gamma_{S_1v_2^{\circ\prime}} - \gamma_{S_1S_2} = \gamma_{S_2v_2^{\circ\prime}} \cos\theta \tag{7}$$

where the γ's are again surface tensions and the prime on the subscript indicates that the saturation vapor pressure of S_2 is different from that of L_2. We again assume that S_1 and S_2 are equilibrium surfaces, so that we may write

$$F_{S_1v_2^{\circ\prime}} - F_{S_1S_2} = F_{S_2v_2^{\circ\prime}} \cos\theta \tag{8}$$

where the F's are again surface free energies.

The maximum reversible work of adhesion of S_2 to S_1 is

$$W_{adh} = F_{S_1^\circ} + F_{S_2v_2^{\circ\prime}} - F_{S_1S_2} \tag{9}$$

Substituting in Equation 9 the value of $F_{S_1S_2}$ from Equation 8 we get

$$W_{adh} = \left(F_{S_1^\circ} - F_{S_1v_2^{\circ\prime}}\right) + F_{S_2v_2^{\circ\prime}}(1 + \cos\theta) \tag{10}$$

This is the equation for the maximum reversible work of adhesion for two solids in contact and is the counterpart of Equation 4 for the case of a liquid in contact with a solid. Our definition of the final solid-solid state as an equilibrium state implies that there are no residual stresses in either solid produced by the solidification of L_2.

Equation 10 could just as well have been derived on the basis of bringing into contact with each other an equilibrium planar surface of solid S_2 and a similarly defined surface of solid S_1 and then separating them in the appropriate fashion.

We showed that if L_2 spreads on S_1, the maximum reversible work of adhesion of L_2 to S_1 is greater than the work of cohesion of L_2. Conversely, if the maximum reversible work of adhesion of L_2 to S_1 is greater than the work of cohesion of L_2, then L_2 must spread (initially) on S_1. We can write, then, from Equations 3 and 6,

$$W_{adh} - W_{coh} = F_{S_1^\circ} - F_{L_2v_2^\circ} - F_{S_1L_2} = Sp \tag{11}$$

Publication Date: January 1, 1964 | doi: 10.1021/ba-1964-0043.ch012

where Sp is the initial spreading coefficient [6, 16, 17].

We said, however, that if $W_{adh} - W_{coh} > 0$, L_2 must (initially) spread on S_1—that is, for spreading to occur

$$F_{S_1}^{\circ} - F_{L_2V_2}^{\circ} - F_{S_1L_2} > 0$$

or

$$F_{S_1}^{\circ} > F_{L_2V_2}^{\circ} + F_{S_1L_2} \qquad (12)$$

This relationship says that for spreading of liquid L_2 on solid S_1 to occur, the surface free energy of S_1 must exceed the sum of the surface free energies of the liquid (in contact with its saturated vapor) and of the solid-liquid interface.

Formation of Interface. Two materials probably adhere, at least initially, because of van der Waals attractive forces acting between the atoms in the two surfaces. Now interfacial strengths, based on van der Waals forces alone, far exceed the real strengths of one or other of the adhering materials. This means that interfacial separation probably never occurs to any sensible extent when mechanical forces are used to separate a pair of materials which have achieved complete interfacial contact (probably a highly unlikely situation), or a number of separate regions of interfacial contact. It follows, then, that breaking a joint mechanically, in general, tells nothing directly about interfacial forces.

Van der Waals forces are operative over very small distances. Hence, in order that materials adhere, the atoms in the two surfaces must be brought close enough together for these forces to become operative. If we had a piece of A (solid) and B (solid) and each had an absolutely smooth (on an atomic scale) planar surface which we then brought together in a perfect vacuum, all attempts to get them apart mechanically would result in failure in the bulk of either A or B. But real surfaces differ from these ideal surfaces in that they are rough and contaminated and both of these imperfections contribute to a greatly decreased real area of contact between the surfaces of A and B. In general, however, where they have achieved contact—that is, where they have been brought close enough for van der Waals forces to become operative—they have adhered, and when they are separated mechanically a little of A remains on B, and B on A, depending on the geometry in the neighborhood of each area of contact. The general reaction based on visual examination is that the solids did not adhere or the failure was in adhesion. The first statement, we believe, is incorrect, because surely some areas of A and B achieved interfacial contact, and the second is incorrect because where the surfaces were not in contact there was no adhesion and it makes no sense to talk about the failure of something that did not exist.

This point of view leads to the conclusion that to get A and B to make a stronger joint we need to increase their real area of contact. This means that one or both of the materials must be made to conform better to the surface roughness of the other. This implies, in a practical sense, that one of the materials should be fluid when placed in contact with the other. However, that one of the materials be liquid is a necessary, but may not be a sufficient, condition for if the liquid makes a

Publication Date: January 1, 1964 | doi: 10.1021/ba-1964-0043.ch012

nonzero contact angle with the solid, its tendency to create a large interfacial area of contact is relatively small. The result is that the liquid may do a great deal of bridging, trap a great deal of air, and achieve little penetration into the surface roughness of the solid, and stress concentrations due to a nonzero contact angle become important. However, if the liquid member spontaneously spreads on the solid, the interfacial area of contact increases, because the liquid can now flow more completely into the micro or submicro pores and crevices in the surface of the solid and can displace adsorbed gases and other contamination. In addition, the zero contact angle tends to minimize stress concentrations. The effect of creating a spontaneous spreading situation, then, is twofold—the real area of contact is increased and stress concentration is minimized [11].

It becomes important now to point up the fact that spreading is a nonreciprocal phenomenon—that is, for two liquids, the fact that pure A spreads on pure B means that pure B positively will not spread on pure A (see, for example, Harkins [14]) and the same appears to be true of adhesion in a practical sense. In a practical sense, if A adheres strongly to B, then B will not adhere strongly to A. What, of course, we really mean is that if we can make a strong joint between A and B when A is the liquid member (subsequently solidified) and B the solid, then it appears that we cannot, in general, make a strong joint when B is the liquid member and A the solid, for reasons mentioned above. It may be possible to make a strong joint if both are fluid simultaneously.

It may appear that we have said that spreading of the liquid member is the *sine qua non* of adhesion and, also, of practical adhesion. In a sense we have, but this requires qualification. From a purely thermodynamic point of view, it makes no difference for an ideal system A-B, in the final state, whether the final state was achieved by making A fluid, or B fluid, or both fluid, or both solid, if we define the final state as being that of complete interfacial contact of A and B. But, in a real or practical sense, the achievement of adhesion and practical adhesion is time-dependent and, in general, it may make a difference how—that is, from which side—we attempt to approach the equilibrium state. If we work from the side of the low-surface free energy solid and the high-surface free energy liquid the rate of approach to equilibrium may be intolerably slow, or in the case of a liquid which sets to a solid (as by cross linking) in a relatively short time span, the rate may become essentially zero. This is the case in the epoxy adhesive–polyethylene joint, to be discussed shortly. If, however, the low surface free energy solid can be made fluid, the rate of approach to equilibrium may be greatly accelerated. The rate of approach to equilibrium may (and, in general, should) be rapid if both phases are fluid simultaneously. Stresses induced by differential shrinkage have been neglected in this discussion. However, we are mainly concerned with the conditions for creation of extensive and proper interfacial contact, and the subject of shrinkage-induced stress concentrations is treated extensively elsewhere [9, 11].

We have specifically mentioned only van der Waals forces in connection with the preceding treatment. This is not to be construed as meaning that other molecular forces may be excluded from participation in adhesion. In the initial process involving the establishment of interfacial contact, all those molecular forces involved in wetting

Publication Date: January 1, 1964 | doi: 10.1021/ba-1964-0043.ch012

phenomena can be considered to be important. Chemisorption is not excluded, but if it is to occur molecular contact must have already been established—that is, van der Waals forces must already be operative. Therefore, any such chemical reaction as does occur, occurs after adhesion is a *fait accompli*. Further, since we believe that sensible interfacial separation does not occur under mechanical influences even when only van der Waals forces are operative, it follows that we do not believe that chemisorption has any positive influence on the mechanical strength of an adhesive joint. It may have negative influence on strength if weak boundary layers [5] are formed. However, chemisorption may increase the permanence of an adhesive joint by retarding or preventing destruction of the interface as by dewetting by moisture, low surface tension liquids, etc.

In order to be able to use Expression 12 it is necessary to determine $F_{S_1}^{\circ}$, $F_{L_2V_2}^{\circ}$, and $F_{S_1L_2}$. There exists a good method only for the determination of $F_{L_2V_2}^{\circ}$, the surface free energy (surface tension) of the liquid, but no satisfactory method for determining directly either $F_{S_1}^{\circ}$ or $F_{S_1L_2}$. Zisman's [27] work on wetting and his concept of γ_c, the critical surface tension of wetting, provide us with some characterization of $F_{S_1}^{\circ}$ or $F_{S_1V_2}^{\circ}$. However, if we are willing to accept the empirical relationship which Zisman has established between γ_c and $F_{L_2V_2}^{\circ}$ (or $\gamma_{L_2V_2}^{\circ}$), it is unnecessary to concern ourselves with either $F_{S_1}^{\circ}$ or $F_{S_1L_2}$. If we admit that γ_{cS_1}, the critical surface tension of wetting, is the surface tension which a liquid, L_2, would have to possess in order just to spread on S_1, then the criterion for spreading, Expression 12, may be replaced by the criterion [13,27].

$$\gamma_{cS_1} > \gamma_{L_2V_2}^{\circ} \tag{13}$$

the terms of which are experimentally much more accessible than the thermodynamic quantities which we have been discussing. Expression 13 provides a useful working relationship. It may be possible to decide, *a priori*, whether A will adhere strongly to B—that is, form a strong joint—or will not, from a knowledge of the parameters γ_{cS_1} and $\gamma_{L_2V_2}^{\circ}$ at the temperature at which the bond is to be made.

Table I gives representative values of γ_{cS_1} and $\gamma_{L_2V_2}$ for a number of polymers. The values of γ_c given have been determined at 20°C. At present, there exist no data concerning the value of γ_c for various substrates at elevated temperatures. Strictly speaking, therefore, predictions based on the above relationship are limited to 20°C. However, since the temperature coefficient of surface tension for a large number of organic materials, as given by Harkins [15], appears to be approximately 0.1 dyne per cm. per °C., the same relative surface tension relationship between liquid and solid will probably exist at somewhat elevated temperature as exists at 20°C.

One further note of caution with respect to the use of the critical surface tension in this context is necessary. The precise value of γ_c

Table I. Critical Surface Tension (γ_c) and Surface Tension (γ_{LV}) of Selected Systems

System	γ_c, Dynes/Cm., 20°C.	γ_{LV}, Dynes/Cm., 25°C.
Teflon FEP	16[a]	-
Teflon TFE	18.5[a]	-
Polyethylene	31[a]	-
Polystyrene	33[a]	-
DER332LC epoxy resin	-	47.2
DER332LC epoxy resin, 100 pbw[b] +DEAPA[c], 7pbw	-	32.9
Fluorinated epoxy resin	-	40.3
Fluorinated epoxy resin, 100 pbw +DEAPA, 7 pbw	-	38.8
DEAPA	-	23.6

[a]Values from [27].
[b]Parts by weight.
[c]Diethylaminopropylamine.

Publication Date: January 1, 1964 | doi: 10.1021/ba-1964-0043.ch012

obtained for a surface is dependent, in general, upon the particular series of liquids used to determine it. A series of liquids which interacts more strongly with a surface will, in general, give a higher γ_c than another series which interacts less strongly with the same surface. One should, therefore, use for prediction the γ_c value obtained by use of a series of liquids which is, in general, characteristic of the liquid material in the system for which the prediction is being made. This is necessary in light of the findings of Fowkes [12], that a low-energy liquid will spread on a high-energy solid only if the intermolecular forces in the solid and the liquid can interact with each other. For example, if a liquid exhibiting only a dispersion force contribution to its surface tension is placed on a solid which exhibits both dispersion and hydrogen bonding forces, then, in general, the only interaction between the two phases will be a dispersion force interaction, and the simple spreading criterion must be modified to take this into account.

Experimental

Experiments concerning the practical adhesion between a conventional epoxy adhesive and a conventional polyethylene illustrate some of the principles which we have been discussing.

Materials. Epoxy resin DER332LC (Dow Chemical Co., Midland, Mich.) is a very pure diglycidyl ether of bisphenol A, having an epoxy equivalent weight of 179 maximum (the pure material would have an epoxy equivalent weight of 170), a total chloride content less than 0.1% by weight, and a viscosity of 6400 centipoises maximum at 25°C.

Diethylaminopropylamine (Miller-Stephenson Chemical Co., Inc., Philadelphia) was distilled under nitrogen through a 6-inch Vigreux column and the first fraction discarded. The product, distilling at 68°C. and 26-mm. pressure, was stored in the dark in tightly stoppered glass containers prior to use.

The epoxy adhesive consisted of 100 parts by weight of the above resin and 7 parts by weight of the diethylaminopropylamine, thoroughly mixed and used immediately.

Polyethylene (Marlex 5003, Phillips Petroleum Co., Bartlesville, Okla.) was formed from powder into 0.009-inch-thick sheets between specularly smooth Mylar sheets in a metal mold at a temperature of 150°C. and pressure of 1000 p.s.i. for approximately 5 minutes. The polymer has a density of 0.95 and a melt index of 0.3.

The above polyethylene was irradiated in 0.009-inch-thick sheet at 21° to 23°C. in a nitrogen atmosphere with 1-m.e.v. electrons to a total dose of 20 megarads to give the material which is termed irradiated or cross-linked polyethylene.

The metal tensile-shear adherends were of 2024-T3 aluminum (Aluminum Co. of America). Their dimensions were 5 by 1 by 1/16 inch. The surface of the aluminum was prepared by first vapor-degreasing in trichloroethylene and then etching for 7 minutes at 65°C. in the following solution:

Sodium dichromate ($Na_2Cr_2O_7 \cdot 2H_2O$)	1 part by weight
Water	30 parts by weight
Sulfuric acid (95%)	10 parts by weight

After etching, the specimens were rinsed for 5 minutes in running tap water and for 1 minute in running distilled water, and then dried in a forced air oven at 60°C. Specimens were stored in desiccators over Ascarite and removed just prior to use.

Procedures. For the measurement of tensile-shear strengths, standard composite test pieces consisting of aluminum–epoxy adhesive–polyethylene sheet–epoxy adhesive–aluminum were prepared for bonding in a special device designed to maintain a half-inch overlap. The thickness of the epoxy adhesive was maintained constant by insertion of a piece of 0.003-inch-diameter gold wire in each glue line between the aluminum and the polyethylene. Clean gloves and tweezers were used in all specimen preparations to avoid possible contamination. Bonding was accomplished, at approximately 20-p.s.i. pressure, by placing stacks of composites in forced air ovens at specified temperatures for 16 hours. The bonded specimens were tested in tensile shear in accordance with ASTM D 1002-53T, except that the strain rate was 0.1 inch per minute.

A DuNouy tensiometer was used to measure the surface tension of the epoxy resin and curing agent. The instrument was calibrated with water and benzene. Prior to each determination, the surface tension of water was measured. Mixtures of the epoxy resin and curing agent were equilibrated for a few minutes after mixing before the surface tension was determined. Since the mixtures had high viscosities, the DuNouy ring was equilibrated in the surface of the liquid for a few minutes at a stress several tenths of a dyne below the point of maximum stress, to permit the material to relax. The break point was approached slowly until rupture occurred. Three readings were taken for each mixture. Deviations of the order of ±0.2 dyne per cm. or less were obtainable by this procedure. The surface tensions were calculated using the appropriate correction parameter of Harkins and Jordan [18].

Publication Date: January 1, 1964 | doi: 10.1021/ba-1964-0043.ch012

Results. Figure 1 shows the effect of the ultimate temperature of bond formation on the tensile-shear strength of the aluminum-epoxy-polyethylene composite structure described previously. It is rather obvious that at temperatures close to 100°C. the epoxy, even though its viscosity is low, has not formed a strong bond with the polyethylene, for the reason, we believe, that it has not achieved extensive interfacial contact with the polyethylene before solidification occurs. If, however, one first solidifies the epoxy at some temperature below 100°C. and then raises the temperature close to, or above, the melting point of the

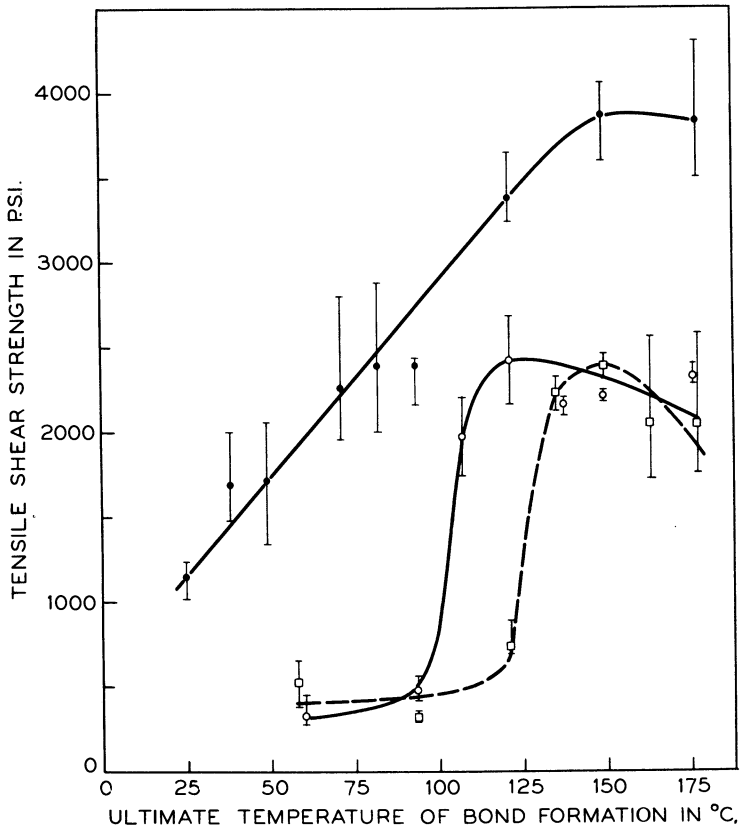

Figure 1. Dependence of bond strength on temperature of bond formation

● Aluminum-epoxy-aluminum composite
□ Aluminum-epoxy-polyethylene-epoxy-aluminum composite
O Aluminum-epoxy–cross-linked polyethylene–epoxy-aluminum composite

Ranges indicated. Results based on five replicates, each point

polyethylene, a striking increase in the bond strength results. This, in fact, occurs (and the bond strengths are a function of the ultimate temperature only) regardless of whether the temperature is immediately raised to the neighborhood of the melting point of the polyethylene while the epoxy is still liquid, or whether the epoxy is first solidified at some temperature below 100°C. and the temperature is then raised. We believe that in these instances the surface energetics are now favorable for spreading of the polyethylene to occur and sufficient time is allowed for extensive and proper interfacial contact to take place. The viscosity of the polyethylene at 145°C. is approximately 10^6 centipoises (determined by stress relaxation method [22]), whereas the viscosity of the epoxy, when it is the liquid member, at 25°C. is approximately 10^3 centipoises. It is interesting to note, therefore, that viscosity of the liquid member apparently is of no real importance in this instance, because sufficient time can be allowed for good wetting by the polyethylene to take place.

The behavior of the cross-linked polyethylene is also particularly interesting. The temperature at which the bond strength of the composite bearing this material begins to rise markedly is some 20°C. below the comparable temperature for the identical un-cross-linked polyethylene, and not above it, as might generally be believed. The explanation for this, we believe, is simple. The crystalline melting point of polyethylene is lowered by irradiation, not raised, as Mandelkern, *et al.* [20] and Marker, Early, and Aggarival [21] have pointed out. The irradiated polyethylene, therefore, spreads at a lower temperature than the unirradiated polymer because its melting point is lower.

The bend strength of the composite bond containing the irradiated polyethylene is remarkable. The aluminum adherends must be bent through an angle of about 110° before failure of the bond occurs. On a number of occasions, bending the specimen has resulted in fracture of one of the aluminum adherends, rather than failure of the bond.

The present generally accepted procedure for structurally bonding polyethylene with an adhesive is to oxidize the polyethylene surface; this raises its surface free energy and improves the wettability of the polyethylene by the adhesive [2]. An improvement in bond strength is thus obtained. We are not, however, aware of any previous work in which the strength levels reported were comparable to those which we have obtained.

Discussion

The deBruyne adhesion rule states [7]: "Provided we use pure or simple substances as adhesives then there is a good deal of evidence that strong joints can never be made by polar adherends with nonpolar adhesives or to nonpolar adherends with polar adhesives." It is possible to support the portion of the rule which deals with nonpolar adherends and polar adhesives on the basis that polar adhesives generally have higher surface free energies than nonpolar adherends, and therefore will wet them very poorly [27]. It is not possible, however, to support the other portion of the rule which deals with polar adherends and nonpolar adhesives, since the surface energetics are favorable in this instance and spreading should result. This portion of deBruyne's adhesion rule must, therefore, be incorrect. That it is incorrect is further

Publication Date: January 1, 1964 | doi: 10.1021/ba-1964-0043.ch012

attested by the fact that we have obtained strong bonds between a cured epoxy adhesive and a number of nonpolar thermoplastics—e.g., polyethylene, polypropylene, Teflon FEP, and polystyrene—also between the above-mentioned thermoplastics and metals such as aluminum, copper, and stainless steel, by the melt technique. DeBruyne has recently stated that he now also believes this portion of his rule to be incorrect [8], and that the rule was simply an expression of the facts as they were known at the time the rule was formulated.

It might be instructive now to develop a more general but practical point of view based on the consequences of nonreciprocity of spreading, and our experiments. Examples of materials which are at present difficult to bond with conventional adhesives without surface modification are: polyethylene, polypropylene, Teflon TFE, Teflon FEP, polystyrene, etc.—that is, the class of nonpolar thermoplastics. They are difficult to bond because they are materials of low-surface free energy, much lower than conventional adhesives. However, because they are of low-surface free energy and because they can be rendered fluid (mobile), as by raising the temperature, they can be made to form strong joints with a large number of suitable materials of higher surface free energy. So far as we have been able to determine, this particular aspect of adhesive bonding has not previously been pointed out, and it is rather startling when one first comes to the realization that materials which are generally believed to be impossible to bond conventionally without surface modification are precisely those materials which, when used as adhesives, form strong joints with a large number of substrates. Recently Korolev *et al.* [19] have discussed practical adhesion between poly (tetrafluoroethylene) and metals in these same terms.

Future Work. The spreadability-adhesion criterion, as we have discussed it, immediately draws attention to low surface tension polymers as potential adhesives for low-surface free energy solids. It is known that low surface tension is associated with the substitution of fluorine for hydrogen in organic materials. This knowledge suggests that useful adhesive materials may result from the appropriate substitution of fluorine or fluorinated side chains for hydrogen in hydrogen-containing polymers. Certain such fluorinated materials might be capable of forming strong joints with such polymers as polyethylene, polypropylene, and Teflon TFE, which cannot now be structurally bonded by conventional adhesives without prior surface modification.

One class of such materials is the fluorinated alkyl esters of acrylic and methacrylic acid, a number of which have been prepared [1]. One of these esters, poly(1,1-dihydropentadecafluoro-octyl methacrylate), has a $\gamma_c \approx 11$ dynes per cm.—less than Teflon TFE or even FEP [4]. Such materials, and others within the general class of unsaturated, appropriately fluorinated, polyesters warrant investigation for use either as thermoplastic hot-melt adhesives, or for cross linking *in situ* to form rigid thermoset adhesives. The saturated, appropriately fluorinated polyesters also warrant investigation as thermoplastic hot-melt adhesives.

Several very interesting classes of materials may also result from proper fluorination of conventional monomeric or polymeric diepoxides. The conventional diepoxides or "epoxies" are extremely useful adhesive materials. The epoxy resin which we have examined in this study has a surface tension of 47.2 dynes per cm. Appropriate fluorination of this

Publication Date: January 1, 1964 | doi: 10.1021/ba-1964-0043.ch012

and similar materials would markedly reduce their surface tensions. We have prepared a diglycidyl ether of bisphenol A (obtained from the Research Laboratories of Allied Chemical, Morris Township, N. J.) in which the pendant methyl groups on the bridge carbon atom were replaced by perfluoromethyl groups. Neither the surface tension nor some other properties were markedly affected by this substitution. This might have been predicted on the basis of the relatively small volume substitution of fluorine in the molecule. Longer fluorinated chains would proportionately affect physical and mechanical properties. It is tempting to speculate that adhesive systems useful for the polyolefins and polystyrene might lie among such polymers.

Acknowledgment

The authors gratefully acknowledge helpful discussions with N. A. deBruyne, Techne, Ltd., Cambridge, England, and with F. H. Stillinger, Jr., Bell Telephone Laboratories, Inc.

Literature Cited

(1) Ahlbrecht, A. H., Reid, T. S., Husted, D. R. (to Minnesota Mining & Mfg. Co.), U. S. Patent 2,642,416 (June 16, 1953).
(2) Allan, A. J. G., J. Polymer Sci. 38, 297 (1959).
(3) Bangham, D. H., Razouk, R. I., Trans. Faraday Soc. 33, 1459 (1937).
(4) Bernett, M. K., Zisman, W. A., J. Phys. Chem. 66, 1207 (1962).
(5) Bikerman, J. J., "The Science of Adhesive Joints," Academic Press, New York, 1961.
(6) Cooper, W. A., Nuttall, W. H., J. Agr. Sci. 7, 219 (1915).
(7) deBruyne, N. A., Aircraft Engr., 18, No. 12, 53 (1939).
(8) deBruyne, N. A., 19th International Congress of Pure and Applied Chemistry, Symposium on Adhesion, London, England, July 1963.
(9) deBruyne, N. A., Houwink, R., eds., "Adhesion and Adhesives," Elsevier, New York, 1951.
(10) Deryagin, B. V., Krotova, N. A., Dokl. Akad. Nauk. SSSR 61, 849 (1948).
(11) Eley, D. D., ed., "Adhesion," Oxford University Press, London, 1961, particularly Chap. 8 and 11.
(12) Fowkes, F. M., ASTM Symposium on Recent Advances in Adhesion Science, Atlantic City, N. J., June 1963.
(13) Fox, H. W., Zisman, W. A., J. Colloid Sci. 5, 514 (1950); 7, 109, 428 (1952).
(14) Harkins, W. D., "Physical Chemistry of Surface Films," Reinhold, New York, 1952.
(15) Harkins, W. D., Davies, E. C. H., Clark, G. L., J. Am. Chem. Soc. 39, 541 (1917).
(16) Harkins, W. D., Feldman, Aaron, Ibid., 44, 2665 (1922).
(17) Harkins, W. D., Grafton, E. H., Ibid., 42, 2534, 2539 (1920).
(18) Harkins, W. D., Jordan, H. F., Ibid., 52, 1751 (1930).
(19) Korolev, A. Ya., et al., Vysokomolekul. Soedin. 4, 1412 (1962).
(20) Mandelkern, L., Roberts, D. E., Halpin, J. C., Price, F. P., J. Am. Chem. Soc. 82, 46 (1960).
(21) Marker, L., Early, Robert, Aggarwal, S. L., J. Polymer Sci. 38, 369 (1959).
(22) Matsuoka, S., private communication.
(23) Skinner, S. V., Savage, R. L., Rutzler, J. E., J. Appl. Phys. 24, 438 (1953).
(24) Voyutskiĭ, S. S., Margolina, Yu. L., Uspekhi Khim. 18, 449 (1949); Rubber Chem. Technol. 30, 531 (1957).
(25) Voyutskiĭ, S. S., Shtarkh, B. V., Kolloidn. Zh. 16, 3 (1954); Rubber Chem. Technol. 30, 548 (1957).

(26) Voyutskiĭ, S. S., Zamaziĭ, V. M., Kolloidn. Zh. 15, 407 (1953); Rubber Chem. Technol. 30, 544 (1957).
(27) Zisman, W. A., in "Adhesion and Cohesion," P. Weiss, ed., Elsevier, New York, 1962.

Received March 28, 1963

13

Hysteresis of Contact Angles in the System Mercury - Benzene - Water

ANTOINE M. GAUDIN and AUGUST F. WITT

Massachusetts Institute of Technology
Cambridge 39, Mass.

Publication Date: January 1, 1964 | doi: 10.1021/ba-1964-0043.ch013

Experiments with a water drop on mercury under benzene in absence of oxygen show an equilibrium contact angle of 119° ± 1° and absence of hysteresis. Under these conditions the dynamic contact angles did not indicate any speed dependence. The same system when saturated with oxygen shows a hysteresis of 110°. pH dependence of hysteresis was found for oxygen-contaminated systems. In the pH range 0 to 4, the hysteresis is nil, increasing to 141° at pH 14. We conclude that contact angle hysteresis is absent in the pure three-phase system. Hysteresis when encountered is attributed to oxidation reactions occurring at the mercury surface.

When a drop of a liquid is placed on a solid surface, the system will try to establish a state of minimum total surface free energy. Depending upon the relative values of the three interfacial tensions involved, the contact angle, θ, between the liquid and the solid phase will vary from 0° to 180°. The correlation between γ and θ is given by Young's equation

$$\gamma_{SG} - \gamma_{SL} = \gamma_{LG} \cos \theta \quad (1)$$

Rayleigh [4] found as early as 1890 that the magnitude of θ often depends upon whether previous to the measurement the liquid phase was advancing or receding over the solid phase. Sulman [5] in 1920 termed the spread between the maximum and minimum contact angles measured in the same system "contact angle hysteresis." Since then many systems have been found with hysteresis values up to 150°. The fact that hysteresis is often overlooked or neglected, added to the difficulty of obtaining good reproducibility, renders the value of many published data doubtful.

In Contact Angle, Wettability, and Adhesion; Fowkes, F.;
Advances in Chemistry; American Chemical Society: Washington, DC, 1964.

Current theories to explain hysteresis of contact angles are primarily based on the concepts of surface roughness, surface heterogeneity, friction, and adsorption phenomena. Unintentional adsorption, or contamination—the result of inadequate experimental technique—is, however, the most frequent explanation. As all systems involving solids are subject to the reasons indicated above for hysteresis, we chose the system mercury-benzene-water, which should be affected only by adsorption phenomena, controllable under proper experimentation. An additional advantage is the fact that all interfacial tensions involved can be measured.

Materials Used

All glassware was cleaned in hot chromic acid, rinsed with hydrochloric acid, and again rinsed with conductivity water.

Water, specific conductance, $K = 6 \times 10^{-7}$ ohm^{-1} per cm.

Benzene, reagent-grade, chemically purified and submitted to zone refining (refractive index 1.5011, 20°)

Mercury, triple distilled, total impurities less than 0.00009 weight %. It was redistilled and stored in a quartz vessel under nitrogen.

Unless otherwise stated, water and benzene were saturated with purified nitrogen and saturated with each other. The atmosphere above the three-phase system under investigation was constantly flushed with nitrogen saturated with water and benzene. The nitrogen, prepurified (99.998% N_2, 0.002% O_2), was passed through activated copper, heated to 300° C., and passed through a concentrated KOH solution. This procedure reduces the oxygen content to less than 5×10^{-4} mole %.

Preparation of System and Experimental Setup

In a borosilicate glass vessel with optically flat walls, mounted on the tilted stage of the microscope table, a drop of water is squeezed on to the surface of mercury from a glass capillary which is part of a micrometer buret. By means of a motor and chain drive connected to the micrometer, the volume of the drop may be increased or decreased at any desired rate. An image of the drop is focused on a glass screen by means of the microscope tilted into horizontal position. To reduce the heating of the system due to light absorption, a blue filter was placed between the microscope lamp and the reaction vessel. This filter arrangement was subsequently replaced by an electrical circuit automatically illuminating the system for 0.1 second, when the drop was photographed by a Bolex reflex camera.

The desired lateral movement of the three-phase interline (Hg - H_2O - C_6H_6) is achieved by changing the drop volume. In continuously recording the volume change of the drop, the so-called "dynamic" advancing and receding contact angles are registered. The system (exclusive of motor) is placed on a heavy steel plate equipped with rubber mounts to reduce extraneous uncontrollable vibrations. Vibrations induced by the motor are a constant factor in all experiments. This arrangement also permits the measurement of "static" contact angles and the investigation of relaxation phenomena. One distinctive feature of this setup is that the speed of lateral movement of the three-phase interline changes continuously. With increasing drop volume, the speed

Publication Date: January 1, 1964 | doi: 10.1021/ba-1964-0043.ch013

of movement of the interline decreases (and vice versa). All experiments, unless otherwise stated, were conducted with a constant rate of drop volume change of 0.0189 cu. mm. per second. Changes in the system were recorded with a 16-mm. Bolex reflex camera with time lapse attachment at a speed of 1 frame every 6 seconds. The films were developed and the contact angles measured with a protractor from enlarged pictures (Figure 1).

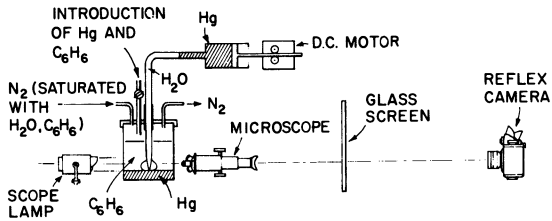

Figure 1. Principles of experimental setup

The cleaned reaction cell is closed with a ground-glass lid and flushed with nitrogen for 20 minutes at a rate of 50 to 100 cc. per minute (STP). Without interrupting the flushing process, benzene (equilibrated with water) is introduced through the top of the cell. Next the rigorously cleaned microburet, which terminates in a capillary about 0.1 mm. in outside diameter, is filled with conductivity water, which is deoxygenated and saturated with benzene. The capillary is now introduced into the reaction vessel so that its end is about 8 mm. from the bottom of the cell. Mercury is then introduced until its surface is about 0.5 mm. from the capillary. After the capillary and the mercury interface have been focused on the glass screen, the system is ready for experimentation.

Experimental Results

Influence of Oxygen. Earlier work by Bartell [1], as well as our preliminary experiments, indicates that the presence of even traces of oxygen in the system greatly influences contact angles and hysteresis. Oxygen is minimized by deoxygenating the whole system and constantly flushing it with purified nitrogen. In two independent experiments, mercury was introduced into the reaction vessel by two extremely different techniques.

A. Mercury was introduced through a glass tubing which reached into the benzene phase. It thus did not come into contact with the gas phase above the benzene surface.

B. Mercury was introduced by passing it in a fine spray through the gas atmosphere above the benzene surface.

The formation of a water drop at a constant rate of volume change of 0.0189 cu. mm. per second, experiment A, produces a dynamic

Publication Date: January 1, 1964 | doi: 10.1021/ba-1964-0043.ch013

advancing contact angle, θ_A, of 119° constant from zero volume to the final volume of 3.4 cu. mm. (frame 30). θ_R, the dynamic receding contact angle, obtained when reducing the drop volume at the same rate, is identical with θ_A down to a volume of 0.795 cu. mm. Over this volume range we observe absence of contact angle hysteresis. When the drop volume is further decreased, θ_R decreases and reaches a minimum value of 106°, corresponding to a maximum hysteresis of 13° at the last frame (Figure 2). A second experiment on the same part of the

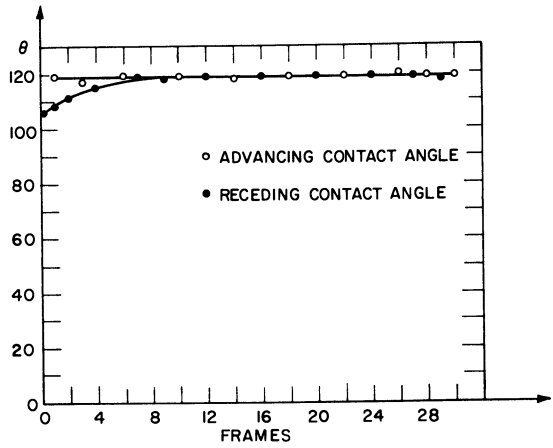

Figure 2. Contact angles in system Hg - C_6H_6 - H_2O

Mercury introduced without contact with gas phase

mercury surface, done immediately after the conclusion of the first, showed identical results. In the portion of this experiment where no hysteresis can be observed, we may reasonably assume that the recorded angle is identical with the equilibrium contact angle. This is confirmed by a calculation of θ by means of Young's equation, based on interfacial tension measurements done by Bartell [2].

In experiment B, where mercury is introduced through the gas atmosphere, an entirely different behavior is encountered (Figure 3). θ_A has now increased from 119° to 149° and hysteresis is observed over the full experiment, reaching a maximum value of 82°. A second experiment on the same surface showed a marked decrease of θ_A to 134°, while θ_R, the receding contact angle, is identical with the one measured in the first experiment. In these experiments the final part of the receding drop was filmed at a rate of 1 frame per second, in order to follow the variation of θ better, while the rest of the experiment was recorded at a rate of 1 frame per 6 seconds.

Assuming that the increased hysteresis, $\Delta\theta$, found in the second experiment is due to contamination of mercury by oxygen and other unidentified gaseous components, we flushed the equilibrated liquids (H_2O and C_6H_6) with oxygen (99.5%) and introduced mercury as in experiment A without bringing it in contact with the gas atmosphere above the

Publication Date: January 1, 1964 | doi: 10.1021/ba-1964-0043.ch013

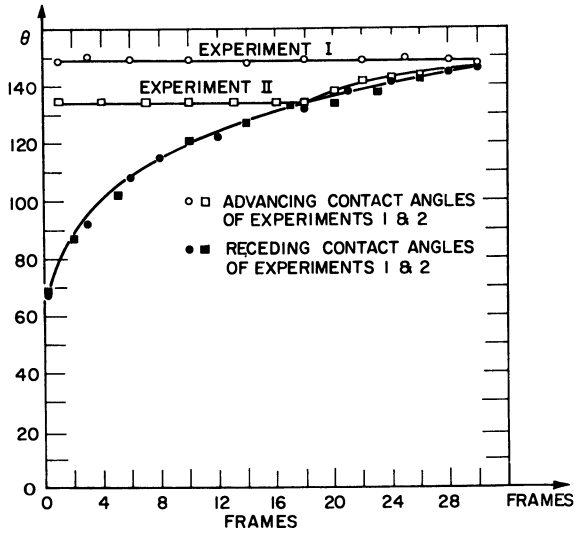

Figure 3. Contact angles in system Hg - C_6H_6 - H_2O

Mercury introduced in fine spray through gas phase

benzene. Hysteresis now was found to be 110° as compared to 13° for the "oxygen-free" conditions (Figure 2) and 82° for the slightly contaminated system (Figure 3).

When the oxygen-saturated, equilibrated liquids were flushed for 20 minutes with purified nitrogen, hysteresis dropped to 80°. Further flushing for 4 hours reduced hysteresis to 38°. Flushing with nitrogen reduces the oxygen content in the system, but no assurance can be given that it removes all oxygen.

Influence of pH. In a series of experiments the behavior of the system was further investigated, when conductivity water was replaced by diluted hydrochloric acid or sodium hydroxide of varying concentration.

Acidic pH Range. The influence of the acid is twofold. There is a slight decrease of contact angles (concentration-dependent) with increasing acid concentration, and hysteresis is absent over a wide range. Table I and Figure 4 show results obtained 6 minutes after contact of the benzene phase with the mercury. In consecutive experiments on the same part of the mercury surface, it was found that after some time a varying degree of hysteresis can be observed at all acid concentrations (Table II). The period over which no hysteresis is detectable is a function of pH. Identical results were obtained when experiment at pH 2 was performed in the inverted system (benzene drop on mercury under water). θ_A and θ_R were 117° and hysteresis was nil.

Basic pH Range. In the pH range from 7 to 14 slight concentration-dependent increase of θ_A occurs, and hysteresis observed in the whole basic pH range increases with increasing base concentration. While the advancing contact angle increases to a maximum of 141°, the receding contact angle decreases steadily and reaches a zero value at pH 13.

Publication Date: January 1, 1964 | doi: 10.1021/ba-1964-0043.ch013

Table I. Effect of pH on Contact Angle Hysteresis in Mercury-Benzene-Water System

pH	θ_A, °	θ_R, °	$\Delta\theta$, °
0	93	93	Nil
1	111	111	Nil
2	116	116	Nil
3	118	118	Nil
4	119	111	8
6	119	104	15
7	119	98	21
9	126	83	43
10	129	80	49
11	130	52	78
12	132	38	94
13	134	0	134
14	141	0	141

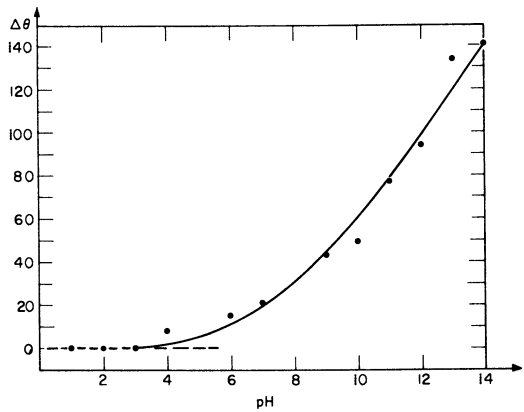

Figure 4. pH dependence of contact angle hysteresis

Table II. Effect of pH on Time Interval Over Which No Hysteresis Can Be Observed

pH	θ_{equil}, °	Period of No Hysteresis, Min.
0	93	45
1	111	34
2	116	25
3	118	24
4	Hysteresis	

Figure 5, A and B, shows in sequence the behavior of a water drop at pH 14. In Figure 5, A, the abscissas are the successive volumes of the drop, but in Figure 5, B, the abscissas represent the diameter of the three-phase interline. The ordinates in both A and B are the observed contact angles. Figure 5, B, shows that the drop expands with constant $\theta_A = 141°$ to an interfacial diameter of approximately 1.0 mm. At this point the volume increase is stopped. During the 18 seconds that elapsed before the drop volume reduction was started, the system showed a slight relaxation phenomenon, which increased the three-phase interline diameter, and slightly decreased θ_A, while the drop volume remained constant (square dots in 5, B). When the drop volume was reduced, θ_R steadily decreased to zero while the interfacial area, Hg-H_2O, remained constant. When θ_R reached zero, a thin film remained on the mercury surface.

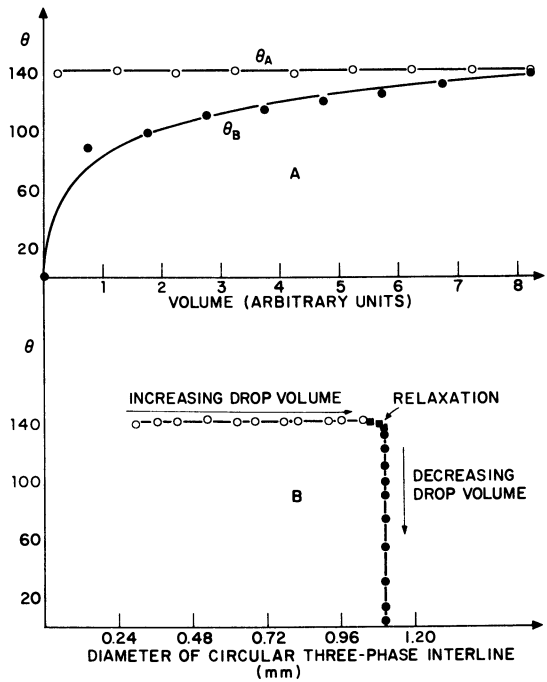

Figure 5. Behavior of H_2O drop at pH 14

A. Contact angle vs. volume
B. Contact angle vs. diameter of three-phase interline

A new experiment done immediately after the first one, on the mercury surface covered with the film left behind from the first experiment, showed a readvancing contact angle of zero. The water drop spread with zero contact angle over this film and was stopped at its end. At this constant diameter the advancing contact angle increased until it again reached its value in the first experiment. When this value

was reached with a further increase of the drop volume, the circular three-phase interline increased its diameter, while θ_A remained constant at 141°, the value of the angle in the first experiment.

At pH 14 when the connection between the film remaining from the first experiment and the glass capillary was broken, the film remained unchanged at the same location of the mercury surface. Readvancing contact angles were zero even after several minutes. At lower pH values, however, the system behaved differently. At pH values less than 13, θ_A decreased but never reached the values of zero recorded at pH 14. When between experiments the water drop was completely sucked back into the capillary and the next experiment started about 30 seconds afterwards, θ_A had again the same value as in the first experiment.

Speed Dependence. All experiments done with the controlled drop volume method are inherently accompanied by a steadily varying speed of lateral movement of the three-phase interline. As the rate of volume change remains constant throughout each experiment, the lateral movement of the three-phase interline decreases with increasing drop volume and increases with decreasing drop volume. For our experiments with a maximal drop volume of 3.4 cu. mm., a drop volume change of 0.0189 cu. mm. per second, and a θ of 119°, the speed (computed over 6 seconds) varied from 0.3×10^{-2} to 0.1 mm. per second.

In these experiments θ_A is independent of the rate of movement of the three-phase interline over the whole speed range. Not so with θ_R. The maximum hysteresis depends not only on the velocity of movement of the interline when the drop is shrinking, but also on the duration of contact at maximal diameter, and the magnitude of the maximal drop volume. Table III, for example, illustrates the effect of changing the duration of contact at maximal diameter.

Table III. Variation of θ with Time of Contact of Water Drop with Mercury Surface (at pH 9.3)

Time of Contact at Maximal Size, Sec.	θ_A, °	θ_R, °	$\Delta\theta$, °
6	129	99	30
180	127	79	48
300	128	68	60
600	128	40	88

Discussion of Results

Oxygen greatly influences the contact angle and hysteresis. In its presence the reaction $4Hg + O_2 + 2H_2O = 2Hg_2^{+2} + 4OH^-$ takes place.

The oxidation according to Gatty and Spooner [3] proceeds stepwise, the first step being the formation of "oxide patches" which have almost free surface mobility. These oxide islands grow in size and finally cover the whole mercury surface as a continuous film, the surface of which no longer has the properties of liquid mercury. The stability of this deposit is significantly influenced by the nature of the electrolyte in contact with it. While basic solutions favor film stability, acidic solutions assist in dissolution of the deposit. Our experiments thus indicate that in the pure system $Hg\text{-}C_6H_6\text{-}H_2O$ there is no

Publication Date: January 1, 1964 | doi: 10.1021/ba-1964-0043.ch013

hysteresis of contact angles. Hysteresis can be observed only when a new phase is formed on the mercury surface. As long as we have a clean mercury surface and thus free mobility of the surface atoms, we can expect instantaneous readjustment to equilibrium conditions upon lateral movement of the three-phase interline and no hysteresis.

Acknowledgment

The authors express their gratitude to the National Science Foundation and its officers for their support of this research.

Literature Cited

(1) Bartell, F. E., J. Phys. Chem. **56**, 453 (1952).
(2) Ibid., p. 532.
(3) Gatty, O., Spooner, E., "Electrode Potential Behavior of Corroding Metals in Aqueous Solutions," p. 111, Clarendon Press, New York, 1938.
(4) Rayleigh, Lord, Phil. Mag. **30**, 397 (1890).
(5) Sulman, H. L., Trans. Inst. Mining Met. (London) **29**, 44-138 (1920).

Received March 26, 1963

14

The Contact Angle at the Gallium-Mercury Interface on Glass

ROBERT J. GOOD, WILLIAM G. GIVENS, and CHARLES S. TUCEK

Space Science Laboratory, General Dynamics/Astronautics
San Diego, Calif.

Publication Date: January 1, 1964 | doi: 10.1021/ba-1964-0043.ch014

Contact angles on glass were obtained from capillary rise measurements and from x-ray observations of menisci in tubes, for the interface between liquid gallium and mercury at 25°C. In a vacuum system with degassed metals and glass, the equilibrium contact angle was zero, and did not change with time. In apparatus exposed to air, the equilibrium contact angle was zero initially, but changed markedly with time, reaching a steady state in about 10 days with an angle of about 100°. The properties of the metals separately lead to expectation of the zero contact angle. The interfacial tension between gallium and mercury, as obtained from the capillary rise measurements, was 37 ± 5 dynes per cm. at 25°C.

A project involving measurement of the interfacial tension between mercury and gallium liquids by the drop weight method is being carried out in this laboratory. For that study it was desirable to be able to predict, and if possible control, the wetting behavior of these metals at the dropping tip. The work reported here was undertaken to further the understanding of the tip wetting.

The usual methods for measurement of contact angle depend on optical observation of the interface, which is impossible in this system. Although the interfacial surface cannot be seen, the line of intersection of the interface with glass is visible because the reflectivity of gallium is higher than that of mercury. In the present work an apparatus was set up in which the contact angle could be deduced from observation of the intersection of a meniscus with a glass tube. Some x-ray observations were also made, which showed the interface directly.

Experimental

The principal technique used was a version of the differential capillary rise method for measurement of interfacial tension. Runs were

In Contact Angle, Wettability, and Adhesion; Fowkes, F.;
Advances in Chemistry; American Chemical Society: Washington, DC, 1964.

made both with the apparatus and metals exposed to air, and in a vacuum system. All work was at 25°C., with both metals in the liquid state.

(Pure gallium melts at 29.78°C., and gallium saturated with mercury at 27°C. [2]. But it is very easy to keep either gallium or gallium saturated with mercury as a supercooled liquid indefinitely, at temperatures 10° or more below the melting point. The fact that the total system was not in thermodynamic equilibrium does not affect the conclusions of this study regarding surface thermodynamic properties such as relative surface tensions which are discussed below.)

Apparatus. The apparatus for use in air is shown schematically in Figure 1.

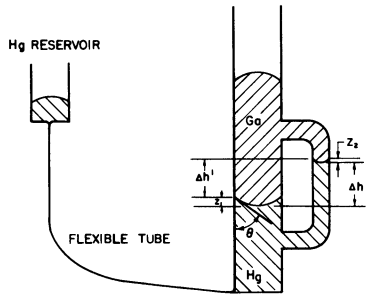

Figure 1. Apparatus for measuring capillary rise at mercury-gallium interface

It was constructed of borosilicate glass. The flexible tube allowed the Hg-Ga interface to be raised or lowered at will, without appreciable vibration of the main tube. Typical tube diameters were about 10 mm. for the large tube and 0.5 to 1.0 mm. for the small tube. Height measurements (by means of a cathetometer, accurate to better than 0.01 mm.) were made at several places around the tube, for each measurement of the position of the interface.

Similar apparatus was used for direct observation of the menisci with x-rays, but the diameter of the larger tube was reduced to about 2 mm., in order to improve definition of the meniscus, in the x-ray photographs.

The two metals were mutually saturated by gentle rocking in a thermostat for at least 24 hours before use. The saturated phases were used for all measurements. (The mercury phase contains about 1.3% gallium, and the gallium phase about 5.8% mercury at 25°C. [2,15].)

The apparatus for performing the experiment in a vacuum is shown in Figure 2. Pure mercury was loaded into bulb H (Figure 2, b), and pure gallium into bulb G, and this portion of the apparatus was attached to a vacuum line by means of ground joint A. The gallium in bulb G was heated to about 400°C. during evacuation. Bulb G was cooled, and the mercury in bulb H distilled into bulb G. Stopcock B was closed and the bulbs were removed from the vacuum line.

The measurement tubes (Figure 2, a) were outgassed under a vacuum of 10^{-6} torr, and with heating of the glass to about 400°C. with a

Publication Date: January 1, 1964 | doi: 10.1021/ba-1964-0043.ch014

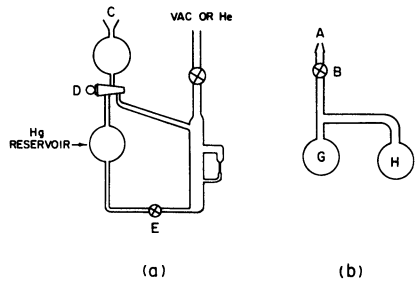

Figure 2. Apparatus for performing experiment in vacuum

gas flame. After saturation, bulb G was attached to the measurement apparatus at joint C. After evacuation stopcock B was opened, and the metals were allowed to flow into the main apparatus. The mercury was directed into the mercury reservoir, and the gallium into the measurement tubes on the right. Finally, mercury was admitted to the cell through stopcock E. The levels of the menisci could be controlled by admitting helium to either leg of the apparatus, and operating stopcock E.

The x-ray equipment was a Norelco industrial unit, with a constant potential source; a Norelco MG150 tube was used, with a focal spot 0.4 mm. square. The maximum difference in x-ray absorption, between mercury and gallium, occurs for around 85-kv. x-rays, and stays reasonably large up to 150 kv. [9]. (A pronounced minimum in the difference occurs somewhat below 85 kv.) So the tube was operated at 150 kv. and 3 ma. A copper filter was employed to remove most of the lower energy radiation and thus increase contrast. Additional copper was used over the smaller tube, to equalize exposure of the two tubes.

The effects of several surface treatments for the glass were examined. In each case the cell was constructed of new glass. The chemical treatments consisted of soaking the cell for 1 hour in the solutions listed below, then rinsing extensively with tap water, followed by distilled water. The cell was then oven-dried at 110°C., cooled to room temperature, and allowed to stand at least 24 hours before use, with no attempt to exclude air or water vapor.

In addition to the blank, which received no special cleaning, treatments with concentrated hydrochloric acid, chromic acid cleaning solution, and 1% Alconox solution (an alkaline detergent) were employed.

It was necessary to use a new cell each time, as removal of the metals with acid, or with alkaline detergent, even though followed by surface treatment, did not return the cell to the same condition as a new one, as evidenced by different capillary rises.

Measurements of the heights of the interfaces in the two tubes, after the mercury level had been raised or lowered with a minimum of vibration, were used to obtain the advancing and retreating angles. An approximation to equilibrium contact angles was obtained by tapping the cell after the interfaces had stopped moving.

Materials. The gallium used was Alcoa grade G-6, stated to be 99.9999% pure. The mercury was obtained from United Mineral and Chemical Co., and was stated to be 99.9999% pure. All glass was Pyrex 7740.

Method of Calculating Results

The direct measurements of contact angles made from the x-ray films need no further discussion. Unfortunately, the interface, and especially its intersection with the glass, could not be defined very sharply; so these measurements were only approximate. The results of the direct measurements were in accord with those made by other methods.

The balance of the results depends on calculation of contact angles from measurements of capillary rise [10]. A value of 41 dynes per cm. for the gallium-mercury interfacial tension, determined in previous work in this laboratory [8], was used in these calculations. The densities of the two saturated phases are 6.28 grams per cc. for the gallium and 13.35 for the mercury [8].

The capillary rise, h—i.e., the height of the center of a curved interface above the reference plane of an infinite plane interface—is given by the expression

$$h = \frac{2\gamma}{g\rho R} \tag{1}$$

for an axially symmetrical curved meniscus, where γ is the interfacial tension, g the gravitational constant, R the radius of curvature at the center of the meniscus, and ρ the density difference between the two liquids.

The shape of an interface is determined by the tube diameter, the contact angle at the wall, the densities, and the interfacial tension (see Figure 1). The radius of curvature at the center and the vertical height, z, of the meniscus from center to edge may be calculated from these four parameters. An accurate numerical computation of meniscus shape is given by Bashforth and Adams [1,3]; and a treatment of large menisci (including numerical tables and approximation formulas) is given by Blaisdell [4]. If the contact angle is θ, and the tube diameter is small enough, the equation

$$h = \frac{2\gamma \cos \theta}{g\rho x} \tag{2}$$

may be used, where x is the tube radius.

In general,

$$h = f(\gamma, \theta, \rho, x) \tag{3}$$

and for the difference in height between the apices of the menisci in tubes 1 and 2,

$$\Delta h = f(\gamma, \theta, \rho, x_1) - f(\gamma, \theta, \rho, x_2) \tag{4}$$

where function f may be obtained from numerical tables [3,4].

Publication Date: January 1, 1964 | doi: 10.1021/ba-1964-0043.ch014

The capillary rise for the interface between these metals with a tube 1.0 cm. in diameter and a contact angle of 0° was calculated as about 0.0064 mm., and so is negligible for our purposes. When the contact angle is other than zero, the rise is even smaller. In a tube with radius 0.5 mm., calculations using the tables of Bashforth and Adams—i.e., Equation 3—showed that for this system Equation 2 yielded a result that was at most in error by 7% for a 0° contact angle. If the tube is smaller or the contact angle is not 0°, the error is less than 7%. Since the measurement error was of the order of a few per cent, Equation 2 could be taken as a satisfactory approximation to Equation 4, for the difference in capillary rise.

It was necessary to make the correction for the meniscus height, z, since z is of the same order of magnitude as h for this system, and its neglect could produce an error as large as 30%.

Contact angles were calculated from the observations of the edges of the menisci in the two tubes, as follows: With reference to Figure 1, the measured height difference is $\Delta h'$. Since the radius of the small tube is much less than that of the large tube, $\Delta h'$ may be used as an approximation for h in Equation 2, and this allows a preliminary value of θ to be calculated. This θ then is used to obtain approximate values of z for each tube, using the Bashforth and Adams tables for the 1-mm. tubes and the approximation formulas given by Blaisdell [4] for the 10-mm. tubes.

Results

Evacuated System. A first, qualitative observation was that, when the system was initially filled with mercury and the gallium added, the line of demarcation between the gallium and mercury moved in a few minutes to the top of the gallium phase. After considerable time had elapsed, from several hours to days, a rather diffuse line of demarcation slowly reappeared, moving rather raggedly down the tube, and reaching a constant level only after 2 or 3 more days. The system behaved as if a film of mercury had formed, or moved in between the gallium and the glass, a film that subsequently moved by solution and diffusion as well as by drainage.

On raising the level of the mercury, the apparent interface responded rapidly, advancing up the tube. But on repeating the retreat of the mercury, again some time was required before the interface could be observed at its equilibrium level. After a week or more of exposure of the glass to the liquid metals, the response of the apparent interface to retreat of the mercury became a little faster, but something of the order of hours was still required.

The difference in heights of the menisci corresponded to a contact angle indistinguishable from zero (measured through the mercury) for both advancing and retreating mercury, both for the case of prior exposure of the glass to the gallium, and for exposure to the mercury phase, before measurements. When oxygen was admitted to the cell, above the gallium, no change was observed in the contact angle over a period of two weeks.

Systems in Contact with Air. Systems exposed to the atmosphere, with or without chemical treatment of the glass, differed from those with the evacuated system, both in equilibrium angles and in rate of at-

Publication Date: January 1, 1964 | doi: 10.1021/ba-1964-0043.ch014

tainment of equilibrium. First, there was no initial spreading of the mercury under the gallium. When the system was initially filled with mercury and the gallium was added on top, a line of demarcation between the phases became visible almost at once. When the mercury was caused to retreat, the new position of the interface became visible within only 2 or 3 hours, and stayed at a constant height. After the mercury had been raised and lowered again, the interface was observed to move within 10 to 15 minutes; and after a day or more of exposure of the glass to the metal, the interface responded within minutes or less. When the mercury was raised, the response was always rapid.

Results obtained from the runs in air are summarized in Table I. The advancing and retreating contact angles showed considerable variations, of the order of ± 30°, throughout the experiments in air. The equilibrium final values were reproducible to within less than 5°; each value reported in Table I was the average of at least 10 readings.

Publication Date: January 1, 1964 | doi: 10.1021/ba-1964-0043.ch014

Table I. Contact Angles for Mercury-Gallium Interface on Borosilicate Glass, Exposed to Air
(All angles measured through mercury)[a]

Surface Treatment		Contact Angle, θ, Degrees	
		Initial	Final
None, or Alconox	Hg retreating	0	80[b]
	Equilibrium	0	100
	Hg advancing	30[b]	120[b]
Chromic acid	Hg retreating	0	95[b]
	Equilibrium	30	105
	Hg advancing	35	115[b]
HCl	Hg retreating	0	
	Equilibrium	0	
	Hg advancing	30[b]	

[a]"Measured through mercury" refers to the arbitrary choice to list angles as reported rather than their supplements, which would be "contact angles measured through gallium." The phrase was not intended to indicate direct measurement of the angle.
[b]Showed large variations, of order of ± 30°.

A strong time dependence was noted in all cases. The initial values were obtained within a few hours after the cell was filled. The initial values for mercury retreating, and for equilibrium, were the same as observed for the evacuated systems—zero. For mercury advancing, the initial contact angle was greater than zero, outside the range of experimental error, only for the chromic acid-washed glass. The contact angles seemed to reach a steady state in about 10 days. There was a difference in the behavior, depending on which metal had been in contact with the glass, described below. This small effect was ignored in the values in the table, which are an average of the "equilibrium" values following mercury advance and mercury retreat.

Observation with the microscope showed that the edge of the meniscus was not perfectly smooth, but was rather jagged (particularly for mercury retreating) which would indicate variations in glass surface, from point to point. As the meniscus was moved, the edge could be observed to move in jumps, rather than smoothly; this observation was in accord with the large hysteresis effect.

An apparatus with tubes of fused silica gave results essentially identical with those of the untreated or Alconox-treated borosilicate glass.

Figure 3, B and C, shows the time dependence of the equilibrium contact angles on Alconox-treated glass in air. The other surface treatments gave generally similar equilibrium results; and the advancing and retreating angles showed similar behavior. Curves B and C (Figure 3) were obtained as follows:

Over a period of days, the tubes were kept filled with the one metal or the other except for the time needed to take measurements—that is, the level of the interface was either raised, so that the glass in the region where the measurements were made was left in contact with the mercury; or else the level was lowered so that the glass was left in contact with the gallium. It was possible to change the behavior from one curve to the other by allowing the other metal to remain in contact with the glass for about 2 days. This effect was observed as late as 20 days after filling the cell. This difference was observed consistently, with each of several cells, even though it was of about the same size as the variation from cell to cell. The curves shown are smoothed curves through the data points for a typical run. The individual points showed a scatter of about 10° for the first few days, and several degrees at later times. The limiting values of the equilibrium angles, 100° and 105°, respectively, are average values for the two cases, and the 5° difference may be considered accurate to about ± 1.5°.

X-ray pictures of cells confirmed the above results. Measurements made on the x-ray negatives for the heights of the capillary rise agreed with above results; and direct observations of the angles, while imprecise, generally confirmed the results from measurements of cappilary rise.

Publication Date: January 1, 1964 | doi: 10.1021/ba-1964-0043.ch014

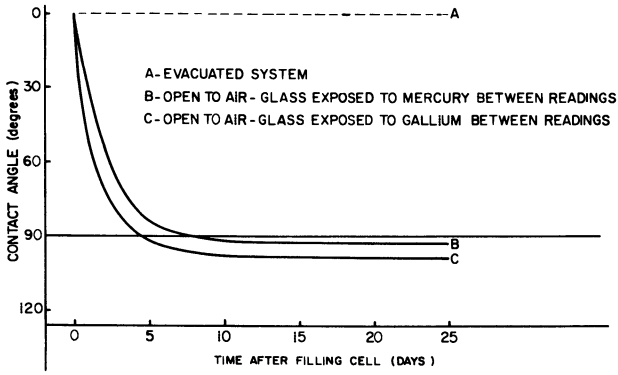

Figure 3. Variation of equilibrium contact angle with time for mercury-gallium interface on glass

The fact that in the x-ray pictures the menisci could be observed directly makes possible an estimate of the interfacial tension from these measurements without the uncertainties associated with observation of the edges. In a case where the contact angles appeared to be zero, the following data were obtained:

Tube diameters, mm.	0.74 and 1.6
Capillary rise (Δh), mm.	1.7 ± 0.2
Calculated interfacial tension, dynes/cm.	37 ± 5

This result is consistent with the data [8] obtained independently by the drop-weight method, γ_{12} = 39.7 dynes per cm. at 30°, and (extrapolated) 41.0 at 25°.

Discussions

Experimental Errors. The chief difficulty in the capillary height measurements was in identifying the line of demarcation between gallium and mercury. Only when the contact angle was well above 30° could a sharp line be observed in both tubes, but even so it was somewhat "ragged." This trouble was most pronounced in the evacuated system, and much more for the retreating than the advancing angle. In addition, the line was sometimes diffuse, particularly for retreating angles near zero and for the evacuated system.

A major source of uncertainty in the calculation was in the assumption that the contact angles in the two tubes were identical. In the case of $\theta \sim 0$ and $\theta \sim 90°$, this assumption was probably justified. But for intermediate values of θ, especially when θ was varying with time, it is not possible to be so certain of the assumption. If the change in contact angle was due to a diffusion - limited heterogeneous reaction, the differences in diffusion path as between the cell legs might lead to a difference in rates of deposition in the two tubes, and to different θ's. Such a possibility was borne out by visual observations, which indicated that, with exposure to air, the interface in the large tube tended to become sharp, and to move freely, in a shorter time than the interface in the small tube.

Results with Evacuated Systems. From the observation of the spreading of mercury "under" the gallium the conclusion may be drawn at once that the spreading coefficient (the negative of the free energy of spreading, ΔF^s) is positive:

$$- \Delta F^s = \gamma_{g,Ga} - \gamma_{g,Hg} - \gamma_{Ga,Hg} > 0$$

where subscript g refers to glass. It may be shown that this sign for the spreading coefficient is to be expected, from the behavior of gallium and of mercury, separately, on glass.

Gallium has a high contact angle on outgassed glass in vacuum [5], and mercury has a relatively low contact angle on glass under the same circumstances [5,13,14,17]. Exact values of the contact angles under these conditions have not been reported. (From Manley's data [13], an estimate may be made that for mercury on outgassed glass, $\theta \sim 70°$. The true value is probably no larger than this number, and may very well be less. Schumacher [14] found a marked dependence of θ on the composition of the glass, in the order, soda lime glass > borosilicate

Publication Date: January 1, 1964 | doi: 10.1021/ba-1964-0043.ch014

glass > fused silica.) Freundlich [7] has treated Young's equation [18] in terms of what he called the adhesion tension, A:

$$\gamma_{sv} - \gamma_{sl} = \gamma_{lv} \cos \theta_{slv} \equiv A_{sl} \tag{5}$$

If the contact angle of mercury on evacuated, baked-out glass is as high as 70°, then A_{sl} is of the order of 150 dynes per cm.; and a lower value of θ would correspond to a value of A_{sl} even larger than that:

$$A_{g,Hg} = \gamma_{g,Hg} - \gamma_{go} = \gamma_{Hg} \cos\theta \geqq 150$$

The contact angle of gallium on evacuated, baked-out glass is above 110°. Since the surface tension of pure gallium is in the range, 700 to 735 dynes per cm. [11,12,16],

$$- A_{g,Ga} = \gamma_{go} - \gamma_{g,Ga} = - \gamma_{Ga} \cos\theta \geq 250 \text{ dynes per cm.}$$

Hence $\gamma_{g,Hg} - \gamma_{g,Ga} \geqq 400$ dynes per cm.

For the liquid-liquid-solid interfacial angle,

$$\text{Cos}\theta_{sl_1l_2} = \frac{\gamma_{sl_1} - \gamma_{sl_2}}{\gamma_{sl_1l_2}} \tag{6}$$

$$= 1 \text{ if } (\gamma_{sl_1} - \gamma_{sl_2}) > \gamma_{l_1}\gamma_{l_2}$$

In this case, γ_{sl_1} and γ_{sl_2} are the liquid-solid interfacial tensions for two saturated liquids, and so differ from the γ_{sl}'s estimated above, on account of adsorption. The necessary adsorption data are not available, and in their absence no firm conclusions can be drawn. However, it seems highly unlikely that adsorption would invalidate the approximation,

$$\gamma_{g,Ga(Hg)} - \gamma_{g,Hg(Ga)} \simeq \gamma_{g,Ga} - \gamma_{g,Hg} \tag{7}$$

by the order-of-magnitude decrease that would be necessary to affect this discussion. So the numerator on the right in Equation 6 can be expected to be of the order of hundreds of dynes, and in any case significantly larger than the 41-dyne denominator. Hence, one would expect $\theta = 0$, and a strongly negative free energy of spreading, as observed.

Systems in Contact with Air. A similar argument could be made to predict the contact angle, if a valid contact angle were available for the gallium-glass-air system. But gallium in air is always covered with an oxide film. (This film no doubt is responsible for the extreme hysteresis of the contact angle. The apparent advancing contact angle of gallium on glass in air may be greater than 120°, and the retreating angle may be 0°, or range up to 50° or more.) Hence it is very difficult to make a valid estimate of the adhesion tension of gallium *vs.* glass in the presence of air.

The experimental result, that the initial mercury-gallium-glass contact angle is zero, shows that qualitatively the argument given above for the evacuated system is also valid for the initial condition of the

Publication Date: January 1, 1964 | doi: 10.1021/ba-1964-0043.ch014

glass-mercury and glass-gallium interfaces—i.e., $\gamma_{g,Hg(Ga)} - \gamma_{g,Ga(Hg)} > 41$ dynes per cm. Since the ultimate equilibrium contact angle is approximately 100°, the final condition must be

$$\gamma_{solid,\ Ga(Hg)} - \gamma_{solid,\ Hg(Ga)} \simeq 5 \text{ to } 10 \text{ dynes per cm.}$$

(The lower figure applied to glass previously exposed to the mercury phase, and the higher, to glass previously exposed to the gallium phase.)

The explanation of the change in contact angle with time is presumably a chemical reaction or adsorption of some molecular species at the metal-glass surface. We can only speculate as to what is adsorbed—the most reasonable species to consider would be some oxide of gallium. The contribution of components of the glass, likewise, can be only the subject of speculation at this time; but the evidence indicates that glass which has been flamed out under vacuum either is inert as far as providing chemical components for an interfacial reaction, or else is inert with regard to adsorption of the active species from the liquid.

Whatever the solid product may be, it seems rather remarkable that the two interfacial tensions *vs.* the solid should be so closely matched, particularly when the interfacial tensions of the two liquids *vs.* fresh glass differ by at least 41 dynes, and probably by several hundred dynes. It may well be, however, that the approximation (Equation 7) is not valid for this new solid product, on account of adsorption of metal atoms.

The effect of prior contact of the glass with the gallium phase was to increase the quantity, $\gamma_{solid,\ Ga(Hg)} - \gamma_{solid,\ Hg(Ga)}$; and the effect of prior contact with the mercury phase is to decrease it. This is not surprising, since, for example, the exposure of the glass to a higher concentration of gallium metal might make the solid "more like gallium," and hence decrease the liquid-solid interfacial tension. But the effect is small, being only about 5 dynes in the adhesion tension. What may be considered more surprising is the reversibility of this change at apparently all stages in the aging process.

Conclusions

The initial contact angle of the mercury-gallium interface on glass is zero, for both glass flamed out under vacuum, and glass exposed to laboratory atmospheres and/or given hydrochloric acid or alkaline detergent treatments.

On glass exposed to a laboratory atmosphere, the contact angle rises, over a period of days, reaching a steady value in the neighborhood of 100°. This behavior must be due to adsorption of some species on the glass, or a chemical reaction.

The zero contact angle and strongly negative initial free energy of spreading, on flamed out, evacuated glass, are in accord with expectations based on the behavior of the pure metals on glass.

An approximate value of the interfacial tension between gallium and mercury was obtained, which agreed within experimental error with a much more accurate measurement made previously in this laboratory.

Publication Date: January 1, 1964 | doi: 10.1021/ba-1964-0043.ch014

Literature Cited

(1) Adam, N. K., "Physics and Chemistry of Surfaces," 3rd ed., Cambridge University Press, London, 1941.
(2) Amarell, G., Ph.D. thesis, University of Karlsruhe, O. Berenz, Waldenstrasse 8, Karlsruhe, Germany, 1958.
(3) Bashforth, F., Adams, J. C., "Attempt to Test the Theories of Capillary Action," Cambridge University Press, London, 1883.
(4) Blaisdell, B. E., J. Math. Phys. **19**, 186, 217, 228 (1940).
(5) Briggs, L. J., J. Chem. Phys. **26**, 784 (1957).
(6) Cochran, C. N., Foster, L. M., J. Electrochem. Soc. **109**, 144 (1962).
(7) Freundlich, H., "Colloid and Capillary Chemistry," Dutton, New York, 1922.
(8) Good, R. J., Opdycke, J. D., Tucek, C. S., Division of Colloid and Surface Chemistry, 139th Meeting, ACS, St. Louis, Mo., 1961.
(9) Grodstein, G. W., "X-Ray Attenuation Coefficients from 10 K.e.v. to 100 M.e.v.," National Bureau of Standards, Circ. 583 (1957).
(10) Harkins, W. D., in "Physical Methods of Organic Chemistry," Vol. I, part 1, A. Weissberger, ed., 3rd ed., Interscience, New York, 1959.
(11) Korolkov, A. M., Bychkova, A. A., Issledovanie Splavov Tsvetnykh Metal., Acad. Nauk SSSR, Inst. Met. im. A.A. Balkova **196**0, No. 2, 122-34.
(12) Mack, G. L., Davis, J. K., Bartell, F. E., J. Phys. Chem. **45**, 846 (1941).
(13) Manley, J. J., Phil Mag. **5**, 958 (1928).
(14) Schumacher, E. E., J. Am. Chem. Soc. **45**, 2255 (1923).
(15) Spicer, W. M., Bartholomay, H. W., Ibid., **73**, 868 (1951).
(16) Timofeevicheva, O. A., Pugachevich, P. O., Dokl. Acad. Nauk SSSR **134**, 840 (1960).
(17) Young, T., Phil. Trans. **1805**, 73.
(18) Ibid., p. 84.

Received April 15, 1963. Work supported in part by the U. S. Atomic Energy Commission under Contract AT(04-3)-297.

Publication Date: January 1, 1964 | doi: 10.1021/ba-1964-0043.ch014

15

Thermodynamics of Wetting of Solid Oxides

WILLIAM H. WADE and NORMAN HACKERMAN

Department of Chemistry
The University of Texas
Austin, Tex.

Publication Date: January 1, 1964 | doi: 10.1021/ba-1964-0043.ch015

This paper surveys the results of a long series of adsorption experiments designed to determine the reasons why experiments of this kind generally have not given reliable information in regard to the obviously relevant surface thermodynamic parameters.

Few thermodynamic adsorption parameters are listed in the International Critical Tables, and rightly so. The literature commonly reveals considerable disagreement between investigators for these parameters, even for surfaces which should be structurally simple.

To understand better the sources of this disagreement, a series of investigations was begun in this laboratory some years ago. Several representative samples of metal oxides were to be used as the adsorbents and the adsorbates were to consist of simple molecular species such as water, alcohols, and hydrocarbons. The object was a broad survey of the thermodynamic adsorption parameters for the various combinations. The integral heats of adsorption and the adsorption isotherms were to be measured, and the integral entropies calculated therefrom. It was hoped to provide an inclusive picture of many of the variables which affect these adsorption parameters. To cite a specific case showing that these studies were necessary, literature data for the heats of immersion of SiO_2 in H_2O [1,2,4,18] show values ranging from 200 to 800 ergs per sq. cm. Since all of these investigators are reputable, a reasonable conclusion is that the surface properties of the adsorbents used differed sufficiently to evoke this spectrum of values.

It was decided to measure the integral heats of adsorption microcalorimetrically, free energies of adsorption by a Gibbs integration of the adsorption isotherms, and integral entropies by numerical difference. Though the results of this survey may be incomplete, they have provided some insight into the specificity of physical adsorption processes.

Several other investigators have been working along similar lines. Whalen has clearly shown that a variation of adsorption heats is to be found in the SiO_2-H_2O system [1δ]. In looking at the data available in the literature, the only correlation one finds in the variation of heats of

In Contact Angle, Wettability, and Adhesion; Fowkes, F.;
Advances in Chemistry; American Chemical Society: Washington, DC, 1964.

adsorption from sample to sample for a particular substrate material—e.g., SiO_2—is a trend showing decreased heats of adsorption with decreased particle size (increased specific surface area).

Along with thermodynamic data acquired from various sources, other recent types of experimental measurement have done much to elucidate the chemical structure of the surface of inorganic metal oxides. The most conclusive measurements have been the infrared studies of these surfaces [3,8,17]. These studies show that surfaces of oxides exposed to atmospheric conditions differ chemically from that of bulk phase. In particular, the surface is covered with strongly bonded hydroxyl groups. Although these groups were thought to exist prior to the infrared measurements [7], these measurements offered the first direct proof of this fact. These OH groups would be expected to modify the surface of an inorganic metal oxide chemically, and promote phenomena such as hydrogen bonding.

Publication Date: January 1, 1964 | doi: 10.1021/ba-1964-0043.ch015

Experimental

The samples of SiO_2, Al_2O_3, and TiO_2 studied have been previously characterized [12,13,14] with regard to impurity and specific surface area. For purposes of uniformity, the surface areas of all the samples studied were measured by Kr adsorption at 77°K. Gel samples were not included, in order to minimize hysteresis effects which would invalidate thermodynamic arguments. In general, the purity of the samples was 99.9%, some samples were less pure, and a few were even purer. The adsorbates—water, methanol, and hexane—were highly pure and, in the case of the organic adsorbents, freed from trace quantities of water by storing over Molecular Sieves.

The calorimeter employed [9] is a twin differential semiadiabatic calorimeter with thermistor temperature-sensing elements. The thermistors are stable to the equivalent of $\pm 2° \times 10^{-6}$ °C. over 30-minute periods. The temperature rise noted on sample breakage varied from $10^{-2°}$ to $10^{-3°}$C. The reproducibility of immersional heats was approximately 2 to 3%. Adsorption isotherms were measured with volumetric adsorption apparatus, previously described [5,6] and the Gibbs integrations to give the integral free energies of adsorption at a relative pressure of 1.00 were done graphically. Heats of adsorption were obtained from the immersional heats by subtraction of the surface enthalpy of the appropriate liquid.

Results and Discussion

Chronologically the SiO_2-H_2O system was studied first. Some of the results of the original calorimetric studies for this system are shown in Figure 1. First, heats of adsorption decrease with increasing specific surface area and, secondly, differences in behavior due to outgassing temperature are obvious. Low-area quartz samples (1.28 sq. meters per gram) show an initial rise in heats of adsorption with increased outgassing temperature, followed by a gradual decrease. This behavior has been noted elsewhere [16]. Here it is attributed to the irreversible loss of surface hydroxyl groups at higher outgassing temperatures; hence to lessened opportunity for hydrogen bonding upon immersion in water. This phenomenon was even more clearly

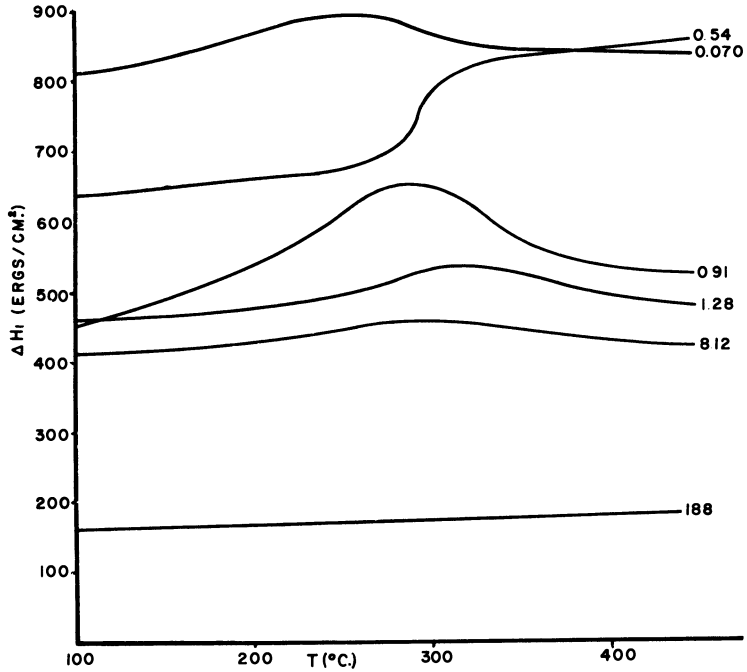

Figure 1. Heats of immersion as a function of outgassing temperature for various quartz samples in water

demonstrated by means of an adsorption isotherm on a low-area quartz sample accidentally heated at 450°C. The adsorptive capacity at relative pressures less than 0.5 was reduced by a factor of 4 until the sample was exposed to boiling water for a week.

The variation of immersional heats of SiO_2 in water with particle size seems at first glance to be a very anomalous effect. The only known difference between these samples is that the samples of very low area are crystalline quartz, whereas the samples of high area are undoubtedly amorphous. To check the importance of the amorphous character of the surface, three experiments were performed.

A sample of low-area quartz (0.07 sq. meter per gram) was ground extensively and samples of various specific surface areas were obtained by sedimentation fractionation. The 8.12 sq. meters per gram sample of Figure 1 is one of the higher area samples generated. Once again, the higher the specific surface area the lower was the heat of adsorption. If it is assumed that grinding increases the thickness of amorphous layer, the correlation between this experiment and the earlier ones is good.

A sample of quartz of relatively low surface area (0.91 sq. meter per gram) was heated to 1500°C., converted to β-crystobolite, and quenched in this crystalline modification by rapid immersion in water. The resultant heats of immersion on this sample also shown in Figure 1 are interesting, in that the heats of immersion are higher than those of

Publication Date: January 1, 1964 | doi: 10.1021/ba-1964-0043.ch015

the parent material. In addition, a step in the vicinity of 300°C. indicates that the rehydration of surface OH groups is rapid and monoenergetic.

An ingot of fused quartz was ground to produce a spectrum of particle sizes which were separated by sedimentation fractionation. Heats of immersion were measured on this series of samples and found [11] to be independent of particle size. The indication is that the grinding process did not notably alter the initially amorphous surface. The heats of immersion of these amorphous samples averaged 370 ergs per sq. cm., somewhat less than that obtained for "quartz" samples with a specific area of ~ 10 sq. meters per gram. This suggests that the surface of quartz samples of higher specific surface area would look completely amorphous to the adsorbate molecule.

Adsorption isotherms were obtained for most of the samples shown in Figure 1 and the integral free energies of adsorption were calculated. The entropies of adsorption were obtained by difference. All these thermodynamic parameters are tabulated in Table I. If the amorphous character of the surface has a direct correlation with the particle size, the entropies of adsorption of the adsorbate molecules would be expected to bear some relation to the underlying periodic structure of the adsorbent. In particular, large entropies of adsorption would be expected for crystalline samples and relatively small entropies of adsorption for the supposedly amorphous substrates. That this relationship is observed is clear from the integral entropies of adsorption listed in Table I.

Table I. Parameters for Water Adsorption

	Surface Area, Sq. M./G.	ΔH_A[a]	ΔG_A	ΔS_A
SiO_2	0.070	729	106	2.09
	0.138	547	128	1.41
	0.910	389	227	0.54
	8.12	334	215	0.40
	188	44	41	0.01
Al_2O_3	2.72	575	202	1.25
	65.2	326	171	0.52
	104	322	206	0.39
	221	236	149	0.29
TiO_2	7.65	608	298	1.04
	10.5	469	248	0.71
	188	231	179	0.17

[a] ΔH_A and ΔG_A are in units of ergs per sq. cm.; ΔS_A in units of ergs/°C. sq. cm.; $\Delta H_A = \Delta H_i - 118.3$.

After obtaining the data on quartz it was felt that the observed phenomena should be established as other than a peculiarity of the quartz system alone. Therefore similar measurements on the Al_2O_3-water [13] and TiO_2-water [14] systems were carried out. The behavior of immersional heats with outgassing temperature and particle size for these two substrates is shown in Figures 2 and 3. These systems

Publication Date: January 1, 1964 | doi: 10.1021/ba-1964-0043.ch015

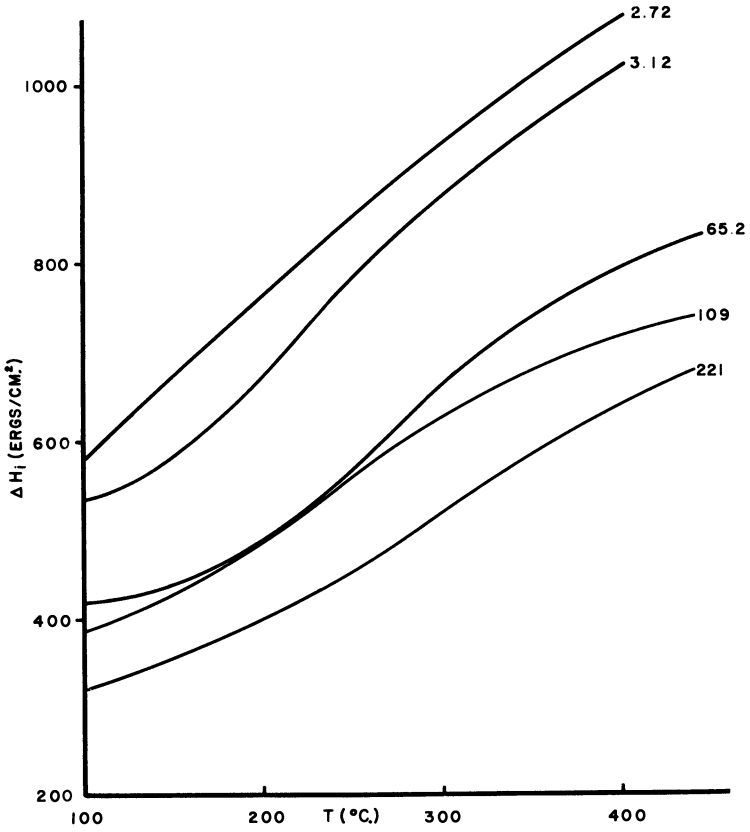

Figure 2. Heats of immersion as a function of outgassing temperature for various samples of Al_2O_3 in water

exhibit similar large variations in immersional heat with particle size, much as was observed for quartz.

The alumina immersional heats show a monotonic increase with outgassing temperature above temperatures where physically adsorbed water should still be bound. This indicates that the rehydration of surface OH groups in the calorimeter was rapid. On the other hand, the TiO_2 samples generally showed behavior commonly found with SiO_2—a decrease in heats of immersion at the higher outgassing temperatures—thus once again indicating irreversible loss of surface OH groups. However, TiO_2 does not appear to be chemically stable at these higher outgassing temperatures and the heats of immersion may be representative of a new chemical species. The TiO_2 data are especially interesting, in that the variation of immersional heats with particle size is regular only if the anatase and rutile samples are considered separately. This indicates a considerable sensitivity of water molecules to the two different underlying crystal structures.

The integral entropies of adsorption for H_2O on many of the Al_2O_3 and TiO_2 samples were also obtained (Table I). The entropies show

Publication Date: January 1, 1964 | doi: 10.1021/ba-1964-0043.ch015

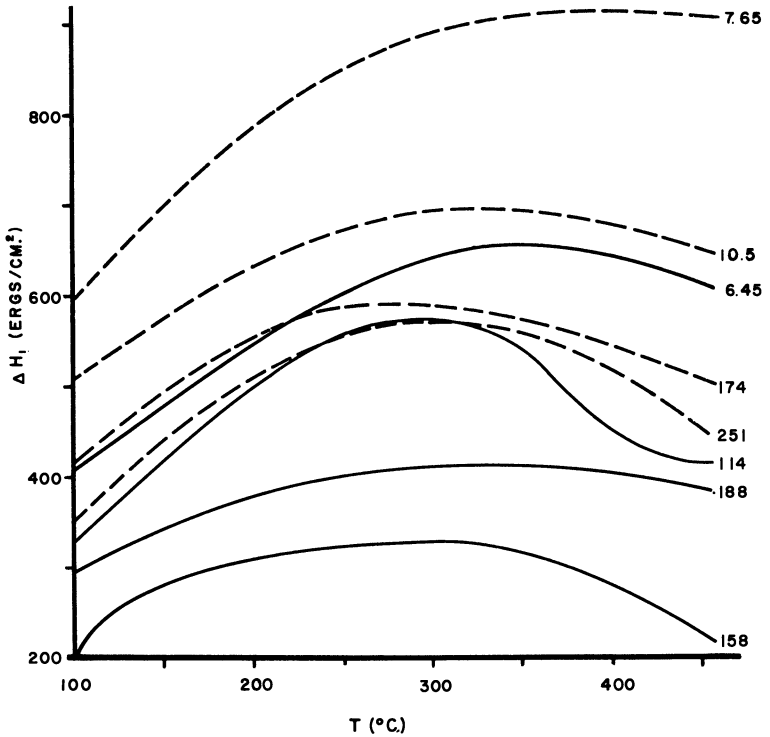

Figure 3. Heats of immersion as a function of outgassing temperature for various samples of TiO_2

---- Anatase
——— Rutile

the same behavior as for SiO_2—a decrease with increasing specific surface area.

Although the variation with particle size appears to be characteristic of powdered samples, this behavior gives some cause for concern, because the samples of alumina and titania were subjected to no distortional forces such as grinding and the variation in surface area was generated primarily by high temperature regulation of the growth process. This suggests that the amorphous character of the surface is an inherent characteristic.

It is possible to explain this variation with particle size if one considers in more detail the nature of the interaction of an ionic lattice with a dipolar molecule. The ion-dipole contribution to the interaction energy is linearly dependent on the electrostatic field strength. Any modification of crystalline to amorphous character should reduce the electrostatic field strength at the surface because of the more random arrangement of positive and negative ions.

A series of measurements was conducted with methanol as the adsorbate, on the premise that MeOH with a lower dipole moment should

Publication Date: January 1, 1964 | doi: 10.1021/ba-1964-0043.ch015

show less variation in immersional heats with particle size. The data are shown in Figure 4 for a series of SiO_2, Al_2O_3, and TiO_2 samples. Although the phenomenon is still evident, there is less variation of immersional heat with particle size than with water on the same adsorbents. Unfortunately, the data for TiO_2 no longer show any clear trend with particle size, probably indicative of specific chemisorption process occurring between methanol and TiO_2 samples. However, for SiO_2 and Al_2O_3 there is a remarkable parallelism between the adsorptive heats of water and methanol, extending even to the behavior of heats of immersion as a function of outgassing temperature for almost every sample. The variation of immersional heats of alumina and methanol at the higher outgassing temperatures is indicative of chemisorption bonding, with a subsequent cleavage of methanol molecules in the first layer to produce two surface species (OH and OMe). The entropies of

Publication Date: January 1, 1964 | doi: 10.1021/ba-1964-0043.ch015

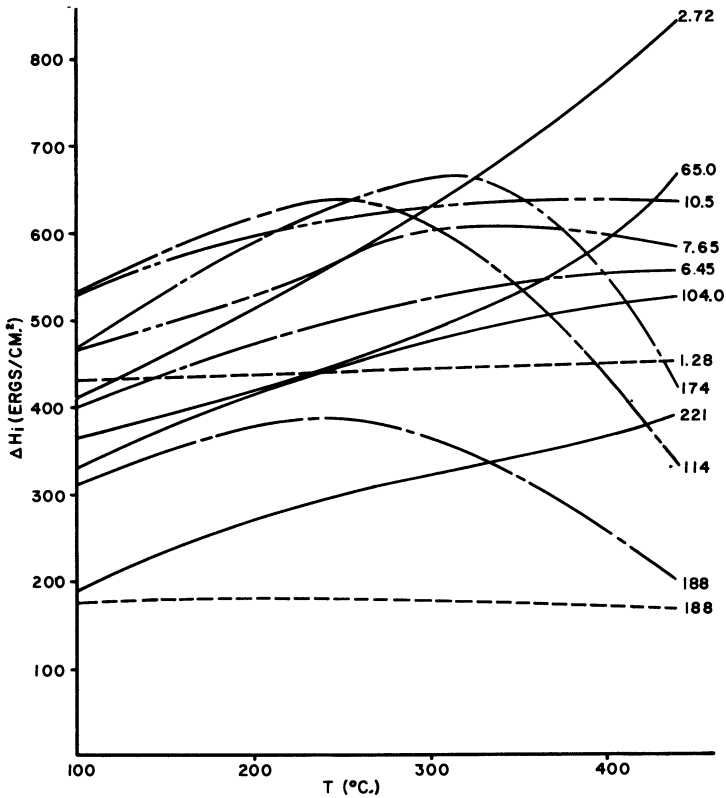

Figure 4. Heats of immersion in methanol as a function of outgassing temperature

——— Al_2O_3
– – – – SiO_2
—·—·— TiO_2

adsorption obtained as described by immersional heats and integration of the adsorption isotherms for the methanol studies are listed in Table II. Here once again we see that the entropy of adsorption decreases with decreasing particle size, as would be expected from previous arguments.

Table II. Parameters for Methanol Adsorption

	Surface Area, Sq. M./G.	ΔH_A	ΔG_A	ΔS_A
SiO_2	1.28	386	130	0.86
	188	132	61	0.24
Al_2O_3	2.72	422	122	1.01
	65.0	348	105	0.82
	104.0	336	125	0.71
	221	194	108	0.29
TiO_2	7.65	453	150	1.02
	10.5	527	125	1.35
	188	307	69	0.80

$\Delta H_A = \Delta H_i - 48.$

To provide a more rigorous test of the nature of the variation with particle size, immersional heats for these samples were measured in hexane. If hexane has no dipole moment, no variation of immersional heat with particle size would be expected. This is not completely true, since there is a small but easily distinguishable variation of immersional heat with particle size for all three types of substrates (Figure 5). To explain this residual variation one must look to second-order effects. Adsorption of a nonpolar molecule in an inhomogeneous electric field generates an induced dipole moment in the adsorbate molecules which can be measured quantitatively in principle by the polarizability of the adsorbate species. One would then expect this additional contribution to the total adsorption energy of hexane to be related to the electrostatic field strength, E, of the surface and the polarizability, α, of the adsorbate by the following equation:

$$W = 1/2\ \alpha\ E^2$$

A quantitative estimation once again would require an estimation of the electrostatic field strength and its variation with particle size. This has been estimated previously [15], but since the electrostatic field strength is such a sensitive function of the distance normal to the surface, the calculation has little quantitative significance.

The lack of variation of immersional heat with outgassing temperature indicates that the hexane molecules are rather insensitive to the chemical nature of the surface and are held primarily by van der Waals forces. The integral entropies of adsorption for a number of adsorbents with hexane are listed in Table III.

Publication Date: January 1, 1964 | doi: 10.1021/ba-1964-0043.ch015

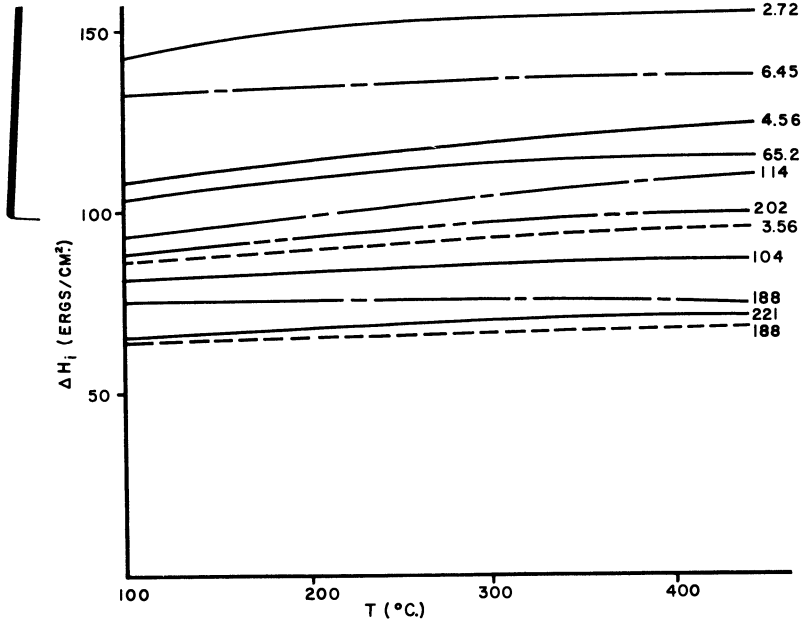

Figure 5. Heats of immersion in hexane as a function of outgassing temperature

——— Al_2O_3
– – – – SiO_2
—·—·— TiO_2

Table III. Parameters for Hexane Adsorption

	Surface Area, Sq. M./G.	ΔH_A	ΔG_A	ΔS_A
SiO_2	188	47	19.0	0.094
Al_2O_3	2.72	133	33.4	0.34
	65.0	89	29.9	0.20
	104	67	44.2	0.076
TiO_2	10.5	119	46.4	0.24
	188	56	34.8	0.071

$\Delta H_A = \Delta H_i - 17.9$.

Conclusions

In processes traditionally referred to as physical adsorption there are considerable sensitivity and selectivity in the systems studied. Although Rhodin's [10] beautiful measurements on copper single crystals show a variation of physical adsorption parameters with crystal face

Publication Date: January 1, 1964 | doi: 10.1021/ba-1964-0043.ch015

exposed, there has been no attempt to repeat these measurements on other systems. The variations observed in our laboratory tend to show how extremely complex simple adsorption processes can be. However, it has been possible to interpret reasonably many of the accrued data in general terms. Unfortunately, many questions remain unanswered.

What is the exact influence of the surface OH groups on the energetics of adsorption? This question cannot be answered without a quantitative estimation of the surface OH coverage. Infrared measurements are restricted in their application to samples of high specific surface area and do not possess sufficient sensitivity for samples of surface area measuring 1 to 10 sq. meters per gram. This is unfortunate, in that samples of high surface area may be somewhat limited in the thermodynamic interpretation because of complications due to interparticle condensation. Until a method is devised for measuring the surface OH coverage quantitatively for low-area samples, many of the interpretations will be open to question. Experimental weight loss measurements have so far been useless in the characterization of low-area samples and no other experimental technique is now available with which to attack this problem.

Some technique must be devised to provide first-hand information on the supposed amorphous character of the surface. This information has been attained up to the present time only by inference.

The perennial objection to surface chemistry measurements based on concentration of impurities in the surface region must be successfully answered. No technique for this is available at present.

Acknowledgment

The authors express their continued appreciation to the American Petroleum Institute for its support.

Literature Cited

(1) Bartell, F. E., Suggitt, R. M., J. Phys. Chem. 58, 36(1954).
(2) Boyd, G. E., Harkins, W. D., J. Am. Chem. Soc. 64, 1190, 1195(1942).
(3) Cuschens, R. P., Pliskin, W. A., Advan. Catalysis 10, 1-56(1958).
(4) Egorov, M. M., Drasilnikov, K. G., Sysoev, E. A., Dokl. Akad Nauk SSSR 108, 103(1956).
(5) Every, R. L., Wade, W. H., Hackerman, N., J. Phys. Chem. 65, 25(1961).
(6) Ibid., p., 937.
(7) Iler, R. K., "Colloid Chemistry of Silica and Silicates," Cornell University Press, Ithaca, N. Y., 1955.
(8) McDonald, R. S., J. Am. Chem. Soc. 79, 850(1957).
(9) Makrides, A. C., Hackerman, N., J. Phys. Chem. 63, 594(1959).
(10) Rhodin, J., J. Am. Chem. Soc. 72, 5691(1950).
(11) Wade, W. H., Cole, H. D., Meyer, D. E., Hackerman, N., Advan. Chem. Ser., No. 33, 35(1961).
(12) Wade, W. H., Every, R. L., Hackerman, N., J. Phys. Chem. 64, 355(1960).
(13) Wade, W. H., Hackerman, N., Ibid., 64, 1196(1960).
(14) Ibid., 65, 1681(1961).
(15) Ibid., 66, 1823(1962).
(16) Whalen, J. W., Advan. Chem. Ser., No. 33, 281(1961).
(17) Yates, D. J. C., J. Phys. Chem. 65, 746(1961).
(18) Zettlemoyer, A. C., Young, G. J., Chessick, J. J., Healey, F. H., Ibid., 57, 649(1953).

Received April 15, 1963.

16

Chemisorption and Dewetting of Glass and Silica

LISBETH TER-MINASSIAN-SARAGA

Laboratoire de Chimie Physique
Faculté des Sciences, Paris, France

Publication Date: January 1, 1964 | doi: 10.1021/ba-1964-0043.ch016

The adsorption of dodecyltrimethylammonium bromide (LNBr) from aqueous solutions on silica and glass slides dewetted by these solutions was measured by using molecules labeled with radioisotopes (C^{14} and Br^{82}). At low LNBr concentrations the counterion, Br^-, was not adsorbed. It was assumed that the LN^+ ions were chemisorbed by cation exchange between the aqueous LNBr solution and the ≡SiOH groups at the surface of silica or glass. The adhesion free energy was measured for these systems. The results were interpreted by assuming that the adhesion free energy may be related to a process of cation exchange between the solid surfaces and a LNBr monolayer adsorbed at the surface of the solution that dewets the solid.

The chemisorption, at the surface of a solid (wet slide or suspension), of surfactants which are completely dissociated when in aqueous solution may depend on the character of the active groups of the solid (acid or basic).

According to Carman [8] and many other authors [17], the surface hydration of collodial amorphous silica results in the formation of one hydroxyl for every silicon atom at the surface; the other three valencies of this atom are saturated by oxygen atoms, in such a manner that the tetrahedral coordination is preserved.

When hydrated silica is brought in contact with water, hydrated silicon atoms or silanol groups may dissociate and form electrically charged ionic sites.

The existence and the sign of the electrical charges are revealed by electrokinetic phenomena [21]. Glass [22], vitreous silica [3, 23], and quartz [19] bear negative charges.

The pK of dissociation of silanol groups is not known. But for the first dissociation of silicic acid:

In Contact Angle, Wettability, and Adhesion; Fowkes, F.;
Advances in Chemistry; American Chemical Society: Washington, DC, 1964.

$$H_4SiO_4 \rightleftharpoons H_3SiO_4^- + H^+$$

the value of pK is 9.8 [11, 17]. It may be inferred that silica behaves as a very weak colloidal acid.

The exchange of mineral cations between silica and many aqueous solutions has been studied recently as a function of pH [1, 12]. It has been shown [1] that the experimental results conform to the law of mass action.

When brought in contact with aqueous solutions of organic salts (dodecyltrimethylammonium bromide [3] or dodecylammonium chloride [19]) of increasing concentrations, the surface electric charge of silica may decrease to zero and even become positive.

The decrease of the electric charge at the silica-solution interface may proceed by the following mechanisms:

The long-chain organic cations of the salts are attracted by electrostatic forces [24] and combine with a negatively charged (ionized silanol) site which becomes neutralized, while another cation (which may be a H^+_{aq} ion) is released from the diffuse Gouy layer.

A cation exchange [19] between the solution and the undissociated (neutral) silanol groups at the surface of silica leads to a decrease of charge in the diffuse Gouy layer, if the groups resulting from this exchange dissociate to a lesser extent than the original silanol groups of the silica-water interface. In this process too a H^+_{aq} ion is released into the solution.

As the end result of both processes is adsorption, we call it "chemisorption." It leads to the "neutralization" of the ionized or ionizable groups of the colloid (silanol groups for silica surfaces). In this process H^+_{aq} ions participate. It should, therefore, be dependent on the pH of the aqueous phase.

The positive electric charge at the surface of silica in contact with the above-mentioned solutions has been ascribed either to the physical adsorption of a second layer of long-chain ions (and of their counterions) on top of chemically bound ions to silica [19, 24] or to the chemisorption on silica from solution [18] of multivalent positively charged micelles.

Greenberg [12] has found by measuring the capacity of cation exchange, with calcium hydroxide, that a maximum of eight silanol groups per 100 sq.A. may be accounted for at the surface of amorphous silica gels. The capacity of exchange was less (about half of the first value) when measured with sodium hydroxide. However, areas per molecule of stearic acid and n-octadecane adsorbed on dry nonporous aerosil from solutions in heptane [5] as well as areas per cation-exchange site of clay minerals [6], which have a planar symmetry, measured by Brooks, lie within the range of 60 to 140 sq. A. Also in this range (40 to 80 sq.A.) lie the values of areas per silanol site, which may be calculated from the results of Young [31].

A peculiar type of adsorption [26] may take place while a glass slide is raised out of a solution of a substituted quaternary ammonium salt, which is a dewetting agent for glass. Adsorbed molecules at the solution-air interface are transferred to the solid surface and are added to the molecules already adsorbed on the solid directly from the solution. Tenebre [26] has called this transfer "complementary adsorption." The densities of molecules adsorbed from the bulk of the solution and those transferred from the free surface of the solution were measured

Publication Date: January 1, 1964 | doi: 10.1021/ba-1964-0043.ch016

separately. It was found that 1.4×10^{14} molecules of tetradecyltrimethylammonium bromide were transferred to 1 sq.cm. of glass from the surface of a solution (2×10^{-4} M). The area per molecule was therefore 70 sq.A.

The free energy of adhesion, τ, glass solution [26], has been related to the surface density of transferred molecules by using the usual definition of the free energy of adhesion, $\tau = \gamma_S - \gamma_{SA} = \gamma_{LA} \cos \theta$ [2,16] and the Gibbs equation as

$$\delta_S - \delta_{SL} = - \frac{d\tau}{\alpha \, kT \, d \ln c} = - \frac{1}{\alpha} \left(\frac{d\gamma_S}{kT \, d \ln c} - \frac{d\gamma_{SL}}{kT \, d \ln c} \right)$$

where δ_S, δ_{SL}, γ_S, and γ_{SL} are the densities and surface tensions at the solid-air (S) and solid-liquid (S/L) interfaces, α is a numerical coefficient ($1 < \alpha < 2$), γ_{LA} is the surface tension of the solution of concentration c, θ is the contact angle, and k and T are the Boltzmann constant and temperature.

The numerical coefficient, α, is related to the process of surface hydrolysis which may take place in monolayers of quaternary ammonium-substituted salts [32], which means that one negatively charged counterion is displaced by a selectively adsorbed hydroxyl ion. When all the counterions have been replaced, $\alpha = 1$ and in the absence of surface hydrolysis $\alpha = 2$.

Earlier, the author showed [28] that the dewetting adsorption amounts to a chemical adsorption by cation exchange between the solid and the adsorption monolayer at the solution-air interface.

A mechanism has been proposed for the dewetting of glass, which is treated as a solid having ionizable groups at its surfaces.

Since then, the dewetting of silica has been extensively studied with solutions of dodecyltrimethylammonium bromide in the presence of HCl and NaOH, as well as the adsorption, δ_S of the dewetting agent at the surface of dewetted vitreous silica.

Experimental Results

Adsorption of LNBr at Surface of Dewetted Vitreous Silica and Glass. The following labeled substances were used: $CH_3(CH_2)_{11}N(CH_3)_2(C^*H_3)Br$ [28] or L^*NBr, and $CH_3(CH_2)_{11}N(CH_3)_3Br^*$ [29] or $LNBr^*$, where $C^* = C^{14}$ and $Br^* = Br^{82}$.

These substances were prepared by the Centre d'Etudes Nucléaires, Saclay, France. The plot of the surface tension *vs.* the concentration of their aqueous solutions did not show a minimum. The critical micelle concentration was equal to 10^{-2} M at 25°C. [32].

Silica slides were made of vitreous silica, heated to 2000°C., and very finely polished. The glass slides were ordinary microscope slides.

The major part of the work was done with slides cleaned by a mixture of $KClO_3$ (crystalline) and H_2SO_4 (liquid) and rinsed carefully with tap water and distilled water.

The slides, while still wet, were immersed rapidly in the solution (Figure 1) [29] for a given period of time, and then taken out slowly (at the rate of 0.2 or 0.1 mm. per minute). They appeared dry. The adsorption of LNBr on them seemed to be independent of the period of

Publication Date: January 1, 1964 | doi: 10.1021/ba-1964-0043.ch016

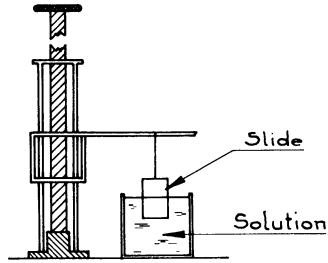

Figure 1. Device for dewetting slides

immersion in solution, but if the slides were removed too quickly from the solution, the results were inconclusive.

After the activity of the β-rays emitted by the labeling atoms had been measured, the adsorption, δ_S, was calculated for the anion (Br^-) or the cation (LN^+), expressed in ions per square centimeter.

The adsorption curve of bromine ions at the surface of glass dewetted by aqueous solutions of LNBr* is given in Figure 2,a. This adsorption was zero when glass was dewetted by dilute solutions (less than 4×10^{-3}M). Analogous results were obtained for the tetradecyl- and hexadecyltrimethylammonium bromides [28].

The amount of chemical adsorption, δ_S, of L^*N^+ on glass dewetted by aqueous solution of L^*NBr was plotted as a function of soap concentration (Figure 2,b) [28]. The curve showed a level P and an inflection point, F. As in the case of adsorption of the bromine ions (Figure 2,a) on glass, the results for LN^+ adsorption were inconclusive when the solutions were near their critical micelle concentration.

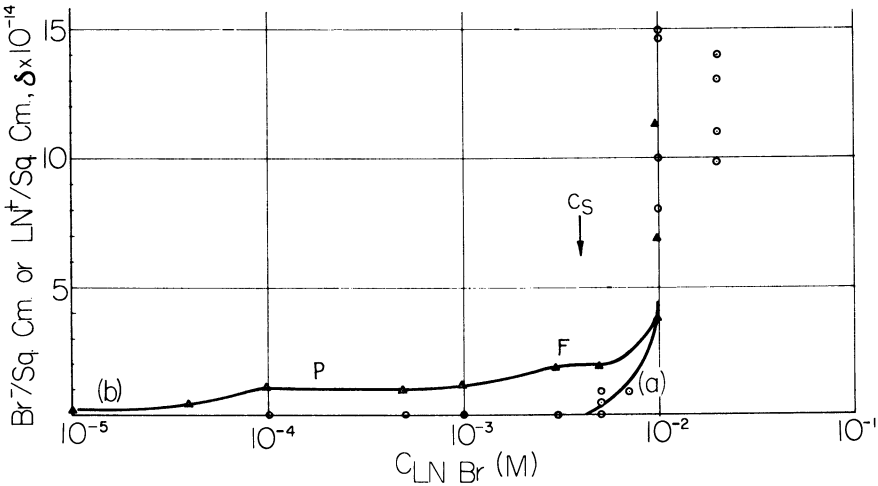

Figure 2. Relation of LNBr concentration in dewetting solution to amount of LN^+ and Br^- at surface of dewetted glass 22–23° C.

A. Adsorbed anions, Br^-
B. Adsorbed cations, LN^+

$c_s = 4 \times 10^{-3}$M

Publication Date: January 1, 1964 | doi: 10.1021/ba-1964-0043.ch016

The amount of chemical adsorption of L^*N^+ on vitreous silica is shown in Figure 3. (The measurements for the silica-HCl solutions are quoted from Fleury's dissertation [10].)

The same samples of silica were dewetted by solutions of L^*NBr at several pH values.

The substituted quaternary ammonium salt is a strong stable electrolyte. It may be inferred that by varying the pH of solution, only the state of the surface of the solid adsorbent has been modified. It is

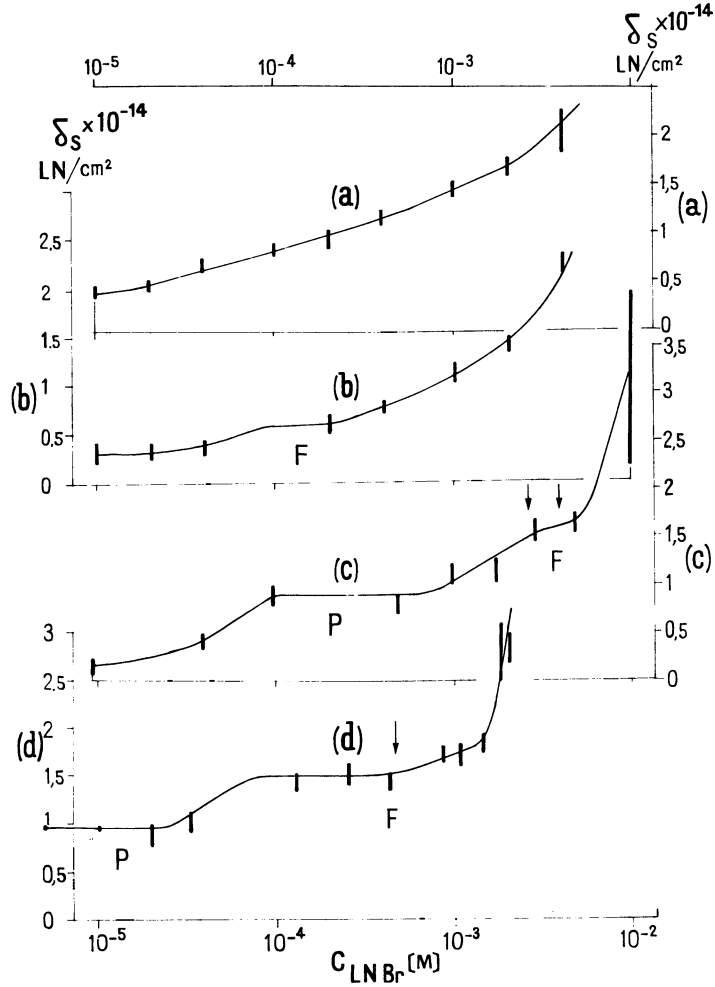

Figure 3. Relation of LNBr concentration in dewetting solution to amount of LN^+ at surface of dewetted silica 22–23°C.

A. In acid environment, 10^{-2}M HCl
B. In dilute acid environment, 10^{-4}M HCl
C. In distilled water → $c_{LNBr} = 2.7 \times 10^{-3}$ and 3.8×10^{-3} M
D. In alkaline environment, 1.2×10^{-2}M NaOH → $c_{LNBr} = 4.7 \times 10^{-3}$ M

assumed that in strong acid solutions (10^{-2} M HCl) silica adsorbs protons [4]; in dilute acid solutions (10^{-4} M HCl) or in contact with distilled water very few silanol groups at the surface of silica are ionized. But in contact with an alkaline solution (1.2×10^{-2} M NaOH) it is probable that most of the surface acid groups of silica are ionized.

Curves c and d of Figure 3 resemble one another as well as curve b of Figure 2. They show a level, P, and an inflection point, F.

The values of δ_S^P and δ_S^F corresponding to P and F of the curves are shown in Table I.

Table I. Chemical Adsorption of L^*N^+ on Silica and Glass

System	$\delta_S^P \times 10^{-14}$	$\delta_S^F \times 10^{-14}$	δ_S^F/δ_S^P
	L^*N^+ per sq. cm.		
Silica/HCl_{aq}, 10^{-2} M	No P	No F	
Silica/HCl_{aq}, 10^{-4} M	No P	0.6	
Silica/H_2O, dist.	0.9	1.6	1.80
Silica/$NaOH_{aq}$, 1.2×10^{-2} M	0.95	1.5	1.61
Glass/H_2O, dist.	1.05	1.9	1.81

The ratio of δ_S^F/δ_S^P values seems to be independent of the nature of the adsorbent. Level P and inflection point F are not observed on the curve referring to the 10^{-2} M HCl solution.

Electrical Charge at Surface of Silica and Glass. The sign of these charges may be determined by studies of electro-osmosis and electrophoresis [21]. Both solids (silica [3] and glass [2]) are negatively charged when in contact with water or dilute aqueous LNBr. For a critical concentration, c_s, of LNBr, lower than the critical micelle concentration of this soap dissolved in water at 22–23°C., the apparent electric charge is zero. For glass $c_s = 4 \times 10^{-3}$ M [27]. For silica two values of c_s (2.7×10^{-3} M [27] and 3.8×10^{-3} M [3]) were found in plain LNBr aqueous solutions. When NaOH was added, the value of c_s was around 4.7×10^{-4} M.

Adhesion Tension Measurements for Silica-Aqueous Solutions of LNBr. Adhesion tensions had previously been measured for such systems by Guastalla [14].

The present investigation was made on silica slides of the same origin as the ones used to study the chemical adsorption of LNBr.

The adhesion tension, τ, was measured with Guastalla's wetting balance [13]. This apparatus was designed according to Wilhelmy's principle [30] for measuring the surface tension of liquids.

A solid slide (silica or glass) was hung on the lever of a torsion balance above the surface of a liquid (pure liquid or solution). The slide was gradually immersed into the liquid while the balance was measuring the force acting on the slide. This force, f, was plotted as a function of the position, h, of the slide (Figure 4). At point a the slide was brought in contact with the surface of a liquid, which, in our case, did not wet the solid completely. The contact angle, θ_e, increased gradually while the slide was being immersed. At point b the immersion or

Publication Date: January 1, 1964 | doi: 10.1021/ba-1964-0043.ch016

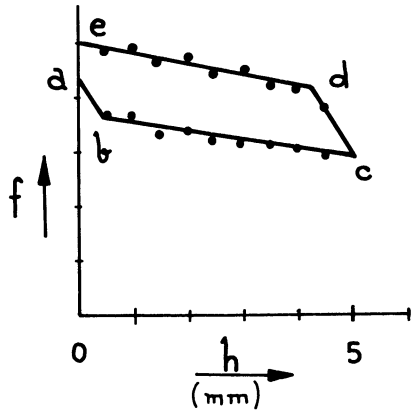

Figure 4. Cycle of wetting of silica slide, LNBr in alkaline solution 24° C.

$$c_{LNBr} = 1.02 \times 10^{-3} M$$
$$c_{NaOH} = 1.2 \times 10^{-2} M$$

advancing contact angle, θ_e, and adhesion "tension," τ_e, were established and remained constant as long as the slide was advancing further into the liquid (point c). The slide was then slowly taken out of the liquid. The angle of contact changed first and at d the emersion adhesion tension, τ_s, and contact angle (receding θ_s angle) were established. They stayed constant while the slide was gradually taken out of the liquid (point e). The hysteresis of this cycle of wetting was given by the difference, $\Delta\tau = \tau_s - \tau_e$. The tensions, τ_s and τ_e, are obtained by extrapolation of the force, f, to h = 0. [More details on this type of experiment are given by Guastalla [13].]

An aging effect for the measured force, f, was observed for the systems studied by Tenebre [26] and myself [29]. After the slide had been lifted 0.5 mm., f decreased and attained a stable value, which was used in tracing the wetting cycles (Figure 4). The adhesion tensions for the systems silica–aqueous solutions of LNBr and silica–alkaline solutions (1.2×10^{-2} M NaOH) of LNBr were measured at 24° C. and plotted as a function of the concentration of LNBr (Figure 5,a and b). For these systems the chemical adsorption is known (Figure 3 and Table I).

A nick appears on Figure 5,b, for a value of concentration $c_{LNBr} = 5 \times 10^{-5}$ M. At about this concentration a discontinuity may be seen on Figure 3,d, showing our results for the chemical adsorption of LN^+.

Between the concentration values 5×10^{-4} M and 10^{-3} M for LNBr the adhesion tension, τ_e and τ_s, curves reach a minimum. The inflection point, F, which can be seen on Figure 3,d, corresponds to a concentration of LNBr in solution equal to 5×10^{-4} M.

The hysteresis of wetting ($\Delta\tau$) is low for the aqueous solutions (in distilled water), a. For the alkaline solutions, b, the hysteresis is larger but does not exceed 10 dynes. (This result was obtained for silica slides which had been soaked overnight in aqueous 4N HCl. Following this treatment the results of adhesion tension measuring became

Publication Date: January 1, 1964 | doi: 10.1021/ba-1964-0043.ch016

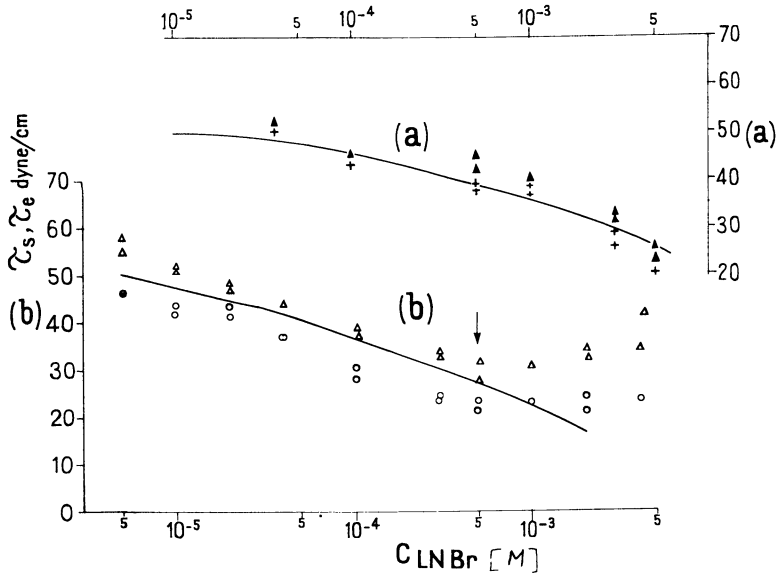

Figure 5. Emersion and immersion adhesion tensions for silica-aqueous solutions of LNBr as a function of LNBr concentration in solution 24° C.

Δ Emersion adhesion tension, τ_s
\+ Immersion adhesion tension, τ_e
——— Calculated adhesion tension, τ_{calcd}
A. Solutions in distilled water
B. Alkaline solutions

$c_{NaOH} + 1.2 \times 10^{-2}$ M. → $c_{LNBr} = 5 \times 10^{-4}$ M

reproducible and the difference, $\Delta\tau$, decreased. The last fact confirmed the view of Okersee and De Boer [20], who had found that silica gels are changed by treatment with 4N aqueous HCl solutions.)

A difficulty arises when the thermodynamic meaning of τ_e and τ_s is examined.

In principle the adhesion tension for a solid-liquid system in thermodynamic equilibrium may be obtained only from a reversible wetting-dewetting cycle.

For the system we studied the hysteresis of wetting was small and independent of the composition of the liquid phase (Figure 5). The average $\tau_{exp} = (\tau_e + \tau_s)/2$ has been therefore here considered to be a reasonable approximation for the equilibrium adhesion tension.

Discussion

The presence of silanol groups, ≡SiOH, at the surface of silica gels has been demonstrated in many ways [17]. It has been supposed that at the surface of glass (≡SiOX) groups exist which may be silanol (X = H) or pseudosilicate groups X = Na, for example.

Publication Date: January 1, 1964 | doi: 10.1021/ba-1964-0043.ch016

When glass is immersed in water, the pseudosilicate groups may hydrolyze and become silanols. Wet glass and silica may then be considered as having surfaces which resemble one another chemically.

In the following interpretation of our results concerning glass and silica, both substances are designated as solid and the ionizable surface group is named $\equiv SiOX$.

The possible constitution of the interface solid-solution of LNBr is represented by Figure 6, where a solid slide is shown emerging from a LNBr solution at a concentration lower than c_s (Figure 2). On the immersed portion the negative charges of the solid may be neutralized partially by fixed cations (LN^+ or H^+) and partially by the ions of the Gouy layer.

The film of liquid thins near the contact line, R (Figure 6). In this region, the $\equiv SiOX$ sites of the solid surface, ionized or un-ionized, may approach very closely the long-chain cations and their counterions, Br^-, belonging to the adsorbed film at the L/A interface. These ions may react with the sites at the S/L interface according to the following relations:

$$\equiv SiOX_{S/L} + LN^+_{L/A} + Br^-_{L/A} \rightleftharpoons \equiv SiOLN_S + X^+_{aq} + Br^-_{aq} \quad (2)$$

$$\equiv SiO^-_{S/L} + X^+_{S/L} + LN^+_{L/A} + Br^-_{L/A} \rightleftharpoons \equiv SiOLN_S + X^+_{aq} + Br^-_{aq} \quad (3)$$

As a result of Reactions 2 and 3, during liquid recession, on the emerging slide one hydrophobic ion LN^+ is adsorbed at the dry S/A interface, while two hydrophilic ions, X^+ and Br^-, desorb into the aqueous phase. Also, during liquid recession the slide crosses the adsorbed layer of LNBr where the concentration of the long-chain ions is very high and where they are oriented in a favorable position for the exchange to take place. Lastly, repulsion of hydrogen ions, from the thin region around line R, by the positively charged long-chain adsorbed ions might bring a local increase in pH compared to the rest of the system.

However, a steric hindrance may be imagined, which may decrease the extent of exchange: When the adsorbed monolayer at the L/A interface is very dilute, cations $LN^+_{L/A}$ at R (Figure 6) may lay their chains down at the surface of the solid and thus cover several active $\equiv SiOX$ sites, which become inaccessible to the organic cations which follow.

This type of steric hindrance decreases when the surface density of the monolayer at the interface L/A increases (Figure 7) as a consequence of increase in the concentration of the solution.

For a solution of concentration c_s corresponding to the inflection point, F (Figure 2), δ_S equals the full capacity of exchange at the surface of the solid.

For silica, δ_S is the same for aqueous solutions (in distilled water) and for alkaline solutions (Table I), but is different from that of glass. The areas per active site $\equiv SiOX$ are, respectively, 52.5 and 65 sq.A. at the surface of glass and silica. These values are close to the values given by Brooks for sodium and calcium montmorillonites and for aerosil [5, 6].

The low "capacity of exchange" (δ^P_S at level P) is equivalent to 110 to 105 sq.A. per $\equiv SiOH$ site for silica and 95 sq.A. per $\equiv SiOX$ site for glass. All these values are comparable to the value found by Tamamushi

Publication Date: January 1, 1964 | doi: 10.1021/ba-1964-0043.ch016

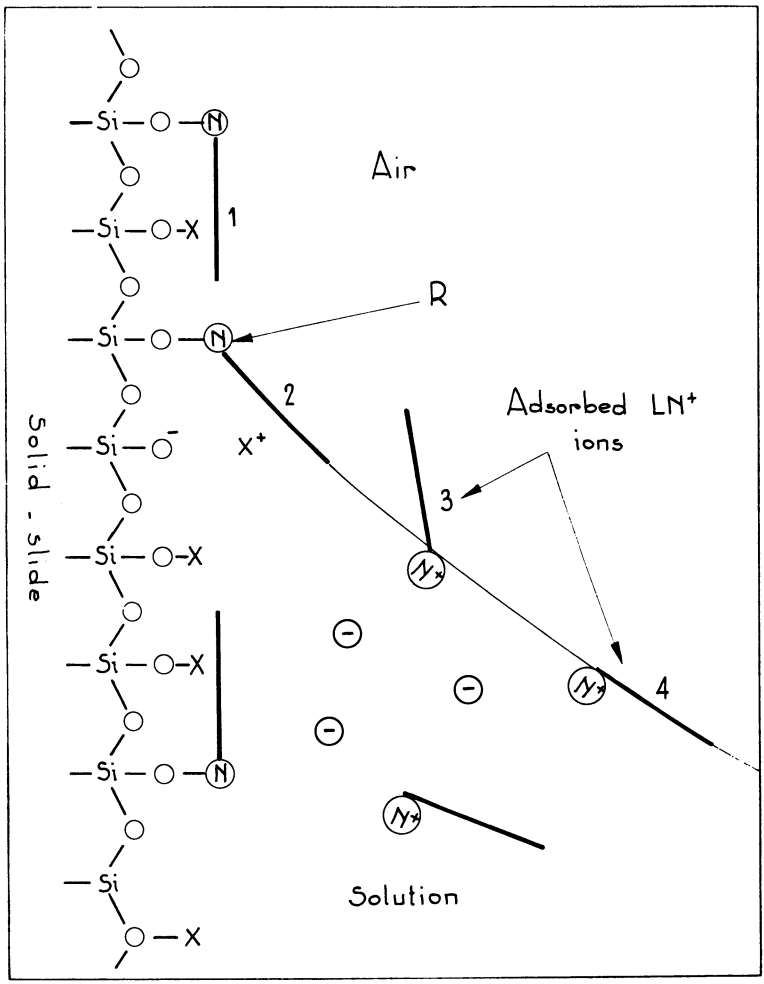

Figure 6. Silica or glass slide emerging from dilute aqueous solution of LNBr

$c_{LNBr} < c_s$, and

$\delta_S = \delta_S^P$ (see Table I)

- θ Anions, Br^-
- × Small cations, H^+ or Na^+
- ⊕ Organic cation, LN^+
- R. Contact line of L/A interface with S/A interface
- Si. Silicon atoms
- O. Oxygen atoms

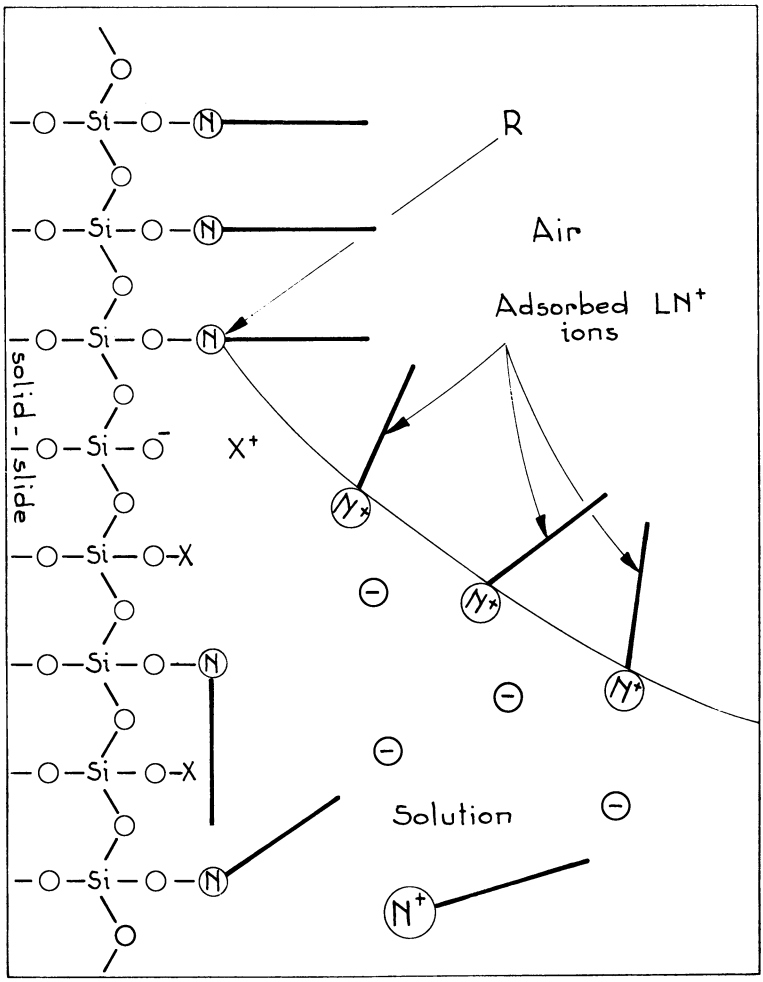

Figure 7. Silica or glass slide emerging from concentrated nonmicellar aqueous solution of LNBr

$c_{LNBr} = c_s$, and

$\delta_S = \delta_S^F$ (see Table I)

θ Anions, Br^-
× Small cations, H^+ or Na^+
⊖ Organic cation, LN^+
R. Contact line of L/A interface with S/A interface
Si. Silicon atoms
R. Oxygen atoms

and Tamaki [25] for dodecylammonium chloride adsorbed at the interface between the aqueous solutions and an ion-exchange resin. They are higher than the value (90 sq.A.) found by Ellison [9] for a lauric acid molecule in films spread at the mercury-air interface.

The molecules seem to be lying at the surface of the adsorbent in all three cases mentioned here.

The variation of the adhesion tension with composition of the liquid phase has been interpreted using the results obtained from chemisorption measurements of LNBr on silica, as follows.

According to Equation 26, calculated values of the adhesion tension may be obtained by integration of this relation.

A graphical integration can be done if the variation of the complementary adsorption, $\delta_S - \delta_{S/L}$, with concentration, c_{LNBr}, has been determined experimentally. The result of this integration is:

$$\tau_{calcd} = \text{cte} - kT \int (\delta_S - \delta_{S/L})\, d \ln c_{LNBr} \qquad (4)$$

where cte is an adjustable parameter.

In the present work the values of δ_S are measured but those of $\delta_{S/L}$ are not known.

However, at the pH of the plain aqueous solutions the amount of cation exchange for silica is very low [1]. As we assume that LN^+ is adsorbed on silica by this process only, $\delta_{S/L} = 0$ in Relation 6. Therefore the integration in 6 can be done when δ_S only has been experimentally determined as a function of c_{LNBr} (Figures 2 and 3).

The constant of integration in Equation 4 was adjusted by using the average value, τ_{exp}, obtained from the receding and advancing adhesion tensions at $c_{LNBr} = 10^{-4}$ M. Then the calculated curve for the adhesion tension silica-aqueous solutions of LNBr is obtained (Figure 5,a). This curve verifies the experimental results satisfactorily.

In the presence of 1.2×10^{-2} M NaOH (high pH) the amount of cation exchange at the S/L interface cannot be neglected. Curve b of Figure 5, however, has been calculated under the assumption that $\delta_{S/L}$ is zero. The constant of integration has been adjusted by using the average of the experimental τ_e and τ_s obtained for silica and a LNBr solution of a concentration equal to 5×10^{-6} M.

For relatively concentrated solutions of LNBr ($c_{LNBr} > 10^{-4}$ M) the calculated curve is different from the experimental one. On the last, a minimum can be seen at about 5×10^{-4} M (Figure 5). According to Relation 26 this minimum corresponds to a complementary adsorption equal to zero.

Variation of the Adhesion Tension Silica-Solution of LNBr, with Composition of Aqueous Phase

The free energy or tension of adhesion, τ, for a solid-liquid system is defined as the difference between the interfacial free energies or tensions at the S/A and S/L interfaces on the contact line R between these two interfaces and the L/A interface. The variation of the adhesion tension with composition of the liquid phase therefore must follow the variations of the corresponding adsorption equilibria (and tensions) at the corresponding interfaces.

Publication Date: January 1, 1964 | doi: 10.1021/ba-1964-0043.ch016

The variation of any interfacial tensions with composition at constant temperature can be written according to Gibbs [15]

$$- d\gamma = \sum_i \Gamma_i^\circ \, d\mu_i \tag{5}$$

where the summation extends over all solute species (ions, molecules, etc.) found in the interfacial region and in the adjacent bulk phases.

Adsorption and Tension at Silica-Aqueous Solution Interface

The aqueous solution contains only the substituted ammonium salt, LNBr. The solute species at the S/L interface (Figures 6 and 7) are:

$$\equiv SiOH,\ \equiv SiO^-,\ \equiv SiOLN,\ OH^-,\ H^+,\ LN^+,\ \text{and}\ Br^-.$$

The bulk concentrations of the species $\equiv SiOH$, $\equiv SiOLN$, and $\equiv SiO^-$ in the solid and aqueous phases are zero. Those of OH^-, LN^+, and Br^- are zero in the solid phase only. Furthermore, equilibria between the different i species and the conditions of electroneutrality in the interfacial and bulk regions impose some additional relations between the chemical potentials, μ_i, which diminish the number of the independent variables. These restrictions are the consequences of:

Equilibrium of formation of silanol groups at the surface of silica in presence of water

$$\boxed{\text{silica}} + H_2O \rightleftharpoons \boxed{\text{silica}}\equiv SiOH \tag{6}$$

$$\mu_{\boxed{\text{silica}}} + \mu_{H_2O} \rightleftharpoons \mu_{\boxed{\text{silica}}\equiv SiOH} \tag{6'}$$

where $\boxed{\text{silica}}$ signifies solid silica and the box represents its surface. Therefore $\boxed{\text{silica}}\equiv SiOH$ represents solid silica which has reacted with water only at its surface to give superficial $\equiv SiOH$ groups. Thus $\boxed{\text{silica}}\equiv SiOH$ is equivalent to

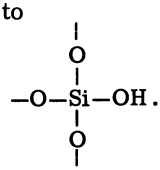

Equilibrium of acid dissociation of silanol groups

$$\equiv SiOH \rightleftharpoons \equiv SiO^- + H^+ \tag{7}$$

$$\mu_{SiOH} = \mu_{SiO^-} + \mu_{H^+} \tag{7'}$$

Equilibrium of the combination of $\equiv SiO^-$ sites with LN^+ ions

$$\equiv SiO^- + LN^+ \rightleftharpoons \equiv SiOLN \tag{8}$$

$$\mu_{SiO^-} + \mu_{LN^+} = \mu_{SiOLN} \tag{8'}$$

Equilibrium for cation exchange by silanol undissociated groups obtained by adding Equation 7 to 8 and 7' to 8'.

$$\equiv SiOH + LN^+ \rightleftharpoons \equiv SiOLN + H^+ \tag{9}$$

$$\mu_{SiOH} + \mu_{LN^+} = \mu_{SiOLN} + \mu_{H^+} \tag{9'}$$

which depends on the concentration of the hydrogen ions in the aqueous phase.

Equilibrium of dissociation of water molecules

$$H_2O \rightleftharpoons H^+ + OH^- \tag{10}$$

$$\mu_{H_2O} = \mu_{H^+} + \mu_{OH^-} \tag{10'}$$

Conditions of electroneutrality. (a) In bulk (aqueous solution)

$$\begin{aligned} c_{OH^-} &= c_{H^+} \\ c_{Br^-} &= c_{LN^+} = c_{LNBr} \end{aligned} \tag{11}$$

(b) At the surface

$$\Gamma^{\circ}_{Br^-} + \Gamma^{\circ}_{SiO^-} = \Gamma^{\circ}_{LN^+} + \Gamma^{\circ}_{H^+} \tag{12}$$

A given capacity of exchange for the silica surface:

$$N = \Gamma^{\circ}_{SiOH} + \Gamma^{\circ}_{SiOLN} + \Gamma^{\circ}_{SiO^-} \tag{13}$$

Constant pH of the aqueous phase

$$\begin{aligned} \mu_{H^+} &= \text{constant} \\ \mu_{OH^-} &= \text{constant} \end{aligned} \tag{14}$$

Constant activity and chemical potential in the bulk phases of water and silica, leading to:

$$\begin{aligned} \mu_{SiOH} &= \text{constant (from 6')} \\ \mu_{SiO^-} &= \text{constant (from 7' and from 14)} \end{aligned} \tag{15}$$

When the concentration of LNBr is varied in the aqueous phase at constant pH, conditions 14, 15, and 9' lead to the following expression for the change in the chemical potential of the superficial $\equiv SiOLN$ groups:

$$d\mu_{SiOLN} = d\mu_{LN^+} \tag{16}$$

Publication Date: January 1, 1964 | doi: 10.1021/ba-1964-0043.ch016

In our particular case the general relation (Equation 5) becomes:

$$- d\gamma_{S/L} = \Gamma^{\circ}_{SiOH}\, d\mu_{SiOH} + \Gamma^{\circ}_{SiOLN}\, d\mu_{SiOLN} + \Gamma^{\circ}_{SiO^-}\, d\mu_{SiO^-} + \Gamma^{\circ}_{H^+}\, d\mu_{H^+} + \Gamma^{\circ}_{LN^+}\, d\mu_{LN^+} + \Gamma^{\circ}_{Br^-}\, d\mu_{Br^-} + \Gamma^{\circ}_{OH^-}\, d\mu_{OH^-} \quad (17)$$

Taking into account all the restrictions mentioned above as well as Equation 16, a relation is obtained for the change in the interfacial $\gamma_{S/L}$ tension with the concentration of the salt LNBr at constant pH, as follows:

$$- d\gamma_{S/L} = \left(\Gamma^{\circ}_{SiOLN} + \Gamma^{\circ}_{LN^+}\right) d\mu_{LN^+} + \Gamma^{\circ}_{Br^-}\, d\mu_{Br^-} \quad (18)$$

The molecular chemical potential of any of the ions in the solution may be expressed as:

$$\mu_i = \mu^0_i(T, p) + kT \ln c_i f_i$$

In the particular case of LNBr solutions where f_i may be considered constant and Conditions 11 are valid, the expressions for the molecular chemical potential of LN^+ and Br^- ions reduce to:

$$\mu_{LN^+} = \mu^0_{LN^+} + kT \ln c_{LNBr}$$

$$\mu_{Br^-} = \mu^0_{Br^-} + kT \ln c_{LNBr}$$

The chemical potentials are then eliminated between the last two equations and Equation 18, which becomes:

$$- d\gamma_{S/L} = \left(\Gamma^{\circ}_{SiOLN} + \Gamma^{\circ}_{LN^+} + \Gamma^{\circ}_{Br^-}\right) kT\, d \ln c_{LNBr} \quad (19)$$

In the present work we neglect any adsorption of pairs of LN^+ and Br^- ions at the silica surface. Therefore $\Gamma^{\circ}_{Br^-} = 0$.

The negative value of the slope of the tangent to the curve of $\gamma_{S/L}$ *vs.* $\ln c_{LNBr}$ is equal to $\delta_{S/L}$, the total amount of long chain ions LN^+, either bound to silica as SiOLN groups or attracted into the diffuse Gouy layer as LN^+:

$$(- d\gamma_{S/L}/kT\, d \ln c_{LNBr}) = \delta_{S/L} = \Gamma^{\circ}_{SiOLN} + \Gamma^{\circ}_{LN^+} \quad (20)$$

Adsorption and Tension at Silica-Air Interface

The solute species at this interface above the line of contact R (see Figures 6 and 7) are ≡SiOH and ≡SiOLN. They are in equilibrium with the solid phase and with the adsorbed monolayers at the L/S and the L/A interfaces. As the films are in equilibrium with the underlying solution, species ≡SiOH and ≡SiOLN are in equilibrium with the solution as well.

The cation exchange between the S/A interface of silica and the aqueous solution may then be described as a three-step equilibrium: a first between the species at the S/A interface and the L/A interface (equilibrium between the corresponding monolayers)

Publication Date: January 1, 1964 | doi: 10.1021/ba-1964-0043.ch016

$$\equiv SiOH_S + LN^+_{L/A} + Br^-_{LA} \rightleftharpoons \equiv SiOLN_S + H^+_{L/A} + Br^-_{L/A} \quad (21)$$

and a second and a third between the species dissolved in bulk and those adsorbed at the L/A interface (corresponding monolayer).

$$LN^+_{aq} + Br^-_{aq} \rightleftharpoons LN^+_{L/A} + Br^-_{L/A}; \; H^+_{L/A} + Br^-_{L/A} \rightleftharpoons H^+_{aq} + Br^-_{aq} \quad (21')$$

The three relations (Equations 21 and 21') are added together and give:

$$\equiv SiOH_S + LN^+_{aq} \rightleftharpoons \equiv SiOLN_S + H^+_{aq} \quad (22)$$

which is an equation for the equilibrium of selective exchange at the S/A interface between one hydrophilic ion, H^+, and a hydrophobic ion, LN^+.

The chemical potentials of the reacting species in (Equation 22) depend on each other and the following restriction has to be taken into account:

$$\mu_{SiOH} + \mu_{LN^+} = \mu_{SiOLN} + \mu_{H^+} \quad (22')$$

Conditions 6, 10, and 11 are still valid. But additional ones are imposed at the S/A interface:

Nondissociation of the groups at the S/A interface: $\left(\Gamma^o_{H^+}, \; \Gamma^o_{LN^+}, \; \Gamma^o_{SiO^-} \text{ are zero}\right)$.

The capacity of exchange is equal to

$$N = \Gamma^o_{SiOH} + \Gamma^o_{SiOLN}.$$

The measured chemisorption is equal to the number of $\equiv SiOLN$ groups

$$\delta_S = \Gamma^o_{SiOLN} \quad (23)$$

For the S/A interface the variation of the interfacial tension with concentration of LNBr at constant temperature and pH (Relation 5) has the following expression:

$$- d\gamma_S = \Gamma^o_{SiOH} \, d\mu_{SiOH} + \Gamma^o_{SiOLN} \, d\mu_{SiOLN} \quad (24)$$

Substituting Equations 14, 16, 22', and 23 into 24 we get an equation analogous to Equation 20.

$$\left(- d\gamma_S / kT \, d \ln c_{LNBr}\right) = \delta_S \quad (25)$$

Subtracting 20 from 25, the slope of the tangent to the curve of adhesion tension *vs.* the logarithm of the concentration of LNBr, is obtained at constant temperature and pH. The expression for this slope is:

$$\left(- d\tau / kT \, d \ln c_{LNBr}\right) = (\delta_S - \delta_{S/L}) \quad (26)$$

Comparison of this relation to that suggested by Tenebre (Equation 1) shows that the parameter α is equal to 1.

Publication Date: January 1, 1964 | doi: 10.1021/ba-1964-0043.ch016

Relations 20, 25, and 26 have been obtained for a system constituted of silica and plain aqueous solutions of LNBr.

The same result can be arrived at when sodium hydroxide is dissolved in the aqueous phase and maintained at a constant concentration (1.2×10^{-2} M) while c_{LNBr} is variable.

It has been shown by Ahrland, Grenthe, and Noren [1] that at the corresponding high pH all the ≡SiOH groups are transformed into ≡SiONa groups. The exchange equilibria (Equations 9 and 22) then become equilibria of exchange between the pseudo-silicate groups, ≡SiONa, and the aqueous solution of LNBr (Figures 6 and 7). Therefore if the symbol H is replaced by Na, the expression obtained at last for the coefficient ($- d\tau/kT \, d \ln c_{LNBr}$) is again Equation 26.

Nomenclature

μ_i = molecular chemical potential of species i

μ_i° = molecular chemical potential (standard) of species i

Γ_i° = surface excess per unit area of species i ([15], equation 9.30.1) in Gouy layer or on solid surface

N = total number of acid sites (silanol) on 1 sq. cm. of silica surface

f_i = activity coefficient of species i in aqueous phase

Conclusions

By using molecules labeled with radioisotopes it is possible to determine the amount of substituted ammonium ions chemically adsorbed (by cation exchange) on glass or silica surfaces from an aqueous solution or from the monolayer adsorbed at the surface of the solution.

The isotherms of adsorption of trimethyldodecylammonium ions on both solids have a two-stepped shape corresponding to an expanded layer at low surface coverages and a compressed layer at high surface coverages. In the expanded layer the paraffin chains of the ions lie on the surface of the solid and may have a screening effect on several nearby silanols, which become inaccessible to other adsorbing ions. In the compressed layer the chains are gradually standing up. At maximum coverage the number of chemisorbed ions equals the number of silanol groups on the solid's surface. Each silanol group occupies 65 sq.A. on the silica surface and 52.5 sq.A. on the glass surface.

The free energy of adhesion or adhesion tension for the system silica-LNBr aqueous solutions has been measured. The model, which explains the above-mentioned peculiarities of the isotherm of chemisorption at the surface of the solids, is confirmed by the results of adhesion tension measurements.

Acknowledgment

The author is indebted to Yolande Hendricks for many stimulating discussions and to A. S. Michaels for helpful suggestions.

Literature Cited

(1) Ahrland, S., Grenthe, I., Noren, B., Acta Chem. Scand. **14**, 1059 (1960).
(2) Bartell, F. E., Bartell, L. S., J. Am. Chem. Soc. **56**, 2205 (1934).
(3) Baruch-Weil, M., Ann. Phys. (13) **4**, 1159 (1959).
(4) Bolt, G. H., J. Phys. Chem. 60, 325 (1956).
(5) Brooks, C. S., J. Colloid Sci. **13**, 522 (1958).
(6) Brooks, C. S., J. Phys. Chem. **64**, 532 (1960).
(7) Bungenberg de Yong., H. G., "Colloid Science," H. R. Kruyt, ed., Vol. II, p. 304, Elsevier, Amsterdam, 1949.
(8) Carman, P. C., Trans. Faraday Soc. **36**, 964 (1940).
(9) Ellison, A. H., J. Phys. Chem. **66**, 1867 (1962).
(10) Fleury, Ph., unpublished results.
(11) Greenberg, S. A., J. Am. Chem. Soc. **80**, 6508 (1958).
(12) Greenberg, S. A., J. Phys. Chem. 60, 325 (1956).
(13) Guastalla, J., "Proceedings of 2nd International Congress," p. 143, Butterworth, London, 1957.
(14) Guastalla, L., Compt. Rend. **243**, 1314 (1956).
(15) Guggenheim, E. A., "Thermodynamics," p. 326, North Holland Publishing Co., Amsterdam, 1949.
(16) Harkins, W. D., Fowkes, F. M., J. Am. Chem. Soc. 60, 1511 (1938).
(17) Iler, R. K., "Colloid Chemistry of Silica and Silicates," Cornell University Press, Ithaca, N.Y., 1955.
(18) Ibid., p. 251.
(19) O'Connor, D. J., Buchannan, A. S., Trans. Faraday Soc. **52**, 397 (1956).
(20) Okersee, C., de Boer, J. H., "Silice," Colloque de l'Association Belge pour Favoriser l'Etude des Verres et des Composés Silicieux, Brussels, Belgium, 1960.
(21) Overbeek, J. Th., "Colloid Science," H. R. Kruyt, ed., Vol. I. p. 194, Elsevier, Amsterdam, 1952.
(22) Rutgers, A. J., de Smet, M., Trans. Faraday Soc. **41**, 758 (1945).
(23) Rutten, F. (Van), J. Chim. Phys. **53**, 3 (1956).
(24) Tamamushi, B., Kolloid Z. **150**, 44 (1957).
(25) Tamamushi, B., Tamaki, D., Trans. Faraday Soc. **55**, 1013 (1959).
(26) Tenebre, L., Mem. Serv. Chim. Etat. 40, 77 (1955); J. Chim. Phys. **53**, 6 (1956).
(27) Ter-Minassian-Saraga, L., Compt. Rend. **249**, 1652 (1959).
(28) Ibid., **252**, 1596 (1961).
(29) Ter-Minassian-Saraga, L., J. Chim. Phys. **57**, 10 (1960).
(30) Wilhelmy, L., Ann. Physik, 9, 475 (1902).
(31) Young, G. J., J. Colloid Sci. **13**, 67 (1958).
(32) Zutrauen, H. A., J. Chim. Phys. **53**, 54 (1956).

Received April 3, 1963.

17

Resistance to Flow in Capillary Systems of Positive Contact Angle

ANTHONY M. SCHWARTZ, CHARLES A. RADER, and ELAINE HUEY

Harris Research Laboratories, Inc.
Washington 11, D. C.

Publication Date: January 1, 1964 | doi: 10.1021/ba-1964-0043.ch017

In capillary systems having an equilibrium contact angle substantially greater than zero, the liquid-solid-vapor boundary line shows a definite resistance against being moved along the solid surface. This resistance is characterized and defined as the critical line force. By determining the pressure necessary to start an index of liquid moving in a tube made of the substrate material, the critical line force values of a series of liquids on Teflon and polyethylene substrates were determined and found to increase linearly as $\cos \theta_{equil}$ decreased. In so far as $\cos \theta_{equil}$ remained a linear function of γ_{LA}, the contact angle hysteresis increased monotonically, but not linearly, with increasing critical line force. These findings support the view that microscopic surface roughness cannot be the sole factor controlling contact angle hysteresis.

This report is concerned with contact angle hysteresis and with a closely related quantity referred to as "critical line force (CLF)." More particularly, it is concerned with the relationship between contact angle hysteresis and the magnitude of the contact angle itself. Two sets of liquid-solid-vapor systems have been investigated to provide the experimental data. One set consists of Teflon [poly(tetrafluoroethylene), Du Pont] and a series of liquids forming various contact angles at the Teflon-air interface. The second set consists of polyethylene and a similar series of liquids. In neither case was the ratio of air to test liquid vapor at the boundary line controlled, but it can be assumed that the ambient vapor phase operative in all the systems was close to an equilibrium mixture.

In capillary systems having a contact angle greater than zero the liquid-solid-air boundary line does not move with complete freedom

In Contact Angle, Wettability, and Adhesion; Fowkes, F.;
Advances in Chemistry; American Chemical Society: Washington, DC, 1964.

along the solid surface. A very familiar example of this resistance to movement is the hanging of raindrops on an ordinarily dirty window pane or of water droplets on the side of a waxed paper drinking cup. It can be measured and specified in terms of a minimum force necessary to start and keep the three-phase boundary line moving. The fact that this force is fundamentally related to contact angle hysteresis is also well recognized, and has been brought out in at least three groups of experimental studies: the movement of liquid drops down an inclined plane due to gravity [9,10]; the dipping and raising of a thin plate through a liquid surface [14]; and the pushing of an index of liquid through a capillary tube by air pressure [17,18].

The exact form of functional relationship between the resistance force and the contact angle hysteresis depends, of course, on the parameters chosen. Rosano has presented an equation based on the plate method [14] and very recently Furmidge [10] has shown the essential relationship between Rosano's equation and the widely used equation for a droplet moving on an inclined plane. Since the total resistance force that must be overcome before the boundary line will move is directly proportional to the length of the line, we can tentatively define a force just necessary to start a unit length of boundary line moving as the critical line force.

Experimental

In studying this critical line force we have chosen to use the device first described by Jamin as shown in Figure 1 [13]. This consists of a horizontally placed cylindrical tube containing a series or "chaplet" of individual liquid indexes separated by air spaces. An air pressure differential is applied across the chaplet, and the velocity of the last index on the low pressure side is noted as a function of increasing pressure differential.

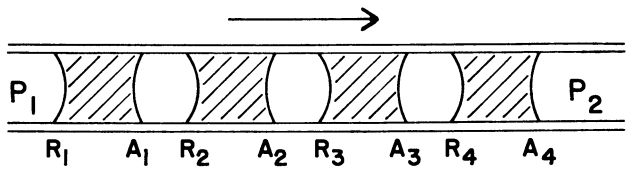

Figure 1. Chaplet of four indexes in capillary tube, subjected to pressure differential $P_1 - P_2$

Direction of motion indicated by arrow

As the pressure differential is applied, the first index on the high pressure side starts to move first, followed in order by the next index, and succeeding indexes, until finally the last index starts to move. As pointed out by Jamin and by Bouasse [2], the pressure differential necessary to bring the whole chaplet into motion increases directly as the number of indexes. This effect was confirmed very early in the study, using a liquid of relatively high contact angle. It was further confirmed, by using tubes of different diameters as well as different numbers of indexes in the chaplets, that the pressure differential necessary to start

Publication Date: January 1, 1964 | doi: 10.1021/ba-1964-0043.ch017

the whole chaplet moving is proportional to the total length of boundary line in the system. This agrees completely with the results Rosano obtained using the dipping plate system. It is evident that the sensitivity of this system can be increased indefinitely by increasing the number of indexes, just as it can in the dipping plate system by increasing the width of the plate.

The method for plotting velocity *vs.* pressure differential, and particularly for determining the minimum pressure necessary to start motion, is given below, and a typical plot is shown in Figure 2. Measuring in the region of relatively high velocity, where the pressure-velocity curve is nearly linear, and then extrapolating back to zero velocity, does not give the true critical pressure necessary to start the index moving. In the low velocity region just above the critical pressure the slope of the pressure-velocity curve decreases markedly with decreasing velocity. This makes the precise determination of critical pressure difficult. We arbitrarily chose the critical pressure as that at which no motion was perceptible in our apparatus over a

Publication Date: January 1, 1964 | doi: 10.1021/ba-1964-0043.ch017

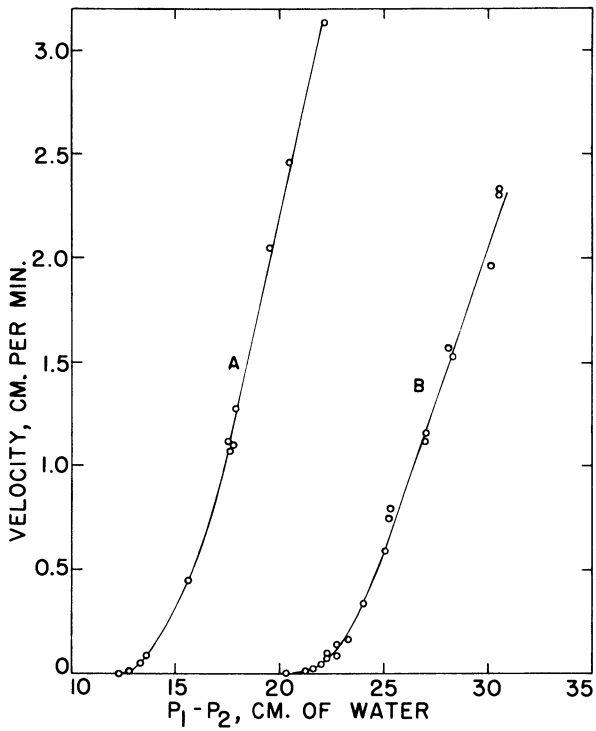

Figure 2. Velocity of advancing polyethylene glycol front vs. pressure differential in Teflon capillary tubes

Determined with chaplets of 10 indexes
A. Tube diameter 0.0624 cm.
B. Tube diameter 0.0378 cm.

period of 30 minutes. This corresponds to a velocity of less than 0.33 micron per minute. In no case where the index had remained stationary for 30 minutes did it move subsequently, within observation periods ranging up to 8 hours. (When the data for the larger Teflon capillary in Figure 2 are plotted as $V^{1/2}$ *vs.* pressure differential, Figure 3 is obtained. This plot strongly suggests that our critical pressure is where we have shown it to be.)

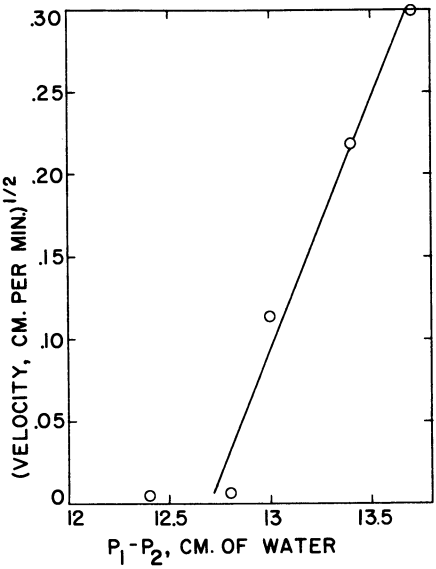

Figure 3. Square root of velocity of advancing polyethylene glycol front vs. pressure differential in Teflon capillary tube

Determined with chaplet of 10 indexes in 0.0624-cm. diameter tube
No movement discerned at $P_1 - P_2 = 12.4$
Point plotted showed maximum possible velocity at which liquid could have been moving

The manner in which an individual index moves was followed by using a viscous liquid and inserting a small portion of dye at one end of the index before starting the movement. The index proceeds forward by rolling away from the tube wall and inward toward its center axis at the rear, while rolling outward from its center axis and onto the tube wall at the front. There is no apparent sliding of liquid along the tube wall. This confirms the observations of West [17] and Yarnold [18] on the movement of mercury indexes in glass tubes. Similar observations showed that partly dyed droplets of high contact angle liquids on tilting plates of Teflon and polyethylene roll rather than slide, confirming the teachings of Frenkel [9] and others.

Publication Date: January 1, 1964 | doi: 10.1021/ba-1964-0043.ch017

The magnitude of contact angle hysteresis depends on the macroscopic roughness of the solid surface, and logical explanations of this effect have been presented by various investigators [15, 16]. It was therefore important in our study to make all measurements of critical pressure on surfaces of identical roughness. This was done by using single pieces of tubing, cleaning them thoroughly before introducing a new liquid, and checking them from time to time with a calibrating liquid (PEG 400). The tubes were also checked for uniformity along their length by placing the chaplets at varying locations and measuring the critical pressure. The variation was found to be within the limits of experimental error. The sections of tubing were chosen for uniformity of diameter and circularity of bore.

All liquids were checked to see that they did not swell, penetrate, or otherwise interact with the substrates. The liquids were chosen to provide a wide range of positive contact angles on the substrates. Most of the liquids were identical with those used on Teflon and polyethylene by Fox and Zisman [6, 8] in their studies of the critical surface tensions of solid surfaces.

When the minimum pressure necessary to move the boundary line $P_1 - P_2$ had been established, the critical line force was calculated as follows:

$$(P_1 - P_2)\pi r^2 = \text{force on chaplet} = f$$

$$\frac{f}{4\pi r n} = CLF$$

The quantity $4\pi r n$ where n is the number of indexes in the chaplet and r is the radius of the tube, is equal to the total length of boundary line in the system. To illustrate the significance of the critical line force, the data of Figure 2 have been replotted using force in dynes per centimeter of boundary line instead of pressure differential as the abscissa (Figure 4). The critical line force is then the value of the force at zero velocity and, unlike the pressure differential, is independent of the tube diameter. If there is any difference between the forces necessary to move the advancing and receding boundaries, at $A_1, A_2, \text{---} A_n$ and $R_1, R_2, \text{---} R_n$, respectively (Figure 1), it does not enter into this calculation. Although there is no *a priori* reason to believe that the two forces are different, it should be borne in mind that the critical line force determined by this procedure is an average of the force per unit length of advancing boundary and the force per unit length of receding boundary.

The experimental work thus consisted essentially in measuring the critical line force of several liquids in representative polyethylene and Teflon tubes. The surface tension of each liquid was checked with a du Noüy tensiometer and the equilibrium contact angles on both polyethylene and Teflon were determined using the method and instrument described by Zisman *et al.* [1, 6, 8]. Plots of surface tension (γ_{LA}) *vs.* cosine of the equilibrium contact angle ($\cos \theta$) on both substrates (Figures 5 and 6) agree well with the data of Zisman and Fox, being linear on polyethylene and showing a slight departure from linearity on Teflon [7]. The critical surface tensions for wetting (plus or minus one standard error of estimate, $\bar{S}_{yx}$) were found to be 31.1 (± 3.7) for polyethylene and 18.5 (± 2.5) for Teflon.

Publication Date: January 1, 1964 | doi: 10.1021/ba-1964-0043.ch017

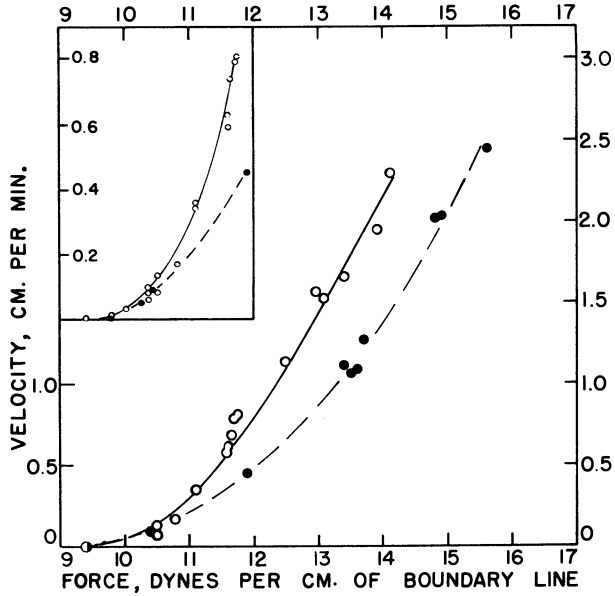

Figure 4. Velocity of advancing front vs. force acting at PEG 400 – air - Teflon line

Chaplets of 10 indexes in Teflon capillaries
● 0.0624-cm. i.d.
O 0.0378-cm. i.d.
Additional points plotted in inset at expanded velocity scale

Materials and Methods

The polyethylene (PE) and Teflon capillary tubes used in these studies were obtained from commercial sources. Teflon spaghetti tubing and polyethylene medical tubing were obtained in several sizes between 11 and 23 mils in nominal inside diameter. The tubing could be satisfactorily cleaned by connecting a length to an aspirator, drawing through it a volume of 95% ethanol equal to at least 50 times the volume of the tubing, and then drawing room air through the tube until it was dry. The cleaned length of tubing was checked for uniformity of inside diameter as follows:

A volume of liquid was introduced at one end of the tube from a microsyringe and then drawn several centimeters into the tube by means of suction applied at the other end. The length of this liquid index (usually chosen to be about 1 cm.) was measured, using a magnifier with a ruled stage, to an accuracy of ± 0.002 cm. The index was moved approximately its own length (by again applying suction) and remeasured. This was repeated until a section of tubing about 50 to 60 cm. long had been found in which the maximum and minimum measured index lengths differed by not more than 2%. The volume of liquid just sufficient to fill 50.0 cm. of this selected length of tubing was determined (to the nearest 0.0001 cc.) using the microsyringe and the average inside diameter of the tubing was calculated. For the critical line

Publication Date: January 1, 1964 | doi: 10.1021/ba-1964-0043.ch017

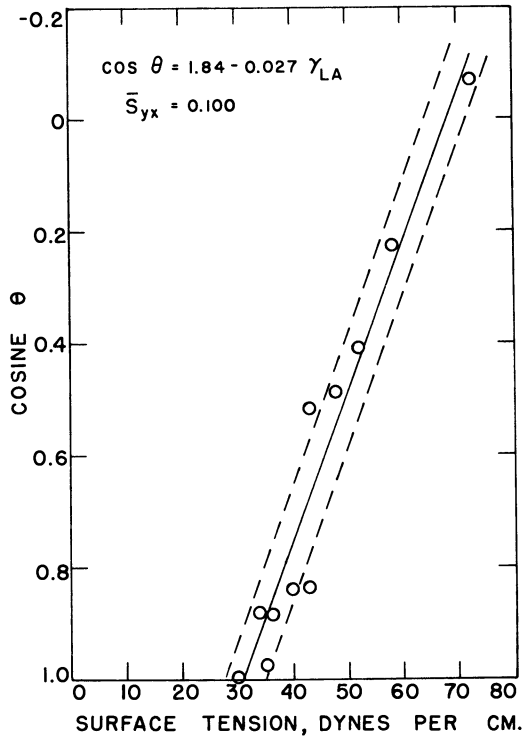

Figure 5. Surface tension vs. cosine of equilibrium contact angle for liquids on polyethylene

force determinations reported herein a piece of Teflon tubing with an inside diameter of 0.0378 ± 0.0005 cm. and a piece of polyethylene tubing with an inside diameter of 0.0364 ± 0.0005 cm. were used.

The liquids were obtained from commercial sources and purified by percolating through Florisil, alumina, or silica gel. The high-boiling liquids were stripped of volatile impurities. The surface tension of each liquid was carefully measured by the ring method, using the correction tables of Harkins and Jordan [12] and Fox and Chrisman [5]. The equilibrium contact angles of the liquids were measured on clean, smooth Teflon and polyethylene surfaces prepared by the heating and pressing techniques described by Fox and Zisman [6, 8].

All measurements were made in a constant-temperature room held at 25° C. and 50% RH. The measured contact angles and surface tensions are given in Table I.

The Apparatus. The apparatus, shown schematically in Figure 7, is designed to move the chaplet in either direction by applying a measured pressure at either end and maintaining the other end at atmospheric pressure.

With stopcock B closed, water can be added dropwise at A to increase the driving pressure in the system. Driving pressure can be

Publication Date: January 1, 1964 | doi: 10.1021/ba-1964-0043.ch017

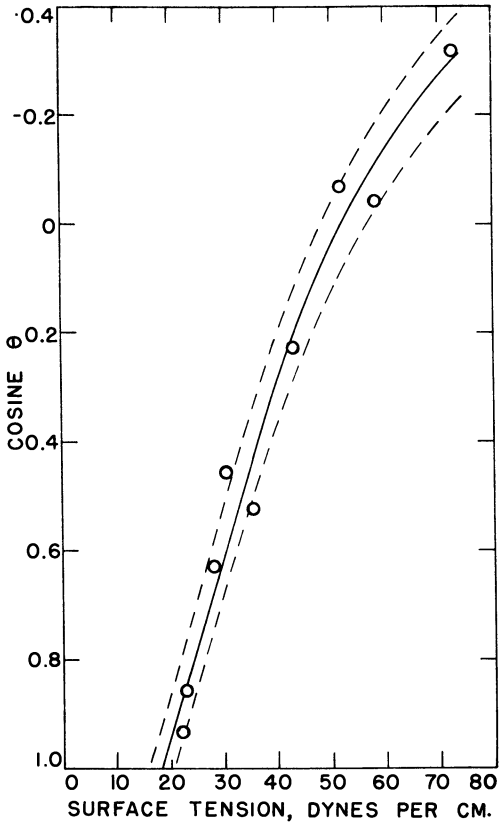

Figure 6. Surface tension vs. cosine of equilibrium contact angle for liquids on Teflon

Standard error of estimate $\bar{S}_{yf(x)} = 0.084$

decreased by closing A and letting water flow out of B. The three-way stopcocks, C and D, allow either end of the capillary tube, T, to be connected to the ballast flask, F, or to be open to the atmosphere.

For ease of handling, T is permanently fastened on a rigid metal scale ruled in millimeters. The capillary tube assembly is mounted on a leveled vibration-free table. Glass tubing is used as much as possible for all connections. Short pieces of Tygon tubing are used at E_1 and E_2, the syringe needles used as connections to the capillary tube.

Procedure for Loading a Chaplet of Liquid Indexes into Capillary Tube. A volume of water was introduced into the separatory funnel, S, and stopcocks A and B were closed. C and D were then opened, so that the system was at room pressure. One end of the cleaned capillary tube was connected at E_1 and C was turned so that E_1 was connected to F. D was then closed. A small volume of liquid was then introduced at the unconnected end of the capillary from a microsyringe. The system

Publication Date: January 1, 1964 | doi: 10.1021/ba-1964-0043.ch017

Table I. Surface Tensions of Test Liquids and Contact Angles on Teflon and Polyethylene

Liquid	Surface Tension, Dynes/Cm.	Contact Angle, Degrees	
		On Teflon	On polyethylene
Water	72.3	108.5	94
Formamide	58.2	92.5	77
1,2,6-Hexanetriol	51.8	94	66
Ethylene glycol	47.7	--	61
Polyethylene glycol 400	43.1	77	59
1-Bromonaphthalene	42.9	--	33.5
Tricresyl phosphate	39.8	--	33
m-Cresol	36.3	--	28
Hexachlorobutadiene	35.3	58.5	13
Tergitol TP-9[a]	33.9	--	28.5
Di(2-ethylhexyl)adipate	30.6	63	--
Di(2-ethylhexyl)phthalate	30.0	--	4.5
Heptanoic acid	27.9	51	Spreads
Di-n-butyl ether	22.8	31	Spreads
1H,1H, 7H-dodecafluoro-1-heptanol	22.1	21	Spreads

[a]Nonyl phenyl polyethylene glycol ether containing 9 moles of ethylene oxide (Union Carbide Chemicals Co.).

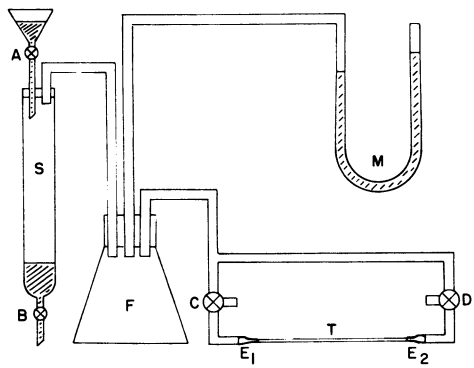

Figure 7. Apparatus for measuring critical line force

A. Water inlet stopcock
B. Water outlet stopcock
C, D. Three-way stopcocks
E_1, E_2. Blunt-end hypodermic syringe needles
F. 2-liter ballast flask
M. Water manometer
S. Separatory funnel
T. Capillary tube

pressure was decreased (by letting water out of B) until this liquid index began moving slowly into the tube. When the slowly moving index had moved in about 0.5 cm., a second index of liquid was introduced from the microsyringe; care was taken not to plug the end of the capillary with the tip of the dispensing syringe. Succeeding indexes were loaded in the same manner until the desired number had been obtained.

As the number of indexes increased, additional amounts of water had to be let out of B in order to reduce the pressure sufficiently to keep the chaplet moving. After the chaplet had been loaded, the system was restored to room pressure and the free end of T was connected at E_2. A pressure differential, $P_1 - P_2$, was established across the chaplet by adding water at A and turning C and D as desired. $P_1 - P_2$ was read on the water manometer, M. The velocity of the front at the low pressure (P_2) side was measured as a function of $P_1 - P_2$. Replicate velocity measurements were made at various places in the tube and with the chaplet advancing in both directions. Low velocities (less than 0.1 cm. per minute) were measured with the aid of a Filar eyepiece on a traveling microscope mounted over the tube. Under this magnification the distance traveled by the front could be measured to an accuracy of 10 microns. The velocity was recorded as zero when no advance was discernible in 30 minutes.

The CLF range (Table II) represents the difference between maximum $P_1 - P_2$ for zero velocity and minimum $P_1 - P_2$ for lowest measured finite velocity.

The number of indexes used in any system was chosen so that $P_1 - P_2$ necessary for motion was always greater than 10 cm. of water. Since the water manometer could be read to the nearest 0.1 cm., the $P_1 - P_2$ values have a precision of ± 2%.

The regression lines in Figures 5 and 8 were calculated by standard procedures [4]. The dashed lines in these figures were plotted at $\pm \bar{S}_{yx}$, the standard error of estimate adjusted for the number of points. The regression curve (best fit) in Figure 6 was judged to be of the form

$$y = k + f(x)$$

with three constants (parabolic). The index of determination is 95.8%, compared with 95.1% obtained with a linear regression plot for the points in Figure 6. The dashed lines in Figure 6 were plotted at $\pm \bar{S}_{yf(x)}$, the standard error of estimate.

Results and Discussion

Critical line force values for the various test liquids on both polyethylene and Teflon are shown in Table II. Plots of these values against cosine of the equilibrium contact angle, $\cos \theta_{equil}$, are shown in Figure 8. The relationship appears to be linear. Thus, the resistance of the boundary line to displacement increases linearly as the cosine of the equilibrium contact angle. In neither case does the regression line calculated from the average CLF values quite pass through the point CLF = 0; $\cos \theta_{equil} = 1$. It seems reasonable to assume on theoretical grounds, however, that CLF will be zero when the contact angle is zero, and a line adjusted to include this point is also shown. This line has the form

Publication Date: January 1, 1964 | doi: 10.1021/ba-1964-0043.ch017

Table II. CLF Values of Test

Liquid	Surface Tension, Dynes/Cm.
Water	72.3
Formamide	58.2
1,2,6-Hexanetriol	51.8
Ethylene glycol	47.7
Polyethylene glycol 400	43.1
Tricresyl phosphate	39.8
m-Cresol	36.3
Hexachlorobutadiene	35.3
Di(2-ethylhexyl) adipate	30.6
Heptanoic acid	27.9
Di-n-butyl ether	22.8
1H, 1H, 7H-dodecafluoro-1-heptanol	22.1

$$CLF = k(1 - \cos \theta_{equil}) \quad (1)$$

The lines for both Teflon and polyethylene remain straight in the region where $\theta_{equil} > 90^\circ$ and $\cos \theta_{equil}$ is negative. The line for Teflon has the steeper slope of the two, and the higher value of k in Equation 1. The CLF values did not change when the direction of motion of the chaplets was reversed repeatedly, suggesting that the solid-air and solid-liquid interfaces achieved equilibrium rapidly.

The relationship between contact angle hysteresis and critical line force in this cylindrical tube system is easily derived from the geometry of the system and the Laplace equation for capillary pressure. It is

$$CLF = \frac{\gamma_{LA}}{2} (\cos \theta_R - \cos \theta_A) \quad (2)$$

where γ_{LA} is the surface tension of the liquid and θ_R and θ_A are the receding and advancing contact angles—i.e., the contact angles at the high and low pressure sides of an index, respectively. This relationship has been pointed out by Yarnold [18]. The quantity we call CLF is called F by Yarnold and is referred to as "a frictional force per unit length of the line of contact and acting at right angles to it, so as to oppose the motion of the liquid over the solid surface."

The relationship between contact angle hysteresis ($\theta_A - \theta_R$) and the equilibrium contact angle is shown in Figure 9. The equilibrium position of the menisci is shown in dotted lines. When the pressure differential, $P_R - P_A$, has increased to the critical point, the menisci are in the position shown by the solid lines but the line boundaries remain at RR' and AA'. A definite volume of liquid, V_R, has been transferred from the receding to the advancing end of the index, where it appears

Publication Date: January 1, 1964 | doi: 10.1021/ba-1964-0043.ch017

Liquids on Teflon and Polyethylene

Cos θ_{equil}		CLF, Dynes/Cm.	
On Teflon	On polyethylene	On Teflon	On polyethylene
-0.3173	-0.0698	13.6 −14.0	9.72−10.6
-0.0436	0.2250	11.8 −11.9	5.66− 6.33
-0.0698	0.4067	10.0 −10.6	5.04− 5.30
---	0.4848	---	2.27− 3.37
0.2250	0.5150	9.4 − 9.8	2.94− 3.38
---	0.8387	---	1.50− 1.64
---	0.8830	---	1.00− 1.11
0.5225	0.9744	6.2 − 6.6	---
0.4540	---	4.58 − 4.64	---
0.6293	Spreads	3.4 − 3.6	---
0.8572	Spreads	2.37 − 2.48	---
0.9336	Spreads	0.076− 0.185	---

as V_A. The functional relationship between V_R (= V_A) and the two cosine differences, (cos θ_R - cos θ_{equil}) and (cos θ_{equil} - cos θ_A), can be worked out by using the parametric equations for a cylindrical tube of radius r = 1.

$$\cos\theta = \frac{2h}{h^2 + 1} \tag{3}$$

$$V = \frac{\pi h^3}{6} + \frac{\pi h}{2} \tag{3a}$$

where h is the height and V the volume of the spherical segment bounded by the plane XX' (insert at left of Figure 9). Only when θ_{equil} is 90° are the cosine differences equal, and θ_{equil} midway between θ_R and θ_A. For all other values of θ_{equil} the cosine differences and the angle differences, (θ_{equil} - θ_R) and (θ_A - θ_{equil}), are unequal.

Using Equations 2, 3, and 3a and the experimentally determined relationships between γ_{LA} and cos θ_{equil} shown in Figures 5 and 6, we have calculated the relationship of CLF to (θ_A - θ_R) and to (cos θ_R - cos θ_A) (Figure 10 and Table III). For polyethylene, where the γ_{LA} *vs.* cos θ_{equil} relationship is linear, both (θ_A - θ_R) and (cos θ_R - cos θ_A) increase monotonically with increasing CLF. In the case of Teflon a similar relationship holds, up to the region where the curve of γ_{LA} *vs.* cos θ_{equil} becomes nonlinear—i.e., where CLF is less than 8 dynes per cm. If the linear relationship describing the lower portion of the curve

Publication Date: January 1, 1964 | doi: 10.1021/ba-1964-0043.ch017

$$\cos \theta_{equil} = 1.635 - 0.0344 \gamma_{LA}$$

is used over the whole range, both $(\theta_A - \theta_R)$ and $(\cos \theta_R - \cos \theta_A)$ increase continuously with CLF (indicated by the dashed lines in Figure 9), just as in the case of polyethylene. The quantitative relationship among θ_{equil}, θ_R, and θ_A is, of course, governed by the interdependency of θ_R and θ_A in this geometric configuration. In the system consisting of a

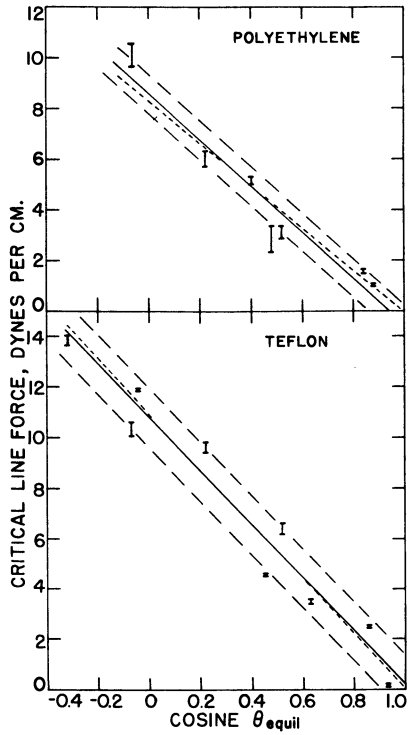

Figure 8. Critical line force vs. cosine of equilibrium contact angle for liquids on polyethylene (top) and Teflon (bottom)

Bars indicate CLF ranges
On polyethylene. CLF = 8.56 - 9.12 cos θ
$\overline{S}_{yx} = 0.86$
On Teflon. CLF = 10.64 - 10.41 cos θ
$\overline{S}_{yx} = 1.21$
Dotted lines adjusted to pass through CLF = 0, cos θ = 1
Equations for these lines are:
CLF = 8.35 - 8.35 cos θ, on polyethylene
CLF = 10.85 - 10.85 cos θ on Teflon

$$CLF = k (1 - \cos \theta_{equil}) \quad (1)$$

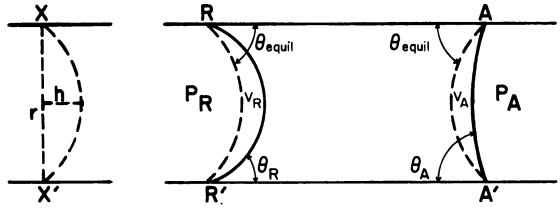

Figure 9. Relation of $\theta_A - \theta_R$ to θ_{equil} in tube of circular cross section

Table III. Relationship of CLF to Advancing and Receding Contact Angles in Teflon and Polyethylene Capillaries

Surface Tension, Dynes/Cm.	Teflon Capillary			Polyethylene Capillary		
	CLF	θ_A	θ_R	CLF	θ_A	θ_R
72.3	14.08	118° 47'	95° 17'	9.35	104° 12'	89° 20'
58.2	12.04	108° 07'	84° 06'	6.14	80° 53'	68° 19'
51.8	10.81	101° 51'	77° 46'	4.72	70° 09'	58° 33'
47.7	---	---	---	3.76	62° 12'	51° 23'
43.1	8.66	90° 28'	66° 48'	2.71	52° 35'	42° 50'
39.8	---	---	---	1.96	44° 39'	35° 54'
36.3	---	---	---	1.17	34° 25'	27° 11'
35.3	6.24	76° 37'	54° 12'	---	---	---
30.6	4.56	65° 34'	44° 39'	---	---	---
27.9	3.56	58° 13'	38° 33'	---	---	---
22.8	1.63	40° 06'	24° 46'	---	---	---
22.1	1.37	36° 46'	22° 20'	---	---	---

rolling (or "sliding") drop on a tilted plane θ_R and θ_A are also interdependent, but the functional form of the dependency is different. In the dipping plate system θ_A and θ_R are independent of each other. It should therefore be possible (provided θ_{equil} can be unambiguously determined) to determine whether or not $(\theta_{equil} - \theta_R) = (\theta_A - \theta_{equil})$ and whether CLF for an advancing boundary is the same as CLF for a receding boundary. This is currently being investigated.

Calculation of Advancing and Receding Contact Angles from Experimentally Determined Relationships among Surface Tension, Equilibrium Contact Angle, and Critical Line Force

To calculate θ_A and θ_R for one of our liquid-solid systems it is necessary first to determine θ_{equil} and $(\cos \theta_R - \cos \theta_A)$, the cosine hysteresis, in the capillary tube.

θ_{equil} is taken directly from Figure 5 or 6 for each test liquid (γ_{LA} is known).

To calculate the cosine hysteresis for each test liquid, it is necessary only to insert numerical values for CLF and γ_{LA} in Equation 2.

Publication Date: January 1, 1964 | doi: 10.1021/ba-1964-0043.ch017

$$CLF = \frac{\gamma_{LA}}{2} (\cos \theta_R - \cos \theta_A) \quad (2)$$

Both CLF and γ_{LA} are linearly related to $\cos \theta_{equil}$, as shown in Figures 5, 6, and 8. On polyethylene, over the entire range of γ_{LA}'s:

$$\cos \theta_{equil} = 1.84 - 0.027 \gamma_{LA} \quad (4)$$

and

$$CLF = 8.35 - 8.35 \cos \theta_{equil} \quad (5)$$

Therefore:

$$CLF = 8.35 - 8.35 (1.84 - 0.27 \gamma_{LA}) \quad (6)$$

Publication Date: January 1, 1964 | doi: 10.1021/ba-1964-0043.ch017

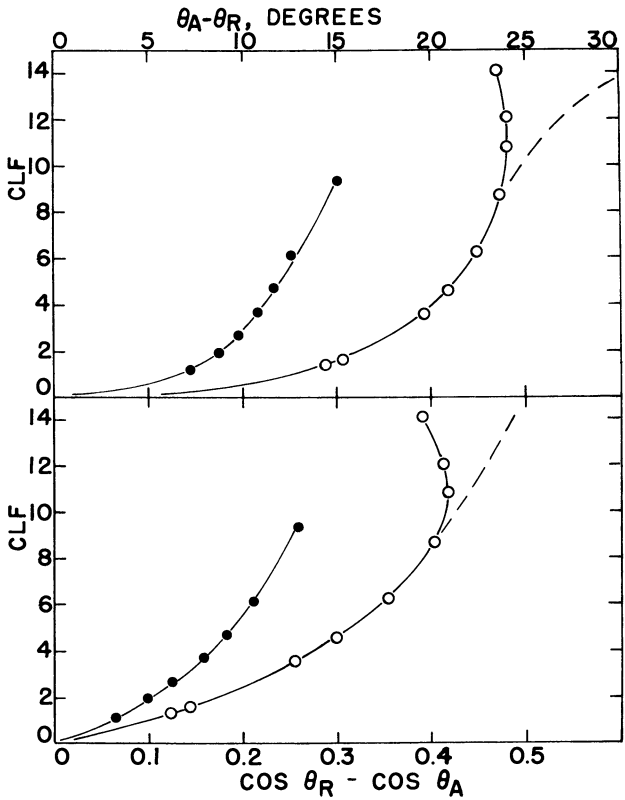

Figure 10. Relation of critical line force to contact angle hysteresis $\theta_A - \theta_R$ (top) and to $\cos \theta_R - \theta_A$ (bottom) for test liquids

● On polyethylene
O On Teflon

On Teflon, for $\gamma_{LA} < 40$ dynes per cm.:

$$\cos \theta_{equil} = 1.635 - 0.0344 \gamma_{LA} \quad (7)$$

and

$$CLF = 10.85 - 10.85 \cos \theta_{equil} \quad (8)$$

Therefore:

$$CLF = 10.85 - 10.85 (1.635 - 0.0344 \gamma_{LA}) \quad (9)$$

For $\gamma_{LA} > 40$ dynes per cm. on Teflon, $\cos \theta_{equil}$ is read on the line plotted in Figure 6, and this value is substituted in Equation 8 in order to determine CLF.

For water ($\gamma_{LA} = 72.3$ dynes per cm.) the cosine hysteresis on polyethylene is thus calculated as follows:

$$(\cos \theta_R - \cos \theta_A) = \frac{2 CLF}{\gamma_{LA}} = \frac{2[8.35 - 8.35 (1.84 - 0.27 \gamma_{LA})]}{\gamma_{LA}} = 0.2568$$

Referring to the insert at the left of Figure 9, for a tube of radius = 1, cos θ and V (the volume of the spherical segment bounded by the the plane XX') are related by:

$$\cos \theta = \frac{2h}{h^2 + 1} \quad (3)$$

$$V = \frac{\pi h^3}{6} + \frac{\pi h}{2} \quad (3a)$$

where h is the height of the spherical segment.

Cos θ and V can be calculated for values of h between 0 and 1 and a graph plotting cos θ *vs.* V can be constructed. (We actually plotted 41 points, taking h in increments of 0.025.) The resultant curved line increases from V = 0 at cos θ = 0 to V = 2.094 at cos θ = 1. For a given value of cos θ the corresponding V can be found on this curve.

To calculate θ_A and θ_R, knowing ($\cos \theta_R - \cos \theta_A$) and θ_{equil}, we start at the point on this V *vs.* cos θ line corresponding to $\cos \theta_{equil}$. The V intercept is V_{equil}. We then move equidistantly from this V_{equil} to $V_{equil} + \Delta V$ and $V_{equil} - \Delta V$ until the difference between the corresponding cosine θ intercepts is equal to the cosine hysteresis, calculated above. These two cosines are $\cos \theta_R$ (at $V_{equil} + \Delta V$) and $\cos \theta_A$ (at $V_{equil} - \Delta V$).

For example, for water on polyethylene, θ_{equil} is found to be 96° 54' ($\cos \theta_{equil} = -0.120$ at $\gamma_{LA} = 72.3$, from Figure 5). The corresponding V_{equil} is -0.094 (volume is taken as negative when θ is $>90°$). The cosine hysteresis is 0.2568, as calculated above. By moving to volumes of -0.197 (-0.094 -0.103) and +0.009 (-0.094 +0.103) we obtain values for cos θ of -0.2452 and +0.0116, whose difference is 0.2568, as desired. The volume of the segment at the advancing front, V_A, is -0.197 and the volume of the segment at the receding front V_R, is +0.009.

Publication Date: January 1, 1964 | doi: 10.1021/ba-1964-0043.ch017

$$\theta_A = \cos^{-1}(-0.2452) = 104^\circ\ 12'$$

and

$$\theta_R = \cos^{-1}(+0.0116) = 89^\circ\ 20'$$

Conclusions

Aside from their factual significance, the above findings shed some light on the causes of contact angle hysteresis. To avoid ambiguity we define this hysteresis as the maximum range of angle which the system can be made to assume without causing the line boundary to move. Thus, the advancing and receding angles may be regarded as incipient dynamic contact angles, and the hysteresis as the difference between the advancing and receding contact angles extrapolated to zero velocity [3]. One of the current hypotheses holds that the contact angle in any highly localized region of the liquid-solid-vapor boundary line has the thermodynamic equilibrium value given by Young's equation and that the surface roughness (localized inclination of the surface plane to the apparent macroscopic surface plane) is solely responsible for the apparent macroscopic hysteresis. It is understood in this argument that the radii of curvature of the irregularities are large compared to the molecular radii. It can be shown, using either the realistic model of Shuttleworth and Bailey [16] or the simplified model of Schwartz and Minor [15], that if this were the case the contact angle hysteresis ($\theta_A - \theta_R$) could increase with increasing θ_{equil} as well as with the degree of roughness. The value of ($\theta_A - \theta_R$) on all surfaces, however, would reach a maximum at $\theta_{equil} = 90^\circ$. Furthermore, systems of θ_{equil} close to zero could show a θ_A of nearly 90° on a surface of sufficient roughness. Our contact angle data are, of course, not gathered directly but are derived from our force measurements. Guastalla [11] has considered the effect of contact angle (θ_{equil}) on the force required to push a liquid-solid-air boundary past an idealized roughness asperity. His analysis indicates that the force reaches a maximum at $\theta_{equil} = 90^\circ$, and that a considerable force can be encountered, on a surface of sufficient roughness, even when θ_{equil} is close to zero.

Since we have shown that this is not the case, we conclude that roughness cannot be the sole cause of the CLF phenomenon or of contact angle hysteresis, although there is no question that it has an effect on the measured values of these quantities.

Literature Cited

(1) Bigelow, W. C., Pickett, D. L., Zisman, W. A., J. Colloid Sci. **1**, 513 (1946).
(2) Bouasse, H., "Capillarité, Phenomènes superficielles," p. 182, Delagraves, Paris, 1924.
(3) Elliott, G. E. P., Riddiford, A. C., Nature **195**, 795 (1962).
(4) Ezekiel, M., "Methods of Correlation Analysis," 2nd ed., Wiley, New York, 1941.
(5) Fox, H. W., Chrisman, C. H., Jr., J. Phys. Chem. **56**, 284 (1952).
(6) Fox, H. W., Zisman, W. A., J. Colloid Sci. **5**, 514 (1950).
(7) Ibid., **7**, 109 (1952).
(8) Ibid., p. 428.

Publication Date: January 1, 1964 | doi: 10.1021/ba-1964-0043.ch017

(9) Frenkel, Ya. I., J. Exptl. Theoret. Phys. (USSR) 18, 659 (1948).
(10) Furmidge, C. G. L., J. Colloid Sci. 17, 309 (1962).
(11) Guastalla, J., "Second International Congress of Surface Activity," Vol. III, p. 143, Academic Press, New York, 1957.
(12) Harkins, W. D., Jordan, H. F., J. Am. Chem. Soc. 52, 1751 (1930).
(13) Jamin, J., "Leçons sur les lois de l'équilibre et du mouvement des liquides dans les corps poreux," Paris, 1861.
(14) Rosano, H. L., "Contribution a l'Etude du Pouvoir Mouillant," Extrait du Memorial des Services chimiques de l'Etat, 1951, Fascicules 3 and 4, Tome XXXVI, Paris, 1953.
(15) Schwartz, A. M., Minor, F. W., J. Colloid Sci. 14, 584 (1959).
(16) Shuttleworth, R., Bailey, G. L. J., Discussions Faraday Soc. 1948 (No. 3), 16.
(17) West, G. D., Proc. Roy. Soc. (London) 86A, 20 (1911-12).
(18) Yarnold, G. D., Proc. Phys. Soc. (London) 50, 540 (1938).

Received March 25, 1963.

18

Coadsorption of n-Octadecane and Stearic Acid on Metal Surfaces

W. P. DOYLE AND A. H. ELLISON

Texaco Research Center
Beacon, N. Y.

Publication Date: January 1, 1964 | doi: 10.1021/ba-1964-0043.ch018

Radioisotopic tracer techniques were applied to study the coadsorption of n-octadecane and stearic acid on a metal surface immersed in a n-octadecane solution of stearic acid. Dual labeling was employed for determining the surface concentrations of both n-octadecane and stearic acid. n-Octadecane was labeled with tritium and stearic acid with carbon-14. The results of half-hour adsorption experiments provide direct proof of coadsorption of polar and nonpolar materials on iron, copper, silver, and platinum surfaces. The films produced on silver and copper by 19-hour adsorption consisted of approximately one molecular layer of stearic acid and two molecular layers of octadecane. A new model is proposed to describe the structure of this thick coadsorbed film.

The composition of the adsorbed film produced on a metal or metal oxide surface as a result of contact with a dilute solution of a long-chain polar solute in a long-chain nonpolar solvent has been the subject of several recent papers [1, 2, 4, 5]. All of these workers conclude that such films are not, as originally believed, monolayers consisting entirely of vertically oriented polar molecules but rather mixed monolayers containing major amounts of solvent coadsorbed with the polar solute.

Zisman and coworkers [2, 5], as a result of their contact potential and wetting angle measurements of films formed by octadecylamine-cetane adsorption, suggest that a mixed monolayer of polar and nonpolar molecules is in a nonequilibrium state and that with time the surface concentration of polar molecules increases and reaches 100%. On the other hand, Ries [4], in studies of the stearic acid-cetane adsorption on metals (oxide) and mica, finds that surface reactivity is a factor. Thus, after extended adsorption time the surface concentration of vertically oriented polar molecules was about 0.3 monolayer on unreactive surfaces and several monolayers on reactive surfaces.

In Contact Angle, Wettability, and Adhesion; Fowkes, F.;
Advances in Chemistry; American Chemical Society: Washington, DC, 1964.

While the concentration of polar molecules in these films has been determined directly by the tracer technique, no similar direct determination of solvent concentration has been carried out.

This work was undertaken, first of all, to measure directly by the radioactive tracer method the amount of n-octadecane solvent present in an adsorbed stearic acid film. It was also our desire to elucidate the structure of these coadsorbed films and determine the effect of adsorption time upon it.

Critical to work in this area is the ability to isolate these films from the generating solution. Zisman's [3] early work provided the "oleophobic" or "retraction" method for this purpose. The application of this method in this work yielded metal samples after adsorption having broad areas of oleophobic or dry surface. However, the few droplets of solution adhering to the area of surface to be counted and the larger amount of solution adhering to the edges and backs of metal samples, which would grossly contaminate the counting equipment, had to be removed by a solvent rinse before radioactive analysis could be carried out. This solvent rinse had little effect on the ability of the tracer technique to provide a clear answer to the main objective of the work.

Publication Date: January 1, 1964 | doi: 10.1021/ba-1964-0043.ch018

Experimental

Stearic acid-1-C^{14} was purchased from the Volk Radiochemical Corp. It was purified by paper chromatography and diluted with Eastman White Label stearic acid to a specific activity of 0.218 millicurie per millimole. Its purity was determined by isotopic dilution. n-Octadecane-1, 2-H^3 was prepared by low pressure hydrogenation of n-1-octadecene over Pd on asbestos, using tritium-labeled hydrogen. Except where noted, the n-octadecane was purified by percolation through silica gel prior to each adsorption experiment. The melting point of this product was 27.5-28°C. and its specific activity was 0.124 mc. per mmole.

The metal samples, 2 × 1 1/2 × 1/8 inches, were polished to a mirror finish on a polishing wheel covered with kitten-ear polishing cloth wet with a suspension of Linde alumina (Type B-5125). Each polished metal sample was covered with an evaporated film of the same metal (1000 A. thick) just prior to use. These films were hydrophillic, indicating the absence of organic contamination.

The purpose of depositing this metal film onto the metal substrate was to cover the alumina embedded in the metal substrate during the polishing operation. Electron diffraction patterns obtained from the metal surfaces showed that the surface was contaminated with alumina before the evaporation step and essentially pure metal after the evaporation. This technique would have shown up any contaminant present in the surface layer (100 A. deep) in excess of about 10%. It is acknowledged that a film of oxide is present on these surfaces.

In each experiment films were produced on two mirrors by immersing them for a measured time in a rectangular cell containing the solution of stearic acid-1-C^{14} (10^{-3} gram per ml.) in n-octadecane-1, 2-H^3. All adsorption studies were carried out at 40°C.

It was desired to produce surfaces comparable to those obtained by Bartell [1] and Zisman [2]—that is, dry films. However, in no case did we obtain a completely dry surface. After the mirrors had been in the

solution for a specified time they were removed and given a 5-second rinse with freshly percolated cyclohexane. Cyclohexane was chosen because its molecular structure was not similar to that of n-octadecane. It was believed that this dissimilarity would reduce the chance for exchange of the unlabeled molecules in the rinse solvent with labeled n-octadecane. The amounts of n-octadecane and stearic acid on the metal surface were then measured by radioactivity assay. Following this, the mirrors were given two additional 1-minute rinses with a good deal of agitation, and were counted after each rinse. The object of the rinses was to see how readily the adsorbed species were removed. In these rinsing procedures the same volume of solvent was always used and the time was closely controlled.

To simplify presentation of the data the values of the surface concentrations of n-octadecane and stearic acid on the duplicate mirrors were averaged. The standard deviation for the surface coverages by acid was 14%; for coverages by octadecane it was 7% after the 5-second rinses and 50% after the other two rinses. Although the 50% standard deviation appears large, the absolute error involved is small, since the surface coverage by octadecane was small after the second and third rinses.

A gas flow Geiger tube was used to count the C^{14} and H^3 radiation from the films. The radiation from C^{14} and H^3 can be distinguished because the energies of the beta-particles emitted in each case, and thus their penetrating powers, are different. C^{14} radiation was detected through a thin Mylar window on the Geiger tube. H^3 radiation does not penetrate this window. The window was removed to count the H^3 and C^{14} radiation combined. The net counting rate for H^3 radiation was obtained by subtracting the C^{14} counting rate (corrected for greater detection efficiency with the window removed) from the combined counting rate. The counting rates were measured to a standard deviation of 3%.

Blodgett monolayers of stearic acid-1-C^{14} and stearic acid-9, 10-H^3 had been previously prepared on silver, platinum, copper, and iron and counted in order to convert counting rate data to monolayers of stearic acid. To calculate surface coverage by n-octadecane it was assumed that vertically oriented n-octadecane molecules would occupy the same cross-sectional area as vertically oriented stearic acid molecules.

Results and Discussion

The first adsorption experiments furnished some interesting results regarding solvent purity. A stock solution of stearic acid-1-C^{14} in n-octadecane-1,2-H^3 was prepared using n-octadecane-1,2-H^3 which had been percolated through silica gel. Ten days later it was observed that the adsorption data did not reproduce the results obtained when the solution was new. Apparently the concentration of labeled polar-oxidation products of n-octadecane had built up during this period to a level where they contributed significantly to the composition of the adsorbed film. To check this point an adsorption experiment was conducted in which silver mirrors were placed for 19 hours in n-octadecane-1,2-H^3 containing no stearic acid. The date from this adsorption experiment, along with results of subsequent cyclohexane rinses, are shown in Table I.

Publication Date: January 1, 1964 | doi: 10.1021/ba-1964-0043.ch018

Table I. Adsorption of Polar Impurities from Stored Octadecane

Rinse Time, Seconds	Fraction of Monolayer of Octadecane-1, 2-H^3 Adsorbed	
	Fresh octadecane	Stored octadecane
5	0.3	0.5
65	0.1	0.4
125	0.0	0.3

Results of an identical adsorption experiment carried out immediately after the initial silica gel treatment of the n-octadecane-1,2-H^3 are included in Table I for comparison.

It is obvious that tritium-labeled polar impurities were formed in the stored solvent. On the basis of these results it was decided to conduct all subsequent adsorption experiments with solutions prepared not more than 2 days before. The authors are aware that experimenters in this field appreciate the general requirement for solvent purity in adsorption experiments. However, it was thought that these data should be presented to emphasize the special importance of solvent purity when studying coadsorption of solvent and solute by tracer techniques and to point out the relatively short time required for impurities to develop.

0.5-Hour Adsorption

In Table II the coverages in equivalent Blodgett layers are given for silver, platinum, copper, and iron samples following a 0.5-hour adsorption in the stearic acid–n-octadecane solution and the subsequent rinse steps. Given also are the coverages of n-octadecane on silver

Table II. Stearic Acid and Octadecane Concentrations in Films Produced by 0.5-Hour Adsorption at 40°C.
(Expressed as equivalent Blodgett monolayers)

	Rinse Time, Seconds	Metal				
		Silver		Platinum	Copper	Iron
		Solvent	Solution [a]			
n-Octadecane	5	0.3	1.2	1.3	0.9	0.4
Stearic acid		-	0.5	0.7	0.7	0.6
Total		0.3	1.7	2.0	1.6	1.0
n-Octadecane	65	0.1	0.2	0.1	0.2	0.2
Stearic acid		-	0.5	0.5	0.6	0.5
Total		0.1	0.7	0.6	0.8	0.7
n-Octadecane	125	0.0	0.0	0.0	0.1	0.1
Stearic acid		-	0.4	0.4	0.5	0.5
Total		0.0	0.4	0.4	0.6	0.6

[a] One sample.

Publication Date: January 1, 1964 | doi: 10.1021/ba-1964-0043.ch018

following a 19-hour adsorption in the pure solvent and the subsequent rinse steps. This run was made for reference, to show the efficiency with which this 5-second rinse removes excess liquid. In comparing these reference data with the data for acid-containing films, it is important to realize that the latter are oleophobic surfaces. Thus the excess liquid being removed consists of loosely adhering droplets which should be more easily removed than the liquid layer produced in the reference run.

It can be seen from Table II that the films remaining on all the metals after the 0.5-hour adsorption and 5-second rinse contain more n-octadecane than can be accounted for on the basis of incomplete removal of excess solution. This is taken to mean that n-octadecane is coadsorbed with stearic acid. The significant removal of n-octadecane by the second and third rinses, compared to the almost negligible removal of stearic acid, indicates that n-octadecane is rather weakly bound on the surface.

19-Hour Adsorption

The results, obtained in the 19-hour adsorption studies using silver and copper mirrors, are tabulated in Table III, with reference data from Table II.

These data provide the same evidence of coadsorbed but loosely bound n-octadecane as seen with the 0.5-hour films. The amounts of both acid and solvent after adsorption and 5-second rinse are, however, significantly greater in the 19-hour films. Higher coverages by solvent only might be attributed to poorer rinsing technique, but the higher coverages by both components must be attributed to increased adsorption of acid and solvent as a result of the longer adsorption time. That an increase in the adsorption of acid is accompanied by an increase in the amount of n-octadecane in the film is additional evidence of solvent coadsorption.

It is unlikely that the observed high total coverages of 3.2 and 3.6 equivalent Blodgett layers can be attributed to surface roughness. Polished surfaces of this type usually have roughness factors of about 1.5.

Table III. Stearic Acid and Octadecane Concentrations in Films Produced by 19-Hour Adsorption at 40°C.
(Expressed as equivalent Blodgett layers)

		Metal		
		Silver		Copper
	Rinse Time, Seconds	Solvent	Solution	
n-Octadecane	5	0.3	2.2	2.4
Stearic acid		-	1.0	1.2
Total		0.3	3.2	3.6
n-Octadecane	65	0.1	0.2	0.2
Stearic acid		-	0.8	1.0
Total		0.1	1.0	1.2
n-Octadecane	125	0.0	0.1	0.1
Stearic acid		-	0.7	0.9
Total		0.0	0.8	1.0

These considerations lead us to believe that these 19-hour films of adsorbed acid and coadsorbed solvent are multilayers. In view of the results with the 19-hour films, the higher than expected total coverages observed with most of the 0.5-hour films are understandable.

For a given adsorption time there was little variation in the amount of acid adsorbed on the different metals. With the 0.5-hour films there was significant variation in the amount of n-octadecane. It is believed that this solvent variation is a result of the difficulty inherent in performing the delicate task of removing by a short rinse all excess solution without removing the very loosely bound coadsorbed solvent.

Conclusions

A revised picture is needed to describe the structure of films composed of coadsorbed polar solute molecules and nonpolar solvent molecules. The close-packed model of Reis implies that the coadsorbed solvent should be relatively tightly bound. That this is apparently not the case is suggested by the ease with which the n-octadecane was removed from all the films. The data show that n-octadecane is more firmly attached to the surfaces on which stearic acid is adsorbed than to surfaces on which no acid is adsorbed. This means that the coadsorbed n-octadecane found is not present in the film as relatively large aggregates of randomly oriented solvent molecules on the surface. These aggregates, if they exist on the surface initially, should have been removed by the 5-second rinse. This is based on the fact that solvent was removed from the silver mirrors which had been immersed in pure n-octadecane containing no stearic acid.

In the case of the 19-hour adsorption studies one might picture these thick films as consisting of a mixture of randomly dispersed acid or soap and solvent. However, if this were true, the rinsing treatments should have removed large amounts of the acid or soap along with the solvent. This was not the case. The fact that large amounts of acid were not removed indicates that the acid is closely associated with the metal surface.

Therefore, we propose a model for coadsorption which is consistent with our results. In our picture of coadsorption nearly all the stearic acid is adsorbed at the metal surface. The rinsing data tend to bear this out. The larger size of the polar head than the hydrocarbon tail of stearic acid results in some space between the hydrocarbon tails of the acid molecules which can be penetrated by solvent molecules. These solvent molecules fit between the stearic acid molecules and are aligned with the hydrocarbon tail of the acid. However, in this picture of coadsorption it is assumed that the entire length of the solvent molecule does not associate with the hydrocarbon moiety of the acid. A portion of the solvent molecule extends beyond the hydrocarbon tail of the acid, and in turn acts as anchor for a second layer of solvent molecules. In this way several layers of solvent molecules could conceivably be built up on a monolayer of adsorbed stearic acid. The solvent molecules in these layers, as described, would tend to be oriented in the same way as the adsorbed acid--that is, vertical to the surface with methyl groups extending outward. If in the last layer out from the surface the hydrocarbon tails are drawn together by van der Waals forces, the result would be a low energy methyl group surface. This picture is consistent with the oleophobic nature of the films. Moreover, the fact that the

Publication Date: January 1, 1964 | doi: 10.1021/ba-1964-0043.ch018

n-octadecane molecules in this model would be available for association with the rinsing solvent accounts for the ease with which the solvent can be removed from the films.

It is our belief that the thick (a few monolayers) oleophobic films containing a volatile component observed by Bartell [1] in his studies of octadecylamine-cetane adsorption on metals are of the same type as observed in this work, the main difference being the lower volatility of n-octadecane than cetane.

The results reported in this paper support the conclusion of Zisman [2, 5] and others [1, 4], that films produced at comparatively short times contain both the polar solute and the nonpolar solvent, but that coadsorbed films are also formed at longer adsorption times. The proposed model describes the primary adsorbed layer next to the metal surface as consisting of nearly 100% adsorbed stearic acid at long adsorption times.

Literature Cited

(1) Bartell, L. S., Ruch, R. J., J. Phys. Chem. 60, 1231 (1956).
(2) Bewig, K. W., Zisman, W. A., Ibid., 67, 130 (1963).
(3) Bigelow, W. C., Pickett, D. L., Zisman, W. A., J. Colloid Sci. 1, 513 (1946).
(4) Cook, H. D., Ries, H. E., Jr., J. Phys. Chem. 63, 226 (1959).
(5) Levine, O., Zisman, W. A., Ibid., 61, 1188 (1957)

Received March 27, 1963.

Publication Date: January 1, 1964 | doi: 10.1021/ba-1964-0043.ch018

19

Electron Microscopic Investigation of the Adsorption of Long-Chain Fatty Acid Monolayers on Glass

L. O. BROCKWAY and R. L. JONES

University of Michigan
Ann Arbor, Mich.

Publication Date: January 1, 1964 | doi: 10.1021/ba-1964-0043.ch019

The formation of monolayers of cerotic, behenic, and stearic acids adsorbed from *cis*-decahydronaphthalene and *n*-hexadecane solutions onto glass was studied by electron microscopy. Platinum preshadowed carbon replicas of the monolayered glass surfaces were examined in a JEM 6-A electron microscope. The acids adsorb initially in discrete patches; the average patch diameter depends on the length of the acid molecule, becoming smaller for shorter acids. The area covered by the unimolecular film increases as the adsorption time or concentration of adsorbate solution increases. Contact angle measurements on partially monolayered surfaces show the contact angle to be dependent upon the fraction of substrate covered. Direct evidence of metastable incorporation of hexadecane in acid monolayers was obtained.

The unique wetting behavior of monolayers of long-chain polar molecules and the fundamental role of fatty acid films in boundary lubrication have led to numerous investigations of the structure of monomolecular layers adsorbed on solid substrates. In a series of studies designed to explain the peculiar wetting properties of these monolayers, Zisman and coworkers [7] established that the most plausible configuration of the adsorbed film is a closely packed array of molecules with the polar groups adsorbed at the solid surface and the hydrocarbon chains projected nearly normal to it in such a way that the outer surface of the monolayer is composed largely of CH_3 groups. They concluded that the outer surface determines the oleophobic and hydrophobic properties of the monolayer [22].

In Contact Angle, Wettability, and Adhesion; Fowkes, F.;
Advances in Chemistry; American Chemical Society: Washington, DC, 1964.

Bigelow and Brockway [6] used reflection electron diffraction and contact angle measurements in a study of the structure and wetting properties of progressively depleted monolayers of several long-chain fatty acids. The monolayers were adsorbed from *n*-hexadecane solution onto microscope slides. Depletion was accomplished by immersing the monolayered slides for varying periods of time in pure hexadecane. They observed that there was an upper limit to the angle of tilt assumed by the acid molecules, which increased from about 2° for behenic acid to approximately 8° for myristic acid. The maximum tilt observed for any one acid did not change with depletion, although the pattern intensity decreased, but it did change from one acid to another.

Epstein [13], who was working at the same time on an electron microscopic study of fatty acid films, postulated the existence of "micelles" in the unimolecular layer to explain the appearance of deposited acid layers; his theory was used to rationalize the molecular tilt observed by Bigelow. Epstein's basic assumption, which is the same as that used by Langmuir [18] in his treatment of stearic acid spread on water, is that the most stable arrangement of polar molecules in a monolayer occurs when the hydrocarbon chains of adjacent molecules are in intimate contact. Since the cross-sectional area of the carboxylic group is somewhat greater than that of the hydrocarbon chain, the implication is that the molecules must tilt toward one another, forming clumps of molecules which have been likened in homely analogy to corn shocks. With increasing size of the micelles the molecules in the outermost ring must show an increasing tilt, an increasing mismatch between the methylene groups in adjacent chains, and a decrease in the energy associated with intermolecular attractions. Accordingly, there will be a certain limiting tilt of the outer molecules and a limiting diameter of the micelles, beyond which it is energetically more feasible for molecules to take part in the formation of a new micelle. The limiting diameter for stearic acid was calculated to be about 100 A. A saturated monolayer then would presumably have a high density of micelles with nearly equal diameters. Incomplete monolayers where fewer polar molecules are adsorbed would ideally have micelles of about the same diameter as those in the saturated monolayer but now separated from one another by some distance. The diffraction patterns of depleted monolayers obtained by Bigelow [6], showing a decreased intensity but no change in basic form when compared to patterns from saturated monolayers, would be consistent with this scheme. Other electron diffraction investigations have given data which are compatible with the micelle theory (Karle [17], Chapman and Tabor [9]).

Ries and Kimball [21] have published micrographs of islands of vertically orientated acid molecules which occur at certain surface pressures in monolayers of fatty acids spread on water. Mathieson [20] examined electron micrographs of replicas of mica surfaces which had been dipped in dilute stearic acid-hexadecane solution; he observed that the stearic acid was present on the surface in patches which were of varying lateral extent but only 25 A. thick. He noted in some instances a tendency toward regular alignment of particles of the shadowing metal on the surface of the acid patches. Mathieson suggests these may indicate the presence of Epstein's micelles in the monolayer.

Publication Date: January 1, 1964 | doi: 10.1021/ba-1964-0043.ch019

This paper describes a systematic study by electron microscopy of adsorbed monolayers of long-chain fatty acids ranging from C_{14} to C_{26}. Improvements in replication techniques and the electron microscopes themselves since the time of Epstein's original work, as well as the successful applications of electron microscopy cited above, gave reason to believe that such an investigation would be a useful supplement to the previous experiments of Bigelow and Brockway in elucidating the structure of the adsorbed films.

Experimental Methods

Adsorbed films showing a smooth variation in contact angle measurements were prepared by dipping freshly cleaned microscope slides for appropriate periods of time into *cis*-decahydronaphthalene (Decalin) solutions containing the acid. Longer fatty acid molecules form stronger monolayers than the shorter members of the acid series, and their additional length should alleviate the problem of resolving the unimolecular film adsorbed on the glass surface. For this reason initial experimentation was begun with a high homolog (cerotic acid) of the fatty acid series. Replicas of slides were prepared and examined in the electron microscope. This process was repeated with acids lower in the homologous series until it became impossible to resolve the adsorbed acid structures. The group of experiments was then repeated using hexadecane as the solvent.

The fatty acids used—cerotic, behenic, stearic, and myristic—were donated by the Chemical Division, Procter and Gamble Co., and were reported at the time of their preparation to be at least 95% pure. The melting points of these acids taken just prior to our film-forming experiments were found to be within 1° to 2° of the literature values. Melting point depression is not an especially sensitive criterion for purity in long-chain fatty acids [10], but since the probable impurities are themselves saturated long-chain acids differing only in chain length, it was concluded that these acids were of sufficient purity for their intended use.

The solvents were *cis*-Decalin and *n*-hexadecane. The former was chosen because it has a bulky, nonlinear molecule not likely to be incorporated in the acid monolayers, high surface tension (32.18 dynes per cm. at 20°C.), relatively low volatility, and appropriate dissolving capacity for the acids used. The solvents were Eastman Kodak practical grade treated to remove adsorbable impurities. They were shaken with concentrated H_2SO_4 until no further discoloration of the organic layer occurred, washed with dilute NaOH, then with water, and finally dried over anhydrous $MgSO_4$. Just prior to their use the solvents were percolated through a column of activated alumina. Drops of the liquids so purified showed no tendency to spread on either strongly alkaline or strongly acidic water [25].

The methylene iodide used for the majority of contact angle measurements was Eastman Kodak White Label grade and was passed through columns of activated alumina before use.

The solutions used for monolayer preparation with their approximate concentration ranges are listed in Table I. Some of the more concentrated solutions approach or exceed the probable saturation

Publication Date: January 1, 1964 | doi: 10.1021/ba-1964-0043.ch019

Table I. Range of Concentrations of Fatty Acid Solutions Used for Monolayer Preparation

Acid	Molar Concentrations of Solutions	
	n-Hexadecane	cis-Decalin
Cerotic acid (C_{26})	$1 \times 10^{-4} - 1 \times 10^{-5}$	$1 \times 10^{-3} - 1 \times 10^{-5}$
Behenic acid (C_{22})	$1 \times 10^{-4} - 1 \times 10^{-5}$	$1 \times 10^{-3} - 1 \times 10^{-5}$
Stearic acid (C_{18})	$1 \times 10^{-3} - 1 \times 10^{-5}$	$1 \times 10^{-3} - 1 \times 10^{-5}$
Myristic acid (C_{14})	----	$1 \times 10^{-3} - 1 \times 10^{-5}$

point. No correction was made for adsorption of the solute on the walls of the container.

Premium grade microscope slides were chosen for use as the adsorbent substrate in these experiments, although glass surfaces are difficult to characterize because of their tendency to be hydrolyzed by water vapor in the atmosphere. Graphic proof of the hydrolysis of lime glass is given by Zarzycki and Mezard [24]; moreover, it has been reported that the adsorption of fatty acids is affected by the extent of surface hydrolysis, and tends to be less on glass surfaces treated so as to reduce the degree of hydrolysis [16]. The contact angle of high surface tension organic liquids on glass is finite in atmospheres where the relative humidity is not zero—e.g., $\theta = 35°$ for CH_2I_2 at approximately 30% relative humidity [19], and may become as large as 60° for CH_2I_2 at higher humidities [12].

Despite these shortcomings, glass has been employed successfully as a substrate by several workers [6,13,17], and the decision was made to use glass here, in order to correlate our experimental findings with those of the previous investigators. A standardized cleaning treatment and drying cycle (described below) were adopted to produce a "standardized" degree of surface hydration. Methylene iodide contact angles measured over a period of several months on the cleaned specimens fell within the range of 40° ± 5° with exceptions amounting to fewer than 1%, even though the humidity in the laboratory was not controlled. The agreement of these angles and the general reproducibility of fatty acid adsorption observed in this work were taken as indication that the cleaning method was adequate.

Methylene iodide contact angles were also measured on glass surfaces which had been immersed for increasing times in Decalin. Immersions of 5 to 10 minutes did not change the contact angle, but an increase in angle to 45° and to 49° was observed after immersion periods of 1 and 10 hours. An examination by electron microscopy of slide replicas revealed no consistent differences between glass surfaces which had been immersed in Decalin and those which had been only cleaned but not immersed, or those examined without cleaning or treatment in the solvent.

Propper Crown Brand microscope slides were scored and broken into pieces approximately 3.8 by 2.5 cm. These pieces were washed in detergent (Tide) and hot water, and then rinsed thoroughly in steaming doubly distilled water. While still wet, the pieces were stacked in weighing bottles in such a fashion that they remained standing upright without having their surfaces touch one another even when the bottles

Publication Date: January 1, 1964 | doi: 10.1021/ba-1964-0043.ch019

were gently shaken or tilted. Enough absolute ethanol was added to cover the stacked pieces. The weighing bottle and its contents were then treated in an ultrasonic cleaning apparatus for 5 minutes. The ethanol was replaced by reagent grade acetone, and the glass pieces were given two successive 5-minute treatments in fresh acetone. During this process, great care was exercised to avoid touching the slides with anything but glass tweezers. The weighing bottles complete with contents were placed in a grease-free oven, and dried 4 hours at 150°C.

The slides were removed from the hot oven just prior to use and attached by a stainless steel spring clamp to the end of a rod which had vertical movement by a rack and pinion mechanism. After a standard cooling period of 1 minute, the slide was run quickly down into the fatty acid solution until about two thirds of its length was immersed in the liquid. After the period of immersion, the slide was withdrawn from the solution as rapidly as possible while allowing good retraction of the solution; this usually required no more than 5 seconds. When short times of adsorption or very dilute concentrations were used, the slide emerged with a film of solution still on its surface. In some instances this film retracted within a few seconds of withdrawal as more acid molecules were adsorbed from the adhering solution. A rather arbitrary definition of wetted surface was adopted; if the solution did not retract from most of the slide's surface within 2 minutes while hanging vertically, it was described as "wetted."

A more quantitative criterion of the wetting tendency of the monolayered slides was obtained by contact angle measurements. Advancing contact angles were measured using the drop-on-plate method. Only drops having less than 0.5-mm. maximum diameter were measured to avoid the complication of gravitational distortion. Hexadecane was used initially, but later methylene iodide, which exhibits larger, easier to measure contact angles was employed. No provision was made to prevent dissolution of the monolayer in the contacting liquid. The contact angles were reproducible to ± 1° (50% confidence level).

Measurements were made at five locations on each specimen: one at the top on the untreated surface, and four at regular intervals across the slide at about the center of the monolayered section. Transversely located sites were chosen because the bottom of the slide is in the solution longest, and for short times of immersion the percentage difference between the adsorption time at the top edge of the monolayered area and at the bottom is not negligible. Surface migration of adsorbed molecules, at least for the time periods ordinarily involved here, was ruled out by comparing the "blank" contact angle measured on these specimens to contact angles measured on untreated slides.

Replicas of these slides were prepared immediately after the contact angle measurements were completed. Saturated monolayers were expected to be stable, but rearrangement in incomplete monolayers, or in monolayers incorporating appreciable amounts of solvent, was considered a definite possibility [2]. Just before the specimen was placed in the evaporator, a water suspension of polystyrene latex spheres of about 0.09-micron diameter was sprayed onto the monolayered surface with a nebulizer. The presence of a sphere in the micrograph allows quick differentiation between holes in a nearly complete film and islands of acid molecules rising above the substrate surface. The spheres

Publication Date: January 1, 1964 | doi: 10.1021/ba-1964-0043.ch019

are a convenient check of the magnification of a micrograph and also are used as a focusing aid in the examination of the replica.

Platinum is much used for shadow-casting because it is highly opaque to the electron beam and yields a finer grain when evaporated than the other heavy metals. The shadowing and replicating technique used in this study was devised by Cook [11] and involves the evaporation of platinum from a resistance-heated carbon rod. It is a convenient and economical method of producing platinum preshadowed carbon replicas, which is claimed by Cook to give shadowing grains smaller than 10 A. and replica resolution of better than 20 A. The shadowing angle was 30°, which gives a shadowing ratio of 1 to 2, and the distance from source to specimen was 12 cm.

The replicas were stripped from the monolayered glass surfaces by gradual immersion in dilute aqueous solutions of HF with the slide at an angle to the liquid surface. The stripped replicas were subsequently washed with distilled water and mounted on copper grids. Stripping was slower for the surfaces which were more wetted—i.e., the ones with fewer acid molecules adsorbed on their surface. From this, it is assumed that the fluoride attack is primarily upon the fatty acid.

A JEM 6-A electron microscope with accelerating voltages up to 100 kv. and capable of a demonstrable 10-A. resolution was used in this study. The instrument was routinely operated at something less than its maximum capabilities; although up to 200,000 × direct magnification was available, most micrographs were taken at 25,000 to 75,000 × and 80 kv.

The percentage of substrate surface covered by the adsorbed monolayer was determined by cross-hatching enlarged prints of micrographs of replicas of the monolayered surface and counting squares. Each replica was carefully scanned in the electron microscope to ensure that the micrograph taken was truly representative of the surface of the specimen. The precision of this method of measurement was estimated by taking micrographs of three different areas of the same replica and then determining the surface coverage in each micrograph. This was repeated with several different specimens of behenic and cerotic acid monolayers; a comparison of results indicates that the estimated probable error (50% confidence level) in a single given measurement is not greater than ± 3%. This method of measuring surface coverage was not practical for many of the specimens examined.

Experimental Results

A representative set of data is presented in Table II. The conditions of adsorption for the individual specimens have been included. Micrographs of these surfaces are shown in Figures 1 through 6.

The glass surfaces were smooth over large areas [8], and in the rare instances where scratches and abrasions did occur, monolayers of the cerotic and behenic acids continued uninterruptedly over a minor surface defect. Stearic acid structures were not observed to do this.

Reflection electron diffraction patterns from glass surfaces treated in hexadecane solutions of cerotic and stearic acids were obtained and compared with diffraction patterns taken by Bigelow [5] of monolayers of the same acids. The agreement was sufficient to conclude that the

Publication Date: January 1, 1964 | doi: 10.1021/ba-1964-0043.ch019

Table II. Contact Angles and Surface Coverage for Monolayers of Fatty Acids Adsorbed on Glass Surfaces (Representative Data)

	Time of Adsorption, Sec.	Molar Concn.	Contact Angle, °	Surface Coverage, %
cis-Decalin Solutions				
Cerotic acid				
CD-1	30	1×10^{-4}	46[a]	10
CD-2	15	1×10^{-3}	59	35
CD-3	30	1×10^{-3}	65	55
CD-4	3 min.	1×10^{-3}	71	95
Behenic acid				
BD-1	30	1×10^{-5}	50[a]	15
BD-2	1-1/2 min.	1×10^{-5}	55	20
BD-3	15	1×10^{-4}	59	30
BD-4	30	1×10^{-4}	65	80
Stearic acid				
SD-1	15	1×10^{-5}	48[a]	--
SD-2	30	1×10^{-5}	53	--
SD-3	30	1×10^{-4}	60	--
SD-4	1-1/2 min.	1×10^{-4}	64	--
n-Hexadecane Solutions				
Cerotic acid				
CH-1	1-1/2 min.	1×10^{-4}	22[b]	10
CH-2	15 min.	1×10^{-4}	29	35
CH-3	45 min.	1×10^{-4}	35	55
CH-4	32 hr.	1×10^{-4}	38	Multilayers
Behenic acid				
BH-1	10	5×10^{-5}	39[b]	--
BH-2	30	5×10^{-5}	41	--
BH-3	1 min.	5×10^{-5}	44	--
BH-4	1-1/2 min.	5×10^{-5}	45	--
Stearic acid				
SH-1	10	1×10^{-4}	56[a]	--
SH-2	30	1×10^{-4}	59	--
SH-3	1-1/2 min.	1×10^{-4}	63	--
SH-4	5 min.	1×10^{-4}	68	--

[a]Contact angle measurements using methylene iodide.
[b]Contact angle measurements using hexadecane.

monolayer structures in the present study are basically the same as those produced in Bigelow's experiments.

Cerotic Acid-*cis*-Decalin Series. The adsorbed clusters of cerotic acid in micrographs CD-1 through CD-3 (Figure 1) are about 30 A. thick as determined from the length of the shadow. Their lateral extent is easily estimated by comparison with the 900-A. polystyrene spheres. In micrograph CD-4 the structures observed are actually holes in an almost complete monolayer.

In this series, there is an approximately linear relation between the observed contact angle and the per cent surface coverage. While

Publication Date: January 1, 1964 | doi: 10.1021/ba-1964-0043.ch019

Publication Date: January 1, 1964 | doi: 10.1021/ba-1964-0043.ch019

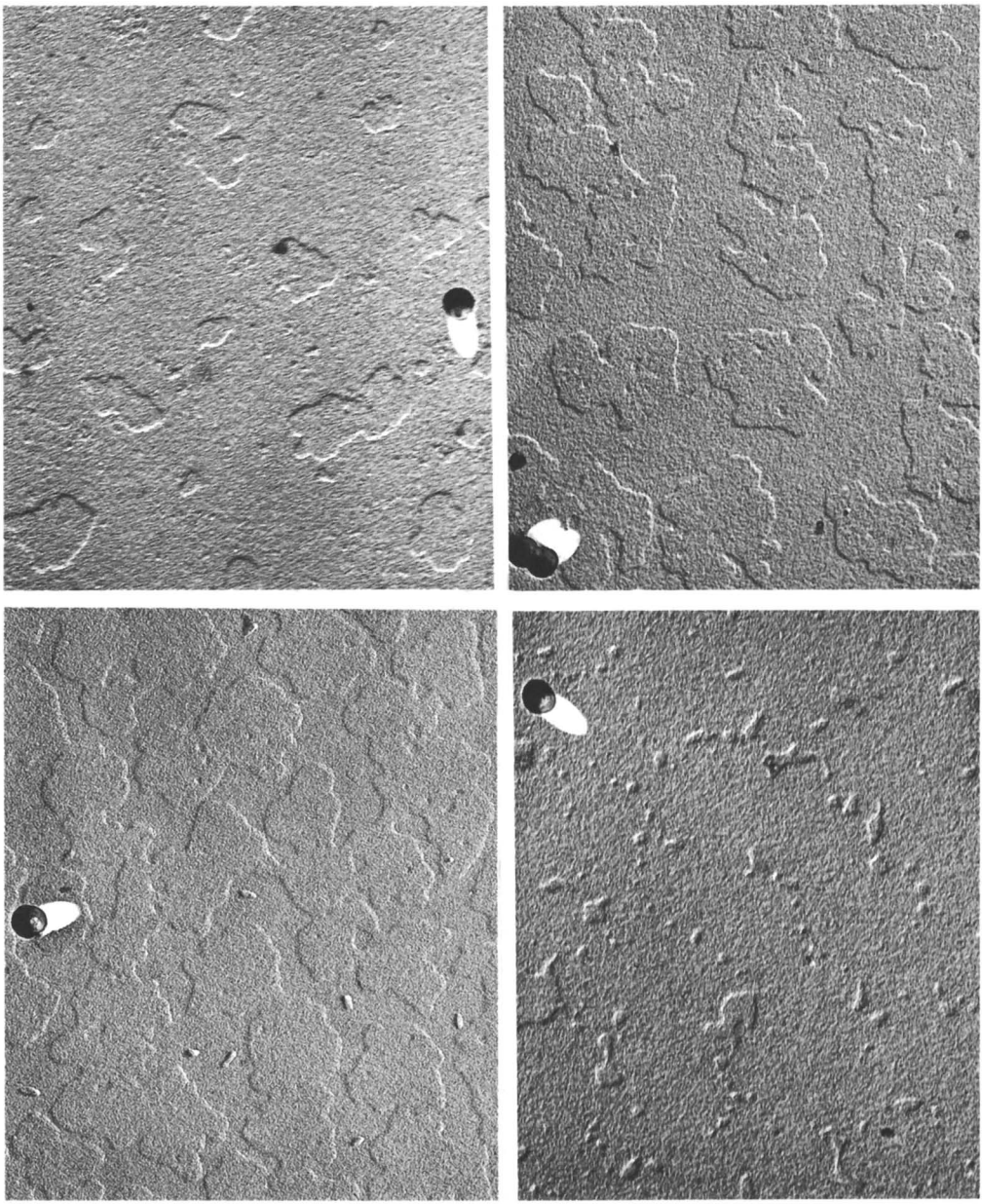

Figure 1. Cerotic acid adsorbed from Decalin (70,000 ×)

Upper left. CD-1. 30 sec. in 1×10^{-4}
Upper right. CD-2. 15 sec. in 1×10^{-3}
Lower left. CD-3. 30 sec. in 1×10^{-3}
Lower right. CD-4. 3 min. in 1×10^{-3}

In Contact Angle, Wettability, and Adhesion; Fowkes, F.;
Advances in Chemistry; American Chemical Society: Washington, DC, 1964.

clean glass is wetted by pure Decalin, specimen CD-1, which is covered by the acid monolayer over only 10% of its surface, is not wetted.

It had been anticipated that there might be a difference in the fine structure of the replica in the area of the adsorbed acid clusters compared to that of the bare glass substrate. Enlarged prints of the best micrographs of this series showed no variation of texture between these areas. When replicas of cleaved mica, which is thought to be structureless, were prepared by the technique used here, they had a similar fine texture; this suggests that the fine structure results from the shadowed replica itself and not from the actual surfaces of the monolayered slides.

Behenic Acid-*cis*-Decalin Series. Micrographs BD-1 through BD-4 (Figure 2) are similar to those of the previous series, except that the adsorbed acid clusters are definitely smaller. A comparison of BD-1 and BD-2 shows that there is some increase in the size of the islands in BD-2, but that there also is an increase in the number of islands of a given diameter. A linear relation between contact angle and per cent coverage is again noted with nonwetting by the solution occurring at low surface coverage.

Stearic Acid-*cis*-Decalin Series. The adsorption process of stearic acid from Decalin (Figure 3) is similar to that of the first two acids, with the trend being to still smaller average island diameters for the several stages of monolayer completion.

Myristic Acid-*cis*-Decalin Series. The micrographs in this series fail to show recognizable clusters of molecules, except in a single instance where clusters of 200-A. diameter could be detected, although contact angles were observed to increase regularly with increasing time of immersion in the solution.

The lack of clearly defined edges separating covered and uncovered portions of the surface probably indicates that the chain length of 14 carbon atoms is not enough to provide a good regular alignment of the molecules at the edges of the clusters, and the absence of shadows does not necessarily mean the absence of molecules.

Cerotic Acid-*n*-Hexadecane Series. For equivalent stages of completion, the diameters of the adsorbed acid patches in CH-1 through CH-3 (Figure 4) are somewhat larger than those observed for cerotic acid adsorbed from Decalin. Multilayers of cerotic acid were found for the first time in this study on specimen CH-4; scanning the replica shows that the substrate is covered by an essentially complete monolayer with multilayered structures scattered over this base film. Two holes in this monolayer as well as a part of a multilayered structure are shown in micrograph CH-4. Shadow length measurements indicate that the layered structure is made up of two molecular layers. In enlarged prints, a faint line demarcating the individual layers is visible in the shadow of the structure.

Contact angles for hexadecane on the partially monolayered slides increase linearly with the per cent surface coverage, but specimen CH-4, which is wholly covered by one or more layers of cerotic acid, gives a contact angle of 38° and not 44°, the angle for hexadecane on a saturated monolayer [6]. It has been previously reported [14] that slides immersed for a long time in fatty acid solutions become decreasingly oleophobic, and that crystals or multilayers are found upon the base monolayer, as is also noted here. If the contact angle decrease

Publication Date: January 1, 1964 | doi: 10.1021/ba-1964-0043.ch019

Publication Date: January 1, 1964 | doi: 10.1021/ba-1964-0043.ch019

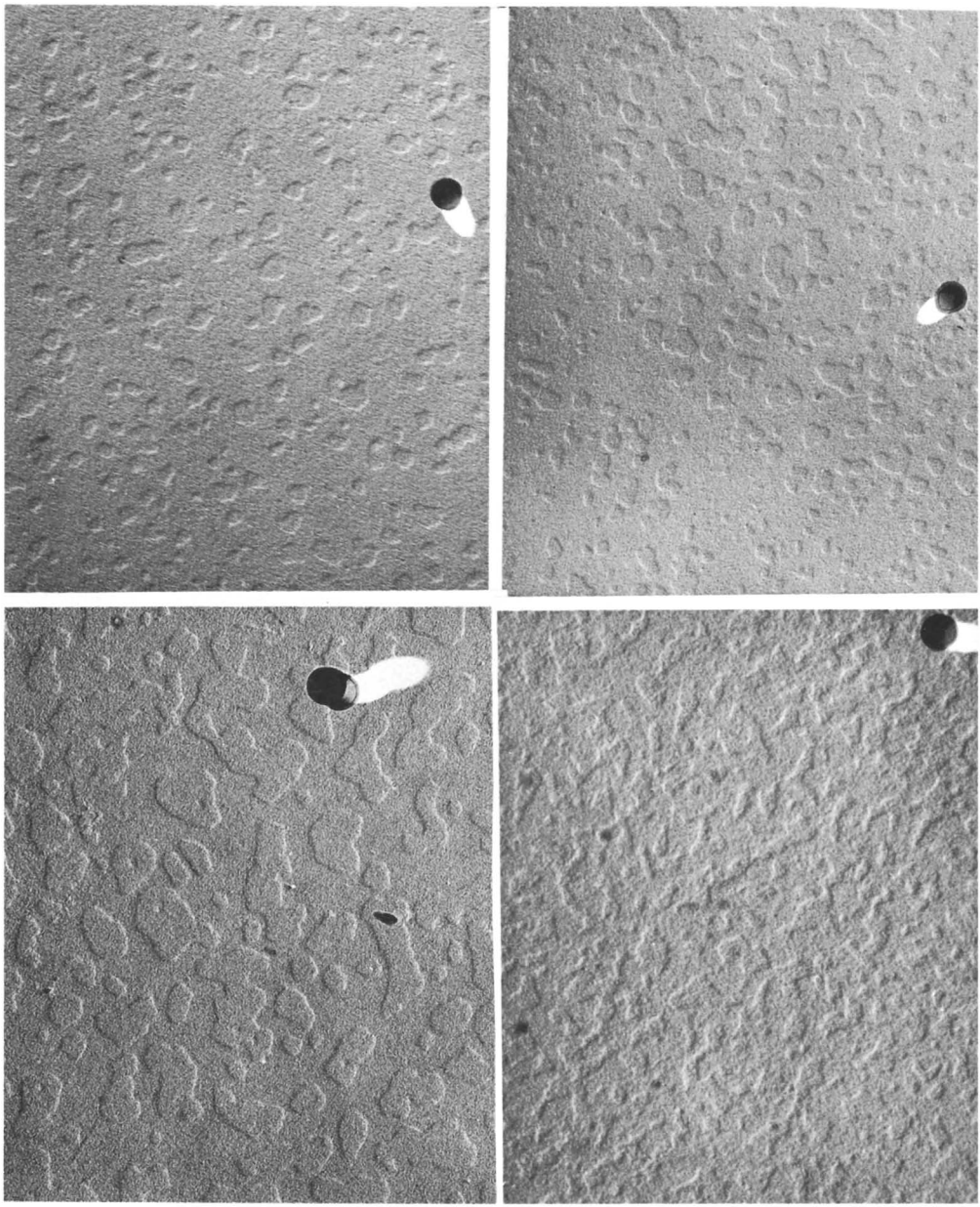

Figure 2. Behenic acid adsorbed from Decalin (70,000 ×)

Upper left. BD-1. 30 sec. in 1×10^{-5}
Upper right. BD-2. 1-1/2 min. in 1×10^{-5}
Lower left. BD-3. 15 sec. in 1×10^{-4}
Lower right. BD-4. 30 sec. in 1×10^{-4}

Publication Date: January 1, 1964 | doi: 10.1021/ba-1964-0043.ch019

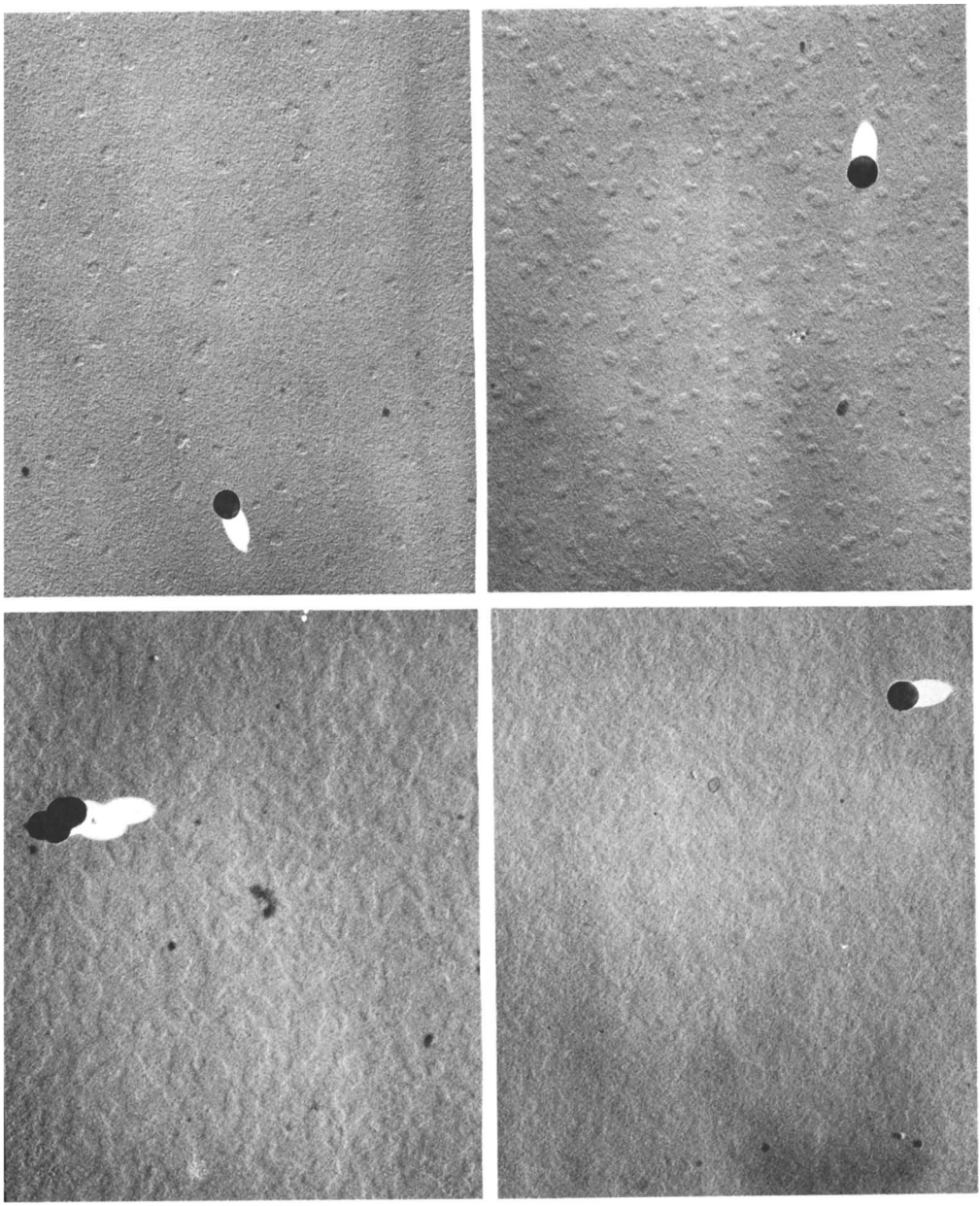

Figure 3. Stearic acid adsorbed from Decalin (70,000 ×)

Upper left. SD-1. 15 sec. in 1×10^{-5}
Upper right. SD-2. 30 sec. in 1×10^{-5}
Lower left. SD-3. 30 sec. in 1×10^{-4}
Lower right. SD-4. 1-1/2 min. in 1×10^{-4}

Publication Date: January 1, 1964 | doi: 10.1021/ba-1964-0043.ch019

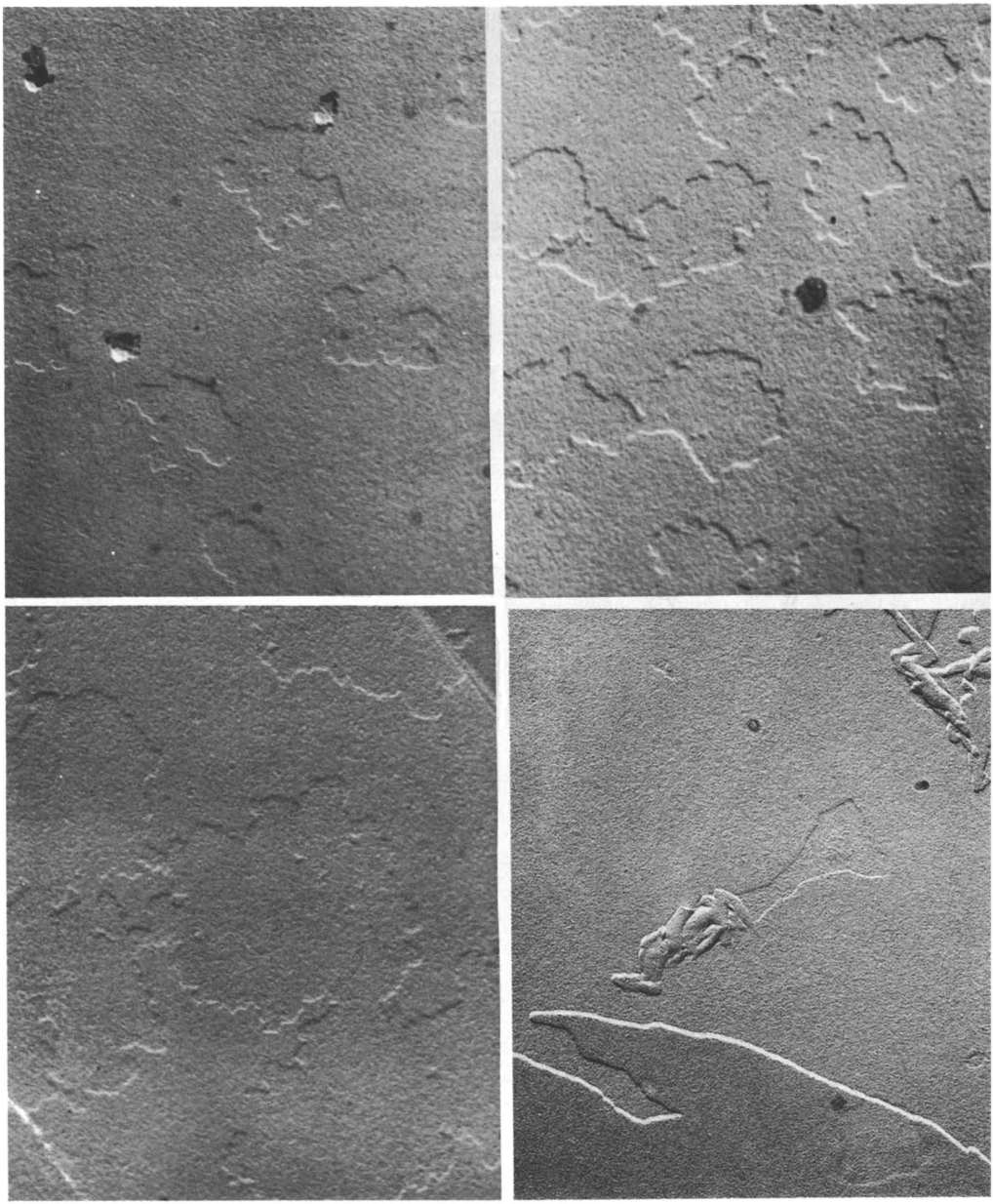

Figure 4. Cerotic acid adsorbed from hexadecane (35,000 ×)

Upper left. CH-1. 1-1/2 min. in 1×10^{-4}
Upper right. CH-2. 15 min. in 1×10^{-4}
Lower left. CH-3. 45 min. in 1×10^{-4}
Lower right. CH-4. 32 hours in 1×10^{-4}

with multilayer formation is explainable as a surface roughness effect only, the observed contact angle of 38° would correspond, applying Wenzel's equation [1], to a surface roughness factor of 1.1.

A faint cloudiness was noticed in the solution when specimen CH-4 was withdrawn after 32 hours' immersion, indicating that a 1×10^{-4} M solution of cerotic acid in hexadecane was actually slightly supersaturated at laboratory temperature. This suggested a short experiment to determine if multilayer formation is really an adsorption phenomenon and not just precipitation from a supersaturated solution. Cleaned slides were immersed for 60 hours in cerotic acid-hexadecane solutions of 1×10^{-6} through 3×10^{-4} M concentration. Contact angle measurements were made on these slides after withdrawal and their surfaces were examined by electron microscopy. A qualitative trend was found: Slides from very dilute solutions withdrew wetted and generally showed discrete acid patches of unimolecular thickness on their surfaces; slides from increasingly concentrated solutions gave increasing contact angles and showed increasing surface coverage by the monolayer until finally an essentially complete monolayer which exhibited a 70° contact angle with CH_2I_2 was adsorbed from the 3×10^{-5} M solution (approximately saturated); slides from saturated solutions showed multilayer configuration and exhibited contact angles less than 70°. There are not sufficient data from this single trial for a final conclusion, but the indication is that the acid solution must approach saturation before extensive multilayer formation will occur.

The rate of adsorption of cerotic acid was much slower from the hexadecane solutions than from the Decalin solutions; this decreased rate is probably at least partially due to the greater viscosity of hexadecane.

Behenic Acid-*n*-Hexadecane Series. The general pattern of the adsorbed acid in this series (Figure 5) can perhaps best be described as a monolayer with well-defined holes, which become smaller as adsorption continues. This structure is clearly shown in BH-3, where the holes at that stage of adsorption range from approximately 200 to 1000 A. in diameter. This mode of adsorption is opposite to that observed for all the preceding acid-solvent pairs, where the polar molecules adsorbed initially in patches which increased in size and perhaps number to form the complete monolayer. The small projections in BH-2 are thought to be from the substrate and not part of the acid structure, because similar projections were occasionally observed on untreated microscope slides.

Behenic acid adsorbs from hexadecane much more rapidly than cerotic acid, and the time required to form adsorbed films exhibiting high contact angles is much shorter. The increase in mobility of the acid molecules in the solution which results from shortening the molecule from C_{26} to C_{22} is not nearly large enough to cause this greatly increased adsorption rate, nor can it be explained in terms of relative concentration (c/c_{sat}), for the relative concentration of the behenic solution was less than half that of the cerotic acid solution. Both the adsorbed acid structure and anomalous adsorption rate are thought to be effects of solvent incorporation during the formation process.

Stearic Acid-*n*-Hexadecane Series. Micrographs of this series (Figure 6) show an adsorbed acid structure more like that found by Epstein than those of any other acid-solvent pair. The tiny clusters in

Publication Date: January 1, 1964 | doi: 10.1021/ba-1964-0043.ch019

Publication Date: January 1, 1964 | doi: 10.1021/ba-1964-0043.ch019

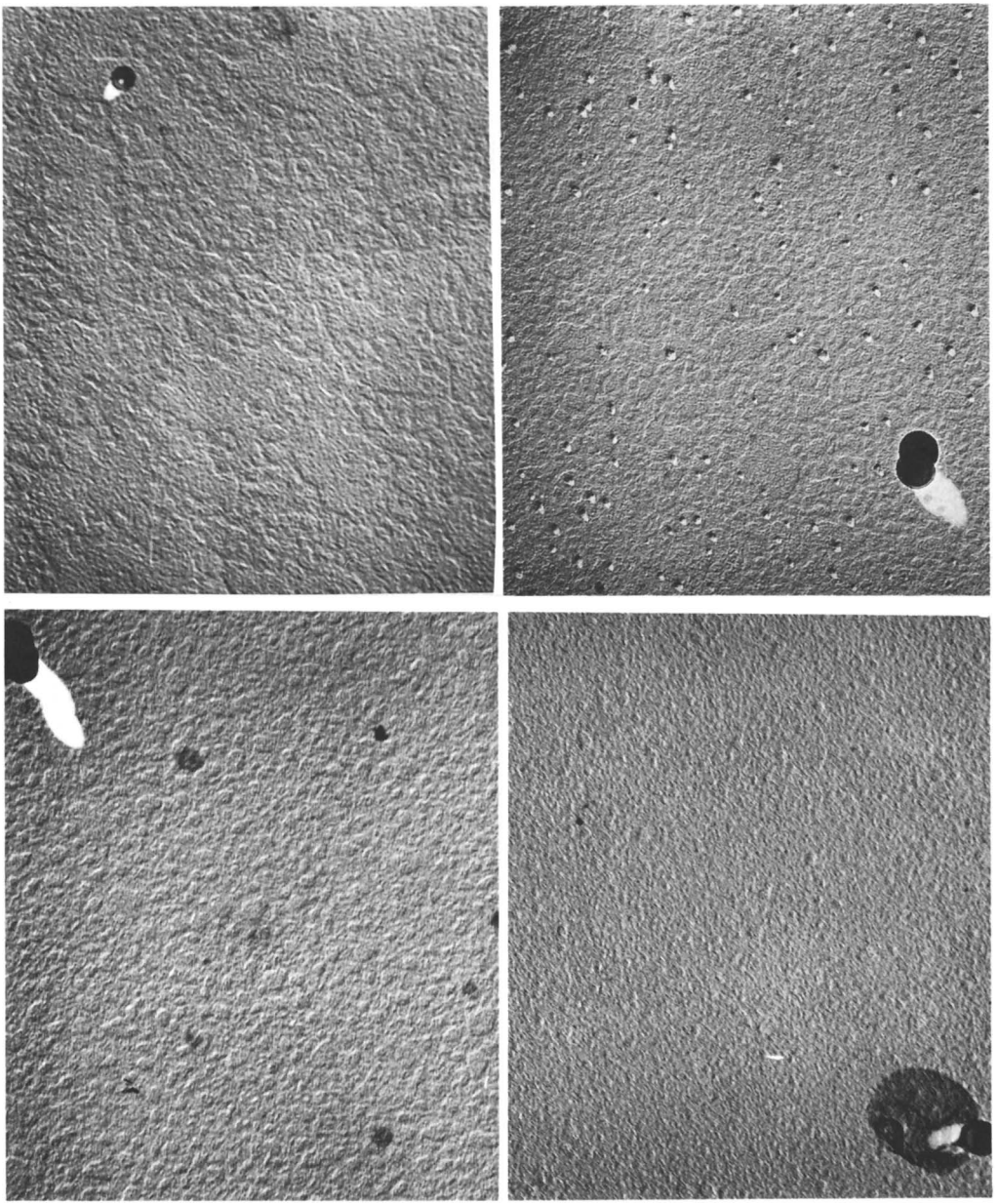

Figure 5. Behenic acid adsorbed from hexadecane (70,000 ×)

Upper left. BH-1. 10 sec. in 5×10^{-5}
Upper right. BH-2. 30 sec. in 5×10^{-5}
Lower left. BH-3. 1 min. in 5×10^{-5}
Lower right. BH-4. 1-1/2 min. in 5×10^{-5}

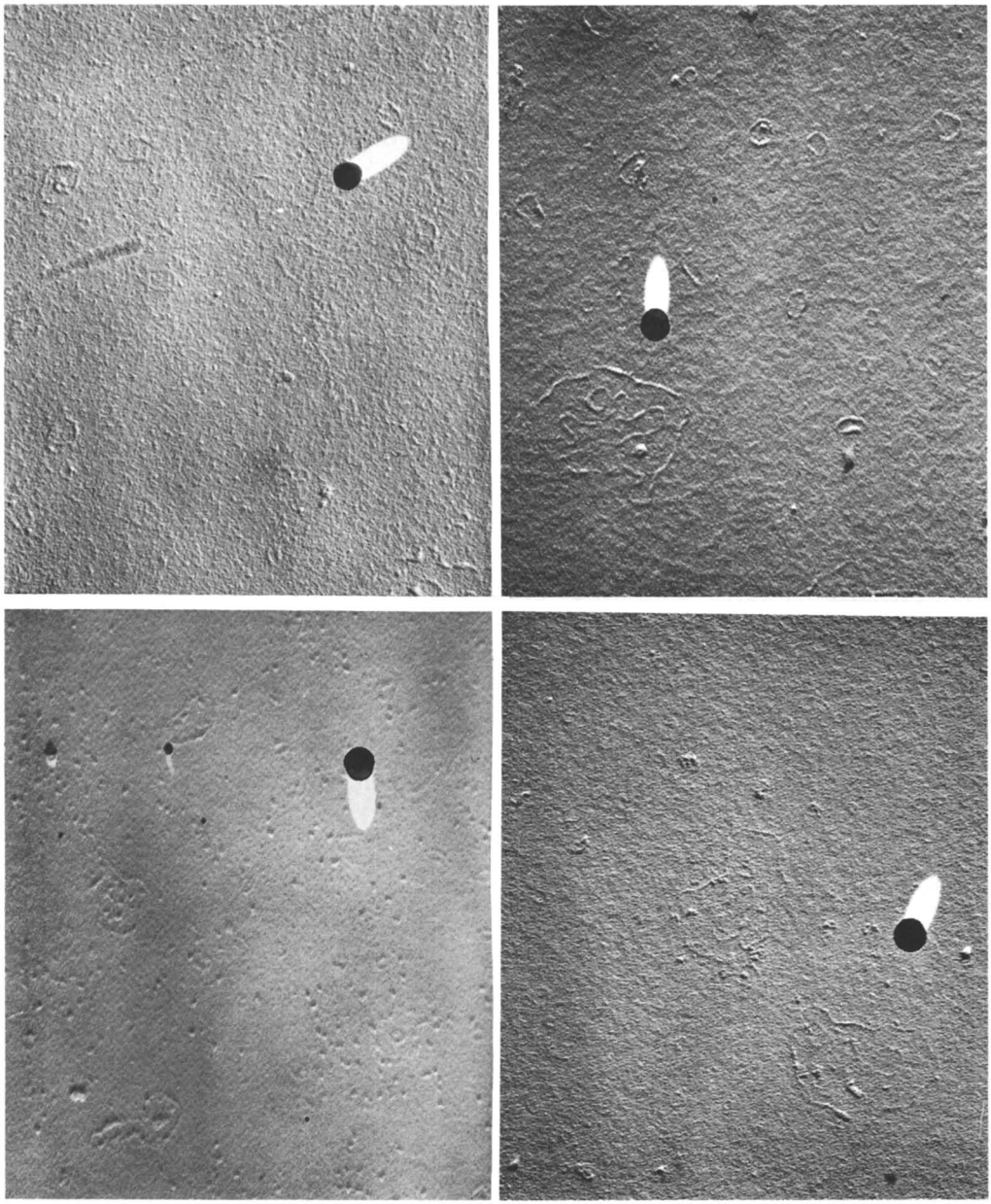

Figure 6. Stearic acid adsorbed from hexadecane (70,000 ×)

Upper left. SH-1. 10 sec. in 1×10^{-4}
Upper right. SH-2. 30 sec. in 1×10^{-4}
Lower left. SH-3. 1-1/2 min. in 1×10^{-4}
Lower right. SH-4. 5 min. in 1×10^{-4}

SH-1 are of about the same diameter and general appearance as his stearic acid micelles, except that here they are more sparsely scattered over the substrate surface; this may be because the monolayers examined by Epstein were saturated, while specimen SH-1 was only partially monolayered. Micrograph SH-4 taken from a more nearly saturated monolayer does not show an increased number of clusters per unit area, however, but instead the surface now seems to be largely covered by less well-defined, wider patches of adsorbed acid. The structure of adsorbed stearic acid in this series is not only dissimilar to that of the other acids, but it is also distinctly different from the structure of stearic acid adsorbed from hexadecane onto mica [20].

The contact angle of CH_2I_2 on the monolayered slides increases linearly as the times of adsorption become greater, but it is no longer possible to estimate surface coverage.

Discussion of Results

A review of the data presented above reveals:

From Decalin solutions, the acid molecules are adsorbed initially in discrete patches which with further adsorption increase in size and number in a fashion dependent on the chain length.

The patches or islands tend to be smaller and more numerous for the shorter acids at the same degree of surface coverage.

From hexadecane solutions, cerotic acid is initially adsorbed in patches or islands, while behenic acid is adsorbed in a network which encloses empty areas or holes; stearic acid initially forms molecular groups of about 100-A. diameter which tend to coalesce into filament-like structures.

In the cases where the fraction of surface area covered could be readily measured, the values showed a linear relation with the contact angle observed with either CH_2I_2 or hexadecane.

Multilayers of cerotic acid showing sharp terrace edges are produced from hexadecane solutions near the saturation point.

The behavior of the fatty acids when adsorbed from Decalin solutions agrees with Epstein's prediction of molecular clusters, although the observed sizes are much larger than predicted. Cerotic acid is able to form extended islands thousands of Angstroms in diameter, and even the islands of stearic acid are 5 to 10 times wider than the 100-A. diameter proposed for them. The trend to smaller islands as the acids become shorter is contrary to an expression derived by Epstein from binding energy considerations for micelles, $D \neq 4.5(18)^4/N^3$ (D = micelle diameter; N = number of carbon atoms in the molecule). The adsorbed acid patches from Decalin solutions do not represent the micelles proposed by Epstein. The possibility that small micelles exist unresolved within these islands has not been eliminated. In the stearic acid-Decalin films the number of islands per unit area increases with surface coverage while the size of the islands is more nearly constant. This result is consistent with Bigelow's observation [5] on the diffraction patterns from stearic acid films from hexadecane of a change in intensity with surface coverage while the shape and tilt of the layer lines remain unchanged.

Perhaps the most striking effect observed in this investigation was the markedly different modes of adsorption of behenic acid from Decalin

Publication Date: January 1, 1964 | doi: 10.1021/ba-1964-0043.ch019

solutions and from hexadecane solutions. Adsorption from Decalin forms initially distinct patches which grow and coalesce to complete the monolayer. When hexadecane is used, the first observable acid structure is a lacelike network of adsorbed molecules enclosing areas of bare substrate which may be as much as 1000 A. in diameter. As adsorption continues, the size of the holes found remaining in the monomolecular film becomes smaller.

Since hexadecane is an unbranched aliphatic hydrocarbon well suited for close alignment along the hydrocarbon chain of the acid molecules within the monolayer, and Decalin is a bulky molecule not suited for this alignment, this difference in capacity for incorporation of solvent molecules explains the difference between the behenic acid films adsorbed from the two solvents. When a sufficient number of behenic acid molecules are adsorbed, they become able to incorporate hexadecane in the monolayer, probably orienting the solvent molecules so that the monolayer exhibits a uniform surface of methyl groups. With longer immersion, the incorporated solvent is replaced by the more strongly adsorbed acid molecules. If the slide is withdrawn before all of the occluded hexadecane has been displaced, the solvent molecules will evaporate out of the monolayer during the replication process, leaving numerous holes. Micrographs BH-3 and BH-4 (Figure 5) show the decrease in the size of these holes as the adsorption times increase.

The suggested formation of a regular upper surface of exposed methyl groups even before the surface is largely covered with acid molecules would account for the rapid rise of contact angle with short immersion times observed for the behenic acid films from hexadecane.

The formation of discrete islands in all of the films from Decalin and in the cerotic acid from hexadecane indicates little solvent incorporation in these films. The increasing tendency toward solvent incorporation suggested for behenic and stearic acid from hexadecane is in agreement with the Bewig and Zisman statement [4] that "adlineation of the solvent is most marked" when the solvent and solute chains are the same length.

Although the appearance of the behenic acid-hexadecane films suggests that the solvent is occluded in aggregates which may be so large as to contain several hundred molecules, this may not be so, for it would imply some sort of very long-range orienting influence on the part of the adsorbed acid. The mechanism of this influence and the reason for its strong dependence upon the relative lengths of the hydrocarbon chains of acid and solvent are difficult to conceive. It is perhaps more plausible that the solvent molecules are entrapped singularly or in small clusters in the monolayer, and that the structures observed here are formed by surface mobile acid molecules as the solvent is pumped out during the replication process.

In Figure 7, some contact angles measured in the several series of experiments have been plotted against the percentages of substrate surface covered. The angles exhibited by methylene iodide and hexadecane on the partially monolayered surfaces fall near straight lines, and an extrapolation of those lines to 0% coverage yields θ_0 values which are close to our observations of contact angles on bare glass. A graph very similar to Figure 7 has been published by Gaines [15], who studied the variation of CH_2I_2 contact angles on fractional monolayers of radioactive stearic acid deposited on several substrates. His data

Publication Date: January 1, 1964 | doi: 10.1021/ba-1964-0043.ch019

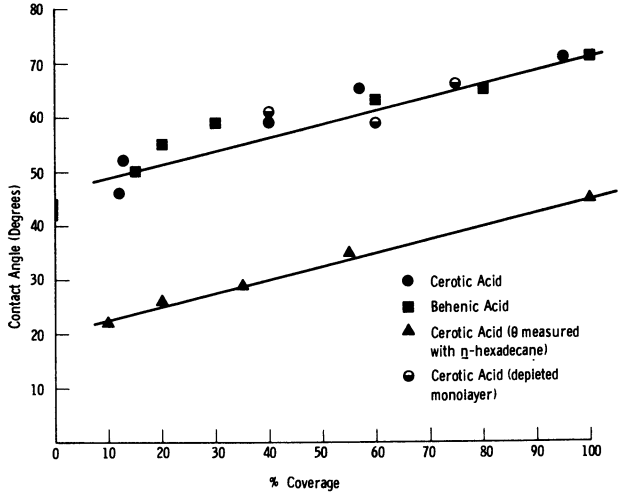

Figure 7. Relation of contact angle to surface coverage

extrapolate to a contact angle of about 40° for zero coverage also, although the partial films in this case were upon chromium, platinum, and mica substrates, and not glass.

The estimated probable errors (50% confidence level) involved in these measurements are rather large, ± 3% for per cent coverage, and ± 1° for contact angles. The fit of the data from the cerotic acid-hexadecane series is appreciably better than that for the Decalin solutions. The reason for this is not known, but it may be because the acid patches formed by cerotic acid adsorbed from hexadecane are larger than the islands from any other solute-solvent combination.

Shafrin and Zisman [23] derived a relation between X and the cosines of the contact angles—i.e., $X = (\cos \theta_x - \cos \theta_0)/(\cos \theta_1 - \cos \theta_0)$, where X is the per cent coverage, and $\cos \theta_x$, $\cos \theta_1$, and $\cos \theta_0$ are cosines of the contact angles exhibited on partially monolayered, completely monolayered, and bare substrates, respectively. The linearity between $\cos \theta$ and X proposed here cannot be distinguished on the basis of the present data from the linearity between θ and X shown in Figure 7. Over the respective ranges of θ for the two liquids used, the angle and its cosine show a linear variation with precision as good as the fit of our surface coverage data to a linear function of θ. Better control of temperature and humidity during substrate acid film preparation and contact angle measurements, and perhaps a choice of contacting liquid affording a greater range of θ from clean to fully covered surface, would be necessary for a test of the X *vs.* θ relation.

An experiment of interest here, because it represents another approach to the problem of quantitatively determining the degree to which the substrate is covered by the adsorbed polar molecule film, has been reported by Bartell and Ruch [2], who employed an ellipsometer to measure the average amount of adsorbed material per unit area. The ellipsometer was calibrated by comparison of the adsorbed films with

Publication Date: January 1, 1964 | doi: 10.1021/ba-1964-0043.ch019

Langmuir-Blodgett monolayers. Among the systems investigated by these workers were monolayers of *n*-octadecylamine adsorbed from hexadecane solutions onto slides cut from chromium-plated ferrotype plates. The amine films were depleted in benzene and contact angles with hexadecane measured and per cent depletions established for the several stages of depletion. In these experiments, the contact angle was observed to be little affected until the coverage was reduced to 40%, at which point the contact angle decreased sharply to zero. Later experiments [3] using contacting liquids of nearly the same surface tension as hexadecane but with bulky molecular structures show a more nearly linear decrease in the contact angle for lightly depleted monolayers, but the contact angle still approaches zero at about 60% depletion.

These results are different from those obtained in the present study. The reason for this discrepancy is not known, although it must lie in a difference between the systems observed or the methods used. The maximum contact angle reported for hexadecane on the octadecylamine film was 40° or about 5° less than reported here for hexadecane on complete films. It seems desirable to make ellipsometer observations on films for which electron micrographs have been obtained.

Acknowledgment

The authors gratefully acknowledge aid in these researches by an Esso Research and Engineering Co. fellowship to the junior author.

Literature Cited

(1) Adamson, A. W., "Physical Chemistry of Surfaces," 1st ed., p. 275, Interscience, New York, 1960.
(2) Bartell, L. S., Ruch, R. J., J. Phys. Chem. 60, 1231 (1956).
(3) Ibid., 63, 1045 (1959).
(4) Bewig, K. W., Zisman, W. A., Ibid., 67, 130 (1963).
(5) Bigelow, W. C., thesis, University of Michigan, 1951.
(6) Bigelow, W. C., Brockway, L. O., J. Colloid Sci. 11, 60 (1956).
(7) Bigelow, W. C., Pickett, D. L., Zisman, W. A., Ibid., 1, 513 (1946).
(8) Calbick, C. J., "1961 Transactions of Eighth Vacuum Symposium and Second International Congress," Pergamon Press, New York, 1962.
(9) Chapman, J. A., Tabor, D., Proc. Roy. Soc. A 242, 96 (1957).
(10) "Chemistry of Carbon Compounds, Aliphatic Compounds," Vol. IA, R. H. Rodd, ed., p. 577, Elsevier, New York, 1951.
(11) Cook, C. F., Jr., Rev. Sci. Instr. 33, No. 3, 359 (1962).
(12) Cottington, R. L., Levine, O., Zisman, W. A., "Effects of Adsorbed Water and Surface Roughness of Glasses of Various Compositions on the Friction and Wear Properties of Adsorbed Fatty Acid and Amine Monolayers," 134th Meeting, ACS, Chicago, III., September 1958.
(13) Epstein, H. T., J. Phys. Colloid Chem. 54, 1053 (1950).
(14) Epstein, H. T., thesis, p. 91, University of Michigan, 1949.
(15) Gaines, G. L., Jr., J. Colloid Sci. 15, 321-39 (1960).
(16) Hare, E. G., Zisman, W. A., J. Phys. Chem. 59, 335 (1955).
(17) Karle, J., J. Chem. Phys. 17, 500 (1949).
(18) Langmuir, I., Ibid., 1, 756 (1933).
(19) Levine, O., Zisman, W. A., J. Phys. Chem. 61, 1068 (1957).
(20) Mathieson, R. T., Nature 183, 1803 (1959).
(21) Ries, H. E., Jr., Kimball, W. A., Ibid., 181, 901 (1958).
(22) Shafrin, E. G., Zisman, W. A., J. Phys. Chem. 64, 519 (1960).

Publication Date: January 1, 1964 | doi: 10.1021/ba-1964-0043.ch019

(23) Shafrin, E. G., Zisman. W. A., "Monomolecular Layers," p. 129, H. Sobotka, ed., AAAS Symposium Publication, Washington, D. C., 1954.
(24) Zarzycki, J., Mezard, R., Phys. Chem. Glasses **3**, 163 (1962).
(25) Zisman, W. A., J. Chem. Phys. **9**, 789 (1941).

Received April 1, 1963.

20

Direct Measurement of Adsorption of Radiostearic Acid onto Vapor-Deposited Metal Films

Effect of Moisture

DONALD C. WALKER and HERMAN E. RIES, Jr.

Research and Development Department
American Oil Co., Whiting, Ind.

Publication Date: January 1, 1964 | doi: 10.1021/ba-1964-0043.ch020

Radiostearic acid was adsorbed from n-hexadecane onto mica and thin vapor-deposited films of iron, gold, and copper that had been exposed to dry and water-saturated helium or air. Adsorption was measured directly and continuously by a recently developed technique. The mica substrate showed essentially zero adsorption. None of the metals adsorbed more than one stable compact monolayer. Iron and gold showed a large difference in adsorption in dry helium or air, but adsorbed about the same amount, 0.2 to 0.5 monolayer, when exposed to either wet helium or air. Copper adsorbed 0.3 to 0.7 monolayer in all atmospheres except wet air, in which it showed a weak adsorption of nine monolayers; rinsing with hexane removed all but one monolayer.

In most techniques for studying adsorption on metals, uniform, clean, and reproducible metal surfaces are difficult to prepare and the adsorption process cannot be followed continuously [2, 3, 4, 7, 10, 11, 16, 18, 21]. Clean and reproducible metal surfaces are also difficult to prepare and maintain in methods that measure adsorption continuously and directly on a metal-coated window of a Geiger tube [1, 6, 7, 13]. A recently developed apparatus and technique provide controlled conditions for the production and maintenance of relatively clean metal films and the precise measurement of adsorption [20]. Metal is evaporated onto a mica window supported within a high-vacuum apparatus; adsorption onto the metal film is measured directly and continuously by a counter tube below the window.

Reported previously were results of the adsorption of radiostearic acid from dilute n-hexadecane solution onto the mica substrate and

In Contact Angle, Wettability, and Adhesion; Fowkes, F.;
Advances in Chemistry; American Chemical Society: Washington, DC, 1964.

100-A. films of iron, gold, and copper that had been exposed to purified dry helium or air [20]. Because the presence of moisture is important in many surface phenomena, corresponding experiments have been conducted in which the metal films were exposed to water-saturated helium or air.

Experimental

Radiostearic acid was adsorbed from a 0.0005 molal solution in n-hexadecane onto mica and 100-A. films of iron, gold, and copper that had been exposed 15 minutes to water-saturated helium or air. All experiments were conducted at 35.0° ± 0.2° C. Seventy hours was allowed for adsorption; duplicate determinations agreed within 0.03 monolayer.

Apparatus and Procedure. The metal films were deposited and adsorption thereon was carried out in a high-vacuum apparatus, as shown in Figure 1. The mica window was supported between two chambers that were evacuated simultaneously to prevent breakage; the window was coated by evaporating metal from a heated filament in the upper chamber. The gas was then admitted to both chambers until the pressure was 1 atm. Valve 3 was closed to isolate the upper chamber, the bottom plate was removed, and the counter tube was positioned under the window. After the film had been exposed 15 minutes to the gas, the solution was admitted and counting was started with an automatic counter-printer system.

The apparatus was calibrated by determining the counting rate of a compact monolayer of the radiostearic acid on the film balance. Such a layer should have the same counting rate as that of a compact monolayer adsorbed on a relatively smooth metal film. The smoothness of

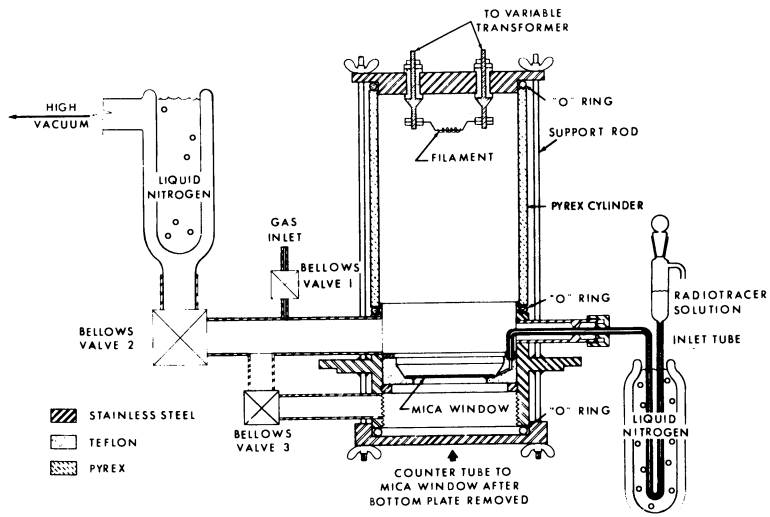

Figure 1. Adsorption apparatus

Publication Date: January 1, 1964 | doi: 10.1021/ba-1964-0043.ch020

vapor-deposited metal films, with respect to adsorption of long straight-chain polar molecules, is apparently close to that of water if optimum rate of deposition and film thickness are used, and if the films are deposited on a flat substrate [20]. Surface potentials of tightly packed monolayers on metals are the same as those of corresponding monolayers on water [8]. Backscattering of the n-hexadecane was assumed to be the same as that of the water.

Vapor deposition of metal films, calibration, and related details of apparatus and procedure have been reported [20].

Materials. The purchased radiostearic acid, $C_{17}H_{35}C^{14}OOH$, was of high purity, as shown by pressure-area isotherms on the film balance. It had a specific activity of 1.5 millicuries per millimole.

The n-hexadecane was distilled twice and passed through a silica gel column under nitrogen to remove polar impurities. A 0.0005 molal solution of radiostearic acid in n-hexadecane was stored under nitrogen in Teflon bottles. Five milliliters of solution was used—enough to cover the mica window to a depth of about 1.5 mm. A depth of 0.015 mm. contained enough radiostearic acid for a continuous monolayer.

For each experiment, a new mica window was prepared from a thin sheet (5 to 7 microns) of cleaved Indian ruby mica. The window was mounted in the adsorption chamber and thoroughly washed with twice-distilled benzene.

Weighed amounts of the metals, in the form of 7- to 15-mil wire at least 99.95% pure, were evaporated from heated tungsten filaments to give a film thickness of 100 A., by assuming the density of the film to be the same as that of bulk metal [12, 19].

The air was purified by passage through concentrated sulfuric acid, Drierite, and a trap cooled with solid carbon dioxide. The helium was passed through two coiled 15-foot borosilicate glass tubes cooled with liquid nitrogen and containing alumina and charcoal, which had been activated previously by heating at 500° C. under vacuum for 24 hours. Immediately before entering the apparatus, each gas was bubbled through water that had been deionized and twice distilled in an all-quartz system.

Results and Discussion

Mica was the least reactive surface studied, probably because it is nearly molecularly smooth and the basal surface of its lattice is essentially a layer of oxygen atoms [3, 9]. Furthermore, it is not readily wetted by water. It did not adsorb stearic acid in wet or dry helium or in dry air [20]. In the presence of wet air, it initially adsorbed about 0.2 monolayer, but adsorption decreased to zero after 40 hours. Desorption to zero may indicate that the water and air, or other impurities on the surface, diffused or dissolved in the n-hexadecane solution.

Iron exposed to the wet atmospheres adsorbed about half a monolayer of stearic acid; in the dry atmospheres, about one monolayer, as shown in Figure 2. Perhaps water reduces the activity of the surface by presenting a water film that is less attractive to stearic acid than either dry iron or iron oxide. Any oxide surface beneath the water film has little influence on adsorption; the iron film exposed to wet air adsorbed only about 0.1 monolayer less than the film exposed to wet helium. A reverse effect to the extent of 0.3 monolayer was observed in dry atmospheres.

Publication Date: January 1, 1964 | doi: 10.1021/ba-1964-0043.ch020

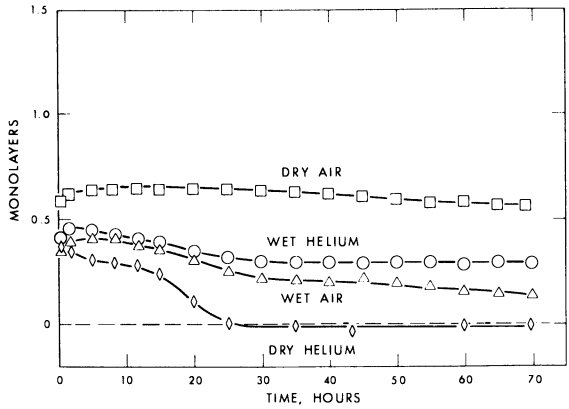

Figure 2. Adsorption of radiostearic acid onto iron films

Adsorption on gold in wet helium or air atmospheres was about half of that in dry air, as shown in Figure 3. The stable adsorption of 0.6 monolayer in dry air may be due to a film of gold oxide [17]. In the wet atmospheres, however, adsorption may have been on a water film on the gold. As with iron, adsorption on gold in wet air was only slightly less than in wet helium. At equilibrium, gold in dry helium did not adsorb radiostearic acid. The initial adsorption and subsequent decrease to zero are more difficult to explain. As was shown earlier [20], high initial surface activity of the gold film [5, 14] did not cause the adsorption. Gold films may hold a small amount of contaminants such as oxygen, water, and gold oxide, which in turn adsorb radiostearic acid. Desorption may then occur because the contaminant diffuses or dissolves in the n-hexadecane solution.

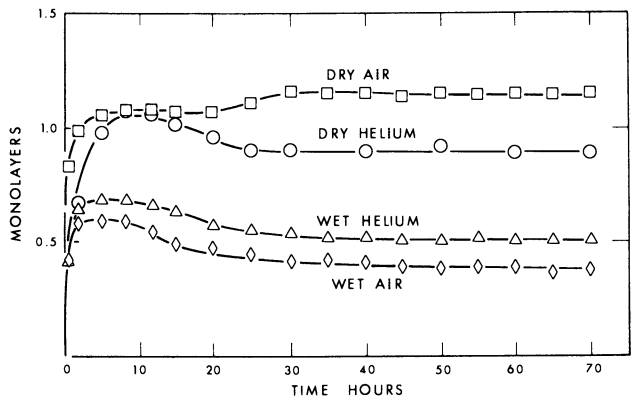

Figure 3. Adsorption of radiostearic acid onto gold films

Publication Date: January 1, 1964 | doi: 10.1021/ba-1964-0043.ch020

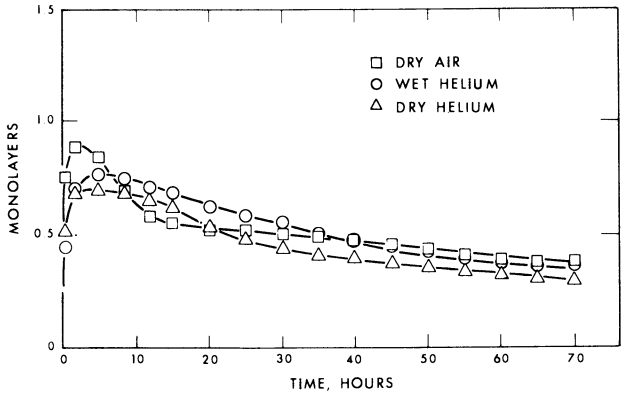

Figure 4. Adsorption of radiostearic acid onto copper films

Adsorption on copper was about the same in wet or dry helium and in dry air, as shown in Figure 4. Slow desorption to about 0.4 monolayer at 70 hours was due to lack of formation of a stable monolayer. Chemical analysis of the liquid layer indicated the presence of copper stearate. The highest initial rate of adsorption was on the copper film exposed to dry air. This suggests that a close-packed monolayer might have been adsorbed if the stearate molecules had remained at the surface. Exposure to wet air for 15 minutes caused an apparently stable adsorption of about nine monolayers at 60 hours, as shown in Figure 5. The stearate molecules were not tightly held, even though they remained at the surface, because rinsing with n-hexane removed all but

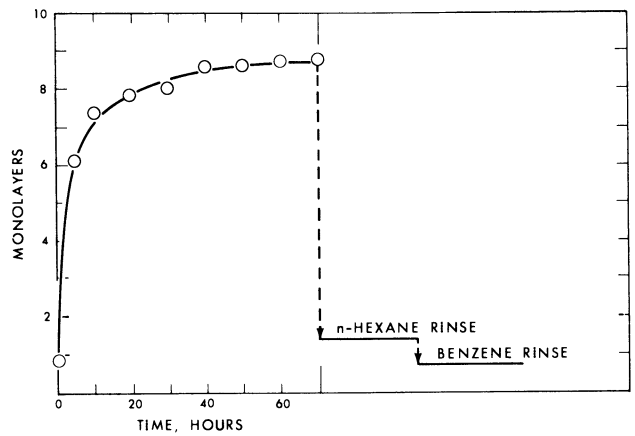

Figure 5. Adsorption of radiostearic acid onto copper film in wet air

Removal by solvents

Publication Date: January 1, 1964 | doi: 10.1021/ba-1964-0043.ch020

about 1.4 monolayers and rinsing with benzene left only 0.8 monolayer. The last monolayer was evidently stable.

Monolayers Adsorbed at 70 Hours

	Iron	Gold	Copper
Helium			
Dry	0.9	0.0	0.3
Wet	0.5	0.3	0.4
Air			
Dry	1.2	0.6	0.4
Wet	0.4	0.2	9.0

Publication Date: January 1, 1964 | doi: 10.1021/ba-1964-0043.ch020

Excluding copper in wet air, the greatest adsorption was about one monolayer on iron in the dry atmospheres; the least, on gold in dry helium. In the presence of moisture, however, iron and gold adsorbed 0.2 to 0.5 monolayer, regardless of whether the metals were exposed to helium or air. Thus, two metals with large differences in reactivity adsorbed about the same amount of radiostearic acid when moisture was present. When adsorption was less than a compact monolayer, the stearic acid molecules may not have been vertically oriented and the effective molecular area was greater. On the other hand, a mixed film containing vertically oriented adsorbate and solvent molecules may have been adsorbed [7, 15].

Initial adsorption-desorption humps were observed in most of the experiments. Perhaps the stearic acid molecules rearranged at the surface to occupy greater area. Another possibility is that some stearic acid was slowly displaced by trace quantities of water or other polar contaminants.

Conclusion

Adsorption of stearic acid onto iron and gold in the absence of moisture was generally consistent with the relative reactivities of the adsorbents, but when moisture was present, the adsorption properties were nearly the same. In no case was there a stable adsorption of more than one compact monolayer. Copper weakly adsorbed nine monolayers in wet air; all but one were easily removed by rinsing. Apparently the first layer of adsorbed molecules is bound more strongly than any succeeding layer; its molecules are the only ones that can be chemisorbed or can react chemically with the surface. When less than a compact monolayer is adsorbed, it may be either a loosely packed monolayer in which the molecules are not vertically oriented, or a mixed monolayer of vertically oriented stearic acid and n-hexadecane molecules.

Acknowledgment

The authors are grateful to B. A. Girman and Joseph Gabor for conducting much of the experimental work.

Literature Cited

(1) Aniansson, G., J. Phys. Colloid Chem. 55, 1286 (1951).
(2) Bartell, L. S., Betts, J. F., J. Phys. Chem. 64, 1075 (1960).
(3) Beischer, D. E., Ibid., 57, 134 (1953).
(4) Bowden, F. P., Tabor, D., "Friction and Lubrication of Solids," p. 214, Oxford University Press, Oxford, England, 1950.
(5) Conrad, M. A., Levy, S., Nature 189, 887 (1961).
(6) Cook, H. D., Rev. Sci. Instr. 27, 1081 (1956).
(7) Cook, H. D., Ries, H. E., Jr., J. Phys. Chem. 63, 226 (1959).
(8) Fowkes, F. W., Ibid., 64, 726 (1960).
(9) Gaines, G. L., Jr., Ibid., 61, 1408 (1957).
(10) Gaines, G. L., Jr., Nature 186, 384 (1960); J. Colloid Sci. 15, 321 (1960).
(11) Hackerman, N., Powers, R. A., J. Phys. Chem. 57, 139 (1953).
(12) Heavens, O. S., Brown, M. M., Hinton, V., Vacuum 9, 17 (1959).
(13) Kafalas, J. A., Gatos, H. C., Rev. Sci. Instr. 29, 47 (1958).
(14) Kramer, J., Z. Physik 125, 739 (1949).
(15) Levine, O., Zisman, W. A., J. Phys. Chem. 61, 1188 (1957).
(16) Shepard, J. W., Ryan, J. P., Ibid., 60, 127 (1956).
(17) Shishakov, N. A., Ibid., 64, 1580 (1960).
(18) Smith, H. A., Fort, T., Jr., Ibid., 62, 519 (1958).
(19) Wainfan, N., Scott, N. J., Paratt, L. G., J. Appl. Phys. 30, 1604 (1959).
(20) Walker, D. C., Ries, H. E., Jr., J. Colloid Sci. 17, 789 (1962).
(21) Young, J. E., Australian J. Chem. 8, 173 (1955).

Received April 3, 1963.

21

The Wettability of a Homologous Series of Nylon Polymers

TOMLINSON FORT, JR.

Fiber Surface Research Section
Textile Fibers Department
E. I. du Pont de Neumours & Co., Inc.
Kinston, N. C.

Publication Date: January 1, 1964 | doi: 10.1021/ba-1964-0043.ch021

The wettability of a homologous series of nylon polymers was studied. Measured contact angles and test liquid surface tensions were used to estimate the critical surface tension of wetting, and the approximate work of adhesion of each test liquid, for each nylon homolog. Polymer wettability decreased with increasing separation of the amide groups in the solid surfaces. However, odd and odd-odd nylons were more easily wet than their even and even-even homologs. Within the odd and even series, wettability was determined by the average nylon number and not by the spacing of the polar groups along the polymer chains. Results are interpreted in terms of the constitutive law of wettability and the morphologies and crystal structures of the nylons.

Some nine years ago, Ellison and Zisman [4] reported their study of the wettability of 6–6 nylon (polyhexamethylene adipamide) and compared their results to those previously obtained on polyethylene [7]. They found that the nylon was more easily wet than the polyethylene, especially by hydrogen-bonding liquids, and attributed these findings to the presence of amide groups in the nylon surface.

Since the time that study was made, a large body of experimental data has accumulated which shows that regular and predictable changes in solid-liquid contact angles result from changes in the outermost layer of atoms in the solid surface. A "wettability spectrum" has been published [14], and the utility of the "critical surface tension of wetting" as an index of solid surface energy has been well established.

This paper uses these concepts to correlate wettability with the surface constitution of a homologous series of nylons. These materials

In Contact Angle, Wettability, and Adhesion; Fowkes, F.;
Advances in Chemistry; American Chemical Society: Washington, DC, 1964.

are of special interest not only because of their commercial importance (at least four members of the series are produced on a large scale), but also because characteristic differences in crystal structure and molecular orientation occur among the different polymer homologs. These differences, as well as the different spacings of the amide groups along the polymer chains, might be expected to lead to significant variations in the contact angles exhibited by hydrogen-bonding liquids on the various nylon surfaces.

Experimental

Polymers. The nylon 11 and polyethylene were commercial materials (Société Organico, Paris, France, and E. I. du Pont de Nemours & Co., Inc., Wilmington 98, Del.). All the other polymers were prepared from the dry salt by bulk melt polymerization. Pertinent data for the samples used are collected in Table I. Amine ends were determined by titration with perchloric acid in 85% phenol-methanol solution and carboxyl ends by titration with sodium hydroxide in benzyl alcohol. Other analyses were by standard methods. Elemental analyses confirmed the identity of the polymers. Each was a pure sample, except nylon 11, which contained 0.26% of an unidentified inorganic material.

Table I. Polymer Analyses

Polymer[a]	Melt Temp., °C.	Amine Ends[b]	Carboxyl Ends[b]	Inherent Viscosity[c]
6–6	252	47.3	75.0	1.13
7–7	201	38.1	91.9	1.23
8–8	206	36.6	78.5	1.08
9–9	182	36.0	93.5	1.01
10–10	192	20.5	182	0.80
6	216	31.8	33.0	1.26
11	183	56.5	287	1.07

[a]In designating nylons, the first number refers to the number of carbon atoms in the diamine component, the second number to the number of carbon atoms in the dicarboxylic acid component. Single numbers refer to poly-Ω-amino acids.
[b]Number of ends per million grams of polymer.
[c]0.5% solution in m-cresol.

Wetting Liquids. The wetting liquids were all reagent grade chemicals, further purified either by distillation or by percolation through silica-alumina adsorption columns until their surface tensions checked reliable literature values [1].

Sample Preparation. Samples of polymer flake were baked in a vacuum oven for 4 hours at 110°C. to rid them of sorbed water. They were then formed into smooth continuous films by pressing small quantities in a Carver press (Fred S. Carver, Inc., 1 Chatham Road, Summit, N. J.) between a stainless steel disk (Planchets Co., Chelsea, Mich.)

Publication Date: January 1, 1964 | doi: 10.1021/ba-1964-0043.ch021

1.25 inch in diameter and 0.012 inch thick and a thin sheet of bright aluminum foil (Aluminum Co. of America, 123 South Broad St., Philadelphia 9, Pa.). The pressing temperature was 10° higher than the polymer's melting point, pressing time was 45 seconds, and the pressure was 4 tons p.s.i.g. The disk–polymer foil "sandwich" was protected by Ferrotype (Sears, Roebuck and Co., Inc., Greensboro, N. C.) plates throughout the film-forming step.

The films were quenched by placing the hot sandwiches on a cold stone laboratory bench top. The aluminum foil was then peeled away, exposing a smooth polymer surface. Measurements were made with the nylons still adhering to the steel disk, since the rigidity of the disk prevented wrinkling of the thin polymer film.

Several methods of cleaning the films were tested. Either washing in a concentrated solution of the detergent Tide, followed by thorough rinsing, or extracting in a Soxhlet apparatus with carbon tetrachloride gave polymer surfaces yielding equal and reproducible contact angles. However, neither treatment was necessary if all metal surfaces which touched the polymer were thoroughly cleaned by solvent extraction prior to the pressing step, and most films were prepared using this latter technique.

Samples were stored in a desiccator, since Ellison and Zisman [4] have shown that nylon wettability is much influenced by moisture sorbed from the atmosphere.

Apparatus, Technique, and Conditions of Measurement. Most contact angles were measured by observing light reflected from the surface of sessile drops of the various test liquids, using a special goniometer and technique [5]. Those few angles which were greater than 90° were measured by drawing tangents to the drop profiles projected onto a screen, as described by Kneen and Benton [12]. In all cases, the recorded data are the maximum reproducible advancing contact angles measured at 22°C. and 65% relative humidity, for each solid-liquid system. Experiments were performed at least in duplicate, on different days and using different pieces of polymer film. Angles were read to the nearest degree, and precision was better than ±2°.

Results

The results are presented graphically in Table II. The wettability of a given polymer decreased as the surface tension of the test liquid was raised and with a given liquid, wettability decreased as the average nylon number (average number of carbon atoms per amide group) rose. However, significant differences were found between the odd- and even-numbered nylon homologs.

The critical surface tensions of wetting, γ_c, of the nylons by hydrogen bonding liquids were estimated by linear extrapolation of graphs of the contact angle cosines *vs.* wetting liquid surface tensions to $\cos \theta = 1$ [7]. These estimates, collected in Table III, range from 43 dynes per cm. for 7-7 nylon to 28 dynes per cm. for polyethylene; the latter figure is 3 dynes per cm. lower than that found by Fox and Zisman [7] but is within the γ_c range of 26 to 37 dynes per cm. recently reported for polyethylene by Wolfram [18].

Values for the approximate work of adhesion, WA, of each polymer for each test liquid are indicated in Table IV. They were calculated

Publication Date: January 1, 1964 | doi: 10.1021/ba-1964-0043.ch021

Table II. Wettabilities of Homologous Nylons

Nylon	Contact Angle, Degrees		
	Water	Glycerol	Formamide
6	70	63	51
6-6	73	61	52
7-7	70	60	50
8-8	86	78	68
9-9	82	69	62
10-10	94	82	72
11	89	79	69
∞ (Polyethylene)	101	86	79

Table III. Critical Surface Tensions of Wetting

Nylon	γ_C, Dynes/Cm.
6	42
6-6	42
7-7	43
8-8	34
9-9	36
10-10	32
11	33
∞ (Polyethylene)	28

from the Young-Dupré equation, $WA = f_{SV^\circ} + \gamma_{LV^\circ}(1 + \cos\theta)$, assuming that f_{SV°, the free energy of immersion of the solid in the vapor, was negligible [6] and that the measured contact angles, θ, approximated the true equilibrium values, θ_E. WA varied as the separation of the amide groups in the polymers changed and was lowest for polyethylene and highest for 7-7 nylon.

Discussion

It was expected that as the average nylon number increased, the contact angles exhibited by hydrogen-bonding liquids on the various surfaces would rise, approaching the wettability of polyethylene as an asymptotic limit (polyethylene might be regarded as nylon ∞). Such

Publication Date: January 1, 1964 | doi: 10.1021/ba-1964-0043.ch021

Table IV. Approximate Works of Adhesion

Nylon	Approximate WA, Ergs./Sq. Cm.		
	Water	Glycerol	Formamide
6	97.0	92.5	94.8
6-6	93.4	94.4	93.5
7-7	96.9	95.4	95.1
8-8	76.1	76.8	79.6
9-9	82.3	86.2	85.1
10-10	67.3	72.4	75.8
11	73.5	75.5	78.6
∞ (Polyethylene)	58.4	67.4	68.9

Publication Date: January 1, 1964 | doi: 10.1021/ba-1964-0043.ch021

behavior would be predicted from consideration of the "constitutive law of wettability" [14] and the Young equation [19], $\cos \theta = \frac{\gamma_{SV} - \gamma_{SL}}{\gamma_{LV}}$ since decreasing the surface density of amide groups in the nylons should reduce the difference between the solid-vapor, γ_{SV}, and solid-liquid, γ_{SL}, interfacial tensions. This behavior was found. However, when γ_C, WA, or θ for any given wetting liquid was plotted as a function of average nylon number (Figure 1), the data fell on not one but two curves.

It was reasoned that the indicated alternation of polymer wettabilities had to result from differences in density, orientation, and/or bonding of the amide groups in the nylon surfaces. Consequently, an attempt was made to relate the observed wettabilities to polymer morphology.

A literature survey revealed that each class of nylon crystallizes to form sheets of polymer chains, with 100% hydrogen bonding between amide groups on adjacent chains in the sheets [10]. To achieve this complete bonding, different crystal habits must be taken by the different classes, as shown in Table V. Diagrams of the hydrogen-bonded sheets for representative members of each class are indicated by Figure 2.

The plane of the hydrogen-bonded sheets in thin nylon films might be expected to correspond to the plane of the films. Diffraction studies have confirmed this arrangement as correct for oriented films made by squashing nylon samples under the wheels of a railway train [2] or by evaporating the solvent from a formic acid solution of 6-6 nylon [9,13]. However, studies by Barriault and Gronholz [1], Burnett and McDevit [3], and Jenckel and coworkers [8] have shown that melt-quenched 6-6 nylon is spherulitic and that the surface of this nylon normally consists of a thin "transcrystalline skin" in which the polymer chains are oriented parallel to the surface but with their hydrogen-bonded planes normal to it. It is significant that the "skin" has been observed in nylon films prepared by melt-pressing between aluminum plates [8], as were

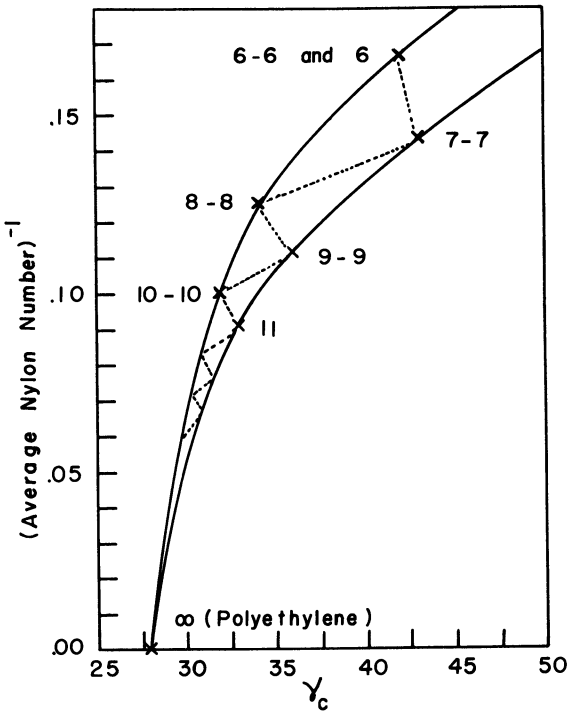

Figure 1. Variation in wettability with average nylon number

Table V. Structure of Crystalline Polyamides

Class of Polyamide	Crystal Habit[a]	Polymer Chains	Reference
Even-even	Triclinic	Planar zigzag	[2]
Odd-odd	Hexagonal	Twisted	[10, 15]
Even (4 and 6)	Monoclinic	Planar zigzag	[2, 17]
Even (>6)	Hexagonal	Twisted	[16, 17]
Odd	Triclinic	Planar zigzag	[10, 16]

[a]Even and even-even nylons are polymorphic. Crystal habit listed is normal stable structure at room temperature.

the samples used in this study. The transcrystalline region is formed as a result of growth from spherulite nuclei which exist at the surface of the polymer. Since the density of these nuclei is always high, coverage of the nylon by the transcrystalline layer is complete, unless quenching is extremely rapid, even if the bulk of the polymer is amorphous in character.

Publication Date: January 1, 1964 | doi: 10.1021/ba-1964-0043.ch021

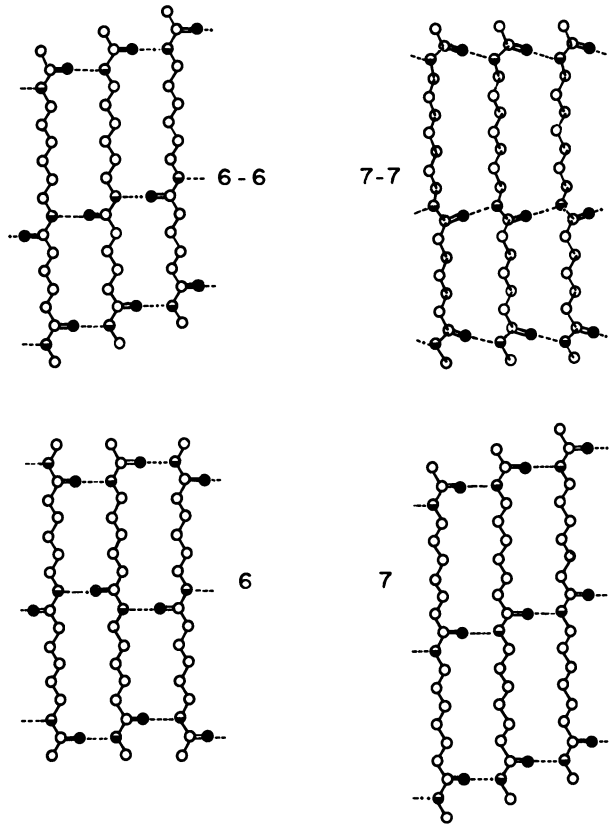

Figure 2. Hydrogen-bonded sheets in representative nylons

O Carbon atoms
● Oxygen atoms
◒ Nitrogen atoms
--- Hydrogen bonds

Contact angle measurements showed that the odd and odd-odd nylons wet easier than their even and even-even homologs, a differentiation not consistent with the crystal structures listed in Table V. However, if the transcrystalline layer extends all the way to the surface of the polymers, so that the edges of the hydrogen-bonded sheets diagrammed in Figure 2 make up the interface, the even and even-even homologs expose, alternately, a keto oxygen and imido hydrogen function, while the odd and odd-odd homologs expose one or the other, but not both. The wettability of the even polyamides would then represent an average for the two kinds of polar groups, while that of the odd polyamides would represent only one of them. Since these would logically be different, the observed variation in wettability could be explained.

Publication Date: January 1, 1964 | doi: 10.1021/ba-1964-0043.ch021

Exposure of the plane of hydrogen-bonded sheets cannot explain the observed wettability differences. If this orientation were taken, the energy of the odd-odd nylons would be increased slightly, relative to that of the other polymers tested, because of the approximately 5% greater amide group density in the "pleated" odd-odd nylon sheets [10]. However, this increase would not seem large enough to account for the wetting results, and the orientation is further disqualified by the fact that nylon 11, which crystallizes with fully extended polymer chains, behaves like its odd-odd and not its even-even homologs.

Finally, it is necessary to consider the effects on wettability of the different separations of the hydrogen-bonded sheets in the extended and twisted chain polymers. These differences are caused by the greater space requirements of the twisted chain structures. Thus, in nylon 6-6 the interplanar distance is 3.7 A. [2] and in nylon 7-7 it is 4.2 A. [11]. Zisman and coworkers [7] have shown that closer packing of hydrocarbon chains leads to more difficult wetting, while closer packing of polar functions has the opposite effect. Since nylons 7-7, 9-9, and 11 all behaved so similarly, the two effects must come near to canceling in the polymers tested.

Acknowledgment

The author thanks I. A. David, Carothers Research Laboratory, Du Pont Co., for preparing the nylon polymers used in this work, and the Du Pont Co. for permission to publish.

Literature Cited

(1) Bariault, R. J., Gronholz, L. F., J. Polymer Sci. **18**, 393 (1955).
(2) Bunn, C. W., Garner, E. V., Proc. Roy. Soc. London **198A**, 39 (1947).
(3) Burnett, B. B., McDevit, W. F., J. Appl. Phys. **28**, 1101 (1957).
(4) Ellison, A. H., Zisman, W. A., J. Phys. Chem. **58**, 503 (1954).
(5) Fort, Tomlinson, Jr., Patterson, H. T., J. Colloid Sci. **18**, 217 (1963).
(6) Fox, H. W., Zisman, W. A., Ibid., **5**, 514 (1950).
(7) Ibid., **7**, 428 (1952).
(8) Jenckel, Von Earnst, Teege, Ernst, Hinricks, Walter, Kolloid Z. **129**, 19 (1952).
(9) Keller, A., J. Polymer Sci. **36**, 361 (1959).
(10) Kinoshita, Y., Makromol. Chem. 33, 1 (1959).
(11) Ibid., p. 21.
(12) Kneen, E., Benton, W. W., J. Phys. Chem. **41**, 1195 (1937).
(13) Scott, R. G., J. Appl. Phys. **28**, 1089 (1957).
(14) Shafrin, E. G., Zisman, W. A., J. Phys. Chem. **64**, 519 (1960).
(15) Slichter, W. P., J. Polymer Sci. 35, 77 (1958).
(16) Ibid., **36**, 259 (1959).
(17) Vogelsong, D. C., Ibid., in press.
(18) Wolfram, E., Kolloid Z. **182**, 75 (1962).
(19) Young, T., Phil. Trans. Roy. Soc. (London) **95**, 65 (1805).

Received April 1, 1963.

22

The Wettability of Road Aggregates with Doped Bituminous Binders

R. P. DRON

Laboratoire Central des Ponts et Chaussées
58 Boulevard Lefebvre
Paris, France

Publication Date: January 1, 1964 | doi: 10.1021/ba-1964-0043.ch022

The ability to coat wet aggregates is connected with immersion adhesion tension and antistripping effect is connected with emersion adhesion tension. These values are measured by Guastalla's wetting balance for the system water-kerosine–mineral slide. Increasing amounts of the studied dope are dissolved in kerosine. Two thresholds of concentration were found. The lower one may be related to the antistripping effect; the higher may be related to the coating of the wet aggregate.

While analyzing the adhesive qualities of binders on aggregates, several authors have pointed out the leading part played by wetting.

Duriez [1] underlines the necessity of considering the ternary system mineral-binder-water to explain the affinity for coating wet materials on the one hand and the stripping of coated materials by water on the other hand. He emphasizes the role played by dopes as modifiers of the absolute value of the adhesion tensions of water and binder on the minerals, which are the motivating factors behind the development of coating, the viscosity of the binder and the roughness of the stone acting as a brake.

Hallberg [4] has shown that, from an experimental point of view, it is of interest to replace the binders by liquid hydrocarbons; this eliminates viscosity, which is an interfering factor. The qualitative sense is not seriously altered, as the chemical properties of the hydrocarbons, which control the wetting phenomenon, are very closely related to the properties of the bituminous binders.

Nevertheless, the experimental method which Hallberg suggests, based on measuring the speed of capillary ascension of the hydrocarbon in sand, does not eliminate the roughness of the mineral.

It is of interest to know the adhesion tensions by direct measurement. According to whether or not the forces put in action by the

In Contact Angle, Wettability, and Adhesion; Fowkes, F.;
Advances in Chemistry; American Chemical Society: Washington, DC, 1964.

surface phenomena are able to overcome the forces of viscosity, evolution or stabilization of the coating state will take place.

These surface actions appear only when water and binder coexist on the mineral and it is necessary, then, to study the phenomenon at the line of contact between the three phases.

Such a knowledge is particularly valuable for the study of the additives known as dopes. The action of the dopes is precisely that of modifying, by surface adsorption, not only the absolute values of adhesion tensions and of interfacial tensions, but also the signs of these forces, which are indicated by a change of the contact angles.

Inspired by Hallberg's method, we have taken up the problem of replacing the binder by a liquid hydrocarbon. However, instead of using sand, we worked with slides of polished minerals in order to eliminate the roughness factor.

As Duriez indicated, it is not necessary to study a great variety of minerals; it is enough to establish a distinction among the acid minerals, composed of silicates, and basic materials (alkaline earth carbonates). Our work proved that there is no essential difference within each of these two categories.

The hydrocarbon chosen is kerosine, which, like asphalt, is of petroleum origin and is sufficiently fluid without being too volatile.

We have been able to define the difference in behavior of the mineral-hydrocarbon-water system according to whether the mineral is initially wetted by water or by hydrocarbon, by utilizing J. Guastalla's wetting balance which permits one to measure successively the immersion, and emersion, adhesion tensions.

Experimental Technique

Guastalla Wetting Balance. This instrument [2,3] allows one to measure the force exerted on a vertical slide (2.5 × 2 cm.) when it is partially immersed in a liquid or, as in the case with which we are concerned, when it is placed perpendicular to the interface of two liquids, the upper part of the slide being in the lighter liquid and the lower part in the heavier one.

The slide is hung on a lever which exerts a torsion on the torsion wire and the distortion is optically amplified by a mirror system (Figure 1). The reading is done on a graduated scale in dynes per centimeter.

The entire torsion balance is mobile in the vertical sense, which allows displacement of the slide either upward or downward, in order to immerse or withdraw it progressively. This shifting is done by means of a drum, where each turn corresponds to a change of level of 1 mm.

Technique of Measurement. A beaker containing water and kerosine is placed under the torsion balance, each layer having a thickness of about 2.5 cm. The slide being studied is hung on the lever and completely immersed in the water layer before the layer of kerosine is floated on top of the water. By turning a knurled knob, the wire is twisted so that the spot indicates zero. The drum is then turned to raise the slide until its upper part comes in contact with the interface. The position of the drum is used as the point of departure for measurements of vertical displacement.

Publication Date: January 1, 1964 | doi: 10.1021/ba-1964-0043.ch022

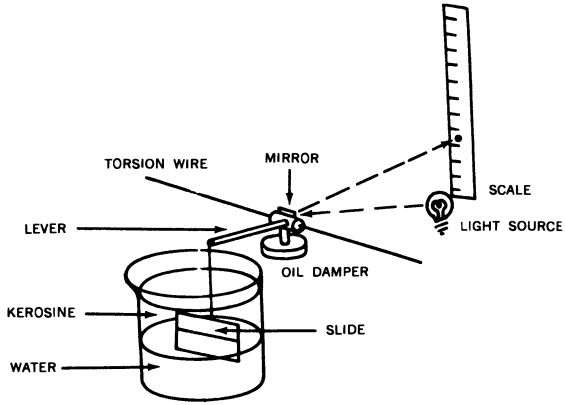

Figure 1. Guastalla's wetting balance

Tracing of Wetting Cycle

The slide is raised progressively, millimeter by millimeter, and the force exerted on it is read on the scale at each position. Equilibrium is obtained after 1 minute.

The force increases progressively for the first few millimeters and then stabilizes. This stable value corresponds to the immersion adhesion tension.

The slide is then progressively lowered; the reading is stabilized at the end of several turns of the drum. This second reading corresponds to the emersion adhesion tension. If the values measured, while the slide is being raised and lowered, are taken into consideration in relation to the number of turns of the drum (in other words, the portion of the slide immersed in the kerosine), a parallelogram is obtained, two sides being horizontal when the slide is extremely thin. Because of the different buoyancies in the two liquids, a slight slope is noticeable and the exact values of the immersion and emersion tensions are obtained by extrapolation to zero (Figure 2).

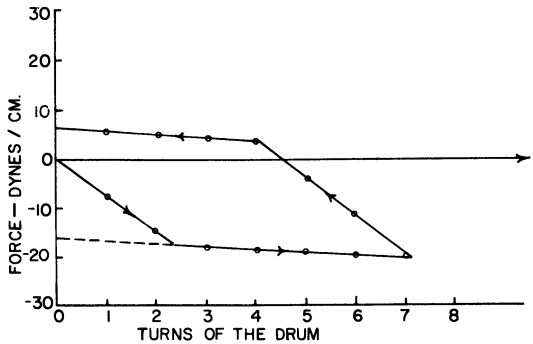

Figure 2. Tracing of wetting cycle

The slide is then replaced by a platinum stirrup (2.5 cm. long) in order to determine the interfacial tension. The tearing free method is employed, as usual, and a direct reading is obtained on this instrument.

The relation between the adhesion and the surface tensions gives the cosine of the contact angle.

Preparation of Slides. A 2.5 × 2 cm. slide, about 0.5 mm. thick, is sawed and ground from a sound and homogeneous part of the stone being studied. It is then polished with finer and finer abrasives and the operation is finished with alumina obtained after 5 hours of sedimentation.

Then, using a diamond point, a small hole is pierced, by scratching, in the middle of the upper edge of the slide, so that it may be hung on the balance.

The slides are cleaned before each experiment by placing them for one hour in methylene chloride vapor, inside a flask topped by a reflux cooler. We verified that this process is sufficient to obtain reproducible measurements (± 1 dyne per cm.).

A Study of Mineral Wetting in Presence of Dopes

Systems Studied. We have made slides of various materials and studied the variations of immersion and emersion adhesion tensions by adding Dinoram S, an amine currently utilized in France for doping road materials and similar to the American Duomeen T, which has an alkyl propylenediamine base.

The water-kerosine interface is always used and the amine is dissolved in the kerosine phase. The action of amine hydrochlorate or amine acetate can also be studied by dissolving them in water.

The slides were cut from quartz crystal and from porphyry and basalt. It was not possible to make slides from calcite crystal because of its extreme cleavability. Figures 3 and 4 show the immersion and emersion tensions on various materials *vs.* the logarithm of the dope concentration. The dashed curve shows the interfacial tension.

Examination of Results. Interfacial Tension. The interfacial tension of water-kerosine is equal to 40 dynes per cm. in the absence of dope. It is not affected by the presence of dope unless its concentration in kerosine increases beyond a certain value, which is approximately 10^{-7} gram per ml. It then decreases linearly *vs.* the logarithm of the concentration and attains very low values which are not measurable when the concentration reaches 10^{-2} gram per ml. The slope of the linear part is:

$$d\tau/d \log c = 12 \text{ dynes per cm.}$$

The immersion adhesion tension is negative and nearly equal in absolute value to the interfacial tension, as long as the dope concentration remains low. It deviates from this value when the concentration attains 10^{-6} gram per ml. The interesting fact is the cancelling out and the change of sign of the adhesion tension for a certain threshold of concentration which changes with the nature of the solid. At high concentration the immersion adhesion tension is equal in value and sign to the interfacial tension.

The curve of immersion adhesion tension concentration ultimately joins the curve of interfacial tension and this means that the contact

Publication Date: January 1, 1964 | doi: 10.1021/ba-1964-0043.ch022

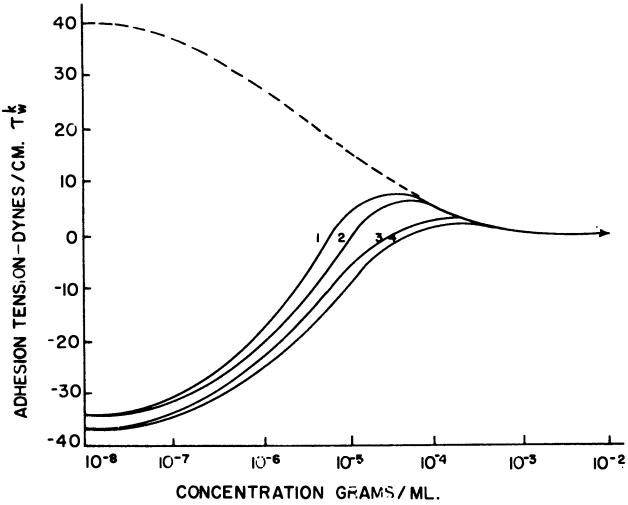

Figure 3. Immersion adhesion tensions

1. Basalt
2. Quartz
3. Porphyry A
4. Porphyry B

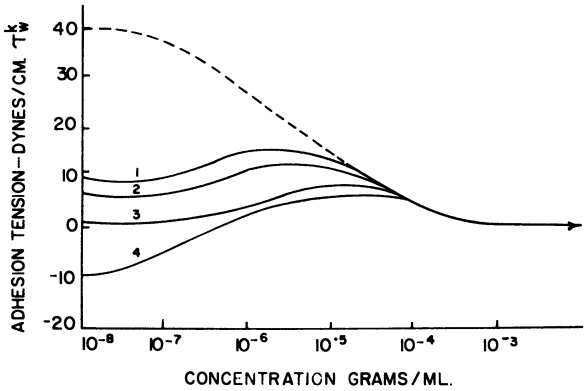

Figure 4. Emersion adhesion tensions

angle becomes nil and the wetting by hydrocarbon is perfect. The emersion adhesion tension varies greatly with the materials in the absence of dope. It is negative in the case of quartz, positive for other materials. It is affected by dope as soon as the concentration attains 10^{-7} gram per ml. and becomes equal to the interfacial tension when the concentration is equal to 10^{-5} gram per ml.

The results are appreciably different when working with amine salts, introduced in the equeous phase.

With amine acetate at a higher concentration (10^{-2} gram per ml.) the interfacial tension is nearly 5 dynes per cm., but the adhesion tensions are close to zero, so that the contact angles are equal to 90°.

With amine hydrochlorate, the problem is still more paradoxical. The adhesion tensions are negative and their absolute values may, in a high dope concentration, be equal to the value of the interfacial tension, but of opposite sign. The solid is, therefore, perfectly wetted by water.

Interpretation of Results

The technological problems relative to the competing of water and binder on the surface of the stone are of two categories.

Problem 1. A wetted stone is to be coated with a binder. This problem arises at the time the macadam is made. Water is to be displaced by the binder on the surface of the mineral. This process is equivalent to the immersion of the slide in the kerosine phase. We must consider, therefore, the immersion adhesion tension.

The immersion tensions of all the materials studied are negative in the absence of dope. Therefore, it is not possible to displace a film of water by the binder in the absence of surface active agents.

When an amine is dissolved in the hydrocarbon phase, a threshold of concentration exists, beyond which the adhesion tension becomes positive. This threshold is characteristic of the efficacy of the dope employed on the mineral. It is equal to the concentration of the dope required for the binder to displace the water off the mineral surface.

When the dope is in its hydrochlorate state and dissolved in the water phase, it acts only on the interfacial tension; its role seems unfavorable from the wetting point of view. A film of water is drawn along the mineral when it is immersed in kerosine, probably because of the adsorption of whole micelles and no longer of isolated molecules as Ter-Minassian found on glass slides [6]. Thus, the outer part of the adsorption coating is hydrophilic instead of lipophilic.

When acetate is utilized, the contact angle is near 90°. The additive acts only to lower the tension and not as a wetting agent.

Problem 2. A different problem appears when the material is set in place on the road and we want to avoid displacement of the binder by water. It is a matter of protecting the structure, if, for example, the laying is followed by rain. This is equivalent to the emersion process and the force of displacement is then the emersion adhesion tension.

The emersion adhesion tensions at the lower concentration of dope indicate different tendencies to spontaneous stripping according to the minerals. The spontaneous stripping can occur only on quartz, for which the adhesion tension is negative.

However, although positive, the emersion adhesion tensions are very low (practically nil in the case of porphyry). Because of the hysteresis (difference between immersion and emersion adhesion tensions) under the effect of outside energy—mechanical action, for example—the binder may be irreversibly replaced by water, and the stripping will continue, leading to the destruction of the structure.

For the quartz, a threshold of concentration of the dope exists, above which the emersion adhesion tension becomes positive and the spontaneous stripping can no longer take place; its value is near 5.10^{-7} gram per ml.

Publication Date: January 1, 1964 | doi: 10.1021/ba-1964-0043.ch022

Conclusions

Measurements of adhesion tensions on polished mineral slides by the Guastalla wetting balance point out certain aspects of the physical mechanism of the wetting of aggregates with doped hydrocarbons in the presence of water.

This technique permits one to determine whether the aggregates are initially wetted by water or by hydrocarbons. The results show that water-wetted materials can be made receptive to coating by adding a certain quantity of amine, and that spontaneous stripping can occur only on very acid minerals and may be prevented by adding a smaller quantity of amine.

Literature Cited

(1) Duriez, M., Construction, special issue (December 1958).
(2) Guastalla, J., J. Colloid Sci. **11**, 623–36 (1956).
(3) Guastalla, J., "Proceedings of Second International Congress on Surface Activity," p. 143, Butterworths, London, 1957.
(4) Hallberg, Sten, Meddelande 78, Statens Väginstitut, Stockholm, private communication, 1950.
(5) Rosano, H. L., Weill, M., "Memorial des Services Chimiques de l'Etat," Vol. 37, part 3, 1952.
(6) Ter Minassian-Saraga, L., 5th Colloquium, "Theorie et Pratique de l'Utilisation des Agents de Surface," Paris, June 1959.

Received April 3, 1963.

23

Surface Activity at Organic Liquid-Air Interfaces

V. The Effect of Partially Fluorinated Additives on the Wettability of Solid Polymers

N. L. JARVIS, R. B. FOX, and W. A. ZISMAN

U. S. Naval Research Laboratory, Washington 25, D. C.

Publication Date: January 1, 1964 | doi: 10.1021/ba-1964-0043.ch023

The present investigation describes the successful modification of the surface properties of polymeric solids by the adsorption of appropriate partially fluorinated compounds at polymer-air interfaces during the formation of the polymer surfaces. The extent of additive adsorption was found to be dependent upon the molecular structure, fluorine content, and solubility of the additives in the solute—i.e., their organophilic-organophobic balance with respect to the solute. Certain effective additives were able to decrease the critical surface tension, γ_c, of such polymers as poly(methyl methacrylate) and polyacrylamide to 20 and 11 dynes per cm., respectively. These low γ_c values correspond to surfaces containing closely packed CF_2 and CF_3 groups.

Many surface properties of solid, smooth polymers are strongly dependent upon the chemical constitution of the surface layer of molecules [25, 26, 27]; therefore, to modify a given surface property it is necessary to alter the chemical composition of the surface in some way. One example of such a modification is the commercial use of controlled oxidation of the surface of polyethylene foil to ensure wetting by and adhesion of polar printing inks [2].

A series of studies of surface activity of soluble and insoluble compounds at organic liquid–air interfaces has been reported by Zisman, Ellison, Bernett, and Jarvis [4, 10, 11, 16, 17, 18]. The most surface active compounds were found to be various fluorocarbon derivatives having the proper organophobic-organophilic balance. If one considers a plastic solid to be either a supercooled liquid or a liquid of very high viscosity, one would expect many of these partially fluorinated compounds also to manifest great surface activity when dissolved in

In Contact Angle, Wettability, and Adhesion; Fowkes, F.;
Advances in Chemistry; American Chemical Society: Washington, DC, 1964.

various polymers, provided sufficient time is allowed for diffusion of the solute to the interface and for adsorption equilibrium to occur. The rate at which one of these surface active agents will adsorb at the polymer-air interface will be primarily determined by the rate of diffusion in the bulk polymer phase. If added to a molten polymer or to a solution of the polymer in a volatile solvent, the surface active agent will be able to diffuse rapidly to the surface as the polymer solidifies or as the solvent evaporates. Once the polymer film is solid, however, it may take hours or days for a significant amount of the additive to migrate to the surface, depending upon the concentration of the additive and the nature of the polymer.

The extent to which a surface active solute adsorbs at a polymer surface will be determined by essentially the same properties that are responsible for their effectiveness in organic liquids—namely, their concentration, ability to lower the surface energy of the system, fluorine content, and solubility or extent of association with the polymeric substrate. By analogy with aqueous systems one might briefly call the combination of these properties in a fluorocarbon derivative its organophilic-organophobic balance. The presence of adsorbed and oriented fluorocarbon groups at the polymer-air interface will not only decrease the surface free energy of the polymer, and thus its wettability, but should modify its coefficient of friction and decrease its adhesive properties as well. It is the purpose of this report to demonstrate the effectiveness of a small concentration of a partially fluorinated additive in changing the surface constitution and reducing the wettability of various polymer surfaces.

Experimental Materials and Methods

The partially fluorinated compounds used in this investigation as surface active additives are listed in Table I.

TABLE I. List of Partially Fluorinated Compounds Used as Surface Active Agents

I	Tris(1H,1H-pentadecafluoro-octyl) tricarballylate
II	3-(Hydroxymethyl)-1,5-pentanediol tris(heptafluorobutyrate)
III	Bis(1H,1H-undecafluorohexyl)-3-methyl glutarate
IV	Bis(1H,1H-pentadecafluoro-octyl) tetrachlorophthalate
V	1H,1H-Pentadecafluoro-octyl ethanesulfonate
VI	Bis(1H,1H-heptafluorobutyl) adipate
VII	18,18,19,19,20,20,21,21,22,22,22-Undecafluorodocosanoic acid
VIII	N,N,N-Dimethyl-3-(n-perfluoroheptanecarboxamido)propyl -3-aminopropionic acid, inner salt

Additives I through VI were prepared in high purity by O'Rear and coworkers at this laboratory [12, 19] and have been used in the previous studies of surface activity at organic liquid–air interfaces [4, 10, 11, 16, 17, 18]. Additives VII and VIII are research preparations donated by the Organic Chemical Department, E. I. du Pont de Nemours & Co., and the Minnesota Mining and Manufacturing Co., respectively. The carefully purified liquids used in the determination of γ_c were selected to give a wide range of surface tensions and a variety of structural types. Sources, methods of purification, and surface tensions of the majority

of these liquids (listed in Tables II to V) have been given in previous reports from this laboratory [20,22]. The 1,1-diphenylethane was a product of Eastman Organic Chemicals, which had been freed from polar impurities by several percolations through a column of Florisil.

Four polymers with different surface compositions were used in this study—polystyrene (PS), poly(methyl methacrylate) (PMMA), polyacrylamide (PAM), and a poly(vinylidene chloride) (PVeC) copolymer (containing 20% polyacrylonitrile). Polystyrene has essentially a hydrocarbon surface, whereas the surfaces of poly(methyl methacrylate) and polyacrylamide contain ester and amide groups, respectively. The surface of the poly(vinylidene chloride) copolymer on the other hand will contain a relatively large number of chlorine atoms. The presence of acrylonitrile in the poly(vinylidene chloride) copolymer improved the solubility characteristics of the polymer for the purposes of this study, but did not appreciably alter γ_c, its critical surface tension of wetting. Values of γ_c of these polymers ranged from 30 to 33 dynes per cm. for polystyrene to approximately 40 dynes per cm. for the poly(vinylidene chloride) copolymer. No attempt was made to determine the crystallinity of the polymer samples, or to correlate crystallinity with adsorption of the fluorocarbon additives.

The poly(methyl methacrylate) used in these experiments was obtained from freshly distilled degassed monomer by bulk polymerization to 30% conversion at 60° C. with azodiisobutyronitrile as initiator. The polymer was purified by two reprecipitations from tetrahydrofuran solution with methanol. After drying at room temperature under vacuum for 24 hours, the material had $\bar{M}_v = 7.76 \times 10^5$. Mass spectroscopic analysis of the volatile material obtained by heating 0.1-gram film samples of the polymer at 110° C. for 4 hours showed 7.4×10^{-7} mole of monomer and traces of methylene chloride solvent, no other volatile material having been evolved. Films of PMMA about 15 microns thick, with and without additives, were prepared in shallow rectangular borosilicate glass dishes by the slow evaporation (for 24 hours or more) at room temperature of methylene chloride solutions of about 0.1 gram of the polymer and appropriate amounts of additive. During most of this time the surface-active compounds were free to diffuse to the polymer-air interface. Traces of solvent were removed by continuous pumping at room temperature an additional 16 hours. Finally, samples were stored in an evacuated desiccator until the contact angle measurements were made, usually within 3 days. In each case there appeared to be no significant change in contact angle with time after the third day.

Polystyrene was prepared from freshly distilled and degassed styrene by bulk polymerization at 50° C. under nitrogen with benzoyl peroxide as the initiator: Conversion was about 50%. After precipitation with methanol, the polymer was purified by two reprecipitations from tetrahydrofuran solution with methanol, exhaustively extracted with methanol, and finally vacuum-dried at room temperature. The polymer had $\bar{M}_v = 1.8 \times 10^5$. Films of this material were prepared from methylene chloride solution in the same way as the PMMA films.

Acrylamide (m.p. 85° C. from ethyl acetate) was polymerized in aqueous solution at about 75° C. in the presence of 2-propanol and potassium persulfate as described by Sorenson and Campbell [23]. The polyacrylamide was further purified by an additional precipitation from

Publication Date: January 1, 1964 | doi: 10.1021/ba-1964-0043.ch023

aqueous solution with methanol and dried in vacuum. Films were prepared by the slow evaporation of water from aqueous solutions of the polymer and additive.

The poly(vinylidene chloride) copolymer (Dow Chemical Co.) contained 80% vinylidene chloride and 20% acrylonitrile. A small amount of a carbonyl-containing compound was the only impurity detected by means of the infrared spectra of a thin film of the copolymer. Films were prepared by the slow evaporation of tetrahydrofuran solutions; otherwise they were handled in the same manner as the PMMA samples.

Smooth surfaces of each polymer were also prepared (without additives) by pressing samples of the powdered polymers against a highly polished stainless steel surface in a Carver press at 16,000 p.s.i. Circular disks 1 inch in diameter and weighing several grams were formed in this way. PS and the PVeC copolymer were compressed at room temperature, PAM at 120° C., and PMMA at 150° C. The pressure was maintained until smooth polymer surfaces were obtained. The mold and stainless steel piston were cleaned prior to use, so that contact angles could be measured on the polymer surfaces without further surface treatment.

The contact angles of the various liquids in Tables II to V on each polymer surface were determined while increasing the volume of the drop, and thus slowly advancing its periphery over the surface. The contact angles on each polymer surface prepared by solvent evaporation were measured through the plane ends of the rectangular borosilicate glass dishes using the method and improved goniometer telescope described previously [13]. All contact angles on PMMA, PS, and PVeC copolymer were measured in air, but to prevent the adsorption of water, contact angle measurements on PAM were made in a dry nitrogen atmosphere.

Every contact angle reported is the average of the values obtained on at least three different drops on a plastic surface, and at least two independent samples of each film were prepared. Contact angles for successive drops on a given polymer surface seldom varied more than 4°; however, somewhat larger differences were sometimes observed between independently prepared samples of the same polymer containing small amounts of certain additives. These variations may have been a function of the age of the solid—i.e., the longer the polymer specimen ages, the greater the amount of additive that may diffuse to the surface. Because of the difficulty involved in measuring small contact angles through the plane ends of the glass sample dishes, contact angles of 5° or less were considered as essentially zero and indicative of spreading for the purposes of this study. Each prepared sample containing an additive was allowed to stand no longer than 4 days before contact angle measurements were made. All measurements were made at 25° ± 1° C. with the relative humidity varying from 15 to 30%, except for PAM.

Experimental Results

Polystyrene. Contact angles of the various pure liquids on polystyrene are given in Table II for surfaces of pure polystyrene prepared by solvent evaporation as well as by compression of the powdered polymer. Values of θ obtained in each case agree well with those

Publication Date: January 1, 1964 | doi: 10.1021/ba-1964-0043.ch023

TABLE II. Contact Angles for Various Liquids on Polystyrene

Liquid	Surface Tension, Dynes/Cm.	Contact Angles, θ, Degrees			
		Pressed disk	Surface by Solvent Evaporation		
		No additive	No additive	4% additive III	10% additive II
Water	72.6	93	96	96	97
Glycerol	63.4	82	84		
Formamide	58.2	76	80		
Thiodiglycol	54.0		63		
Methylene iodide	50.8	[a]	[a]		
Arochlor 1242 (trichlorobiphenyl)	45.3	18	16		
1-Bromonaphthalene	44.6	18	15		
Tricresyl phosphate	40.9	14	18	16	18
Hexachloropropylene	38.1	11	14		
1,1-Diphenylethane	37.7	12	12		
tert-Butylnaphthalene	33.7	Spr.[b]	Spr.		
Dicyclohexyl	32.8	Spr.	Spr.		
Bis(2-ethylhexyl) orthophthalate	31.3	7	10	12	14
Squalane	29.5		6		
Hexadecane	27.6	Spr.	Spr.	6	9
Tetradecane	26.7	Spr.	Spr.	Spr.	Spr.

[a]Polymer dissolved in methylene iodide.
[b]Contact angle less than 5°.

reported by Ellison and Zisman [9], as shown in Figure 1. This agreement indicates that the polystyrene surfaces formed by solvent evaporation were essentially free of contamination, for the presence of a modest fraction of a monolayer of residual methylene chloride solvent at the interface would have significantly decreased the contact angles [8] below those reported in Table II. The plot in Figure 1 of cos θ *vs.* surface tension, (γ_{LV°), for various pure liquids indicates that γ_c for polystyrene is between 30 and 35 dynes per cm., the range previously reported as the best estimate of the critical surface tension of polystyrene [9, 24].

The fluorocarbon additives I through VII listed in Table I were added in varying concentrations to solutions of polystyrene in methylene chloride. Each was added in concentrations up to at least 1% by weight of polymer, while the pentanediol (II) and 3-methylglutarate (III) derivatives were added in concentrations up to 10 and 4%, respectively. In every case where only 1% additive was present there was no perceptible change in the wetting behavior of the polystyrene surface. Even at the higher concentrations, additives II and III had only a slight effect on the wettability of polystyrene, the most significant change being that hexadecane now gave definite, measurable, contact angles. The ineffectiveness of these additives in polystyrene is a result of their low solubilities in the polymer. Each additive contains one or more highly polar ester or acid group, which in combination with the high fluorine content of the molecule tends to cause low solubility in nonpolar

Publication Date: January 1, 1964 | doi: 10.1021/ba-1964-0043.ch023

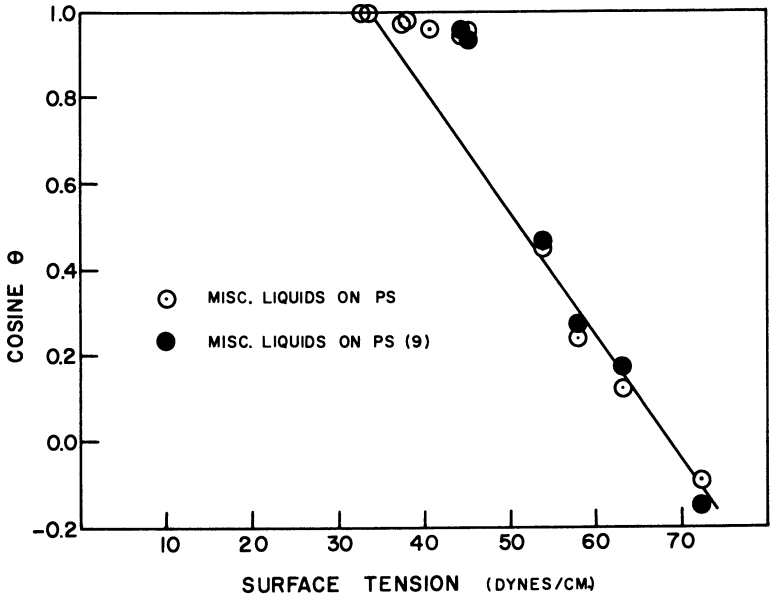

Figure 1. Cos θ vs. γ_{LV}° for various pure liquids on polystyrene surfaces

liquids. In most instances the additives were so insoluble in the polystyrene that they either separated as another phase as the solvent evaporated or formed cloudy, opaque films. Evidently, in order to modify the surface of polystyrene by adsorption of surface active molecules, it will be necessary to find partially fluorinated compounds that are more soluble in polystyrene.

Poly(methyl Methacrylate). The contact angles of the various liquids on PMMA surfaces are given in Table III. The surfaces of PMMA (without additives) prepared by the two independent techniques were initially studied exactly as prepared, without any attempt to clean the newly formed surfaces. Significant differences were observed between contact angles on these two surfaces, the specimen prepared by solvent evaporation exhibiting much higher contact angles with some liquids than the pressed disks. However, after the surface prepared by solvent evaporation was washed with detergent, rinsed profusely with distilled water, and dried, contact angles were obtained which agreed within the limits of experimental error with those measured on the pressed disk, and were in better agreement with values reported in the literature. Craig, Berry, and Peyton [7] have reported a contact angle of 78° for water on clean PMMA, in very good agreement with that reported here for the clean surface. Therefore, the surface of the PMMA prepared by solvent evaporation had been contaminated by an easily removed film. It is unlikely that the contamination came from the solvent, for samples of polystyrene prepared from the same batch of solvent and by the same technique did not show evidence of such contamination. It is concluded that the film removed by cleaning originated from a small

Publication Date: January 1, 1964 | doi: 10.1021/ba-1964-0043.ch023

Publication Date: January 1, 1964 | doi: 10.1021/ba-1964-0043.ch023

TABLE III. Contact Angles of Various Liquids on Poly(methyl Methacrylate)

Liquid	Surface Tension, Dynes/Cm.	Contact Angle, θ, Degrees						
		Pressed disk	Surface Formed by Solvent Evaporation					
		No additive	No additive	No additive (after cleaning)	0.2% additive I	0.5% additive I	0.5% additive II	1.0% additive II
Water	72.6	80	94	76	96	96	96	97
Glycerol	63.4	69	88	69	89	91	96	
Formamide	58.2	64	75	63	79	85	85	
Thiodiglycol	54.0	47	63	46	59	59	61	
Methylene iodide	50.8	41	43	42	42	46	45	51
1-Bromonaphthalene	44.6	16	16	18	17	18	15	
Tricresyl phosphate	40.9	19	20	24	24	26	32	
Hexachloropropylene	38.1	Spr.	Spr.	Spr.	Spr.	Spr.	Spr.	
1,1-Diphenylethane	37.7	Spr.	Spr.	Spr.	Spr.	Spr.	10	
tert-Butylnaphthalene	33.7	Spr.	Spr.	Spr.	10	11	8	
Dicyclohexyl	32.8	Spr.	Spr.	Spr.	41		6	40
Bis(2-ethylhexyl) orthophthalate	31.3	Spr.	8	6	19	18	20	
Squalane	29.5	Spr.	26		44	44	21	47
Hexadecane	27.6	Spr.	14	Spr.	48	52	19	39
Tetradecane	26.7		11	Spr.	45	48	15	36
Dodecane	25.4		Spr.	Spr.	43	44	9	33
Decane	23.9				37	39	Spr.	31
Octane	21.8				23	29		23

In Contact Angle, Wettability, and Adhesion; Fowkes, F.; Advances in Chemistry; American Chemical Society: Washington, DC, 1964.

amount of impurity in the PMMA sample which had adsorbed at the polymer-air interface as the solvent evaporated. A similar accumulation of impurity would not be expected to occur at the surface of the pressed disk, because of the slower rate of diffusion in the solid polymer.

From the contact angles in Table III, cos θ *vs.* γ_{LV} was plotted in Figure 2 for clean PMMA. From the intercept it is seen that γ_c is approximately 39 dynes per cm., well within the range of 33 to 44 dynes per cm. recently reported by Wolfram [24]. Ellison and Zisman [9] also obtained a critical surface tension of between 39 and 40 dynes per cm. for poly(ethylene terephthalate), another polymer containing a large number of carboxylic ester groups.

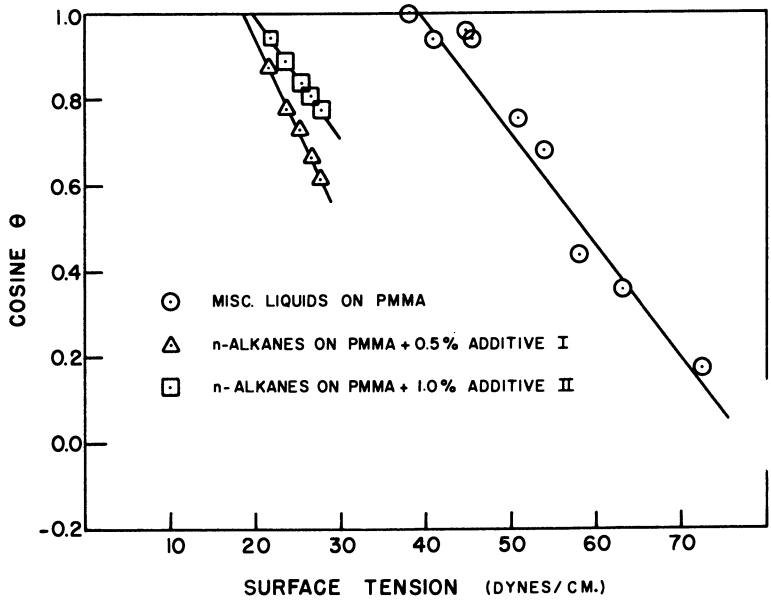

Figure 2. Cos θ vs. γ_{LV}° for various pure liquids on poly(methyl methacrylate) surfaces

The following fluorinated compounds were added to PMMA: tricarballylate (I), pentanediol (II), and 3-methylglutarate (III) derivatives. Additive I was added in concentrations up to 0.5% by weight of polymer, while II and III were added in concentrations up to 1.0 and 2.0%, respectively. Contact angles were measured on PMMA films containing fluorinated additives without prior cleaning of the film surface, as in many cases washing with a detergent removed significant amounts of the adsorbed additive. The trace of impurity in the PMMA discussed in the previous paragraph was not considered important here, since in the competitive adsorption between it and one of the highly surface active fluorinated solutes, the latter would probably be the dominant species adsorbed. Therefore, an additive was considered effective only if it increased θ above the values reported in Table III for PMMA

Publication Date: January 1, 1964 | doi: 10.1021/ba-1964-0043.ch023

prepared without additives by solvent evaporation. Additive III appeared to be so soluble in PMMA that even a 2.0% concentration resulted in essentially no change in the wetting properties of the polymer. However, additives I and II brought about significant changes in the wettability. The fact that identical concentrations of these additives in methylene chloride did not cause a similar change in the wettability of polystyrene indicates that this effect is truly related to the surface activity of the additives in the polymer and not to their surface activity in the evaporating solvents.

The fluorinated tricarballylate (I) was very surface active in PMMA and at a concentration of only 0.2% had apparently reached its maximum adsorption at the polymer-air interface. As is shown in Table III, θ did not increase further when the concentration was increased to 0.5%. However, significant changes in θ were observed only for the high surface tension polar liquids and the low surface tension nonpolar liquids; those having intermediate properties exhibited contact angles identical to those measured on the additive-free PMMA. Previous work on the behavior of these additives when dissolved in organic liquids [17] indicates that the observed effect arose from the ability of the sessile drop to dissolve the film of additive accumulated in the surface of the polymer. Even if the entire fluorocarbon monolayer beneath a drop was dissolved, the concentration within the drop would still be too low to reduce the liquid surface tension. Essentially then we would have a situation analogous to a pure liquid drop resting on the additive-free PMMA.

Additive II did not show the same surface activity in PMMA as the tricarballylate (I), for 0.5% caused only moderate changes in θ, and only when 1.0% had been added did θ approach values obtained with additive I. At the higher concentrations the polymer films containing the pentanediol derivative (II) tended to wrinkle badly and pull away from the bottom of the glass dish; therefore reliable measurements of θ were difficult to make and hence fewer are reported. Again, the most significant changes in θ occurred for the very polar and nonpolar liquids.

In many studies of wettability Zisman and coworkers have used the contact angles of a series of n-alkanes as a convenient means for determining γ_c for low energy solid surfaces [5, 6, 13, 20]. In Figure 2 are plotted the cos θ *vs.* γ_{LV}° curves for the n-alkanes on PMMA surfaces containing 0.5% additive I and 1.0% additive II. The critical surface tensions with additives I and II were 19 and 20 dynes per cm., respectively, representing a decrease of about 20 dynes per cm. from the value of γ_c obtained with the additive-free surface. Since the γ_c values of 19 and 20 dynes per cm. are very close to that of 18 dynes per cm. reported by Fox and Zisman [13] for the n-alkanes on polytetrafluoroethylene surfaces, it is apparent that a number of perfluoroalkane groups are present in the outermost part of the surface phase with the principal axis of each carbon-carbon chain parallel to the surface.

Poly(vinylidene Chloride) Copolymer. Contact angles observed on poly(vinylidene chloride) copolymer surfaces prepared by solvent evaporation are given in Table IV, along with the values obtained on highly polished surfaces of compressed disks of the additive-free powdered polymer. Values of θ exhibited by the various liquids on each type of

Publication Date: January 1, 1964 | doi: 10.1021/ba-1964-0043.ch023

TABLE IV. Contact Angles of Various Liquids on Poly(vinylidene Chloride) Copolymer

Liquid	Surface Tension, Dynes/Cm.	Contact Angle, θ, Degrees			
		Pressed disk	Surface by Solvent Evaporation		
		No additive	No additive	1.0% additive I	1.0% additive IV
Water	72.6	81	85	86	100
Glycerol	63.4	67	72	72	92
Formamide	58.2	65	70	71	82
Thiodiglycol	54.0	42			
Methylene iodide	50.8	27	27	29	50
Arochlor 1242 (trichlorobiphenyl)	45.3	11	Spr.	8	23
1-Bromonaphthalene	44.6	9	9	Spr.	
Tricresyl phosphate	40.9	10	11	12	30
Hexachloropropylene	38.1	Spr.	Spr.	Spr.	
1,1-Diphenylethane	37.7	Spr.	Spr.	Spr.	
tert-Butylnaphthalene	33.7	Spr.	Spr.	Spr.	
Dicyclohexyl	32.8	Spr.	Spr.	Spr.	
Bis(2-ethylhexyl) orthophthalate	31.3	Spr.	Spr.	Spr.	20
Hexadecane	27.6	Spr.	Spr.		44
Tetradecane	26.7				41
Dodecane	25.4				36
Decane	23.9				27
Octane	21.8				11

PVeC copolymer surface are in good agreement, generally within the limits of experimental error. These values of θ are very similar to those reported previously by Ellison and Zisman [8] on a poly(vinylidene chloride) surface, which for comparison are plotted in Figure 3 along with the present results. The plot of cos θ *vs.* γ_{LV}° in Figure 3 shows the critical surface tension of the additive-free PVeC copolymer surface to lie between 38 and 44 dynes per cm.

Fluorinated compounds I, III, IV, and V were dissolved in tetrahydrofuran solutions of the PVeC copolymer in concentrations up to 1% by weight of the polymer. Of these additives, the 3-methyl glutarate (III), ethanesulfonate (V), and tricarballylate (I) derivatives failed to modify the wettability of the polymer surface. However, the tetrachlorophthalate derivative (IV) caused a marked decrease in the wettability of the polymer (see Table IV, last column). In Figure 3 the graph of cos θ *vs.* γ_{LV}° for the n-alkanes on the resulting surface shows that γ_c is between 20 and 21 dynes per cm., which is close to the characteristic γ_c value of poly(tetrafluoroethylene), 18 dynes per cm. It is apparent that the polymer surface is rich in the fluorinated aliphatic chains of the solute and that the presence of the chlorine atoms in the tetrachlorophthalate molecule has increased the solubility of the additive in the highly chlorinated PVeC copolymer. The presence of the chlorine groups in the tetrachlorophthalate derivative thus gave it a more suitable organophilic-organophobic balance than was present in additives I, III, and V.

Publication Date: January 1, 1964 | doi: 10.1021/ba-1964-0043.ch023

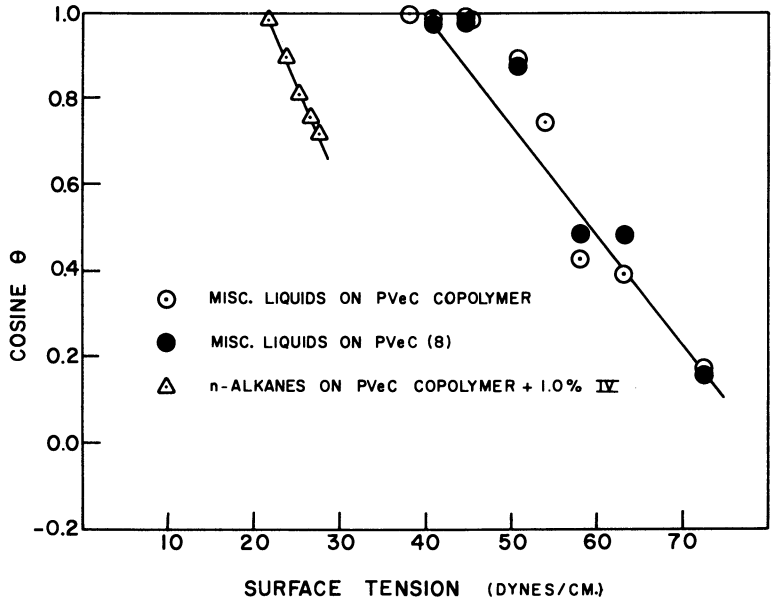

Figure 3. Cos θ vs. γ_{LV}° for various pure liquids on surfaces of poly(vinylidene chloride) copolymer (containing 20% polyacrylonitrile)

Polyacrylamide. In Table V are listed the contact angles of the various liquids on polyacrylamide. On account of the high water solubility of this polymer, extremely low contact angles were observed for water, approaching zero with time. Glycerol and formamide also appeared to interact with PAM, and failed to give reproducible contact angles. Contact angles of the remaining liquids, obtained in a dry nitrogen atmosphere, were reproducible (Table V). The contact angles observed on the clean PAM surface are somewhat larger than might have been predicted on the basis of the polymer's chemical composition. If the amide groups are exposed at the surface, one would expect the polymer to have a critical surface tension about as high as PMMA or nylon [9], whose γ_c values are about 40 dynes per cm. On the other hand, if the amide groups are not exposed, the γ_c for PAM would be closer to that of polyethylene, approximately 31 dynes per cm. The plot of cos θ *vs.* γ_{LV}° for the pure liquids on additive-free surfaces does not give a well defined γ_c. If a line is drawn through the points representing the liquids with surface tensions greater than 35 dynes per cm., and is drawn parallel to corresponding lines in Figures 1 to 3, it indicates a γ_c somewhere between 35 and 40 dynes per cm. However, if this is the true γ_c of the surface, the liquids with surface tensions below 35 dynes per cm. should have spread.

This anomalous wetting behavior of the low surface tension liquids on additive-free PAM may indicate that the polymer surface is contaminated. The most probable contaminant on the surface of this water-soluble polymer would be a layer of strongly adsorbed water, which is

Publication Date: January 1, 1964 | doi: 10.1021/ba-1964-0043.ch023

TABLE V. Contact Angles of Various Liquids on Polyacrylamide
(Values obtained in dry N_2 atmosphere)

Liquid	Surface Tension, Dynes/Cm.	Contact Angle, θ, Degrees — Surface by Solvent Evaporation			
		No additive	0.6% additive VIII	1.2% additive VIII	1.0% additive VIII[a]
Water	72.6				
Glycerol	63.4				
Formamide	58.2				
Thiodiglycol	54.0	28		84	
Methylene iodide	50.8	47	91	93	95
Arochlor 1242 (trichlorobiphenyl)	45.3	33	87	86	83
1-Bromonaphthalene	44.6	33	86	87	85
Tricresyl phosphate	40.9	31	87	87	85
Hexachloropropylene	38.1	Spr.	39	42	59
1,1-Diphenylethane	37.7	22	82	82	82
tert-Butylnaphthalene	33.7	20	80	78	78
Dicyclohexyl	32.8	19			
Bis(2-ethylhexyl) orthophthalate	31.3	20	78	77	76
Squalane	29.5		76	74	74
Hexadecane	27.6	14	71	71	70
Tetradecane	26.7	11	68	68	67
Dodecane	25.4		66	65	64
Decane	23.9		62	62	60
Octane	21.8		57	56	54

[a]Additive VIII added to monomer prior to polymerization.

not removed by drying under vacuum at room temperature. To determine whether or not adsorbed water will influence the contact angle, surfaces of PAM prepared by solvent evaporation, and by pressing the dried powder into disks, were exposed for several hours to atmospheres of varying relative humidity. The contact angles of methylene iodide on both surfaces were observed to increase from 47° to 58° as the relative humidity rose from 0 to 99%, while the contact angles of hexadecane increased from 14° to 31° over the same relative humidity range. This behavior is analogous to the increase in methylene iodide contact angle with increasing hydration of a silicate surface that was observed by Shafrin [21]. On the basis of these experiments the finite contact angles of the low surface tension liquids on additive-free PAM surfaces may be explained by the presence of adsorbed water.

The incorporation of a fluorocarbon additive in PAM presented a somewhat different problem than the previous polymers, inasmuch as it required a fluorinated additive that has some solubility in water. The partially fluorinated additives, I to VII, are insoluble in water and fail to disperse in the polymer when added to aqueous solutions; rather they form a separate phase and settle to the bottom of the sample dish. Additive VIII was therefore selected for use in this polymer, as Guenthner and Vietor [14] have shown that it was soluble in water up to 1% by weight. Each of the samples containing the additives was handled

Publication Date: January 1, 1964 | doi: 10.1021/ba-1964-0043.ch023

in the same manner as the additive-free surface, so that all would have about the same exposure to water vapor. In this way differences in wettability were observed, even though we were unable to determine the precise critical surface tension for the polymer itself. It subsequently was found that the contact angles on the films containing additive VIII did not seem to be susceptible to the presence of the small amounts of water vapor in the atmosphere, and did not change significantly upon standing in the room at 15 to 20% relative humidity up to several hours. The contact angles on PAM containing 0.6 and 1.2% of additive VIII given in Table V show that even 0.6% additive dramatically increased the contact angles of the liquids on the polymer surfaces. Contact angles for the n-alkanes approached those reported for surfaces consisting largely of $-CF_3$ groups [6, 15, 20, 22]. A plot of cos θ *vs.* γ_{LV}° (see Figure 4) using the data for the n-alkanes shows that for this surface γ_c is 10.4 dynes per cm. There was no further decrease in γ_c when the additive concentration was increased from 0.6 to 1.2%, indicating that even at the lower concentration maximum adsorption of the additive had developed at the interface.

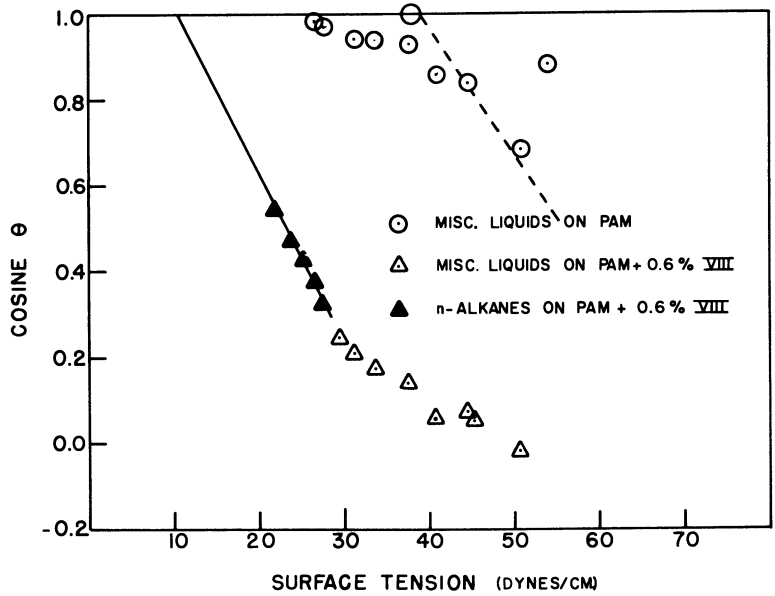

Figure 4. Cos θ vs. γ_{LV}° for various pure liquids on polyacrylamide surfaces

Besides being added to aqueous solutions of PAM, additive VIII was also added to a solution of the acrylamide monomer prior to polymerization. After polymerization, the PAM was purified as described earlier and films were prepared by solvent evaporation with no further addition of surface active additive VIII. The contact angles given in the last column of Table V for the organic liquids on this film correspond, within the limits of experimental error, to those obtained

when the additive was added to an aqueous solution of the polymer just prior to formation of the film.

Discussion

Small amounts of appropriate fluorine-containing compounds, 1% by weight or less, significantly modified the wetting properties of several polymer surfaces. The fluorine-containing surface active agents were equally effective when added to the monomer prior to polymerization or to solutions of the polymer in a volatile solvent. If one considers the polymer as a liquid of very high viscosity, it should be immaterial how the additives are incorporated in the polymer, provided sufficient time is allowed for diffusion of the solute to the interface. The less viscous the polymer, the more rapidly adsorption equilibrium will be attained. One further property of a film formed by this technique is that it should be self-healing—that is, any surface active molecules lost from the film will be replaced by the diffusion of additional material into the interface. The rate of self-healing will be dependent upon the rate of diffusion of the fluorocarbon derivatives in the bulk polymer, and may be accelerated by heating the solid polymer or otherwise lowering its viscosity.

It is apparent from this study that in many ways the problems involved in selecting surface active agents for polymeric systems are analogous to those of finding surface active agents for any organic liquid, the primary difference being the slow rate of diffusion of the additives in the polymer. The problem of surface activity in a polymeric system is thus a logical extension of the previous studies of surface activity in organic liquids, the effectiveness of a specific additive in a polymer being dependent upon its organophilic-organophobic balance with respect to that polymer. In the present study only fluorocarbon derivatives were used as surface active additives, but many hydrocarbons as well as silicone compounds would also be expected to show some surface activity in polymers. The primary advantage of a fluorine-containing compound is that it will cause a much greater decrease in surface free energy, and thus give a polymer surface a lower wettability. A critical surface tension of 10 to 11 dynes per cm. was observed for PAM containing only 0.6% by weight of a fluorinated additive, while PMMA and the PVeC copolymer had γ_c values of approximately 20 dynes per cm. when small amounts of appropriate additives were present at the interface. The critical surface tensions of PMMA and the PVeC copolymer were thus reduced 20 dynes per cm., while that of PAM was lowered at least 25 dynes per cm. These large decreases in critical surface tension reflect the change in surface composition which has taken place, the polymer molecules being replaced in the interface by closely packed CF_2 and CF_3 groups.

The presence of a closely packed layer of adsorbed molecules at a polymer surface will have a marked effect on many of its surface properties, such as friction, adhesiveness, and wettability. These properties of an adsorbed film have already found some application in industry. Allan [1] has demonstrated that small amounts of oleylamide incorporated in polyethylene foil will diffuse to the surface of the foil and greatly reduce the friction and adhesion between sheets of the plastic. A committee from the Piedmont Section of the American

Publication Date: January 1, 1964 | doi: 10.1021/ba-1964-0043.ch023

Association of Textile Chemists and Colorists recently [3] described the incorporation of small amounts of fluorocarbon derivative in a polymeric material normally used to treat textiles for water repellency. They observed that the fluorocarbon preferentially adsorbed at the interfaces and decreased the γ_c values to 16 to 18 dynes per cm. Their films clearly showed the ability to self-heal, for when the initially adsorbed layer was deliberately scraped off, additional molecules quickly adsorbed at the interface when the polymer matrix was recured at an elevated temperature. The usefulness of adsorbed films of surface active molecules is thus apparent, and one may expect wide application of this technique to specific problems. The present study, in combination with previous investigations of wettability and surface activity in organic liquids, forms an excellent guide for the design and synthesis of further surface active agents for polymeric systems.

Acknowledgment

The authors thank L. G. Isaacs of this laboratory for preparing the polymer films that were studied.

Literature Cited

(1) Allan, A. J. G., J. Colloid Sci. 14, 206 (1959).
(2) Allan, A. J. G., J. Polymer Sci. 38, 297 (1959).
(3) American Association of Textile Chemists and Colorists, Piedmont Section, Am. Dyestuff Reptr. 52, 83 (1963).
(4) Bernett, M. K., Jarvis, N. L., Zisman, W. A., J. Phys. Chem. 66, 328 (1962).
(5) Bernett, M. K., Zisman, W. A., Ibid., 64, 1292 (1960).
(6) Ibid., 66, 1207 (1962).
(7) Craig, R. G., Berry, G. C., Peyton, F. A., Ibid., 64, 541 (1960).
(8) Ellison, A. H., Zisman, W. A., Ibid., 58, 260 (1954).
(9) Ibid., p. 503.
(10) Ibid., 60, 416 (1956).
(11) Ibid., 63, 1121 (1959).
(12) Faurote, P. D., Henderson, C. M., Murphy, C. M., O'Rear, J. G., Ravner, H., Ind. Eng. Chem. 48, 445 (1956).
(13) Fox, H. W., Zisman, W. A., J. Colloid Sci. 5, 514 (1950).
(14) Guenthner, R. A., Vietor, M. L., Ind. Eng. Chem. Prod. Res. Develop. 1, 165 (1962).
(15) Hare, E. F., Shafrin, E. G., Zisman, W. A., J. Phys. Chem. 58, 236 (1954).
(16) Jarvis, N. L., Zisman, W. A., Ibid., 63, 727 (1959).
(17) Ibid., 64, 150 (1960).
(18) Ibid., p. 157.
(19) O'Rear, J. G., Sniegoski, P. J., Naval Research Lab., NRL Rept. 5795 (July 18, 1962).
(20) Schulman, F., Zisman, W. A., J. Colloid Sci. 7, 465 (1952).
(21) Shafrin, E. G., private communication.
(22) Shafrin, E. G., Zisman, W. A., J. Phys. Chem. 66, 740 (1962).
(23) Sorenson, W. R., Campbell, T. W., "Preparative Methods of Polymer Chemistry," p. 179, Interscience, New York, 1961.
(24) Wolfram, E., Kolloid Z. 182, 75 (1962).
(25) Zisman, W. A., Advan. Chem. Ser., No. 43, 1 (1963).
(26) Zisman, W. A., "Constitutional Effects on Adhesion and Abhesion," General Motors Research Symposium on Adhesion and Cohesion, July 25, 1961.
(27) Zisman, W. A., "Decade of Basic and Applied Science in the Navy," NRL Rept. 4932, May 15, 1957, ONR Decennial Symposium, Washington, D. C., March 19, 1957.

Received March 27, 1963.

24

Prevention of Liquid Spreading or Creeping

Marianne K. Bernett and William A. Zisman

U. S. Naval Research Laboratory, Washington 25, D. C.

Publication Date: January 1, 1964 | doi: 10.1021/ba-1964-0043.ch024

Spreading of liquids over solid surfaces can be prevented by three approaches: The liquid can be inherently nonspreading in its pure state, it can be made nonspreading by addition of carefully selected solutes, or the solid surface can be modified by coating it with substances of low surface energy. Requirements for nonspreading oils for watches and fine instruments are discussed in terms of the basic mechanism of spreading and wetting, the effect of chemical composition on spreading, and the use of oleophobic additives. The solid surface can be modified by monolayer coatings. These sometimes can be too readily removed, whereas coatings of selected fluorinated polymers remain effective when laid down in the form of a circular ring surrounding the oil drop.

In the lubrication of large machinery the whole bearing is usually surrounded by a viscous lubricant which is continually renewed at determined intervals of time. Conditions for the lubrication of watches, clocks, and many indicating meters, however, are quite different, since the oil in the watch must be left in the bearing for months or even years, and during this long interval must remain in the form of a drop without spreading away. Thus, the most important requirement for a good watch oil is its retention in a small droplet at the lubricating point over long periods of time. By the seventeenth century, certain bearings of watches and clocks consisted of a steel pivot rotating on a ruby or sapphire, each lubricated with a tiny drop of a nonspreading oil.

Practice today is not much different, except that synthetic corundum (α - Al_2O_3) has replaced the natural gems. Until about 30 years ago, nonspreading clock oils had been obtained mainly by various refining procedures from porpoise jaw, blackfish, olive, neat's-foot, and bone oils by procedures which were more or less considered as trade secrets. The principal difficulties with these products were their tendencies to evaporate, to thicken, and to deposit gums. Batches of oil from the same source were often too variable in nonspreading and stability

In Contact Angle, Wettability, and Adhesion; Fowkes, F.;
Advances in Chemistry; American Chemical Society: Washington, DC, 1964.

properties, effective product control was rare, and oil specifications were inadequate. During the twentieth century Woog [27, 28] and Bulkley and Snyder [8] found that on addition of small concentrations of oleic or stearic acid as well as olive, castor, and lard oil, the spreading tendency of refined oils on polished steel, brass, and jewel bearing material was decreased. They concluded that this reduced spreading tendency was due to a very thin coating deposited on the bearing surface. Woog [27, 28] developed and patented a process in which a dilute solution of the fatty acid in a volatile solvent was used to coat the bearing surfaces with a thin film or "epilame" of fatty acid. Some refined oils suitable for watch lubrication did not spread on such a film-coated surface. Since the film, however, was removed whenever the bearing was cleaned with a solvent, a new film treatment was necessary after every cleaning. In mass production, therefore, the process did not justify itself, especially since this process also promoted increased oxidation.

As the supply of effective, high-quality clock oils became increasingly meager and the cost mounted accordingly, several clock manufacturers started research on clock oils and their synthesis. The best known American investigation, supported first by the Elgin National Watch Co. and later during World War II by the Navy Bureau of Aeronautics, was conducted by Barker and coworkers [1, 10] of the Mellon Institute. During an extensive search among organic liquids with the requisite physical and chemical properties for clock lubricants, including nonspreading at subzero temperatures, they prepared several hundred synthetic compounds and 185 blends [10]. They developed a useful synthetic clock oil (N-28) which was acceptable to the military late in World War II and was the basis for military clock oils used since [21]. Despite this success, lower vapor pressure, better oxidation stability, lower freezing point, and lower cost were desired. In addition, at the end of World War II there still was no theory offered to explain the nonspreading of either these synthetic oils or the formerly used natural products.

In the decade after the war, Zisman and coworkers at the U. S. Naval Research Laboratory investigated the surface chemistry of the spreading of oils and other liquids on solids and by 1958 had published an essentially complete picture of the various mechanisms involved. In another paper Zisman [29] has reviewed our present knowledge of the molecular mechanisms and theory relating to the wetting of solid surfaces.

Prevention of Spreading by Oleophobic Additives

It has been established that the spreading tendency of a liquid decreases with increase of its contact angle, θ, on the respective solid surface and that the cosine of the contact angle bears a linear relationship to the surface tension of the liquid, γ_{LV°. The relation between contact angle θ, surface tension γ_{LV°, and work of adhesion W_A is given by the classic Dupré equation [13]

$$W_A = \gamma_{LV^\circ} (1 + \cos \theta) + f_{SV^\circ}$$

where f_{SV° stands for the specific free energy decrease on immersion of the solid in the saturated vapor of the liquid. Nonvolatile liquids

Publication Date: January 1, 1964 | doi: 10.1021/ba-1964-0043.ch024

exhibiting nonzero contact angles (liquids useful for clock oils) have negligible f_{SV° values [30]. The Dupré equation demonstrates that maximum adhesion of the droplet of oil can be expected when γ_{LV° is as large and θ as small as possible; in qualitative agreement, it has been found that all of the useful clock oils have γ_{LV° values above 35 dynes per cm. at 20°C. and θ values smaller than 15°.

Pure liquids exist which are inherently nonspreading on high-energy surfaces. The background on the wettability of low-energy surfaces [29] has proved essential in explaining the spreading properties of these liquids on high-energy surfaces. The pure nonspreading liquids can be grouped into three classes. The first class, the autophobic liquids [18], is exemplified by molten stearic acid, octyl alcohol, tricresyl phosphate, and trichlorodiphenyl [26]. The first molecules of these liquids to come in contact with the solid adsorb instantly to form a monomolecular film whose critical surface tension of wetting is less than the surface tension of the liquid, thus preventing it from spreading upon its own adsorbed film. The second class is comprised of numerous esters which, although able to spread completely on metal surfaces, are unable to spread on glass, silica, and sapphire. The ester hydrolyzes immediately upon adsorbing on these hydrated solid surfaces [15]; of the two products of the hydrolytic reaction, the one having the greater average lifetime of adsorption remains to coat the surface with a close-packed monolayer, thereby blocking further progress of the hydrolysis reaction. If this protective monolayer has a critical surface tension of wetting which is less than the surface tension of the liquid ester, nonspreading results—i.e., the ester is unable to spread upon the adsorbed film of one of its own hydrolyzed products.

It can now be understood why many of the early clock oils could be made from such raw materials as porpoise jaw oil, blackfish oil, bone oil, and olive oil. Such substances are rich in fatty acid esters whose hydrolysis, though slight, releases fatty acids and alcohols capable of serving as effective oleophobic film-forming solutes. A third class of nonspreading liquids may exist, comprised of those liquids whose surface tensions are so high and adhesional energies so low that the energy of adhesion is smaller than that of cohesion and spreading is thus thermodynamically impossible—i.e., the Harkins spreading coefficient is negative. If such liquids exist, they differ from autophobic liquids in not leaving a film behind them when rolled over a horizontal polished solid surface [26].

By utilizing the principles responsible for the nonspreading qualities of pure liquids, ways can be devised to impart those same qualities to spreading liquids. This result can be achieved by the addition of selected solutes which act in either of two manners. The first approach is based on the ability of the solute to adsorb on a high-energy surface and form a monolayer with a critical surface tension of wetting less than the surface tension of the original liquid. Having modified the higher-energy surface, this monolayer then prevents the liquid from spreading on that surface. When the liquid involved is an oil, the solute is said to make the oil become "oleophobic" to the solid surface, and the solute is called an oleophobic additive [6, 7, 14, 25, 32]. If the liquid surface tension is below 24 dynes per cm., the oleophobic additive must be a fluorocarbon or silicone derivative; if it is above 24 dynes per cm., a fatty acid or other paraffinic polar compound will be effective. When the liquid

Publication Date: January 1, 1964 | doi: 10.1021/ba-1964-0043.ch024

surface tension is above 30 to 32 dynes per cm., a branched-chain or cyclic hydrocarbon derivative can be used as the polar solute.

The second approach is based on the addition of a more volatile solute which creates a surface tension gradient at the edge of an oil drop that opposes the spontaneous spreading of the oil. This method is reported by Bascom, Cottington, and Singleterry [2]. The use of oleophobic additives as a means of obtaining nonspreading properties presents a number of problems, such as their limited solubility in many oils, or the necessity of using very low concentrations of the additive so that θ will not become so large as to cause inadequate adhesion. When θ is kept small enough to be below 15°, the additive concentrations necessary are often so low that any careless handling of the lubricant during storage or pouring from one container to another may cause a significant decrease in the oleophobic property because of the adsorption by the active ingredient on the walls.

Synthetic clock oils have been and can readily be found from among the aromatic esters of aliphatic alcohols or acids [1, 12, 15]; some have high enough surface tensions to be autophobic, and many are nonspreading because their hydrolytic products adsorb to form low-energy surface films. The introduction of aromatic rings in the molecular structure always increases the slope of the curve of viscosity *vs.* temperature and hence decreases the temperature range over which the oil can be used, a difficulty evident in the work of Barker *et al.* [1], O'Rear [22], and Portnoy *et al.* [24]. Recent results of Cottington, Murphy, and Singleterry [11] on the control of oil spreading by the use of certain silicone additives capable of adsorbing as monolayers on high-energy surfaces have shown a new route to making nonspreading oils. Their results have already led to the development of a useful clock oil from an ester containing only one aromatic ring [23].

One of the unexpected results of the long-term NRL study of spreading and wetting was to dispel an old, widely held, belief that a good lubricating liquid has better wetting and adhering qualities to a bearing surface than a poor lubricant. It was shown that the ability of liquids to spread on metals has no necessary relation to their lubricating properties [17, 19, 31, 32]. On the one hand some liquids, such as tricresyl phosphate, have exceptionally good boundary lubricating properties but do not spread on clean metals. For this reason, clock oils containing tricresyl phosphate are in use, but they have steep viscosity *vs.* temperature graphs and the fault that even the slightest decomposition will liberate corrosive phosphoric acid. On the other hand, liquids like the dimethyl silicones have inadequate boundary lubricating properties, yet spread freely on all clean metals. In general, it can be shown that the molecular structural requirements for good spreading ability are very different from those for good boundary lubrication properties.

Control of Spreading through Modification of Surface

The previously reviewed investigations of spreading and wetting make it possible to give a simple and fundamental explanation of the epilame treatment of Woog [27, 28]. Essentially the epilame is a modification of the substrate surface. A close-packed adsorbed monolayer of a higher fatty acid, such as stearic acid, has a γ_c value of 24 dynes per cm. Any oil or other liquid having a surface tension, $\gamma_{LV}°$, at 20°C.

Publication Date: January 1, 1964 | doi: 10.1021/ba-1964-0043.ch024

greater than 24 dynes per cm. would therefore be nonspreading on such a monolayer, and the equilibrium contact angle would be greater the larger the difference from liquid surface tension to critical surface tension.

The epilame treatment can be improved greatly by applying our present knowledge of the constitutional laws of wetting. Since a silicone resin coating on a solid surface can be prepared having a γ_c value as low as 24 dynes per cm. [11, 30], such a coating can be used in place of the fatty acid as the epilame. It is possible to lay down such a silicone coating on a metal or gem from an air-drying lacquer or dilute benzene solution; thus, an effective and more durable epilame treatment can be made using such a silicone air-drying varnish. An immediate advantage would be the less destructive action of many solvents used in cleaning watches and clocks to the silicone coating than to Woog's epilame of stearic acid.

Another way to prevent spreading of the instrument oil is to use one of several commercially available fluorinated polymers whose low γ_c values render them especially attractive for such application. Suitable coatings can be made from Teflon (polytetrafluoroethylene), FEP Teflon (a commercial copolymer of tetrafluoroethylene and hexafluoropropylene), or fluorinated esters of poly(acrylic) or poly(methacrylic acid); their γ_c values are 18.5 [16], 17.0 [3, 4], 11.1, and 10.6 dynes per cm. [5], respectively. Each such coating will prevent the spreading of any lubricating liquid known. However, one essential precaution must be observed in using such coatings. Since these liquids have such low γ_c values, the drop of oil placed on top of the coating will have a contact angle so large that the adhesion of the liquid to the coating will be inadequate, and a slight jar of the instrument might detach the oil drop. This difficulty can readily be avoided, however, by applying the fluorocarbon resin coating in the form of a circular ring surrounding the oil drop. If the oil in the middle portion does not rest on the coating, there will be adequate adhesion to the bearing surface.

Techniques for Depositing Coatings. Teflon coatings are normally applied from a dispersion in water [12]; in applying them there is usually difficulty with the requirement of a brief bake at temperatures around 700°F. in order to sinter the Teflon particles, obtain good film adhesion, and eliminate the water and additives. This treatment is often impractical in the manufacture of many instruments. The coating procedure is more advantageous with FEP Teflon [20], since its melting point of 545°F. is much lower; in addition, small bearings may be coated by immersing each in a fluidized bed of the hot polymer powder [9].

A more generally applicable and simpler method, which does not require any heat treatment, can be used with either of the fluorinated polymers prepared as research products by the Minnesota Mining and Manufacturing Co. The chemical formulas of the respective monomers investigated at NRL are $C_7F_{15}CH_2OCOC(CH_3)=CH_2$, 1*H*, 1*H*-pentadecafluoro-octyl methacrylate (polymer A), and $C_8F_{17}SO_2N(C_3H_7)C_2H_4OCOCH=CH_2$, 2-(*N*-propylperfluoro-octane sulfonamido) ethyl acrylate (polymer S), whose properties have been described [5]. These low surface-energy films can be readily laid down from a solution in an appropriate solvent such as xylene hexafluoride or benzotrifluoride which, after slow evaporation, leaves a suitable coating. A fine camel's-hair brush can be used to paint bands of any desired width (such as 1 to 3 mm.)

Publication Date: January 1, 1964 | doi: 10.1021/ba-1964-0043.ch024

around a circular area surrounding the bearing of sufficient size to contain the oil drop.

These fluorinated materials have the additional advantage of not being readily dissolved by any of the cleaning solvents commonly used in the instrument field. Organic solvents such as xylene, petroleum ether, or AMSCO 140 solvent (140°F. flash point aliphatic solvent manufactured by American Mineral Spirits Co.) had no adverse effect on polymer A coatings on stainless steel, brass, and aluminum disks when totally immersed for 3 weeks at ambient temperature. Ammonia-containing aqueous watch cleaning solutions are capable of detaching the coating after prolonged immersion without dissolving it (Extra Fine Solution, L and R Manufacturing Co., started to loosen the film edges on a stainless steel disk after 2 days' immersion and completely detached the film after 2 weeks; Concentrate Cleaning Solution, Zenith Cleaning Fluid Co., had the same effect, but after an immersion period of 4 weeks). Fluorinated solvents, such as Freon TF (b.p. 117.6°F.), understandably act as good solvents on the polymer.

To determine the applicability of these coatings for instrument-oil barriers for drops of either spreading or nonspreading watch oils, spreading tests were made on three smooth surfaces of 18/8 stainless steel, fused borosilicate glass, and synthetic sapphire. The surfaces were freshly cleaned according to the procedure described by Fox, Hare, and Zisman [14]. Small rings of a fluorocarbon coating were deposited on each surface by the above-mentioned techniques. Three drops of each of the five chemically diverse spreading oils (freshly percolated to remove any polar impurities) and of one synthetic nonspreading oil (Table I) were placed in the uncoated center of the ring, one drop

Table I. Oils Observed for Spreading in Uncoated Center of Fluorinated Polymer Rings

Spreading Oil	Surface Tension (γ_{LV}°) at 25°C., Dynes/Cm.	Source
Bis (2-ethylhexyl) sebacate	30.1 (20°)	Rohm and Haas
Bis (1H, 1H, 7H-dodecafluoroheptyl) 3-methyl glutarate	24.6	Naval Research Laboratory
Silicone DC 200 (20 cs. at 25°C.)	20.6	Dow Corning
Petroleum lubricating oil MS 3042	28.9	Esso Standard Oil
Ucon Fluid DLB-140E	29.1	Union Carbardide Chemical Co.
Nonspreading clock oil 14-L-16	32.3	Lehigh Chemical Products Co.

to a ring. These oils were then observed periodically while stored in a dust-free closely confined chamber at 20°C. Each oil drop spread

Publication Date: January 1, 1964 | doi: 10.1021/ba-1964-0043.ch024

initially over the uncoated surface within each circle and it did this for each of the three different surfaces used, until it came in contact with the inner rim of the ring-shaped coating of the fluorinated polymers.

Figure 1 shows the results after 100 days for the stainless steel substrate. All oil drops, with the exception of one system, still remained confined within the rings after 100 days. The one exception was

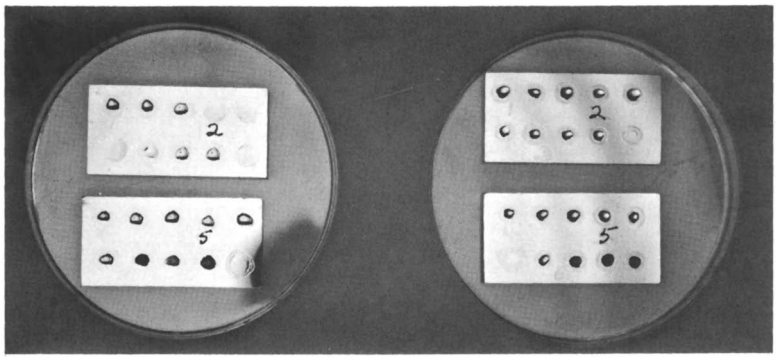

Figure 1. Three drops of each of six oils after 100 days at 20°C. on stainless steel confined by polymer S (left) and polymer A (right)

Only oil 2 for polymer S spread

observed with the fluorinated ester drops, bis(1*H*, 1*H*, 7*H*-dodecafluoroheptyl) 3-methyl glutarate, which spread over the coating of polymer S only (Figure 1, upper left, series 2), regardless of the nature of the substrate surface. After 3 to 4 days, this oil began to creep over the inside rim of the coating, and then it slowly continued over the whole width of the band, and remained there for the 100-day observation period. On stainless steel the oil drop never passed the outer rim of fluoropolymer S; on glass the oil reached the outer rim of about half the band, but never did on the opposite half; on sapphire, one of the three drops of the fluorinated oil spread after 90 days beyond the outer circumference onto the clean surface.

The reason why only the fluorinated ester drops spread over one of the fluorinated coatings can be explained by mutual attraction promoted by the structural and chemical affinity of the two fluorine-containing organic compounds. It had been established [5] that the fluorinated side chains of polymer S are sterically less closely packed and have more freedom of rotation than those of polymer A; they may thus permit some lateral penetration of the closely related fluoro chains of the glutarate ester, whereas polymer A with its tight array of side chains is impervious to such penetration. The fluorinated ester exerts a slight solvent action on polymer S, but not on polymer A, when the polymer is totally immersed in the ester for periods longer than 10 days at ambient temperature, or 2 days at 50°C.

Lubricants are required to remain nonspreading at subzero as well as high temperatures in modern instruments. After 100 days at 20°C., the above-mentioned specimens were therefore subjected to cycling between + 50° and -20°C. for 24 hours at each temperature,

Publication Date: January 1, 1964 | doi: 10.1021/ba-1964-0043.ch024

to observe if spreading could be induced or whether the adhesion of the coatings remains acceptable. After 20 full cycles (40 days), all liquids with the exception of the fluoroester were still contained within the rings of polymer S. On sapphire and glass some of the liquid drops, especially nonspreading clock oil 14-L-16, had slightly flattened out, whereas on stainless steel the drop shape remained unaltered. Most of the liquids began to creep over the containing bands of polymer A after two full cycles but did not go beyond them even after the 20 full cycles. Again the drops on stainless steel showed the least effect. These observations may indicate that the coefficient of expansion of polymer S is not so different from those of steel, glass, and sapphire, that it adversely affects its adhesion to these materials. Coatings of polymer A, however, are more susceptible to temperature changes; this is evidenced by the spreading of almost all oils to the rim of the polymer ring on sapphire and glass. The adhesion relative to stainless steel is much greater, as shown by the almost unchanged shape of the oil drops after full cycling.

Conclusions

Liquid spreading can be prevented by three approaches:

1. Use of a pure nonspreading liquid.
2. Modification of a spreading oil through additive agents. Selected solutes can be added which act either as additives of low surface tension capable of adsorbing as monolayers whose critical surface tension is lower than the surface tension of the liquid; or as additives of higher volatility which create a surface tension gradient.
3. Modification of the solid surface. The surface can be completely coated by monolayers of low surface energy compounds on which oil drops having higher surface tension will not spread, or covered with narrow ring coatings of insoluble polymers of low surface energy, such as fluorocarbon derivatives, which surround the oil drop.

Since the nonspreading oil feature can be obtained by the surrounding ring-shaped coating of a fluorocarbon resin, the nonspreading requirement of the oil is not essential. Hence, it becomes possible to employ any one of the many available spreading-type lubricating oils (such as petroleum, polyethers, or aliphatic diesters) which fulfill to a higher degree than present clock oils all of the other important requirements of such oils—i.e., small temperature coefficient of viscosity, low pour point, lowest possible evaporation rate, and low cost as well as excellent boundary lubricating properties, rust inhibition, and oxidation stability.

Literature Cited

(1) Barker, G. E., Alter, G. E., McKnight, C. E., McKleven, J. R., Hood, D. M., ASTM Bull., No. **139**, 25 (March 1946).
(2) Bascom, W. D., Cottington, R. L., Singleterry, C. R., Advan. Chem. Ser. No. 43, 355 (1963).
(3) Bernett, M. K., Zisman, W. A., J. Phys. Chem. 64, 1292 (1960).
(4) Ibid., 65, 2266 (1961).
(5) Ibid., 66, 1207 (1962).

(6) Bigelow, W. C., Glass, E., Zisman, W. A., J. Colloid Sci. **2**, 563 (1947).
(7) Bigelow, W. C., Pickett, D. L., Zisman, W. A., Ibid., **1**, 513 (1946).
(8) Bulkley, R., Snyder, G. H., J. Am. Chem. Soc. **55**, 194 (1933).
(9) Checkel, R. L., Modern Plastics **36**, 125 (1958).
(10) Chem. Eng. News **23**, 524 (1945).
(11) Cottington, R. L., Murphy, C. M., Singleterry, C. R., Advan. Chem. Ser. No. 43, 341 (1963).
(12) DuPont Co., Fabrics and Finishes Division, "Teflon Finishes," New Product Tech. Bull. **1**, 6th ed. (May 1956).
(13) Dupré, A., "Théorie Méchanique de la Châleur," p. 369, Gauthier-Villars, Paris, 1869.
(14) Fox, H. W., Hare, E., Zisman, W. A., J. Colloid Sci. **8**, 194 (1953).
(15) Fox, H. W., Hare, E., Zisman, W. A., J. Phys. Chem. **59**, 1097 (1955).
(16) Fox, H. W., Zisman, W. A., J. Colloid Sci. **5**, 514 (1950).
(17) Gunderson, R. C., Hart, A. W., "Synthetic Lubricants," Reinhold, New York, 1962.
(18) Hare, E. F., Zisman, W. A., J. Phys. Chem. **59**, 335 (1955).
(19) Kobe, K. A., McKetta, J. J., "Advances in Petroleum Chemistry and Refining," Vol. II, Chap. 2, "Trends in Lubricants," by W. A. Zisman and C. M. Murphy, Interscience, New York, 1959.
(20) Mallouk, R. S., Thompson, W. B., SPE **14**, 42 (October 1958).
(21) Military Specification MIL-L-3918, Aug. 29, 1955.
(22) O'Rear, J. G., "Synthesis and Characterization of Esters for Nonspreading Lubricants," Naval Research Lab., Rept. **3891** (August 1951).
(23) O'Rear, J. G., U. S. Naval Research Laboratory, Washington 25, D. C., private communication.
(24) Portnoy, S., Verderame, F., Messina, J., Gisser, H., Ind. Eng. Chem., Chem. Eng. Data Ser. **3**, 287 (1958).
(25) Shafrin, E. G., Zisman, W. A., J. Phys. Chem. **64**, 519 (1960).
(26) Timmons, C. O., Zisman, W. A., "A Study of Autophobic Liquids on Platinum by the Contact Potential Method," Naval Research Lab., NRL Rept. 6020 (1963).
(27) Woog, P., Compt. Rend. **181**, 772 (1925).
(28) Woog, P., "Contribution à l' Etude du Graissage Onctuosité," Delagrave, Paris, 1926.
(29) Zisman, W. A., Advan. Chem. Ser., No. 43, 1 (1963).
(30) Zisman, W. A., "Constitutional Effects on Adhesion and Abhesion," in "Symposium on Adhesion and Cohesion," P. Weiss, ed., Elsevier, New York, 1962.
(31) Zisman, W. A., Ind. Eng. Chem. **45**, 1406 (1953).
(32) Zisman, W. A., "Relation of Chemical Constitution to the Wetting and Spreading of Liquids on Solids," in "A Decade of Basic and Applied Science in the Navy," Office of Naval Research, 1957.

Received March 27, 1963.

25

Effect of Polar-Nonpolar Additives on Oil Spreading on Solids, with Applications to Nonspreading Oils

ROBERT L. COTTINGTON, CHARLES M. MURPHY, and CURTIS R. SINGLETERRY

U. S. Naval Research Laboratory
Washington 25, D. C.

Publication Date: January 1, 1964 | doi: 10.1021/ba-1964-0043.ch025

Nonspreading oils can be prepared from many lubricating oils by proper choice of an adsorbable additive, but an additive that makes one oil nonspreading may cause violent spreading of another. This anomalous spreading is produced by surface tension gradients resulting from adsorptive depletion of additive along the edge of the drop. Oily contamination of a surface may also cause spreading of an otherwise nonspreading oil. Since contamination rarely produces a critical surface tension above 30 dynes per cm., a practical nonspreading oil should have a surface tension above this value. Effective additives for nonspreading include the silicones, fluoroesters, amine–organic acid salts, high molecular weight organic acids, alcohols, or amines, and some oil-soluble soaps. A predeposited film of a polysiloxane prevents the spreading of most oils on metal surfaces.

For an important group of applications the spreading characteristic of a lubricating oil may be as important as its viscosity, oxidation stability, or boundary lubricity. This has long been recognized by watchmakers, who require an oil that will not spread from jewel bearings to the hair spring, where it may alter the escapement rate. Jeweled bearings in meters for military electrical equipment require a similar lubricant. The nonspreading property of oil is also important because it minimizes evaporation; a drop of oil after spreading may expose as much as a thousand times the original surface. A drop of a good nonspreading oil will remain almost undiminished on a test plate for a year or more, whereas a spreading oil of equal volatility will be lost completely within one or two weeks. A spreading oil film is also undesirable

In Contact Angle, Wettability, and Adhesion; Fowkes, F.;
Advances in Chemistry; American Chemical Society: Washington, DC, 1964.

because it promotes the collection of dust and lint which absorb additional oil. The nonspreading characteristic of instrument lubricants may be expected to assume additional importance as problems emerge in maintaining highly instrumented missiles in instant readiness over a period of years. Nonspreading oils may also find critical uses in satellite instruments, which cannot be relubricated, and which are sometimes exposed to evaporation in a high vacuum.

Nonspreading oils are not new [1, 2, 8, 10, 11]. Earlier work in this laboratory [6] has established criteria for spreading or nonspreading of liquids on solid surfaces. This work [18] explains the behavior of watch oils that have already been developed by empirical methods and provides the basis for a rational approach to the formulation of instrument oils to meet more exacting requirements.

Such an approach must choose between the attempt to synthesize a truly autophobic liquid having suitable physical properties and the search for additive-oil combinations that will be reliably nonspreading. The truly autophobic liquids reported to develop contact angles greater than 3° are aromatic phosphates or halides. Since such compounds have large viscosity-temperature coefficients, the most promising approach to the preparation of nonspreading oils with better low-temperature properties would appear to be a basic study of the effect of surface active additives on the spreading behavior of nonautophobic oils. The results of such a study should provide rational guidance for the formulation of nonspreading oils from available low-temperature lubricants of the spreading type.

The present investigation has established that almost any oil can be made nonspreading on clean and smooth stainless steel or sapphire surfaces by the inclusion of a proper additive. However, unsuitable additives may sometimes accelerate rather than prevent spreading. This report describes the diverse wetting phenomena observed with oil solutions of polar-nonpolar molecules and identifies the properties favorable to the formulation of a stable nonspreading lubricant. It also examines new possibilities for preventing spreading by predepositing silicone coatings in a manner somewhat analogous to the "epilame" treatment of bearings with stearates and/or stearic acid.

Publication Date: January 1, 1964 | doi: 10.1021/ba-1964-0043.ch025

Experimental

Materials. The bis(2-ethylhexyl)sebacate (EHS) used in this study was prepared from lubricant grade diester by fractionation in a molecular still and percolation through Florisil adsorbent before use. The other aliphatic esters were research preparations which were percolated through Florisil before use. The fluoroesters were pure materials prepared at this laboratory for other purposes [5, 7, 12], and repercolated through Florisil before use. The fluoroester prepared from a telomer alcohol, bis(1H,1H,7H-dodecafluoroheptyl) 3-methyl glutarate, is referred to as fluoroester I, that prepared from an alcohol terminated by a perfluoromethyl group (1H,1H-undecafluorohexyl alcohol) as fluoroester II, and tris(1H,1H,4H-hexafluorobutyl)tricarballylate as fluoroester III.

The squalane (2, 6, 10, 15, 19, 23-hexamethyltetracosane) was material represented to have an iodine number of 7.5 or less (Eastman No. 7311). It was treated with concentrated sulfuric acid, washed, and

percolated through silica gel and Florisil before use. The absence of polar impurities was shown by its nonspreading on clean water. The pristane (2, 6, 10, 14-tetramethylpentadecane) was a commercial sample which was twice percolated through silica gel and Florisil. The cetane (n-hexadecane) was a highly pure material which was percolated through silica gel and Florisil before use. Isopropylbiphenyl, supplied by the Monsanto Chemical Corp., was percolated through alumina and Florisil before use. The isopropyl 1,9-diphenylnonane was a research sample supplied by the California Research Corp. [15] and percolated through alumina and Florisil before use. It was a mixture of the meta and para isomers. The Grade 1010 petroleum oil was a light aircraft engine oil supplied under specification Mil-0-6081/B(ASG). It was percolated through alumina, fuller's earth, and Florisil.

The DC 510 silicone was material supplied commercially by the Dow Corning Corp. It was used after percolation through Florisil, except where the nonvolatile residue from stripping in a molecular still is specified. This residue was also percolated through Florisil before use. The dimethyl silicone (DC 200), the moderately phenylated DC 550, and the highly phenylated DC 710 were obtained from Dow Corning; they were percolated through alumina and Florisil before use. The fluorosilicone was a sample supplied by Dow Corning Corp. under the designation QF-1-0065. It had a nominal viscosity of 1000 cs. and was percolated through alumina and Florisil.

Procedure. Wetting behavior was studied mostly on stainless steel surfaces (304 SS: 18% Cr, 8.0% Ni, 2.0% Mn, 0.75% Si) which formed the ends of short cylinders 3/4 inch in diameter and 1/2 inch long. Special care was exercised to prepare the test pieces from bar stock containing a minimum of microscopic inclusions and voids. The cylinders were ground to exact height and polished on a pitch lap to a high mirror finish. The surface was cleaned immediately before use by a light polishing with γ-alumina on a metallographic wheel, rinsed with hot distilled water, and dried at room temperature. Sapphire and fuzed quartz surfaces were cleaned in the same manner before use. Oil droplets were applied to test surfaces with a freshly flamed platinum wire. The drops commonly had initial diameters of 0.03 to 0.10 cm. and were observed under a metallurgical microscope with vertical incident illumination.

Contact angles of 5° or more were measured with a contact angle goniometer. Angles of less than 5° were determined by measurement of the spacing of interference bands generated by monochromatic light on the slope adjacent to the drop edge. This technique permits a precision of 0.1° or better with such small angles. True nonspreading edges were readily distinguished from the edges of slowly spreading drops by the different appearance of the first interference band; this band was sharp and spaced uniformly with the adjacent bands for true nonspreading, but was widened and displaced outwards from uniform spacing in the case of slow-spreading liquids.

The test surface with the oil drop in place was protected from aerosols and dust during observation and storage by enclosing it in a glass cylinder 3 mm. larger in diameter and 2 mm. higher than the test piece. The upper end of the glass cylinder was covered with a standard microscope cover slip through which observations were made. The small volume of air enclosed and the very low head room between the test

Publication Date: January 1, 1964 | doi: 10.1021/ba-1964-0043.ch025

surface and the cover slip reduced aerosol contamination so that test drops could be studied over storage periods of as long as 12 months. Experience indicates that oily aerosols—e.g., from tobacco smoke—are a major source of contamination for clean surfaces.

Results and Discussion

Preliminary experiments revealed four typical patterns of behavior for oil solutions of additives which adsorb strongly at the oil-metal interface:

1. The solution was nonspreading and developed a reproducible contact angle which decreased only moderately during several months' storage of the test assembly at room temperature (Figure 1).
2. The solution spread initially in the same way as a pure oil, but eventually retracted from the wetted area to form many small drops with finite contact angles (Figure 2).
3. The drop exhibited a substantial contact angle, but skated over the surface at a rate of several millimeters per minute. It refused, however, to cross any previous track in its gyrations.
4. The drop spread "catastrophically" at a rate two or three orders of magnitude faster than drops of pure oils of comparable viscosity. In such cases, the spreading liquid formed an intricate dendritic pattern, a series of rapidly growing lobes about the drop circumference, or a reticulated pattern containing parallel threads of liquid obviously related to polishing directions on the solid surface. These patterns, after a few hours of development, were stable, and exhibited finite contact angles at the oil margins (Figure 3).

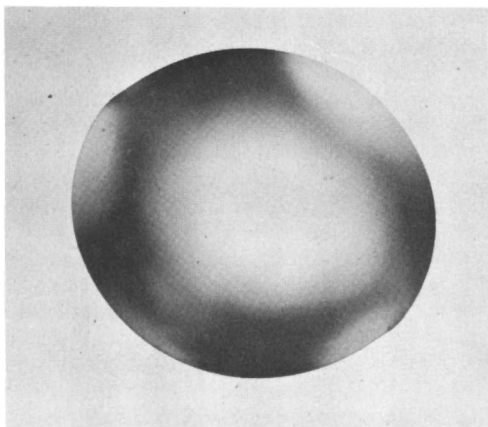

Figure 1. A nonspreading droplet

Squalane containing 0.1% DC 510 silicone, after 30 days

Spreading Anomalies. The anomalous spreading behaviors of types 2, 3, and 4 that are exhibited by some liquids containing strongly adsorbed

Publication Date: January 1, 1964 | doi: 10.1021/ba-1964-0043.ch025

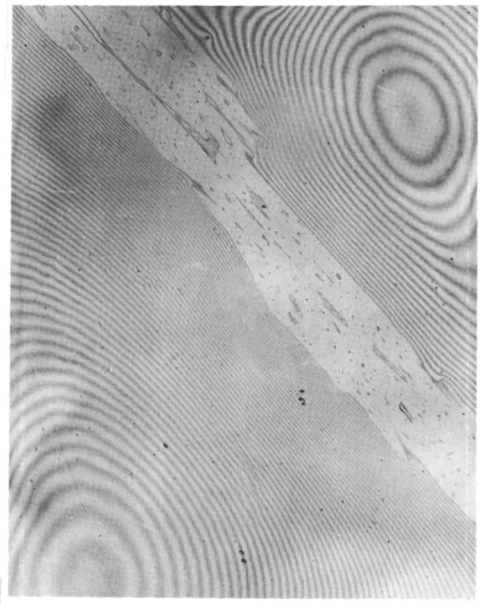

Figure 2. Retraction after initial spreading

Bis(2-ethylhexyl) sebacate containing 1% of sodium dinonylnaphthalene sulfonate

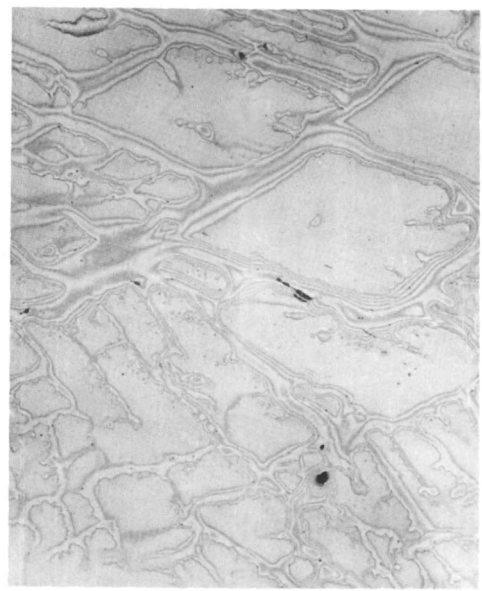

Figure 3. Dendritic spreading of bis (3,5,5-trimethylhexyl) sebacate containing 1% of DC 510 silicone

Publication Date: January 1, 1964 | doi: 10.1021/ba-1964-0043.ch025

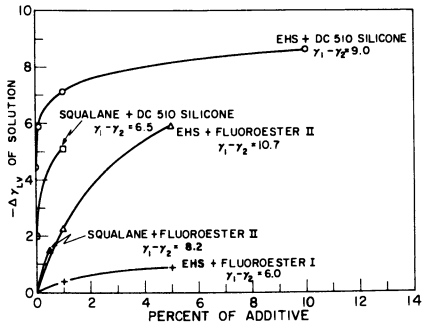

Figure 4. Surface tension lowering in squalane and in bis(2-ethylhexyl) sebacate as a function of concentration of surface active solute

$\gamma_1 - \gamma_2$. Difference between the surface tension of major component and that of liquid added to reduce surface tension

additives need to be clearly understood if such effects are to be avoided in practical formulations of nonspreading oils. The information in Tables I, II, and III and Figure 4 suggests the following explanations for the various behaviors.

Stable spreading behavior of type 1 results when the additive has only a small effect on the surface tension, γ_{LV}, of the oil but deposits a monolayer whose critical surface tension, γ_c, is smaller than γ_{LV}, so that the solution exhibits a substantial contact angle against the adsorbed monolayer. Several such systems are shown in Tables I, II, and III, with data for the decrease in γ_{LV} of the liquid produced by the specified additive. Stable nonspreading compositions result when dimethyl (or lightly phenylated) silicones are added to aliphatic hydrocarbons and when fluoroesters are added to bis(2-ethylhexyl) sebacate. Other examples not included in the table are barium dinonylnaphthalene sulfonate in isopropylbiphenyl and a moderately phenylated (DC 550) silicone in isopropyl-1,9-diphenylnonane. The significant common feature of these systems is that the additive lowers the surface tension of the pure liquid by not more than 5 to 6 dynes per cm.

Normal spreading with delayed retraction to droplets (type 2 spreading) is characteristic of nonvolatile additives which do not lower the surface tension of the solution significantly and whose monolayers at the solid interface have γ_c only slightly smaller than γ_{LV}. Type 2 spreading is understandable if we recall that all the oils studied with nonspreading additives spread normally on metals in the absence of the adsorbed monolayer. It must be assumed that at the instant of application a "foot" or meniscus of oils turns outward at the base of the drop to form a zero contact angle with the solid surface. If the adsorption of additive from this thin film is insufficient to make the critical surface

Publication Date: January 1, 1964 | doi: 10.1021/ba-1964-0043.ch025

Table I. Spreading of Oils Containing DC 510 Silicone on Clean Stainless Steel

Liquid	% Silicone	Spreading Behavior	Surface Tension, γ_{LV}, at 25°C.		
			Base oil	Soln.	$-\Delta\gamma_{LV}$
Pristane	1.0	NS[a]	25.5	23.4	2.1
n-Hexadecane	1.0	NS	27.3	23.6	3.7
Squalane	1.0	NS	27.8	22.7	5.1
1010 petroleum oil	1.0	NS	28.7	23.6	5.1
Bis(3,5,5-trimethylhexyl) sebacate	1.0	Slight spr.	28.4	22.5	5.9
Polypropylene glycol	1.0	Rapid dendritic	29.2	-	-
Trimethylolpropane tri-n-alkanoate	1.0	Rapid dentritic	29.6	22.8	6.8
Bis(2-ethylhexyl) sebacate	1.0	Slight dendritic	30.3	23.2	7.1
Isopropylbiphenyl	0.1	Strong dendritic	34.8	24.1	10.7

[a]NS— Nonspreading.

tension of the surface less than the surface tension of the oil solution, spreading will continue. As the bulk of the droplet passes over the zone of unsaturated adsorption, more additive will be deposited to saturate the monolayer, which will then have $\gamma_c < \gamma_{LV}$, although spreading still continues at the drop margin. The thin film of oil above the monolayer eventually breaks and retracts into irregular droplets. In other cases the ultimate nonspreading may result from *in situ* hydrolysis of an ester to give acids or alcohols which adsorb to form a low energy oil-solid interface after the drop has spread.

Type 3 behavior, in which nonspreading drops move about spontaneously over the surface, is observed for several oils containing amine salts of fluorinated acids. Since there may be some free amine present in the oil, it is suspected that the evaporation of amine vapor from the drop is nonuniform because of air convection; this nonuniformity causes slight differences in the surface tension, so that the surface film flows toward the point of higher surface tension. Such a flow carries along the bulk oil underneath and produces a self-propagating movement of the drop along a straight path. The self-propagation results because the new surface generated on the trailing side of the drop will have a lower surface tension than the surface on the advancing edge. The significance of additive evaporation for this phenomenon is supported by the fact that a second sample, when held at 60°C. for two weeks, lost its nonspreading property and its mobility, and spread normally.

Such mobile behavior has also been noted for drops of squalane and isopropyl-1,9-diphenylnonane supported, respectively, on the adjacent faces of a polished metal disk and a glass cover slip 1 mm. above it. If the drop of squalane (surface tension 27.8 dynes per cm.) is centered on the disk and the drop of the aromatic hydrocarbon (surface tension 34.4 dynes per cm.) on the underside of the cover slip above it is displaced from

Publication Date: January 1, 1964 | doi: 10.1021/ba-1964-0043.ch025

Table II. Effect of Surface Active Solutes on the Spreading Behavior of Bis(2-ethylhexyl)sebacate. (γ_{LV} of pure ester. 30.3 dynes/cm. Experiments on polished stainless steel)

Additive	Additive Concn., Wt. %	Spreading Behavior	$-\Delta\gamma_{LV}$ of Soln.
DC 200 silicone, 70 cs.	0.01	NS, low θ	4.9
	0.1	NS, low θ	
DC 200 silicone, 20 cs.	0.1	Dendritic spr.	
DC 200 silicone, 5 cs.	1.0	Dendritic spr.	
DC 510, silicone 50 cs., stripped sample	0.1	Dendritic spr.	5.9
	1.0	NS, low θ	7.1
	10.0	Slow spr.	8.6
	40.0	Mod. spr. dendritic	9.1
DC 550 silicone, 100 cs.	1.0	Slow spr.	
Fluorosilicone, 1000 cs.	0.01% (sat)	Slow spr.	
Fluoroester I[a]	1.0	NS, low θ	0.4
	5.0	NS, low θ	0.9
Fluoroester II[b]	1.0	NS $\theta = 17°$	2.3
Fluoroester III[c]	1.0	NS	
Barium dinonylnaphthalene sulfonate	2.0	Normal spr., then retracts to irregular drops	0.2
11-H-Eicosofluoroundecylic acid plus dimethyldodecylamine	1.0	NS; self-mobile drops which leave oleophobic trail	0.2
Pentadecafluoro-octanoic acid plus dimethyldodecylamine	1.0	NS; self-mobile drops $\theta = 50°$. Spreads after 2 wk. at 60°C.	0.0

[a]Bis(1H,1H,7H-dodecafluoroheptyl)3-methyl glutarate.
[b]Bis(1H,1H-undecafluorohexyl)3-methyl glutarate.
[c]Tris(1H,1H,4H-hexafluorobutyl)tricarballylate.

Table III. Effect of Additives on the Spreading Behavior of Squalane on Stainless Steel

Oil	Additive	Additive Concn., %	Spreading Behavior	$-\Delta\gamma_{LV}$
Squalane $\gamma_{LV} = 27.8$	DC 510 silicone	0.01	Marginal, 2 of 3 tests were NS	2.0
		0.1	NS	
		1.0	NS, $\theta = 21°$	5.1
		9.5	NS	
	Fluoroester II[a]	0.5	NS	1.5

[a]Bis(1H,1H-undecafluorohexyl)3-methyl glutarate.

Publication Date: January 1, 1964 | doi: 10.1021/ba-1964-0043.ch025

the center by 2 mm., the interchange of vapor between the two drops will lower the surface tension of the isopropyl 1,9-diphenylnonane and raise the surface tension of the squalane on the sides of the drops nearest each other. As a result of the surface tension imbalance across each drop, the aromatic hydrocarbon will move away from the squalane drop, but the latter will move in the same direction, so that one drop appears to pursue the other. Since both of these compounds have vapor pressures low enough to permit their use as the stationary phase in gas-liquid chromatography, this experiment shows that extraordinarily small differences in surface tension are sufficient to produce bulk movements of oil if the surface tension gradient can be maintained over an interval of minutes or hours.

The rapid dendritic (or lobar) spreading of type 4 is characteristic of oils containing a strongly surface active additive which lowers the surface tension of the additive-containing oil by 5 dynes per cm. or more, and which is also strongly adsorbed at the oil-solid interface. The dendritic pattern usually follows the direction of microscratches produced during polishing. It is believed that spreading occurs initially along these capillary scratches, which are effectively open capillaries with a radius of curvature of only a few hundred angstroms. A liquid forming a contact angle of less than 90° with the solid will spread along such a capillary, even though it may be nonspreading on a plane surface. The filling of such capillaries is not directly observable with an optical microscope, but indirect evidence is obtainable after the oil has had time to diffuse over the metal surface adjacent to the scratches. A breath pattern of the surface then reveals a network of hydrophobic bands which eventually fuse into a continuous hydrophobic ring outside the drop.

Capillary spreading occurs with all nonspreading oils, but in the absence of unusual surface tension effects, the process slows or stops within 1 mm. or so as the oil reaches dead ends in the scratch structure or as the viscous drag on oil moving through long capillaries starves the advancing front. The total volume of oil removed from the drop is then negligible. However, if the surface tension lowering agent originally present is strongly adsorbed at the metal surface, the surface-to-volume ratio in the tiny capillary may be so great as to permit extensive depletion of additive from the oil advancing through the capillary. This raises the surface tension of the oil in the capillary with respect to the central drop, which produces a surface flow outward along the capillary. The viscous drag of this flowing film carries additional oil beneath it toward the tip of advancing liquid [Marangoni effect (13,14)]. This flow may lead to the formation of an actual mound of oil near the outer end of the capillary. Thus surface tension gradients produced by adsorption from thin advancing films of liquid provide a powerful mechanism for the transport of bulk oil along a solid surface. The changes in surface tension which may result from adsorption can be estimated from Figure 4, in which the change in surface tension of the solution, $\Delta \gamma_{LV}$, is plotted against the concentration of additive present.

The whole dendritic spreading process is relatively rapid; after one or two hours the pattern becomes nonspreading and may remain unchanged for weeks. In the absence of scratches a related depletion process may occur along the edge of the main drop in a random way to initiate lobes which spread most rapidly at the point furthest from the

Publication Date: January 1, 1964 | doi: 10.1021/ba-1964-0043.ch025

main drop. Such lobar spreading is usually slower and less extensive than the typical dendritic spreading along scratches. Oils which show dendritic spreading on polished stainless steel or sapphire are either nonspreading or develop lobar patterns when applied to scratch-free surfaces of blown or melt-drawn glass.

It is clear that the formulation of a nonspreading oil requires a discerning choice of the amount and nature of the adsorbable additive. It should be appreciably soluble in the base oil over the temperature range contemplated, it should adsorb promptly from the leading edge to give a film from which the oil retracts, and it should lower the surface tension of the base oil by less than 5 dynes per cm. In addition, it should not be more volatile than the base oil, and should not be altered by hydrolysis or oxidation in such a way as to increase the free surface energy of the adsorbed film. Polydimethyl siloxanes and their slightly phenylated analogs are useful only with aliphatic oils having surface tensions below about 29 dynes per cm. The moderately phenylated 550 silicone, on the other hand, was found to produce a stable nonspreading composition giving a contact angle of 14° when added to isopropyl-1,9-diphenylnonane (γ_{LV} = 34.4). Although bis(2-ethylhexyl) sebacate is nonspreading on a predeposited film of the 510 silicone (Table VI), a 1% solution of this silicone in the same ester spreads on clean steel; the film initially adsorbed from this solution is clearly not equivalent to one prepared from the silicone in a volatile hydrocarbon solvent. The behavior of the fluoroesters as additives probably depends upon trace

Publication Date: January 1, 1964 | doi: 10.1021/ba-1964-0043.ch025

Table IV. Effect of Surface Contamination or Roughness on Behavior of Nonspreading Oils

	Spreading Behavior			
Surface	Squalane + 1% DC 510	Bis(2-ethylhexyl)-sebacate + 5% fluoroester II[a]	P_1[b]	MIL L 3918[c]
Polished stainless steel	NS	-	NS	NS
Abraded stainless steel (600 A paper)	Slight spr.	Slight spr.	Slight spr.	NS
Naval brass, clean	NS	NS	Slight lobes	NS
Brass, not cleaned	Slight spr.	Slight spr.	NS	NS
Chrome plate, not cleaned	Lobes	Lobes	Slight spr.	NS
1020 steel, not cleaned (smooth)	Slight spr.	Slight spr.	Slight spr.	NS
Surface tension of solution, dynes/cm.	22.7	24.4	28.3	32.3

[a] Bis(1H,1H-undecafluorohexyl)3-methyl glutarate.
[b] Experimental nonspreading oil containing 97.75% bis(2-ethylhexyl)sebacate, 1.0% barium dinonylnaphthalene sulfonate, 1.0% fluoroester II, and 0.25% phenolic oxidation inhibitor.
[c] Military specification nonspreading oil.

hydrolysis to give strongly adsorbed fluorinated alcohols or half esters. The purified ester was nonspreading even shortly after percolation, but it has been shown [6] that esters are readily hydrolyzed by the water normally adsorbed at an alumina surface; a similar behavior on the oxidized stainless steel surface is probable. The fluoroesters are promising additives for the ester-type oils most likely to satisfy low temperature requirements because they produce much smaller lowerings of the surface tension of the diesters than the methyl silicones give, but nevertheless deposit low energy adsorbed films. The present work has examined representatives of a few classes of additives; further work using the guidelines set forth may produce more nearly optimum combinations than are reported.

Effect of Organic Surface Contaminants on Performance of Nonspreading Oils. An examination of the behavior of nonspreading formulations on oil-contaminated, shop-soiled, or abraded surfaces, as summarized in Table IV, indicates that practical nonspreading oils must have surface tensions above 30 dynes per cm. This restriction is understandable in terms of the concept of the critical surface tension, γ_c, and the established laws for spreading pressure and the spreading of one liquid on another. These relations are illustrated in Table V, which records spreading data for a variety of liquids on some low energy surfaces. If a solid surface is covered with a thin film of organic material which exposes aromatic or oxygenated structure at the air interface, the critical surface tension, γ_c, may readily exceed 30 dynes per cm. Since aliphatic hydrocarbon liquids do not have surface tensions above 30 dynes per cm., any oil having such a base must spread upon the contamination. The behavior of aliphatic diester oils, which usually have surface tensions in the range of 30 to 32 dynes per cm., will be marginal in the presence of organic contaminants. Oils having higher surface tensions than the aliphatic esters do not spread on such surfaces.

Pretreatment with Silicone Films to Prevent Oil Spreading. Films of stearic acid or metal stearates have been used to prevent spreading of oil in watch and clock mechanisms [4, 16, 17]. In the present work it has been noted that silicones are readily and rapidly adsorbed on stainless steel, brass, sapphire, quartz, and glass to form films over which none of the oils studied will spread. The silicones have been reported to adsorb to give films several times as thick as a stearic acid monolayer [9]. The silicones are much more resistant to oxidation than are aliphatic carbon structures, and have low volatility, so that silicone films may be expected to have long useful lives. The critical surface tension of a dimethyl silicone film is about 23 dynes per cm., which is closely comparable with γ_c for stearic acid or stearate films. Tests showed that nonspreading behavior persisted for test drops that have been in contact with the silicone-treated surface for 9 months. All of the base oils studied were nonspreading on a film adsorbed from DC 510, a lightly phenylated methyl phenyl polysiloxane.

Films of the silicones having different degrees of phenylation can be arranged in a series according to increasing γ_c of the treated surface. DC 550 and DC 710 silicones spread on their own films, but not on films from silicones having a lower degree of phenylation (Table VI).

Silicone films are readily deposited from extremely dilute benzene solutions, so that films of submicron thickness can be formed uniformly

Publication Date: January 1, 1964 | doi: 10.1021/ba-1964-0043.ch025

Table V. Spreading Behavior of Various Oils

Liquid	Surface Tension	Teflon
		18
Fluoroester II[b]	19.6	Spreads
Squalane + 1% DC 510	22.7	42
Fluoroester I[c]	24.3	19
n-Hexadecane	27.3	46
EHS[a] + 1% fluoroester II	28.0	58
EHS + 1% fluoroester I	29.9	62
Mil-L-3918	32.3	68
Isopropyl-1,9-diphenylnonane	34.4	73
Methylene iodide	50.3	88

[a]Bis(2-ethylhexyl)sebacate.
[b]Bis(1H,1H-undecafluorohexyl)3-methyl glutarate.
[c]Bis(1H,1H,7H-dodecafluoroheptyl)3-methyl glutarate.

and reproducibly either by dipping the instrument into a very dilute solution and draining, or by applying a light film of the dilute solution as an aerosol spray. Such films could be renewed at the time of cleaning the instrument by including a very small amount of a suitable silicone in the cleaning solvent.

Table VI. Contact Angles of Various Liquids on Silicone Films over a Stainless Steel Substrate[a]

Liquid	Contact Angle° on DC 200	DC 510	DC 550
DC 200 silicone	-	-	Spreads
DC 510 silicone	9	-	-
DC 550 silicone	26	11	-
DC 710 silicone	47	31	12
Squalane	43	25	-
Bis (2-ethylhexyl) sebacate	48	25	ca. 3
Isopropyl 1,9-diphenylnonane	56	31	25
Methylene iodide	77	-	48
Water	95		
n-Octane	6		
n-Decane	13		
n-Dodecane	24		
n-Tetradecane	30		
n-Hexadecane	35		

[a]Films prepared by adsorption from bulk silicone oil, followed by repeated washing with benzene.

Publication Date: January 1, 1964 | doi: 10.1021/ba-1964-0043.ch025

and Reference Liquids on Some Low Energy Surfaces

Contact Angle, θ on				
Octadecyl amine monolayer on SS	Phenyl stearic monolayer on SS	$Ba(DNNS)_2$ monolayer on SS	Polyethylene	Thin film EHS[a] on SS
Critical Surface Tension				
22	ca. 28	29	32	ca. 31
26	Spreads	Spreads	Spreads	-
18	Spreads	Slow spr.	Spreads	-
49	18	16	4	-
39	Spreads	Spreads	Spreads	-
41	Spreads	Spreads	Spreads	-
45	ca. 4	12	Spreads	-
50	17	20	8	7
53	29	31	9	13
69	55	-	52	-

The silicone film responsible for the nonspreading was not removed by repeated washing in benzene. It appears desirable to use a silicone of relatively high molecular weight to reduce volatility and to decrease the rate of lateral flow. The film should be kept below 300 A. to reduce lateral flow as well as to minimize dust collection by the treated surface. The utilization of thicker resin-type films for the control of oil spreading is described in another report from this laboratory [3].

Literature Cited

(1) Barker, G. E. (to Elgin Watch Co.), U. S. Patent 2,355,616, (Aug. 15, 1944), 2,412,956 (Dec. 24, 1946), 2,583,200 (Jan. 22, 1952).
(2) Barker, G. E., Alter, G. E., McKnight, C. E., McKlveen, J. R., Hood, D. M., ASTM Bull. 138 (1946).
(3) Bernett, M. K., Zisman, W. A., Advan. Chem. Ser., No. 43, 332 (1963).
(4) Bulkley, R., Snyder, G. H., J. Am. Chem. Soc. 55, 194 (1933).
(5) Faurote, P. D., Henderson, C. M., Murphy, C. M., O'Rear, J. G., Ravner, H., Ind. Eng. Chem. 48, 445 (1956).
(6) Fox, H. W., Hare, E. F., Zisman, W. A., J. Phys. Chem. 59, 1097 (1955).
(7) Jarvis, N. L., Zisman, W. A., Ibid., 64, 150, 157 (1960).
(8) O'Rear, J. G., "Synthesis and Characterization of Esters and Ethers for Nonspreading Lubricants," Naval Research Lab., Rept. 3891 (Aug. 21, 1951).
(9) Perkel, R., Ullman, R., J. Polymer Sci. 54, 127 (1961).
(10) Peterman, R., Schweiz. Arch. Angew. Wiss. Tech. 26, 45 (1960).
(11) Portnoy, S., Verderame, F. D., Messina, J., Gisser, H., J. Chem. Eng. Data 3, 287 (1958).
(12) Romans, J. B., Singleterry, C. R., Ibid., 6, 56 (1961).
(13) Scriven, L. E., Sternberg, C. V., Nature 187, 186 (1960).

(14) Thomson, James, Phil. Mag. (4), 10, 330 (1855).
(15) Wilgus, D. R., Ettling, A. C., Pino, M. A., J. Chem. Eng. Data 6, 106 (1962).
(16) Woog, P., Compt. Rend. 181, 772 (1925).
(17) Woog, P., "Contribution a l'Étude du Graissage Onctuosite," Delagrove, Paris, 1926.
(18) Zisman, W. A., Advan. Chem. Ser., No. 43, 1 (1963.)

Received April 1, 1963.

26

Dynamic Surface Phenomena in the Spontaneous Spreading of Oils on Solids

WILLARD D. BASCOM, ROBERT L. COTTINGTON, and CURTIS R. SINGLETERRY

U. S. Naval Research Laboratory
Washington 25, D. C.

Publication Date: January 1, 1964 | doi: 10.1021/ba-1964-0043.ch026

A study by interference microscopy and ellipsometry shows that the spontaneous spreading of nonpolar liquids on smooth, clean metal surfaces is characterized by the advance from the bulk liquid of a primary film less than 1000 A. thick, usually followed by a thicker secondary film. The movement of the secondary film results from a surface tension gradient across the transition zone between the primary and secondary films. This gradient is produced by the unequal evaporative depletion from these two regions of a volatile contaminant having a lower surface tension. If the volatile contaminant has a higher surface tension than the main component, the gradient is reversed, and the liquid recedes. Removal of the volatile constituents eliminates the secondary but not the primary spreading. Liquid may also spread by capillary flow in microscratches.

The tendency of certain liquids to spread spontaneously or "creep" over solid surfaces is sometimes desirable and sometimes a distinct annoyance. Lubrication engineers must often rely upon the creep of oils to carry the lubricant to surfaces which otherwise would be inaccessible. On the other hand, the ease with which some liquids will creep out of a container and contaminate the surrounding area can be most disconcerting. The spontaneous spreading of liquids over solids is not simple, and it presents an intriguing problem in surface chemistry which has not received the detailed attention it deserves.

Three previous studies of spontaneous spreading are pertinent to this present investigation: Sir William Hardy's studies [9], the somewhat later work of Bangham and Saweris [2], and the recent studies by Zisman and coworkers [8] of liquids spreading on polar surfaces.

In Contact Angle, Wettability, and Adhesion; Fowkes, F.;
Advances in Chemistry; American Chemical Society: Washington, DC, 1964.

Hardy, in his classic study of boundary lubrication, gave careful attention to the spreading of drops of water and of various polar organic liquids on clean surfaces of glass and steel. He observed that a sensibly invisible film of liquid about 1 micron thick spreads from a drop and that this primary spreading may or may not be followed by spreading of the drop itself. These two distinct processes Hardy termed the primary and secondary spreading, respectively, and he arrived at some interesting conclusions concerning the nature of the primary film. It was his opinion that this film is usually many molecules thick and that it has a surface tension greater than that of the liquid itself. This primary film he termed "contractile," in that it pulls the liquid drop out to form a secondary spreading. He also concluded that the primary film is formed only by deposition of liquid from the vapor.

Bangham and Saweris observed the behavior of various liquids on freshly cleaved mica. They found that of the many polar and nonpolar liquids observed on this surface in air only a few would spread spontaneously, and that none would spread when the surrounding atmosphere was saturated or supersaturated with vapor. Their conclusions were essentially the same as Hardy's, except that they believed the primary film could be formed by surface diffusion of molecules from the drop edge as well as by deposition from the vapor.

Zisman and coworkers studied the spreading of liquids on both the nonpolar surfaces of organic solids and the polar surfaces of metals, oxides, and glass. They determined experimentally that for nonpolar surfaces of organic solids and for close-packed monolayers of organic molecules adsorbed on polar solids there exists a critical surface tension of wetting, γ_c, characteristic of the surface [16]. Liquids having surface tensions greater than the value of γ_c of any given solid surface will not spread on that solid. Their experiments with polar solids demonstrate that organic liquids will usually spread on these surfaces, unless the liquid forms a monolayer that has a γ_c value lower than the surface tension of the liquid itself [8].

The experimental work of the present investigation deals exclusively with hydrocarbons showing zero contact angles on the surfaces studied. Their spontaneous spreading behavior on both horizontal and vertical surfaces was observed by interference microscopy and ellipsometry, which allowed the study of the topography of the spreading films in considerable detail. The spreading of these liquids is characterized by the formation of an extremely thin primary film, much thinner than the 1 micron suggested by Hardy, and often but not invariably followed by a much thicker secondary film. An important aspect of the geometry of spreading films revealed by interference techniques is the development of a ridge between the primary and secondary regions of the film. This observation, along with a careful study of the effect on spreading of surface roughness, the chemical constitution of the solid surface, and the chemical composition of the liquid, permits us to propose a mechanism of spontaneous spreading. The mechanism is entirely consistent with the experimental results and satisfactorily explains why certain liquids that have a zero angle with the solid show no tendency to spread spontaneously and why certain others actually recede.

Any explanation of the observed spreading behavior must account for the fact that a film of liquid many hundreds of molecules deep can

Publication Date: January 1, 1964 | doi: 10.1021/ba-1964-0043.ch026

spread upward against gravity over an already developed primary film of the same liquid. Hardy and Bangham believed that spontaneous spreading of the secondary film occurs because the liquid in the primary film ahead of it has a higher surface tension. They attributed this higher surface tension to interaction between the molecules of the primary film and the solid substrate, even though the surface of the primary film was many molecules away from the liquid-solid interface. Zisman, however, shows that the exterior surface of a close-packed monolayer of a compound such as stearic acid on a polar solid has a critical surface tension characteristic of the exposed methyl end groups, and nearly the same as the critical surface tension of a paraffin crystal face exposing similar groups. This finding argues against long-range effects of a polar solid on the surface tension of an overlying liquid. This paper reports experimental results which suggest an alternate source of surface tension gradients capable of producing the observed spreading phenomena, develops a mechanism for bulk transport in liquid films, and describes further experiments designed to test the ability of the theory to predict spreading behavior.

Publication Date: January 1, 1964 | doi: 10.1021/ba-1964-0043.ch026

Experimental Methods

Metal Surfaces. The stainless (18-8) steel plates used to study vertical spreading were 1/4 inch thick, cut in 1 × 2 inch rectangles, and machine-ground on all sides; one face was polished to an optical mirror finish. Prior to each experiment all surfaces of the plate were cleaned of adsorbed polar contamination by polishing on a metallographic wheel with alumina powder suspended in water and then rinsed in a strong stream of distilled water to remove adhering particles. The plate was placed on end on a washed piece of filter paper, covered, and allowed to dry. The presence of surface contamination could be detected by the tendency of the water film to retract and drain irregularly from the affected area. In such an event the plate was recleaned. For studies of horizontal spreading, stainless steel disks 3/4 inch in diameter and 3/4 inch high were prepared with one face highly polished. They were cleaned and handled in the same manner as the rectangular plates.

Evaporated films of Nichrome metal deposited on glass microscope slides were also employed. The glass slides were cleaned by chemical methods and then by glow discharge in the evaporation chamber. Nichrome wire was evaporated onto the glass to give an opaque coating.

Spreading Liquids. The liquids whose spreading behaviors were observed are listed in Table I, with their surface tensions and viscosities at 25°C.

The surface tensions were determined by the ring method with appropriate corrections [7,10] and the viscosities were measured in an Ostwald-Cannon capillary viscometer.

Polar impurities were removed from the organic liquids by percolation through columns of activated Florisil adsorbent. The absence of polar contamination was assumed if a drop of the percolated liquid would not spread on a clean water surface. Passage of the alkyl aromatic liquids through Florisil did not always achieve sufficient purification; some required passage through fuller's earth adsorbent as well.

Table I. Surface Tensions and Viscosities of Spreading Liquids

Liquid	Surface Tension, Dynes/Cm.	Kinematic Viscosity, Centistokes
Aliphatic hydrocarbons		
Hexane	18.4	0.46
n-Hexadecane	27.6	4.0
Pristane (tetramethylpentadecane)	25.6	7.3
Squalane (hexamethyltetracosane)	27.6	26.8
Squalene (hexamethyltetracosahexene)	31.0	17.0
Aromatic hydrocarbons		
Dodecylbenzene	31.5	21.7
Polyamylnaphthalene	32.2	101.6
Amylbiphenyl	34.2	17.4
Liquid polymers		
Polyisobutylene[a]	28.3	346.0
Polychlorotrifluoroethylene (Kel F)[b]	27.4	49.4
Polychlorobiphenyl (Arochlor 1221)[c]	41.8	6.7
Methyl silicone oils[d]		
7-cs. oil	19.2	6.9
7-cs. oil, fraction	19.4	7.5

[a]Amoco Chemicals Corp.
[b]Minnesota Mining and Mfg. Co.
[c]Monsanto Chemical Co.
[d]Dow Chemical Co.

Soap Adsorbates. The barium salt of dinonylnaphthalene sulfonic acid, $Ba(DNNS)_2$, was prepared by metathesis of the sodium salt with barium chloride [3].

An aqueous solution of potassium perfluorodecanoate was prepared by dissolving 0.016 gram of the free acid into 10 ml. of distilled water and exactly neutralizing with aqueous potassium hydroxide. The resulting solution was diluted with distilled water to a concentration of 3×10^{-4} mole per liter of the potassium salt.

Observation of Spreading by Interference Microscopy. Profiles of the liquid films were plotted from photomicrographs of the interference bands taken with conventional microphotographic equipment. The light source was a mercury vapor lamp from which the mercury green line, 5460 A., was isolated by a filter mounted so it could be moved out of the light path to permit observation of the film with polychromatic illumination. For the observation of films on vertical surfaces a metallographic microscope was mounted in a horizontal position on an optical bench. The metal specimens were supported vertically from the lower end of a rod adjustably mounted on a separate carriage. Another carriage positioned beneath the specimen bore a table whose vertical location was alterable by a rack and pinion movement. This table carried

Publication Date: January 1, 1964 | doi: 10.1021/ba-1964-0043.ch026

a small beaker of the liquid under study. A draining film was formed by bringing the table and beaker up until the plate was about three-quarters wet by the liquid. The beaker was sufficiently wide so the plate could be kept away from the meniscus curvature near the beaker walls. The immersion was done slowly and smoothly, so that the liquid surface formed a horizontal line across the face of the plate. Drainage was initiated by lowering the beaker with as smooth a movement as possible by squeezing the table and the supporting carriage between the thumb and forefinger in the manner of pulling the trigger of a gun. The film drainage was particularly sensitive to any jerky or hesitant movement in lowering the beaker. Unusual edge effects were not propagated into the central area of observation. The geometry of the liquid at the bottom edge of the plate had no detectable effect on the upper part of the film if the bottom edge was more than 2 cm. from the section studied. The usual practice was to keep the lower end of the plate touching the surface of the liquid.

All spreading experiments were performed at 25°C. in a constant temperature room. The metal plates and disks were allowed to come to thermal equilibrium before an experiment commenced. The steel disks on which horizontal spreading was studied were protected from airborne dust and aerosols by a covered glass cell through which the spreading liquid could be observed microscopically. The vertical steel plates and coated slides were not enclosed, but ellipsometric determination of the rate of contamination indicated that it required nearly a day for a layer 10 A. thick to accumulate, whereas observations on the vertical plates were limited for the most part to the first 4 or 5 hours.

It was not always possible to determine the film profile unambiguously from a single interference photograph when the film of liquid developed a ridge or a ridge and a trough. Progressive changes in bandwidths on a given photograph were sometimes helpful in indicating the presence of a maximum or minimum, which could then be confirmed by viewing the film with polychromatic illumination and noting the sequence of interference colors.

Ellipsometric Determination of Film Thickness. The principal use of the ellipsometer was to study the upper edge of the films on vertical plates where the thickness became less than 1000 A. and could not be observed with the interference microscope. The ellipsometric measurement of film thickness is described in the literature [4,6]. For the purposes to which the technique was applied here, the approximate equation given by Drude [6] relating the film thickness and refractive index with the optical parameters of the incident and reflected light was entirely adequate. In order to use the Drude approximations it was necessary to assume the refractive index of the liquid film to be the same as that of bulk liquid. These approximate equations are highly inaccurate for film thickness greater than 100 A.

The films studied with the ellipsometer were of uniform thickness in the horizontal direction, but varied in thickness continuously in the vertical direction. It was therefore desirable that the area of film viewed by the instrument be as narrow as possible in the vertical direction, so that the film thickness in the observed area would be nearly constant. The aperture of the instrument was therefore reduced to a narrow horizontal slit by cementing two pieces of razor blade edge across the 1-mm. opening to leave a 0.2-mm. space between them. Any further

Publication Date: January 1, 1964 | doi: 10.1021/ba-1964-0043.ch026

reduction in the slit width diminished the light intensity beyond the working sensitivity of the instrument.

When viewed through a relatively wide aperture (1×2 mm.), regions of the film having thickness greater than $\lambda/4$ exhibited interference bands in nearly the same position as the interference bands observed with unpolarized, normal incident light. Although there is not an exact correspondence between the bands observed in the two different ways, the interference bands retained their identity and did not move significantly even with a complete change of setting of the quarter-wave plate and analyzer of the instrument. Therefore, an approximate film thickness was computed from these bands, taking account of the angle of incidence imposed by the ellipsometer.

Results

Publication Date: January 1, 1964 | doi: 10.1021/ba-1964-0043.ch026

The spreading of selected organic liquids of high molecular weight was observed on both horizontal and vertical surfaces by interference microscopy. Liquids having low vapor pressures were taken, so that evaporation of the spreading liquid would have a negligible effect on film thickness. This choice provided relatively viscous liquids whose spreading was slow and conveniently observed. The choice of spreading liquids was limited to relatively nonpolar materials, because molecules having highly polar functional groups are generally adsorbed on metal surfaces to form monomolecular films over which the liquid cannot spread [8].

The behavior which was found characteristic of many liquids on horizontal surfaces is illustrated by the photomicrographs in Figure 1, A, for a drop of squalane on a polished, stainless steel disk. From measurements of interference band spacing and of bandwidths, the film profiles for each photograph were plotted as in Figure 2. The dome-shaped profile initially assumed by the drop had within an hour developed a plateau region and was advancing with the leading edge at a small angle to the solid surface. After 3 hours the drop still maintained an apparent angle with the solid and a ridge had developed behind the leading edge. The individual profiles could not be drawn to an experimental intercept of the horizontal axis, because the first-order interference band corresponds to a liquid layer about 1000 A. thick.

Careful examination of these drops revealed that a thin film of liquid invisible with the interference microscope extended out ahead of the apparent edge of the spreading liquid. The actual angle of contact with the solid is therefore zero and not a finite angle, as the interference photographs might suggest. Breath patterns formed by breathing over the spreading drop indicated that the outer edge of the film was distinctly ahead of the first-order interference band. These experiments also showed that the advancing edge of this invisible film was close to the visible edge during the initial stages of spreading but that the distance between them increased as the liquid spread. The presence of this very thin film was also demonstrated by placing ahead of the visible edge minute drops of another liquid, such as isopropyl-1,9-diphenylnonane, having a surface tension higher than that of squalane. When placed on the invisible film, such drops would immediately retract from the spreading liquid, but when placed on a clean metal surface they would spread uniformly in all directions.

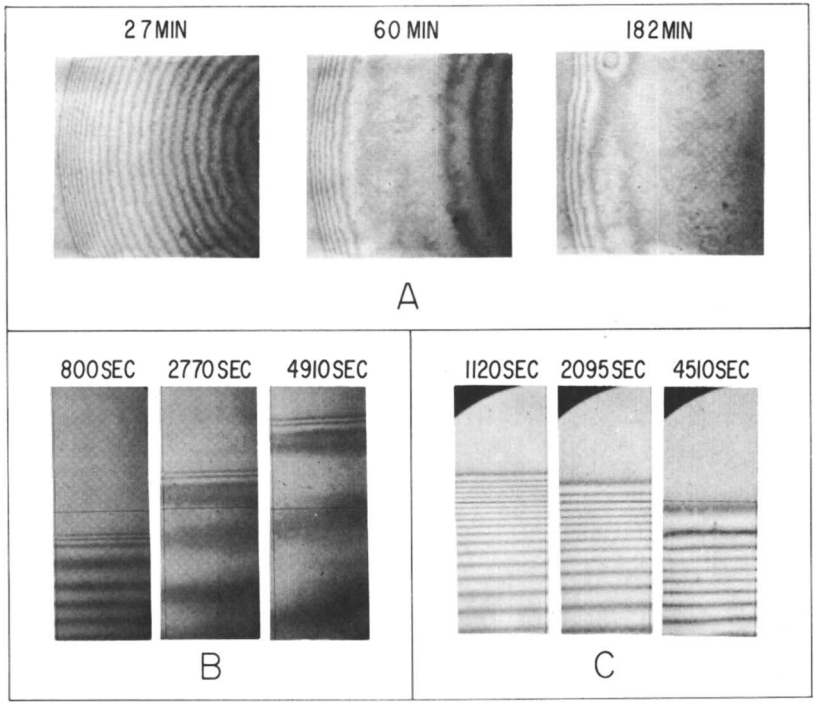

Figure 1. Interference photomicrographs

A. Squalane drop spreading on horizontal steel surface
B. Squalane film spreading up vertical steel plate
C. Film of polyamylnaphthalene receding from vertical steel plate

The upward spreading of liquid on vertical surfaces was in many respects similar to the behavior observed on horizontal surfaces. Photomicrographs of squalane on a polished stainless steel plate are presented in Figure 1, B; the upward spreading of the edge is evidenced by the progressive displacement of the first-order interference fringe from the stationary reference line. The film profiles plotted in Figure 3 were drawn from the corresponding interference photomicrographs. The dashed lines in this and all the other figures represent the profile for purely hydrodynamic drainage calculated from an equation given by Jeffreys [11],

$$x = \frac{g}{\nu} h^2 t \qquad (1)$$

Here x is the distance along the plate measured from the initial position of the liquid surface when drainage began, h is the film thickness, t is the time of drainage, and ν is the kinematic viscosity of the liquid. This equation was derived for laminar flow from a vertical plate without including the effect of surface forces, and so by superimposing the calculated profiles on the experimental film profiles it is immediately evident to what extent surface forces have disturbed the hydrodynamic drainage of the liquid.

Publication Date: January 1, 1964 | doi: 10.1021/ba-1964-0043.ch026

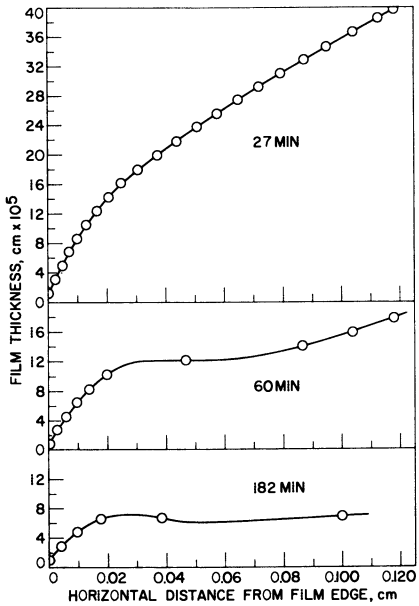

Figure 2. Profiles of edge of squalane drop spreading radially on horizontal steel surface

Film thickness magnified 250 ×

The position of the liquid surface when drainage began, which corresponds to the point on the plate from which the hydrodynamic profile is drawn (x = 0), was determined by plotting the displacement of the film edge from the reference line against the time of drainage. The displacement was a reasonably linear function of the time, so that the data could be extrapolated to t = 0 and the intercept taken as the initial position of the liquid surface. The horizontal scale of film thickness has been expanded 250-fold by the choice of coordinate scales. The actual slopes, therefore, lie much closer to the vertical than the figures suggest. The film profile, if plotted to equal scales in the two dimensions, would have been almost indistinguishable from the edge of the figure.

Inspection of the film profiles shows that the apparent angle of contact of the upper edge of the film with the plate and the progressive development of a ridge of liquid at the leading edge resemble the spreading phenomena observed on horizontal surfaces. For this particular experiment this geometry was maintained through the first 6000 seconds, after which there was a gradual decline in the maximum height of the ridge and the apparent angle of contact. As had been observed for drops of squalane on horizontal surfaces, breath patterns and indicator drops demonstrated the presence of liquid ahead of the first-order interference band of squalane films on vertical plates.

The extent and thickness of the primary film, which was invisible with the interference microscope but detectable by breath patterns,

Publication Date: January 1, 1964 | doi: 10.1021/ba-1964-0043.ch026

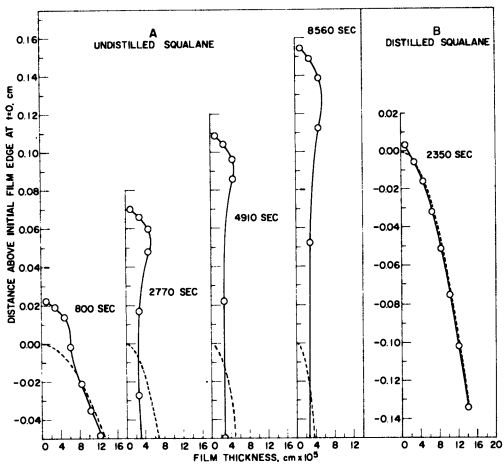

Figure 3. Film profiles for squalane spreading up vertical steel plates

A. Undistilled
B. Distilled
Film thickness magnified 250 ×

were investigated directly with the ellipsometer. Quantitative ellipsometric measurements indicated that in the early stages of spreading the primary film was particularly thin and extended only a short distance ahead of the first-order interference band. A region of the plate from the first-order interference band to 8 mm. above it was scanned with the ellipsometer after 1 and 5 hours of drainage. The settings for the instrument over this entire region were the same as for light reflected from the bare steel substrate. Evidently the primary film does not extend far enough beyond the first interference band at these times to allow resolution of its width by the 0.2-mm. slit of the ellipsometer.

Successful quantitative measurements of the thickness of the squalane primary film were possible after 18 and 42 hours of drainage. The film profiles determined from these measurements are shown in Figure 4. The film thickness was measured at various distances from a reference line drawn on the metal plate. The points plotted at about 1200-A. thickness correspond to the first-order interference fringe. These measurements demonstrate a sharp change in the slope of the film and also a tendency for the primary film to thicken over the 24-hour period. Undoubtedly there is some error in the measurement of film thickness where the thickness is changing abruptly and also near 100 A., where the Drude calculations of film thickness are invalid.

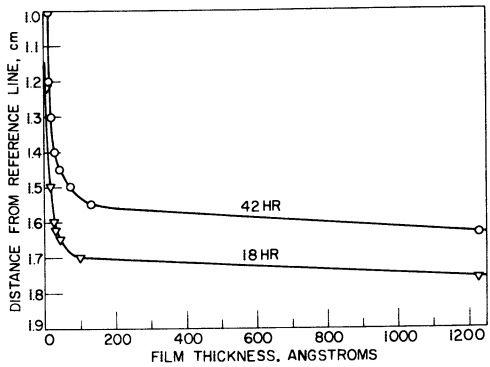

Figure 4. Ellipsometrically determined profile of leading edge of squalane film spreading up vertical steel plate

Film thickness magnified 100,000 ×

However, such errors would not alter substantially the inference of an abrupt change in film slope just outside the first interference fringe.

The presence of a ridge near the leading edge of a spreading film conflicts with the equilibrium configuration required by surface tension and gravity for liquid forming a zero contact angle with a plane solid surface. To explain the presence of a ridge it is necessary to look for transient phenomena of a dynamic rather than a static character. However, a static experiment was found which proved particularly helpful in defining the conditions required for the formation of a ridge of liquid at the leading edge of spreading films. Specifically, a ridge was observed at the upper edge of films draining from vertical plates when upward spreading had been prevented by forcing the edge of the film to assume a finite contact angle with the plate. To do this a narrow band of potassium perfluorodecanoate monolayer was deposited across a clean metal plate about three quarters of the distance from the bottom edge by touching the plate with a silk string wet with an aqueous solution of the soap. It was already known that squalane will not spread on a close-packed monolayer of these perfluorinated molecules. The plate was dipped into a vessel of squalane until the barrier was in the liquid surface and drainage was initiated by lowering the vessel from this position.

The profiles of a squalane film draining from a perfluorodecanoate barrier are presented in Figure 5. The film established itself some distance below the visible residue left by the aqueous soap solution, presumably at the edge of the perfluorodecanoate monolayer. The presence of the barrier entirely prevents spreading and imposes a contact angle of slightly over 1° on the upper edge of the film. A ridge of liquid developed at the upper edge of the film and this geometry was maintained for the 72 hours during which the film was observed. Below the ridge the drainage corresponds closely to that predicted for purely hydrodynamic flow.

Publication Date: January 1, 1964 | doi: 10.1021/ba-1964-0043.ch026

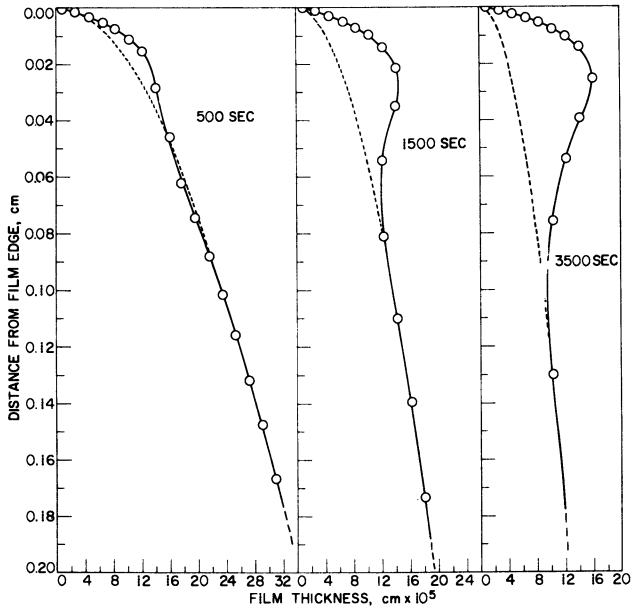

Figure 5. Film profiles of squalane film draining from perfluorodecanoate barrier on vertical steel plate

Film thickness magnified 250 ×

In a second experiment drainage was initiated from about 1 mm. below the region of the barrier. At first the upper edge of the squalane film spread in the same manner as the film shown in Figure 3, but when the liquid reached the barrier the upward spreading of the film ceased. However, there was a sustained flow of liquid from the film below up to the stationary edge where the liquid formed into a ridge. This ridge reached the same dimensions as the one observed at the upper edge of draining films that originated at the barrier. This experiment demonstrated the spontaneity of ridge formation whenever the surface of the liquid was forced to assume a finite contact angle with the plate. The explanation of ridge formation by spreading squalane then requires some dynamic mechanism which will maintain a nearly constant slope of the advancing edge of the secondary film in the face of the zero contact angle required for a spreading liquid.

Effect of Volatile Constituents. A large part of the spontaneous spreading behavior observed for squalane and other liquids was found to be due to the presence of materials which had a greater volatility than the main constituent but were otherwise chemically similar. This was first suspected when it was found that different batches of squalane had very different spreading behaviors, even though each batch had been carefully cleaned of polar contaminants. When a batch of squalane was molecularly distilled, three fractions were obtained having slightly higher volatilities than the main fraction (Table II, A). Removing these

Publication Date: January 1, 1964 | doi: 10.1021/ba-1964-0043.ch026

Table II. Properties of Distillation Fractions

Fraction	Temp. Range, °C.	Volume, Ml.	Surface Tension, Dynes/Cm.	Refractive Index
		A. Squalane		
	1 - 4μ Hg			
Original	-	500	28.2	1.4523
1	30 - 50	1.5	26.5[a]	1.4451
2	50 - 60	7.5	27.5	1.4461
3	60 - 65	27	28.5	1.4510
4	65 - 70	55	28.6	1.4525
5	70 - 80	355	28.6	1.4525
Residue	-	54	28.6	1.4525
		B. Polyamylnaphthalene		
	8 mm. Hg			
Original	-	250	32.2	1.5479
1	175	5	32.9	1.5590
2	175 - 178	15	32.2	1.5515
3	179 - 186	50	32.4	1.5530
4	187 - 190	15	32.9	1.5543
Residue	-	115	31.8	1.5460

[a]Determined by maximum bubble pressure method.

volatile materials reduced drastically the rate of upward spreading on a vertical plate and eliminated any evidence of ridge formation at the advancing edge (Figure 3, B). In Figure 6, A, the vertical distance spread is plotted as a function of time for a distilled and an undistilled squalane. The rate of spreading—i.e., the slope of the plot—was relatively large, about 2.5×10^{-5} cm. per second, for the undistilled material; over the same time interval the rate of spreading of the stripped material was nearly zero. The spreading rate for the undistilled squalane appears nearly constant in Figure 6, A, but after 20 hours had decreased to 0.05×10^{-5} cm. per second.

Experiments were made to determine to what extent the original spreading behavior of the distilled squalane could be reinstated by adding to the stripped material various amounts of saturated hydrocarbons more volatile than squalane itself. In Figure 6, B, the spreading rate of distilled squalane is compared with the rates for 10% mixtures of this purified material with distilled *n*-hexane, distilled *n*-hexadecane, and pristane, a branched, saturated hydrocarbon having a slightly higher molecular weight than hexadecane. These three hydrocarbons were chosen because they have volatilities greater than squalane, the difference being greatest for hexane. The hexadecane and pristane have nearly the same boiling point, but the surface tension of pristane is 25.6 dynes per cm., whereas hexadecane has a surface tension of 27.6 dynes per cm. Addition of hydrocarbons of lower molecular weight restored spontaneous spreading behavior to squalane but not in proportion to the volatility of the additive. Despite their comparable volatilities, pristane mixtures spread nearly twice as fast as the hexadecane

Publication Date: January 1, 1964 | doi: 10.1021/ba-1964-0043.ch026

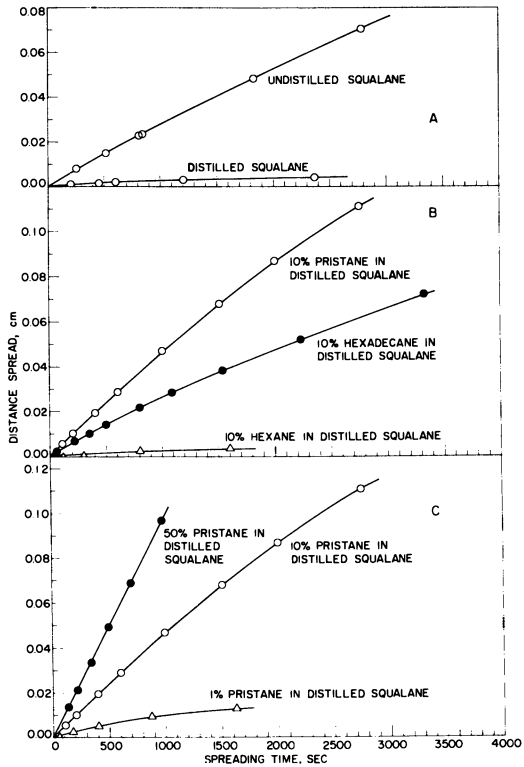

Figure 6. Comparison of distance spread vs. time on vertical steel plates

A. Distilled and undistilled squalane
B, C. Various mixtures of hydrocarbons in distilled squalane

mixture. Evidently, the surface tension of the more volatile component is also of importance. The highly volatile hexane, on the other hand, had no noticeable effect on the spreading behavior of the distilled squalane. Figure 6, C, shows that increasing the concentration of pristane increased the spreading rates, but the rate of the 50% pristane mixture was not five times the rate of the 10% mixture.

The invisible or primary film that had been detected in advance of spreading squalane was not eliminated by distilling the liquid but was, at any given time, distinctly further ahead of the apparent edge of a film of distilled liquid than of undistilled liquid. After about an hour of draining and spreading on a vertical plate, breath patterns revealed liquid on the surface 3 or 4 mm. in front of the stationary visible edge of distilled squalane, whereas at this relatively early time no primary

film was detectable by this technique ahead of the advancing edge of a film of undistilled squalane.

The radial spreading of squalane on horizontal surfaces also was markedly reduced after distillation. Figure 7 shows that, after an initial gravitational spreading, drops of distilled and undistilled squalane both reach nearly constant spreading rates, which are less than half as great for the distilled as for the undistilled liquid. As on the vertical plates, the advancing edge of the stripped squalane showed no ridge formation. Breath patterns demonstrated a primary film considerably ahead of the drop of distilled squalane.

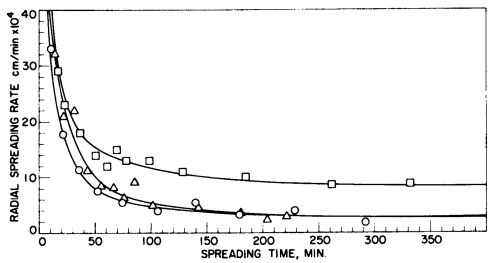

Figure 7. Radial spreading rates of squalane drops on horizontal steel surfaces

□ Undistilled squalane
○ Distilled squalane
△ Undistilled squalane surrounded by nearly saturated vapor

Further evidence that spontaneous spreading is associated with the evaporation of volatile components from the liquid appeared when it was found that the spreading tendency of undistilled squalane could be reduced to that of the distilled material by saturating the surrounding air with vapor from the liquid. This was demonstrated by applying a film of undistilled squalane to the inside of the glass cell enclosing the test specimen. Figure 7 shows that such a drop in an atmosphere nearly saturated with its own vapor spread at a rate almost identical with that of the distilled squalane.

To test the generality of the observations on the spreading of squalane, spreading tests were made with a variety of viscous nonpolar liquids, including a group of polymeric materials. To ensure scratch-free and reproducible surfaces, these spreading experiments were made on Nichrome films vacuum-deposited on microscope slides. The spreading behavior grouped these liquids into three classes.

Group I. Liquids which spread upward, exhibiting a primary film and a secondary film with nearly constant slope at the leading edge (n-hexadecane, pristane, squalane, squalene, polychlorobiphenyl, and the polymer liquids: polymethylsiloxane, polyisobutylene, and polytrichloroethylene).

Publication Date: January 1, 1964 | doi: 10.1021/ba-1964-0043.ch026

Group II. Liquids whose edge remains stationary except for the development of a zero contact angle and a primary film above the original boundary (dodecylbenzene and highly purified liquids containing only a single molecular species).

Group III. Liquids whose edge appears to recede from the original boundary, but leaves a primary film and shows a zero contact angle (amylbiphenyl and polyamylnaphthalene).

In group I the rate of upward spreading and the volume of liquid lifted above the original boundary varied widely but showed no simple correlation with structure or viscosity. The film profiles for films of these liquids at about 1000 seconds of drainage are given in Figure 8

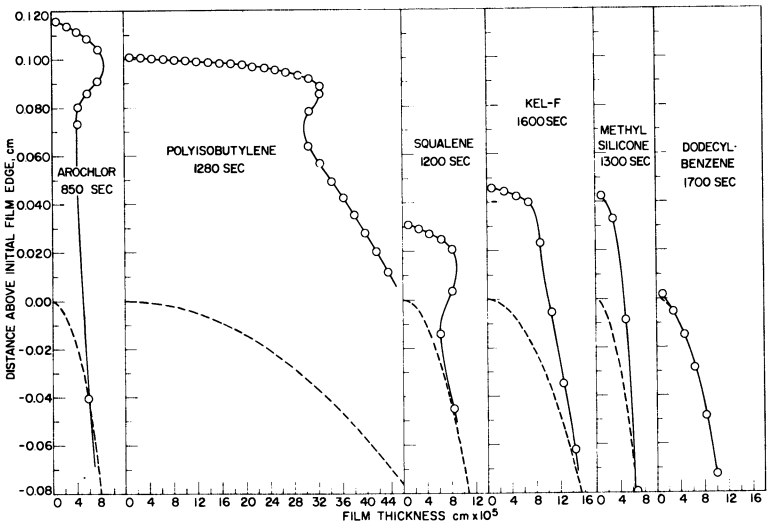

Figure 8. Film profiles for various liquids spreading upward on vertical Nichrome surfaces

Film thickness magnified 250 ×

and their spreading rates can be seen in Figure 9. The polymeric liquids, which are known to consist of mixtures of macromolecules of differing molecular weight and volatility, showed some of the most spectacular upward spreadings—e.g., polyisobutylene, most viscous of the liquids examined, had one of the highest spreading rates. A 7-cs. dimethylsiloxane isolated from a higher molecular weight oil as a narrow distillation fraction spread much less vigorously (Figure 9,A) than a commercial dimethyl silicone of the same viscosity.

Both group II and group III liquids were alkyl aromatic hydrocarbons known from their methods of preparation to be mixtures of molecules having different alkyl substitution and molecular weight. Liquids of group III had an unusual receding behavior (Figure 1,C, Figure 10,A). No true contact angle greater than zero was formed; the broadening of

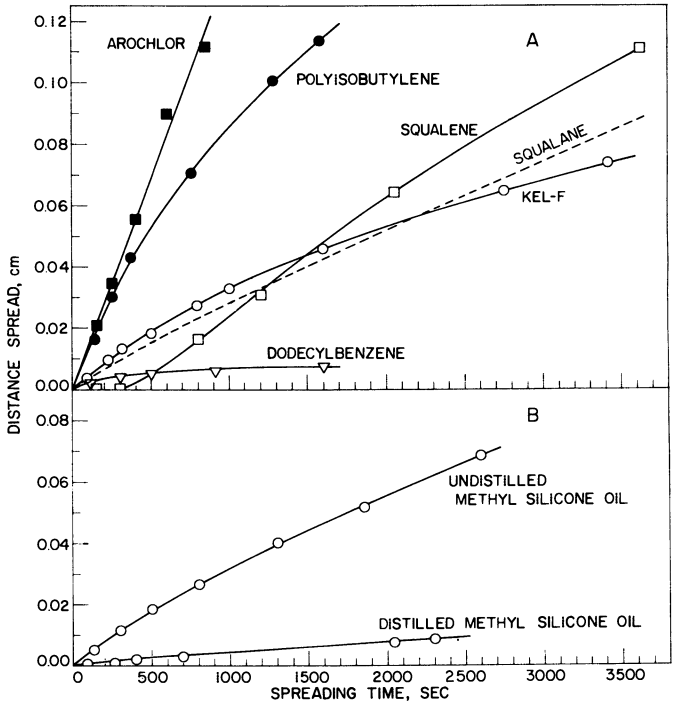

Figure 9. Comparison of distance spread vs. time for various liquids

A. Comparison of different structural types
B. Effect of degree of heterogeneity of polydimethyl silicone liquid

the first interference band showed that the liquid surface approached the plane of the solid asymptotically. A drop of the polyamylnaphthalene on a horizontal stainless steel surface spread initially under gravity, but spreading stopped after a few minutes. The drop was dome-shaped, but showed no definite contact angle with the surface. The recession of the apparent boundary reported here is not to be confused with the much more common retraction of liquids which form definite contact angles. Fractional distillation of the polyamylnaphthalene reduced its tendency to recede on a vertical surface, and one of the forerun fractions even spread upward slightly (Figure 10, B). Table II shows that the surface tensions of the main fractions remaining after stripping of volatiles from squalane and from polyamylnaphthalene differed from those of the original fluids by only 0.4 dyne/cm. in each case. However, the surface tension of the squalane was increased by stripping, while that of the polyamylnaphthalene was lowered. Another significant fact was that the heat from a concentrated light source, when directed to strike one side only of the drop on a horizontal surface, accelerated the spreading of group I liquids and the recession of group III liquids.

Publication Date: January 1, 1964 | doi: 10.1021/ba-1964-0043.ch026

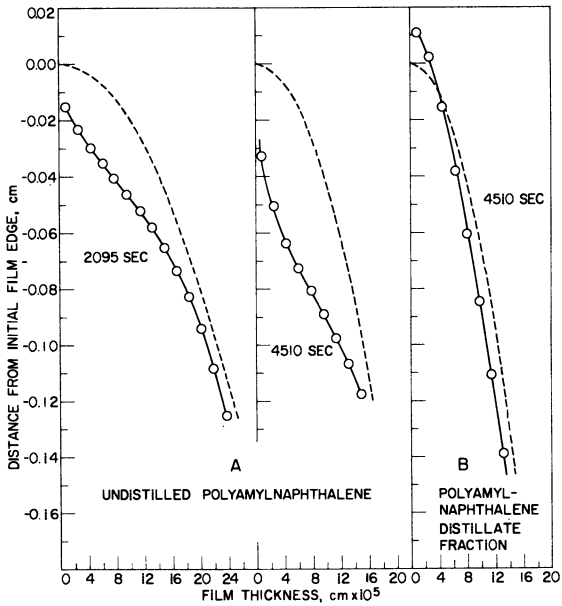

Figure 10. Film profiles on vertical steel plates

A. Undistilled polyamylnaphthalene
B. Fraction distilled from polyamylnaphthalene
Film thickness magnified 250 ×

Effect of Surface Finish of Solid on Rate of Spreading. The stainless steel surfaces employed in this study were optically polished on a pitch lap. They appeared scratch-free at 50 × magnification with bright-field illumination, but microscratches could be detected with dark-field lighting. The plates were cleaned between tests by polishing on metallurgical felt charged with fine alumina. Although their surfaces appeared highly polished to the unaided eye, microscopic investigation showed that both the number and the depth of the scratches increased by almost an order of magnitude with repeated cleaning. Differences noted in the spreading of a given liquid up new and repolished surfaces prompted the use of melt-drawn microscope slides, on which Nichrome had been vacuum-deposited. These surfaces showed no microscratches in dark-field illumination.

The effect of random surface scratches (ca. 1.0 microinch r.m.s. hill height in the worst specimens) was to increase by as much as 50% the spreading rate of liquids that spread, but roughness did not cause spreading of the "nonspreading" squalane obtained by distillation. Increased spreading rates on rough surfaces were usually associated with smaller constant slopes at the edge of the secondary film. The effect of scratches was examined more specifically by comparing

spreading rates on plates treated to obtain a strong pattern of unidirectional scratches parallel or perpendicular to the direction of spreading. Figure 11 shows that scratches in the direction of spreading accelerate the rate, while those at right angles to the oil movement reduce the spreading rate slightly below that on the smooth Nichrome-coated slide. When these experiments were repeated with distilled squalane, this liquid was not induced to spread by a favorable scratch configuration.

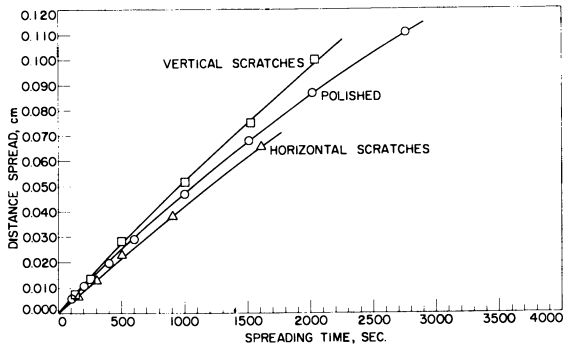

Figure 11. Effect of directional scratches on distance spread vs. time for 10% pristane in distilled squalane on vertical steel plates

Effect of Surface Energy of Solid on Spreading. It was to be expected that spreading rates and spreading geometries for a given liquid were essentially the same on the two metal surfaces, Nichrome and stainless steel. We were surprised to encounter essentially the same rate and spreading geometry on a stainless plate coated with a close-packed monolayer of barium dinonylnaphthalene sulfonate. Such a surface has been shown to have a critical surface tension for spreading of 29 dynes per cm., closely comparable with that for a polyethylene surface [3]. This value of γ_c is only a minor fraction of the surface energy for a clean metal oxide surface. Tests with a 0.5% solution of barium dinonylnaphthalene sulfonate in squalane ruled out the possibility that the monolayer was desorbed by the advancing oil. It appears that, given a liquid that wets a solid at a zero contact angle, the surface energy of the substrate is not an important factor in determining the rate of secondary spreading.

Discussion

A systematic explanation of the spreading phenomena observed requires consideration of mechanisms which will account for the invariable advance of a primary film, and relate the presence of volatile impurities to the spreading of secondary films and the frequent development of a ridge at their leading edge, account for the distinct recession of some liquids from a boundary at which they exhibit a zero contact angle, and explain the upward transport of significant amounts of liquid in films a micron or more thick.

Publication Date: January 1, 1964 | doi: 10.1021/ba-1964-0043.ch026

In the case of the slightly volatile liquids studied, the primary film is considered to advance largely by surface diffusion. While evaporation from squalane occurs at 25°C., the rate is so low that the amount transferred across an 0.08-cm. air gap between plane parallel surfaces of squalane and clean stainless steel during 72 hours is not great enough to be measurable with the ellipsometer. This instrument is capable of detecting the deposition of a monolayer or more of the hydrocarbon on clean steel. DeBoer [5] has pointed out that the energy of activation for the lateral motion of a physically adsorbed molecule is significantly smaller than that required for desorption to the vapor phase. The few surface diffusion constants of large organic molecules which have been measured appear to be of the same order of magnitude as the self-diffusion constants of similar molecules in the liquid phase [19]. This magnitude appears adequate to account for the observed rates of advance of the primary film. These rates will vary with the concentration gradient between bulk film and clean metal, and, more significantly, with the gradient resulting from differences in the energy of adsorption of the organic molecules on bare metal oxide and on a monolayer or more of the liquid species. Thus the crowding of the primary film by advancing bulk liquid sharpens the gradients and promotes faster diffusional advance. When the advance of bulk oil ceases, diffusion widens the primary film, reduces the gradient, and slows the diffusion rate.

Another factor which modifies the spreading rate of the primary film is the presence of microscratches or other microroughness on mechanically polished surfaces. These scratches are often 1000 A. or less wide and have width-depth ratios of no more than 10 [14]. The radius of curvature of such a trough may be as small as 1×10^{-5} cm. The pressure difference across a concave squalane surface wetting such a scratch will be of the order of kilograms per square centimeter. It is sufficient to induce rapid flow of oil along the bottom of the scratch until the radius of the oil surface in the scratch approaches infinity. Such open capillaries fill well ahead of the true diffusional advance of the primary film. Liquid spreads laterally from them by surface diffusion, so that a breath pattern reveals a network of squalane-wetted strips ahead of the slow moving film boundary.

The secondary film advances over a primary film which is generally more than a monolayer thick. Both the experimental results and a consideration of the nature of the primary film indicate that differences between the surface energy of the clean solid and the surface tension of the liquid do not contribute materially to upward movement of the secondary film against gravity. It is believed that its movement results from a surface tension gradient produced in and near the advancing edge by differential exhaustion of a more volatile species, this exhaustion being greater the thinner the film. If the loss of volatile species raises the average surface tension of the liquid, surface tension will be highest in the primary film, decreasing to that of the original liquid mixture as the film becomes thicker. As a result of this surface tension gradient the surface of the film will be drawn upwards; the effect will extend as far as the gradient itself. This movement of the surface layer will necessarily entrain some of the underlying liquid in accordance with hydrodynamic principles. As shown by Figure 12, the movement of liquid is greatest in the layer nearest the surface, which tends

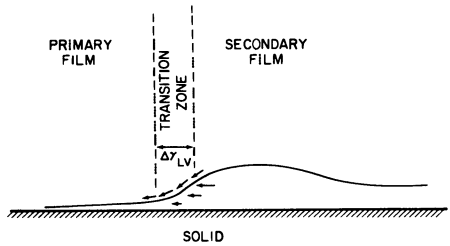

Figure 12. Schematic representation of flow pattern responsible for secondary spreading

to increase the slope of the advancing edge of the secondary film. The process continues until this effect is balanced by gravity and the tendency of surface curvatures to be ironed out by surface contraction. This balance produces a steady-state slope or false contact angle which decreases slowly over many hours, as the more volatile component is exhausted from the bulk film. Such quasi-constant slopes are an invariable feature of rapid spreading.

This explanation for the upward migration of thick liquid films is not new; it was advanced over a hundred years ago by Thomson [18] to explain the "tears of strong wine" phenomenon. He suggested that the creep of liquor up the glass wall was due to a surface tension gradient maintained by progressive depletion of alcohol from the ascending film. We are not aware that this explanation has been extended before to the spreading of low-volatile liquids.

This explanation of spreading is in agreement with the data reported. Since the time of Thomson there has been considerable study of phenomena ascribed to surface tension gradients and often referred to as Marangoni effects [15]. There has also been some quantitative analysis of flows produced by surface tension gradients [12,13]. The spreading rate of squalane is dramatically reduced by removal of more volatile components in a molecular still. The fractions removed have lower surface tensions than either the original mixture or the undistilled residue. Spreading of the purified squalane is enhanced by the addition of either hexadecane or pristane, which have higher and comparable volatilities and lower surface tensions than squalane. The increase in spreading rate is a function of the amount of volatile liquid added; for equal concentrations of either liquid the rate is increased more by pristane, which has a lower surface tension than hexadecane.

The complete failure of the 10% hexane-squalane mixture to spread is disconcerting until the rates of exhaustion of the various liquids from a thin film are examined quantitatively. Making reasonable assumptions about evaporation rates and diffusional transport of the volatile component through the solution, it can be shown that half of the hexane would be lost from a film 10 microns thick in 1 second. Half exhaustion of hexadecane from an equally thick film would require several hours. Thus the surface tension gradients produced by the evaporation of hexane disappear before any detectable flow of the viscous squalane has occurred.

In calculating the depletion rates of hexane and hexadecane from films of their mixtures with squalane it was assumed that the squalane is for all practical purposes nonvolatile, that the mixture of hydrocarbons behaves ideally, and that loss from a given film thickness is not replenished by lateral diffusion of solute from adjacent liquid. The calculated depletion times represent minimum values, since the failure of any of the assumptions would lower the rate of loss. It was also calculated that a very slight concentration gradient between the surface and the base of the film would cause transport of solute to the surface as rapidly as it was removed by evaporation, so that the difference between the bulk and surface concentration is not an important factor in the spreading mechanism.

A more critical test of an evaporatively induced surface tension gradient as an explanation of spreading behavior is afforded by the alkyl aromatic liquids, which either do not spread or actively recede from their original boundary while maintaining a zero contact angle. In the case of the alkyl biphenyls and the alkyl naphthalenes the fractions of lower molecular weight and higher volatility have higher surface tensions than the major high boiling component. This is because polyaromatic structures give higher surface tensions than aliphatic structures, and the proportion of polyaromatic component in the polyalkyl naphthalenes and biphenyls decreases as the size of the aliphatic substituent is increased.

Figure 13 shows that the relation between molecular weight and surface tension for the alkyl polyaromatics is the inverse of that for

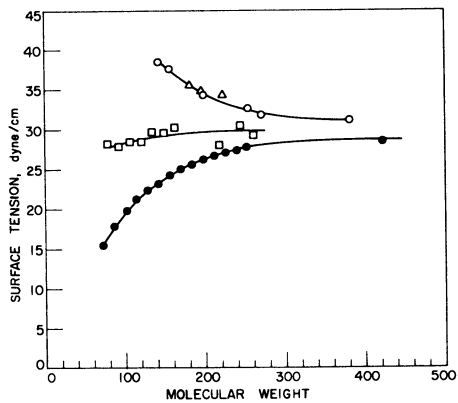

Figure 13. Change in surface tension with molecular weight for various groups of hydrocarbons

● n-Alkanes
□ Alkyl benzenes
○ Alkyl naphthalenes
△ Alkyl biphenyls

aliphatic hydrocarbons. As a result of this inverse relation the surface tension of the primary film is reduced by evaporative loss of the more volatile component and the surface flow is from the primary film towards the bulk liquid. This flow pattern causes the film edge to recede on the vertical plate and opposes the normal radial flow-out under gravity of drops on horizontal surfaces. Figure 13 also reveals why the alkyl benzenes show little tendency to advance or recede; there is almost no variation in surface tension with the degree of alkyl substitution in this particular series, so that loss of lower homologs by evaporation does not produce significant surface tension gradients.

The formation of a ridge of thicker film is a common but not an invariable characteristic of rapid spreading; its cause is clarified by considering the case in which a ridge developed at the upper edge of a stationary vertical film. This occurred when a barrier to spreading was placed above a squalane film by depositing a band of potassium perfluorodecanoate monolayer. The squalane moved upward until it reached the edge of the barrier, where it developed a stable contact angle of about 1°. Liquid continued to flow up the plate, however, until a distinct ridge developed. This ridge then persisted unchanged for many hours, while the film below drained away in the manner required by the Jeffrey equation.

The equilibrium contact angle formed by the squalane film at the barrier film edge requires explanation, since it differs from the zero angle normally found on clean metal surface or the near 80° contact angle to be expected for squalane on a perfluorodecanoate monolayer [17]. The small angle results because the edge of the barrier is not a straight line on the molecular scale but is a series of micropeninsulas and bays. The edge of the squalane is dragged against the peninsulas by the advance of liquid over clean steel at either side until a contact angle develops at the peninsula tip. The existence of the contact angle about the tip creates a local thickening of liquid film at this point. The action of surface tension to minimize the liquid surface thickens adjacent sections of the film, so that these also develop a finite angle at the film barrier. The apparent contact angle observed is the average of these effects when the angle developed becomes just sufficient to support the liquid retained in the resultant ridge. Given a small but stable contact angle representing an equilibrium of surface forces, ridge formation can be seen to follow as a further consequence of this equilibrium. Because of the weight of liquid it must support, the upper surface of the film curves downward from the angle imposed at the barrier. The situation is crudely analogous to that of a flexible rod attached to a vertical wall at a fixed angle and progressively loaded at points away from the wall. A mechanical equilibrium must ultimately be reached at which surface forces balance the weight of liquid that is restrained from draining by the fixed slope at the upper edge of the film. In principle, the equilibrium shape of the ridge can be determined analytically from the general equation for the mechanical equilibrium of an interface in a gravitational field [1], but such a calculation is involved and has not been undertaken.

Once it is clear that ridge formation is a consequence of a previously established slope at the film boundary, the appearance of such a ridge at the leading edge of rapidly spreading liquids is readily understood. In the moving film the surface tension gradient resulting from

Publication Date: January 1, 1964 | doi: 10.1021/ba-1964-0043.ch026

evaporative depletion creates and maintains the necessary fixed angle, and a ridge forms. If the rate of upward liquid transport below the ridge is sufficient to maintain the spreading film at a thickness as great as that of the required ridge, the secondary film will advance as a plateau rather than a ridge. As spreading continues, this rate of transfer below the film edge diminishes and the ridge is accentuated.

When a drop of liquid is allowed to spread on a smooth horizontal surface similar phenomena are observed, but the spreading pattern is modified because the gravitational forces are much smaller and operate to promote spreading rather than to oppose it. There is an initial gravity-driven spreading during the first few minutes, after which the hydrostatic head becomes negligible in comparison with viscous resistance or with the surface tension gradients which develop. The primary and secondary films then appear and ridges or plateaus form as in the case of upward spreading. Oils purified by removal of more volatile components spread extremely slowly and maintain the characteristic domed profile of a static drop. A liquid containing volatile impurities of lower surface tension, on the other hand, usually takes the form of a plateau a few microns thick, which thins as spreading continues, but maintains uniform thickness within one or two wavelengths of light. This leveling is a logical consequence of the spreading mechanism proposed, since any variation in film thickness creates a surface tension gradient tending to pull liquid into the thinner portions.

The observation in this work and by Bangham [2] that, in the presence of nearly saturated vapor the spontaneous spreading tendency of a drop is suppressed, is entirely consistent with the proposed mechanism. The evaporative depletion of solute from the liquid edge is prevented by the presence of surrounding vapor.

The observed spreading behaviors were promoted by surprisingly small differences in surface tension between the primary and secondary films. The lot of undistilled squalane which spread most vigorously had a surface tension of 27.6 dynes per cm. The surface tension of purified squalane is 28.6 dynes per cm., which indicates that, at the advancing film edge of impure squalane, the maximum possible difference in surface tension between the primary and secondary films is 1 dyne per cm. if all the more volatile components were lost from the primary film. Since the surface tension gradients are small, contaminants having comparable volatilities but minor differences in their surface tensions may produce significantly different spreading rates. A 10% solution of pristane in squalane has a surface tension of 28.3 dynes per cm., while a 10% solution of hexadecane in squalane has a surface tension of 28.5 dynes per cm. Since the surface tension of the purified squalane is 28.6 dynes per cm. and pristane and hexadecane have comparable volatilities, the potential driving gradient for spreading of the pristane solution is approximately three times that for the hexadecane solution.

The similarity between the spreading behavior of impure squalane on clean stainless steel and on steel coated with a monolayer of barium dinonylnaphthalene sulfonate provides further support for the explanation of spreading offered here. The surface energy of the monolayer-coated steel is only a fraction of that for the clean oxide-coated surface, but the monolayer's critical surface tension for spreading, 29 dynes per cm., is above the surface tension of the squalane. Consequently

Publication Date: January 1, 1964 | doi: 10.1021/ba-1964-0043.ch026

the latter gives a zero contact angle and forms a primary film on the monolayer. Since secondary spreading occurs over a primary film in both cases, the explanation proposed requires the spreading behavior on the two surfaces to be similar, and is in agreement with experiment.

Another support for the theory is furnished by the contrasting behaviors of the boundaries of drops of squalane and of polyamylnaphthalene when one side of each drop is warmed by a concentrated light beam. The heated boundary of the squalane drop spreads ahead of the unheated boundary on either side, while the heated edge of the drop of alkyl aromatic liquid recedes even more rapidly than the adjacent boundary. Evidently the heat, in each case, accelerates the process of evaporative depletion and thereby augments the surface tension gradient already present. If only the decrease in surface tension due to the increased temperature were operative, the heated squalane film should also have receded.

An interesting example of surface tension flow induced by temperature effects alone has been noted in thin films of silicone liquids on horizontal glass or metal plates heated to 400°C. Because of the great difference between the temperature of the plate and the air above it, there is a sharp vertical temperature gradient in the liquid film. The surface of any thin spot in the film will be hotter and have a lower surface tension than thicker portions near it. Consequently the film is unstable and the liquid draws up into small droplets, distributed over a much thinner film against which they nevertheless show zero contact angles. The droplets spread as soon as the temperature is lowered.

The theory of spreading proposed makes it possible to select additives for almost any liquid to enhance or counteract its tendency to spread. Experiment verified that undistilled squalane could be made nonspreading for several days by the addition of 5% of isopropylbiphenyl. The latter has a surface tension 7 dynes per cm. higher and a boiling point 50°C. lower than squalane, so that evaporation at the edge of a film lowers the surface tension relative to the bulk liquid mixture instead of raising it. The polymethylsiloxane liquids are often troublesome because of their excessive spreading, but the addition of small amounts of a more volatile methyl phenyl silicone having a higher surface tension prevented spreading for 2 to 3 weeks.

Publication Date: January 1, 1964 | doi: 10.1021/ba-1964-0043.ch026

Practical Implications

The spreading phenomena reported here have more than academic significance; they modify or control the performance of liquids in lubrication, in surface coating, and in the application of insecticides.

In the lubrication of ball bearings, oil is transported by surface creep from the grease supply to the raceway; this creep is favored by the molecular heterogeneity of ordinary petroleum oils, whose more volatile components have lower surface tensions than the total oil mixture. If one undertakes to lubricate with a radiation-resistant alkyl aromatic oil, however, the situation may be reversed, and the deliberate inclusion of a minor amount of an oil of lower surface tension is indicated. The recession phenomena reported for silicone liquids on a 400° surface remind us that at the high temperatures and temperature gradients existing in some military equipment oil films may be expected

to migrate away from the hottest points on the surface, which may be where the lubricant is needed.

In the spray application of thin coatings it is important that the droplets spread quickly to cover bare islands on the surface; the results of this study point the way to formulations in which a high spreading rate is assured by the choice of solvents of suitable volatility and surface tension. Similar considerations apply to the spraying of disinfectants and insecticides.

The excessive creeping tendency that causes polymeric liquids such as polyisobutylene and the methyl silicones to contaminate their surroundings can be counteracted by the addition of small amounts of a suitably chosen liquid.

Literature Cited

(1) Adam, N. K., "Physics and Chemistry of Surfaces," 2nd ed., p. 9, Oxford Univ. Press, London, 1938.
(2) Bangham, D. H., Saweris, Z., Trans. Faraday Soc. **34**, 554 (1938).
(3) Bascom, W. D., Singleterry, C. R., J. Phys. Chem. **65**, 1683 (1961).
(4) Bateman, J. B., Harris, M. W., Ann. N.Y. Acad. Sci. **53**, 1064 (1951).
(5) deBoer, J. H., "The Dynamical Character of Adsorption," p. 90, Oxford Univ. Press, London, 1953.
(6) Drude, P., "The Theory of Optics," Longmans, Green New York, 1902.
(7) Fox, H. W., Chrisman, C. H., Jr., J. Phys. Chem. **56**, 284 (1952).
(8) Fox, H. W., Hare, E. F., Zisman, W. A., Ibid., **59**, 1097 (1955).
(9) Hardy, W. B., "Collected Works," p. 38, 667, Cambridge Univ. Press, Cambridge, England, 1936.
(10) Harkins, W. D., Jordan, H. F., J. Am. Chem. Soc. **52**, 1751 (1930).
(11) Jeffreys, H., Proc. Cambridge Phil. Soc. **26**, 204 (1930).
(12) Levich, V. G., "Physicochemical Hydrodynamics," Prentice-Hall, Englewood Cliffs, N. J., 1962.
(13) Pearson, J. R. A., J. Fluid Mechanics **4**, 489 (1958).
(14) Samuels, L. E., in "Surface Chemistry of Metals and Semiconductors," H. C. Gatos, ed., p. 100, Wiley, New York, 1960.
(15) Scriven, L. E., Sternling, C. V., Nature **187**, 186 (1960).
(16) Shafrin, E. G., Zisman, W. A., J. Phys. Chem. **64**, 519 (1960).
(17) Ibid., 66, 740 (1962).
(18) Thomson, J., Phil. Mag. **10** (4th ser.), 330 (1855).
(19) Volmer, M., Adhikari, G., Z. Physik. Chem. **119**, 46 (1926).

Received April 1, 1963. Portion of a thesis submitted to the Graduate School of Georgetown University in partial fulfillment of the requirements for the M.S. degree in chemistry.

INDEX

A

Publication Date: January 1, 1964 | doi: 10.1021/ba-1964-0043.ix001

B

C

D

Publication Date: January 1, 1964 | doi: 10.1021/ba-1964-0043.ix001

Publication Date: January 1, 1964 | doi: 10.1021/ba-1964-0043.ix001

Q

R

Publication Date: January 1, 1964 | doi: 10.1021/ba-1964-0043.ix001

S

T

V

Publication Date: January 1, 1964 | doi: 10.1021/ba-1964-0043.ix001

W

Y